MONASH University

SPRAY COATED NANOCELLULOSE FILMS
PRODUCTION, CHARACTERIZATION
AND APPLICATION

**Thesis in the fulfilment of the requirement for the degree of
Doctor of Philosophy in Chemical Engineering**

Kirubanandan Shanmugam

M.A.Sc (Engg)

Department of Chemical Engineering

Faculty of Engineering

Monash University

May 2019

THIS PAGE HAS BEEN INTENTIONALLY LEFT BLANK

Dedicated to

High Performance Fibre Materials Group,

Bioresource processing Research Institute of Australia,

Department of Chemical Engineering,

Monash University,

Australia

THIS PAGE HAS BEEN INTENTIONALLY LEFT BLANK

Copyright notice

Kirubanandan Shanmugam

General Declaration

This thesis contains no material which has been accepted for the award of any other degree or diploma at any university or equivalent institution and that, to the best of my knowledge and belief, this thesis contains no material previously published or written by another person, except where due reference is made in the text of the thesis.

Signature: …………………

Print Name: Kirubanandan Shanmugam

Date: 27th May 2019

TABLE OF CONTENTS

List of Chapters

List of Appendices

MONASH UNIVERSITY
Thesis including published works declaration

I hereby declare that this thesis contains no material which has been accepted for the award of any other degree or diploma at any university or equivalent institution and that, to the best of my knowledge and belief, this thesis contains no material previously published or written by another person, except where due reference is made in the text of the thesis.

This thesis includes 2 original papers published in peer reviewed journals (Chapter 2 and 3), 1 submitted publication (Chapter 4), 2 unpublished publications (Chapter 5 and 6). The core theme of the thesis is Spray Coated Nanocellulose films: Production, Characterization and Applications. The ideas, development and writing up of all the papers in the thesis were the principal responsibility of myself, the student, working within the Department of Chemical Engineering, Monash University under the supervision of Associate Professor Warren Batchelor, Professor Gil Garnier, Monash University and Assistant Professor Swambabu Varanasi, Indian Institute of Petroleum & Energy , India.

(The inclusion of co-authors reflects the fact that the work came from active collaboration between researchers and acknowledges input into team-based research.)

In the case of chapter 2 and 3 my contribution to the work involved the following:

Thesis Chapter	Publication Title	Status	Nature and % of student contribution	Co-author names, Nature and % of co-author contribution	Co-author(s), Monash student Y/N
2	Rapid preparation of smooth nanocellulose films using spray coating.	Published	60% Key Ideas, experimental works, data analysis and drafting first manuscript	Swambabu Varanasi (5%), Gil Garnier (5%), and Warren Batchelor (30 %) for Reviewing and Editing	N
3	Flexible spray coating process for smooth nanocellulose film production.	Published	60% Key Ideas, experimental works, data analysis and drafting first manuscript	Hamid Doosthosseini (10%) for experiments and writing, Swambabu Varanasi (5%), Gil Garnier (5%) for reviewing, and Warren Batchelor (10%) for reviewing and editing.	N
4	Nanocellulose films as air and water vapour barriers: A recyclable and biodegradable alternative to polyolefin packaging	Published	60% Key Ideas, experimental works, data analysis and drafting first manuscript	Hamid Doosthosseini (5%) for writing, Swambabu Varanasi (5%), Gil Garnier (5%) for reviewing, and Warren Batchelor (15%) for reviewing and editing.	N

I have renumbered sections of submitted or published papers in order to generate a consistent presentation within the thesis.

Student signature: S. Kirubanandan   **Date:** 27th May 2019

The undersigned hereby certify that the above declaration correctly reflects the nature and extent of the student's and co-authors' contributions to this work. In instances where I am not the responsible author I have consulted with the responsible author to agree on the respective contributions of the authors.

Main Supervisor signature: **Date:**   10/10/19

THIS PAGE HAS BEEN INTENTIONALLY LEFT BLANK

THIS PAGE HAS BEEN INTENTIONALLY LEFT BLANK

ACKNOWLEDGEMENTS

ABSTRACT

Nanocellulose (NC) is a biodegradable, renewable and sustainable material. It has strong potential to use as a functional material in various applications such as barriers, coatings, electronics and biomedical applications. Key limitation for its commercial application is the lack of an efficient method to roll to roll preparation of nanocellulose films. Therefore, development of a rapid method for the fabrication of NC films is required to meet their high demand.

Vacuum filtration is a commonly used method to prepare NC films. However, the film preparation is not time efficient because of the high drainage time and difficulty in separation of wet film from filter after drainage. In this thesis, a novel method to prepare a smooth NC film using spray coating was developed, which is delineated in the first chapter. The NC fibre suspension is sprayed on a metal surface, imitating the spraying of a paint. This work highlights that film preparation time is unaffected by the target basis weight. NC films with the basis weight (weight per unit area) and thickness ranging from 50 to 200 g/m^2 and 84 μm to 243 μm, respectively were prepared just by varying the NC suspension concentration. One side of this film, which is in contact with the metal surface (stainless-steel plate) was smooth, having the RMS roughness of 389 nm evaluated over a 1 cm^2 inspection area with an optical profiler and 81.1 nm with an inspection zone of 100 $μm^2$ from AFM. Lastly, film was prepared with high manufacturing speeds, with each film only taking a minute of operator time to form the sheet, independent of the mass per unit area of the film. However, the evaporation of water from the spray coated wet film took more than 24 hours in air drying and 1 hour in an oven at 105 °C. The removal of water from the wet films severely limits the production rate in the spraying process.

In the second chapter, the optimization of spraying process parameters is explained and also the range of mechanical properties and bulk properties of the spray coated NC film is listed. Additionally, the experimental set up configurtions to enhance the uniformity of spray coated NC films and their properties is explained. In the first set of experiments, conveyor velocity varied while keeping NC suspension concentration fixed at 1.5 wt. %. In the next two set of experiments, NC suspension was varied, while keeping conveyor speed fixed at either 0.32 or 1.05 cm/s. By varying speed and solid concentration, spray-coating was found to allow efficient production of films with basis weights ranging from 38 to 187 g/m^2, with the film thicknesses ranging from 59 μm to 243 μm, respectively. It was found that, there is a universal linear relationship between the thickness and basis weight, independent of the process conditions. Film uniformity is also noticeably dependent on the spraying process. The uniformity index of spray coated NC films, relative to vacuum filtered films, increased with conveyor speed at 1.5 wt. % solid concentration and was independent of solid concentration at low speed. Forming at a higher speed of 1.04 cm/s produced a maximum in uniformity in the concentration range from 1.5 to 1.75%, with these films being more uniform than

conventional films produced through vacuum filtration. The most uniform films produced by spraying also had a tensile index (TI) of 79 Nm/g comparable to (TI) 72 Nm/g of films produced via vacuum filtration. With an understanding of these parameters and effects, this method was demonstrated to be a more time efficient alternative method to produce NC films, than vacuum filtration. The research shows that the properties of the films produced by spraying can be much more easily tailored to the required application.

In the third chapter, the recyclability of spray coated NC films and the barrier performance of recycled NC films was investigated. The strength of recycled films retained 70 % of the virgin films. Due to poor hydrogen bonding between nanofibrils and hornification, a drop in strength of recycled fibres was observed. The water vapour permeability (WVP) of recycled NC film approximately doubled and increasing to 1.29×10^{-10} g.m^{-1}. s^{-1} Pa^{-1} which is still comparable to synthetic plastics such as Polyethylene (PE), Plasticized PVC, Oriented Nylon 6 and Polystyrene (PS). The formation of agglomerates during recycling due to the poor breakdown of the fibre could be the probable reason for the decrease in barrier performance. The optical uniformity measurements of recycled NC film confirms a drop in uniformity of the film at smaller length scales and an increase in uniformity at larger length scales, compared with virgin NC film. The retained strength and barrier properties and facile re-processability of the spray coated NC films promise a sustainable and recyclable alternative to conventional polyolefin packaging.

Commonly, Commercial Sodium Montmorillonite (MMT) is added to NC films to enhance the barrier properties of the composite. However, operation time to prepare NC/MMT composites increases enaroamoulsy. In fourth chapter, a time efficient method to prepare NC/MMT composites is delianated. It was found that the operation time to form composite film is less than 1 minutes independent of MMT concentration in NC suspension. However, the removal of water from the wet composite film consumed more than 24 hours via air drying. Water vapour permeability (WVP) of spray coated composites from the raw NC decreased initially with MMT loading and then increased with MMT addition above 5 wt. %. This could be due to the aggregation of MMT when the loading higher than 5 wt. %. The sodium from of the MMT allows to swell and exfoliate in the composite and is another reason for elevation of WVP. The water vapour permeability of the spray coated homogenized composites decreased with MMT loading from 5 wt. % to 20 wt. % and then increased due to the aggregation and swelling characteristic of Sodium MMT. At the optimal addition level, lowest WVP achieved with spraying method is 8.3×10^{-12} g/m.s.pa when sprayed at 2.4 wt. %, which included 20 wt. % MMT and 2 wt. % NC. The XRD measurements showed that the MMT were aligned in the plane of the film and were strongly interacting with the cellulose nanofiber matrix, as the interlayer spacing increased from 11.78 to 14.16 Å. The tensile index results showed the composites had good strength, stiffness and were significantly flexible. Considering the barrier performance and

strength of the nanocomposites, spray coated nanocomposites can perform as an effective barrier material, and spraying has the potential for the scalable process.

The spray coated NC film has two unique surfaces with a shiny and glossy smooth surface contacting the stainless steel surface and a rough side exposed to air. In this chapter, methods to enhance the smoothness of NC films was delineated. The three parameters controlling the roughness of the resultant NC films were the roughness of the substrate surface, the fibril diameter of the NC and Carboxymethylcellulose (CMC) addition. The aerial average roughness (Sa) on the smooth side of NC film was evaluated and varied between 1055±8 nm and 402±23 nm. The aerial RMS roughness (Sq) on the smooth side of NC film varied between 1400±269 nm and 550±36 nm at an inspection area of 0.07 mm^2. High-pressure homogenization reduces the nanofibril diameter of NC depending on the number of passes. When homogenized NC was used to spray NC films, the surface roughness decreased. The Sa of homogenized NC film varied from 1125nm to 362±14 nm and Sq varied from 1517 nm to 470± 20 nm. This compares with the Sa and Sq of 4 wt. % CMC and 1.75 wt. % NC composite film which varies from 396±28 nm to 262±26 nm and 507±34 nm to 335±117 nm, respectively. The controlling order of roughness of NC films is CMC addition>fibril diameter of NC> base substrates. The addition of CMC in the NC suspension decreases the surface roughness of the NC film. As a result, the fibril network formed a smoother film compared to a film without the presence of CMC. This study has shown that spraying of NC on base surfaces produces a smooth NC film and its smoothness was engineered via varying base surface and reducing fibre diameter of cellulose fibrils or adding CMC in NC suspension. These films could be potentially used in electronic applications.

To sum up, the spraying method on stainless steel surface is a rapid process to form film. The time taken for drying the spray coated wet film is a limitation in this method. This method is a potential alternative for roll-to-roll preparation of NC films and composites with smooth and glossy surface. It is not limited with only this NC material and could also make any films or composites from fibrous biopolymers.

LIST OF PUBLICATIONS

The following published and submitted papers are the outcome of this thesis and each chapter in this thesis published as individual research papers. The sections of these published papers have been renumbered as chapters in order to generate a consistent presentation within the thesis... Papers in the published format are included as Appendix II.

ORIGINAL RESEARCH PUBLICATIONS

1. Shanmugam, K., Varanasi, S., Garnier, G., & Batchelor, W. Rapid preparation of smooth nanocellulose films using spray coating. Cellulose, 24, 7 (2017): 2669 -2676.

2. Shanmugam, Kirubanandan, Hamid Doosthosseini, Swambabu Varanasi, Gil Garnier, and Warren Batchelor. Flexible spray coating process for smooth nanocellulose film production. Cellulose 25, 3 (2018): 1725-1741.

3. Kirubanandan Shanmugam, Hamid Doosthosseini, Swambabu Varanasi, Gil Garnier, Warren Batchelor, Nanocellulose Films as Air and Water Vapour Barriers: A Recyclable and Biodegradable Alternative to Polyolefin Packaging. Sustainable materials and technologies. December 2019.

4. Kirubanandan Shanmugam, Maisha Maliha, Vikram Singh Raghuwanshi, Swambabu Varanasi, Gil Garnier, Warren Batchelor, Flexible Process to produce Nanocellulose – Montmorillonite Composite via Spray Coating, would be submitted to Journal of Cleaner Production, Elsevier.

5. Kirubanandan Shanmugam, Humayun Nadeem, Christine Browne, Gil Garnier and Warren Batchelor, Engineering Surface Roughness of Nanocellulose Film via Spraying to Produce Smooth NC Substrates would be submitted to Colloid and Surfaces, Elsevier.

BOOK CHAPTER

1. Kirubanandan Shanmugam, Christine Browne, Gil Garnier and Warren Batchelor, Nanocellulose and its composites films – applications, properties, preparation methods and limitations – a literature review, will be submitted as Book chapter for Nanoscale Processing, Elsevier: Editor: Prof Sabu Thomas and Dr. Preetha,

CONFERENCE EXTENDED ABSTRACT

1. Kirubanandan Shanmugam, Hamid Doosthosseini, Swambabu Varanasi, Gil Garnier, Warren Batchelor, Effect of Recycling on the properties of nanocellulose –Barrier and Mechanical Properties. International Paper Physics Conference at PaperCon, Indianapolis, IN, USA, May 5-8, 2019.

RELATED CO-AUTHORED JOURNAL PAPERS

The following co-authored manuscripts are produced from my tenure of graduate studies and are also an application of spray coating in other areas of nanocellulose science and technology.

1. C. Czibula , C. Ganser , M. Kratzer , F. Brumbauer , M. Kräuter , K.Shanmugam , W. Bachelor , M. Penn , M. Ebner , M. Pramstrahler , F. Pilat , T. Chien , R. Schennach , B. Friedel and C. Teichert, "Silver Nanowires: A Versatile Tool For conductive paper" 16th Fundamental Research Symposium "Advances in Pulp and Paper Research, Oxford 2017".Pembroke College, Oxford, UK. 3rd – 8th September 2017.

2. Aysu Onur, Kirubanandan Shanmugam, Aaron Ng, Gil Garnier, Warren Batchelor, Cellulose fibre- perlite depth filters with cellulose nanofibre top coating for improved filtration performance, Volume 583, 20 December 2019.

3. Humayun Nadeem, Mahdi Naseri-Nosar, Kirubanandan Shanmugam, Christine Browne, Gil Garnier, Warren Batchelor, Production of Environmentally Friendly and Time Proficient Nanocellulose Films via Spray Coating, would be submitted to Journal of Cleaner Production, Elsevier.

4. Humayun Nadeem, Mahdi Naseri-Nosar, Kirubanandan Shanmugam, Christine browne, Gil Garnier, Warren Batchelor, Energy and Time Efficient NC based composite films produced via Spray coating for Packaging and Optical Applications would be submitted to Journal of Cleaner Production, Elsevier.

LIST OF FIGURES

Chapter 1

Chapter 4

Chapter 5

Chapter 6

LIST OF TABLES

Chapter 1

Chapter 2

Chapter 4

Chapter 6

LIST OF ABBREVATIONS

AFM	Atomic force microscopy
3D	Three dimensional
AS/NZS	Australian/New Zealand Standard
ASTM	American Society of Testing and Materials
AUC	Area under the curve
CMC	Carboxyl methyl cellulose
CNF	Cellulose nanofibre
LBL	Layer by Layer
LDPE	Low density poly ethylene
MFC	Micro fibrillated cellulose
MMT	Montmorillonite
MWCO	Molecular weight cutoff
NC	Nanocellulose
NFC	Nano fibrillated cellulose
OLED	Organic Light Emitting Diode
OP	Oxygen Permeability
OSSC	Ordinary stainless steel circular
OSSS	Ordinary stainless steel square
OTR	Oxygen transmission rate
PAA	Poly acrylic acid
PAE	polyamideamine-epichlorohydrin
PE	Polyethene
PLA	Poly (lactic acid)
PP	Poly Propylene
PPF	Paper Perfect Formation
PS	Polystyrene
PTFE	Poly tetrafluoroethylene
PV	Photovoltaic
PVA	Poly (vinyl alcohol)
PVC	Polyvinyl chloride
PVDC	polyvinylidene
R2R	Roll to Roll Coating
RFID	Radio-frequency identification

RFV	Relative formation value
RH	Relative humidity
RMS	Root mean square
SEM	Scanning electron microscopy
SP-NC	Spray coated nanocellulose film
SSS	Super polished stainless steel
SW	Silicon wafer
TAPPI	Technical Association of the Pulp and Paper Industry
TEM	Transmission electron microscopy
TEMPO	2,2,6,6-Tetramethylpiperidin-1-yl)oxyl
	2,2,6,6-Tetramethylpiperidin-1-yl)oxidanyl
TI	Tensile Index
TMA	Trimethyl ammonium
UV	Ultraviolet
VF-NC	Vacuum filtered nanocellulose film
WVP	Water vapour permeability
WVTR	Water vapour transmission rate
XRD	X-ray diffraction

LIST OF NOMENCLATURE

%	percentage
ν	Velocity of conveyor
B	Basis weight of NC film
cc	cubic centimetre
Cm^3	Cubic centimetre
C_o	Concentration of NC suspension
g	grams
Gpa	Giga pascal
kg	Kilogram
kPa	Kilo pascal
m	meter
$\dot{m}$	Mass flow rate
m^2	Square metre
m^3	Cubic meter
min	minutes
mm	Millimetre
mm^2	millimetre square
MPa	Mega pascal
nm	Nanometre
Nm	Newton meter
ŋ	Efficiency factor in spray coating experimental set up
^oC	Degree Celsius
s	Seconds
Sa	Average Roughness
Sa_{film}	Average Roughness of NC film
Sq	RMS Roughness
Sq_{film}	RMS Roughness of NC film
SRabase	Average roughness of base surface
SRqbase	RMS roughness of base surface
w	Film width
Wt.	Weight
μm	Micrometre

THIS PAGE HAS BEEN INTENTIONALLY LEFT BLANK

CHAPTER 1

INTRODUCTION AND LITERATURE REVIEW

THIS PAGE HAS BEEN INTENTIONALLY LEFT BLANK

CHAPTER 1 – INTRODUCTION AND LITERATURE REVIEW

CONTENTS

NANOCELLULOSE AND ITS COMPOSITE FILMS APPLICATIONS, PROPERTIES, PREPARATION METHODS AND LIMITATIONS – A LITERATURE REVIEW

1.1. ABSTRACT

Nanocellulose (NC) is a biodegradable nanomaterial produced from lignocellulosic biomass. Mechanical, chemical or enzymatic processes are normally used for defibrillation of wood fibres into nanofibrils. It is a network of fibrillar cellulosic material in which there is a very wide range of fibrillar diameter. This material has unique characteristics leading to potential applications in fabricating various functional materials. These nanomaterials can be used as a base substrate or in coatings, as an alternative for synthetic plastic substrates and plastic laminates. These nanomaterials possess good barrier properties, although often still inferior to synthetic plastics, excellent mechanical strength and is biodegradable NC films and their composites have been used in developing functional materials such as barrier materials, substrates for printing circuits in flexible electronics, barrier coatings on the paper and paper board etc., In addition, there is a potential demand for NC films and composites to replace or eliminate conventional plastics. There are many methods available to prepare free-standing NC films and composites and these are critically reviewed and addressed in this chapter. Conventional methods are seen to be time-consuming, and unable to produce outstanding quality films, and hence set limitations on commercialization. Therefore, a rapid process to produce the NC films is required to meet the potentially large requirement for packaging and other functional material.

1.2. KEYWORDS

Nanocellulose; Nanocomposites; Applications; Oxygen permeability and Water Permeability.

1.3. INTRODUCTION

Synthetic plastics are extensively used in developing functional materials such as barrier layers on cellulosic substrates, packaging films and substrates for printed electronics. However, they have poor recyclability, biodegradability and plastic waste are potentially harmful to the environment. To overcome this limitation with plastics, cellulose substrates are used in the construction of various functional materials.

Cellulosic fibre products such as paper and paperboard are equal predominant with synthetic plastic materials. It is biodegradable and therefore safe for the environment. The

hydrophilic nature of cellulose macro fibres limits the specific application in various fields. In packaging, cellulose fibre products are a recyclable and biodegradable material. Cellulose fibre substrates have large pores and high affinity towards water and water vapour, which produces have poor water vapour and oxygen barrier performance.

To note, the barrier performance of these materials declines with increasing humidity. To mitigate these limitations, the cellulose fibre products are often associated with plastics, wax and/ or aluminium, for enhancing their barrier properties. However, these materials suffer from environmental issues, as difficult and inefficient to recycle. Recently, cellulose nanofibers such as nanocellulose (NC) plays a predominant role in material development due to its properties such as good strength and high specific area and aspect ratio.

Cellulose is the most predominant fibrous biopolymer among natural materials and is readily obtainable. It has good mechanical strength and stiffness. In addition to that, it is biodegradable and recyclable. Cellulose from plant sources such as wood, grass, agricultural and lignocellulosic waste is a potential for replacing plastics and provides a platform for resolving many issues such as reduction of oil stocks, synthetic plastic pollution, and carbon footprint. This is a renewable and non-toxic, eco-friendly material and biocompatible in nature. The source of cellulose via the photosynthesis process in plants is estimated to be from 10^{11}–10^{12} tonne per annum [2]. Microbial fermentation is an alternative way to produce bacterial cellulose.

Cellulose is used in regenerated cellulose fibres, and in cellulose ethers and esters. These materials are used as additives, coating materials, thickeners, stabilizers, binders and fillers in foods, pharmaceutics, sanitary, and textile etc., Due to its mechanical properties and barrier performance, it plays a major role in developing packaging materials such as papers and paper boards. The presence of surface hydroxyl groups in the cellulose gives a platform of chemical modification, resulting in tailoring its properties and functionality. The reduction of cellulose macro fibres via mechanical, chemical and enzymatic processing into cellulose nanofibers has potential benefits and drastically changes its characteristics from macro fibres [3]. Nanocellulose (NC) consists of entangled cellulose nanofibrils several micrometres long containing both amorphous and crystalline regions. These regions are well connected through intra and intermolecular bonds. The crystalline domain of the cellulose is maintained by hydrogen bonding and Van der Waals forces among the hydroxyl groups in the cellulose fibrils. The twists and torsions are present in the amorphous structure. The reduction of cellulose

fibres into nanofibrils increases its inter-fibrillar bonds permitting a strong compact network and drastically increases its strength, E-modulus, viscosity, optical properties and barrier performance. It is an eco-friendly material used for various applications. NC has high aspect ratio, forming a compact fibrous network with a considerable density via strong interfibrillar bonds. The fibrous network of NC acts as a good barrier against oxygen, comparable to Low density polyethylene (LDPE), High density poly ethylene (HDPE) and Poly Proylene (PP). However, Nanocellulose has only moderate barrier properties against water vapour, something which can be improved by incorporation of inorganics [4] in cellulose fibrils [5].
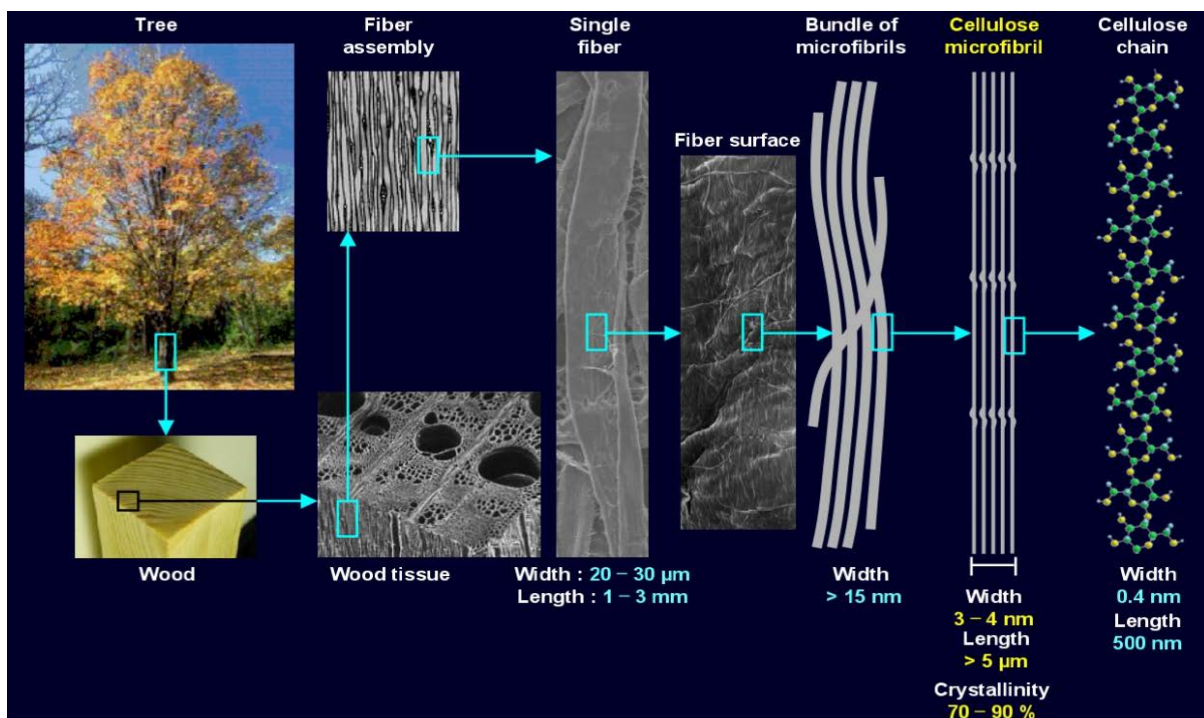
Figure 1 - Hierarchical Structure Of Cellulose From Wood To The Molecular Level Cellulose, Obtained From Isogai, 2011 [1]
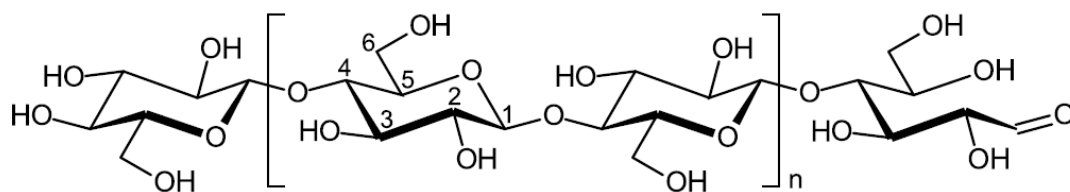
Figure 2-Molecular Structure of Cellulose, obtained from Nechyporchuk *et al,* 2016 [6]
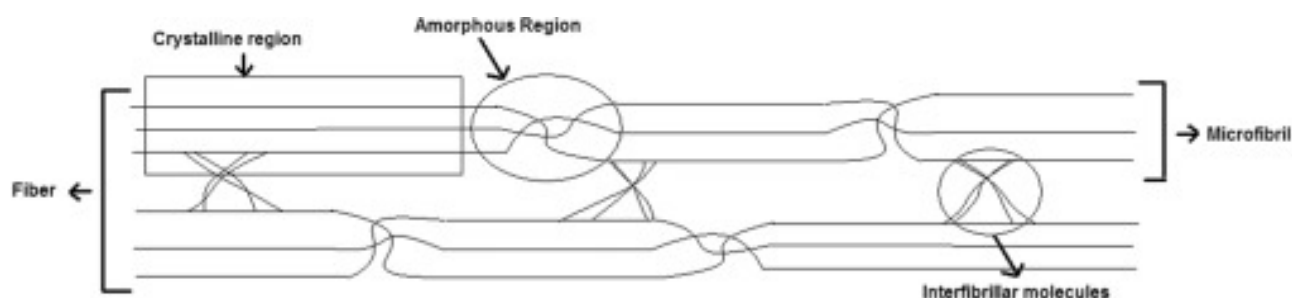
Figure 3-Crystalline And Amorphous Regions Of Cellulose, obtained from Abdul Khalil et al, 2016 [7]

Cellulose is a linear carbohydrate polymer with repeating units of Cellobiose, a disaccharide with the formula $C_{12}H_{22}O_{11}$, consisting of two β-glucose molecules linked by a $\beta (1 \rightarrow 4)$ bond. As a natural polysaccharide, it is susceptible to microbial and fungal degradation. It is found as an assembly of cellulose fibrils chains forming well-organized fibre wall in the wood. Figure1 shows the organisation of cellulose fibres from wood to a single fibre and figure 2 shows the structure of cellulose and surface hydroxyl groups. Figure 3 shows cellulose containing two domains namely crystalline and amorphous regions.

The nomenclature of cellulosic nanomaterials has not been reported uniformly in the literature. As per the TAPPI Standard WI 3021, Cellulose nanomaterials are specified with various terms such as Cellulose nanomaterial, cellulose nano-object, cellulose nanostructured material, cellulose nanofiber, cellulose nanocrystal, cellulose nanofibril [8]. The fibre diameter of raw cellulose was reduced via mechanical, chemical and enzymatic processing resulting in the formation of nanocellulose. The term micro-fibrillated cellulose (MFC) refers to the product produced via the delamination of wood fibres by mechanical pressure with chemical or enzymatic treatment. The term MFC is consistent with nanofibrils, micro fibrils and nano fibrillated cellulose [2] with diameter from 10 nm to 100 nm , fibril length in the range from 500 to 10000 [9] and an aspect ratio of 100 [10]. It is composed of formed cellulose semi-microcrystalline fibrils generally produced via high-pressure homogenization of pulp from wood [11].

1.3.1. NANOCELLULOSE – A NOVEL FIBROUS MATERIAL

Nanocellulose (NC) can be classified into three types of (1) cellulose nanocrystals (CNC), [12] cellulose nanofibrils also called as nanofibrillated cellulose (NFC) and [12] Bacterial cellulose (BC) [13]. In this thesis, Nanocellulose in the form of cellulose nanofiber which is an entangled fibrous network of micro and nanofibrils has been used. NC contains

both amorphous and crystalline regions. These regions mainly contribute to functionality of materials prepared from NC. Nano-fibrils have high aspect ratio. Figure 4 shows the cellulose nanofibrils after two pass high pressure homogenization and the diameter of cellulose nanofibrils after this condition is ˜20 nm. The properties of NC are high elastic modulus (150 GPa) and high tensile strength (10 GPa) [13, 14]. Its properties are controlled by their cellulose fibrils' diameter and length. The aspect ratio of the cellulose fibrils depends on the source, processing method and particle type. The source of NC also decides its properties such as applicability and functionality in various fields [13].
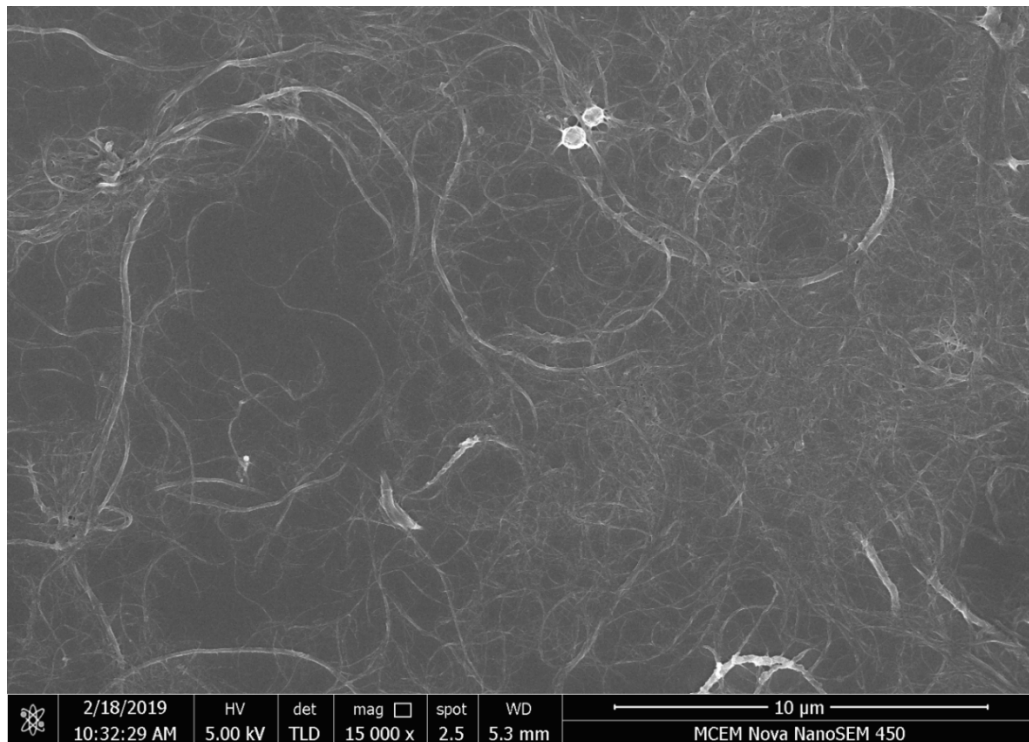
Figure 4 - SEM Micrograph of Nanocellulose (CELISH KY-100S treated with 2 Pass High-Pressure Homogenization).

1.3.2. CHARACTERISTICS OF NANOCELLULOSE

Nanocellulose has unique diameter distribution of cellulose fibrils having several micrometres in length [15]. Due to the presence of heterogeneous regions such as crystalline and amorphous regions in the fibre chain [16]. The crystalline region contributes mostly to the functionality of materials such as barrier and composites materials [9]. The fibril diameter distribution of NC and its aspect ratio depends on the source, pre-treatment processing and fibrillation method etc., and indirectly controls its rheological and interfacial properties.

The diameter and aspect ratio of NC can be evaluated via an image analysis of micrographs collected from SEM, TEM and AFM. Sedimentation of NC fibres is also performed to evaluate their gel point. Gel point is defined as the lowest solid concentration at which a continuous network of fibres exhibits mechanical stability under load. It is a transition point from a highly dilute solution of NC fibres into a concentrated suspension. At this state, nanofibrils in the suspension forms a compact network of fibres due to hydrogen bond between fibres. This network is known as the threshold of connectivity. Beyond this concentration, the NC suspension loses its mechanical strength due to insufficient contact of fibres with each other. This property depends on the aspect ratio of nanocellulose fibres. This characteristic has an important effect on the drainage time in vacuum filtration for NC film fabrication [17], [18]. The sedimentation method has been used to evaluate an aspect ratio for homogenized NC fibres in the research described in this thesis.

The notable properties are lightness in weight, optical transparency, chemical functionality and modification, dimensional stability and good barrier properties. Nanocellulose has potential compatibility with other materials like bio- natural polymers, proteins and living cells for biomedical applications and developing composites. The surface hydroxyl groups on NC provide an active site for various chemical modification and functionalization. The rheological behaviour of NC plays a major contribution in the coating process for producing barrier layers on the paper substrates and its shows pseudoplastic under shear thinning fluids [19].

1.3.3. SCOPE OF LITERATURE REVIEW

The predominant objective of this chapter is to review critically NC and NC composite film production and identify the research gaps and find the possible ways to rapidly form NC films. The potential applications for nanocellulose film and its composites as a barrier, as fire and flame retardant layers, smooth films, membranes and other applications will also be discussed. Additionally, Nanocellulose as sustainable barrier materials and the need for improvements in its barrier performance against water vapour, with a particular focus on developing composites with nanoclay, have been addressed. This chapter gives a critical review of the methods of nanocellulose film and nanocellulose composite films development from nanocellulose with nanoclay, including its advantages and disadvantages. The effects of various parameters on the rapidity of film making through spray coating process have been investigated. The optimization of the spray coating process to form a uniform NC film and to tailor the surface smoothness have been studied.

1.4.   NANOCELLULOSE PRODUCTION

The large sources of cellulose are wood, seed fibres (for example, cotton, coir etc.), bast fibres (flax, hemp, jute, ramie etc.) and grasses (bagasse, bamboo etc.)., The least source of cellulose are marine animals (tunicate), algae, fungi, invertebrates and bacteria [20]. Wood is the predominant feedstock of cellulose and is classified into hardwood and softwood. Apart from cellulose as a main constituent, hemicellulose, lignin and inorganic salts are also present in the wood. The principal difference between hardwood and softwood is the complexity in the structure with the level of heterogeneity in cellulose fibrils [21].

The fibres of cellulose processed from the hardwood pulp were harder to fibrillate into nanocellulose than that of the pulp from softwood. High pressure homogenization of hardwood pulp causes fluctuations of pressure in the homogenizer as well as clogging in the equipment. The hardwood pulp is more likely to form fibre aggregates during the processing than a softwood pulp. A high number of passes was required to break these aggregates. The structure of hardwood resists normally fibrillation process and only the ourter layer of the cell wall is subjected to fibrillation. In other words, the surface of fibres from hard wood were fibrillated into cellulose nanofibres [22].Hardwood fibres are more rigid than that of softwood having a high Runkel ratio, i.e. thick fibre wall relative to internal diameter [23]. It is reported that the processing of softwood to produce NC consumes less energy than that of hardwood as a feedstock [22].

It is reported the used hardwood pulp produced from either gum, maple, oak, eucalyptus, poplar, beech or its mixture utilised for NC production. The softwood pulp from produced from the northern spruce and Scots pine were used as feedstock for NC production. When processing of hard wood for manufacturing of nanofibres, the processing step/number of passes in high-pressure homogenization increased and requires high energy for fibrillation. The energy input for the production of NC from bleached eucalyptus kraft pulp through mechanical fibrillation varies from 5 to 30 kWh/kg [22, 23].Similarly, low energy is required for non- woody feedstocks such as grasses and marine sources to produce NC. These feedstocks contain low lignin with a more suitable cellulose structure for purifying and fibrillating the cellulose [6]. Recently, agricultural and food waste have also proved to be a potential feedstock for producing NC via a chemical-free process [24].

It is a significant challenge to fibrillate the microfibrils into nanofibrils through the refining process. Refining processes can be classified into the mechanical, chemical and

enzymatic processes. Before refining of microfibrils, the fibres are subjected to a pre-treatment such as de-lignification, to reduce the energy required for refining and produce high-quality nanofibers. De-lignification is the isolation of lignin in the lignocellulosic biomass. In this process, lignin is depolymerised by a pulping process and the solubilized lignin and hemicellulose in the biomass is removed by washing. Further delignification can be achieved via bleaching with chemical agents. During these pre-treatments, cellulose can undergo mechanical and chemical changes. The pre-treatments produce high-quality cellulose fibres, effectively removing non-cellulosic constituents. The disintegration of cellulose fibrils is promoted through the pre-treatment, reducing the aggregation of fibres to prevent clogs in further fibrillation process. As a result, the fibrillation into nanofibers is improved and minimized energy consumption [7].

1.4.1. MECHANICAL PROCESS

The most common mechanical treatment of cellulose fibres into nanofibers is primarily disintegration. Grinding is a feasible method for production of NC. In the grinding operation, the fibres are pressed between rotor and stator disc in the system and fibres are disintegrated due to the frictional forces and high impact by grinding action. This method has no clogging in the process and does not required any pre-processing of fibres. Recently, high intensive homogenization is reported as a novel method to produce nanofibers from cellulose macro fibres and its particles. However, it is an energy consuming method and demands approximately 25,000 kWh per tonne of the production of micro fibrillated cellulose. These methods are suitable for scaling up for production of NC. In high pressure homogenization, the critical factors namely pressure, NC solid concentration and number of passes control the consumption of energy [5]. The various methods of mechanical disintegration of fibres are reported in Table 01. It summarizes the concept of cellulosic fibres reduction, its isolation methods, its advantages and disadvantages [10].

The comparative study on the energy consumption of micro fibrillated cellulose production reveals that the micro fibrillated cellulose from homogenizer has high specific area and the films prepared from homogenized micro fibrillated cellulose has the good barrier performance such as lowest water vapour transmission rate reported to 3.81 x 10^{-4} mol /m^2.s. However, homogenization consumes high energy to produce micro fibrillated cellulose [25].

The high consumption of energy for the production of micro-fibrillated cellulose is a significant factor hindering the development of green based packaging materials from these

materials. The order of energy consumption for producing MFC to make films is high pressure homogenization> micro fluidizer > grinder with pre-treatment of fibres [26, 27].

Table 1 - Mechanical Refining for Production of Nanocellulose [10]

Methods for Isolation of Cellulosic Fibres	The concept of reduction of Size	Advantages	Disadvantages	Reference
High-Pressure Homogenization	High impact shearing forces reduce fibre size	Quick, Effective and continuous process. Good Reproducibility. Could control the degree of defibrillation	Clogging Pre-treatment of fibres required High Passing time and High Energy consumption Rise in temperature of suspension.	[28] [10]
Micro Fluidization	An intense collision with high impact led to the splitting of macro fibres into nanofibrils.	Less clogging Uniformity in size Lesser cycles	Not suitable for scale-up	[28]
Micro Grinding	The macro fibres are pressed in the gap between the stator and rotor disc in the grinder. High impact and frictional forces disintegrate the fibres into fibrils	Less energy and cycle No pre-treatment of fibres	cost is expensive Difficult in replacement of internal parts such as disk The crystalline nature of nanocellulose is reduced	[10]
High-Intensity ultrasonication	Sound energy is utilized to disintegrate macro fibres into nanofibrils.	High Power output and The high efficiency of defibrillation	Lab Scale application	[10]
Refining	High Shearing forces used for disintegration	-	-	[10] [29]
Cryo-Crushing	The refined macro fibres are treated with liquid nitrogen and it freezes the water in the fibres and then subjected to high impact grinding for disintegration.	High disintegration performance	Ice formation	[30] [9] [10]
Steam Explosion	The suspension is heated at high pressure and then vented into a vessel with low pressure. It is a type of explosion for reduction of fibres.	-	Chemical pre-treatment required	[31] [10]

1.4.2. CHEMICAL PROCESS

Mechanical disintegration of macro fibres is an energy consuming process, and this could be one of the stumbling blocks for scaling up the process. Nowadays, the demand for cellulosic materials is exponentially increasing in both research and industry. Therefore, an energy efficient process is required to scale up production of nanocellulose [6]. Chemical or enzymatic processes often allow nanocellulose to be produced with less energy input and improves fibrillation efficiency [10]. Various types of chemical processing of cellulosic nanofibers are presented, with their disadvantages and advantages in the following Table 2.

Table 2-Chemical processing for Nanocellulose [10]

Serial No	Chemical Methods	Reaction Mechanism	Advantages	Disadvantages
1	TEMPO –Oxidation	Oxidation of C6 hydroxyl groups into carboxyl groups and partially into aldehydes.	Shorter Reaction time	TEMPO is a poisonous and expensive chemical reagent
2	Periodate Chlorite Oxidation	Oxidation of the vicinal hydroxyl groups in the C2 and C3 positions	Increases Carboxyl Group	Weakens the structure of cellulose Long Reaction time
3.	Carboxymethylation	Incorporating carboxymethylated cellulose to the fibres. Enhancing anionic groups, Reduction of fibre friction, disintegration into fibrils	Improved fibrillation Reduced energy consumption	Thinner NFC produced

Table 2 summarizes the reaction mechanism of each chemical method for cellulose fibrillation into nanocellulose. These processes are also pre-treatments of cellulose fibres pulp suspension from wood or any other cellulose based feed stocks. For example, the nanocellulose was prepared via TEMPO oxidation and then subjected to high pressure homogenization for further fibrillation to produce cellulose nanofibrils.

1.4.3. ENZYMATIC PROCESS

Enzymatic processes can be used to produce the NC from cellulosic biomass. Enzymatic hydrolysis involves the cleavage of glycosidic bonds in the structure of the cellulose fibres. The classical enzymes are cellobiohydrolases that attack the crystalline region of cellulose, and endoglucanases that attack the amorphous or disordered region of cellulose. The subsequent fibrillation efficiency of NC production depends on the contact time of the enzymatic treatment and concentration of enzymes during the processing [10].The advantages of enzymatic hydrolysis are good fibrillation, reduced clogging of fibrils in the mechanical process, and less energy consumed in this processing.

1.5.   APPLICATION OF NC FILMS

The small dimension of Nanocellulose (i.e. fibre diameter and length) and its large surface area provided a great opportunity to develop it into a more functional material for various applications [32, 33]. Nowadays, the demand for NC is increasing due to several key technical applications. For example, NC film is rapidly growing in importance. In brief, NC film is a transparent, dense packing of cellulose nanofibrils offering good barrier performance and lower surface roughness than paper, leading to the development of many functional materials. Therefore, it can be used in high performance packaging, and can play as a good substrate for flexible & printable electronics, low cost diagnostics and organic displays. Although NC film's applications are many, in this chapter we restrict discussion to a few major applications.

1.5.1. BARRIER APPLICATIONS

Barrier materials are widely utilised for preventing the physical, chemical and microbiological deterioration of foods, nutrients, drinks, pharmaceuticals and cosmetics. Barrier materials require low gas and water permeability to protect the contents from the external influences and to preserve the flavour and nature of the packaged product [34]. Commonly used barrier materials are glass, metal such as aluminium and tin and synthetic plastics made from fossil fuels. These have good barrier properties and strength, but are not biodegradable and recyclable [35] [36]. Nowadays, the packaging materials should have low gas and water vapour permeability.

Synthetic plastic films and sheets are predominant in the current conventional practice. After use, these films are thrown away as waste in landfill resulting in a threat to the environment. The recycling of these synthetic plastics is an expensive process and retaining its barrier performance after recycling is problematic.

Cellulosic fibre products such as paper and paperboard are alternative flexible packaging materials that are biodegradable in the environment. However, the hydrophilic nature of cellulose limits the water vapour-barrier properties and oxygen barrier properties of paper. Due to the large pore sizes and high affinity towards water and its vapour, it has poor barrier performance [37]. Cellulosic fibre products are alternative flexible packaging materials that are biodegradable. However, their hydrophilic nature limits the water vapour-barrier properties and oxygen barrier properties in high humidity environments (> 65% Relative humidity) such as in frozen conditions. To mitigate these limitations, paper and paperboards

can be coated with plastics, wax or extruded aluminium to increase their barrier properties. However, these composite materials are very difficult to recycle.

Nanocellulose has good barrier properties due to its fibrous network [13] and crystalline region. The cellulose nanofibrils in the dense network form a compact structure reducing the passage of water vapour and oxygen. This complex fibrous network increses the permeation pathway for oxygen and water vapour, thus resulting a barrier against these permeants. Further the barrier performance of nanocellulose film can be enhanced by increasing tortuosity through incorporating montmorillonite clay in the fibreous network. NC film has low oxygen permeability (OP) due to the complex entanglement of fibrils [37]. The OP of NC film is reported to be 0.004 $cm^3.\mu m.m^{-2}.day^{-1}.kPa^{-1}$[38]. This OP value is quite comparable with synthetic plastics such as polyvinylidene (PVDC) (OP- 0.1-3 $cm^3.\mu m.m^{-2}.day^{-1}.kPa^{-1}$) [39], poly(vinyl chloride) (PVC) (20-80 $cm^3.\mu m.m^{-2}.day^{-1}.kPa^{-1}$) [39]. The water barrier properties of NC films is also extremely good under dry conditions although it is less effective in high humidity [26] Therefore, NC is a potential alternative for synthetic plastics in barrier application [40]. The source of fibres for making NC films, their chemical composition, physical structure, and the pretreatment methods used to produce the nanocellulose have an effect on their barrier performance [9].

1.5.2. PRINTED ELECTRONICS

Cellulose substrates such as paper are sustainable and low-cost substrates for developing functional materials such as printed electronics, solar cells [41], Radio- Frequency Identification Device (RFID) tags, Organic Light Emitting Diode (OLED)s, photovoltaic (PV) cells, printed diagnostics, batteries, memory cards etc [42]. Paper substrates is also used in the fabrication of transistors and super capacitors. However, paper is a porous substrate, highly susceptible to moisture absorption and has high surface roughness. Their properties limit the utilization of paper in the construction of electronic materials. The surface roughness of paper-based substrates varies from 2 to10 microns and this range of roughness limits the performance of solar cells [43]. Nanocellulose is considered as a base substrate for developing printed electronics due to the much lower surface roughness of the NC film [44]. NC provides smoothness on the substrates, is thermally stable and provides good barrier against water and air for the construction of flexible electronic device.

1.5.3. OTHER APPLICATIONS

The surface and mechanical properties of nano-fibrillated cellulose can be tailored. Films made from nanocellulose can have various outstanding mechanical, optical and structural properties and these properties are useful in fabricating various functional materials such as cellulose nanocomposites [45], inorganic nanocomposites [46], organic Transistors and conducting materials [47], Immunoassays and Diagnostics materials [48]. As a result, it is used in the field of photonics, as a surface modifier,, in nanocomposites, biomedical scaffolds and optoelectronics [13]. Recently, NC films have become one of the most promising high-performance functional materials potentially used as filters for removal of virus [49], adsorbents, catalysts [50], cell culture substrate, thermal insulator and drug carrier for drug delivery system [51]. Moreover, due to the barrier performance of nanocellulose and size, it is used to functionalize base sheets via creating barrier layers as a coating or to make freestanding sheets/films and nanocomposites [6]. The application of nanocellulose developed via academic research have increased rapidly. There are no nanocellulose film in commercial application and in practice. But there are commercial products such as TEMPO nanocellulose in Japan, Pure nanocellulose manufactured in Canada, USA etc. There are companies namely CelluForce, Kruger, Performance Bio Filaments in Canada, VTT in Finland, and InoFib in France for commercial production of Nanocellulose. Nanocellulose is an available feedstock for films development. There is a demand for a rapid manufacturing method for NC film. In particular, the demand for barrier application NC film to replace synthetic plastics in practice is urgent [52]. Table 3 summarizes the application of NC depending on its quantity in various fields. Figure 5 shows the products developed with NC in High-performance Fibre material Group, Department of Chemical Engineering, Monash University, Australia.
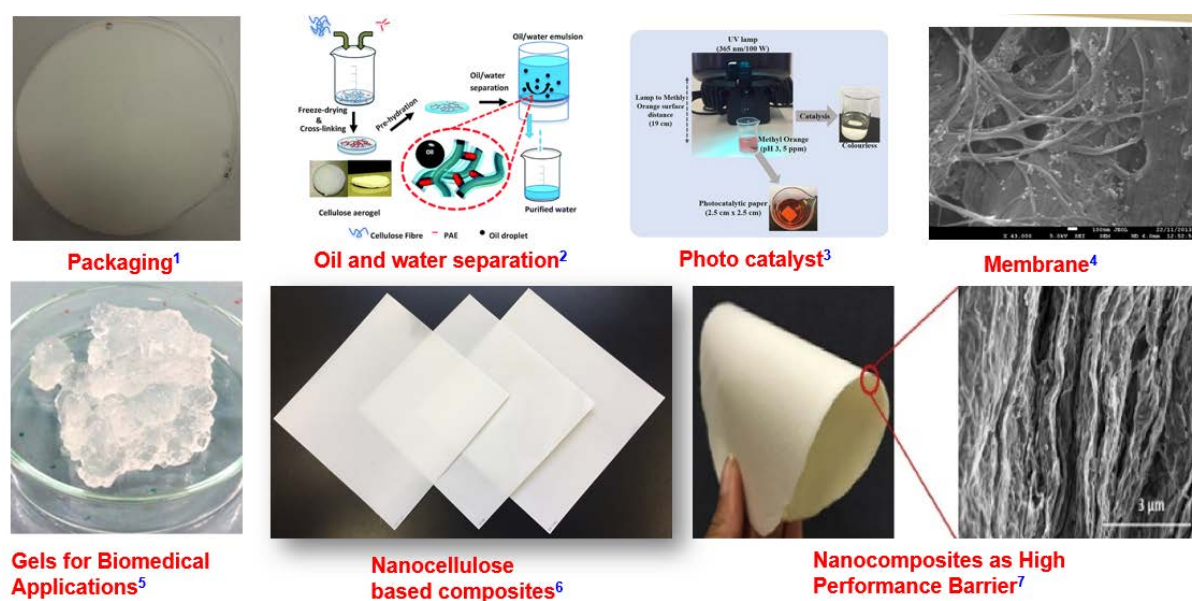
Figure 5- Applications of Nanocellulose Into Functional Materials From High-Performance Fibre Material Research Group, BIOPRIA, Monash University, Australia.

{1}. K.Shanmugam et al, Cellulose, 2017, 24, 7, 2669–2676. , {2} Z. he et al, RSC Adv., 2016, 6, 21435-21438.{3} U.M. Garusinghe et al, Scientific Reports, **8**, 2306 (2018) {4}. V. Swambabu et al, Chemical Engineering Journal 265 (1) 2015. {5}. Mendoza et al, J Colloid Interface Sci. 2018 1;509:39-46. {6} Maliha, 2018 {7}. U.M. Garusinghe et al, Colloids and Surfaces A, 540, 2018, 233-241.

1.5.4. PRODUCTS OF HIGH-PERFORMANCE FIBRE MATERIAL RESEARCH GROUP, MONASH UNIVERSITY.

1.5.4.1. PACKAGING

An homogenized NC film from MFC was prepared, via vacuum filtration, with an air permeance less than 0.003 µm/Pa.S, confirming that it is a good impermeable film for packaging applications [53]. The water vapour transmission rate WVTR and oxygen transmission rate OTR of the NC film at 23°C and 50% RH were 44.7 g/m^2.day and 20.1 cc/m^2.day respectively [54]. These values confirmed that a vaccum filtered NC film can be a good barrier.

1.5.4.2. OIL AND WATER SEPERATION

Crosslinking between nanocellulose and polyamideamine-epichlorohydrin (PAE) was used to produce an aerogel filter using a freeze drying cross linking method. The NC based aerogel filter was capable of de-emulsification of oil water mixture producing 100% oil water

separation efficiency even after 10 cycles of usage and yielding 98.6 % oil water surface free emulsion [55].

1.5.4.3. PHOTO CATALYST COMPOSITE

This composite was developed from nanocellulose -polyamide-amine-epichlorohydrin (PAE)-TiO_2 nanoparticles via vaccum filtration, and was designed as a photo catalyst for treatment of waste water. Figure 6 shows that the titanium dioxide in the composite degrades 95% of methyl orange dye in water in 150 min under UV light irradiation. The NC fibre network with PAE strongly hold TiO_2 nanoparticles and avoid the release of nanoparticles into the waste water. This composite can be used as a recylable , low cost photo catalyst membrane for waste water treatment [56].
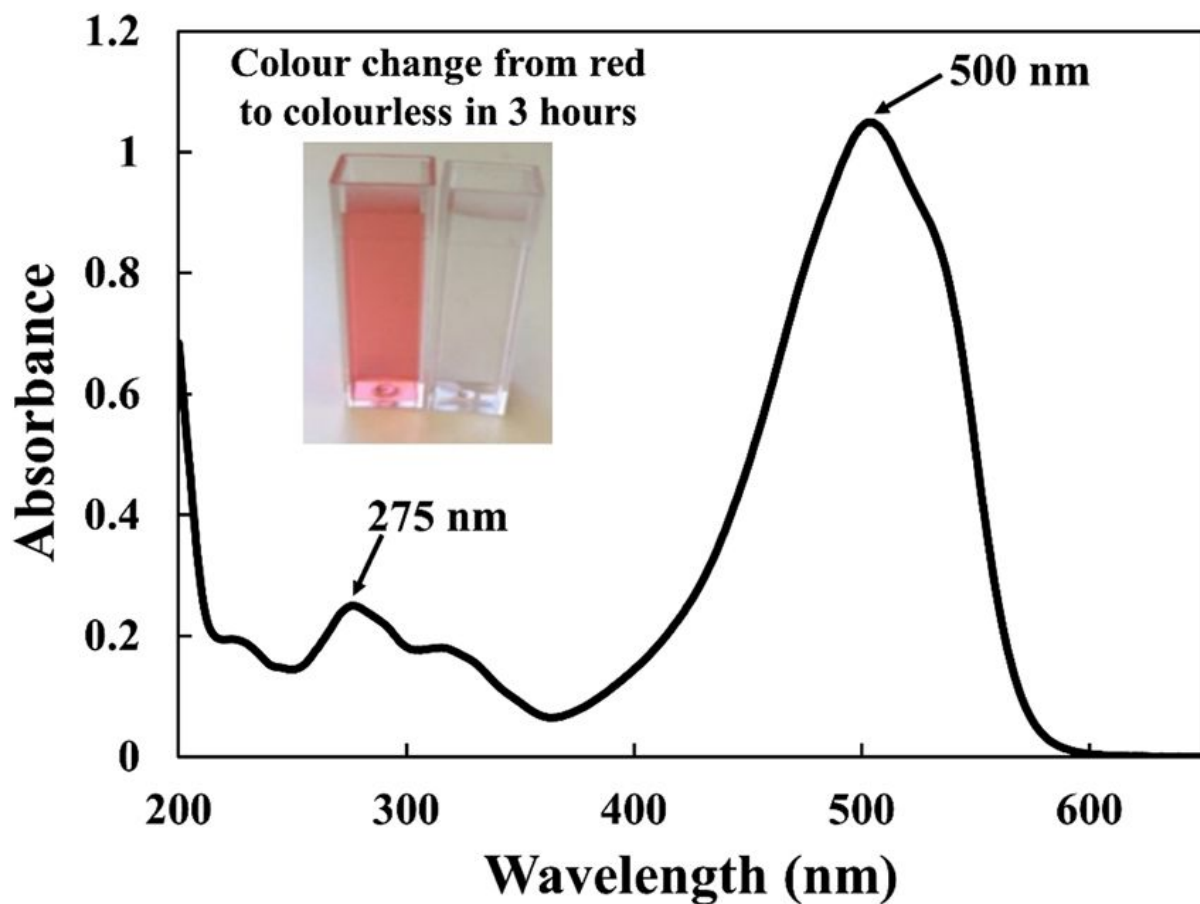
Figure 6- The Degradation of Methyl Orange Solution by TiO_2-MFC Composite as Photo Catalyst. The Spectrum Indicates Two Absorption Maxima. The Colour Of Dye Solution Reduced Using Photocatalysis Composite. The image obtained from Garusinghe *et al* 2018 [56].

1.5.4.4. MEMBRANE

Cellulose nanofibre membranes can be an alternative to synthetic plastic membranes and they are recyclable and biodegradable. In this case, the novel composite was prepared via vaccum filtration and the composite was produced with nanocellulose, silica nanoparticles (NP) and polyamide-amine-epichlorohydrin (PAE).The size of silica nanoparticles were 22 nm and NP acted as a spacer for controlling the pore of the composite. The function of PAE in the composite was to adhere with the negativly charged silica nanoparticles and promote the wet strength of composite. This composite membrane has a water flux of 80 L/m^2/hour, LMH and Molecular weight cutoff,MWCO of 200 kDa. The quantity of silica nanoparticle could be altered to tune the pore size. The composite funtions as membrane and can be used mainly in ultrafiltration applications [57].

1.5.4.5. GELS

Nanocellulose can be converted via TEMPO oxidation method, into hydrogels and gels for numerous biological and medical appliocations. Nanocellulose gels can be used for separation of protein via elctrophoresis and in diagnostics for bioseparation [58]. Nanocellulose hydrogels and gels are also suitable substrates for 3D cell culture for producing microenvironment for cell growth, tissue engineering scaffolds and drug delivery vehicles [59]. Carboxylated nanocellulose via TEMPO oxidation can be converted into foam structures as super adsorbent material (SAM) [60].

1.5.4.6. ANTI-MICROBIAL NANOCOMPOSITES

Anti-microbial nanocellulose composites using an anti-microbial agent phenyl bismuth bis (diphenyl phosphinate), via vacuum filtration [61] and spraying [62] were developed. These composites can act as anti-microbial packaging materials, biomedical bandages, and anti-microbial coating on the surface. Recently, Bismuth based anti-microbial agents has been shown to have broad spectrum activity against pathogens including antimicrobial resistant species. The anti-microbial potential of the 5 wt. % bismuth loaded composite was shown by the 15 mm zone of inhibition against both gram negative microorganisms such as *Escherichia coli* (E. coli) and *Pseudomonas aeruginosa* (P. aeruginosa), gram positive bacterium such as *Staphylococcus aureus* (S. Aureus), antimicrobial resistant pathogens namely *Vancomycin-resistant Enterococcus* (VRE) and *Methicillin-resistant Staphylococcus aureus* (MRSA). The WVP of the same composite was evaluated to be 4.4 x 10^{-11} g/Pa.s.m, comparable with synthetic plastics [62].

1.5.4.7. HIGH PERFORMANCE NANOCOMPOSITES

NC based nanocomposites for high performance barrier material were developed via an *in-situ* precipitation process. In this method, calcium carbonate nanoparticles were precipitated via a chemical reaction between sodium carbonate and calcium chloride in the NC film to yield a low permeability porous composite. The precipitated nanoparticles reduced the pore volume of the NC film, resulting in the low permeance of the composite. Figure 7 shows the difference between pure NC film and in-situ precipitated composite prepared from 0.2 M solutions and the presence of $CaCO_3$ nanoparticles interior of the composite. The WVTR and OTR of 1 wt. % $CaCO_3$ precipitated in NC film were 4.7 g/m^2.day and 2.7 cc/m^2.day respectively at 23°C and 50% RH. The tensile strength and E-Modulus of this composite were 91.96 ±14.99 MPa and 4.6 GPa respectively, confirming good strength and stiffness [54].
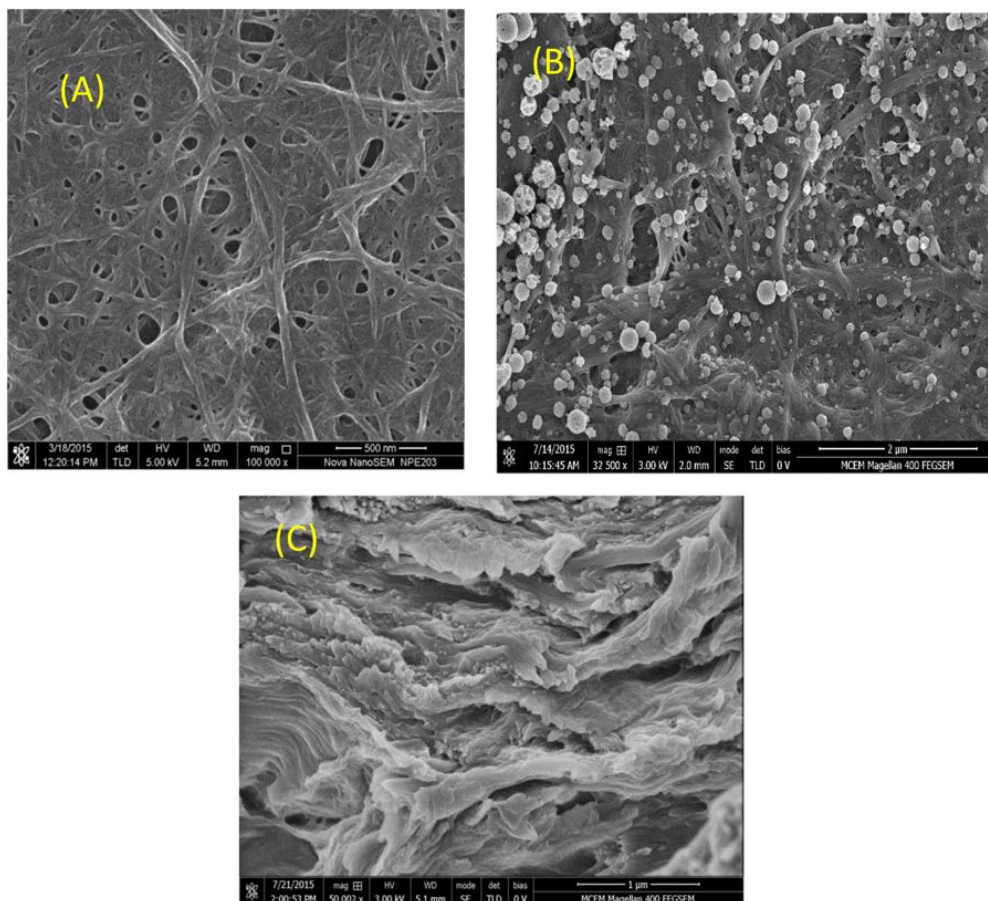
Figure 7 - SEM Micrographs of CNF Film and It's Composite Via In-Situ Precipitation Of Nanoparticles. (A) Pure CNC Film and (B and C) Surface and Cross Sectional View of Composite prepared via in-situ precipitation. The image obtained from Swambabu et al, 2018 [54].

High performance membranes were also achieved with a nanocellulose (NC)-Silicon –Di- Oxide , SiO_2 composite fabricated with a conventional vacuum filtration method. The pore size of the composite was reported to be less than 100 nm. The porosity of the composite could be tailored by varying SiO_2 loading in the NC suspension [63]. Similarly, a NC- Montmorillonite (MMT) composite was developed via vacuum filtration for packaging application. The WVP of the homogenised NC – MMT composite was reported to be 6.33±1.5 g.µm/m^2.day.kPa with 23.1 wt.% MMT comparable with synthetic plastics [4].

Table 3 - Application of NC [10]

Highly Consumption of NC	Low Consumption of NC	Novel and Under Development
Paper Production Process Strength Additives Barrier Layers Glossy surface Reduction of paper grammage Produce Smart Packaging Binding filler	Insulators Protection against sound and Heat	Medical, Industrial and Environmental Areas Biodegradable Sensors Membranes for air and water filtration
Coating and Films Co-binder and Thickener for paper coating Nanofiltration Membranes Barrier Films	Aerospace Industries Advanced Composite Materials Structures Interiors	Construction Field Reinforcement Fibres
Cement Processing Concrete Additive	Petroleum Aerogels Oil and gas processing	Electronics Smooth Substrates for flexible electronics Conducting substrates Recyclable Organics LED Photovoltaics
Automotive industry Composite Materials	Rheological Modifier Functional Pigments and Paint Products	Cosmetics
Packaging Composites Films Fillers	Construction Composites	Packaging Intelligent barrier materials
Printing Paper Good quality of printing		Films for photonics
Cosmetics Hygiene and absorbent products Textiles		3D Printing Tissue Engineering Scaffold

1.5.5. NANOCELLULOSE-MMT COMPOSITES AND THEIR APPLICATIONS

Although NC film is a flexible, strong, biodegradable and sustainable material. It has specific limitations in oxygen and water vapour permeability at high humidity where the pore size of NC film is increased by the swelling of the cellulose nanofibrils. Formation of flocs is a limitation in the preparation of nanocellulose films. To overcome this problem in the production of NC films, NC has been combined with polyelectrolytes [18] or nano inorganics to form composites [4]. One of the most important applications of NC is to develop composites with nano-inorganics [4, 64, 65]. The platelets of nano inorganics interact with cellulose nanofibrils network and fill their pores forming the composite with drastically enhanced properties These composites have specific applications as barrier, fire retardant, membrane and heat insulating materials. The incorporation of nanoclay into NC fibre network enhances its mechanical and barrier properties [4]. The nano-inorganics interact with cellulose nanofibrils promoting the functionality of the composite [64] [65]. The functionality of the composites can be enhanced by filling the pores in cellulose fibrous network resulting in good barrier composites, by forming aggregates in cellulose network resulting in fire retardant material, or by tuning the pores of cellulose fibrous network in membrane applications [57, 63] [66]. Table 4 summarizes the potential use of NC based composites.

1.5.5.1. BARRIER COATING

Nanocellulose–MMT suspension can be used for coating to produce a composite barrier layer on the cellulose substrates. The composite barrier coating lowers the oxygen and water vapour permeability of the sheet. 5 wt. % MMT and 1.4 wt. % NC coating on base sheet with thickness of $22 \pm 0.5\mu m$ and with a coat weight of 29 ± 0.5 g/m^2 has a WVTR of 8 ± 0.3 g m^{-2} day and OTR of 36400 ± 1100 cm^3 m^{-2} day. With only 1.4 wt. % NC coating on a base sheet with thickness $11 \pm 0.3\mu m$ and coat weight 9.9 ± 0.2g/m^2 had a WVTR of 24 ± 0.7 g m^{-2} day and OTR was above measurable range. Hence the 5 wt. % addition of MMT in NC suspension causes a significant decrease in WVTR and brought OTR in the range [67].

1.5.5.2. MEMBRANE

NC-MMT can be used for construction of membranes. For example, MMT in membranes can adsorb cationic dyes in the waste water and act as a cation exchanger for water treatment. Additionally, these composites can be used for the removal of heavy metals in waste water [68], [69].

Table 4-Application of NC based Nanocomposites [70]

Field of Applications	Functions of nanocomposites
Composites and Plastics	Shelf life extension
	Heat resistance
	Dimensional stability
Paper and Packaging	Intelligent packaging,
	See-through packaging;
	Ultra-violet screening packaging;
	Anti-microbial packaging;
Medical Application	Drug delivery and controlled release;
	Scaffold in tissue engineering;
	Implants
Barrier Properties	Shelf life extension;
	Down-gauging of films;
	Oxygen scavenger;
Electronics	Time-temperature integrator;
	Freshness indicator;
	Gas and Leakage detector;
	Sensors for food monitoring;
	Signal processor for biochemical pathways
Aerogel	Self-healing material

1.5.5.3. FLAME AND FIRE-RETARDANT

The development of non-toxic sustainable flame and fire retardants to replace synthetic materials is a challenging task. Cellulose-based flame- and fire-retardant materials are a green and sustainable alternative to halogen based retardant materials which are a toxic hazard that can cause halogen compounds to enter the food chain. Recently, nanocellulose has been shown to be capable of meeting the requirements of flame retardant material when used as a base substrate for nanocomposites. The nanocellulose provides a fibre network for clay platelets, which are embedded to form the composite and provide the fire resistance. The fibrous network gives toughness and strength to the composite [66] [71]

The addition of nano-clay is another approach to tailor the properties of composites for flame fire retardant properties [66]. The OP of 5 wt.% MMT composite film prepared via casting is 0.006 mL μm m^{-2} day^{-1} kPa^{-1} at 0 % RH and its mechanical strength is 18 GPa of E-Modulus

and 509 MPa tensile strength. Increasing the MMT to 50 wt.% in the composite decreases its OP to 0.0008 mL µm m^{-2} day^{-1} kPa^{-1}. However, the mechanical strength of the composite film decreased at 50 wt.% of MMT loading. These composite could be used as gas barrier material [72].

The 50 wt. % MMT–50 wt. % NC composite in a continuous fibrous network of nanocellulose formed via vacuum filtration has also been investigated. The strength of this composite was 124 MPa and 8.7 GPa of E. Modulus. The OTR of the pure NC film was 0.048 cm^3 mm m^{-2} day^{-1} atm^{-1} at 50% RH and 17.8 cm^3 mm m^{-2} day^{-1} atm^{-1} at 95% RH. By comparison the OTR of 50 wt. % MMT–50 wt. % NC composite was 0.045 and 3.5 cm^3 mm m^{-2} day^{-1} atm^{-1} at 50 % and 95% RH respectively. The OP of pure NC film was increased by 370% from 50 % RH to 95%. In the case of composite, the increase in OP was only 13 % from 50 % to 95% RH. This demonstrates that the addition of MMT into fibrous structure formed a composite with potential gas barrier and flame retardancy properties [66]. Both 30 wt. % and 50 wt. % MMT in NC composite demonstrated a good fire retardancy material. Flammability test and calorimetry confirmed self-extinguishing properties. The oriented MMT in the NC fibrous network hinders diffusion of oxygen and ignition process [71].

1.6. PROPERTIES OF NANOCELLULOSE FILMS

The physical properties of NC film are related to their thickness, basis weight, density and porosity. These properties strongly rely on the properties of cellulose nano-fibrils such as their diameter and aspect ratio and the method of fabrication [73].

1.6.1. THICKNESS AND BASIS WEIGHT

The thickness and basis weight of NC film affects numerous properties such as strength, density and barrier performance. The method used to fabricate the NC film also controls its characteristics and properties. In vacuum filtration, the thickness of NC films varies from 50 to 100 µm and basis weight varies from 60 to 80 g/m^2 [53]. The dewatering time in the forming process increases when NC suspension concentration is increased for higher basis weight NC film. Casting, a simple method, gives a non uniform NC film due to shrinkage and wrinkles formed. Cast NC films are produced with thickness varying from 5 to 30 µm [74].

1.6.2. APPARENT DENSITY

The density of the fibrous network in NC film controls the barrier and mechanical properties [75]. The density of the NC film is controlled by fibril interactions and film processing. The NC film preparation method controls film density by agglomeration and non-uniformity in the surface of NC film. The clumps of cellulose nanofibers during processing of NC film affects its density. Partial homogenised or non-homogenised NC can produce a drop-in density of film in vacuum filtration. The NC film produced with homogenization of fibres shows densification with lower thickness due to the packing of nanofibrils. The mean densities of micro fibrillated cellulose ,MFC film via vacuum filtration was 820 kg/m^3 [53].

1.6.3. FILM UNIFORMITY

In the processing of cellulose fibres products such as paper and paper board, the quality of the film/sheet is evaluated by its uniformity. This property is a confirmation for evaluating uniformity of NC film. This property affects directly surface quality, strength and printability of the film [76]. A paper perfect formation tester is used to estimate relative formation value (RFV) of the sheet/film. The RFV measures the uniformity of NC film. If the RFV is ≥ 1, the film has good uniformity, if it is < 1, the film is said to have worse formation [77]. In the studies described in this thesis we have used this measure to evaluate the formation of NC film via spraying and to make comparisons with the film produced from vacuum filtration.

1.6.4. MECHANICAL PROPERTIES

The strength of NC film is important in maintaining functions of NC films in barrier materials, membrane and composite. NC films should have enough support for the matrix. The fibres in the NC film form a compact network with hydrogen bonds between neighbouring fibres developing the strength and modulus and high density of the film. The strength of the NC film also depends on a number of factors such as diameter and length of fibrils, source of biomass and quality of interaction with fibres in a network. The strength of NC film depends on the fabrication methods and cellulose nanofibrils characteristics. The mechanical properties of nanocellulose film prepared by various methods are summarized in Table 5. Table 5 shows that spraying is the fastest method to form NC films and properties achieved by spraying are similar to those of film from conventional methods such as vaccum filtration.

1.6.5. BARRIER PROPERTIES

Cellulose nanofibers are able to form a compact fibrous structure that plays a role in barrier performance .When comparing with other synthetic plastics and other natural polymers, nanocellulose has low oxygen permeability and reasonable water vapour permeability. Figure 8 shows oxygen permeability (OP) and water vapour permeability (WVP) of conventional synthetic films and biopolymer films, confirming the notable barrier performance of nanocellulose comparing with other biopolymers [40]. Oxygen and water vapour permeability are the main barrier properties of NC film and Figure 8 reveals that the barrier properties of NC film is better than that of other biopolymers. Figure 9 shows the diffusion pathway of NC against oxygen and water vapour. However, Figure 9 was unable to review 3-Dimensional movements of water vapour and gas around the cellulose nanofibers. The predominant mechanism is diffusion around the cellulose nanofibers. Generally, the gas will pass around the circumference of the fibre not along the length of the fibre. The permeating gas will tend to take the shortest path than the longest path.

Table 5-Properties of NC films [78]

Fabrication Method	Time Consumption Film formation	Elastic modulus GPa	Tensile strength MPa	Tensile Index Nm/g	Basis Weight g/m²
Spraying of NC On nylon fabric	10–27 min	17.5–21	50–150	45–104	13.7–124
Membrane filtration	NA	10.7–13.7	129–214	NA	NA
Vacuum Filtration	10 mins	NA	NA	94	56.4
Filtration (Fabric Filter)		15.7–17.5	104–154	129–146	17–35
Membrane filtration	55 min	13.4±0.2	232	-	56
Paper Filtration	2880 mins	10–10.6	127–135	-	-
Membrane Filtration	-	11.9±0.8	135±18		62.4
Filtration on Fabric	60 – 180 mins	8.1–11	121–230	-	55

1.6.5.1.   OXYGEN PERMEABILITY (OP)

The permeation of oxygen and other gases including volatile organic compounds can degrade the quality of foods. The atmospheric oxygen can react with the carbon- carbon double bond of the unsaturated fatty acids in oils and fats resulting in rancidity. Because NC films have low OP they can provide good barriers to protect the foods. It can increase the shelf life of foods by avoiding the formation of unwanted chemical reactions such as oxidation and assist the retention of the flavour of food and its fragrances. The oxygen permeability of nanocellulose film is evaluated and compared with the synthetic plastics in Table 6. The data for OP of synthetic plastics and nanocellulose films are shown in Table 6 [40]. This table also shows the effect of relative humidity on NC film and carboxymethylated NC film compared with synthetic plastics. At low RH%, NC film has low OP, but it increases with increasing %RH.

The increment is quite comparable with conventional synthetic plastics. Table 7 reports water vapour permeability of biopolymer films and conventional synthetic plastics films.
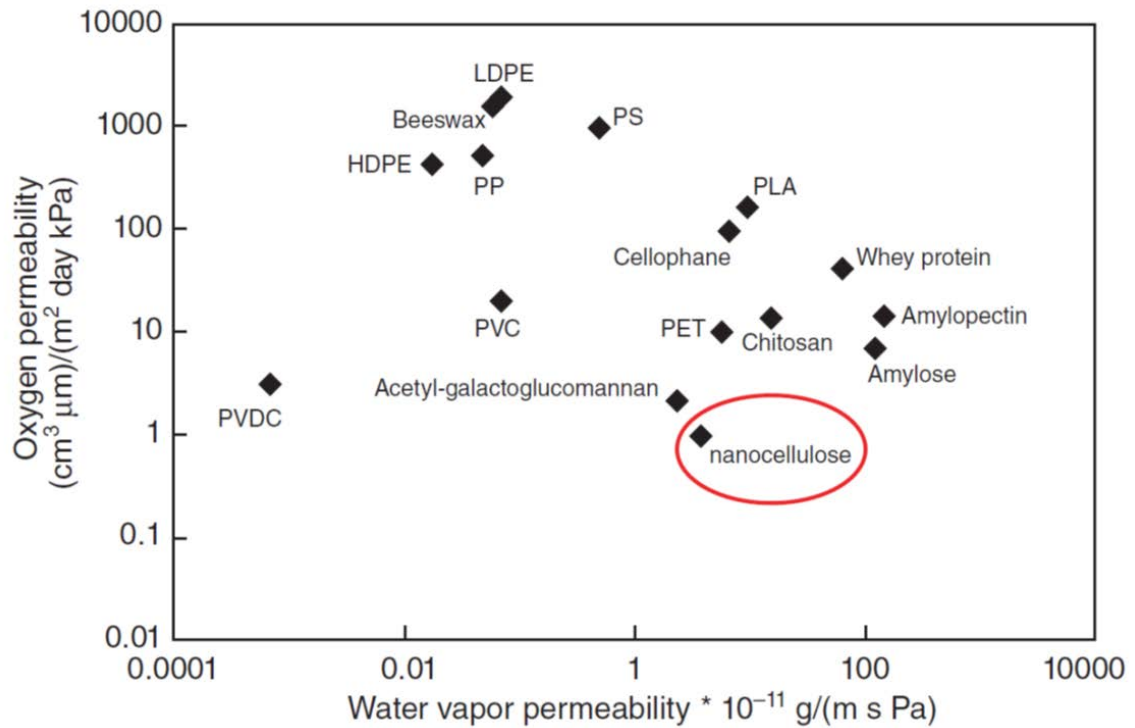
Figure 8-Overview of Barrier Materials, obtained from Aulin et al 2011 [5]. The Oxygen permeability was measured at 23°C and 50% RH.
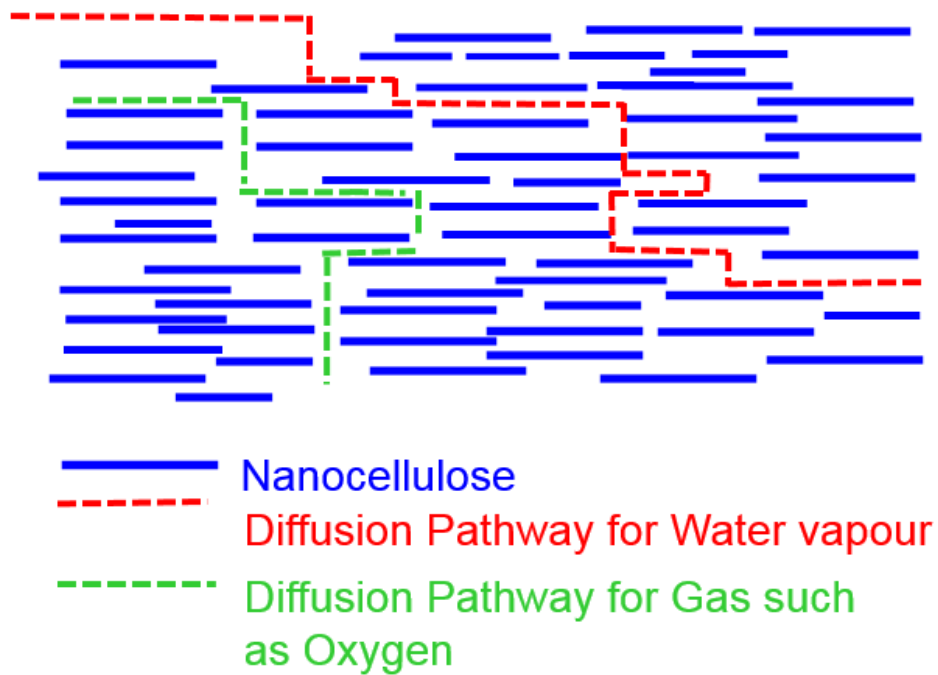
Figure 9-Simple diagram of the structure of NC film giving it good barrier performance against oxygen and water vapour ((Nair, 2014 #109)

Table 6-Oxygen Permeability of NC and Synthetic Plastics [40]

Materials	OP (cc μm/m² day KPa)	Conditions
NC	0.6	65% RH
NC carboxymethylated	0.0006	0% RH
NC Carboxy methylated	0.85	50% RH
Cellophane	0.41	0% RH
Polyethene (PE)	50–200	50% RH
Polyvinylidene chloride (PVdC)	0.1–3	-
Polyvinyl alcohol (PVOH)	0.20	0% RH
Ethylene vinyl alcohol (EVOH)	0.01–0.1	0% RH

Table 7. Water vapour permeability of biopolymer films and conventional synthetic plastics films:

Type of Film material	Water vapour permeability (WVP) 10^{-11} g/m.s.Pa	Test conditions	Reference
Polyvinylidene Chloride (PVDC)	0.0007 – 0.0024	38°C, 0-90% RH	[79]
LDPE	0.07 -0.1	38°C, 0-90% RH	[79]
PP	0.05	38°C, 0-90% RH	[79]
PS	0.5	38°C, 0-90% RH	[79]
Bee wax	0.06	25°C,0-100%	[79]
Cellophane	6.9	25°C,0-90%	[79]
Chitosan	13	25°C,76.2%	[80]

NC film provides a good barrier against oxygen up to 65% RH [37]. In this range, the nanocellulose film shows comparable barrier performance with synthetic polymers [81]. Hence, the nanocellulose are suitable for dry foods packaging. Dense NC films, obtained by structuring to obtain more and higher entanglements of nanofibrils provide a more closed surface, and a complex internal tortuous diffusion path, with reduced gas and water vapour permeability [82]. The crystalline regions in particular, contribute to increased impermeability [83].

1.6.5.2.   LIMITATIONS OF NC WITH RESPECT TO OP

The OP of NC film is very low and comparable with synthetic plastics at 0 % RH. But it increased with RH% and above 65 RH% it is not as good. When comparing with synthetic plastics, NC has excellent oxygen barrier performance at 0%RH and reasonable barrier performance at higher humidities of 50% or 65 % RH. The performance is at least an order of magnitude better than polyethylene across this range. At low humidity, NC film is rigid and

with good resistance. At higher RH, It becomes rubbery and viscous due to the high moisture content which softens the cellulose nanofibrils and weakens the cellulose chains. As a consequence, the interfibrillar space is increased and the local deformation permits increased permeation of oxygen molecules across the film [37]. The OP of NC film is 0.6 cc $\mu m/m^2$ day kPa at 65 % RH, 0.85 cc $\mu m/m^2$ day kPa at 50 % RH and 0.011 $(cm^3\mu m)/(m^2$ day kPa) at 0% RH. The OP of micro fibrillated cellulose, MFC at various humidities and in comparison, with synthetic plastics is shown in Table 8. Table 9 confirms that the OP of cellulose nanofiber, the OP of CNF film decreases with increased thickness of the film and increases with RH [84].

Table 8-OP of MFC [75]

Material	OP $(cm^3\mu m)/(m^2$ day kPa)	Relative humidity (%)
MFC	0.011	0
MFC	3.52 - 5.03	50
PET	10 - 50	50
PLA	184	0
LDPE	1900	50

Table 9-Reported oxygen permeability of selected carboxymethylated nanofibril (CNF) films

Material	OP $(cm^3.\mu m)/$ $(m^2$ .day.kPa)	Film thickness μm	Conditions
CNF (carboxymethylated)	0.009	2.54	0% RH
CNF (carboxymethylated)	0.0006	3.19	0% RH
CNF (carboxymethylated)	0.85	3.19	50% RH

1.6.5.3. WATER VAPOUR BARRIER PROPERTIES:

Paper and paper board are cellulose fibre-based substrates giving mechanical support to protect contents, but they have poor resistance against water vapour and oxygen due to the presence of large pore size and the hydrophilic nature of the cellulose fibres. Nanocellulose has a fibrous network with small pores and shows reasonable resistance against water vapour. The incorporation of cellulose reinforcing materials into the cellulose fibrous network has enhanced barrier performance reasonably and reduced the water vapour permeability [37].

1.6.5.4. MECHANISM OF BARRIER PERFORMANCE

To understand the barrier mechanism of NC film, the diffusion of oxygen and water vapour from high concentration to low concentration separated by an NC film has three following steps namely

1. Permeating molecules adsorbed on the NC film's surface
2. Diffusion of these molecules through the interior of the film.
3. The molecule desorbed from the other side of the NC film.

The permeability through a NC film mostly depends on diffusion rate internal to the film.

Equation 1- Permeability of gas or water vapour through films

$$P = D * S$$

Where P is the permeability, D is the diffusion coefficient and S is the solubility coefficient.

The permeability coefficient P is evaluated from the application of Henry's Law of Solubility to Fick Laws of diffusion and is given by

Equation 2-Permeability coefficient

$$P = D * S = \frac{q * l}{A * t * \Delta P}$$

Where q is the amount of gas or water vapour passing through the film, l is the flow path or thickness, A is the cross-sectional area, t is time, and p is the pressure difference across the film [40].

The relative permeability of the composite film is given by

$$\frac{P}{Po} = \frac{1 - \emptyset}{\tau}$$

Where P = Permeability of the composite film

Po = Permeability of pure film (no filler in the film)

$\emptyset$ = Volume fraction of the filler

τ = Tortuosity of the composite

The permeability of the composite is inversely proportional to tortuosity. Tortuosity is effectively tailored by the type of nanoclay used as filler in the composites, its aspect ratio , aggregation of clay in the composite such as intercalation and exfoliation and orientation of the clay in the composite sheet/film either in plane or misaligned."[85]

The mechanism of barrier performance against gas is also explained as follows. Generally, films from hydrophilic polymers are good barriers against oxygen and grease in dry conditions. Nano cellulose films consist of a large amount of hydrogen bonds and is capable to form good film [86]. Nanocellulose film has the capacity to reduce the permeation of oxygen or volatile compounds. Its gas barrier properties can be used for extending the shelf life of foods and avoiding food contamination [87]. The dense packing of the cellulose nanofibrils in the nanocellulose film prevents the penetration of oxygen and other gaseous molecules across the film.

At higher relative humidity, the oxygen permeability of carboxymethylated nanocellulose film prepared via solvent casting increased exponentially. "The plasticizing and swelling of the cellulose nanofibrils with the water is the main reason for this effect" [40]. The porosity of nanocellulose film is another main factor for oxygen permeation for their barrier performance. The oxygen transmission rate [88] of the film decreased with the thickness of the film. The mechanism behind these effects is the increase in the tortuous pathway via increasing thickness of the film, which improves the barrier performance of the film. The pores at the surface of the film are not connected well and the surface acts as an impermeable film for oxygen penetration. The internal structure of the nanocellulose film such as crystalline region and amorphous region in cellulose nanofibrils contributes to the barrier performance. The crystalline region are impermeable to gases and dense amorphous regions will resist gas

permeation [84]. The fibril size is another factor in barrier performance through the formation of compact film.

The solubility of the gases is also a major factor determining the barrier performance of nanocellulose films. Oxygen and nitrogen are non-polar gases with poor solubility in the hydrophilic nanocellulose polymer resulting in a good barrier against these gases [87].

The oxygen permeability of the film made from biopolymers is given by the following equation

$$P = \frac{j\,(\Delta x)}{A\,(\Delta p)}$$

P is the oxygen permeability coefficient of the biopolymer film in amol/m s Pa. amol is 10^{-18} mol. J is the transmission rate of oxygen through the film (in amol/s), Δx is the film thickness (in meter), Δp is the differential partial pressure across the film in Pa and A is the surface area of the film in m^2 [89].

1.7.   METHODS FOR IMPROVING THE BARRIER PERFORMANCE

Methods available for enhancing barrier performance of NC films are chemical modification of the cellulose fibrils, use of additives, coating on the film, curable cross linking treatment of fibres and keeping residual lignin in the NC [87]. Apart from these methods, incorporation of montmorillonite, MMT or similar nanoparticles influence the water vapour resistance of the NC films [90]. Vermiculite added into NC film increased its oxygen resistance even at high humidity conditions [91]. Adding MMT into biopolymers to develop nanocomposites, improve their strength and thermal stability. Moreover, MMT or similar clays with high aspect ratio [87] provide good reinforcement for bio polymeric matrices [92].

The common clay used in developing composite is bentonite also known as montmorillonite (MMT). "It is an alumina-silicate layered clay hydrated. This structure consists of an edge-shared octahedral sheet of aluminium hydroxide between two silica tetrahedral layers" [93]. Figure 10 shows the structure of MMT. It is a potential filler at the nanoscale, which provides reinforcement in the nanocomposite and offers a high surface area with a large aspect ratio from 50 to 1000 [94]. It is a di-octahedral clay with 2:1 layer linkage. MMT is a rigid and impermeable filler. The 5 wt.% MMT is a permissible concentration used as food additives in Australia and no adverse effects on human health [95]. Nanocomposites from nanocellulose and MMT has low oxygen and water vapour permeability [96]. Apart from the barrier performance of nanocomposite, incorporation of clay in the biopolymer network

promotes its mechanical properties and increased the glass transition and thermal resistance. However, adding clay in the nanocellulose reduces the transparency of NC film [87].

Sodium Montmorillonite is derived from bentonite which has 10 to 20% of impurities of other natural minerals such as feldspar, calcite, silica, and gypsum [97]. Montmorillonite is the main constituent of Bentonite and its common characteristics is agglomeration of platelets into packages of lamellas, which results in an irregular form. Natural bentonite is non – swellable clay due to the presence of calcium and magnesium ions. Alkaline activation is a process to convert Ca^{++} into Na^{++} in MMT. The alkaline activation is a cation exchange process of MMT with soda ash (sodium carbonate) to replace Ca++ and Mg ++ with Na++ in MMT. Sometimes the high content of Mg++ in MMT can affect the swelling and rheological properties of MMT [98]. The activated Na++ - MMT can swell and exfoliate in the preparation of composites.

The types of clay used in the preparation of nanocomposites decides their barrier performance [99]. Clays are broadly classified as swellable and non-swellable. The non-swellable clays include kaolinite and illite etc., the montmorillonites are swellable and the examples are bentonite and vermiculite. The phenomena of swelling and shrinking of MMT depend on the interlayer cations such as Na+, Ca++ and Mg++ in MMT. MMT is another form of bentonite containing exchangeable interlayer cation such as Na++ or Ca++ with Mg++. The natural form of Ca++ MMT, known as calcium bentonite, has low swelling characteristics. When converted to the sodium form, the Na++ ion greatly increases water absorption and the weaker linkage enhances exfoliation. The effect of the Na++ or Ca++ interlayer cations is not explored so far in terms of their barrier performance. However, it is expected that because of their different swelling characteristics, these metallic ions would significantly affect their barrier performance especially water vapour permeability of the composite [100].

1.7.1. ROLE OF CLAYS INTO THE NANOCELLULOSE NETWORK

The packaging industry prefers low-cost additives and eco-friendly materials that should be universally accepted for easy processability by industry. Layered inorganics used as additives are two-dimensional, usually about 1 nm in thickness and several microns in length depending on the types of silicates or clays. As already discussed the tortuosity of NC film is increased through clay particles sitting in the diffusion path of the film, and the the barrier performance and potential of the given nanocomposite is thus improved [101].
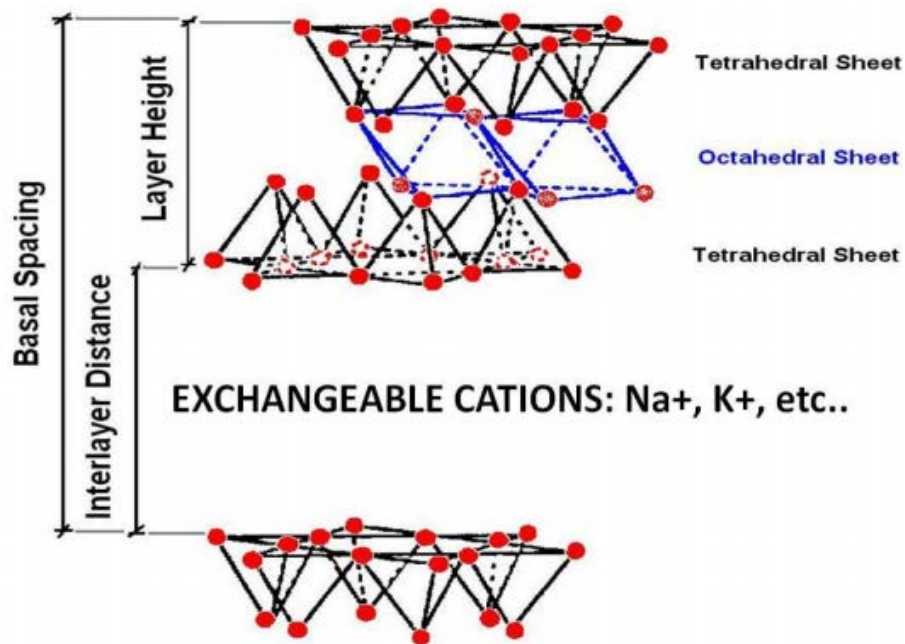
Figure 10-Structure of MMT. The image obtained from [102]

1.7.2. STRUCTURE OF NANOCELLULOSE COMPOSITE

There are three types of structure in composites, namely phase separated nanocomposites, intercalated nanocomposites and exfoliated nanocomposites as shown in Figure 11. The method of fabrication of composites, the configuration of clay platelets and the fibril size of the nanocellulose control the structure of the composite and its barrier performance. In phase separated nanocomposites, clay platelets exist in a tactoid structure where the polymer and clay platelets are not mingled. As a result, clay platelets are aggregated in the composite resulting in the formation of a macroscopic composite with poor barrier performance. In the second type of composite, the clay platelets are intercalated with polymer fibres. The nanocellulose fibres penetrate the interlayer region of the nanoclay platelets resulting in the formation of an ordered structure with a multilayer of alternative NC/clay layers at nanometre scale. In the exfoliated structure, the clay platelets are well delaminated and distributed in the interior of the nanocellulose region of the nanocomposite and extensive nanocellulose penetration into the layer of clays is observed [101, 103]. Figure 11 shows the orientation of clay platelets in nanocomposites and how this affects barrier mechanism.
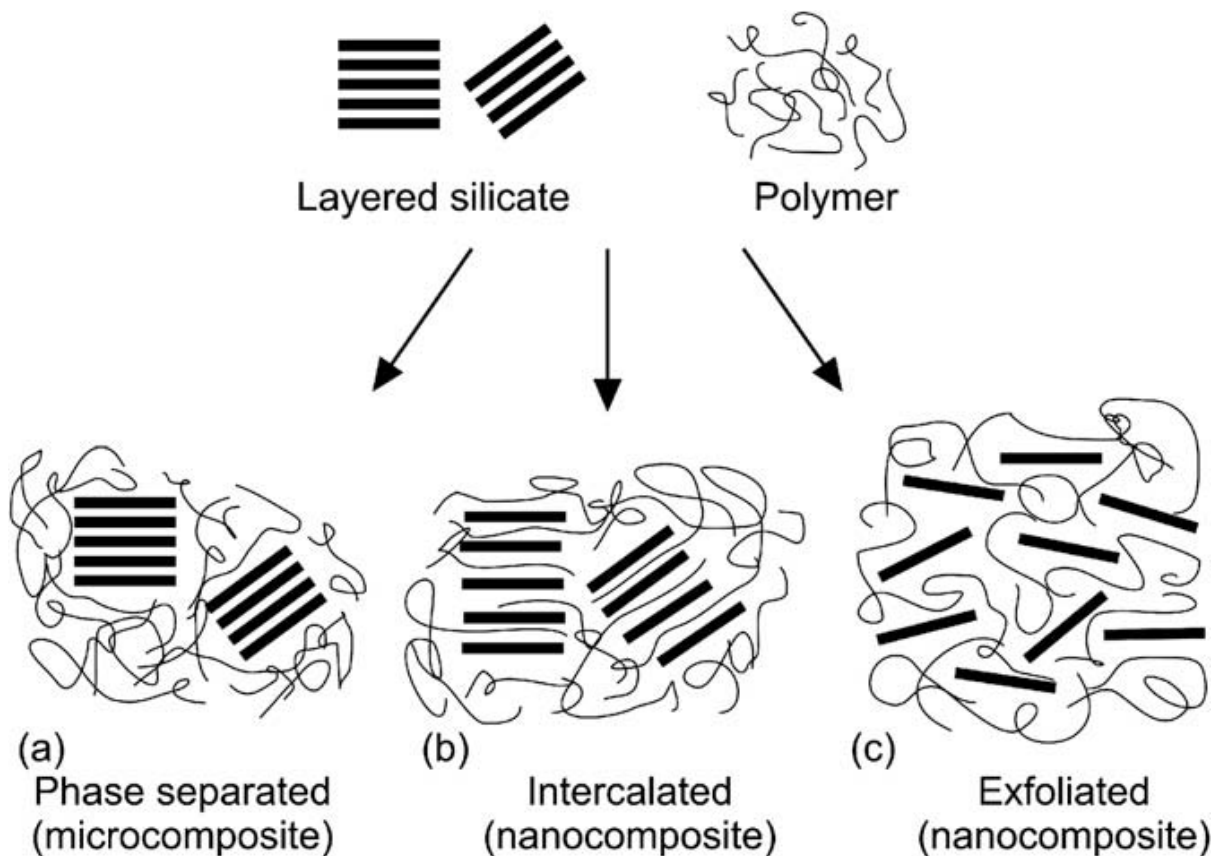
Figure 11-Structure of nanocomposite. The image obtained from Alexandre, M et al , 2000 [104]

1.8. FABRICATION METHODS

NC films/composites can be used in various applications "hence the demand for NC films/composites is rapidly increasing". The market for NC is predicted to reach USD 700 million by 2023 as NC demand increases at a compound annual growth rate of more than 33%, especially increasing in the pulp and paper sector [52]. However, the commercialization of these products is limited by the existing methods for preparing NC films/composites. The key issue is processing time, and therefore, a rapid and flexible process to handle high NC suspension concentration is required to prepare free-standing NC film with properties such as strength, barrier properties and roughness required for specific functionalities.

Methods used for the fabrication of free-standing nanocellulose films/ composites are solvent casting, spin coating, Roll to Roll (R2R) coating, layer by layer assembly, vacuum filtration and spraying. Vacuum filtration is now considered as a conventional laboratory method for NC film fabrication.
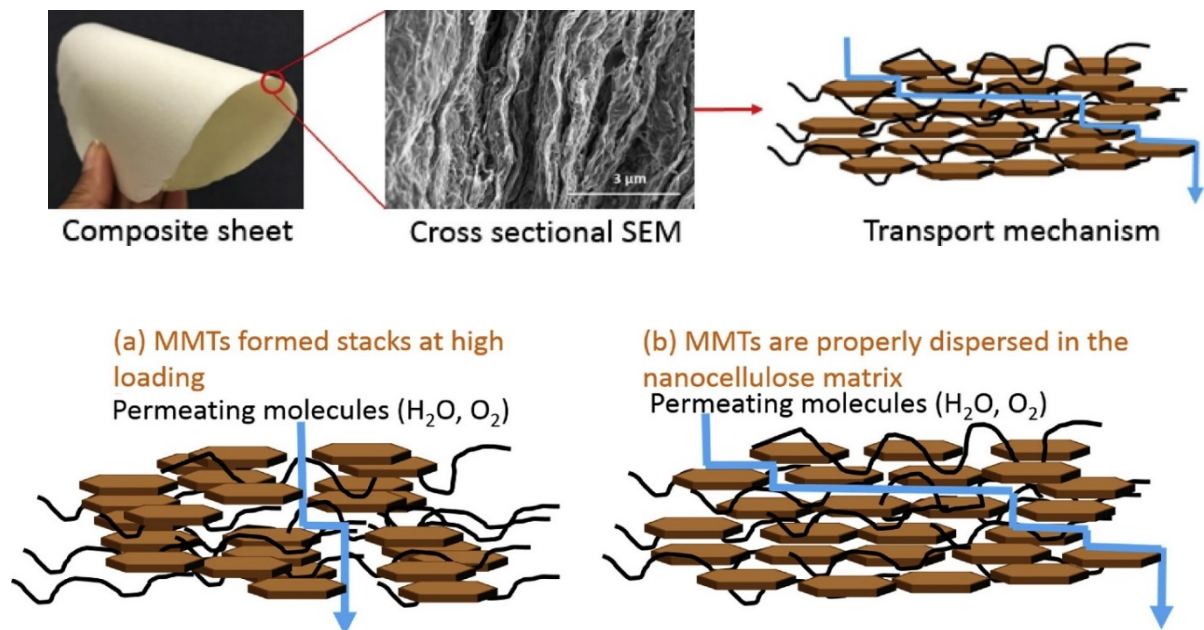
Figure 12-Mechanism of Barrier Performance in Nanocomposites. This image obtained from Garusinghe et al, 2018 [54]

1.8.1. SOLVENT CASTING

Solvent/Solution casting is a laboratory scale technique for NC film fabrication. In this method, NC suspension is poured on a glass or plastic Petri dish. The solvent is evaporated from the poured suspension on the substrate under standard laboratory conditions [105]. Freeze-drying of the cast suspension is another option., The time taken for forming the films varies from a minimum of 3 days to a week, depending on the concentration of NC suspension and the thickness of suspension according to Aulin .C *et al*, 2010 [84]. The higher the water content of the NC suspension the more time is required for evaporation. The suspension consistency normally used in solvent casting varies from 1.13 wt. % to 2 wt. % NC content.

This simple method controls the uniformity of NC film through the thickness and basis weight of the film. After drying, films generally tend to shrink and wrinkle, resulting in poor uniformity of the NC film that affects its strength and other characteristics. Good distribution of the NC in the suspension is also required to achieve quality films and sheets [74].

Casting is also a common laboratory scale method for producing clay–nanocellulose composites. Using suitable base surface, the key factor is proper dispersion of the clay in the

suspension, required to avoid the stacking and aggregation of clay in the composites. The proper dispersion of MMT clay in the suspension is required to avoid aggregation of MMT clay which causes poor barrier performance of the composite [4, (Guo, 2018 #308, 106]. Therefore, an additional step is required to improve the dispersibility of clay platelets in the NC suspension, prior to formation of the composite [87, 88]. The clay dispersibility can be promoted by intensive agitation such as by stirring and shear mixing. Recently, ultra-sonication has also been used to provide a good dispersion of nanoclay in suspension and break the nanoclay clusters or aggregates. However, this may not be a solution for large scale production of composites [4] .

Several examples of cast films are worth noting. Cast composites from vermiculite nanoplatelets in homogenized NC showed good oxygen and water vapour barrier properties and achieved good tensile strength and stiffness[91]. A cast composite of cellulose foam with homogenized NC and Tween 80- 2.5 wt.% MMT achieved a WVP of 216000 g μm m^{-2} day^{-1} KPa^{-1} , a strength of 13.1±1.7 MPa and a Young's modulus of 0.455 GPa [107]. The low WVP and high strength was due to the composite containing a lower loading of MMT.

The composite from the casting of poly (vinyl alcohol) PVA- Poly acrylic acid (PAA) – NFC – 50 wt. % Sodium MMT achieved a WVP of 105 g μm m^{-2} day^{-1} KPa^{-1} a strength of 190±11 MPa and a modulus of 15.9±0.3 GPa [108]. The cast composite showed better WVP and good strength due to the presence of biodegradable polymers and high content of MMT. The biodegradable polymer (PAA) promoted the dispersion of clay particles and crosslinking between PVA and PAA [65]. NFC – vermiculite composite prepared via two pressure homogenization stages followed by solution casting was reported to have a WVP of 60 g μm m^{-2} day^{-1} KPa^{-1} a tensile strength of 244±24 MPa with a modulus of 17.3±0.4 GPa [91]. The processing time for forming the composite film via casting consumed days and is considered as a huge constraint for commercialization.

In solvent casting, the suspensions containing nanocellulose and clay platelets are mixed together for better dispersion, allowing swelling of the clay layers. Therefore, the clay platelets interacted with the fibrous network of the film yielding a good barrier composite film [64]. Similarly to the casting of pure nanocellulose film, the time to dry the cast wet film takes more than 3 days. However, this method causes aggregation or clusters of clay platelets in the composite from other polymers [106]. Therefore, an additional step is required in improving the interaction of clay platelets with NC suspension through enhancing dispersibility of clay to

form composite [106, 109].The clay dispersibility could be promoted by an intensive stirring and shear mixing. Recently, ultra-sonication used to provide a good dispersion of nanoclay in suspension and break the nanoclay clusters or aggregates. However, it may not be a solution for large scale production of composites [4]. Solution blending followed by casting has drawbacks of a time-consuming process, the challenge in forming a composite with aggregation of clay platelets. It has required an additional process to disperse and exfoliate the clay to produce the composite at laboratory scale.

1.8.2. SPIN COATING

Spin coating is a technique for producing freestanding thin nanocellulose film with nanometric thickness. Spin-coated thin NC films have been used for investigating the interaction of biological molecules with NC[110]. In this method, high-speed spinning is applied to remove the excess NC suspension, thus leaving ultra-thin NC films. This is not a scalable method that can meet the commercial requirements of NC film as per the current demand [105]. However, it is a suitable method to make films for looking at biomolecule interaction with cellulose fibrils at laboratory scale. Spin coating was also used to produce cellulose nanomaterial layers as a film on the polypropylene. A 1 μm thin layer of CNC coating on the UV treated Poly Propylene (PP) film reduced oxygen permeability by 39% compared to uncoated PP[111]. Spin-coated CNC films promote their gas barrier functionality and multilayered coated CNC films can be used in gas separation and as barrier material [112].

1.8.3. ROLL TO ROLL COATING

The Roll to Roll Coating (R2R) has been used to produce NC film [74] and NC barrier layers on cellulose substrates to enhance the mechanical and barrier properties [113]. In making films this way, NC is coated evenly on pre-treated substrates, normally plastic films. The spreading of NC is controlled and adheres to the substrate followed by drying under a controlled environment. The NC films are then detached from the substrate and pressed. The NC film prepared via this method has no shrinkage. The average roughness of NC film made this way is 400 nm on the side exposed to the plastic substrate and 800 nm on the free side. This is a scalable method for producing translucent, smooth and densely packed NFC film. The time required for making the film is 15 minutes [74]. The OTR of NC film was less than 0.1 $cm^3/m^2/d$ (0% RH; 15 μm thickness) and tensile strength of 200 MPa, while water vapour barrier was not reported. The coating weight of NC using R2R can vary from 0.1 to 400 g/m^2.

The quality of NC film can be controlled by various parameters such as NC solid concentration, wettability of NC suspension on the substrates and velocity of webs etc.

1.8.4. LAYER BY LAYER ASSEMBLY

This method deposits macromolecules and nanoparticles containing charged groups in solution to form a film ranging in thickness from nanometre to microns. This method can be used to produce thin functional film and for coating of nanocellulose for specific functionality. One application used a thickness of the film of 5µm [114] and reported a surface roughness of 9 nm. It is not a scalable process for commercial production of NC films.

In the past three decades, Layer –By-Layer assembly carried out at mild reaction conditions has been used as a technique for surface engineering of cellulose fibre sheets. The size and shape of the substrate do not affect this process. The drying of coating on the substrates is a time consumption and but not reported in the literature. The film produced via this process can be-flexible in composition, with tailorable thickness and stable performance. The composite's thickness can be engineered via multiple coatings on the surface of base substrates. The multilayer coating of MMT on the base substrates affects the strength of the composites and can cause aggregation of MMT Layer-by layer coating of MMT on biodegradable polymer sheet enhanced its barrier performance including giving a low oxygen permeability [85]. The surface coating of MMT on sisal fibre cellulose microcrystals via this method was utilised to develop a flame retardant material [115].

1.8.5. VACUUM FILTRATION

Vacuum filtration is a well-documented method for forming NC films just as its use in cellulosic fiber sheets such as paper and paper board. In the laboratory method, NC suspension is poured into a column which contains a metal mesh as a filter at the bottom. A wet film of NC fibres is formed on the mesh. The sequences involved in the preparation of NC film via vacuum filtration are shown in figure 13. The retention of NC on the filter depends on the mesh size and its pore size; however, smaller mesh size generally increases the drainage time in the filtration process. The filter medium in vacuum filtration for production of nanocellulose film are hydrophilic polytetrafluroethylene (PTFE) membrane having pore size 0.1 [116], Millipore filter membrane which has pore size of 0.65µm [15], Poly amide filter cloth [75], cellulose filter membrane [117], woven filter fabrics [118] and copper wire having opening of 125 µm [53]. When using the woven filter fabrics, it is essential to use a solids content high

enough that the fibres form an interconnected network. The wet NC film is formed on the mesh and subjected to air or drum drying.

The time required for laboratory sheet production via filtration has varied significantly, depending on the fibre and filter medium. The time for filtration varied from 45 mins [117] to 3 or 4 hours [116] when the fine filter medium was used. This filtration time can be reduced to 8 min when the filter medium with large pores such woven fabric is used together with a higher vacuum [118]. The NC used here was relatively coarse. Reducing the fibre diameter by homogenisation increased the filtration time to 10 minutes to produce a film with a basis weight of 60 g/m^2 [53].

It is a conventional method to produce NC films. However, it has a limitation in that the drainage time increases with basis weight of the film. The increase of thickness and basis weight of the film with drainage time is exponential. The thickness of NC film produced via the filtration varies from 50 to 100μm. The notable issue in this method is the separation of the film from the filter after couching. Sometimes a filter mark is imprinted on the NC film affecting the uniformity of the film [74]. Although this method can achieve excellent barrier and mechanical properties [53], preparation time is a bottleneck for scaling up the process for commercialization of NC film.
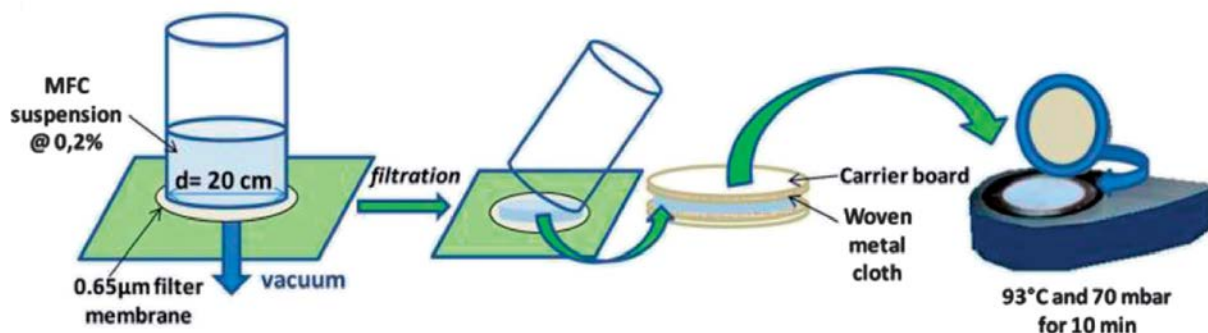
Figure 13 - Vacuum Filtration for NC Film Fabrication. Reprinted adapted with permission from Sehaqui et al 2010 [117]

1.8.6. NANOCOMPOSITE VIA FILTRATION

Vacuum filtration is a conventional cellulose fibre / cellulose based composite sheet making process in which the suspension of cellulose nanofibrils with nano-inorganics is collected on the filter to form the composites. The wet composite on the filter are couched

and followed by pressing and drying process. In the mixing stage, inorganics are well distributed into the 3D fibrous network.

The MMT–NC composites have been produced via vacuum filtration and reported low oxygen and water vapour permeability [4, 65, 96]. The WVP of MMT –NC composites via filtration are reported to be 13.3 ± 2.0 g μm/m^2 .day.kPa with 16.7 wt. % of MMT loading in the composites. Increasing MMT in 0.2 wt. % of NC suspension increase drainage time in the filtration process and high constraint for commercialization. A composite film from 25 wt. % Clay loaded in *Eucalyptus* NC and *P. radiata* NC and prepared via vacuum filtration resulted in WVTR of the composites ranging from 183 to 197 g/m day. [100]. Increasing the clay loading from 0 wt.% to 25 wt.% reduced WVTR from 299 to 197 in *P. radiata* NC composites and from 285 to 183 in Eucalyptus NC composites [119]. The processing time for composites was not reported.

1.8.7. IMPREGNATION PROCESSES

This method has been used to develop composites at the laboratory scale. In this method, a thin cellulose film was initially produced via membrane filtration. The film was then impregnated with nanoparticles in a solvent carrier. The composite was shown to have excellent dimensional stability, flame retardancy and strength [120]. The barrier performance of the composites via impregnation was not reported.

1.8.8. HOT PRESSING

Hot pressing is used to develop nanocellulose – inorganics composite for barrier applications. Hot pressing is a final step applied after filtration. It is reported to perform at a temperature of 105°C and pressure of 150 bar. Time consumption of pressing step can be 3 to 4 hours including cooling and heating of the composites.The WVP of Trimethyl ammonium –modified nanofibrillated cellulose and layered silicate (TMA-NFC/Mica R120) was 2200 g μm m^{-2} day $^{-1}$ KPa^{-1} at a condition of 23 ° C and 50% RH. The strength of this hot-pressed composite was 104±5 MPa with Young's modulus of 10.3±1.1 GPa [119]. The WVP of a TMA-NFC/Vermiculite composite was 1400 g μm m^{-2} day $^{-1}$ kPa^{-1}, with a strength of 135±5 MPa and a modulus of 10.3±1.1 GPa [121].

1.8.9. SPRAY COATING

Spray coating is a bench scale technique for fabricating nanocellulose film. This method is used to develop free-standing films by spraying on to a solid surface either permeable [78, 122] or impermeable [123] . Spraying allows contour coating and the coating is performed contactless with the surface [124]. In addition to that, the coating process is not influenced by the surface's topography [124]. It is reported that the strength of spray coated film is comparable with the cast film [125].

Figure 14 shows the sequences involved in the spraying process. In spraying process, the mechanism consists of the formation of spray jet of the liquid and then atomization of the sprayed jet into the mist of the liquid. The atomization involves two mechanisms namely liquid lamella disintegration and disintegration of the liquid jet. The fine droplets formed from atomization coalesce on the contact surface and a film is formed on the base surface. Spraying of these biopolymers onto the solid surface causes coalescence of sprayed droplets due to the film-forming properties of the polymers via hydrogen bonding [126]. The film that is formed on the surface can be peeled from the substrates after drying.
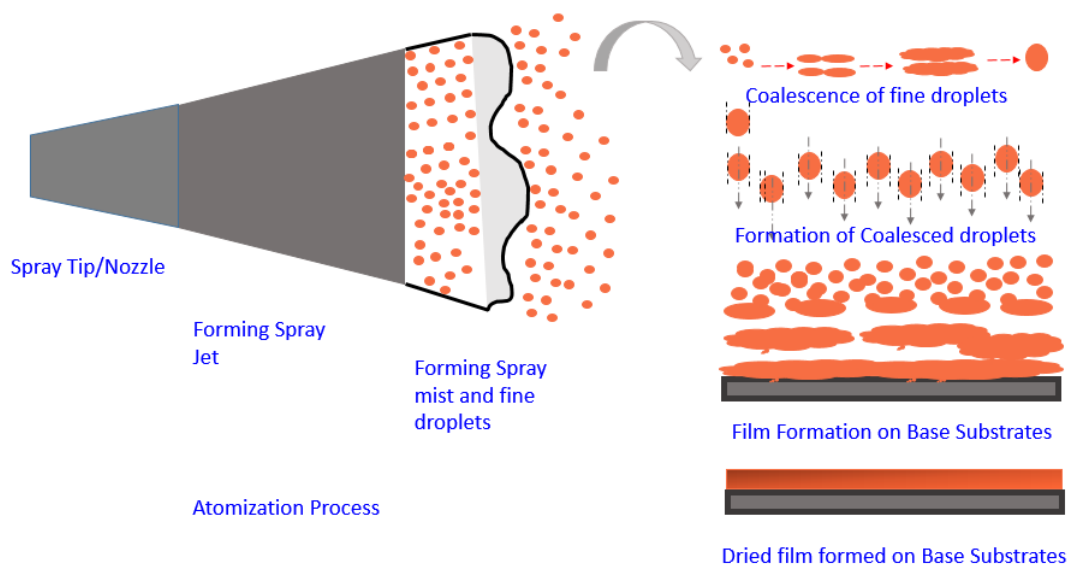
Figure 14 - Mechanism of Spraying

Compared with laboratory and conventional methods for NC film making, spraying was initially reported to create a coating layer either on cellulosic substrates or solid surfaces. Spraying of nanocellulose on a paper substrate has been performed to enhance its barrier and mechanical properties [127] [122]. Similarly, spraying NC on nylon fabric was attempted to make free-standing nanopaper as barrier materials [78]. The spray coating of chitin and

cellulose nanofibers onto poly lactic films has been performed to enhance barrier performance and mechanical properties [128] . In this thesis, the preparation of free-standing NC film via spraying is the focus. This method can be classified into two approaches - spraying on a permeable substrate or spraying on an impermeable substrate.

1.8.9.1. SPRAYING OF NC ON PERMEABLE SUBSTRATES

Spraying can provide a good range of coat basis weight significantly higher than filtration. The spraying process is independent of the NC suspension concentration provided the suspension remains within the sprayable viscosity. Spraying of NC is a method that has been investigated for creating barrier layers on cellulosic fibrous substrates [122] by spray coating an homogeneous layer of NC on paper substrates [122]. Up to 2 wt. % NC was used for spraying, thus reducing the water to be removed in subsequent drying.

1.8.9.2. SPRAYING OF NC ON IMPERMEABLE SUBSTRATES

Spraying of NC on smooth and polished solid surfaces has been investigated to produce free-standing NC film. Recently, spraying of micro-fibrillated cellulose (MFC) on a preheated metal surface was used to produce MFC film with 3D structures [123]. The basis weight and thickness of the film varied from 59 to 118 g/m^2 and 46 to 68µm respectively. The limitations in this method were cracks and wrinkles formed on the surface of the NC film. In this investigation, the amount of water was reduced but spraying with both 4.5 wt. % and 9 wt. % NC caused the formation of a disturbed spray jet due to the gel nature of the MFC. Consequently, the cracked film was produced [123]. The replication and evaluation of surface roughness of spray coated NC film from the base surface was not reported. In another investigation, ethyl cellulose was well dispersed in water with addition of plasticizer and the liquid was sprayed on Teflon plates. The spraying produced a uniform and reproducible cellulose film with tensile strength better than cast films [125]. The spraying of cationic chitin fibres and anionic cellulose nanofiber on poly lactic acid (PLA) films was investigated to promote barrier performance. The multilayer spray coating of these fibrous materials on PLA reduced O$_2$ permeability but had a lower haze than when spray coated with only chitin nanofiber or cellulose nanofiber [128].

1.8.9.3. LIMITATIONS IN SPRAYING OF NC ON PERMEABLE SURFACE

Using spray coating [78] , an NC suspension was sprayed on a permeable nylon fabric substrate having opening size of 20.4µm, 14 % open area and 470 mesh size and then vacuum filtration was used to remove the excess water from the spray coated NC layer on the

nylon fabric. This spraying method is a time-consuming process as it took 10 to 20 minutes. The report detailed that the NC films were made with 5 pass homogenized NC suspension with fixed consistency of 2 wt. %. The surface roughness of the NC film and the effect of suspension consistency on the properties of the NC film were not reported. The thickness and basis weight of the NC film were varied from 10μm to 72μm and 13.7 g/m^2 to 124 g/m^2 respectively by varying the speed of the conveyor in the experimental set up from 0.5 to 3 m/ minutes. The constant MFC slurry flow from the nozzle of spray system was 0.75 kg/min. After spraying, the time taken for filtration varied from 15 sec to 90 sec. After dewatering, the wet MFC film was placed between new nylon fabrics and two blotting papers and two pass compressed with a 3 kg roll, and vacuum dried at 90° C. The time taken for drying a 55 g/m^2 film and another thicker film were 10 and 25 mins respectively. The nylon fabric imprints on spray-coated nanopaper was reported, however not these markings were not evaluated. The effect of the base surface on the properties of NC film was not investigated [78]. Figure 15 shows a typical operation of the spray coating process.

Spraying process produced high thickness and basis weight of the NC film or barrier layers on the cellulosic substrates compared to vacuum filtration. Spraying homogenized micro-fibrillated cellulose onto a nylon fabric moving on a conveyor belt set at a speed of 0.5 m/min, yielded 124 g/m^2 of the NC film. The spray coated films is good in Young's Modulus having 18 GPa and its air permeability is reported to be < 0.7 nm Pa^{-1} s^{-1} [78]. Spraying has not so far been used to make discrete NC film. The effect of suspension consistency on the sheet quality produced by spraying is yet to be investigated in comparison to hand sheets made by vacuum filtration. The effect of suspension consistency and spray process variables on the important qualities of NC films such as uniformity, surface roughness and smoothness, thickness and coat weight are to be investigated.

1.8.9.4. SPRAY COATING FOR COMPOSITES LAYER DEVELOPMENT

Recently, the spraying of nanocellulose with inorganics onto permeable substrates such as paper and cardboard has been found to be a simple approach for developing composites barrier layers. This approach permits the coating of a larger surface area and reduces operation time [122] [129].
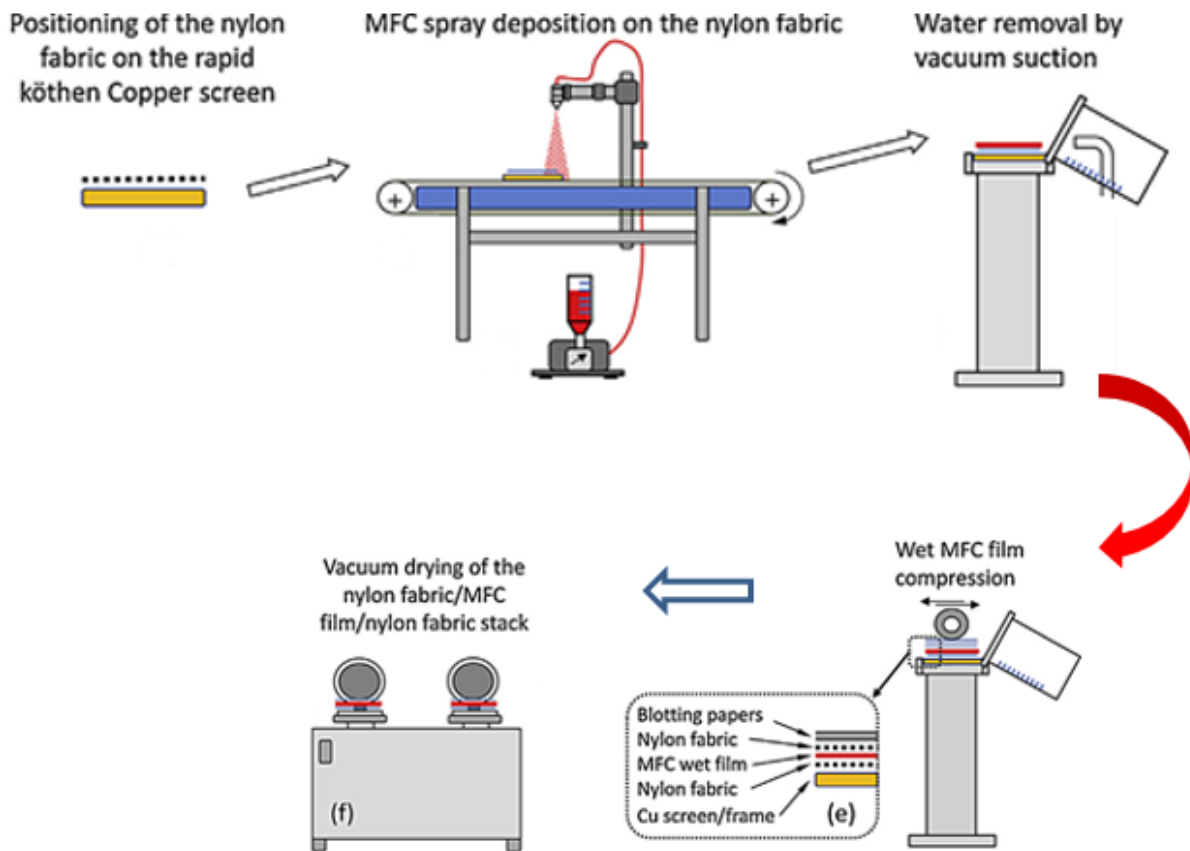
Figure 15-Spray Coating to Prepare NC Film. The image obtained from Beneventi et al, 2015 [69]

MFC -SiO$_2$ composites have been developed via spray coating with operation time on a base sheet of almost 310 cm^2 of less than 30 minutes for spraying, independent of SiO$_2$ concentration. SiO$_2$ was added in the range 0 to 33 wt. % in the spraying suspension, tailoring the properties of the composite. The coating layer weight on the cellulosic substrates was controlled by varying the velocity of the conveyor in the experimental setup and the inorganics content in the NC suspension. These composites produced a material impermeable to air, confirming its good barrier performance [129]. Similarly, a composite made up of graphite and MFC as an electrode were developed via spraying [130].

Spraying of cellulose nanofibrils with nanoclay (MMT) on a Kraft paper and printing paper as base cellulosic substrates were developed and increased its barrier properties against oxygen and water vapour and tensile strength. The operation time for producing the composite barrier layers on the paper were 30 sec and 50 sec for clay suspension varying from 0 wt. % to 5 wt. %. At 3 wt. % and 5 wt. % clay composite layer with basis weight of 22

and 29 g/m^2 the oxygen barrier permeance was 88600±2000 and 36400±1100 cm^3 m^{-2} day respectively. The water vapour barrier performance of these composites was reported to be 14 and 8 gm^{-2} day. The time consumed for 19 and 29 μm thickness of barrier layer on paper was less than 30 sec in the spraying process [67]. In this process, the water in the sprayed suspensions was removed by vacuum filtration. Peeling the layer as a film from the base surface was a challenge. Surface treatment of the substrates such as wetting, and corona discharge treatment was required to enhance the wettability between substrates and cellulose nanofibrils. NC concentration was varied between 1 wt. % and 2 wt. % NC but the effect of NC suspension concentration on the properties of composite layers was not investigated. Some surface non-uniformity of composite layers such as agglomeration was observed.

Layered spray coating of cationic chitin fibres and anionic cellulose fibres on the PLA films has also been investigated. This method provided alternative multi-layer coating of these fibres on PLA film to tune its barrier properties and mechanical properties. The OP of composite layer with PLA film is 22 cm^3 μm/m^2/day/kPa at 50% RH compared to that of the plain PLA film which was OP 70 cm^3 μm/m^2/day/kPa at 50% RH. The WVTR of the composite layer with PLA film is reported to be 60 g -water/m^2/day at 50 % RH, slightly lower than the WVTR of pure PLA film [128].

1.8.9.5. SPRAY COATING FOR DEVELOPING FREE-STANDING NANOCOMPOSITE

Recently, spraying is a rapid process to produce NC film and its operation time less than 30 mins [78]. Spraying is an effective method for producing composites and therefore implemented to make NC–MMT Composite. Generally, Free standing NC films have been prepared using either vacuum filtration or casting. Both methods are time-consuming processes and required from 10 minutes to 3 days for the film to form and it's drying and wrinkling is also limitations in these processes. The operation time for nanocomposite via vacuum filtration required minimum of 24 hours to 4 days. Additionally, there are shortcomings in the separation of the film from the filter. The handling of the peeled wet film was difficult before dried. This is also a conventional method which has limitations in tailoring the basis weight and thickness of the composites.

1.8.9.6. PROS AND CONS OF THE DIFFERENT METHODS

In summary, casting methods are too slow and the quality of the film, because of wrinkling is a major difficulty. In filtration methods, the time required is excessive, limiting the

range of suspension concentrations permissible. In addition, peeling is a challenge and filter marking is a problem. While spraying appears a good option because it is quicker, studies on spraying methods for fabricating NC sheet have not explored sprayable limits of NC suspension. The effect of base surface on the surface properties of NC film has not so far been explored, and the effect of NC suspension and spraying parameters on the uniformity of NC films has not been investigated.

1.8.9.7. IDEAL REQUIREMENT OF PREPARATION OF NC FILMS

When compared to synthetic plastics films, the manufacturing rate of NC films is very slow [87]. Rapid manufacturing of NC films will facilitate their applications in packaging, as air and water filters, membranes and films for tissue engineering applications. Ideally, for commercial preparation of NC films methods must be able to

- Increase film performance in water vapour and oxygen barrier properties via preparation method
- Tailor the thickness and basis weight of the NC film via processing method without affecting operation time
- Engineer the strength and bulk properties of NC film by varying the NC suspension concentration without affecting operation time in the method
- Produce a film with an outstanding uniformity
- Permit composites with the addition of nanoparticles not affecting the process variables in the method.
- Produce NC film in a single step to avoid further processing such as dewatering, vacuum drying, couching of the wet film.
- Produce a smooth nanocellulose film and engineer their roughness for developing potential material without any additional treatment in the methods

1.9. RECYCLABILITY OF NANOCELLULOSE FILMS

Packaging sustainability requires recyclable packaging films and minimizing the carbon footprint and environmental pollution. Safety and sustainability are the important requirement in engineering food packaging materials [7]. The toxicity of cellulosic fibres is very low based on low genotoxicity against hepatocytes and aquatic species. Like cellulose macro fibres, NC is also biodegradable and does not enter or interfere into the food chain [7] [131].

Nanocellulose is susceptible to microbial degradation in the environment. Cellulose is a substrate for cellulose expressing species such as fungi and bacteria and the small size of cellulose nanofibrils exposes it in the environment for microbial action. Therefore, nanocellulose can be a biodegradable, sustainable barrier material. Cellulose nanofibers are obtainable from resources that are renewable and widely available around the world. Nanocellulose satisfies the sustainable packaging concepts defined by the Sustainable Packaging Alliance (SPA). Table 10 shows the sustainability potential of nanocellulose in packaging applications. The important aspect of sustainability of nanocellulose film is energy usage of nanocellulose production and recycling for film production.

Table 10 - Sustainability features of Cellulosic nanofibers [119]

Principle	Strategies of Sustainable Packaging	Cellulosic nanofibers in Packaging
Effective	Minimization of generation of Waste	Biodegradable
		Recyclable
		High abundance
	Maximum functionality	Potential for recyclability and reusability
		Light in weight
		High strength and stiffness
		Excellence in durability
		High barrier performance
	Cost Effective	Abundance
		Recyclable
		Reusable
Efficient	Maximize products to packaging ratio	High Potential
		Durable
		Flexible nature
	Maximize materials efficiency	Potential for recycling with very minimal degradation
Cyclic	Recyclable Reusable Biodegradable	Natural Biopolymer
Clean/Safe	Minimal airborne and waterborne emissions to environment Minimize greenhouse gas emissions Reduce toxicity and litter impacts	Minimal Ecological Impact with cellulose nanofibers Minimal Greenhouse gas emissions Biodegradable nature, effective disposal after use.

Cellulose fibres contains high amount of hydrogen bonds to maintain the fibrous network and different level of hierarchy in wood. The energy required for breaking the inter-fibrillary hydrogen bonding in the cellulose is very large. This requirement ranges from 19 to 21 MJ/Kg mol. In mechanical homogenization for large scale production of nanocellulose, the energy consumption varied from 20000 to 30000 kWh/ ton. The energy requirement for nanocellulose production from a bleached eucalyptus pulp through the grinding process was in the range from 5 to 30 kWh/kg. For reduction of energy consumption for production of nanocellulose, chemical or biological treatment were used to reduce the energy consumption to 1000 kWh/ton [132].

Mechanical fibrillation is the common method for production of nanofibers and is highly consuming around approximately 70000 kWh/tonne [9]). The chemical treatments such as TEMPO -oxidation, carboxymethylation and enzymatic treatment are used to minimize the energy requirements for nanocellulose production. TEMPO treatment rapidly reduced the energy consumption nearly from 194400 kWh/tonne (for repeated passes in homogenizer used) to 1944 kWh/tonne [1]. However, longer chemical treatment is required and some of the chemical process are harmful. The enzymatic treatment of fibres and followed by mechanical fibrillation is higher than that of chemical treatment of fibres with mechanical process [24].

The energy consumed for nanocellulose production via various mechanical process is in the order high pressure homogenization> micro fluidization > grinder. The energy required for processing nanocellulose with pre-treatment was reported ˜ 9,180 kJ/kg for the micro fluidization whereas 9,090 kJ/kg for the grinder 31,520 kJ/kg for the homogenizer [26, 27].

Nanocellulose can be proved as the feed stock for developing barrier films and could be an alternative for synthetic plastic films. When energy analysis for manufacturing nanocellulose film comparing with synthetic plastic film, it consumes ten times more energy consumed [133, 134]. The research on nanocellulose production with low energy consumption is being developed.

Cellulose fibre substrates such as paper and paper board are recyclable, renewable, and biodegradable, but show poor barrier performance against oxygen and water vapour due to the presence of large pores in the fibrous network. To improve the barrier performance of cellulose fibres substrates, lamination and extrusion with synthetic plastic have been performed, but, recycling of these coated substrates has shown to be problematical [135]. In

laminated and composite mixtures of many packaging materials, the layers are strongly bonded and the recycling of this material is an effort [87].

It is also mentioned that the recycling of polyolefin films such as low density polyethylene (LDPE) consumed more than half of the energy required for production of virgin polyolefin films [136]. This compares with the recycling of nanocellulose, where the energy required for recycling is negligible compared to the energy consumed for the virgin NC production [133]."

The NC coated LDPE was mechanically recycled into a second life barrier material. The Roll to Roll coating was used to coat NC on LDPE. During recycling, the LDPE and agglomerates from NC coatings were mixed together and formed a recycled film. The OTR of 1.4 g/m^2 coat weight of pure NC on virgin LDPE film and recycled film were 37±4 cc/m^2/day and 924±47 cc/m^2/day, respectively. The WVTR of pure NC on virgin LDPE film and recycled film were 0.9±0.1 g/m^2/day and 2.0±0.2 g/m^2/day at a condition of 23°C and 50% RH, respectively. The barrier properties of recycled film was decreased after recycling and insignificant by the effect of NC agglomerates [137]. This concluded the possibility of recycling of NC coating on the LDPE film which has been investigated in the present thesis with the focus of recycling of free-standing NC film and its effect on the barrier performance.

1.10. SURFACE ENGINEERING OF NANOCELLULOSE FILMS

The roughness of nanocellulose film is one of the important criteria for developing functional material from nanocellulose. The surface roughness of the film normally controlled by the diameter distribution of nano fibril in the film and the processing method. The minimal surface roughness (high level of smoothness) is required for constructing flexible electronics. Because the conductive ink should spread on the surface of the substrate to avoid any discontinuity in the ink layers. In addition to that, spreading and penetration of the conductive ink on the substrates should be minimal on substrates for printed electronics [138]. Spreading and penetration of conductive ink on the surface of NC film depends mainly on their surface roughness.

The method of NC film preparation is another approach to tailor its surface roughness. The smooth surface and texture of the base surface like plastic material can be replicated on the nanocellulose film [139] [140] either solvent casting method or roll to roll method. The average roughness of the NC film via roll to roll method is ˜450 nm on the base surface side

and ~800 nm on the free side of the film [74]. The surface roughness of NC film via vacuum filtration as a conventional method is 418 nm on free side and 331 nm on the filter side [141]. Sometimes, the NC film via filtration contains filter markings on the surface of the film affecting its roughness. The average roughness of plastic as the base surface is ~ 400nm. From this review, it is an objective to develop a rapid method to prepare smooth NC films for developing functional electronic devices.

The parameters controlling the surface roughness of nanocellulose film have been investigated in this thesis. The fibril size distribution in the nanocellulose network and base surface roughness are the main parameters controlling the surface roughness and declared superficially in the previous work [74]. But the main objective in this spray coating work is to tailor the surface roughness of the film via spraying of NC on the different substrates having high to lowest surface roughness. Through this objective, it is necessary to understand what factors playing in the smoothness and how this film with lowest smoothness can be used for different applications such as flexible electronics and solar cells etc,.

1.11. PERSPECTIVE AND CONCLUSION

Recently, nanocellulose films and their composites have potential applications in various fields. Predominantly, these sheets have been implemented in barrier applications, air filters, and anti-microbial sheets, substrates for electronics and light emitting diodes etc., and replacing synthetic plastics in practice. The methods for production of NC film in practice has time-consuming and limited in rate of production. The properties of NC films and their composites mostly depends on the preparation methods.

Through a critical review of the literature, this chapter demonstrates a need of rapid production of NC film and its composites. This rapid process should be flexible in tailoring the pure NC film and its composite's properties for specific functionality. The barrier and mechanical performance of NC film from spraying as a rapid process in film formation should be evaluated and compared with NC film from filtration. Comparing with other methods, spraying provides fast formation of NC film on the base surface. The spray coated film's barrier performance and strength was improved through adding nano-inorganics to make nanocomposite.

1.12. GAPS IN KNOWLEDGE

The following research gaps are observed and will be investigated through this research:

1.12.1. RESEARCH GAPS

1. *Fundamental studies of spraying nanocellulose on the metal surface:*

Spraying NC on the stainless-steel surface is to make NC film as a concrete concept and to evaluate the sprayable limits of NC suspension. The range of thickness and basis weight of NC film via adjusting NC suspension is to be investigated in the spraying process.

2. *Effect of basis weight and thickness of the NC film on its mechanical properties:*

So far the effect of basis weight on the bulk and mechanical properties of the NC film has not been investigated. In addition, the effect of the NC suspension concentration to be sprayed on the uniformity of the nanocellulose sheet is not understood. The mechanical properties of spray coated nanocellulose sheet in comparison with the nanocellulose film prepared via vacuum filtration are not understood. Questions which arise are - What range of materials can be produced and how can the process be controlled to produce films with the required properties? How does spraying of different suspension concentration of nanocellulose affect the properties of the film? Can spray coated process be adapted to make continuous or standalone sheets to replace the conventional vacuum filtration process?

3. *Effect of recycling on the spray coated NC film on its mechanical and barrier properties*

The effect of recycling on strength and barrier performance of NC films is so far not investigated.

4. *Effect of additives on the nanocellulose suspension to make nanocomposite and its effect on mechanical and barrier properties*

The effect of forming the cellulose nanofiber-inorganic composites by spraying to improve barrier properties and mechanical properties of the nano-composite is not understood so far. The interaction of additives with nanocellulose film has been hardly investigated and further it is not clear how additive nanoclay affects the mechanical and barrier properties of the sheet. The interaction between nanoclay and inorganic nanoparticles with nanocellulose is not understood, and how this addition of nanoclay/nanoparticles affects mechanical and barrier properties remains obscure.

5. *Effect of Substrate roughness on NC film*

The effect of substrate roughness of NC film when spraying NC on substrates having low to high roughness has not been explored so far. The preparation of low roughness NC film

via spraying, the engineering of the roughness of NC film and what parameters are controlling the surface roughness of NC film have not been explored so far.

1.13. RESEARCH OBJECTIVE

This doctoral thesis consists of three main objectives. First is the development of a proof of concept of spraying of NC on the polished metal surface to make free standing NC film. Second is to extend the flexible spraying for multiple NC film preparation, to characterize NC film and the recyclability of spray coated NC film into a potential barrier material. Finally, it aims to demonstrate applications of spray coating to develop nanocomposite and smooth NC film for specific application.

The specific research goals are

1. Investigate the effect of NC suspension to make NC film via spraying of NC on polished impermeable surface and compare the uniformity of the film via thickness of film with the film via vacuum filtration.
2. Investigate the effect of spraying process variables on the uniformity and properties of NC film
3. Investigate the effect of recycling of spray coated NC film into a potential barrier material
4. Develop NC-MMT composite via spraying and evaluate its barrier and mechanical properties and compare with composites from vacuum filtration.
5. Engineering the roughness of NC film via spraying of NC on different substrates and investigate controlling parameters for roughness.

1.14. THE SCOPE OF THE WORK

Rapid Preparation of NC film Via Spraying - Concept

Considering time consumption in existing methods for NC preparation, a fast process to fabricate NC film is required. The method should be able to handle the high concentration of NC suspension to tailor the basis weight and thickness of NC film. The operating time should be independent of NC suspension. It is necessary to investigate and compare the quality of NC film prepared via vacuum filtration and spray coating.

Flexible Process of spraying for multiple NC film preparation

Spray coating of NC on a polished metal surface has been transcribed into a full-fledged and flexible process and it is proposed to investigate process parameters affecting the spraying process and NC film. The properties of spray coated NC film should be compared with the film via vacuum film to evaluate the performance of spraying. The effect of process variable on the uniformity of NC film and its strength should be investigated via modifying the configuration of spray coating experimental setup and varying suspension NC concentration.

Recyclability of Spray Coated NC film

Spraying may fulfil the fast production of NC film but raise a question about whether spray coated NC film could be recyclable into a potential barrier material or not. The effect of recycling on the properties of spray coated NC film will be investigated.

Application of spray coating

An objective of the work is to develop an application of spraying that can produce NC-MMT nanocomposite as a barrier material and secondly to produce super rough and super smooth NC film via spraying of NC on different substrates.

Developing Composite

In spray coating to prepare NC–MMT composite, the effect of MMT loading on the operation time for the spraying process and barrier performance and strength of the composite will be investigated The performance of spraying will be evaluated by the comparison with vacuum filtration for the same composite production.

Developing Smooth NC film

The effect of the smooth impermeable surface on the NC film via spraying in controlling the parameters of the roughness of NC film will be investigated.

1.15. THESIS OUTLINE

Chapter 1: Nanocellulose film and its composites -Production and Limitations – A literature review

In chapter 1, a literature review on the spraying of nanocellulose on permeable and impermeable surfaces, its advantages and disadvantages, and other forms of NC film production are discussed. The potential applications for nanocellulose film and its composites as barrier materials, substrates for printed electronics and filters will also be discussed. The research objectives in the form of knowledge gaps are also developed in this chapter.

Kirubanandan Shanmugam, Gil Garnier and Warren Batchelor, "Nanocellulose film and its composites: Preparation, applications and limitations" - the chapter for A book on Nanoscale Processing, Elsevier Editor: Prof Sabu Thomas, Vice Chancellor, M G University India.

Chapter 2: Rapid Preparation of smooth nanocellulose films using spray coating

A novel rapid method for spraying nanocellulose on a stainless-steel plate to prepare a smooth film has been developed. This is an alternative to vacuum filtration, which has the drawbacks of high drainage time and difficulties arising from the filter and a hard to handle film. This work highlights that the films with weight per unit area ranging from 50 to 200 g/m^2 could be prepared, with the basis weight easily controlled from the suspension solids concentration. This film also possesses large-scale surface smoothness, with the side in contact with the steel plate having an RMS roughness of 389 nm over a 1 cm^2 inspection area. Lastly, film production is achieved with high manufacturing speeds, with each sheet only taking a minute of operator time to produce, independent of the mass per unit area of the sheet.

Shanmugam, K., Varanasi, S., Garnier, G., & Batchelor, W. Rapid preparation of smooth nanocellulose films using spray coating. Cellulose, 24, no 7 (2017) 2669 -2676.

Impact Factor -3.8

Chapter 3: Flexible Spray Coating Process for Smooth Nanocellulose Film Production

This chapter mainly focuses on the characteristics of spray coated nanocellulose film compared with the vacuum filtrated nanocellulose sheet. This chapter especially addresses the mechanical properties and bulk properties of the spray coated nanocellulose film. Additionally, the experimental set up is optimised to enhance the uniformity of spray coated sheet and other properties. Film uniformity was also noticeably dependent on the parameters in the spraying process. The research shows that the properties of the films produced by spraying can be much more easily tailored to to the required application.

Shanmugam, Kirubanandan, Hamid Doosthosseini, Swambabu Varanasi, Gil Garnier, and Warren Batchelor. "Flexible spray coating process for smooth nanocellulose film production." Cellulose 25, no. 3 (2018): 1725-1741.

Impact Factor -3.8

Chapter 4- Smooth nanocellulose films as air and water vapour barrier: a sustainable alternative to polyolefin packaging

This chapter focuses on the barrier properties of spray coated nanocellulose films as a potential replacement for synthetic barrier materials. This research also investigates the recyclability of nano-cellulose (NC) films. Nano-cellulose sheets, created via spraying, were evaluated for barrier performance and strength and were recycled into similar products, using standard laboratory papermaking techniques. The recycled sheets retained 80% of tensile strength and significant barrier performance and although the water vapour permeability (WVP) increased by 5×10^{-11} g.m^{-1}.s^{-1} Pa^{-1} from the WVP of vacuum filtered NC film of 4.97×10^{-11} g.m^{-1}.s^{-1} Pa^{-11}, the recycled NC film still had acceptable performance for most packaging applications. The retained strength and barrier properties and facile re-processability of the product promise a sustainable and recyclable alternative to conventional polyolefin packaging. This provides a very attractive opportunity for the packaging industry.

Kirubanandan Shanmugam, Hamid Doosthosseini, Swambabu Varanasi, Gil Garnier, Warren Batchelor, Smooth nanocellulose films as air and water vapour barrier: a sustainable alternative to polyolefin packaging, Sustainable materials and technologies, Elsevier.Dec 2019.

Chapter 5- Nanoclay –Nanocellulose composite via spraying

The nanocomposite from nanocellulose and nano clay will be prepared by the spray coating method. The effect of nanoclay addition on mechanical and barrier properties of the sheet will be investigated. Additionally, the interaction of nanoclay with nanocellulose will be evaluated as a function of the aspect ratio and hydrophobicity of the sheet. Spraying could be capable of producing the sheet with a very high nanoclay loading (>30%) with respect to fibres content in the suspension. Critical issues to be addressed include the structure size and orientation of the nanoclay within the nanocellulose fibrous network and the relationship to barrier performance. This work is my fifth chapter of my thesis.

Kirubanandan Shanmugam, Maisha Maliha, Vikram Singh Raghuwanshi, Swambabu Varanasi,Gil Garnier, Warren Batchelor, Flexible Process to produce Nanocellulose – Montmorillonite Composite via Spray Coating, will be communicated to Journal of Cleaner Production, Elsevier.

Impact Factor -6.160.

Chapter 6 – Optimization of Surface Roughness of Nanocellulose Film

Spraying of nanocellulose on the stainless-steel plate produced a smooth nano cellulose film. In the work in this chapter, it is planned to spray nanocellulose on the different surfaces which have low to high surface roughness, as well as to vary the fibre diameter by processing the nanofibres with high pressure homogenisation to quantify the factors controlling the surface roughness of the nanofibre sheet.   The surfaces used to make smooth nanocellulose films include ordinary stainless steel , super mirror stainless steel and silicon wafer. The factors that control the surface roughness and uniformity of nanocellulose film, including nanofibre diameter, substrate surface roughness and processing conditions, will be investigated in the 6th chapter of the thesis.

Kirubanandan Shanmugam, Humayun Nadeem, Christine Browne, Gil Garnier and Warren

Batchelor, Engineering the smoothness of nanocellulose film via spraying, will be communicated to Colloid and Surfaces, Elsevier.

Impact Factor -5.1

Chapter 7 – Conclusion and Future Perspective

This chapter explores the advantages of spray coating as a flexible process to manufacture smooth nanocellulose films and nanocomposites and addresses its limits and discusses the prospects for scaling up into an industrial scale. The thesis is then concluded with future applications of spray coating in material processing and development.

1.16. REFERENCES

1. Isogai, A., T. Saito, and H. Fukuzumi, TEMPO-oxidized cellulose nanofibers. Nanoscale, 2011. **3**(1): p. 71-85.

2. Klemm, D., F. Kramer, S. Moritz, T. Lindström, M. Ankerfors, D. Gray, and A. Dorris, Nanocelluloses: A New Family of Nature-Based Materials. Angewandte Chemie International Edition, 2011. **50**(24): p. 5438-5466.

3. Dufresne, A., Nanocellulose: a new ageless bionanomaterial. Materials Today, 2013. **16**(6): p. 220-227.

4. Garusinghe, U.M., S. Varanasi, V.S. Raghuwanshi, G. Garnier, and W. Batchelor, Nanocellulose-montmorillonite composites of low water vapour permeability. Colloids and Surfaces A: Physicochemical and Engineering Aspects, 2018. **540**: p. 233-241.

5. Aulin, C. and T. Lindström, Biopolymer coatings for paper and paperboard. Biopolymers–New Materials for Sustainable Films and Coatings, 2011: p. 255-276.

6. Nechyporchuk, O., M.N. Belgacem, and J. Bras, Production of cellulose nanofibrils: A review of recent advances. Industrial Crops and Products, 2016. **93**: p. 2-25.

7. Abdul Khalil, H.P.S., Y. Davoudpour, C.K. Saurabh, M.S. Hossain, A.S. Adnan, R. Dungani, M.T. Paridah, M.Z. Islam Sarker, M.R.N. Fazita, M.I. Syakir, and M.K.M. Haafiz, A review on nanocellulosic fibres as new material for sustainable packaging: Process and applications. Renewable and Sustainable Energy Reviews, 2016. **64**: p. 823-836.

8. Standard Terms and Their Defination for Cellulose Nanomaterial WI 3021, in TAPPI STANDARD. Technical Association of the Pulp and Paper Industry.

9. Lavoine, N., I. Desloges, A. Dufresne, and J. Bras, Microfibrillated cellulose–Its barrier properties and applications in cellulosic materials: A review. Carbohydrate polymers, 2012. **90**(2): p. 735-764.

10. Osong, S.H., S. Norgren, and P. Engstrand, Processing of wood-based microfibrillated cellulose and nanofibrillated cellulose, and applications relating to papermaking: a review. Cellulose, 2016. **23**(1): p. 93-123.

11. Wågberg, L., G. Decher, M. Norgren, T. Lindström, M. Ankerfors, and K. Axnäs, The build-up of polyelectrolyte multilayers of microfibrillated cellulose and cationic polyelectrolytes. Langmuir, 2008. **24**(3): p. 784-795.

12. Kalia, S., A. Dufresne, B.M. Cherian, B.S. Kaith, Av, #233, L. rous, J. Njuguna, and E. Nassiopoulos, Cellulose-Based Bio- and Nanocomposites: A Review. International Journal of Polymer Science, 2011. **2011**.

13. Abitbol, T., A. Rivkin, Y. Cao, Y. Nevo, E. Abraham, T. Ben-Shalom, S. Lapidot, and O. Shoseyov, Nanocellulose, a tiny fiber with huge applications. Current Opinion in Biotechnology, 2016. **39**: p. 76-88.

14. Zolin, L., Electrode Preparation Exploiting the Spray Coating Technique, in Large-scale Production of Paper-based Li-ion Cells. 2017, Springer International Publishing: Cham. p. 77-94.

15. Henriksson, M., L.A. Berglund, P. Isaksson, T. Lindström, and T. Nishino, Cellulose Nanopaper Structures of High Toughness. Biomacromolecules, 2008. **9**(6): p. 1579-1585.

16. Kangas, H., P. Lahtinen, A. Sneck, A.-M. Saariaho, O. Laitinen, and E. Hellén, Characterization of fibrillated celluloses. A short review and evaluation of characteristics with a combination of methods. Nordic Pulp & Paper Research Journal, 2014. **29**(1): p. 129-143.

17. Raj, P., S. Varanasi, W. Batchelor, and G. Garnier, Effect of cationic polyacrylamide on the processing and properties of nanocellulose films. Journal of colloid and interface science, 2015. **447**: p. 113-119.

18. Li, Q., P. Raj, F.A. Husain, S. Varanasi, T. Rainey, G. Garnier, and W. Batchelor, Engineering cellulose nanofibre suspensions to control filtration resistance and sheet permeability. Cellulose, 2016. **23**(1): p. 391-402.

19. Bilodeau, M., D. Bousfield, W. Luu, F. Richmond, and M. Paradis. Potential applications of nanofibrillated cellulose in printing and writing papers. in Proceedings of the 2012 TAPPI International Conference on Nanotechnology for Renewable Materials, Montreal, QC, Canada. 2012.

20. Varshney, V.K. and S. Naithani, Chemical Functionalization of Cellulose Derived from Nonconventional Sources, in Cellulose Fibers: Bio- and Nano-Polymer Composites: Green Chemistry and Technology, S. Kalia, B.S. Kaith, and I. Kaur, Editors. 2011, Springer Berlin Heidelberg: Berlin, Heidelberg. p. 43-60.

21. Wiedenhoeft, A.C. and R.B. Miller, Structure and function of wood. Handbook of wood chemistry and wood composites, 2005: p. 9-33.

22. Stelte, W. and A.R. Sanadi, Preparation and characterization of cellulose nanofibers from two commercial hardwood and softwood pulps. Industrial & engineering chemistry research, 2009. **48**(24): p. 11211-11219.

23. Wang, Q., J. Zhu, R. Gleisner, T. Kuster, U. Baxa, and S. McNeil, Morphological development of cellulose fibrils of a bleached eucalyptus pulp by mechanical fibrillation. Cellulose, 2012. **19**(5): p. 1631-1643.

24. Varanasi, S., L. Henzel, S. Sharman, W. Batchelor, and G. Garnier, Producing nanofibres from carrots with a chemical-free process. Carbohydrate Polymers, 2018. **184**: p. 307-314.

25. Spence, K.L., R.A. Venditti, O.J. Rojas, J.J. Pawlak, and M.A. Hubbe, Water vapor barrier properties of coated and filled microfibrillated cellulose composite films. BioResources, 2011. **6**(4): p. 4370-4388.

26. Spence, K.L., R.A. Venditti, O.J. Rojas, Y. Habibi, and J.J. Pawlak, A comparative study of energy consumption and physical properties of microfibrillated cellulose produced by different processing methods. Cellulose, 2011. **18**(4): p. 1097-1111.

27. Siró, I. and D. Plackett, Microfibrillated cellulose and new nanocomposite materials: a review. Cellulose, 2010. **17**(3): p. 459-494.

28. Kalia, S., S. Boufi, A. Celli, and S. Kango, Nanofibrillated cellulose: surface modification and potential applications. Colloid and Polymer Science, 2014. **292**(1): p. 5-31.

29.   Bilodeau, M., D. Bousfield, W. Luu, F. Richmond, and M. Paradis. Potential applications of nanofibrillated cellulose in printing and writing papers. in TAPPI international conference on nanotechnology for renewable materials. 2012.

30.   Chakraborty, A., M. Sain, and M. Kortschot, Cellulose microfibrils: a novel method of preparation using high shear refining and cryocrushing. Holzforschung, 2005. **59**(1): p. 102-107.

31.   Abraham, E., B. Deepa, L. Pothan, M. Jacob, S. Thomas, U. Cvelbar, and R. Anandjiwala, Extraction of nanocellulose fibrils from lignocellulosic fibres: A novel approach. Carbohydrate Polymers, 2011. **86**(4): p. 1468-1475.

32.   Pääkkö, M., M. Ankerfors, H. Kosonen, A. Nykänen, S. Ahola, M. Österberg, J. Ruokolainen, J. Laine, P.T. Larsson, O. Ikkala, and T. Lindström, Enzymatic Hydrolysis Combined with Mechanical Shearing and High-Pressure Homogenization for Nanoscale Cellulose Fibrils and Strong Gels. Biomacromolecules, 2007. **8**(6): p. 1934-1941.

33.   Abe, K., S. Iwamoto, and H. Yano, Obtaining Cellulose Nanofibers with a Uniform Width of 15 nm from Wood. Biomacromolecules, 2007. **8**(10): p. 3276-3278.

34.   Massey, L.K., Introduction, in Permeability Properties of Plastics and Elastomers (Second Edition), L.K. Massey, Editor. 2003, William Andrew Publishing: Norwich, NY. p. 1-56.

35.   Tukker, A., Plastic waste-feedstock recycling, chemical recycling and incineration. Rapra Rev Rep, 2002. **13**(4): p. 1-10.

36.   Davis, G. and J.H. Song, Biodegradable packaging based on raw materials from crops and their impact on waste management. Industrial Crops and Products, 2006. **23**(2): p. 147-161.

37.   Wang, J., D.J. Gardner, N.M. Stark, D.W. Bousfield, M. Tajvidi, and Z. Cai, Moisture and Oxygen Barrier Properties of Cellulose Nanomaterial-Based Films. ACS Sustainable Chemistry & Engineering, 2018. **6**(1): p. 49-70.

38.   Fukuzumi, H., T. Saito, T. Iwata, Y. Kumamoto, and A. Isogai, Transparent and high gas barrier films of cellulose nanofibers prepared by TEMPO-mediated oxidation. Biomacromolecules, 2008. **10**(1): p. 162-165.

39.   Lange, J. and Y. Wyser, Recent innovations in barrier technologies for plastic packaging—a review. Packaging Technology and Science: An International Journal, 2003. **16**(4): p. 149-158.

40.   Nair, S.S., J. Zhu, Y. Deng, and A.J. Ragauskas, High performance green barriers based on nanocellulose. Sustainable Chemical Processes, 2014. **2**(1): p. 23.

41.   Wang, F., Z. Chen, L. Xiao, B. Qu, and Q. Gong, Papery solar cells based on dielectric/metal hybrid transparent cathode. Solar Energy Materials and Solar Cells, 2010. **94**(7): p. 1270-1274.

42.   Malinen, M. and J. Kuusisto, Research, development and commercialisation activities in printed intelligence. VTT Technical Research Centre of Finland, 2010: p. 4-6.

43.   Hübler, A., B. Trnovec, T. Zillger, M. Ali, N. Wetzold, M. Mingebach, A. Wagenpfahl, C. Deibel, and V. Dyakonov, Printed paper photovoltaic cells. Advanced Energy Materials, 2011. **1**(6): p. 1018-1022.

44.   Hu, L., G. Zheng, J. Yao, N. Liu, B. Weil, M. Eskilsson, E. Karabulut, Z. Ruan, S. Fan, and J.T. Bloking, Transparent and conductive paper from nanocellulose fibers. Energy & Environmental Science, 2013. **6**(2): p. 513-518.

45.   Henriksson, M. and L.A. Berglund, Structure and properties of cellulose nanocomposite films containing melamine formaldehyde. Journal of Applied Polymer Science, 2007. **106**(4): p. 2817-2824.

46.   Mörseburg, K. and G. Chinga-Carrasco, Assessing the combined benefits of clay and nanofibrillated cellulose in layered TMP-based sheets. Cellulose, 2009. **16**(5): p. 795-806.

47.   Chinga-Carrasco, G., D. Tobjörk, and R. Österbacka, Inkjet-printed silver nanoparticles on nano-engineered cellulose films for electrically conducting structures and organic transistors: concept and challenges. Journal of Nanoparticle Research, 2012. **14**(11): p. 1-10.

48.   Orelma, H., I. Filpponen, L.-S. Johansson, M. Österberg, O.J. Rojas, and J. Laine, Surface Functionalized Nanofibrillar Cellulose (NFC) Film as a Platform for Immunoassays and Diagnostics. Biointerphases, 2012. **7**(1): p. 61.

49.   Metreveli, G., L. Wågberg, E. Emmoth, S. Belák, M. Strømme, and A. Mihranyan, A Size-Exclusion Nanocellulose Filter Paper for Virus Removal. Advanced Healthcare Materials, 2014. **3**(10): p. 1546-1550.

50.   Koga, H., E. Tokunaga, M. Hidaka, Y. Umemura, T. Saito, A. Isogai, and T. Kitaoka, Topochemical synthesis and catalysis of metal nanoparticles exposed on crystalline cellulose nanofibers. Chemical Communications, 2010. **46**(45): p. 8567-8569.

51.   Huang, L., X. Chen, T.X. Nguyen, H. Tang, L. Zhang, and G. Yang, Nano-cellulose 3D-networks as controlled-release drug carriers. Journal of Materials Chemistry B, 2013. **1**(23): p. 2976-2984.

52.   The Global Market for Nanocellulose to 2030: Cellulose nanofibers, Cellulose nanocrystals and Bacterial cellulose particles, I. Future Markets, Editor. 2018. p. 325.

53.   Varanasi, S. and W.J. Batchelor, Rapid preparation of cellulose nanofibre sheet. Cellulose, 2013. **20**(1): p. 211-215.

54.   Varanasi, S., U. Garusinghe, G.P. Simon, G. Garnier, and W. Batchelor, Novel In-situ Precipitation Process to Engineer Low Permeability Porous Composite. Scientific Reports, 2018. **8**(1): p. 10747.

55.   He, Z., X. Zhang, and W. Batchelor, Cellulose nanofibre aerogel filter with tuneable pore structure for oil/water separation and recovery. RSC Advances, 2016. **6**(26): p. 21435-21438.

56.   Garusinghe, U.M., V.S. Raghuwanshi, W. Batchelor, and G. Garnier, Water Resistant Cellulose – Titanium Dioxide Composites for Photocatalysis. Scientific Reports, 2018. **8**(1): p. 2306.

57.   Varanasi, S., Z.-X. Low, and W. Batchelor, Cellulose nanofibre composite membranes – Biodegradable and recyclable UF membranes. Chemical Engineering Journal, 2015. **265**: p. 138-146.

58.   Mendoza, L., T. Gunawardhana, W. Batchelor, and G. Garnier, Nanocellulose for gel electrophoresis. Journal of Colloid and Interface Science, 2019. **540**: p. 148-154.

59.   Curvello, R., V.S. Raghuwanshi, and G. Garnier, Engineering nanocellulose hydrogels for biomedical applications. Advances in Colloid and Interface Science, 2019. **267**: p. 47-61.

60.   Mendoza, L., L. Hossain, E. Downey, C. Scales, W. Batchelor, and G. Garnier, Carboxylated nanocellulose foams as superabsorbents. Journal of Colloid and Interface Science, 2019. **538**: p. 433-439.

61.   Werrett, M.V., M.E. Herdman, R. Brammananth, U. Garusinghe, W. Batchelor, P.K. Crellin, R.L. Coppel, and P.C. Andrews, Bismuth Phosphinates in Bi-Nanocellulose Composites and their Efficacy towards Multi-Drug Resistant Bacteria. Chemistry–A European Journal, 2018. **24**(49): p. 12938-12949.

62.   Maliha, M., Antimicrobial Organobismuth (III) phosphinate- Nanocellulose composites-Confirmation report. 2018, Bioprocessing Research Institute of Australia, Department of chemical engineering, Monash University, Australia.: Faculty of Engineering Monash University Australia.

63.   Garusinghe, U.M., S. Varanasi, G. Garnier, and W. Batchelor. Preparation and characterization of silica nanoparticle-cellulose nanofibre composites. in Asia Pacific Confederation of Chemical Engineering Congress 2015: APCChE 2015, incorporating CHEMECA 2015. 2015. Engineers Australia.

64.   Bardet, R., C. Reverdy, N. Belgacem, I. Leirset, K. Syverud, M. Bardet, and J. Bras, Substitution of nanoclay in high gas barrier films of cellulose nanofibrils with cellulose nanocrystals and thermal treatment. Cellulose, 2015. **22**(2): p. 1227-1241.

65.   Spoljaric, S., A. Salminen, N. Dang Luong, P. Lahtinen, J. Vartiainen, T. Tammelin, and J. Seppälä, Nanofibrillated cellulose, poly(vinyl alcohol), montmorillonite clay hybrid nanocomposites with superior barrier and thermomechanical properties. Polymer Composites, 2014. **35**(6): p. 1117-1131.

66.   Liu, A., A. Walther, O. Ikkala, L. Belova, and L.A. Berglund, Clay Nanopaper with Tough Cellulose Nanofiber Matrix for Fire Retardancy and Gas Barrier Functions. Biomacromolecules, 2011. **12**(3): p. 633-641.

67.   Mirmehdi, S., P.R.G. Hein, C.I.G. de Luca Sarantópoulos, M.V. Dias, and G.H.D. Tonoli, Cellulose nanofibrils/nanoclay hybrid composite as a paper coating: Effects of spray time, nanoclay content and corona discharge on barrier and mechanical properties of the coated papers. Food Packaging and Shelf Life, 2018. **15**: p. 87-94.

68.   Olivera, S., H.B. Muralidhara, K. Venkatesh, V.K. Guna, K. Gopalakrishna, and Y. Kumar K, Potential applications of cellulose and chitosan nanoparticles/composites in wastewater treatment: A review. Carbohydrate Polymers, 2016. **153**: p. 600-618.

69.   Anirudhan, T., J. Deepa, and J. Christa, Nanocellulose/nanobentonite composite anchored with multi-carboxyl functional groups as an adsorbent for the effective removal of Cobalt (II) from nuclear industry wastewater samples. Journal of colloid and interface science, 2016. **467**: p. 307-320.

70.   Sharma, A., M. Thakur, M. Bhattacharya, T. Mandal, and S. Goswami, Commercial Application of Cellulose Nano-composites-A review. Biotechnology Reports, 2019: p. e00316.

71. Carosio, F., J. Kochumalayil, F. Cuttica, G. Camino, and L. Berglund, Oriented Clay Nanopaper from Biobased Components
Properties. ACS applied materials & interfaces, 2015. **7**(10): p. 5847-5856.

72. Wu, C.-N., T. Saito, S. Fujisawa, H. Fukuzumi, and A. Isogai, Ultrastrong and high gas-barrier nanocellulose/clay-layered composites. Biomacromolecules, 2012. **13**(6): p. 1927-1932.

73. Herrick, F.W., R.L. Casebier, J.K. Hamilton, and K.R. Sandberg. Microfibrillated cellulose: morphology and accessibility. in J. Appl. Polym. Sci.: Appl. Polym. Symp.;(United States). 1983. ITT Rayonier Inc., Shelton, WA.

74. Peresin, M.S., J. Vartiainen, V. Kunnari, T. Kaljunen, T. Tammelin, and P. Qvintus. Large-scale nanofibrillated cellulose film: an overview on its production, properties, and potential applications. in Book of abstracts international conference of pulping, papermaking and biotechnology. 2012.

75. Syverud, K. and P. Stenius, Strength and barrier properties of MFC films. Cellulose, 2008. **16**(1): p. 75-85.

76. Wahjudi, U., G.G. Duffy, and R.P. Kibblewhite, An evaluation of three formation testers using radiata pine and spruce kraft pulps. Appita journal, 1998. **51**(6): p. 423-427.

77. Su, J., W.K.J. Mosse, S. Sharman, W.J. Batchelor, and G. Garnier, Effect of tethered and free microfibrillated cellulose (MFC) on the properties of paper composites. Cellulose, 2013. **20**(4): p. 1925-1935.

78. Beneventi, D., E. Zeno, and D. Chaussy, Rapid nanopaper production by spray deposition of concentrated microfibrillated cellulose slurries. Industrial Crops and Products, 2015. **72**: p. 200-205.

79. Morillon, V., F. Debeaufort, G. Blond, M. Capelle, and A. Voilley, Factors affecting the moisture permeability of lipid-based edible films: a review. Critical reviews in food science and nutrition, 2002. **42**(1): p. 67-89.

80. Rhim, J.-W. and P.K. Ng, Natural biopolymer-based nanocomposite films for packaging applications. Critical reviews in food science and nutrition, 2007. **47**(4): p. 411-433.

81. Muramatsu, M., M. Okura, K. Kuboyama, T. Ougizawa, T. Yamamoto, Y. Nishihara, Y. Saito, K. Ito, K. Hirata, and Y. Kobayashi, Oxygen permeability and free volume hole size in ethylene–vinyl alcohol copolymer film: temperature and humidity dependence. Radiation Physics and Chemistry, 2003. **68**(3-4): p. 561-564.

82. Belbekhouche, S., J. Bras, G. Siqueira, C. Chappey, L. Lebrun, B. Khelifi, S. Marais, and A. Dufresne, Water sorption behavior and gas barrier properties of cellulose whiskers and microfibrils films. Carbohydrate Polymers, 2011. **83**(4): p. 1740-1748.

83. Lagaron, J., R. Catalá, and R. Gavara, Structural characteristics defining high barrier properties in polymeric materials. Materials science and technology, 2004. **20**(1): p. 1-7.

84. Aulin, C., M. Gällstedt, and T. Lindström, Oxygen and oil barrier properties of microfibrillated cellulose films and coatings. Cellulose, 2010. **17**(3): p. 559-574.

85. Ben Dhieb, F., E.J. Dil, S.H. Tabatabaei, F. Mighri, and A. Ajji, Effect of nanoclay orientation on oxygen barrier properties of LbL nanocomposite coated films. RSC Advances, 2019. **9**(3): p. 1632-1641.

86. Paul, D.R. and L.M. Robeson, Polymer nanotechnology: Nanocomposites. Polymer, 2008. **49**(15): p. 3187-3204.

87. Hubbe, M.A., A. Ferrer, P. Tyagi, Y. Yin, C. Salas, L. Pal, and O.J. Rojas, Nanocellulose in Thin Films, Coatings, and Plies for Packaging Applications: A Review. BioResources, 2017. **12**(1): p. 2143-2233.

88. Mitragotri, S. and J. Lahann, Physical approaches to biomaterial design. Nat Mater, 2009. **8**(1): p. 15-23.

89. Gontard, N., R. Thibault, B. Cuq, and S. Guilbert, Influence of relative humidity and film composition on oxygen and carbon dioxide permeabilities of edible films. Journal of Agricultural and Food Chemistry, 1996. **44**(4): p. 1064-1069.

90. Liu, A. and L.A. Berglund, Clay nanopaper composites of nacre-like structure based on montmorrilonite and cellulose nanofibers—Improvements due to chitosan addition. Carbohydrate Polymers, 2012. **87**(1): p. 53-60.

91. Aulin, C., G. Salazar-Alvarez, and T. Lindström, High strength, flexible and transparent nanofibrillated cellulose–nanoclay biohybrid films with tunable oxygen and water vapor permeability. Nanoscale, 2012. **4**(20): p. 6622-6628.

92. Priolo, M.A., D. Gamboa, K.M. Holder, and J.C. Grunlan, Super gas barrier of transparent polymer− clay multilayer ultrathin films. Nano letters, 2010. **10**(12): p. 4970-4974.

93. Jochen, W., T. Paul, and M.D. Julian, Functional Materials in Food Nanotechnology. Journal of Food Science, 2006. **71**(9): p. R107-R116.

94. Uyama, H., M. Kuwabara, T. Tsujimoto, M. Nakano, A. Usuki, and S. Kobayashi, Green Nanocomposites from Renewable Resources: Plant Oil−Clay Hybrid Materials. Chemistry of Materials, 2003. **15**(13): p. 2492-2494.

95. Drew, R. and T. Hagen, Nanotechnologies in food packaging: an exploratory appraisal of safety and regulation. Prepared for Food Standards Australia New Zealand. Science Media Centre New Zealand: New Zealand, 2016.

96. A., G.A. and L.H. R., Rational Design of Nanocomposites for Barrier Applications. Advanced Materials, 2001. **13**(21): p. 1641-1643.

97. Uddin, F., Montmorillonite: An Introduction to Properties and Utilization. Current Topics in the Utilization of Clay in Industrial and Medical Applications, 2018: p. 1.

98. Ohrdorf, K.-H. and H. Flachberger, Chapter 1 - Processing of calcium montmorillonites for use in polymers, in Polymer Nanoclay Composites, S. Laske, Editor. 2015, William Andrew Publishing: Oxford. p. 1-25.

99. Sothornvit, R., J.-W. Rhim, and S.-I. Hong, Effect of nano-clay type on the physical and antimicrobial properties of whey protein isolate/clay composite films. Journal of Food Engineering, 2009. **91**(3): p. 468-473.

100. Odom, I., Na/Ca montmorillonite: properties and uses. Society of Mining Engineers Transactions, 1987. **282**.

101.   Azeredo, H.M.C.d., Nanocomposites for food packaging applications. Food Research International, 2009. **42**(9): p. 1240-1253.

102.   Do Nascimento, G.M., Structure of Clays and Polymer–Clay Composites Studied by X-ray Absorption Spectroscopies, in Clays, Clay Minerals and Ceramic Materials Based on Clay Minerals. 2016, IntechOpen.

103.   Silvestre, C., D. Duraccio, and S. Cimmino, Food packaging based on polymer nanomaterials. Progress in Polymer Science, 2011. **36**(12): p. 1766-1782.

104.   Alexandre, M. and P. Dubois, Polymer-layered silicate nanocomposites: preparation, properties and uses of a new class of materials. Materials Science and Engineering: R: Reports, 2000. **28**(1-2): p. 1-63.

105.   Herrera, M., Preparation and characterization of nanocellulose films and coatings from industrial bio-residues. 2015, Luleå tekniska universitet.

106.   Guo, F., S. Aryana, Y. Han, and Y. Jiao, A Review of the Synthesis and Applications of Polymer–Nanoclay Composites. Applied Sciences, 2018. **8**(9): p. 1696.

107.   Ahmadzadeh, S., A. Nasirpour, J. Keramat, N. Hamdami, T. Behzad, and S. Desobry, Nanoporous cellulose nanocomposite foams as high insulated food packaging materials. Colloids and Surfaces A: Physicochemical and Engineering Aspects, 2015. **468**: p. 201-210.

108.   Spoljaric, S., A. Salminen, N. Dang Luong, P. Lahtinen, J. Vartiainen, T. Tammelin, and J. Seppälä, Nanofibrillated cellulose, poly (vinyl alcohol), montmorillonite clay hybrid nanocomposites with superior barrier and thermomechanical properties. Polymer Composites, 2014. **35**(6): p. 1117-1131.

109.   Beyer, G., Nanocomposites: a new class of flame retardants for polymers. Plastics, Additives and Compounding, 2002. **4**(10): p. 22-28.

110.   Su, J., V.S. Raghuwanshi, W. Raverty, C.J. Garvey, P.J. Holden, M. Gillon, S.A. Holt, R. Tabor, W. Batchelor, and G. Garnier, Smooth deuterated cellulose films for the visualisation of adsorbed bio-macromolecules. Scientific reports, 2016. **6**: p. 36119-36119.

111.   d'Eon, J., W. Zhang, L. Chen, R.M. Berry, and B. Zhao, Coating cellulose nanocrystals on polypropylene and its film adhesion and mechanical properties. Cellulose, 2017. **24**(4): p. 1877-1888.

112.   Herrera, M.A., A.P. Mathew, and K. Oksman, Gas permeability and selectivity of cellulose nanocrystals films (layers) deposited by spin coating. Carbohydrate Polymers, 2014. **112**: p. 494-501.

113.   Kumar, V., A. Elfving, and B. Nazari. Roll-to-roll coating of cellulose nanofiber suspensions. in 18th International coating science and technology symposium. 2016.

114.   Karabulut, E. and L. Wågberg, Design and characterization of cellulose nanofibril-based freestanding films prepared by layer-by-layer deposition technique. Soft Matter, 2011. **7**(7): p. 3467-3474.

115.   Wei, C., S. Zeng, Y. Tan, W. Wang, J. Lv, and H. Liu, Impact of layer-by-layer self-assembly clay-based nanocoating on flame retardant properties of sisal fiber cellulose microcrystals. Advances in Materials Science and Engineering, 2015. **2015**.

116. Nogi, M., S. Iwamoto, A.N. Nakagaito, and H. Yano, Optically Transparent Nanofiber Paper. Advanced Materials, 2009. **21**(16): p. 1595-1598.

117. Sehaqui, H., A. Liu, Q. Zhou, and L.A. Berglund, Fast preparation procedure for large, flat cellulose and cellulose/inorganic nanopaper structures. Biomacromolecules, 2010. **11**(9): p. 2195-2198.

118. Zhang, L., W. Batchelor, S. Varanasi, T. Tsuzuki, and X. Wang, Effect of cellulose nanofiber dimensions on sheet forming through filtration. Cellulose, 2012. **19**(2): p. 561-574.

119. Honorato, C., V. Kumar, J. Liu, H. Koivula, C. Xu, and M. Toivakka, Transparent nanocellulose-pigment composite films. Journal of Materials Science, 2015. **50**(22): p. 7343-7352.

120. Hazarika, A. and T.K. Maji, PROPERTIES OF WOOD POLYMER NANOCOMPOSITES IMPREGNATED WITH MELAMINE FORMALDEHYDE-FURFURYL ALCOHOL COPOLYMER AND NANOCLAY. CELLULOSE CHEMISTRY AND TECHNOLOGY, 2017. **51**(3-4): p. 363-377.

121. Thao Ho, T.T., T. Zimmermann, W.R. Caseri, and P. Smith, Liquid ammonia treatment of (cationic) nanofibrillated cellulose/vermiculite composites. Journal of Polymer Science Part B: Polymer Physics, 2013. **51**(8): p. 638-648.

122. Beneventi, D., D. Chaussy, D. Curtil, L. Zolin, C. Gerbaldi, and N. Penazzi, Highly Porous Paper Loading with Microfibrillated Cellulose by Spray Coating on Wet Substrates. Industrial & Engineering Chemistry Research, 2014. **53**(27): p. 10982-10989.

123. Magnusson, J., Method for spraying of free standing 3D structures with MFC: Creation and development of a method. 2016.

124. Czerwonatis, N., Spray coating–a contactless coating process for paper finishing. 2008, Ph. D thesis, Technical University Hamburg-Harburg.

125. Obara, S. and J.W. McGinity, Properties of Free Films Prepared from Aqueous Polymers by a Spraying Technique. Pharmaceutical Research, 1994. **11**(11): p. 1562-1567.

126. The Basics of Airless Spraying. 2016: www.graco.com. p. 44.

127. Seob Lee, K., C. Geun Kim, J. Lee, T.J. Lee, and J.-Y. Ryu, Studies on Application of Spray of Nano-fibrillated Cellulose to Papermaking Process. Vol. 47. 2015.

128. Satam, C.C., C.W. Irvin, A.W. Lang, J.C.R. Jallorina, M.L. Shofner, J.R. Reynolds, and J.C. Meredith, Spray-coated multilayer cellulose nanocrystal—chitin nanofiber films for barrier applications. ACS Sustainable Chemistry & Engineering, 2018. **6**(8): p. 10637-10644.

129. Krol, L.F., D. Beneventi, F. Alloin, and D. Chaussy, Microfibrillated cellulose-SiO2 composite nanopapers produced by spray deposition. Journal of Materials Science, 2015. **50**(11): p. 4095-4103.

130. Beneventi, D., D. Chaussy, D. Curtil, L. Zolin, E. Bruno, R. Bongiovanni, M. Destro, C. Gerbaldi, N. Penazzi, and S. Tapin-Lingua, Pilot-scale elaboration of graphite/microfibrillated cellulose anodes for Li-ion batteries by spray deposition on a forming paper sheet. Chemical Engineering Journal, 2014. **243**: p. 372-379.

131.   Xue, Y., Z. Mou, and H. Xiao, Nanocellulose as a sustainable biomass material: structure, properties, present status and future prospects in biomedical applications. Nanoscale, 2017. **9**(39): p. 14758-14781.

132.   Bharimalla, A.K., S.P. Deshmukh, P.G. Patil, and N. Vigneshwaran, Energy efficient manufacturing of nanocellulose by chemo-and bio-mechanical processes: a review. World Journal of Nano Science and Engineering, 2015. **5**(04): p. 204.

133.   Li, Q., S. McGinnis, C. Sydnor, A. Wong, and S. Renneckar, Nanocellulose life cycle assessment. ACS Sustainable Chemistry & Engineering, 2013. **1**(8): p. 919-928.

134.   Jackson, S., T. Bertényi, and M. Ashby, Recycling of plastics. ImpEE Project, Department of Engineering, University of Cambridge, 2006.

135.   Bugnicourt, E., M. Schmid, O.M. Nerney, J. Wildner, L. Smykala, A. Lazzeri, and P. Cinelli, Processing and Validation of Whey-Protein-Coated Films and Laminates at Semi-Industrial Scale as Novel Recyclable Food Packaging Materials with Excellent Barrier Properties. Advances in Materials Science and Engineering, 2013. **2013**: p. 10.

136.   Choi, B., S. Yoo, and S.-i. Park, Carbon Footprint of Packaging Films Made from LDPE, PLA, and PLA/PBAT Blends in South Korea. Sustainability, 2018. **10**(7): p. 2369.

137.   Vartiainen, J., S. Pasanen, E. Kenttä, and M. Vähä-Nissi, Mechanical recycling of nanocellulose containing multilayer packaging films. Journal of Applied Polymer Science, 2018. **135**(19): p. 46237.

138.   Torvinen, K., J. Sievänen, T. Hjelt, and E. Hellén, Smooth and flexible filler-nanocellulose composite structure for printed electronics applications. Cellulose, 2012. **19**(3): p. 821-829.

139.   Chinga-Carrasco, G., D. Tobjörk, and R. Österbacka, Inkjet-printed silver nanoparticles on nano-engineered cellulose films for electrically conducting structures and organic transistors: concept and challenges. Journal of Nanoparticle Research, 2012. **14**(11): p. 1213.

140.   Tammelin, T., A. Salminen, and U. Hippi, Method for the preparation of NFC films on supports. WO, 2013. **2013060934**: p. A2.

141.   Shanmugam, K., S. Varanasi, G. Garnier, and W. Batchelor, Rapid preparation of smooth nanocellulose films using spray coating. Cellulose, 2017. **24**(7): p. 2669–2676.

CHAPTER 2
RAPID FORMATION OF SMOOTH
NANOCELLULOSE FILMS USING SPRAY
COATING

THIS PAGE HAS BEEN INTENTIONALLY LEFT BLANK

CHAPTER 2 -RAPID FORMATION OF SMOOTH NANOCELLULOSE FILMS USING SPRAY COATING

CONTENTS

RAPID FORMATION OF SMOOTH NANOCELLULOSE FILMS USING SPRAY COATING

Kirubanandan Shanmugam, Swambabu Varanasi, Gil Garnier and Warren Batchelor

Department of Chemical Engineering, Australian Pulp and Paper Institute, Monash University, Melbourne, Vic 3800, Australia.

Address correspondence to E-mail: Warren.Batchelor@monash.edu

2.1. ABSTRACT

Spraying of nanocellulose (NC) on a solid surface to prepare films is an alternative technique to vacuum filtration, which requires a long drainage time and produces films which can sometimes be difficult to separate from the filter. This letter reports a rapid preparation technique for nanocellulose films using a bench scale system spray coating nanocellulose suspension onto stainless steel plates. After spraying NC suspension onto a smooth steel plate travelling on a constant velocity conveyor, the films can be dried directly on the plates using standard laboratory procedures, reducing film formation time and greatly decreasing the operator time required to produce each film. However, drying of wet NC film is still a time consuming step and consumes more than 24 hours in air drying. By adjusting the suspension consistency, we were able to reproducibly make films with a basis weight ranging from 52.8 ± 7.4 to 193.1 ± 3.4 g/m^2 when spraying on to a plate moving at a velocity of 0.32 cm/sec. The operator preparation time for the nanocellulose film was 1 min, independent of the NC film's basis weight, which compares to production times reported in the literature of 10 min using filtration techniques. The films made by spray coating showed higher thickness, but comparable uniformity, to those made by vacuum filtration. Optical profilometry measurements showed that over a 1 cm x 1 cm specimen area for inspection that the surface roughness in Root Mean Square (RMS) of the NC film is only 389 nm on the spray coated side in contact with the steel plates, compared to 2087 nm on the outside surface. Thus, the reduction in preparation time for producing the nanocellulose film recommends this spray coating technique as a rapid and flexible method to produce NC films at the laboratory scale.

2.2. KEYWORDS

Nanocellulose (NC), Spray Coating, Nanocellulose Film, Uniformity, Roughness

2.3. INTRODUCTION

Nanocellulose is a promising renewable, biodegradable nanomaterial available in large quantities in nature. The interest in nanocellulose material is growing due to outstanding properties such as high specific strength, thermal stability, hydrophilicity, and easy chemical functionalization. Nanocellulose materials can provide an excellent alternative material for most plastic films which have limitations in recycling and biodegradability. Films prepared from nanocellulose have outstanding mechanical, optical and structural properties enabling the fabrication of many functional materials and devices such as organic transistors and conducting materials [1], or immunoassays and diagnostics tests [2]. The surface chemistry of nanocellulose can be easily tailored for applications such as photonics, biomedical scaffolds, optoelectronics and developing barrier materials [3]. Recently, nano cellulose film has been investigated for use as filters [4] [5], adsorbents, catalyst [6] , cell culture substrates, thermal insulators and drug carriers [7].

Even though the nanocellulose films have potential uses in many areas, progress and applications are significantly hindered by the difficulty of simply and reproducibly preparing cellulose nano cellulose films both at the laboratory and industrial scales. Stand-alone nanocellulose films have been prepared using either vacuum filtration or casting. Casting is a time-consuming process which typically requires three days for the film to dry and wrinkling is difficult to control [8]. Vacuum filtration is a considerably quicker process when compared to the casting method. Laboratory film preparation time for light weight films less than 60 g/m^2 has been reduced from three to four hours [9] to 10 minutes [10, 11] by increasing the solids content above the gel point and using polyelectrolytes to increase the size and strength of the flocs to reduce filter resistance. However, there can be significant issues in separating the film from the filter and subsequent handling before it is finally dried. Vacuum filtration is also a manufacturing method with a limited range of film basis weight as the filtration time increases exponentially with film thickness and basis weight.

Spraying of nanocellulose on permeable substrates is an alternative technique for making nanocellulose films that has been used to produce continuous nanocellulose films by spraying onto a fabric or to produce composite laminates by spraying onto a base sheet [12]. Spraying has significant advantages such as contour coating and contactless coating with the base substrate. The topography of the surface of the base substrate does not influence the coating process. The range of basis weight achievable with spraying is much higher than has

been obtainable with filtration. A maximum mass of the film of 124 g/m^2 was obtained by spraying nanocellulose onto a nylon fabric running at a speed of 0.5 m/min [13]. So far, spraying of nanocellulose on fabric or paper has been used to prepare sheets and barrier layers, respectively. Spraying has also been used to prepare multilayer nanocomposites for electrodes [14] [15].

Spraying of cellulose microfibres onto impermeable substrates has also been investigated. In a recent study, spraying was used to produce free-standing micro-fibrillated cellulose film with 3D structures on preheated metal surfaces [16]. The spray coated MFC film had a basis weight from 59 to 118 g/m^2 and thickness of the sheet varied from 46 to 68µm. The major reported disadvantage of the approach was the formation of cracks in the film. In an earlier study, ethyl cellulose dispersed in water with plasticizer was sprayed on the Teflon plates and produced a uniform film with enhanced tensile strength and elastic modulus than a cast film [17]. However, this method required extensive pre-treatment of the cellulose prior to spraying in comparison to our method, where the cellulose nano fibrils are directly used for spraying without additional preparation.

Spraying can also be performed at a higher solids content compared to filtration, reducing the amount of water to be removed by drying. Spraying has not so far been used to make discrete films for laboratory investigations, or for small scale products. It is still an open question about the film quality produced by spraying compared to handsheets made by laboratory vacuum filtration. It is the purpose of this paper to describe a new and efficient method for the laboratory production of nanocellulose films by spraying nanocellulose directly onto smooth steel plates. The nanocellulose films thus formed can subsequently be dried in many ways: in air under restraint, heat contact, etc. The uniformity of spray coated nanocellulose films is evaluated by thickness mapping and then compared with the thickness mapping of a nanocellulose film prepared via vacuum filtration.

2.4. EXPERIMENTAL METHOD

2.4.1. MATERIALS

The nomenclature for nanocellulose has not been reported in a consistent manner in the previous scientific investigations. As well as nanocellulose (NC), it is also called micro fibrillated cellulose (MFC), cellulose nano-fibrils, cellulose micro-fibrils and nano-fibrillated cellulose (NFC). In this paper, we use Nanocellulose (NC) as the generic term for all the cellulose nanomaterials used.

NC (Cellulose nanofibrils) supplied from DAICEL Chemical Industries Limited (Celish KY-100S) was used to prepare films. The NC used was supplied from DAICEL Chemical Industries Limited (Celish KY-100S) at 25% solids content. DAICEL NC (Celish KY-100S) has cellulose fibrils with an average diameter of ˜73 nm with a wide distribution of fibre diameter, a mean length of fibre around 8μm and an average aspect ratio of 142 ± 28 [[18]]. DAICEL KY-100S is prepared by micro fibrillation of cellulose with high-pressure water. The crystallinity index of DAICEL nanocellulose was measured to be 78% [[19]].

NC samples were used at consistencies ranging from 1.0 to 2.0 wt. %, prepared by diluting the original concentration of 25 wt. % with distilled water and mixing for 15,000 revolutions in a disintegrator. The viscosity of the NC suspension was evaluated by the flow cup method, which evaluates coating fluid flow through an orifice, to be used as a relative measurement of kinematic viscosity, with the results expressed in seconds of flow time in DIN-sec.

2.4.2. PREPARATION OF NANOCELLULOSE FILMS THROUGH SPRAY COATING AND VACUUM FILTRATION METHODS:

The experimental system for a laboratory scale spray coating system is shown in Figure 1. The NC suspension was sprayed on a circular stainless steel plate moving on a variable speed conveyor using a Professional Wagner spray system (Model number 117) at a pressure of 200 bar. The type 517 spray tip gave an elliptical spray jet. The spray jet angle and beam width are 50° and 22.5 cm, respectively. The spray distance is 30.0±1.0 cm from the spray nozzle to the circular steel plate. The conveyor was operated at a constant speed of 0.32 cm/sec for the spraying of NC on the plate surface. During the spraying, the pressure driven spray system was run for 30 seconds before forming the first film, so as to allow the system to reach equilibrium.
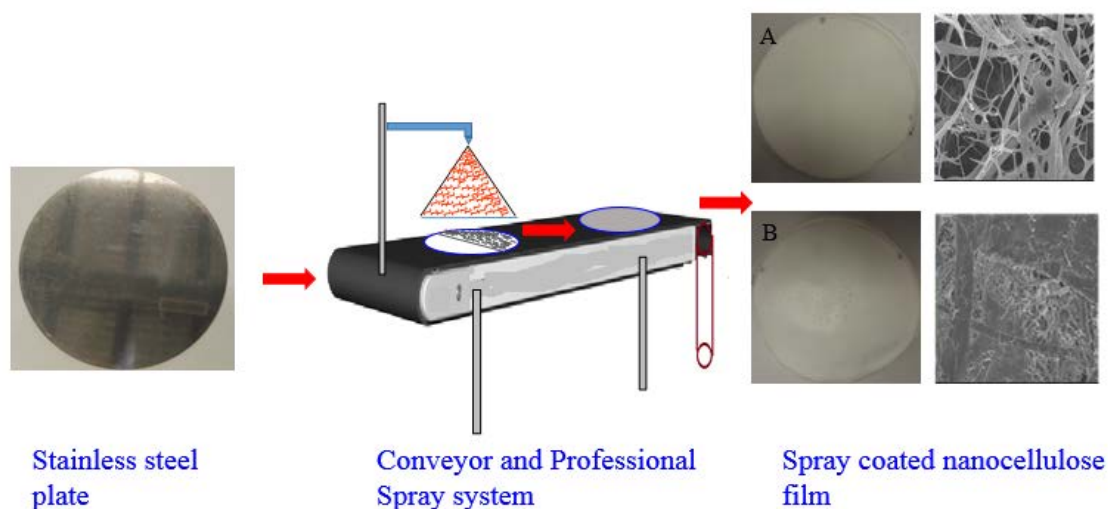
Figure 1. Experimental set up for Laboratory Scale Spray Coating System for Preparation of Nanocellulose Film. (A) The rough surface of the NC film, (B) The smooth surface of the NC film.

After spraying, the film on the plate was dried under restraint at the edges for at least 24 hours. The NC film can then be readily peeled from the stainless steel plate and stored at 23^0C and 50% RH for further testing. For comparison, NC films were also prepared using vacuum filtration method as reported in [10]. In brief, 1000 g of NC suspension with 0.2 wt. % concentration was poured into a cylindrical container having a 150 mesh filter at the bottom and then filtered until it formed a wet film on the mesh. The wet film was carefully separated using blotting papers and then dried at 105^0C in a drum drier for around 10 minutes. The film prepared by this method is used as a reference film to compare the uniformity and thickness of the spray coated film. The basis weight (g/m^2) of each NC film was calculated by dividing the weight of the film, after 4 hours drying in the oven at a temperature of 105 °C, by the film area.

There has been considerable research on the application of free standing cellulose nanofiber films. Applications investigated include those for packaging [10], either as free standing films or laminates on the base sheet [12], filtration membranes ((Varanasi, 2015 #91) and biomedical applications such as drug delivery bio templates for tissue regeneration or base substrates for cell cultures. The qualities of the NC film that make it suitable for these

applications can include uniformity in thickness, good barrier properties and strength and good surface smoothness. The spraying of NC on steel substrates produces film having bi-functional surfaces namely a rough surface and a smooth surface. The smooth surface of the film would be a good platform for use as a base substrate for developing electronic materials where the lowest smoothness of substrates is required.

As part of the initial work in this thesis, the spraying of NC on the packaging paper was attempted to improve the barrier performance. The air permeability of the coated paper decreased with increasing coating weight of NC. However, the wrinkling of coated layer of NC on the base sheet was observed as a limitation in this attempt. The spraying of an anionically modified NC on the surface of the filter/membrane is used to increase the adsorption of cationic molecules in solution. The flux of the filter and the performance of filter can be engineered by the coat weight of nanocellulose on the filter. The coat weight of NC on the filter can be tailored by spraying process. [20]

2.4.2. 1. EVALUATION OF THICKNESS DISTRIBUTION AND THICKNESS MAPPING:

The NC film thickness was measured utilizing L&W thickness analyzer (model no 222). The circular NC film was divided into six regions and thickness was measured in six evenly spaced locations in each region. The thickness mapping of a centre square region of the circular film is done by plotting a contour plot using Origin Pro 9.1. The visual explanation is given in Figure 2. The mean thickness of all the films is plotted against the suspension concentration of nanocellulose. The mass of the film per unit area is evaluated for various concentration of nanocellulose sprayed on the stainless steel plate.

2.4.2.2. EVALUATION OF TENSILE STRENGTH AND AIR PERMEANCE

The strength of the nanocellulose films were evaluated by an Instron model 5566. The test specimen were 100 mm in length and 15 mm width and were conditioned for 24 hours at 23°C and 50% RH. The barrier properties of the 100.5 g/m^2 spray coated film and film prepared via vacuum filtration were evaluated by air permeance through an L&W Air permeance tester.
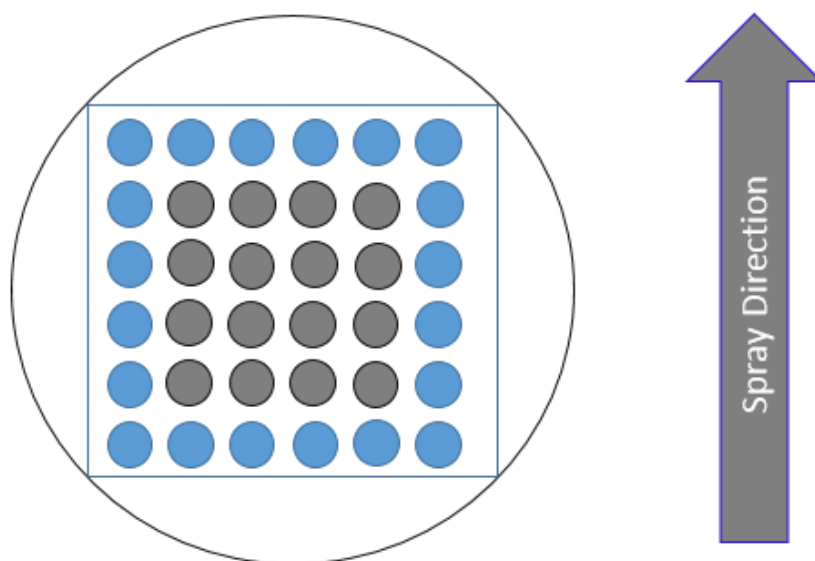
Figure 2. Mapping of thickness of the NC film. The thickness is measured in the centre region of the film. The square section of centre part of the film is used for contour plotting. The grey points are used for mapping to confirm the uniformity of the film.

2.4.2. 3. SURFACE TOPOGRAPHY OF NANOCELLULOSE FILM

The surface morphology and topography of the iridium coated NC film were measured with a FEI Novo SEM. The images of both surfaces of the nanocellulose films are captured at magnifications from 500 to 50,000 in secondary electron mode-II. Furthermore, the surface roughness of both sides of the film at nanoscale was evaluated by atomic force microscopy (JPK Nanowizard 3) and optical profilometry (Bruker Contour GT-I).

2.5. RESULT AND DISCUSSION
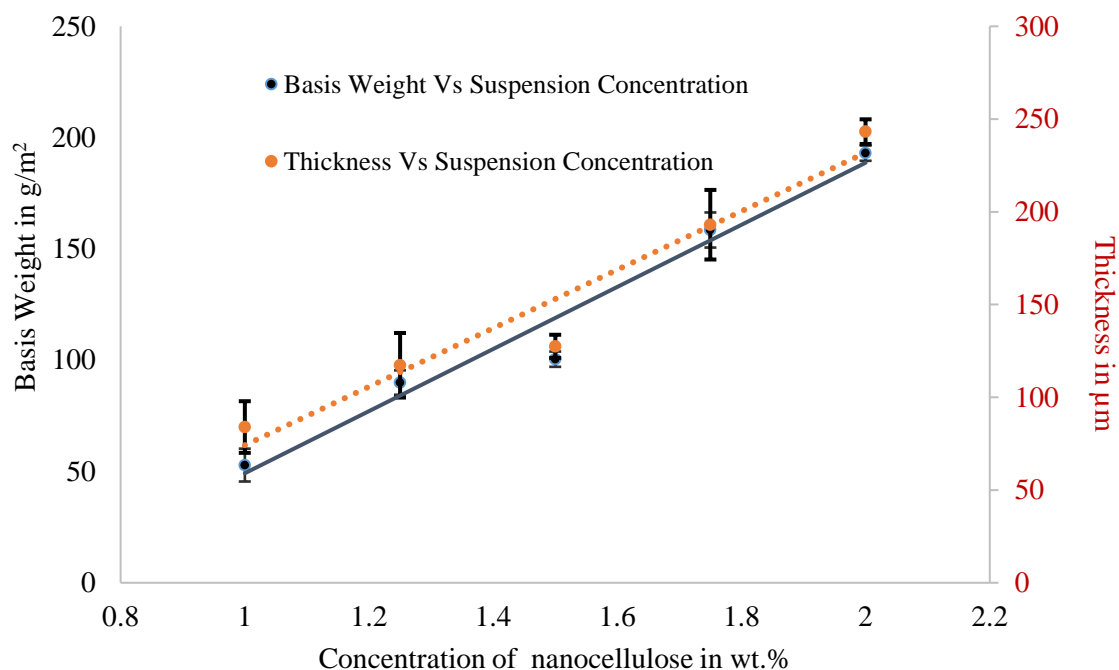
Figure 3. Effect of suspension concentration on the basis weight and thickness of the nanocellulose film prepared using spray coating.
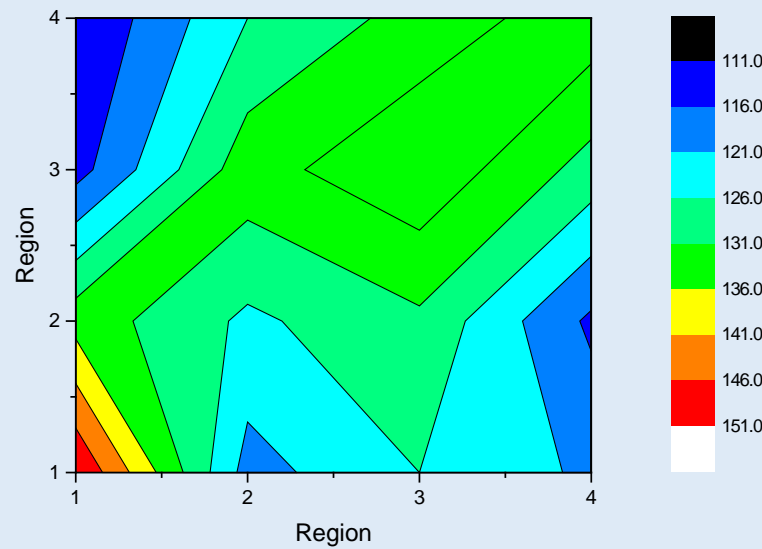
The operational range for spraying NC suspension was between 1.0 wt. % and 2.0 wt. %. Below 1 wt. %, the suspension was too dilute and flowed over the metal surface producing an uneven film, which was difficult to peel from the plate after drying. Above 2 wt. %, the suspension becomes too viscous to spray. The lower and upper limits, corresponded to NC suspension viscosities of 17.0±0.6 and 32.2±0.9 DIN sec, respectively.

Figure 3 shows the effect of NC suspension concentration on the basis weight and mean thickness of the film. Each point is the average of 4 replicates of NC film with the error bars providing the standard deviation. Both film basis weight and thickness increased approximately linearly with increasing NC concentration. Basis weight ranged from 52.8±7.4 to 193.1±3.4 g/m^2 by spraying suspension with a concentration of 1.0 and 2.0 wt. %, respectively. The significant reduction in variability is most likely due to the more rigid suspension at 2.0 wt. % consistency, which produces a more stable suspension sprayed onto

the surface of the plate. The film thicknesses were 83.9±13.9µm and 243.2±6.6 µm for the lowest and highest consistencies.

Figure 4 presents the contour plot of the thickness distribution of the 1.5 wt. % spray coated film compared with a film made by the established method of vacuum filtration. The basis weight of the film prepared by spray coating and vacuum filtration are almost identical at 100.5±3.4 g/m^2 and 95.2±5.2 g/m^2, respectively. The direction of conveyor movement was from bottom to top. Compared to spray coating, vacuum filtration required a much higher dewatering time of 15 minutes to produce the film. When compared to the film made from vacuum filtration, the spray coated nanocellulose film is slightly thicker, even when correcting for the slight difference in basis weight. The apparent density of the spray coated film and film prepared via vacuum filtration were 793 and 834 kg/m^3, respectively. In addition, there is a somewhat wider distribution of thickness for the spray-coated film. The thickness of the NC film prepared via vacuum filtration process and spray drying were 113.4± 5.4 µm and 127.1± 12.1 µm, respectively. The uncertainties give the standard deviation of the distribution of measured thickness.
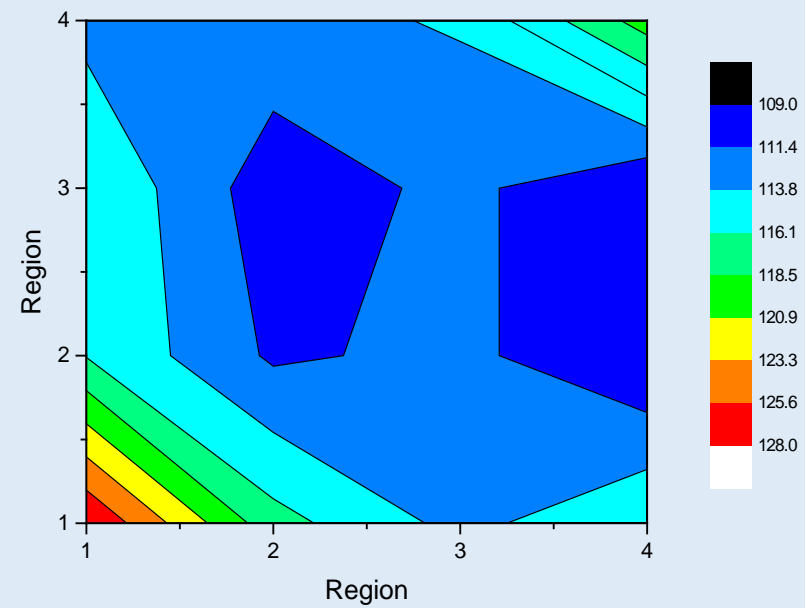
Figure 4. Thickness Distribution of the NC films –Spray coated at Conveyor velocity of 0.32cm/sec and Vacuum Filtration
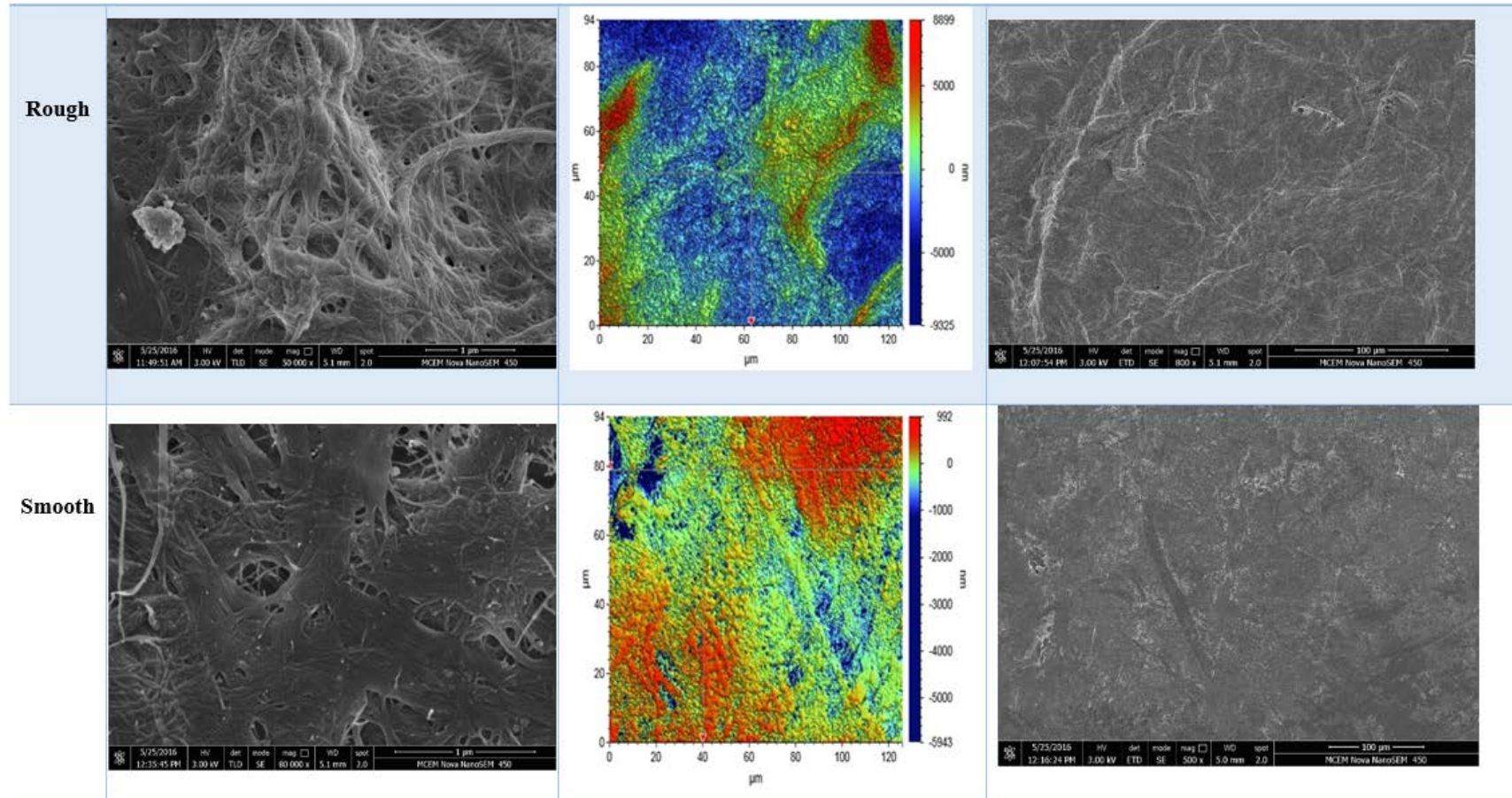
Figure 5. SEM and optical profilometry images of the rough and smooth surfaces of sprayed NC film

Figure 5 shows the surface morphology and topography of both sides of the spray coated NC film investigated by scanning electron microscopy and optical prolifometry of the surface of NC film. The AFM images are given in the supplementary material. At all the length scales investigated, the surface in contact with the stainless steel plate is notably smoother and less porous than the reverse side, where some fibre clumps from the suspension were retained on the film surface as it dried. Visually the smooth surface of the sprayed film has a glossy, shiny appearance. The RMS roughness from the AFM images of the rough side is 414.0 nm for 10μm x10μm film area and 51.4 nm for 2μm x 2μm film area whereas the RMS surface roughness of the smooth side is only 81.1 nm for 10μm x10μm film area and 16.7 nm for 2μm x 2μm film area. AFM measurements of the film prepared by filtration are also given in the Supplementary information and show the sides had a surface roughness of 417.7nm (Side 1) and 330.8 nm (Side 2) at an inspection are of 10μm x10μm, which is approximately the same as the rough side of the film prepared by spray coating. Similarly, the RMS roughness of the spray-coated NC film measured using the optical profilometry at an inspection area of 1 cm x 1 cm is 2087 nm on the rough side and 389 nm on the spray coated side when comparing with NC Film prepared via vacuum filtration which had a RMS roughness of 2673 nm on side 1 and of 3751 nm on side 2.

The results reported in this investigation confirm that laboratory scale spraying NC on a stainless steel plate is viable for the rapid preparation of NC film with a basis weight ranging from 53 to 193 g/m^2. The basis weight of the NC film was readily controlled by the concentration of nanocellulose suspension sprayed.

In our investigation of spraying, the processing time was 50.2 seconds to spray 15.9 cm diameter films, independent of the basis weight from 53 to 193 g/m^2. The quickest time reported in the literature for sheet/film formation with filtration was from work in our group (Varanasi & Batchelor, 2013) , where 2.8 minutes was required for filtering a low basis weight of 56.4 g/m^2, formed from 0.6 wt. % suspension. In contrast, the 95.1 g/m^2 film formed at 0.2 wt. %, made for the work in this paper, took 15 minutes to filter.

When the mechanical properties of the spray-coated and vacuum filtered films were compared, it was found that spray-coated films were the same within the uncertainties. The tensile index of a 104.03 g/m^2 of film prepared via vacuum filtration was 62.3±3.4 Nm/g while the tensile strength of the 100.5 g/m^2 of spray coated nanocellulose film was 60.2±1.5 Nm/g.

The tensile stiffness values were also the same within uncertainties at 946±86 and 941±78 kN/m, for the spray coated film and film prepared via vacuum filtration, respectively. The uncertainties give the 95% confidence interval. It is interesting to note that the tensile index of the 100 g/m^2 film prepared via vacuum filtration is somewhat lower than 60 g/m^2 film made via vacuum filtration or spray coating/filtration of 72 Nm/g [21] and 79 Nm/g [13], respectively . The air permeance of both the spray coated and vacuum filtered films were less than the measurement limit of the instrument of 0.003 µm/Pa.s. This value confirms that the spray coated sheet is highly impermeable.

The current spray coating method is innovative because it allows the production of flat films with uniform thickness. These films require less operator time to produce than films prepared either by filtration or spraying onto porous media ([13]) and can be prepared without cracking unlike the moulded structures produced by [16]. In addition, in contrast to Obara & McGinity, 1994, [17] we have created a cellulose film with one very smooth surface without regenerating or in any way chemically treating or modifying the cellulose.

After filtering, the nanocellulose films can often be difficult to separate from the filter, taking additional time to complete the transfer to the blotting paper without destroying the film. Drying the filtered film then requires repeatedly manually feeding the film into a rotating drum dryer until dry, with the overall process taking at least 10 minutes from the start of filtration. In the spray coating method, the drying time for nano cellulose films in ambient conditions is from 24 hrs to 48 hrs, which is reduced to 30-60 minutes when drying in an oven at 105°C. While the total time to prepare and dry a film is longer with spray coating onto a stainless steel plate, the key strength of the method is the reduction in operator time. Leaving aside, the preparation of the nanocellulose suspension, which is common for the two methods, preparing ten 100 g/m^2 films requires less than 9 minutes of operator time with spraying compared to 220 total minutes with filtration.

2.6. CONCLUSION

We have developed a method of spraying a nanocellulose suspension onto a polished stainless steel to rapidly make smooth films with a basis weight ranging from 50 to 200 g/m^2, simply by adjusting the suspension consistency. This method greatly reduces the operator time to produce films. Further, spray-coating on to stainless steel creates a two-sided film structure with a very smooth surface in contact with the stainless steel plate.

2.7. ACKNOWLEDGEMENT:

2. 8. REFERENCES

1. Chinga-Carrasco, G., D. Tobjörk, and R. Österbacka, Inkjet-printed silver nanoparticles on nano-engineered cellulose films for electrically conducting structures and organic transistors: concept and challenges. Journal of Nanoparticle Research, 2012. **14**(11): p. 1-10.

2. Orelma, H., I. Filpponen, L.-S. Johansson, M. Österberg, O.J. Rojas, and J. Laine, Surface Functionalized Nanofibrillar Cellulose (NFC) Film as a Platform for Immunoassays and Diagnostics. Biointerphases, 2012. **7**(1): p. 61.

3. Abitbol, T., A. Rivkin, Y. Cao, Y. Nevo, E. Abraham, T. Ben-Shalom, S. Lapidot, and O. Shoseyov, Nanocellulose, a tiny fiber with huge applications. Current Opinion in Biotechnology, 2016. **39**: p. 76-88.

4. Metreveli, G., L. Wågberg, E. Emmoth, S. Belák, M. Strømme, and A. Mihranyan, A Size-Exclusion Nanocellulose Filter Paper for Virus Removal. Advanced Healthcare Materials, 2014. **3**(10): p. 1546-1550.

5. Varanasi, S., Z.-X. Low, and W. Batchelor, Cellulose nanofibre composite membranes – Biodegradable and recyclable UF membranes. Chemical Engineering Journal, 2015. **265**: p. 138-146.

6. Koga, H., E. Tokunaga, M. Hidaka, Y. Umemura, T. Saito, A. Isogai, and T. Kitaoka, Topochemical synthesis and catalysis of metal nanoparticles exposed on crystalline cellulose nanofibers. Chemical Communications, 2010. **46**(45): p. 8567-8569.

7. Huang, L., X. Chen, T.X. Nguyen, H. Tang, L. Zhang, and G. Yang, Nano-cellulose 3D-networks as controlled-release drug carriers. Journal of Materials Chemistry B, 2013. **1**(23): p. 2976-2984.

8. Shimizu, M., T. Saito, H. Fukuzumi, and A. Isogai, Hydrophobic, Ductile, and Transparent Nanocellulose Films with Quaternary Alkylammonium Carboxylates on Nanofibril Surfaces. Biomacromolecules, 2014. **15**(11): p. 4320-4325.

9. Nogi, M., S. Iwamoto, A.N. Nakagaito, and H. Yano, Optically Transparent Nanofiber Paper. Advanced Materials, 2009. **21**(16): p. 1595-1598.

10. Varanasi, S. and W.J. Batchelor, Rapid preparation of cellulose nanofibre sheet. Cellulose, 2013. **20**(1): p. 211-215.

11. Zhang, L., W. Batchelor, S. Varanasi, T. Tsuzuki, and X. Wang, Effect of cellulose nanofiber dimensions on sheet forming through filtration. Cellulose, 2012. **19**(2): p. 561-574.

12. Beneventi, D., D. Chaussy, D. Curtil, L. Zolin, C. Gerbaldi, and N. Penazzi, Highly Porous Paper Loading with Microfibrillated Cellulose by Spray Coating on Wet Substrates. Industrial & Engineering Chemistry Research, 2014. **53**(27): p. 10982-10989.

13. Beneventi, D., E. Zeno, and D. Chaussy, Rapid nanopaper production by spray deposition of concentrated microfibrillated cellulose slurries. Industrial Crops and Products, 2015. **72**: p. 200-205.

14. Krol, L.F., D. Beneventi, F. Alloin, and D. Chaussy, Microfibrillated cellulose-SiO2 composite nanopapers produced by spray deposition. Journal of Materials Science, 2015. **50**(11): p. 4095-4103.

15. Zolin, L., Electrode Preparation Exploiting the Spray Coating Technique, in Large-scale Production of Paper-based Li-ion Cells. 2017, Springer International Publishing: Cham. p. 77-94.

16. Magnusson, J., Method for spraying of free standing 3D structures with MFC: Creation and development of a method. 2016.

17. Obara, S. and J.W. McGinity, Properties of Free Films Prepared from Aqueous Polymers by a Spraying Technique. Pharmaceutical Research, 1994. **11**(11): p. 1562-1567.

18. Varanasi, S., R. He, and W. Batchelor, Estimation of cellulose nanofibre aspect ratio from measurements of fibre suspension gel point. Cellulose, 2013. **20**(4): p. 1885-1896.

19. Raj, P., A. Mayahi, P. Lahtinen, S. Varanasi, G. Garnier, D. Martin, and W. Batchelor, Gel point as a measure of cellulose nanofibre quality and feedstock development with mechanical energy. Cellulose, 2016. **23**(5): p. 3051-3064.

20. Aysu, O., Engineering Cellulose Fibre Composites For Liquid Filtration. Doctoral Thesis, Monash University 2019.

21. Varanasi, S. and W. Batchelor, Superior non-woven sheet forming characteristics of low-density cationic polymer-cellulose nanofibre colloids. Cellulose, 2014. **21**(5): p. 3541-3550.

CHAPTER 3

FLEXIBLE SPRAY COATING PROCESS FOR SMOOTH NANOCELLULOSE FILM PRODUCTION

THIS PAGE HAS BEEN INTENTIONALLY LEFT BLANK

Contents

FLEXIBLE SPRAY COATING PROCESS FOR SMOOTH NANOCELLULOSE FILM PRODUCTION

Kirubanandan Shanmugam, Hamid Doosthosseini, Swambabu Varanasi, Gil Garnier, Warren Batchelor

Bioresource Processing Research Institute of Australia, Department of Chemical Engineering Monash University, Melbourne, Vic 3800, Australia.

*Corresponding Author, E-mail: Warren.Batchelor@monash.edu

3.1. ABSTRACT

A novel rapid method for high throughput production of smooth nanocellulose (NC) films by spray coating was communicated recently. In this method, we employed spray coating to produce wet films on stainless steel plates moving on a conveyor, forming free-standing films with interesting structural, mechanical and surface properties upon drying. In this research, we investigate the range of mechanical and physical properties of nanocellulose films prepared by spraying. Furthermore, a comparison with NC films prepared via conventional vacuum filtration was conducted to evaluate the suitability of this method as an alternative film preparation process. One set of experiments was completed where the solids concentration of the suspension was fixed at 1.5 wt. % and the conveyor velocity was varied, while two series of experiments were completed where the solids concentration of the suspension was varied and the conveyor speed was fixed at either 0.32 or 1.05 cm/s. By varying speed and solids concentration, spray-coating was found to allow efficient production of films with basis weights ranging from 38 to 187 g/m^2, with film thicknesses ranging from 58.4 μm to 243.2 μm, respectively. There was a universal linear relationship between the thickness and basis weight, independent of the process conditions. The optical uniformity of film was also noticeably dependent on the spraying process. The optical uniformity index of films, relative to vacuum filtered films, increased with conveyor speed at 1.5 wt. % solids concentration and was independent of solids concentration at low speed. Forming at the higher speed of 1.05 cm/s produced a maximum in optical uniformity in the range 1.5 to 1.75 wt. %, with these films being more uniform than conventional films produced through vacuum

filtration. The most uniform films produced by spraying also had a similar tensile index to films made via vacuum filtration. With an understanding of these parameters and effects, we demonstrate this method to be a more time efficient alternative method to produce uniform films where the properties can be tailored to the required application.

3.2. KEYWORDS:

Spray coating; Nanocellulose; Nanocellulose film; Optical Uniformity; Strength.

3.3. INTRODUCTION

Throughout the past decade, there has been notable growth in the use of micro fibrillated cellulose/nanocellulose films as sustainable substrates for the development of a variety of functional materials [1]. The literature on this topic has confirmed the applicability of nanocellulose films for nanocomposites, anti-microbial films and barrier materials [2] among others. Films made from nano cellulose are strong and show good oxygen barrier properties; they also have the capacity for a broad range of chemical modifications which can attain varied and desirable properties. Additionally, this material is biodegradable, renewable, non-toxic and readily available in large quantities [3].

Nanocellulose films are commonly prepared using either vacuum filtration, whereby fibre suspensions are filtered using a mesh filter and fibres gather in the form of a film, or casting, where the suspension is poured onto a surface and left to dry. Casting is a very time-consuming process as it typically requires three days for drying and can cause wrinkling of the film which is difficult to control [4]. It is another laboratory method used for producing nanocellulose film [5]. The strength of cast nanocellulose films is quite lower than that of films prepared using vacuum filtration method, which is a conventional process in paper-making industries [6]. Vacuum filtration is quicker than casting, however, time consumption is still significant [7]. There are also difficulties in separating the film from the filter mesh and subsequent handling before final drying.

Modifications have improved filtration by increasing the solids content above the gel-point to reduce filtration time, increasing the size of the filter openings to reduce filter resistance and by using polyelectrolytes [8]. Laboratory film preparation time for light weight

films less than 60 g/m^2 has been reduced from three or four hours [9] to 10 minutes [10, 11]. Despite these modifications, there are still significant issues as larger filter openings can result in a loss of material rendering it difficult to control the basis weight of the product and decreasing yield. Vacuum filtration processes reported in literature require a film preparation time ranging from 45 mins to 3 or 4 hrs [9] when finer filters are used. In addition, bulky cellulose film preparation via vacuum filtration is challenging; dewatering time increases exponentially with increased basis weight leading to high operation and labour costs. As such, the range of film basis weights that can be manufactured is limited.

Recently spraying nanocellulose (NC) has emerged as a viable alternative method of NC film preparation [12], [13], while a rapid laboratory scale method for spray coating of NC suspension on a polished stainless steel (SS) plates to create free-standing recyclable films has been reported. Spray coating results in a very uniform deposition layer of nanocellulose on the base surface; the amount of NC increases with an increase in the suspension concentration or decrease in the velocity of the conveyor. Most significantly, spraying can substantially decrease operating time [14].

The present work investigates the effects of process variables on the properties of free-standing NC films prepared by spraying on stainless steel plates. The effects of conveyor velocity, NC suspension concentration and setup configuration are evaluated. The properties of spray coated films are compared with films prepared via vacuum filtration and the effects of process parameters on these properties are quantified. The spraying of nanocellulose on the base surface is hypothesized to produce a stable and uniform distribution of nanocellulose, leading to free-standing films of high optical uniformity. Obtaining quantifiable relationships between process parameters and product properties will allow for tuning product properties such as uniformity and designing processes for desired products.

3.4. EXPERIMENTAL METHOD

3.4.1. MATERIALS

Micro-fibrillated cellulose, also commonly referred to as Nanocellulose in this paper was used for film preparation. Both spray coating and the conventional vacuum filtration methods were employed. From here on, Nanocellulose will be referred to as NC; nano-

cellulose films prepared by vacuum filtration, VF-NC; and Spray coated films, SC-NC. NC was supplied from DAICEL Chemical Industries Limited (Celish KY-100S) with an initial concentration of 25 wt. % cellulose fibres. DAICEL NC has fibrils with an average diameter of ˜ 70 nm with a wide distribution of fibril diameter, mean length of fibre around 8μm and an average aspect ratio of 142 ± 28. The crystallinity of the NC sample was measured as 78% [15]. NC was diluted to the concentration ranges from 1.00 wt. % to 2.50 wt. % and disintegrated in a Messmer disintegrator Model MK III C for 15000 revolutions at 3000 RPM. The viscosity of the NC suspension was evaluated by the flow cup method, i.e. measuring coating fluid flow through an orifice as a relative measure of kinematic viscosity expressed in seconds of flow time in DIN-Sec.

3.4.2. SPRAY COATING

NC suspension was sprayed onto stainless steel plates using Professional Wagner spray system (Model number 117). The experimental set up for spray coating is shown in Figure 1. It is mainly consisting of variable speed conveyor and pressure driven spray system with a knob for adjusting/controlling spray pressure. The spraying of nanocellulose is performed on two different geometries like square stainless steel square plate (220mm x 220mm) and circular plate (Diameter -159 mm). Experiments were conducted in 3 series.

In experimental series 1, the spray jet angle was 50° and the spray width was 30 cm at a spray distance and pressure of 200 bar, respectively. Suspension concentration was kept constant at 1.5 wt.% and conveyor speed was varied from 0.25 cm/s to 0.59 cm/s. 30s time was allowed for pressure driven spray system to reach steady state [14].

In experimental series 2, the spray system setup was similar to series 1; however, the conveyor speed was kept constant at 0.32cm/s and suspension concentration was varied from 1 wt.% to 2 wt.%.

In experimental series 3, the conveyor system was changed, as was spray nozzle to attain a jet angle of 30° and beam width of 22.5cm at a spray distance of 50.0±1.0 cm and 100 bar pressure. The conveyor speed was kept constant at 1.05 cm/s and suspension concentration varied from 1.5 wt. % to 2.5 wt. %.

After spraying, each film was dried on its plate for 24 to 48 hours at ambient conditions, and subsequently removed from the plate and stored at 23^0C and 50% RH before testing.

3.4.3. VACUUM FILTRATION

NC films were prepared using vacuum filtration as reported previously [10]. In brief, NC suspension with 0.2 wt. % concentration was poured into a cylindrical container with 125 mesh at the bottom and filtered, forming a wet film on the mesh. After couching, the wet film was carefully separated using blotting papers, wet pressed at 0.4MPa by sheet press (Type 5-1, AB Lorentzen & Wettre) for 7 mins and drum dried at 105°C. The drying of the film took up to 10 mins. The film prepared by this method is used as a standard reference film to compare the optical uniformity and strength of the spray coated film.

3.4.4. CHARACTERIZATION OF THE NC FILMS:

3.4.4.1. BASIS WEIGHT OF NC FILMS

The basis weight was evaluated by weighing a standard area of the film after 4 hours drying in the oven at a temperature of 105°C.

3.4.4.2. THICKNESS OF NC FILMS

The thickness of the spray coated films was determined using a Thickness Tester Type 21 from Lorentzen & Wettre AB, Stockholm, Sweden. The thickness was measured for at least 36 points on each of the spray coated and vacuum filtered NC films and averaged. The thickness of NC film was measured according to Australian/New Zealand standard method 426.

3.4.4.3. APPARENT DENSITY

The apparent density of the NC films was evaluated through dividing basis weight by mean thickness of the film and followed Australian/New Zealand standard method 208.

3.4.4.4. TENSILE STRENGTH

An Instron model 5566 was used to measure the tensile strength of the NC films. The tensile strength test samples were 100 mm in length and 15mm width. The samples of NC films are equilibrated and conditioned for at least 24 hours at 23°C and 50 % RH before dry tensile testing based on the Australian/New Zealand Standard Methods 448 and 437s. All thickness and tensile tests were done at 23°C and 50 % RH. The samples were tested at a constant rate of elongation of 10mm/min. The Tensile Index (TI)of the samples was calculated from the tensile strength (expressed in Nm^{-1}) divided by basis weight (gm^{-2}). The mean value was obtained from six to seven valid tests and the error bars in plots indicate standard deviation. The elastic modulus was calculated from the maximum slope in the stress-strain curve determined by the software.

3.4.4.5. SURFACE INVESTIGATION

The surface morphology and topography was studied using Scanning Electron Microscopy of iridium coated NC-films. Images were sampled at magnifications of 500x to 50,000x in secondary electron mode-II of FEI Novo SEM 450 for Spray Coated NC film and FEI Magellan 400 FEGSEM for NC film prepared via vacuum filtration. The surface roughness of NC films were evaluated by the Parker Print Surface Roughness Tester (M590 Testing machines Inc), Atomic force microscopy (JPK Nanowizard 3) and optical profilometry (Bruker Contour GT-I).

3.4.4.6. FORMATION ANALYSIS

The optical uniformity of NC film was measured by the Paper Perfect Formation (PPF) Tester (Op Test Equipment Inc, Canada), which measures the optical uniformity of light transmitted through the sample. In brief, the PPF consists of a black and white camera based image analyser and uses a CCD camera interfaced with 256 gray levels and 65 μm/pixel resolution. The analyser uses a diffuse quartz halogen light source with IR filters and automatic intensity control. The PPF classifies formation quality over 10 length scales ranging from 0.5 mm to 60mm. The data reported here is the Relative Formation Value (RFV) of each component relative to one of the films made by vacuum filtration, which was used as a

reference film. Three to six films were measured for each condition, with the results averaged. RFV value less than 1 means that the optical uniformity of the NC film tested is worse than the reference film at that length scale.

3.5. RESULTS

The operational range of the conveyor's velocity, from 0.25 cm/ sec to 0.59 cm/sec, was studied in series 2 of SC-NC experiments where the effects of velocity were studied and suspension concentration was kept constant at 1.5 wt.%. Within these bounds, basis weight ranged from 49.1±5.4 to 102.2±7.5 g/m^2 and thickness ranged from 70.5±2.9 to 130.3±11.3μm. Figure 2 shows the results for Series 2. At low velocity from 0.37 cm/sec to 0.25 cm/sec, the basis weight of the film is relatively constant at ~100±3 g/m^2 for 1.5 wt. % consistency, representing a limit to the amount of suspension that remains on the plate after spraying. The plateau in film basis weight with reducing speed indicates that the carrying capacity of the plate has been reached and that excess material is likely to be flowing off the plate. Interestingly no such flow is observable in the films after they have dried, either in the thickness profiles reported in our previous paper [14] or, as will be discussed later, in the transmitted light images captured to measure optical uniformity. The most likely explanation is that the fluid on the plate has levelled while the plate is held stationary as the film dried.
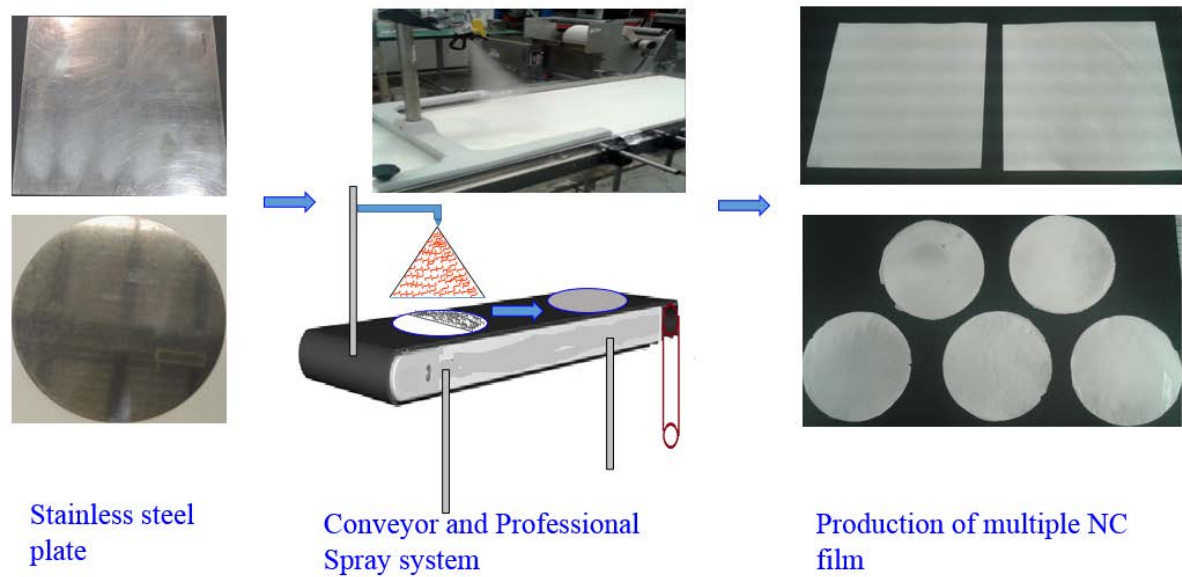
Figure 1: An Experimental Setup for spraying NC suspension on a stainless steel plate to make multiple films.

Beyond 0.37 cm/sec, the basis weight of the film decreases as velocity increases in inverse proportions. In other words, less NC is deposited on the stainless steel when moving at a faster speed, resulting in the formation of a low basis weight NC film due to low suspension consistency of the NC suspension.
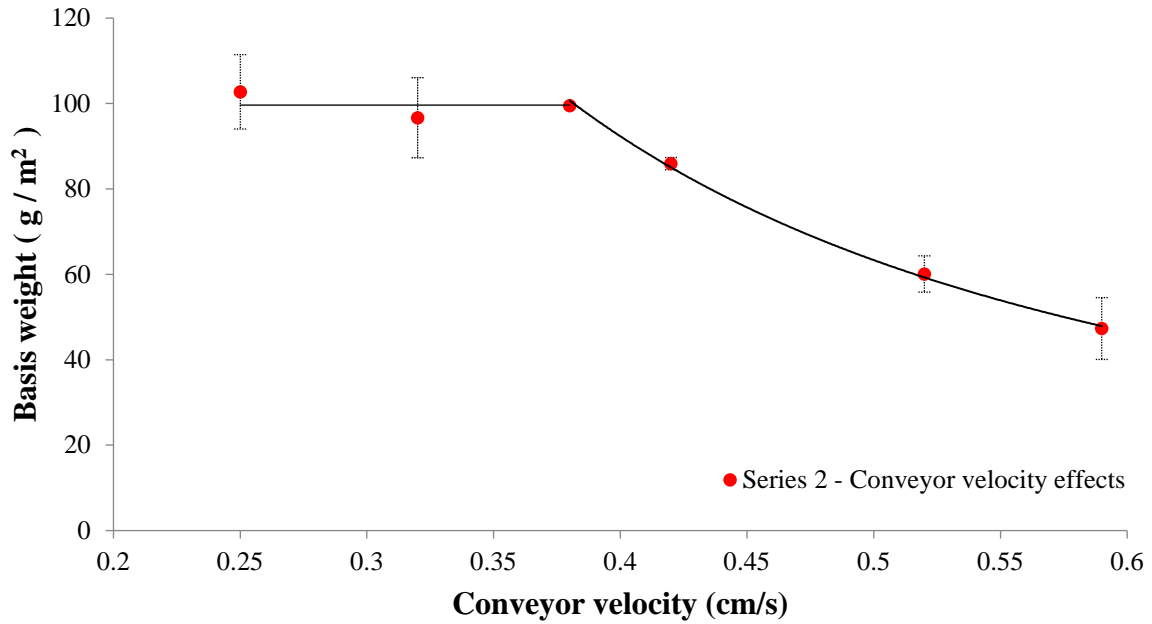
Figure 2 - Influence of the conveyor velocity on the basis weight of SC-NC

The basis weight and thickness of NC films are controlled by the velocity of the conveyor and the consistency of the suspension. Assuming constant flow output of the spray system and positive displacement pump, it may be assumed that deposited mass per unit time would have a positive linear relation with suspension consistency, C_0. From the spray system manual, the spray flow is estimated to be 1.00 litre/min or $\dot{m}$=17x10^{-3} kg/s, assuming a suspension density of 1000 kg/m^3. If the film width is w, the mass consistency is C_0 (kg fibre/kg of suspension) and the conveyor velocity is v then the film basis weight, B, is given by the equation 1.

$$B = \eta \frac{C_0}{v} \frac{\dot{m}}{w} \qquad (1)$$

Where η is an efficiency factor, which includes losses from spraying over the width of the plate, suspension flow and any reduction in flow as suspension viscosity increases.

Figure 3 shows data for three series of experiments of SC-NC demonstrating basis weight as a function of C_0/v. It can be seen that in series 3, the optimized configuration shows

a higher value for x, representing a higher efficiency in the process, which is the result of decreased pressure, change of nozzle and change in setup configuration. The negative values for the y-intercept represent losses of constant value, such as aerosol loss of material. It should be noted that in calculation of trend line for series 2, values below conveyor velocity of 0.38 cm/s were not considered. From Figure 2, it was inferred that maximum deposition is reached at 0.38 cm/s and lowering velocity further results in any additional material flowing off the steel plates.
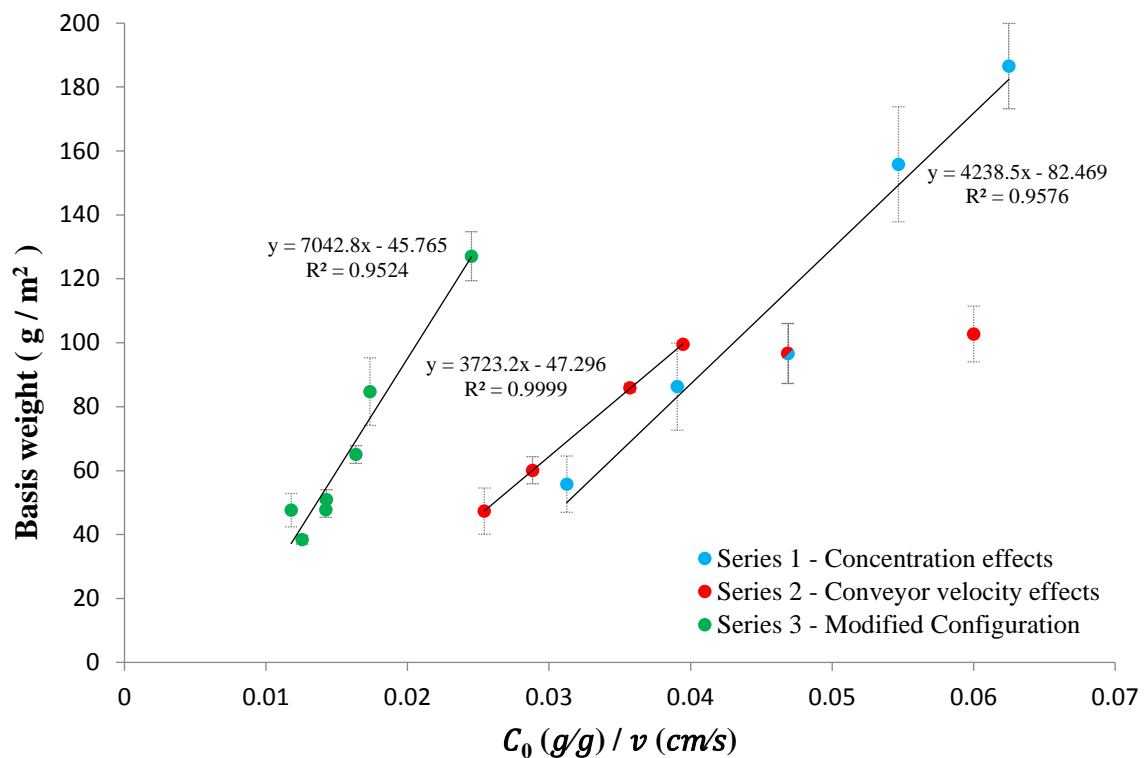
Figure 3 – Basis weight as proportional to $\dfrac{c_0\,(^g/_g)}{v\,(^{cm}/_s)}$

When the results for thickness are plotted in Figure 4, it can be seen that there is a linear relation between thickness and basis weight of films. This relationship is maintained irrespective of configuration and process parameter changes.
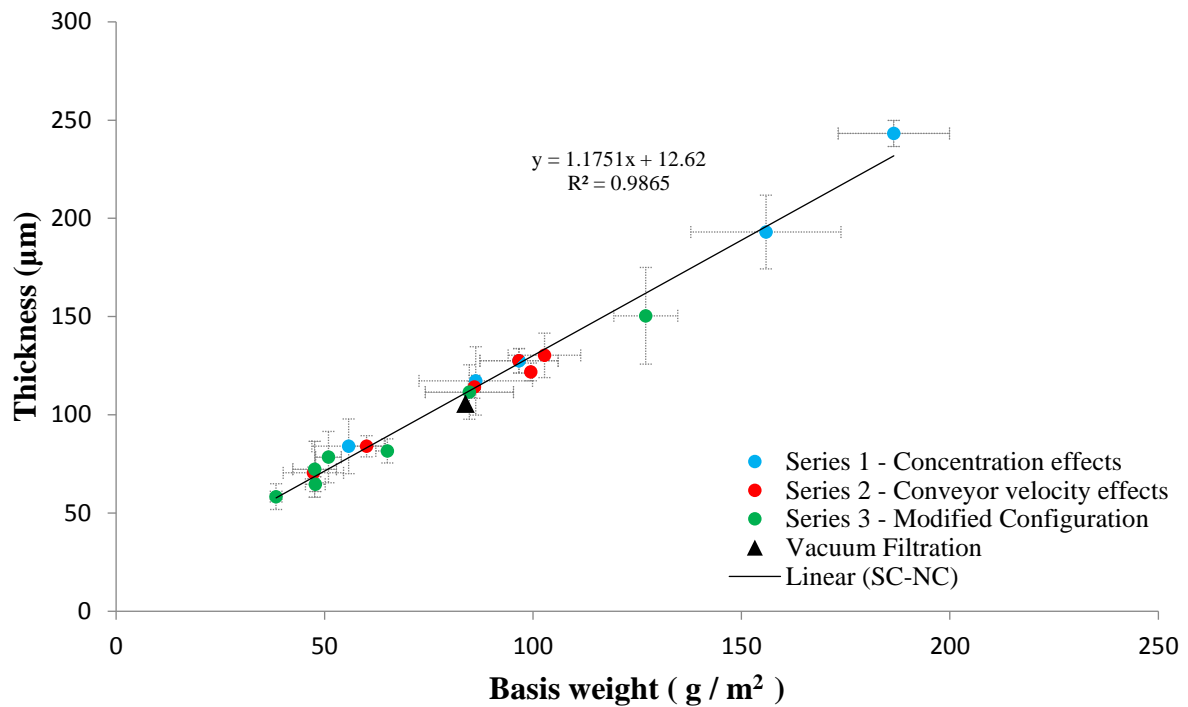
Figure 4 - Effect of NC suspension concentration and Velocity of conveyor on Basis weight and thickness of spray coated NC film

The basis weight and thickness of the NC film can be tailored by two parameters, namely NC concentration and conveyor velocity. Though both can be varied independently, the relationship between thickness and basis weight is a characteristic of these SC-NC films. The figures show that the thickness of VF-NC also lies on the same trend line, irrespective of the fundamentally different production procedure. To calculate the error bars for thickness, all the values measured for a given film were averaged. The average values for the set of films was then used to calculate the overall average shown here, with error bars calculated as the standard deviation of these film averages. The basis weight was only measured once for each film.

The apparent density of films was calculated based on the basis weight and mean thickness of NC films. Figure 5 shows the apparent density as a function of basis weight. It can be seen that for films of basis weight around or higher than 100 g/m^2, apparent density is constant. However, for lower basis weights, apparent density is lower demonstrating the effects of agglomerates and surface non-uniformity fibre clumps which become more

significant as basis weight is decreased. This is also reflected by the non-zero y-intercept in Figure 4.
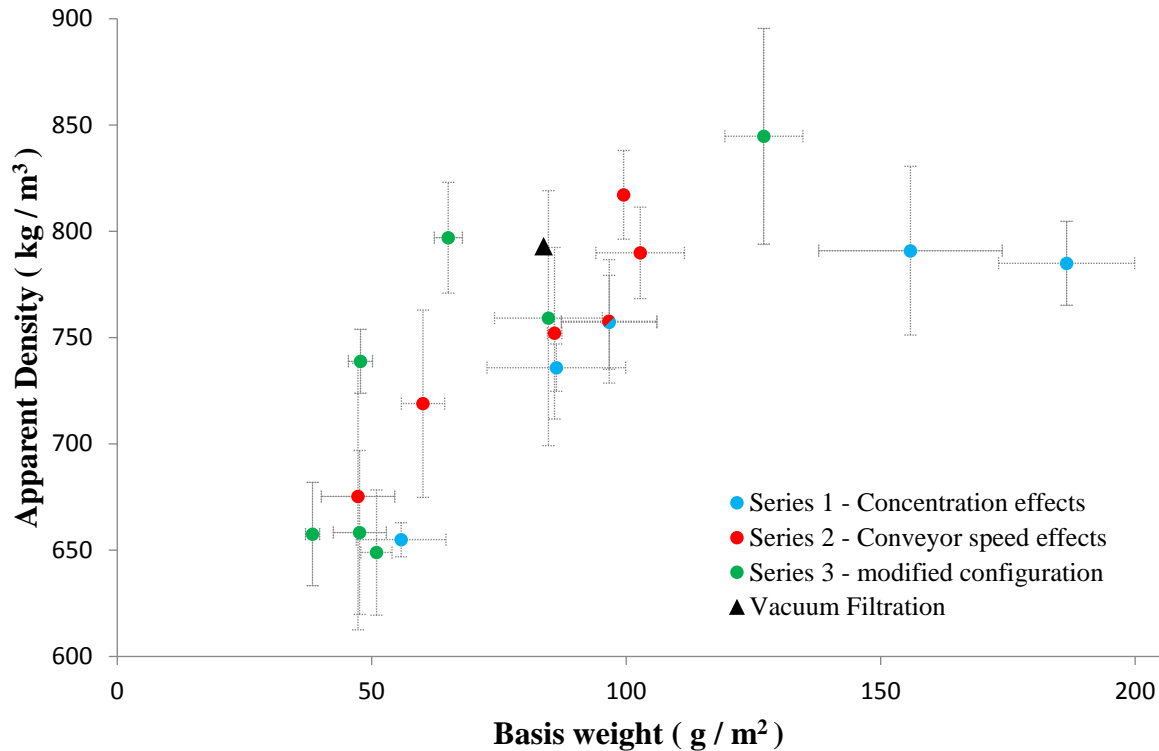

Figure 5 – Relationship between Apparent Density and Basis weight of the films.

The apparent densities of Spray Coated NC film (SC-NC) having basis weight close to 100 g/m^2, (99.5±0.1 g/m^2, 102.7±8.7 g/m^2) are 817.2±20.9 kg/m^3 and 789.9±21.5 kg/m^3 respectively. Measurements for Vaccum Filtered NC films (VF-NC) of 100 g/m^2 were found to be 822.5±14.6 kg/m^3, within the same range and comparable to SC-NC considering the uncertainties.

3.5.1. OPTICAL UNIFORMITY

Within the operational range of the conveyor and spray system, the effects of both velocity and suspension concentration were studied. These parameters were found to distinctly affect the optical uniformity of the films obtained. The optical uniformity of nanocellulose films were quantified at different length scales and analysed with the relative

values defined using one of the VF-NC films as a reference. To simplify the presentation, the results are presented as firstly the average of all inspection zone sizes smaller than 1.8mm and secondly of all inspection zone sizes between 1.8 and 12 mm. It should be noted that some spray coated films contain air bubbles and visible ripples, as can be observed in Figure 10 and 11. These reduce the measured optical uniformity, although the contribution of bubbles and ripples, in comparison to flocculation driven non-uniformity, is hard to quantify. Our major interest here is to use the measurement to identify the experimental conditions where the optical uniformity is equivalent to or better than the films formed through vacuum filtration. The uniformity of the smaller components of formation of the film tends to strongly influence the print quality while larger components of the film influence its strength.

Figure 6 and Figure 7 show the optical uniformity of SC-NC films, at large and small inspection zones, respectively, as a function of conveyor velocity at 1.5 wt. % suspension concentration. Detailed graphs can be found in the supplementary information.
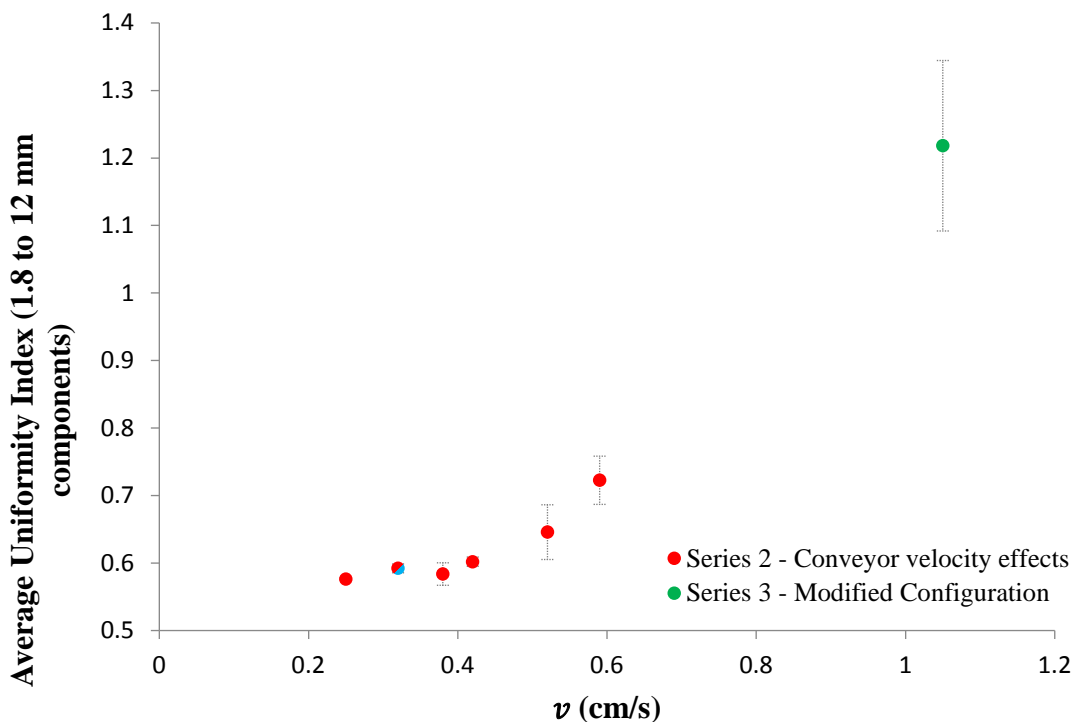

Figure 6 – Average Optical Uniformity Index of larger components (1.8mm to 12mm) as a function of conveyor velocity with vacuum filtered film as a reference
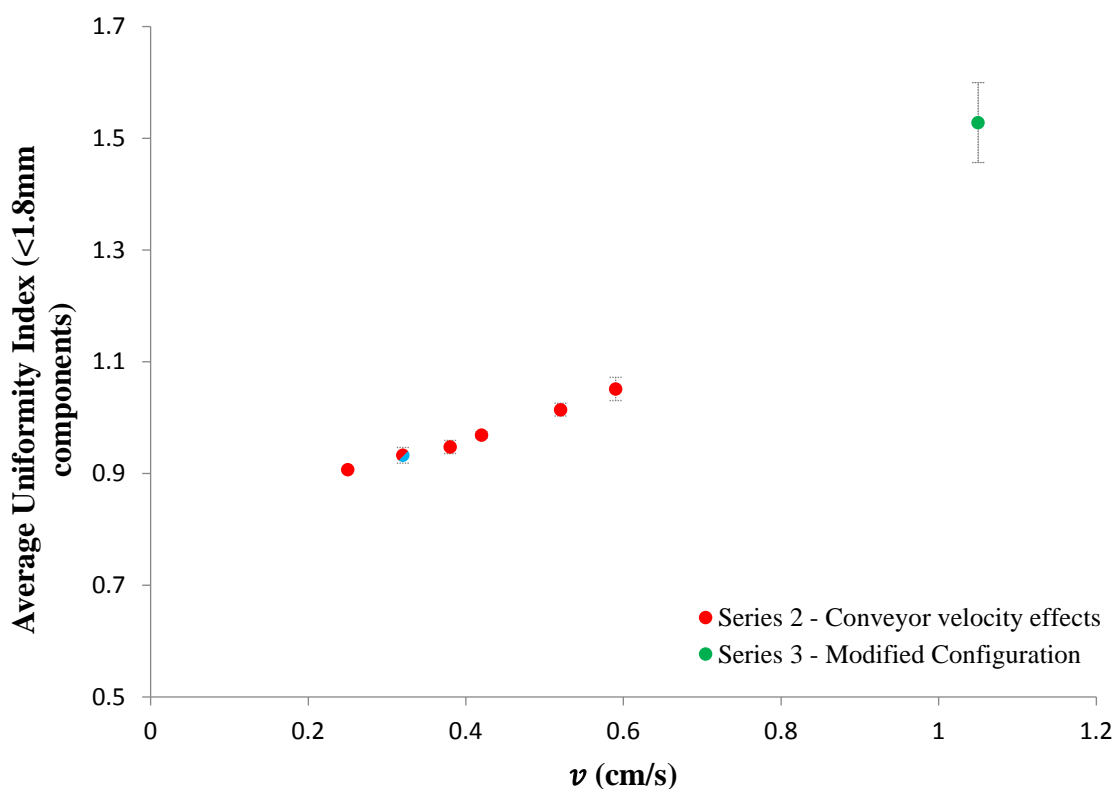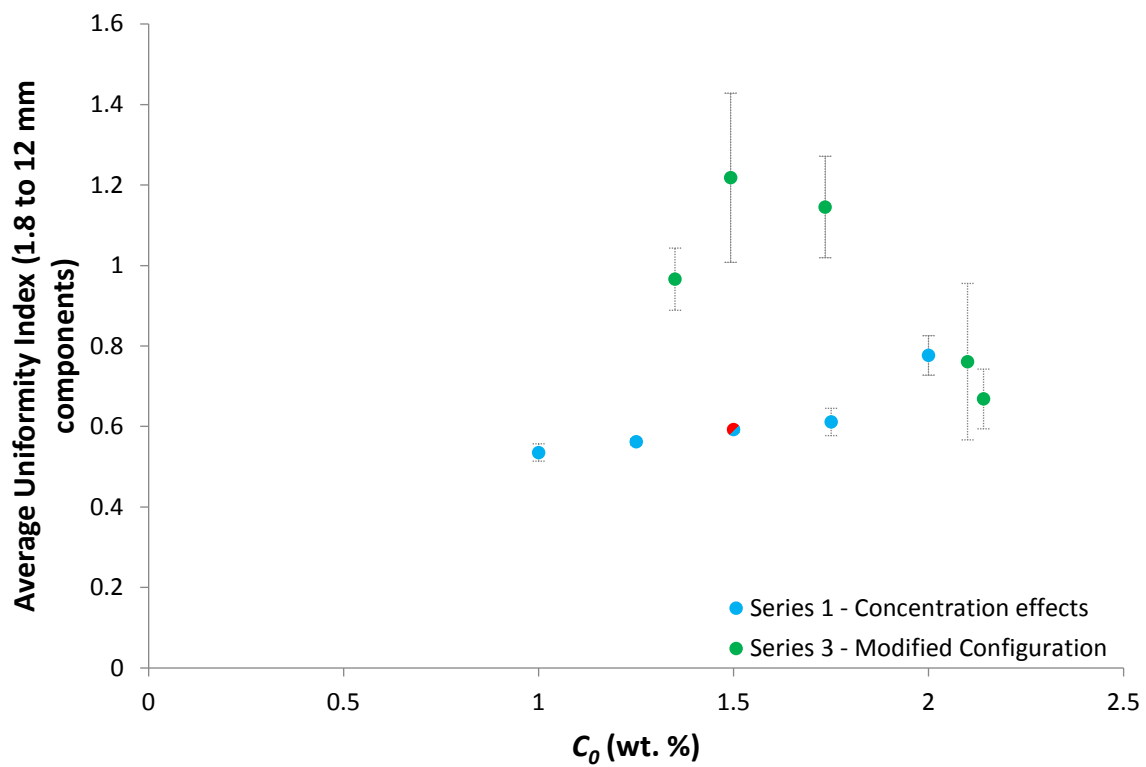
Figure 7 – Average Optical Uniformity Index of smaller components (<1.8mm) as a function of conveyor velocity with vacuum filtered film as a reference

The results show that as conveyor velocity increases, the films obtained are more uniform in both larger and smaller component sizes. The relative optical uniformity of all SC-NC is higher for smaller components than for larger components.

Figure 8 and Figure 9 show the optical uniformity of SC-NC films as a function of suspension concentration at their respective constant velocities (0.32m/s for series 2 and 1.05cm/s for series 3), detailed graphs can be found in the supplementary information.

Figure 8 - Average Optical Uniformity Index of larger components (1.8mm to 12mm) as a function of suspension concentration with vacuum filtered film as a reference
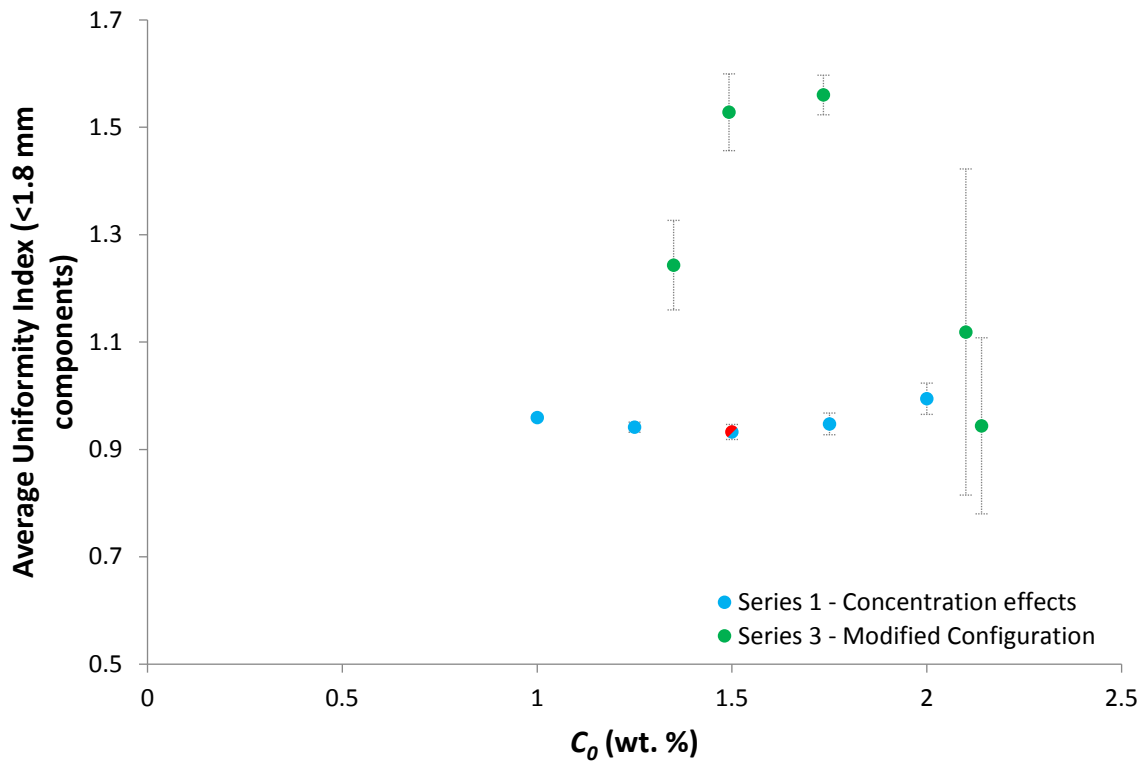
Figure 9 - Average Optical Uniformity Index of smaller components (<1.8mm) as a function of suspension concentration with vacuum filtered film as a reference

With increasing suspension concentration, an increased amount of agglomerated fibres is expected which would lead to lower optical uniformity. However, a thicker film with higher basis weight is obtained at higher concentrations leading to more overlapped fibres and higher optical uniformity. This compound effect determines the variation in optical uniformity as a function of concentration. Figure 8 shows that at a constant velocity of 0.32 cm/s, higher optical uniformity in larger components is observed with increasing suspension concentration. This trend seems to be less pronounced for smaller components in Figure 9.

One of the vacuum filtered NC films was used as a reference for all the Paper Perfect Formation comparisons and all data were normalised by the reference film value at each length scale. The values for the vacuum filtered films in Figures 6-9 are all close to but not equal to 1.0 as the complete set of data for all vacuum filtered films was averaged, including the one reference NC film.

Results for series 3 show no universal trend in optical uniformity with the change of concentration, however, it is noteworthy that these films made at an increased velocity of 1.05 cm/s show higher uniformities in general. This was also demonstrated in Figure 6 and Figure 7. It is shown that to attain constant basis weight films, operating at higher velocities and higher suspension concentration creates more uniform films across all component sizes.

With the modified configuration operating at a higher conveyor velocity in series 3, the range of uniformities is as high as and above that of the VF-NC film; the spray coated NC film no longer visually shows the presence of non-uniformities and contains pinholes, whereas these could be observed for series 1 and series 2 experiments.
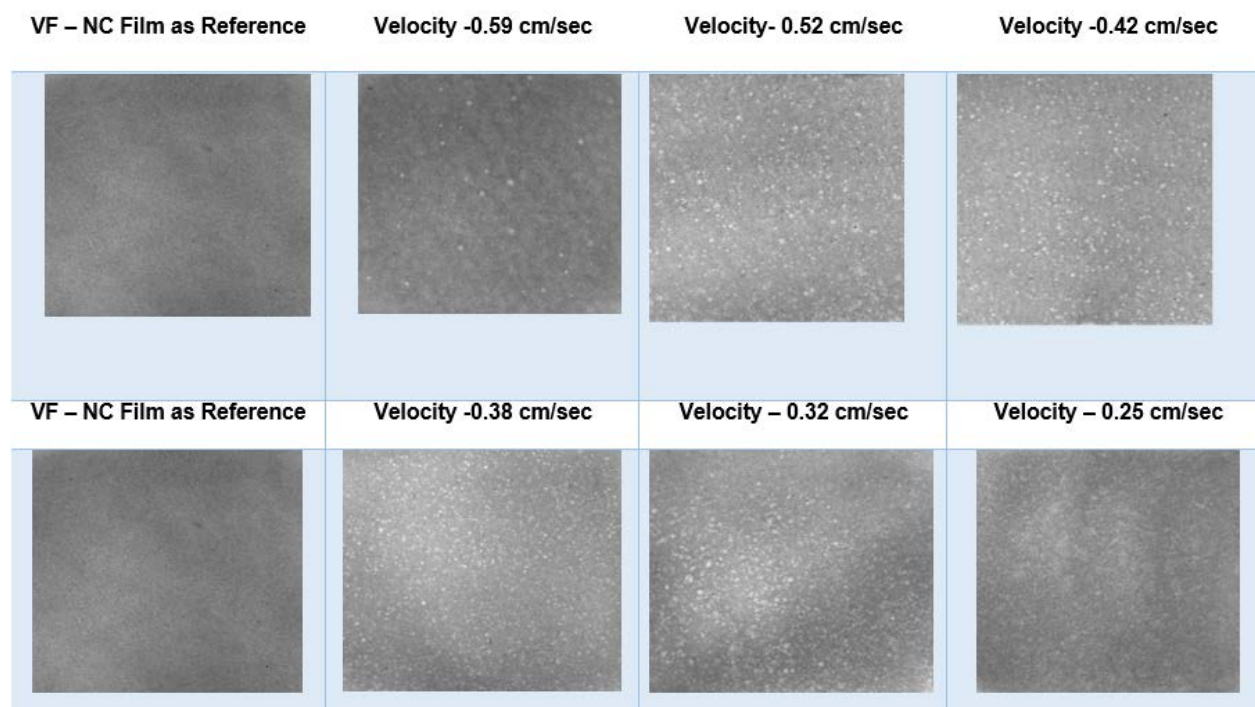

Figure 10 – Paper formation test for Nanocellulose films prepared spray coating at a different velocity (series 2).

Figure 10 and 11 shows the images captured by the Paper Perfect Tester of NC films prepared via spray coating and vacuum filtration. Each image was recorded of an area of 6.75 cm X 6.75 cm. The optical uniformity of formed NC film worsened upon decreasing suspension concentration and the velocity of the conveyor, especially at larger components around 5mm.

Additionally, the 1 wt. % NC spray coated film has ripples in the film while the surface of the film remains smooth. The ripples are formed by the transverse flow of the 1 wt. % suspension NC on the stainless steel plate after the spray impacts the surface. This problem was overcome by increasing the suspension concentration.
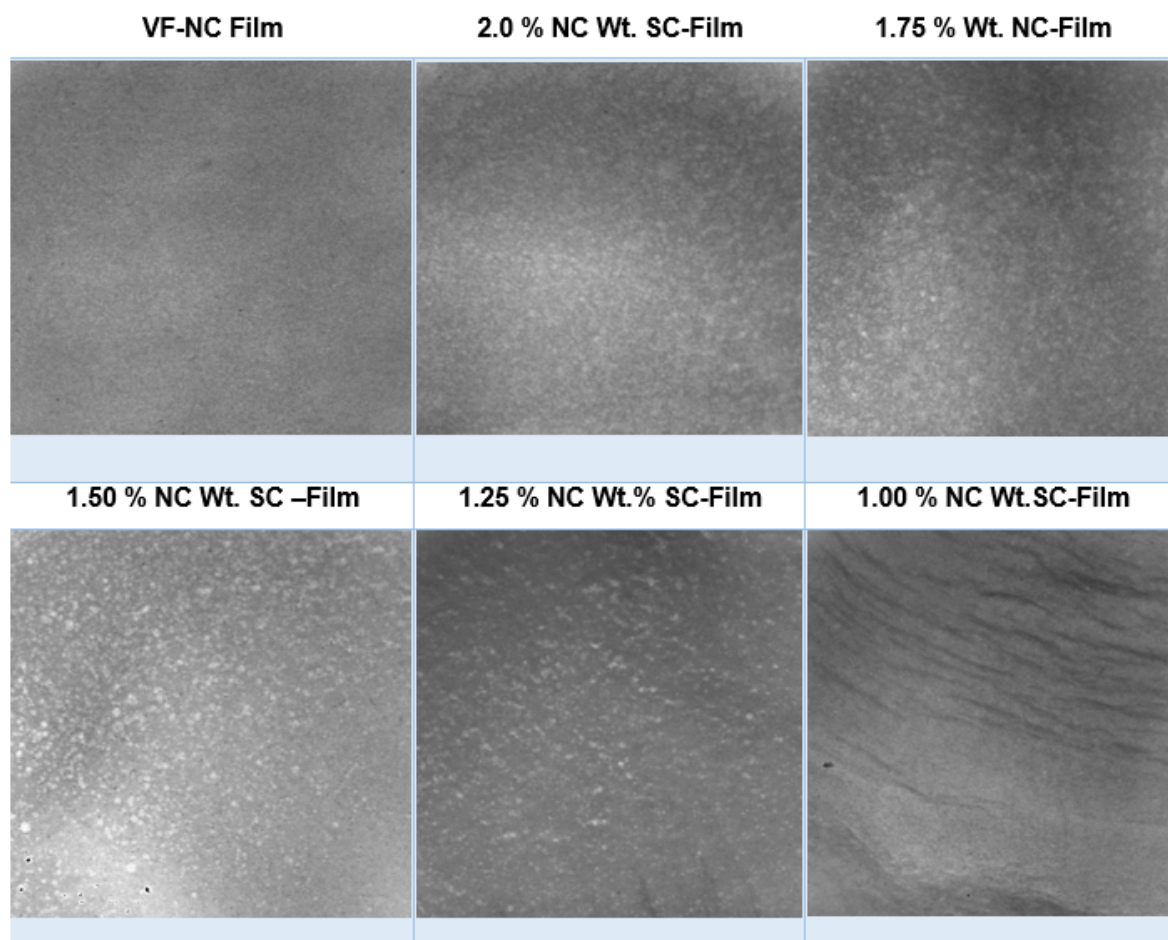

Figure 11 –Paper formation test for NC –Film Prepared via spraying different NC Concentration (Series 1)

It can also be seen that apart from the ripples at low solids concentration, there is no evidence of fluid flow during the forming process, even though the plateau in film basis weight with decreasing velocity, shown in Figure 2, strongly suggests that such flow must be occurring. As we previously mentioned, the most likely explanation for the apparent discrepancy is that the fluid film on the plate has levelled while the plate is held stationary during drying.

VF-NC Film   1.75 wt. % SC- NC Film 1   1.72 wt. % SC-NC Film 2
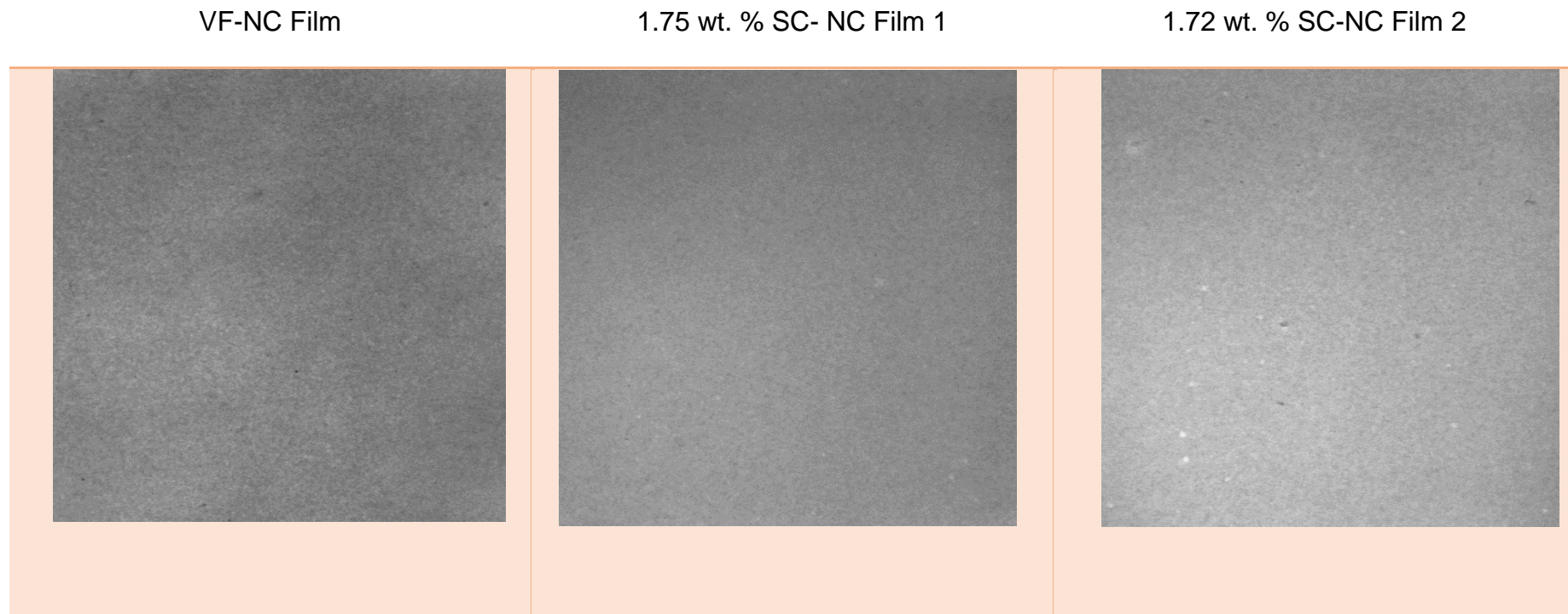

Figure 12 – Paper formation test for Spray coated NC Film prepared via Modified Configuration (Series 3).

Figure 12 shows the spray coated film prepared via modified configuration and the films are free from glossy points and surface irregularities. Figure 1, 2, and 3 in the supplementary information reveal the relative formation value of each component of spray coated NC films prepared via adjusting NC concentration and velocity of the conveyor and related to the NC film prepared via vacuum filtration. RFV value of NC film from series 1 is mostly lower than 1 and the NC film made 1.75 wt. % is higher than 1 confirming good optical uniformity and formation quality in the film.

3.5.2. MECHANICAL PROPERTIES

The mechanical properties of NC films were investigated by tensile strength testing. Fig 13 shows the tensile index of SC-NC as a function of basis weight and error bars concluding the standard deviation of six films. The actual Load Vs Strain curves of the spray coated films are available in the supplementary information. It can be seen that there is some indication that for series 2, a higher tensile index of a film is associated with a higher basis weight. However, considering standard deviation of measurements, no statistically meaningful difference can be inferred between series 1 and series 2. It can be seen that the SC-NC films from series 3, using the higher spraying efficiency configuration, show somewhat higher tensile strengths, with values equivalent to VF-NC. This is probably due to the higher optical uniformity of these films compared to the series 1 and series 2 films.

Higher basis weight films are significantly more rigid. This was investigated by evaluating the relationships between stress and strain, represented in Figure 14 as Elasticity (E-modulus). The relationship between the E-modulus and basis weight was found to be linear over the basis weight range investigated.
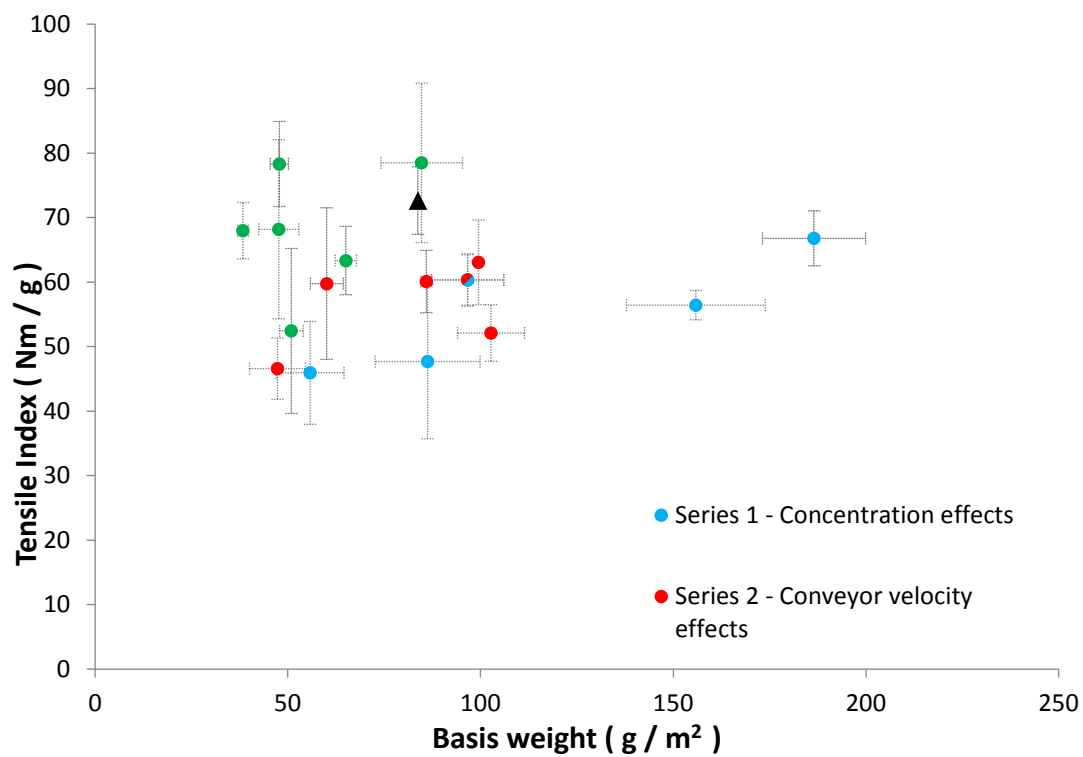
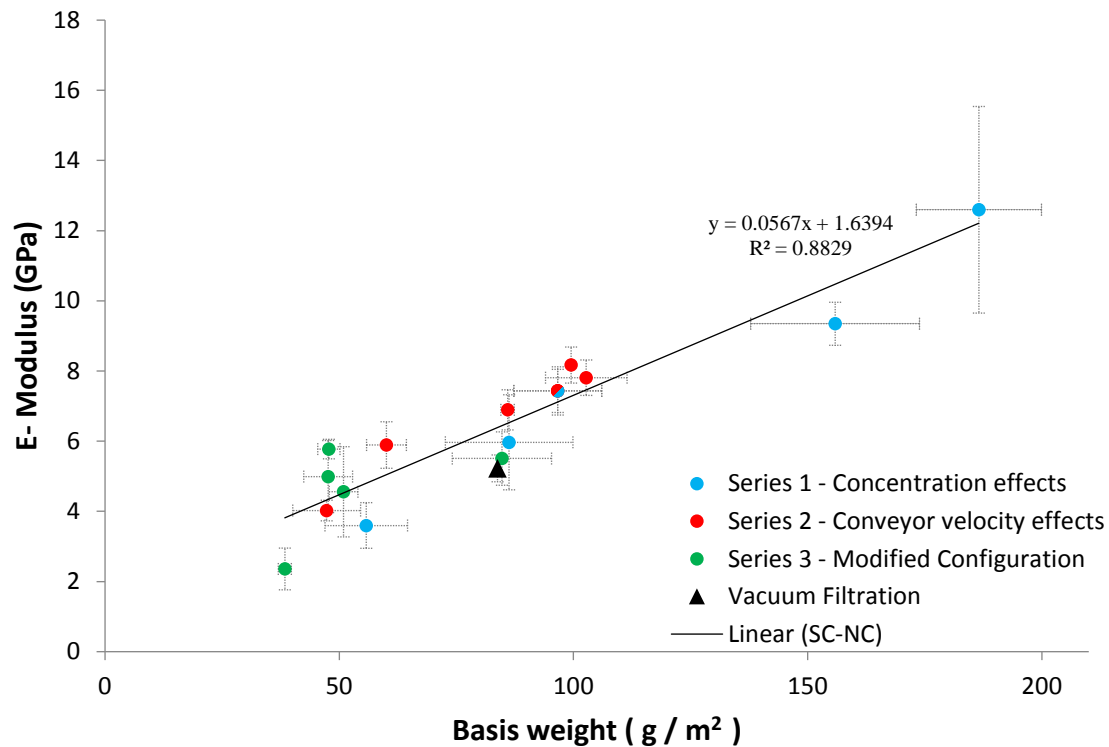Figure 13 - Tensile Index of NC films as a function of basis weight.

Figure 14 – Elastic modulus of NC films as a function of basis weight

Figure 14 shows the elastic modulus of NC films against its basis weight, showing a linear increase with increasing basis weight. The E-modulus of the 83.8 g/m² VF-NC film is 5.22±0.38 GPa, which is slightly lower than that of SC-NC films of similar basis weight. One effect that is certainly contributing to this result is that Figure 5 shows that film density increases with the basis weight rising from 650 to 850 kg/m³ as basis weight increases. This increase in density will reduce the cross-sectional area for a given basis weight, thus increasing strength, even if the breaking load has not changed. The second effect that may be important is that a denser fibre network will produce a higher number of fibre-fibre bonds, which for films from conventional cellulose fibres from wood has been theoretically and experimentally established to increase elastic modulus due to an improvement in the stress transfer efficiency in the network [16]. To clarify the effects of density, the data in Figure 14 has been recalculated as the tensile stiffness index which is independent of thickness and has been plotted against film density and added as Figure 9 in the supplementary information.

Figure 15 shows the SEM images of the NC films surfaces. It can be seen that the rough side of spray coated NC film is more porous than that of smooth side. Additionally, the spray coated NC film are of similar roughness to vacuum filtered films on the air side, while being much smoother on the spray coated side. The surface roughness of 100.5±3.4 g/m^2 and 95.2±5.2 g/m^2 NC film measured via Parker surface instrument reveals 10.7±0.4μm on the rough side and 6.1±1.8μm on smooth side (95% confidence interval) for the spray coated (series 1 condition) compared with 10.67±0.3 μm on filter side and 9.88±0.15 μm on the free side of the vacuum filtered NC film.

Figure 16 and 17 shows the optical profilometry images of both surfaces of spray coated (100.5±3.4 g/m^2 via series 1) and vacuum filtered (95.2±5.2 g/m^2) NC films. The nanoscale RMS surface roughness of the spray coated NC film evaluated via an optical profiler (20 X magnification with an inspection area of 235 μm x 310 μm is 2371 nm on the rough side and 682 nm on a smooth side. The smooth side roughness is much lower compared with the vacuum filtered film, where the roughness at filter side and free sides are 2877 nm and 4253 nm respectively.

We previously reported AFM measurements of the spray coated (100.5±3.4 g/m^2 via series 1) NC film showed a RMS surface roughness of 414.0 nm for 10μm x10μm film area and 51.4 nm for 2μm x 2μm film area on the rough side. This compared with a RMS roughness of only 81.1 nm for 10μm x10μm film area and 16.7 nm for 2μm x 2μm film area on the spray coated side. When compared with the vacuum filtered 95.2±5.2 g/m^2 NC film, the sides had a surface roughness of 417.7nm (Filter side) and 330.8 nm (air side) at an inspection area of 10μm x10μm, which is approximately the same as the rough side of the film prepared by spray coating [14].

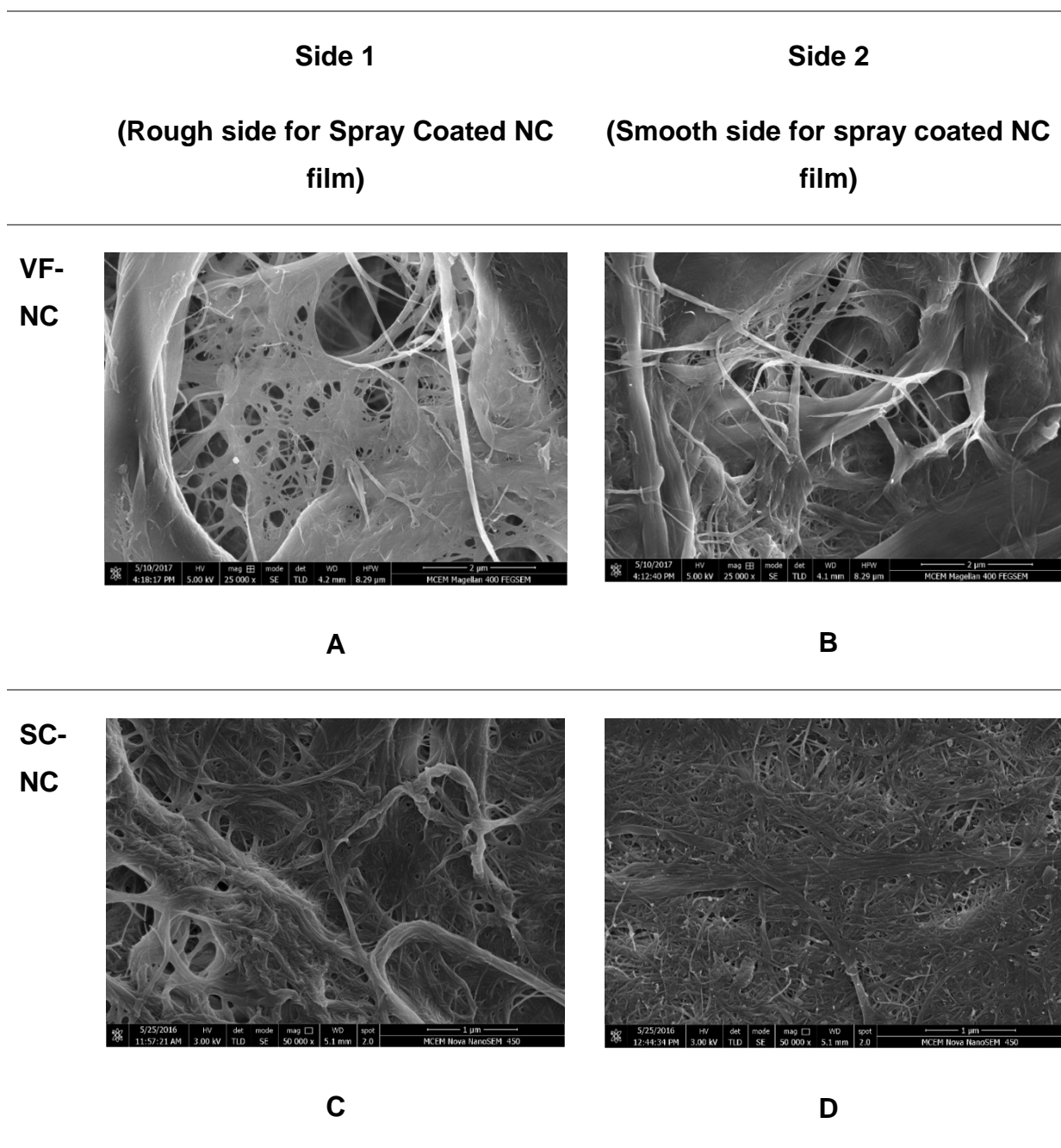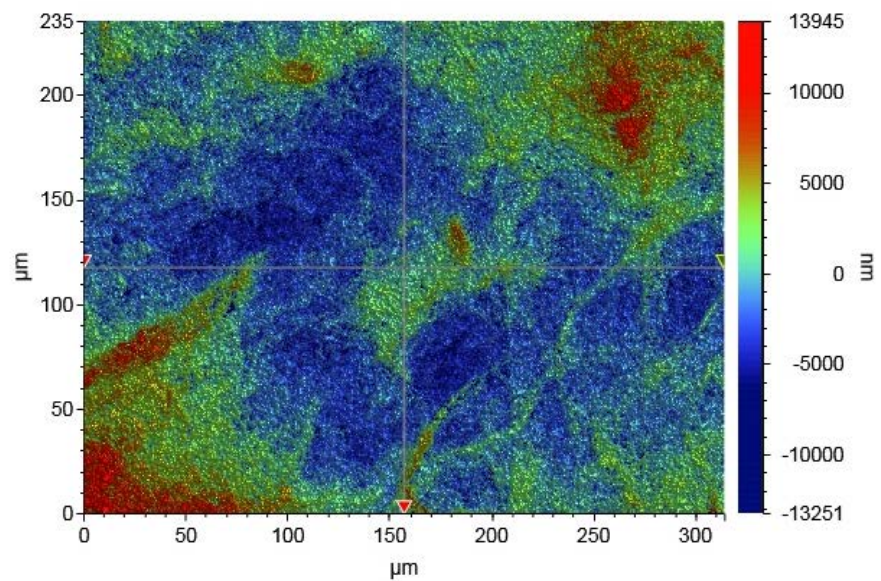|	**Side 1**	**Side 2**
	(Rough side for Spray Coated NC film)	**(Smooth side for spray coated NC film)**
VF-NC		
	A	**B**
SC-NC		
	C	**D**

Figure 15 – SEM micrographs of (A, B) two sides of VF-NC films, (C) the rough side of SC-NC film and (D) smooth side of SC-NC film.
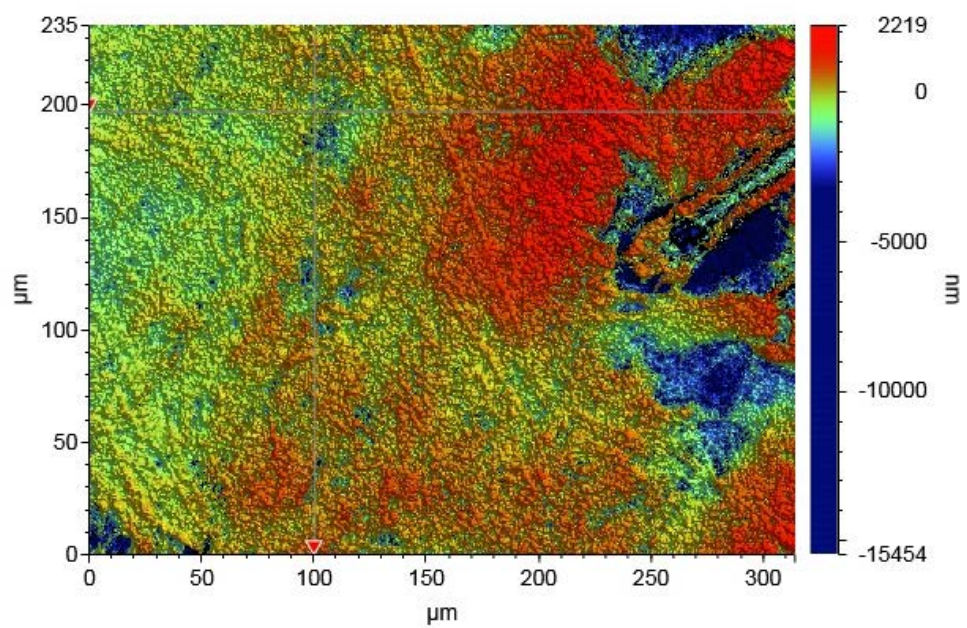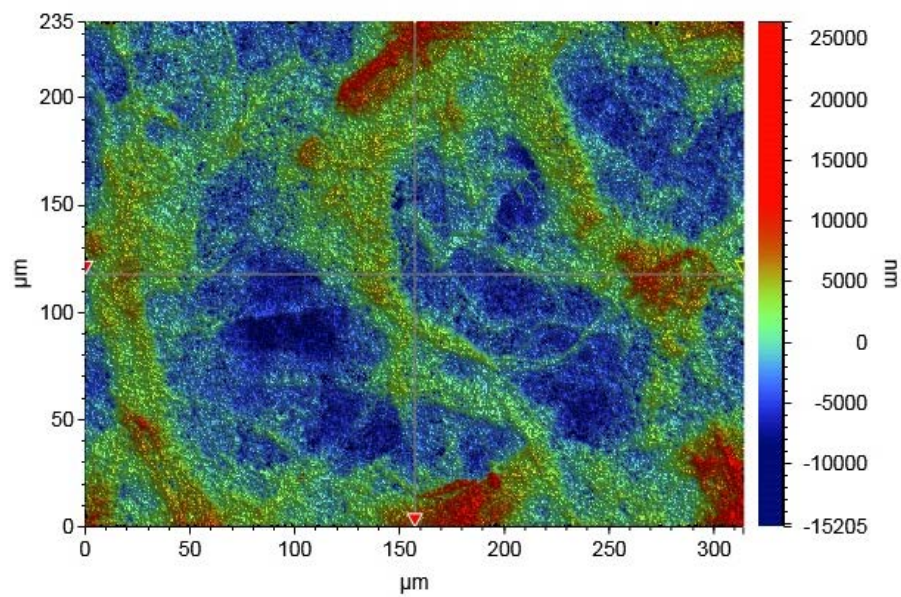
Rough

Smooth

Figure 16 – Optical Profilometry Images of Both Surface of Spray coated NC Film -20 x magnification
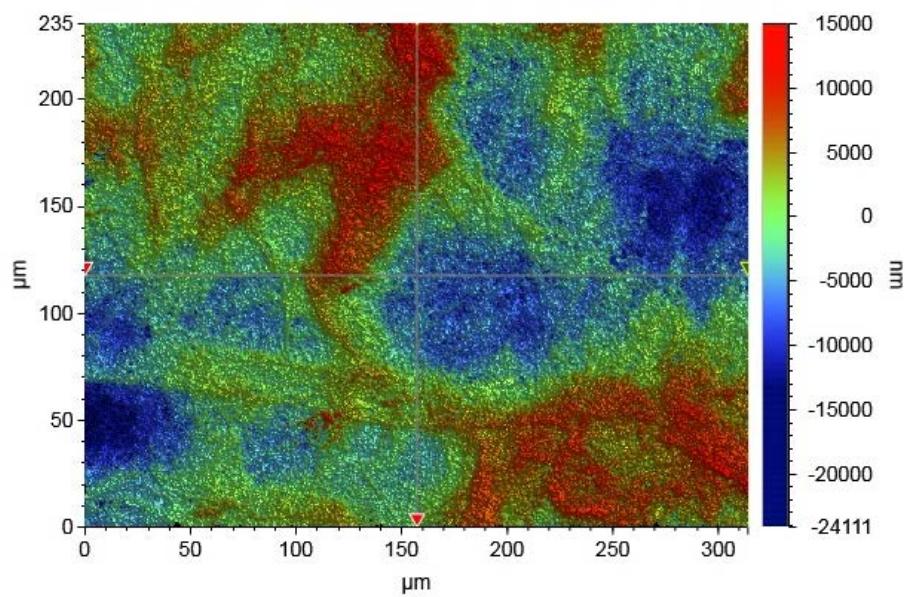
Side 1

Side 2

Figure 17 – Optical Profilometry Images of Both Surface of Vacuum Filtered NC Film- 20X Magnification.

3.6. DISCUSSION

Spray coating has been proven to be a rapid and scalable method for the preparation of NC films, rendering it an exciting alternative for vacuum filtration which has many limitations [14]. To fully understand this process and allow for its implementation, a deeper understanding of the process parameters and properties of spray coated NC film was required, which this research addresses. Various combinations of conveyor velocity and suspension concentration can be used to produce the film with a given basis weight. Film density and E- Modulus were shown to be linearly related to basis weight of the film, but it was not possible to control film density and E- Modulus independently of each other. It was shown that thickness and basis weight are linearly related, independent of the process (whether vacuum filtration or spray coating) or experimental setup. Spray coating produced NC films with very reproducible thickness and basis weight between films, as shown in Figure 05. Our previous publication also showed good thickness uniformity within the films, demonstrating the suitability of the spraying process as an alternative to vacuum filtration [14].

Certain properties of NC films, including printability and strength, are strongly interlinked to the optical uniformity of the NC film [8]. The optical uniformity of the films was evaluated with a PPF tester, which evaluates the NC film over a range of length scales from 0.5 mm to 39 mm reporting a formation values as a ratio to the reference film which was film prepared via vacuum filtration.The optical uniformity of spray coated NC films were shown to be adjustable via changing NC concentration and varying velocity of the conveyor. It was found that increasing suspension concentration and conveyor velocity both increase the optical uniformity within different ranges of component size and that under optimal conditions, the optical uniformity of the spray-coated films was comparable to the reference NC film produced by vacuum filtration. It is noteworthy that with increased conveyor velocity, the operating time is also proportionally decreased.

The most uniform NC films were prepared by spray coating at the highest velocity of 1.05 cm/s using the modified setup. The images are shown in Figure 12. Figure 16 shows that its optical uniformity evaluated by the PPF is better than the vacuum filtered NC films at both small and large inspection sizes.

In comparison to vacuum filtration, spraying of NC suspension produced films of similar density and mostly lower tensile strength and elasticity. The process setup was shown to have an effect on these properties, correlating lower tensile strength and elasticity with a lower apparent density for series 1 and 2.

A change of nozzle, optimized setup configuration and operation at a decreased pressure in series 3 resulted in a slight increase in the apparent density and an increase in the tensile index of the films to be approximately equal to that produced by vacuum filtration. Notably, the optical uniformity of NC film via modified configuration is actually better than the reference NC film via vacuum filtration. This indicates a change in the formation of a wet film on the stainless steel plate resulting in a more compact structure. It should also be noted that with the optimized configuration, waste was decreased allowing for higher throughput and rapid production of films.

Previous data on spray coating of NC on nylon fabric [12], showed the tensile index of spray coated NC film ranging from 45 to 104 Nm/g, within the range of the data reported here. However, these literature values are reported for homogenized NC which show better fibrillation potentially leading to an increase in mechanical strength [17].

The strength of the spray coated NC film could be tailored by adjusting NC concentration or varying the velocity of the conveyor. In the case of vacuum filtration, the forming of film with high basis weight requires high dewatering time and tailoring film properties is a challenging task.

3.7. CONCLUSION

Spray coating, a rapid method to produce a strong, dense and robust NC films was examined in depth and process parameters were studied. Basis weight of NC films can be easily tailored with combinations of conveyor velocity and suspension concentration. The strength of the spray coated NC film is up to 45% lower than the strength of NC film via vacuum filtration and the optical uniformity of the spray coated film could be controlled by the adjusting the process setup. Under optimum conditions, both measured optical uniformity and strength were comparable to films prepared by vacuum filtration. The results confirm spraying to be a

suitable alternative for fabricating NC films, allowing for high throughput mass production and the tailoring of properties for desired characteristics or applications.

3.8. ACKNOWLEDGEMENTS

3.9. REFERENCE

1.   Abitbol, T., A. Rivkin, Y. Cao, Y. Nevo, E. Abraham, T. Ben-Shalom, S. Lapidot, and O. Shoseyov, Nanocellulose, a tiny fiber with huge applications. Current opinion in biotechnology, 2016. **39**: p. 76-88.

2.   Dufresne, A., Nanocellulose: a new ageless bionanomaterial. Materials Today, 2013. **16**(6): p. 220-227.

3.   Klemm, D., F. Kramer, S. Moritz, T. Lindström, M. Ankerfors, D. Gray, and A. Dorris, Nanocelluloses: A New Family of Nature-Based Materials. Angewandte Chemie International Edition, 2011. **50**(24): p. 5438-5466.

4.   Shimizu, M., T. Saito, H. Fukuzumi, and A. Isogai, Hydrophobic, Ductile, and Transparent Nanocellulose Films with Quaternary Alkylammonium Carboxylates on Nanofibril Surfaces. Biomacromolecules, 2014. **15**(11): p. 4320-4325.

5.   Rebouillat, S. and F. Pla, State of the Art Manufacturing and Engineering of Nanocellulose: A Review of Available Data and Industrial Applications. Journal of Biomaterials and Nanobiotechnology, 2013. **Vol.04No.02**: p. 24.

6.   Sehaqui, H., A. Liu, Q. Zhou, and L.A. Berglund, Fast preparation procedure for large, flat cellulose and cellulose/inorganic nanopaper structures. Biomacromolecules, 2010. **11**(9): p. 2195-2198.

7.   Siró, I. and D. Plackett, Microfibrillated cellulose and new nanocomposite materials: a review. Cellulose, 2010. **17**(3): p. 459-494.

8.   Varanasi, S. and W. Batchelor, Superior non-woven sheet forming characteristics of low-density cationic polymer-cellulose nanofibre colloids. Cellulose, 2014. **21**(5): p. 3541-3550.

9.   Nogi, M., S. Iwamoto, A.N. Nakagaito, and H. Yano, Optically Transparent Nanofiber Paper. Advanced Materials, 2009. **21**(16): p. 1595-1598.

10.   Varanasi, S. and W.J. Batchelor, Rapid preparation of cellulose nanofibre sheet. Cellulose, 2013. **20**(1): p. 211-215.

11.   Zhang, L., W. Batchelor, S. Varanasi, T. Tsuzuki, and X. Wang, Effect of cellulose nanofiber dimensions on sheet forming through filtration. Cellulose, 2012. **19**(2): p. 561-574.

12. Beneventi, D., E. Zeno, and D. Chaussy, Rapid nanopaper production by spray deposition of concentrated microfibrillated cellulose slurries. Industrial Crops and Products, 2015. **72**: p. 200-205.

13. Beneventi, D., D. Chaussy, D. Curtil, L. Zolin, C. Gerbaldi, and N. Penazzi, Highly Porous Paper Loading with Microfibrillated Cellulose by Spray Coating on Wet Substrates. Industrial & Engineering Chemistry Research, 2014. **53**(27): p. 10982-10989.

14. Shanmugam, K., S. Varanasi, G. Garnier, and W. Batchelor, Rapid preparation of smooth nanocellulose films using spray coating. Cellulose, 2017. **24**(7): p. 2669–2676.

15. Raj, P., A. Mayahi, P. Lahtinen, S. Varanasi, G. Garnier, D. Martin, and W. Batchelor, Gel point as a measure of cellulose nanofibre quality and feedstock development with mechanical energy. Cellulose, 2016. **23**(5): p. 3051-3064.

16. Niskanen, K., Paper Physics, Papermaking Science and Technology Book 16. Fapet Oy, Helsinki, 1998: p. 57.

17. Syverud, K. and P. Stenius, Strength and barrier properties of MFC films. Cellulose, 2008. **16**(1): p. 75-85.

CHAPTER 3

NANOCELLULOSE FILMS AS AIR AND WATER VAPOUR BARRIERS

A RECYCLABLE AND BIODEGRADABLE ALTERNATIVE TO POLYOLEFIN PACKAGING

THIS PAGE HAS BEEN INTENTIONALLY LEFT BLANK

Contents

NANOCELLULOSE FILMS AS AIR AND WATER VAPOUR BARRIERS: A RECYCLABLE AND BIODEGRADABLE ALTERNATIVE TO POLYOLEFIN PACKAGING

Kirubanandan Shanmugam, Hamid Doosthosseini, Swambabu Varanasi, Gil Garnier, Warren Batchelor

Bio resource Processing Research Institute of Australia,

Department of Chemical Engineering, Monash University, Melbourne, Vic 3800, Australia.

Address correspondence to E-mail: warren.batchelor@monash.edu

4.1. GRAPHICAL ABSTRACT

4.2. ABSTRACT

Synthetic polymer packaging is neither reprocessable, renewable nor biodegradable and is difficult to recycle into useful barrier materials. Cellulose fibre based packaging is renewable, easily reprocessable, recyclable and biodegradable, however, it is a poor barrier material both before and after recycling, especially against air and water vapour. Nanocellulose (NC), formed by breaking down cellulose fibres into nanoscale diameter fibres, is a renewable alternative to synthetic polymer packaging barrier layers. This research investigates the recyclability of virgin NC films. Nanocellulose films were recycled and prepared into films, using standard dispersion-based laboratory papermaking techniques through mixing and vacuum filtration of the resultant suspension. The recycled films retained ˜70 % of the strength of the virgin films. Although the water vapour permeability (WVP) approximately doubled, increasing to 1.29 x 10^{-10} $g.m^{-1}.s^{-1}$ Pa^{-1}, it is still comparable to synthetic polymer packaging materials such as Polyethylene(PE), Plasticized PVC, Oriented Nylon 6 and Polystyrene (PS). SEM micrographs reveal no fibre agglomeration and no damage to the fibres during the recycling process. The optical uniformity measurements of recycled NC film confirms a drop in uniformity of the film at smaller length scales and an increase in uniformity at larger length scales, compared with virgin NC film. The retained strength and barrier properties combined with easy reprocessability of the product promises a sustainable and recyclable alternative to conventional polyolefin packaging, providing a very attractive alternative for the packaging industry.

4.3. KEYWORDS

Nanocellulose; Vaccum Filtration; Recycling; Water vapour permeability; Uniformity; Tensile Index

4.4. INTRODUCTION

The development of sustainable and recyclable barrier materials for packaging is a critical challenge arising from pressing environmental concerns with the widespread use of non-sustainable petroleum-derived polymers in the food, pharmaceutical, electronics and other industries. Sales of packaging materials is forecasted at US$997 billion by 2020 with a market growth of ~3.5% per year [1]. Presently, glass, aluminium, tin and petroleum-based polymers are extensively used as packaging materials. Throughout the industry, polyolefins

have been widely adopted due to their effective barrier properties and simple and cheap processing. Despite these desirable properties, the majority of polyolefin packaging is not re-processable into their original form or into high value products. Petroleum polymers are neither sustainable nor biodegradable; their extensive use has had severe ecological impacts. Consequently, their disposal still raises environmental concerns and recycling requires complex and costly processes. Moreover, the recycle process involving blending the synthetic polymers into a processable melt is very dependent upon the chemical composition and molecular weight of the components; further, volatile organic compounds are emitted which can impact plants, animals and humans. The heat required for thermal recycling of plastics also generates various oxides of carbon that are the most responsible for global warming. Current polyolefin films cannot be reprocessed into the original product, as the recycled product would not yield suitable barrier properties [2-4]. During recycling process, the mixing of different polymers together leads to a reduction in the quality and properties of the recycled plastic. Moreover, chemical compounds from synthetic packaging materials can affect the quality of food when exposed to post-packaging processes [5] and cause food contamination [6, 7].

It is therefore imperative to pursue novel materials for packaging applications to address the ecological and environmental concerns with cost-effective, readily available and sustainable solutions. Bio-based polymers can produce humidity, oxygen and grease barriers for sustainable, biodegradable and compostable packaging [8]. Previously, bio-based materials have been processed into films, significantly enhancing shelf life and quality of foods and reducing waste from packaging. However, such biodegradable polymers have poor barrier performance and are noticeably brittle. As such, complications in processing these materials, such as low heat distortion, render them too expensive for industrial scale use [9].

Cellulose fibre-based packaging materials, such as boxes, cartons and paper are renewable, recyclable and biodegradable but are poor barriers to oxygen and water. Laminating with polymers, such as LDPE, can yield products with sufficient barrier performance, but at the expense of recyclability and biodegradability [4].

One solution to improving the sustainability of paper-polymer laminates is to replace the polyolefin layer with a film of nanocellulose (NC). Nanocellulose is directly produced by defibrillating fibres from pulp and wood into their structural constituent [10]. NC can have widths ranging from 5 - 75 nm and lengths exceeding 5 μm. Nanocellulose fibrils show strong

nanoscale interaction resulting in a high mechanical strength material with high resistance to diffusion. Nanocellulose and its composites were shown to have outstanding barrier properties against oxygen, air and and reasonable barrier properties to water vapour [11]. Nanocellulose can be obtained at low cost from renewable feedstocks, such as wood, rendering it particularly attractive for the development of sustainable barrier materials; the wealth of research on NC has grown exponentially over recent years [12, 13]. Though often hypothesized to be recyclable, the reprocessability of NC films has never been demonstrated.

This objective of this study is to evaluate the reprocessability and full recyclability of virgin NC films into a recycled NC film via vacuum filtration. By evaluating the barrier properties of virgin NC film and the effects of recycling on the barrier performance and strength of NC film, we aim to demonstrate that NC film is easily reprocessable and fully recyclable, and a suitable alternative to conventional packaging materials.

4.5. MATERIALS AND METHODS

The nomenclature for nanocellulose has not been reported consistently in the literature. As well as nanocellulose (NC), it is also called micro-fibrillated cellulose (MFC), cellulose nano-fibrils, cellulose micro-fibrils and nano-fibrillated cellulose (NFC). In this paper, we use NC as the generic term for the cellulose nanomaterials used. The NC used was supplied from DAICEL Chemical Industries Limited (Celish KY-100S) at 25% solids content. DAICEL NC (Celish KY-100S) has cellulose fibrils with an average diameter of ˜ 73 nm with a wide distribution of fibre diameter, a mean length of fibre around 8μm and an average aspect ratio of 142 ± 28 [14]. DAICEL KY-100S is prepared by micro fibrillation of cellulose with high-pressure water. The crystallinity index of DAICEL nanocellulose was measured to be 78% [15]. NC suspensions were prepared using by diluting the original concentration of 25 wt. % to 1.5 wt. % with de-ionized water and disintegrating for 15,000 revolutions at 3000 rpm in a disintegrator.

4.5.1. PREPARATION OF NANOCELLULOSE FILM BY VACUUM FILTRATION

The Virgin NC films were prepared using the conventional vacuum filtration method using British Handsheet Maker (BHM) as reported in the literature [16]. 600 ml of NC suspension with 0.2 wt. % concentration was poured into a cylindrical container having a 150 mesh filter at the bottom and filtered to form a wet film on the mesh. The wet film was carefully

separated using blotting papers and subsequently dried at 105^{0}C in a drum drier for around 10 minutes.

4.5.2. RECYCLING OF NANOCELLULOSE FILM

Recently, a spray coating method to produce NC films on a smooth and polished stainless steel surface was developed and this method is capable of spraying NC suspension with high solids [17]. To make the large quantity of films required for recycling, we prepared 40 films according to this method [17, 18] by spraying onto a smooth stainless steel plate on a moving conveyor at a fixed velocity 0.32 cm/sec using a Professional Wagner spray system (Model number 117) at a pressure of 200 bar. The type 517 spray tip used in spray system produce an elliptical spray jet and the spray jet angle and beam width are 50° and 22.5 cm, respectively. The spray distance is 30.0±1.0 cm from the spray nozzle to the circular steel plate. After spraying, the film on the plate was dried under restraint at the edges for at least 24 hours.

After drying, the nanocellulose films were dispersed and suspended in water following TAPPI standard T205 SP-02, where the films were torn into pieces of 1cm x 1cm dimensions and soaked in de-ionized water for 24 hours. The soaked films were disintegrated for 75,000 revolutions at 3000 rpm in a disintegrator Model MK III C. The obtained suspension was then made into films according to the vacuum filtration method explained above. Figure 1 shows the method of recycling of spray-coated nanocellulose films.
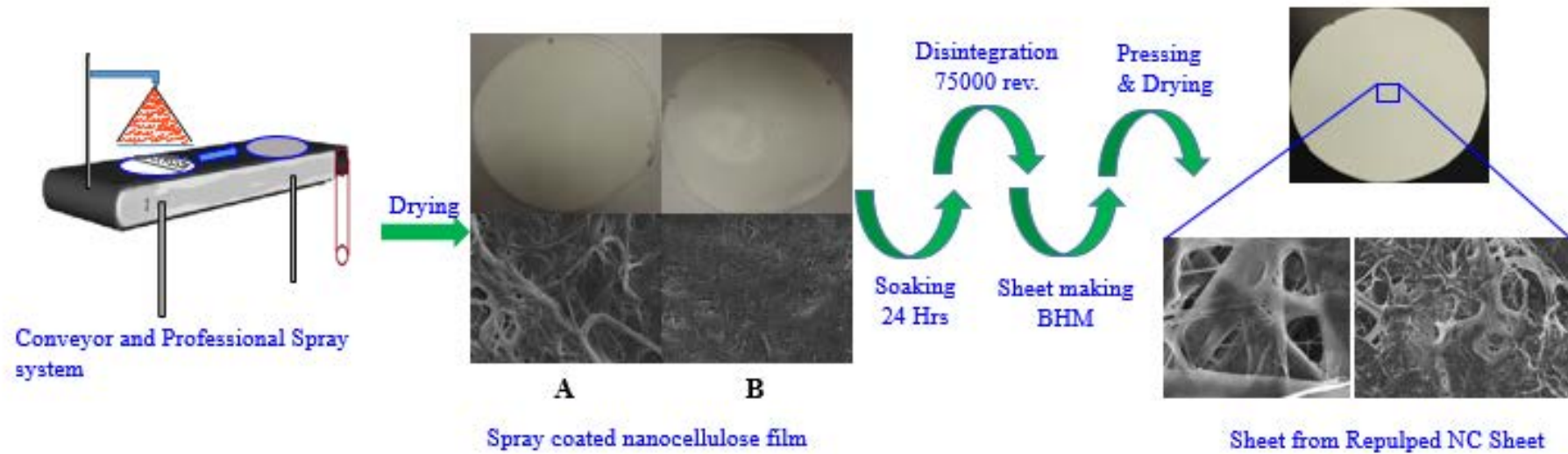
Figure 1 - Method on recyling of spray coated virgin nanocellulose films

4.5.2.1. EVALUATING NC FIBRE DIAMETER

A drop of 0.2 Wt.% of recycled or virgin nanocellulose suspension was cast on the silicon chip and then dried in a controlled laboratory environment. The dried suspension on the silicon chip is coated with iridium layer. Its surface was studied using secondary electron mode-II with FEI Magellan 400 FEGSEM for NC film at a voltage of 5 KV. The micrographs are taken at 1μm and 10μm. The diameter distribution of the raw nanocellulose fibres and recycled NC fibres were measured with Image J. The data are reported average diameter of NC with 95% confidence interval is expressed. The supplementary information gives the micrographs and the diameter distribution histograms of virgin and recycled nanocellulose fibres.

4.5.3. EVALUATING NC FILM PROPERTIES

All prepared virgin and recycled NC films prepared were stored at 23^0C and 50% RH for 24 hours prior to further testing.

4.5.3.1. BASIS WEIGHT

The basis weight (g/m^2) of each nanocellulose film was calculated by dividing the weight of the film, after 4 hours drying in the oven at a temperature of 105 °C, by the film area.

4.5.3.2. THICKNESS OF NC FILMS

The thickness of the virgin and recycled NC films was determined using a Thickness Tester Type 21 from Lorentzen & Wettre AB, Stockholm, Sweden. The thickness of each NC film was evaluated at fifteen points and averaged. The thickness of NC film was measured according to TAPPI T 411, 2015.

4.5.3.3. APPARENT DENSITY

The apparent density of the NC films was evaluated through dividing basis weight by mean thickness of the film.

4.5.3.4. AIR PERMEABILITY

The air permeance of dried NC films was measured with an L&W air permeance tester with an operating range from 0.003 to 100 μm/Pa.S. The mean value of air permeance

evaluated from 3 different areas of each NC film was reported. The Technical Association of the Pulp and Paper Industry (TAPPI) standard T 460 is used to measure the air permeance of the films.

4.5.3.5. WATER VAPOUR PERMEABILITY

Water vapour permeability (WVP) was evaluated according to the American Society of Testing and Materials (ASTM) standard (E96/E96M-05) method using anhydrous Calcium Chloride ($CaCl_2$). In this method, NC film was dried for 24 hours at a temperature of 105 °C in an air oven. ˜40 g of dried anhydrous $CaCl_2$ was added into the cups and covered by the NC films. The increase in weight of the cups is caused by the absorption of water vapour by $CaCl_2$ in the cups through NC film. Test sample was weighed for every standard interval of time. The variation in weight of the cups with time was noted and the WVTR calculated from the slope of the line between weight and time. The water vapour transmission rate were carried out at 23°C and 50 % Relative Humidity (RH). The water vapour transmission rate (WVTR) of NC film are normalised with thickness of the NC film and converted into WVP. The mean value of three replicates of each virgin NC film was reported. The value of four different recycled NC films were reported.

4.5.3.6. FILM UNIFORMITY ANALYSIS

The uniformity of the NC films were evaluated using the Paper Perfect Formation (PPF) Tester (OpTest Equipment Inc, Canada) which measures the optical uniformity of light transmitted through the sample. In brief, the PPF consists of a black and white camera based image analyser and uses a CCD camera interfaced with 256 gray levels, 65 μm/pixel resolution. The analyser uses a diffuse quartz halogen light source with IR filters and automatic intensity control. The PPF classifies formation quality over 10 length scales ranging from 0.5 mm to 60mm. The data reported here is the Relative Formation Value (RFV) of each component relative to one of the films made by vacuum filtration, which was used as a reference film. Three films were measured for each condition, with the results averaged. RFV value less than 1 means that the optical uniformity of the NC film tested is worse than the reference film at that length scale.

4.5.3.7. SURFACE PROPERTIES

The surface roughness of the NC films was evaluated by Parker surface instrument and optical profiler (Bruker Contour GT-I). The raw image from Optical profilometry is processed with the Gwyddion 2.49 software to accurately evaluate RMS of NC film. Surface topography of the film was studied using secondary electron mode-II with FEI Magellan 400 for virgin and recycled NC film.

4.5.3.8. MECHANICAL PROPERTIES

The strength of both virgin and recycled NC films were evaluated by an Instron model 5566 using test specimens of 100 mm length and 15 mm width, conditioned for 24 hours at 23°C and 50% RH before dry tensile testing based on the Australian/New Zealand Standard AS/NZS 1301.448S-2007. All thickness and tensile tests were done at 23°C and 50 % RH. The samples were tested at a constant rate of elongation of 10mm/min. The Tensile Index (TI of the samples was calculated from the tensile strength (expressed in Nm^{-1}) divided by basis weight (gm^{-2}). The mean value was obtained from six to seven valid tests and the error bars in the plots indicate standard deviation.

The zero span tensile index of the films were evaluated with a Pulmac Troubleshooter using six samples 1.5 cm wide and 0.5cm long for each test [19]. In brief , six samples of NC film were required for an individual investigation. A specimen of NC film was placed in the central clamping area of the tester and two other samples were kept under the two back steps of the clamping jaws to ensure proper jaw alignment under pressure. After each test, the samples were removed and replaced. Before the zero-span testing, optimum clamping pressures were determined. An optimum clamping pressure of 70 psi was used for nanocellulose film samples.

4.6. RESULTS

4.6.1. AIR PERMEABILITY

The air permeability of the virgin NC film was less than 0.003 μm/Pa.S, which is the detection limit of the instrument, confirming the film is highly impermeable for packaging application. The air permeance of the recycled NC film was 0.0045 μm/Pa.S, which still provides a good impermeable film for packaging material.

4.6.2. NC FILM DENSITY

The relationship between film density and basis weight is shown in Figure 1, for all the sheets made in this study. The effects of reprocessing can be seen in a change in apparent density as shown in Figure 2. The apparent density of NC films from virgin fibres is higher, demonstrating that a less compact structure is formed after recycling. It is noteworthy that the same process was used to make both the recycled film and virgin film by vacuum filtration, therefore, the decrease in apparent density after recycling is attributed to fibre properties and not to process.
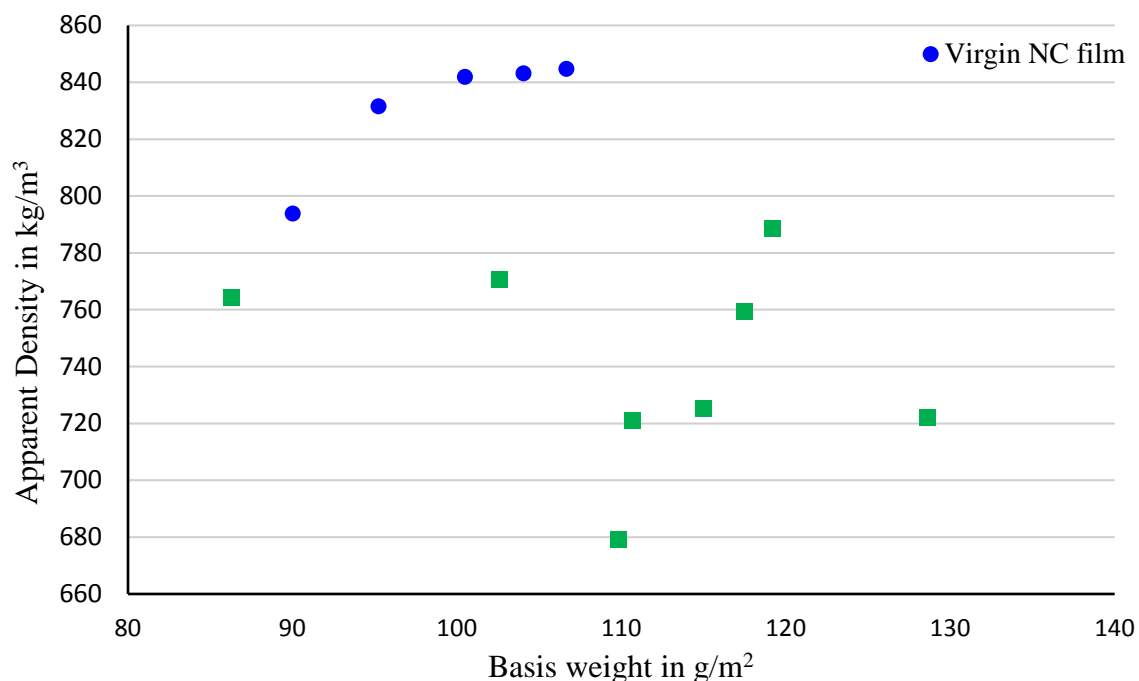

Figure 2: Effect of recycling on the density of the NC films.

The density of the NC film is approximately the same and independent of the NC film basis weight for both the recycled and virgin NC film, but it is statistically lower for the recycled NC film. The reason for the reduced density of recycled NC film is probably the formation of larger aggregates in the nanocellulose fibrous network that has hindered the compaction of the fibre network. As a result, recycled NC films have formed larger pores, which has caused an increase in permeation of water vapour and air through the pores. Drying of recycled cellulose fibres and fibre hornification may also have reduced the fibre swelling capacity and

decreased the conformability of recycled fibres, which will also reduce the compaction of the fibre web as the film forms. This will also reduce the film density.

4.6.3. WATER VAPOUR PERMEABILITY (WVP):

The Water Vapour Permeability (WVP) was measured in triplicate for all samples. The results are compared in Figure 3 as a function of film basis weight. Figure 2 shows that recycled cellulose films show higher WVP than the virgin NC films, with an average increase of approximately 7.5 x10^{-11} g.m^{-1}.s^{-1} Pa^{-1}.
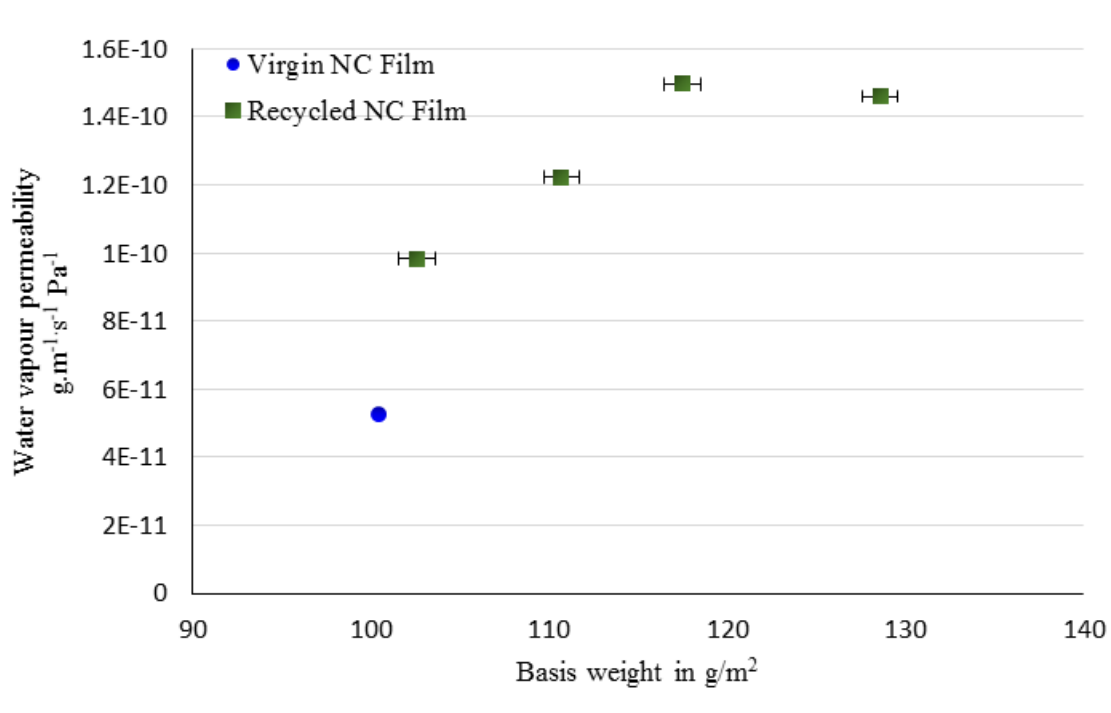

Figure 3: Water Vapour permeability of Virgin and Recycled NC Film against basis weight of the film.

Agglomerates from the incomplete breakdown of recycled films into separated nanofibers, produce non-uniformity in the film and will increase the size of both the surface and bulk pores elevating water vapour permeability and air permeance over than that of virgin NC film. These floc aggregates will also have a poorer bond to the separated cellulose fibrils resulting in a weaker recycled NC film. Additionally, the presence of agglomerates reduces

the total surface area available for bonding thereby limiting film density, uniformity and compactness of the fibril network.

The formation test concludes the good uniformity of recycled NC films compared to the virgin NC film. Figure 4 also interprets that recycled film is less uniform than that of the virgin NC film at lower inspection tiles of 15 mm and more uniform for areas greater than 15 mm.

4.6.5. MECHANICAL PROPERTIES OF THE RECYCLED FILM

The tensile strength of the virgin and recycled NC films was measured at both standard 100 mm test spans, in an Instron, and at zero-span. The zero span tensile index is a measure of the nanofibre film strength over a very short span [19]. Figure 5 showed that the tensile index, at both long and short spans has decreased by 30 % and ˜ 28%, respectively, for the recycled film compared to the virgin film.

A loss in mechanical strength is expected in recycling of conventional cellulose fibres due to poorer hydrogen bonding between fibres and their hornification. The tensile index of the recycled film is affected by weaker inter-fibre bonds due to reduced conformability of the cellulose fibres [20].
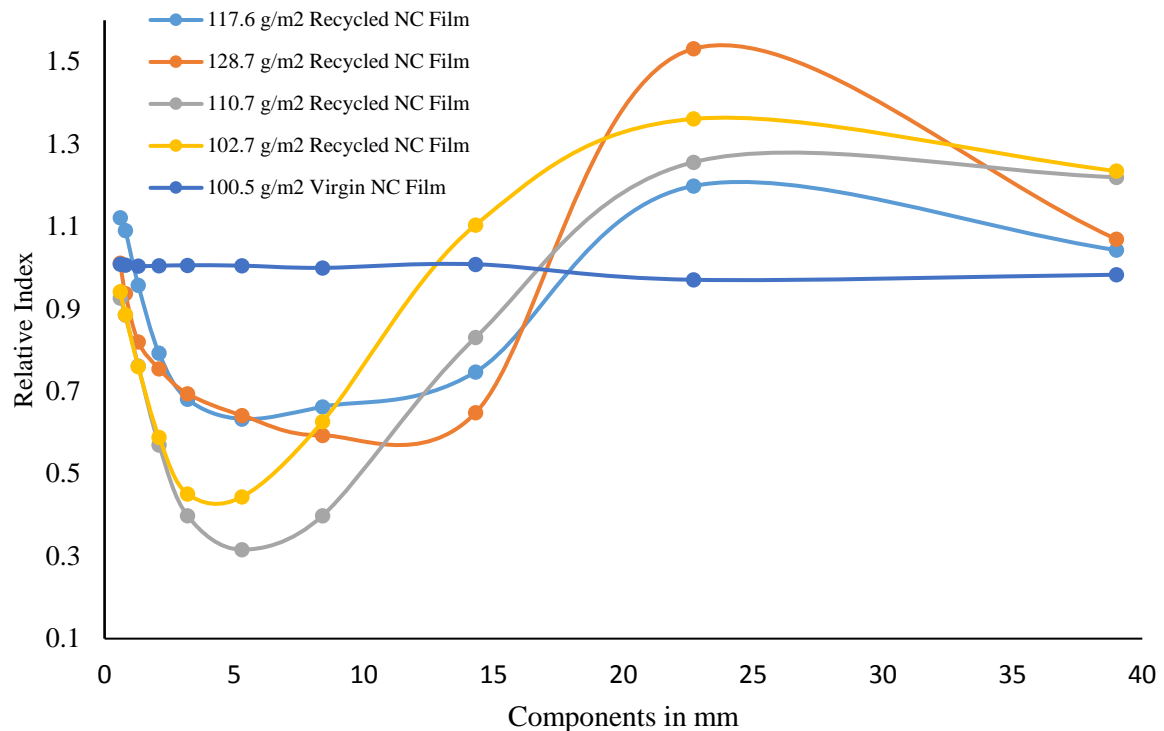
4.6.4. FILM UNIFORMITY ANALYSIS

Figure 4: Formation of Recycled NC film and its comparison with Virgin NC film.

4.6.6. EFFECT OF RECYCLING ON CELLULOSE FIBRILS AND CELLULOSE FILM UNIFORMITY

The effect of recycling on the nanocellulose fibres was evaluated with surface morphology, topography and diameter of the fibres measured with SEM micrographs. Figure 6 shows SEM micrographs of the NC fibres before and after recycling, showing a wide distribution of fibre size in each sample. The average diameter of the nanocellulose was 69.8± 11.3 nm before recycling and 69.6± 12.6 nm after, showing no evidence of agglomeration at lower inspection area. SEM micrographs in Figure 5 show a more compact structure after recycling, but no increase in average fibre diameter.
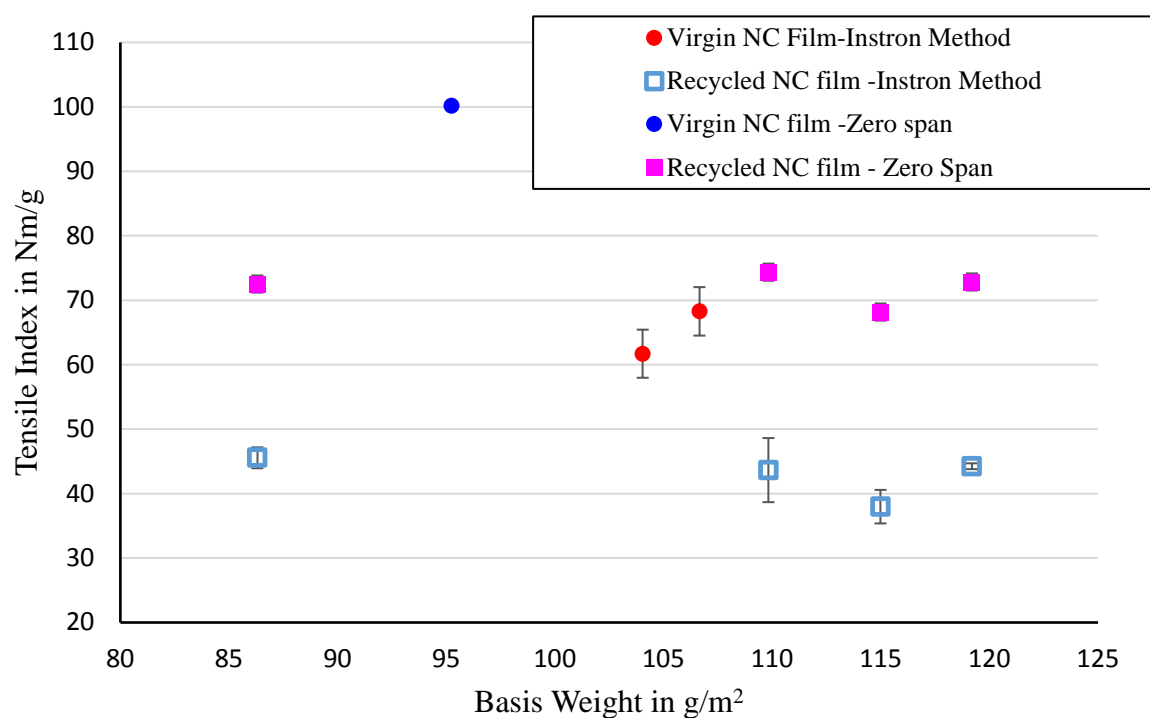
Figure 5:   Effect of basis weight and preparation process on Tensile Index and Zero Span Tensile Index of NC Film via Vacuum Filtration and recycled film.

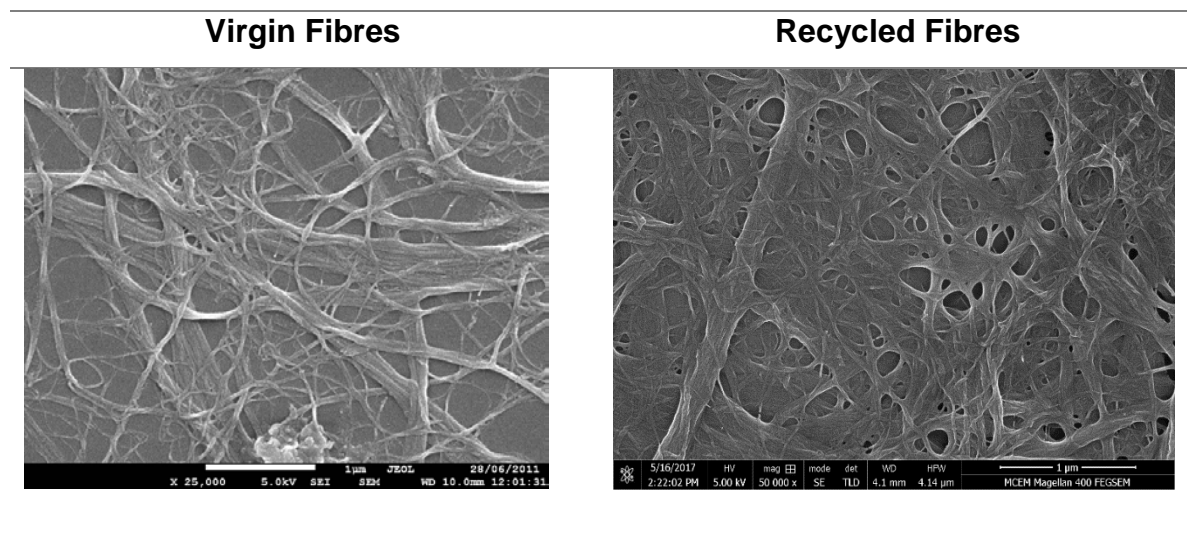| Virgin Fibres	Recycled Fibres

Figure 6: Scanning Electron Micrograph of nanocellulose before and after recycling.

The surface topography and morphology of recycled films were evaluated by SEM micrographs and compared with virgin NC films in Figure 7. The recycled films retained fibre

morphology and topography, showing no significant damage to fibres. Cellulose fibrils were randomly distributed and orientated. In the recycled film, some larger pores were observed and might be a reason for elevating air permeance and water vapour transmission. The additional micrographs of both virgin and recycled NC fibres and NC film from virgin and recycled NC fibres from 1 to 100 µm are in the supplementary information.

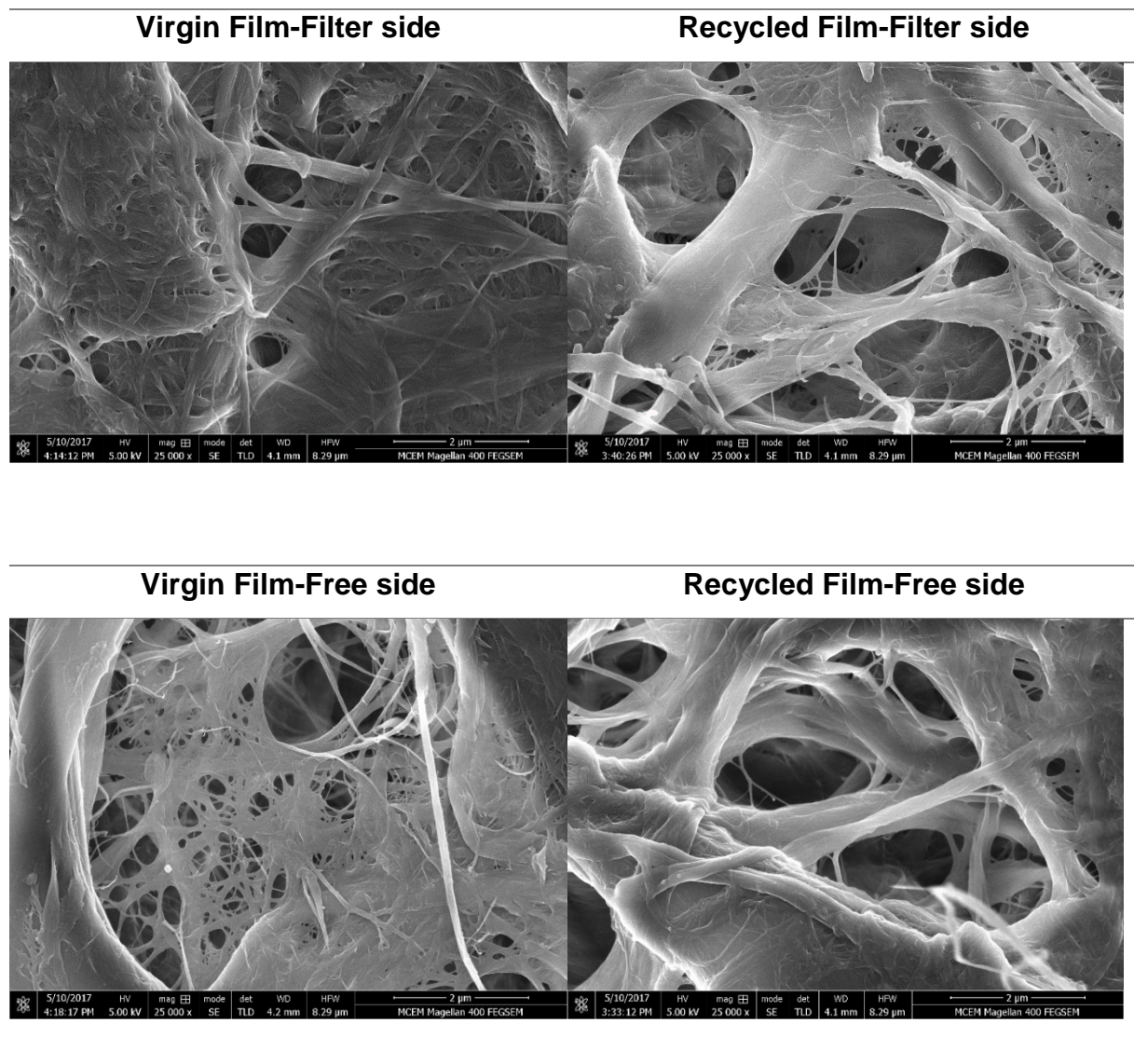**Virgin Film-Filter side**   **Recycled Film-Filter side**

Virgin Film-Free side   **Recycled Film-Free side**

Figure 7: SEM Micrographs of Virgin and Recycled NC films 1µm and 2µm scale bar.

4.6.7. SURFACE ROUGHNESS INVESTIGATION

Figure 8 shows the surface roughness of the recycled and virgin NC films measured using optical profilometry. For an inspection area of 125.7μm x 94.2μm, the RMS roughness of the recycled film was found to be 2624 nm and 3116 nm on filter side and free side showing a similar roughness to the values of 2445 nm on filter side and 3113 nm on free side after recycling. Previously published data shows RMS roughness at 2673 nm and 3751 nm for NC film via vacuum filtration [17]. The additional images (5X magnification) of Optical profilometry for virgin and recycled NC are in the supplementary information, concluding the similar surface roughness for virgin and recycled NC film.
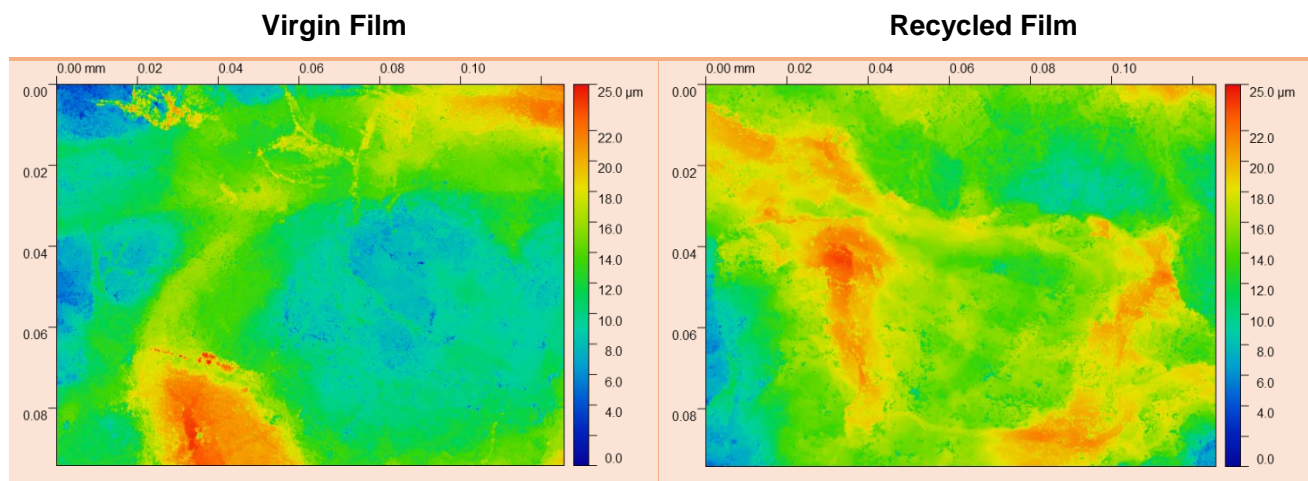
Virgin Film   **Recycled Film**

Figure 8: Optical Profilometry of Free side of NC Film and Recycled NC Film (50 X Magnification).

4.7. DISCUSSION

The effect of recycling on the NC fibres and NC films was tested at a range of length scales, and is summarised in Table 1. The effect of recycling on virgin NC fibres is predominantly observed at larger inspection areas affecting its properties such as zero-span strength, strength, WVP, air permeability and optical uniformity.

The change in the properties of recycled NC fibres cannot be explained by the traditional model of fibre hornification on recycling, which impacts the bonding between fibres and mostly reduces the strength of NC film. Our best explanation is that some of the agglomeration in initial film preparation has not been fully broken down, leaving small flakes.

These flakes of material are probably at the 100 micron or so scale. If the structure is partly composed of flakes of materials connected with NC fibres, then this will not pack together as well as individual fibres, thus lowering density, reducing uniformity, and lowering strength at multiple length scales, while at the same time increasing permeability, with only a moderate decrease in density.

However, these effects are limited and recycling does not undermine the applicability of the reprocessed product, which is still both strong, with reasonable barrier performance. It should be noted that the properties of the recycled film might be further improved by optimising the recycling conditions and processing.

Table 1 – Effect of Recycling on Properties of NC fibres

Measurement Technique	Area examined	Effect of Recyling compared to virgin fibres
SEM Measurement of Fibre diameter	1 micron scale bar	None
SEM Measurement of Film Surface	2 micron scale bar	Nothing conclusive
SEM Measurement of Film Surface	10 micron scale bar	None
Optical Profilometry roughness	100 x 90 microns	None
SEM Measurement of Film Surface	100 micron scale bar	None
Film thickness	159 mm Diameter of film	Higher thickness at the same basis weight (g/m^2)
Zero-span strength	Estimated 300 micron span length	30 % Less
PPF tester of optical uniformity	1-15 mm inspection areas 16-39 mm inspection areas	Decrease in uniformity at lower areas of Inspection Increase in uniformity at higher areas of Inspection
Water Vapour Permeability	63.5 mm diameter circle of film	Higher permeability ˜ Doubled WVP
Air permeability	50 cm^2 sample	Higher permeability: permeability increased above the detection limit of the instrument.
Tensile strength via Instron Method	100 mm test span	30% less strength

Possible strategies could be to increase the disintegration time or to use well established chemistry from the paper recycling process to improve the separation of the fibrils [21]. Homogenisation of the disintegrated fibres could also be used; this was an effective technology to break down clay agglomerates within a cellulose nanofiber suspension [22].

These additional processes could also reverse the effects of larger aggregates formation. Mixing recycled and virgin NC fibres could also produce films with enhanced barrier performance due to substantial increase of narrow pores in the films. From this investigation, it has been determined that fibrils are not impacted in the micro scale by recycling, retaining their structure and size. A limited negative impact on WVP and air permeability is observed and is likely due to the small agglomerates. This may have reduced the strength, although other factors such as hornification may be playing a role.

The potential of the recycled NC film as a packaging material can be evaluated through comparing with numerous synthetic and other cellulose polymers. The WVP of virgin NC films and recycled films of approximately 100 g/m^2 are 4.97 x10^{-11} and 9.83 x 10^{-11} g/m.s.Pa, respectively. This is somewhat above WVPs for plastic packaging materials. For example, Ethylene-vinyl acetate (EVA), Polyamide (PA) , Polycarbonate (PC), Low Density Poly-Ethylene (LDPE) and Poly Propylene (PP) have been reported at 3.41x10^{-12}, 7.54 x10^{-12} , 6.78 x10^{-12} , 8.75*10^{-13} and 2.94 *10^{-13} g/m.s.Pa respectively [[5] , Data taken http://usa.dupontteijinfilms.com]. However, this difference can be overcome by using NC films of higher thickness. The standard thickness of plastics reported falls between 15 to 25 microns, whereas the thickness of standard 100 g/m^2 films prepared in this work are approximately 100 microns, which then attains WVTRs lower than that of PA and PC and almost equal to that of EVA. This demonstrates the applicability of recycled products and the suitability of the recycling process. The recycled NC films also have comparable WVP with the virgin NC films of cellulose nanofibrils (CNF) of 8.12 x 10^{-11} and acetylated CNF of 6.35*10^{-11} g/m.s.Pa previously reported in Rodionova, 2011 [23]. The full set of data is given in a table in supplementary information ,promising recycled NC film as a suitable alternative for synthetic packaging.

The strength of the recycled films is also impacted by the effects of recycling on fibres, however the recycling process retained 70% of film tensile strength. This, too, could possibly be further enhanced by procedures discussed above. The micrographs of recycled films confirm the presence of intact fibres. The roughness of the recycled film is similar to a film prepared via vacuum filtration and that of the rough side of the vacuum filtered NC Film. This is critical as the surface roughness and network of pores in NC films are controlling parameters in barrier performance and a change in roughness can cause differing behaviour in wettability of the NC surfaces [24].

Moreover, the recycling process used here is an eco-friendly and chemical free process and the simplicity and efficiency of reprocessing, i.e. soaking and disintegration, and ease of upscaling for recycling processes demonstrate the unique advantages obtained herein. Recycled NC film obtained can serve as an alternative to synthetic polymers where recycling and reprocessing is not possible or very difficult.

While plastics, such as LDPE are low cost and easy to fabricate into a desired form, they are produced from by-products of fossil fuel. Such plastics are neither renewable nor biodegradable and are a serious threat to the ecosystem. 322 million tonnes of plastics produced every year and a substantial fraction of accumulates as waste in the environment as it is not biodegradable [25]. Recently the European Union has introduced new rules to reduce the amount of single-use plastics in applications such as packaging, which will reduce the cost advantages of plastic packaging [26, 27]. Biopolymers are a potential choice to replace fossil-fuel derived plastics. However, biopolymers such as starch, chitosan have neither good enough strength nor appreciable barrier performance. Therefore, NC fibres, with better strength and barrier performance are being actively developed as barrier layer alternatives to conventional plastics [28].

Preliminary energy consumption analysis on a comparison of spray coating with vacuum filtration concludes that spray coating consumes 0.15 MJ for spraying 1 kg of dry NC film, compared with vacuum filtration which requires 0.56 MJ/kg. The energy required for spraying the film is similar to that required to form a conventional film of Low-Density Polyethylene (LDPE).

The production of nanocellulose consumes ten times more energy than conventional packaging films [29, 30], although significant research is being conducted to lower the energy consumption. In addition, it should be noted that the full scale production of NC is still in the early stages of development and that estimates of energy consumption have often been derived using laboratory scale production. Recent analysis has suggested that substantial savings in energy could be expected as production facilities are scaled up [31]. Growing biomass for nanocellulose will also have significantly higher land-use and water consumption, than is required to produce polyolefin products. From this particular comparison, it could easily conclude that conventional packaging films are more sustainable and the sustainability trade-off between petroleum-derived and bio-based derived packaging may only conserve the non-renewable resources. However, when it comes to recycling, only two third of the packaging

films could be recycled and rest ends up in landfill or released to the environment [32]. Waste from packaging materials will overburden the landfills in the near future and poses significant environmental concerns. Work to include the impacts of plastic waste in life-cycle analysis is still in the very early stages of development [32]. It is also interesting to note that the recycling of polyolefin films such as LDPE consumes more than half of the energy in comparison to the energy required to produce these virgin films [33]. In contrast, the energy consumption for recycling nanocellulose is negligible in contrast to the energy emission owing to its production [29]. Thus, considered the end of life analysis, nanocellulose could be more sustainable and greener owing to its ease of recycling when compared to conventional packaging films, and certainly is worthy of active development.

The case here would be less common, such as when manufacturing rejects and offcuts are recycled directly into barrier layers within the manufacturing process. More common would be the recycling of composite products after use, where it is unlikely that the nanocellulose barrier layer would be separated in order to separately recycle it. Under these circumstances, the nanocellulose would be recycled within the general paper recycling stream. There have been several laboratory studies that suggest that small amounts of nanocellulose can be added to a conventional fibre furnish and will be retained during papermaking. For example, 1% of nanofibers were added into the furnishing of newsprint grade pulp to improve high retention rate and tensile strength of the paper [34, 35].

4.8. CONCLUSION

Virgin NC films of low permeability and high uniformity were manufactured by standard approch. Virgin NC films were recycled using standard paper testing techniques and formed into films again. Results confirm that some of the agglomeration in initial film formation has not been fully broken down, leaving small flakes. Partly composed of flakes did not pack together as well as individual fibres, thus lowering density, reducing uniformity, and lowering strength. However, the recycled NC barrier materials retained ˜70% of the tensile strength and showed limited reductions in barrier performance, still able to perform acceptably for most synthetic packaging applications. Nanocellulose films can now provide an alternative to conventional packaging, and readily recycled and reprocessed into a potential barrier material. This process leads to global sustainability by replacing non-renewable polluting synthetic plastic packaging and laminates with a product that can be recycled directly into a barrier material or could be used in the conventional paper recycling process.

4.9. ACKNOWLEDGMENTS

4.10. REFERENCES

1. Smithers Pira. *The Future of Global Packaging to 2020.* 2015 14 December 2015; Available from: http://www.smitherspira.com/industry-market-reports/packaging/the-future-of-global-packaging-markets-to-2020.

2. Davis, G. and J.H. Song, *Biodegradable packaging based on raw materials from crops and their impact on waste management.* Industrial Crops and Products, 2006. **23**(2): p. 147-161.

3. Tukker, A., *Plastic waste-feedstock recycling, chemical recycling and incineration.* Rapra Rev Rep, 2002. **13**(4): p. 1-10.

4. Bugnicourt, E., M. Schmid, O.M. Nerney, J. Wildner, L. Smykala, A. Lazzeri, and P. Cinelli, Processing and Validation of Whey-Protein-Coated Films and Laminates at Semi-Industrial Scale as Novel Recyclable Food Packaging Materials with Excellent Barrier Properties. Advances in Materials Science and Engineering, 2013. 2013: p. 10.

5. Bhunia, K., S.S. Sablani, J. Tang, and B. Rasco, Migration of Chemical Compounds from Packaging Polymers during Microwave, Conventional Heat Treatment, and Storage. Comprehensive Reviews in Food Science and Food Safety, 2013. 12(5): p. 523-545.

6. Lau, O.-W. and S.-K. Wong, *Contamination in food from packaging material.* Journal of Chromatography A, 2000. **882**(1–2): p. 255-270.

7. Lickly, T.D., K.M. Lehr, and G.C. Welsh, *Migration of styrene from polystyrene foam food-contact articles.* Food and Chemical Toxicology, 1995. **33**(6): p. 475-481.

8. Hubbe, M.A., A. Ferrer, P. Tyagi, Y. Yin, C. Salas, L. Pal, and O.J. Rojas, Nanocellulose in Thin Films, Coatings, and Plies for Packaging Applications: A Review. BioResources, 2017. 12(1): p. 2143-2233.

9.   Tharanathan, R.N., *Biodegradable films and composite coatings: past, present and future.* Trends in Food Science & Technology, 2003. **14**(3): p. 71-78.

10.   Azeredo, H.M.C., M.F. Rosa, and L.H.C. Mattoso, *Nanocellulose in bio-based food packaging applications.* Industrial Crops and Products, 2017. **97**: p. 664-671.

11.   Aulin, C., M. Gällstedt, and T. Lindström, *Oxygen and oil barrier properties of microfibrillated cellulose films and coatings.* Cellulose, 2010. **17**(3): p. 559-574.

12.   Bras, J. and S. Saini, *8 - Nanocellulose in functional packaging A2 - Jawaid, Mohammad*, in *Cellulose-Reinforced Nanofibre Composites*, S. Boufi and A.K. H.P.S, Editors. 2017, Woodhead Publishing. p. 175-213.

13.   Abdul Khalil, H.P.S., et al., *A review on nanocellulosic fibres as new material for sustainable packaging: Process and applications.* Renewable and Sustainable Energy Reviews, 2016. **64**: p. 823-836.

14.   Varanasi, S., R. He, and W.J. Batchelor, *Estimation of cellulose nanofibre aspect ratio from measurements of fibre suspension gel point.* Cellulose, 2013. **20**(4): p. 1885-1896.

15.   Raj, P., A. Mayahi, P. Lahtinen, S. Varanasi, G. Garnier, D. Martin, and W. Batchelor, Gel point as a measure of cellulose nanofibre quality and feedstock development with mechanical energy. Cellulose, 2016. 23(5): p. 3051-3064.

16.   Varanasi, S. and W.J. Batchelor, *Rapid preparation of cellulose nanofibre sheet.* Cellulose, 2013. **20**(1): p. 211-215.

17.   Shanmugam, K., S. Varanasi, G. Garnier, and W. Batchelor, Rapid preparation of smooth nanocellulose films using spray coating. Cellulose, 2017. 24(7): p. 2669–2676.

18.   Shanmugam, K., H. Doosthosseini, S. Varanasi, G. Garnier, and W. Batchelor, Flexible spray coating process for smooth nanocellulose film production. Cellulose, 2018. 25(3): p. 1725–1741.

19.   Varanasi, S., H.H. Chiam, and W. Batchelor, *Application and interpretation of zero and short-span testing on nanofibre sheet materials.* Nordic Pulp and Paper Research Journal, 2012. **27**(2): p. 343.

20.   Delgado-Aguilar, M., Q. Tarrés, M.À. Pèlach, P. Mutjé, and P. Fullana-i-Palmer, Are Cellulose Nanofibers a Solution for a More Circular Economy of Paper Products? Environmental Science & Technology, 2015. 49(20): p. 12206-12213.

21.   M. Hietala, K. Varrio, L. Berglund, J. Soini, and K. Oksman, "Potential of municipal solid waste paper as raw material for production of cellulose nanofibres," *Waste Management,* vol. 80, pp. 319-326, 2018/10/01/ 2018.

22. U. Garusinghe, S. Varanasi, V. S. Raghuwanshi, G. Garnier, and W. J. Batchelor, "Nanocellulose-Montmorillonite Composites of Low Water Vapour Permeability," *Colloids & Surfaces A-Physicochemical & Engineering Aspects,* vol. 540, pp. 233-241, 2018.

23. Rodionova, G., Lenes, M., Eriksen, Ø., & Gregersen, Ø. (2011). Surface chemical modification of microfibrillated cellulose: improvement of barrier properties for packaging applications. Cellulose, 18(1), 127-134.

24. Samyn, Pieter. "Wetting and hydrophobic modification of cellulose surfaces for paper applications." Journal of Materials Science 48.19 (2013): 6455-6498.

25. Milios, Leonidas, Aida Esmailzadeh Davani, and Yi Yu. "*Sustainability Impact Assessment of Increased Plastic Recycling and Future Pathways of Plastic Waste Management in Sweden.*" Recycling 3.3 (2018): 33.

26. European Commission, *Single use of Plastics.* 2018, 28 May 2018; Available from: https://ec.europa.eu/commission/news/single-use-plastics-2018-may-28

27. European Commision, Technical report on " A european strategy for plastics in a circular economy" 2018; Available from: http://ec.europa.eu/environment/circular-economy/pdf/plastics-strategy-brochure.pdf

28. Kim, Joo-Hyung, et al. "*Review of nanocellulose for sustainable future materials.*" International Journal of Precision Engineering and Manufacturing-Green Technology 2.2 (2015): 197-213.

29. Li, Qingqing, Sean McGinnis, Cutter Sydnor, Anthony Wong, and Scott Renneckar. "*Nanocellulose life cycle assessment.*" ACS Sustainable Chemistry & Engineering 1, 8 (2013): 919-928.

30. Jackson, Sue, and T. Bertényi. "Recycling of plastics." ImpEE Project, Department of Engineering, University of Cambridge, 2006; Available from; http://www-g.eng.cam.ac.uk/impee/topics/RecyclePlastics/files/Recycling%20Plastic%20v3%20PDF.pdf.

31. Piccinno F, Hischier R, Seeger S, Som C (2018) Predicting the environmental impact of a future nanocellulose production at industrial scale: Application of the life cycle assessment scale-up framework Journal of Cleaner Production 174:283-295 doi:https://doi.org/10.1016/j.jclepro.2017.10.226

32. Rydz, J., Musioł, M., Zawidlak-Węgrzyńska, B., & Sikorska, W. Present and Future of Biodegradable Polymers for Food Packaging Applications. In Biopolymers for Food Design (pp. 431-467).

33. Choi, Bulim, Seungwoo Yoo, and Su-il Park. "Carbon Footprint of Packaging Films Made from LDPE, PLA, and PLA/PBAT Blends in South Korea." Sustainability 10.7 (2018): 2369.

34. Guimond, R., B. Chabot, K.N. Law, and C. Daneault, The Use of Cellulose Nanofibres in Papermaking. Journal of Pulp and Paper Science, 2010. 36: p. 55-61.

35. Kajanto, I. and M. Kosonen, The potential use of micro-and nanofibrillated cellulose as a reinforcing element in paper. Journal of Science & Technology for Forest Products and Processes, 2012. 2(6): p. 42-48.

CHAPTER 5

FLEXIBLE PROCESS TO PRODUCE NANOCELLULOSE –MONTMORILLONITE COMPOSITES VIA SPRAY COATING

THIS PAGE HAS BEEN INTENTIONALLY LEFT BLANK

Contents

FLEXIBLE PROCESS TO PRODUCE NANOCELLULOSE –
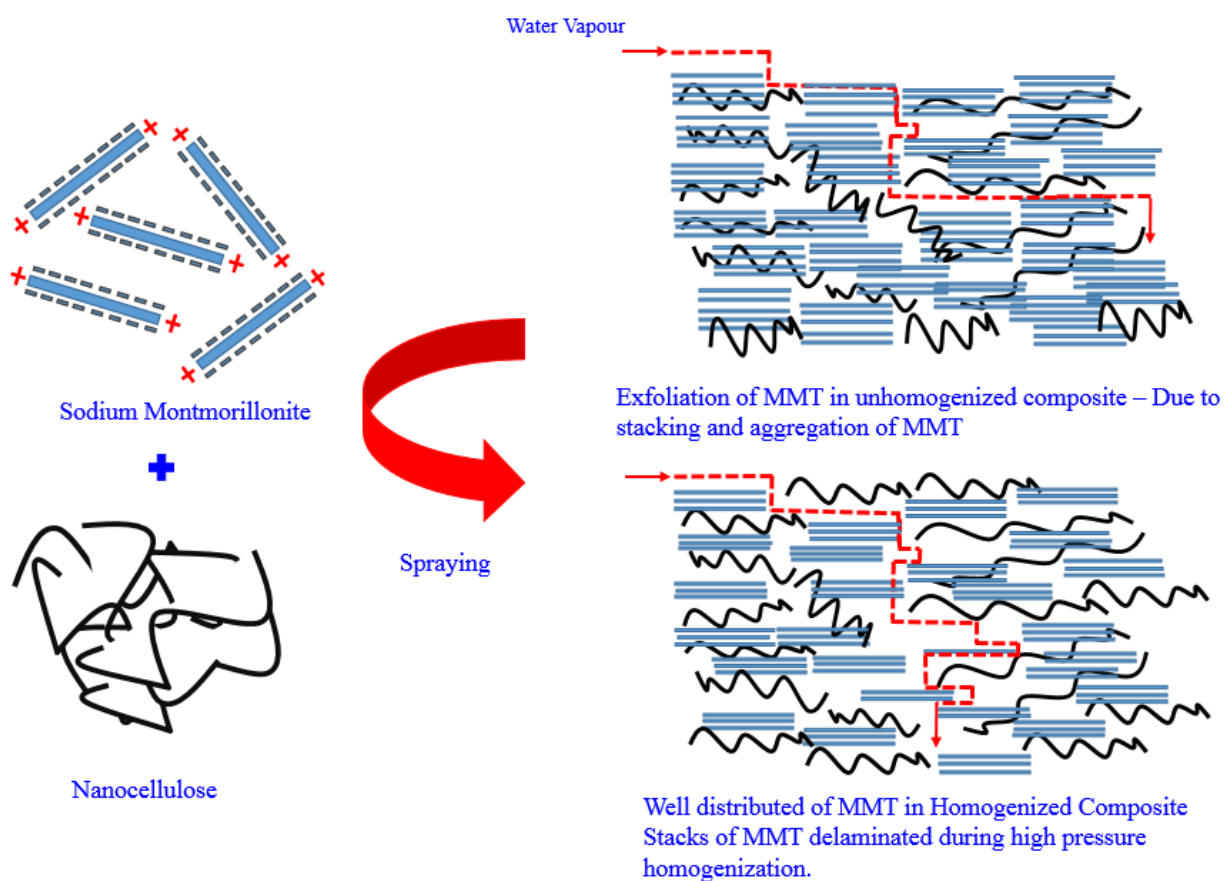
MONTMORILLONITE COMPOSITES VIA SPRAY COATING

Kirubanandan Shanmugam, Maisha Maliha, Vikram Singh Raghuwanshi, Swambabu Varanasi, Gil Garnier, Warren Batchelor.

Department of Chemical Engineering, Bioresource Processing Research Institute of Australia (BioPRIA), Monash University, Melbourne, Vic 3800, Australia.

*Corresponding Author, E-mail: Warren.Batchelor@monash.edu

5.1. GRAPHICAL ABSTRACT

Water Vapour

Sodium Montmorillonite

+

Nanocellulose

Spraying

Exfoliation of MMT in unhomogenized composite – Due to stacking and aggregation of MMT

Well distributed of MMT in Homogenized Composite Stacks of MMT delaminated during high pressure homogenization.

5.2. ABSTRACT

Plastic pollution is widely considered as a serious environmental threat. Cellulose nanofibers are one of the most promising candidates for developing high-performance paper-based packaging that is renewable, recyclable and biodegradable. While cellulose nanofiber films have very low oxygen permeability, their water vapour permeability is significantly higher than conventional packaging plastics, such as LPDE. In this study, water vapour permeability was decreased by forming composites of cellulose nanofibers and inorganic nanoparticles, such as Montmorillonite clay. However, the addition of the nanoparticles further reduces the already poor drainage when layers are formed through vacuum filtration. This paper reports a new method for spray-coating a cellulose nanofiber-Montmorillonite layer composite to improve both the ease of preparation and to reduce the water vapour permeability. The maximum solids content that could be sprayed for the nanofiber alone was 2.25 wt. %, compared to 0.3 wt. % typically used in vacuum filtration. Spraying at high solids content increased the water vapour permeability by 49.4 % over vacuum filtration, due to the agglomeration of the nanofibers, which also reduced the sheet density by 193 kg/m^3. The permeability could be reduced below that achieved with vacuum filtration by adding up to 20 wt. % Montmorillonite and dispersing Montmorillonite with NC suspension in a high pressure homogeniser with two pass homogenization. With Montmorillonite addition above 20 wt. %, the water vapour permeability of the composite started to increase due to aggregation of the Montmorillonite. XRD measurements showed that the Montmorillonite particles were aligned in the plane of the sheet and were strongly interacting with the cellulose nanofiber matrix as the interlayer spacing increased from 11.78 to 14.16 Å. At the optimal addition level, the best performance achieved with spraying was a water vapour permeability of 8.3×10^{-12} g/m.s.pa when spraying at 2.4 total wt. %, reducing the required water removal during drying by 291 kg water/kg dry product, compared to forming the equivalent sheet using vacuum filtration at 0.3 wt. %. All composites had good strength, stiffness and flexibility. The spraying process is of industrial interest as it is scalable and easy to engineer the properties of composite via varying the MMT content.

5.3. KEYWORDS

Spray coating; Nanocellulose; Montmorillonite; Nanocomposites; Homogenization; Water vapour permeability and mechanical properties

5.4. INTRODUCTION

Synthetic plastics are dominant in conventional packaging materials because of the ease of processing and excellent barrier performance against air, water vapour, oxygen, carbon dioxide and water [1]. These are not biodegradable and cause severe environmental issues such as landfilling, harmful recycling process with the emission of toxic gases and plastic microparticulate pollution. A sustainable approach with natural materials is required to combat these problems.

Natural biopolymers are used in packaging due to their sustainability and biodegradability. Cellulose is the most abundant natural fibre biopolymer. It is a renewable, eco-friendly biomaterial and has good mechanical properties. Cellulose also offers easy and varied chemical functionalization. Materials made of cellulose macrofibres such as paper, paperboards, container board and shipping sacks have been widely used as packaging for mechanically protecting food and sensitive products [2]. Yet paper based materials have poor barrier performance due to large pores allowing a significant amount of gas and water vapour to pass through, resulting in oxidation and short shelf-life of foods and drugs. The barrier performance of the cellulose macrofibres could be tailored by coating with wax or laminating with synthetic plastics such as LDPE or Polypropylene (PE). However, these layers are not recyclable nor reprocessable. Cellulose nanofibres such as nanocellulose (NC) can be used to enhance the barrier properties, with the benefit of offering a platform for recyclability and reusability leading to a sustainable pathway. Nanocellulose consists of cellulose nanofibrils forming a fibrous matrix of compact structure, thereby offering outstanding rigidity, tensile, flexural strength and barrier properties. The cellulose nanofibrils in NC fibrous network have high aspect ratio with the fibril diameter varying from 5 to 100 nm and length of a few microns. They form a high compact network by entanglement via hydrogen bonding. The compact fibril network structure of NC film has been shown to perform as a barrier against air and water vapour and offer a promising alternative to synthetic packaging materials [3].

NC film provides a good barrier against oxygen. However, it suffers from a high water vapour permeability (WVP) under medium and high humidity environments due to its hydrophilic nature. The cellulose fibre-fibre bond in the fibril network swells through absorption of water vapour. The weakened fibrous network decreases the diffusion pathway for water vapour. As a consequence, WVP of NC film increases [4] and the stability of cellulose fibril deteriorates [5]. To improve the WVP of NC, inorganic fillers were incorporated into the fibrous

matrix and the presence of layered nanoclays in the NC matrix produced a high-performance nanocomposite which increased the tortuosity of the diffusive path for a water vapour/gas molecule, resulting in high barrier performance [6]. These nanocomposite are stiff and strong with good elastic modulus and low gas permeability [7], and form a fibre matrix network of dispersed clay platelet aggregates in the nanocomposite [8].

One of the most promising inorganic fillers is Montmorillonite (MMT), an alumina-silicate layered clay hydrated bentonite [9] functioning as nanofiller. It produces a structure in the composite that forces the transfer of air/oxygen/ water molecules to follow a very tortuous path resulting in lower permanence [10]. High-performance NC-MMT composites were prepared via vacuum filtration previously [11]. However, the time for forming nanocomposite via vacuum filtration is irrealistic as it varied from a minimum of 24 hours to 4 days. This NC-MMT composite had low water vapour permeability of 6.3 g.µm/m^2 .day. kPa., at 23.1 wt.% loading of MMT. Sometimes the nanoparticles were not retained during the dewatering stage of vacuum filtration, thereby resulting in poor and unpredictable properties. Another limitation is separation of the film from the filter's surface and subsequent handling before drying. As a conventional manufacturing method, a limited range of film basis weight of the composite can be made as the filtration time increases exponentially with film thickness and basis weight [12].

Recently, a rapid spray coating method has been implemented to produce nanocellulose films [12] [13] and nanocellulose composites such as graphite carbon black-micro fibrillated cellulose as an electrode [14] and SiO_2-microfibrillated cellulose nanopaper. When producing SiO_2- microfibrillated cellulose nanopaper, it has an operation time of less than 30 minutes, varying SiO_2 between 0 to 33 wt. % into the suspension. It can result in tailorable properties of composite [15]. Vacuum filtration was applied after spraying. In their method, the conventional process of transferring and dewatering the composite by vacuum filtration was followed by drying [15]. Spraying is a novel process to develop nanocomposites and tailor their properties through the addition of specific nanoparticles or nanofillers in NC suspension. The operation time for spraying is independent of NC concentration and nanoparticle loading in the suspension. This work investigates making high-performance nanocomposites via spraying and develops a scalable, high performance barrier layer, with much lower processing time than currently available alternatives.

5.5. MATERIALS AND METHODS

5.5.1. MATERIALS

5.5.1.1. NANOCELLULOSE

The reported nomenclature for cellulose nanomaterial is not consistent in the scientific literature. As per Shanmugam *et al* 2019 [16], Nanocellulose is also called as micro fibrillated cellulose (MFC), cellulose nanofibrils, cellulose microfibrils and nanofibrillated cellulose (NFC). Nanocellulose as a generic term is used in this scientific communication. DAICEL Chemical Industries Limited Japan was supplied Celish KY-100S grade nanocellulose which has 25 wt. % solids content and 75 wt. % moisture. The average diameter of cellulose nanofibrils in Celish KY-100S is reported to be ˜ 70 nm and a mean length of fibre is evaluated to be 8μm and an aspect ratio of 142±28 [17].

5.5.1.2. NANOCLAY

Cloisite Na++ is a pure Montmorillonite (MMT) powder provided by BYK Additives and Instruments, Germany through IMCD Australia Limited. The dry particle size of Cloisite Na++ is < 25 μm (d_{50}), the packed bulk density is 568 g/l. X-Ray results confirm d_{001} of 1.17 nm.

5.5.2. PREPARATION OF MMT-NANOCELLULOSE SUSPENSION

NC suspension of 2 wt. % was prepared by the addition of 80 g of DAICEL KY100S into 920 g of deionised water and disintegrated for 15,000 revolutions at 3000 rpm. The nanoclay addition is based on fibre (dry solid content) in the nanocellulose and was varied at 5 wt. %, 10 wt. %, 20 wt. % and 30 wt. % of the NC content. The required quantity of pure MMT powder was added into a beaker in fume cupboard to avoid inhalation of any MMT powder. Initially, the weighed MMT was suspended into 1500 g of distilled water and mixed well.160 g of NC was then added into this solution for disintegration. After disintegration of NC with MMT, distilled water was added to make 2 wt. % NC suspension with the additional loading of MMT.

5.5.3. HOMOGENIZATION

Homogenization of NC-MMT suspension was used to disperse the MMT within the NC suspension and reduction of NC fibril diameter. The 2 wt. % NC- with MMT ranging from 5 wt. % to 30 wt. % in suspension was fibrillated in GEA Niro Soavi (laboratory scale) high-

pressure homogeniser at 1000 bar in the first pass and 800 bar in 2nd pass before spraying of homogenised suspension for nanocomposite fabrication.

5.5.4. SPRAYING OF NANOCLAY - NC SUSPENSION:

The experimental setup for the laboratory scale spray coating system is shown in Figure 1. The pure unhomogenized and homogenised 2 wt. % NC were sprayed on the stainless steel plates to make pure NC films. Similarly, NC suspension with MMT loading varying from 5 wt. % to 30 wt. % was used for making composites.

The NC-MMT composite can be prepared through spray coating as reported for preparation of pure nanocellulose film. In this method, spraying nanocellulose NC – MMT suspension on the stainless steel plate on a moving conveyor which has velocity of 1.25±0.25 cm/sec. The professional spray system Wagner Pro 117 was used for spraying suspension at a discharge pressure of 200 bar. In the spray system, an elliptical spray jet with an angle of 50° from the spray nozzle 517 has a coverage of 22.5 cm suspension on the base surface. The spray head from the spray nozzle to the square stainless steel plate was used 50±1 cm. The steady state in the spraying suspension to form the film can be performed by allowing the spray system run for 30 seconds to avoid any discontinuity in the spray jet. The wet spray coated composite film on the stainless steel plate was dried under standard laboratory conditions at 24 hours. The dried film was peeled from the stainless steel plate for evaluating barrier performance and characterizations.
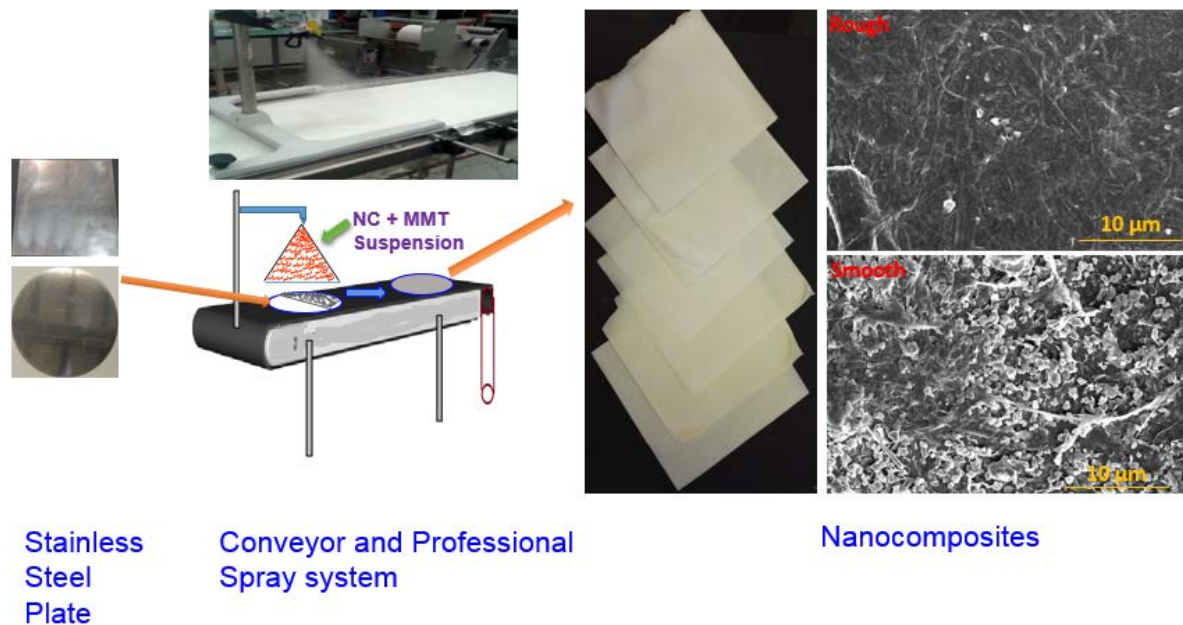
Figure.1. Experimental set up for spraying of NC suspension with MMT for developing nanocomposite

5.5.5. CHARACTERIZATION OF FREE-STANDING NANOCOMPOSITE:

All spray coated nanocomposites were conditioned at 23°C and 50% RH for 24 hours prior to further testing.

5.5.5.1. APPARENT DENSITY OF COMPOSITES:

Australian/New Zealand standard method AS/NZS 1301.426s:2015 is used to evaluate the apparent density of the spray coated composites. The density of the composite is calculated by the ratio between basis weight and mean thickness of the composite. The thickness of the spray-coated nanocomposites were determined using a Thickness Tester Type 21 from Lorentzen & Wettre AB, Stockholm, Sweden. Approximately 25 points on each nanocomposite film were considered and averaged to find mean thickness via descriptive statistics. Australian/New Zealand standard method AS/NZS 1301.426S:1994 was considered as the protocol to measure the thickness of the spray coated composite.

5.5.5.2. AIR PERMEANCE OF NANOCOMPOSITE:

The L&W air permeance tester which has a measuring range from 0.003 to 100 µm/Pa.S was used to investigate the air permanence of the spray coated composite. The mean value of air permeance evaluated from 3 different areas of each NC film was reported. The Technical Association of the Pulp and Paper Industry (TAPPI) standard T 460-om-2 has been used to measure the air permeance of the films.

5.5.5.3. WATER VAPOUR PERMEABILITY OF NANOCOMPOSITE:

ASTM standard (E96/E96M-05) method was used to evaluate the water vapour permeability of the composites. This test was normally carried out 23°C and 50% relative humidity. The principle is the weight gained by calcium chloride in the cup relating to the water transmission rate of the composite. Before the testing, the composites were dried for at least 24 hours at a temperature of 105 °C in an air oven. This drying method of composites helps to remove any residual moisture present in the composite. The cup was filled with 40 g of dried anhydrous $CaCl_2$. The composites were used to cover the cups. The mass of the cups was increased though by $CaCl_2$ in the cups through the composite. The weight of the test specimen was evaluated for every 4 hours. The increase in weight of the cups with every time interval was recorded. The water vapour transmission rate (WVTR) is defined as the slope of the line between the weight of moisture absorbed in $CaCl_2$ in the cup and time. The WVTR of composites were normalised with thickness of the composites and converted into water vapour permeability (WVP). The mean value of three parallel tests of each NC-MMT composites were reported.

5.5.5.4. MECHANICAL PROPERTIES OF COMPOSITES:

An Instron model 5965 was used to evaluate the mechanical strength of the spray-coated composite.The dimension of test specimens is 100 mm length and 15 mm width, conditioned for 24 hours at 23°C and 50% RH before dry tensile testing based on the Australian/New Zealand Standard Methods AS/NZS 1301.448s:2007. All testing investigation were carried out at 23°C and 50 % RH. As per AS/NZS 1301.448s:2007, 10mm/min elongation rate was considered for testing the specimen. The tensile index (TI in Nm/g) of the samples was calculated from the tensile strength (expressed in Nm^{-1}) divided by basis weight (gm^{-2}). The mean value was obtained from six to seven valid tests and the error bars in plots indicate 95% confidence intervals.

5.5.5.5. XRD INVESTIGATION OF COMPOSITES:

X-Ray diffraction was conducted on MMT (Closite Na++) powder, all types of pure NC film and composites using a D8 Advance with DAVINCI Design. The source for X-Rays is from Cu Kα Radiation runs at 40kV and 40mA. The 0.02° step size and 2°/min scan speed were used to scatter the radiation from the instrument. The range for diffraction angle for investigation of orientation of MMT in the composite varied from 2° to 34°.

Bragg's law was used to evaluate the interlayer spacing of MMT. The equation for Bragg's law was given below,

$$d = n\lambda/\ 2\ \text{Sin}\ \Theta \tag{1}$$

Where the d-spacing (nm) is the interlayer spacing, λ is the wavelength of X-Ray beam (nm) and Θ is the angle of incidence, n is the order of diffraction.

5.5.5.5.1. EVALUATION OF AREA UNDER THE PEAK IN XRD SPECTRUM:

The area under the first peak in the XRD spectrum was evaluated with Origin Software Pro 9.1. The base line was first removed by the software. The corrected spectrum was then fitted with the Gaussian- Lorentzian fit to find area under first peak under MMT region.

5.6. RESULTS

A series of composites were prepared by spray coating nanocellulose (NC)-montmorillonite (MMT) suspensions varying in terms of composition and concentration onto metallic surface. The spray coated nanocomposites are flexible, foldable and of uniform thickness. The composites are increasingly yellowish in colour as increased MMT content, due to absorption spectra of MMT in the nanocomposites. In this section, the physical, barrier and mechanical and of the composites formed are characterized as a function of process and composition.

5.6.1. BARRIER PERFORMANCE

5.6.1.1. MATERIAL PROPERTIES

Water vapour permeability (WVP) for spray coated nanocomposites with different addition of MMT is shown in Figure 2. The performance of WVP of nanocomposite prepared by spraying technique is compared with the data of composites made via vacuum filtration

[11]. The error bars indicate the 95 % confidence interval of three composites film for each group.

For sprayed composites, the WVP of the unhomogenized composite with 5 wt.% MMT loading is 1.18±0.05 x 10^{-11} g/Pa.s.m which is less than half the value of 2.5±0.12 × 10^{-11} g/Pa.s.m for the pure NC films. Beyond this loading, WVP increases to 3.3±0.07 × 10^{-11} g/Pa.s.m at 30 wt. % MMT loading. On the other hand, with additional high-pressure homogenization of NC suspension prior to spraying, the films obtained show a decrease in WVP up to 20 wt. %, after which a slight rise in the WVP is observed. The WVP results can be explained because the MMT particles aggregates are broken down by homogenization increasing the tortuous pathway for the permeance of water vapour resulting in an overall reduction in WVP. However, the WVP of both types of composites show higher WVP when produced by spraying, compared with similar films by vacuum filtration [11].
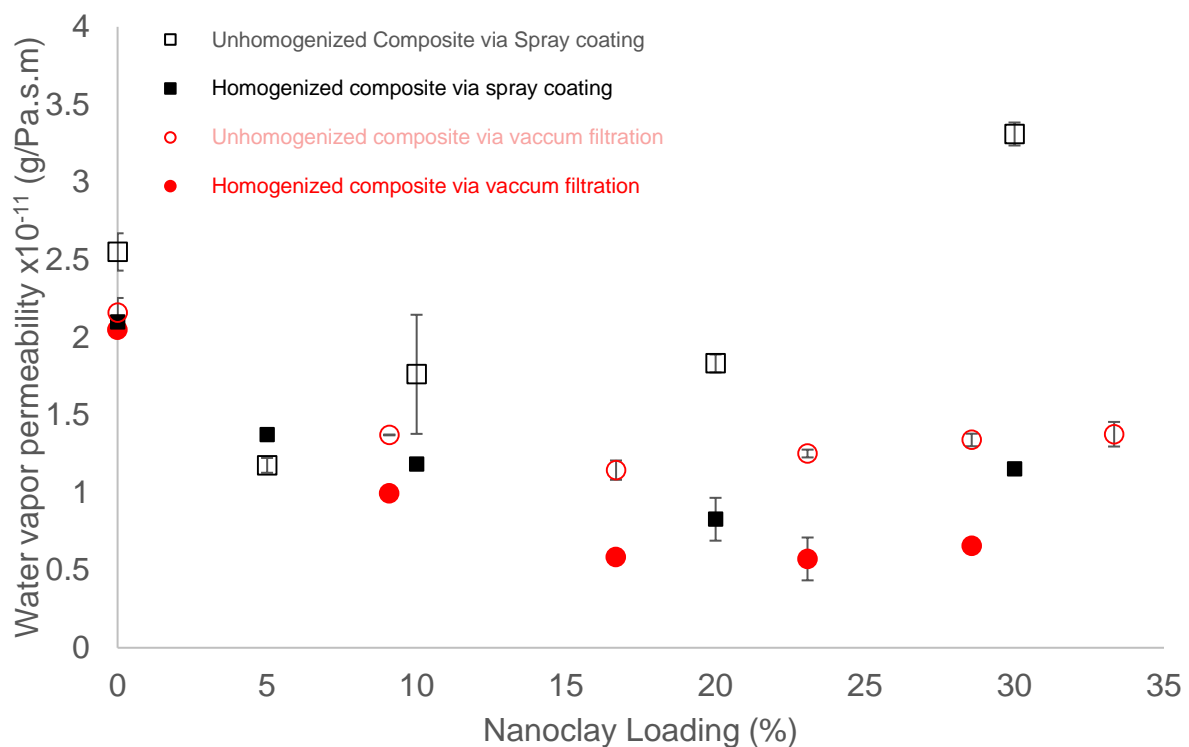
Figure.2. Water vapour permeability of nanocomposites via spray coating. The WVP of the composites made via vacuum filtration was taken from [11]

Figure 3 shows the effect of MMT loading on the apparent densities of MMT-NC composites via spraying of suspension with and without homogenization. The data for similar composites prepared by vacuum filtration [11] are also presented for comparison.

The apparent density of all composites prepared by vacuum filtration is higher than that of the corresponding samples from the spray coating process, including the pure NC films. Nanofibers in the spray-coated pure films tend to form small agglomerates leading to a reduction in packing. In spray coated composites, the density is also reduced with high MMT loading. The MMT forms bigger stacks which disrupts the packing in the structure, reduces the density and increases the water vapour permeability. At lower loading, the MMT is able to fill gaps within the fibrous structure and therefore density increases as the MMT has higher density than cellulose.
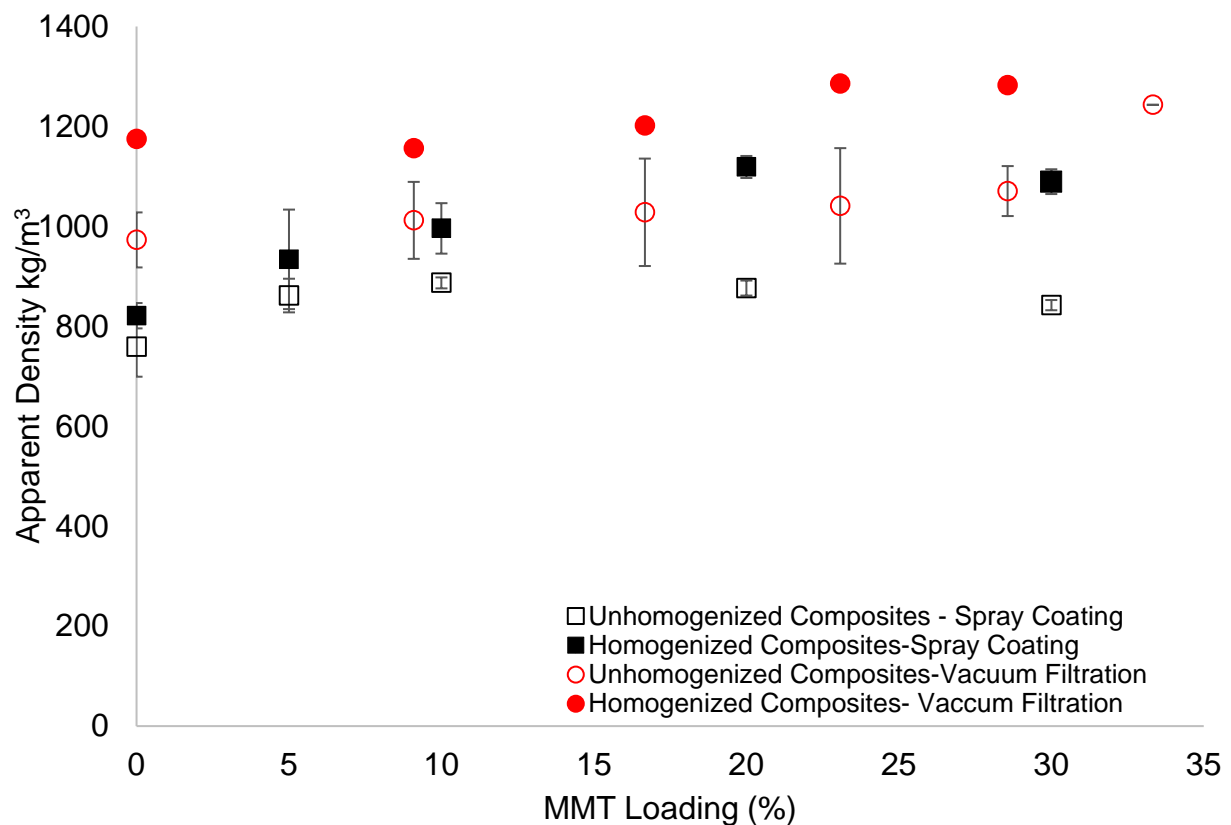
Figure. 3. Effect of MMT Loading on the apparent density of the nanocomposite

In addition, the apparent density of the homogenized composites is higher than that of the unhomogenized one for both vacuum filtration and spray coating methods. The dispersion

of MMT in NC suspension and the high aspect ratio of cellulose nanofibrils could affect and control the apparent density. The variation in the apparent density is also caused by the preparation of NC-MMT suspension. Clay platelets in the suspension can aggregate and stack. After reduction of cellulose fibrils via two pass high-pressure homogenization, these MMT stacks are broken down, well dispersed and mixed with reduced cellulose nanofibrils suspension resulting in higher density composites.

Figure S-1 in supplementary information shows the SEM micrograph of rough side and smooth side of 30 wt. % NC –MMT homogenized composite and pure homogenized NC film. The surface of the composite shows scattered MMT in the NC network. After homogenization of NC suspension with MMT, the diameter is reduced and the MMT is dispersed in the NC network. This forms a good compact fibrous network resulting in less porous films. Figure S-2 in supplementary information shows the cross-sectional view of SEM micrographs on composites indicating the MMT particles with the cellulose nanofibrils of the fibrous matrix. It is confirmed with XRD analysis of the composites.

5.6.1.2. SUSTAINABILITY OF THE COMPOSITES

Spray coated NC composites have higher WVP compared with composites prepared via vacuum filtration. This is due to lowering density in spray coated NC film via agglomeration of fibres. The reason for this elevation in WVP for sprayed composites is the aggregation and stacking of MMT within the NC fibres, which is more dominant at higher loading for unhomogenized nanocomposites. In homogenized composites, the stacked MMT in NC suspension is delaminated and broken down during high pressure homogenization and platelets well distributed with cellulose nanofibrils creating a tortuous pathway for water vapour penetration. As a result, WVP of these composites decreased as MMT loading increased. The WVP value of the composite reaches a minimum of $8.28 \pm 0.01 \times 10^{-12}$ g/Pa.s.m at 20 wt. % of MMT loading. Further increase of MMT loading enhances WVP of the composites.

The air permeability of all samples is less than 0.003 µm/Pa.s, which is the lowest detection limit of the instrument. This air permanence of the nanocomposite with this value confirms that the composite film is highly impermeable for barrier materials applications.

5.6.2. STRUCTURE OF SPRAYED COMPOSITE

XRD investigation on spray-coated composites shows the orientation of MMT in the NC fibrous network. Figure 4 shows XRD patterns of pure NC and homogenized composite

with MMT loading varying from 5 to 30 wt.%. Pure NC has no characteristic peak in the range of 2 ° to 10 °. The area under the curve (AUC) provides information on the amount of MMT present in the composite and increases with MMT loading. The AUC of the first peak is chosen because of MMT produces a peak from 2 ° to 10 °, representing the spacing between MMT layers. The AUC increase sharply from the Pure MMT to 10wt. % loading in both composites. The reason for this is that the MMT is aligned in the plane in the sheets. In a powder, MMT is aligned randomly and only the platelets that happen to be lying flat will contribute to the diffraction pattern. The AUC of the first peak of XRD spectrum versus MMT loading for the unhomogenized and homogenized composites are shown in Figure S3 and S4 added in the supplementary information.

Figure 5 shows the effect of MMT loading on the d-spacing of MMT in the composites. The d- spacing of pure MMT is evaluated to be 11.78 Å from the diffraction peak at $2\theta = 7.5°$ using equation 1. The orientation of MMT platelets in the composite shows a peak in this range. The interspacing of MMT platelets barely varies from 14.72 A° to 14.16 A° in the homogenized composites as the MMT content increased from 10 wt. % to 30 wt. %, revealing the strong interaction of MMT platelets with cellulose nanofibers. The interspacing is constant and independent of MMT loading, except for the 5 wt. % homogenized composite. The diffraction peak of MMT in 5 and 10 wt. % unhomogenized composites are 6.056° and 6.199° respectively. There is no peak for the 5 wt. % homogenised sample and a peak at 6.056° for the 10. wt. % homogenized composites. The absence of peak in 5 wt. % homogenised composite suggests that MMT platelets completely broke down and dispersed in the NC fibrous matrix. The composite beyond 5 wt. % gave a peak due to the stacking of MMT platelets and alignment in the plane of the NC film. Thereafter, peak positions increased slightly with MMT content for both types of composites. This means that all the MMT will contribute to the scattering, whereas with pure MMT only the small fraction of platelets orient in the plane will contribute.
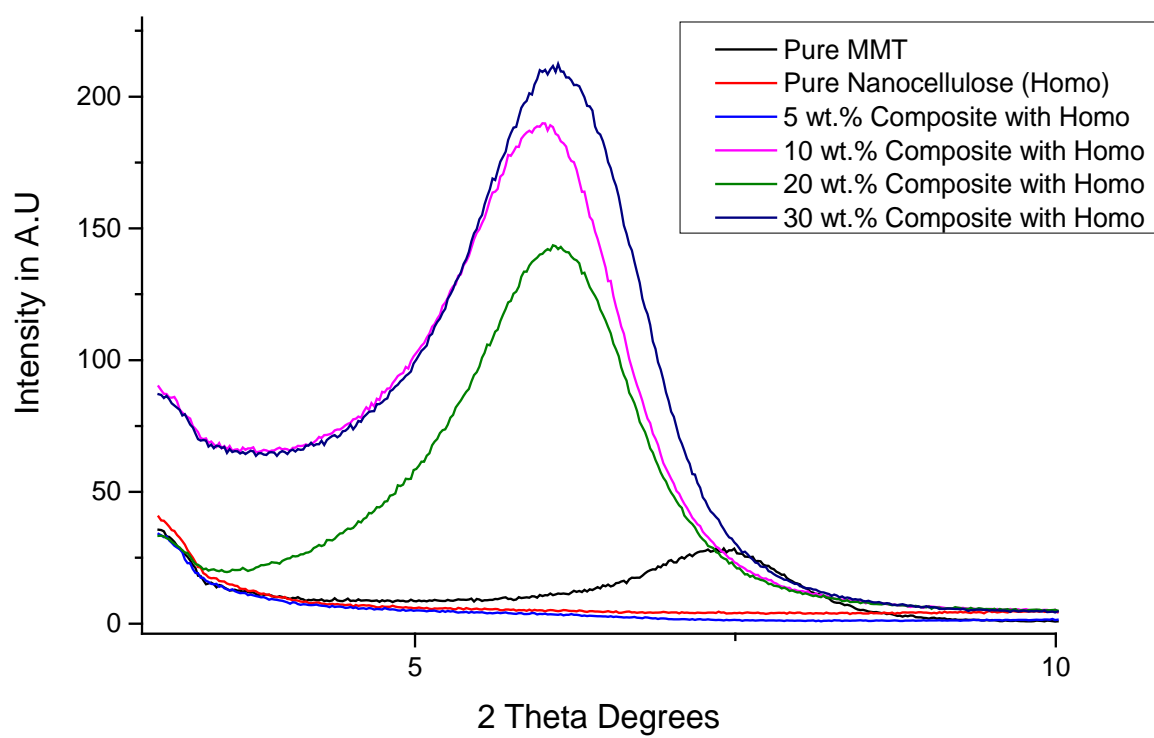
Figure.4. First peak of XRD spectrum of homogenised nanocomposites
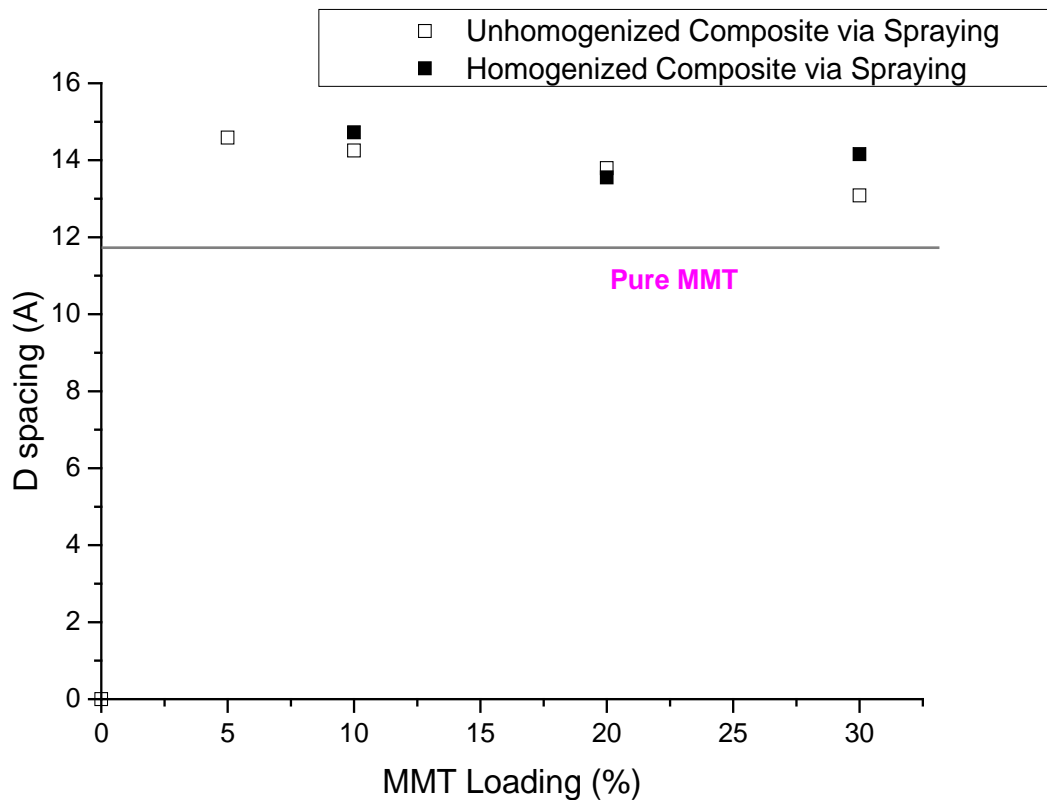
Figure. 5. Effect of MMT loading on d-spacing of MMT in the first peak of nanocomposite of XRD spectra.

5.6.3. MECHANICAL PROPERTIES

The effect of MMT content and fibrillation (homogenization) on the mechanical properties of the nanocomposite are investigated. Figure 6 shows the tensile index of the composites, both unhomogenized and homogenized. The tensile index of the composites is increased for up to 5 wt. % MMT loading and barely reduced from 10 wt. % loading of MMT. The error bars indicate the 95% confidence interval.

The homogenized composites always have a higher strength than those made without mechanical treatment. The higher tensile index of the homogenized composite is due to the fibrillation of the nanofibers during the homogenization treatment. The average diameter of NC after high-pressure homogenization is ˜20 nm with an aspect ratio of 286 [11]. Even after 15 wt. % MMT addition, the tensile index of the composite is still equal to or higher than either the homogenised or unhomogenised pure film. The increase in strength shows that the MMT

is bonding to the CNF and is not just present as a passive filler. The tensile strength and E-modulus of spray coated composites are shown in Figure S5 and S6 in the supplementary information.
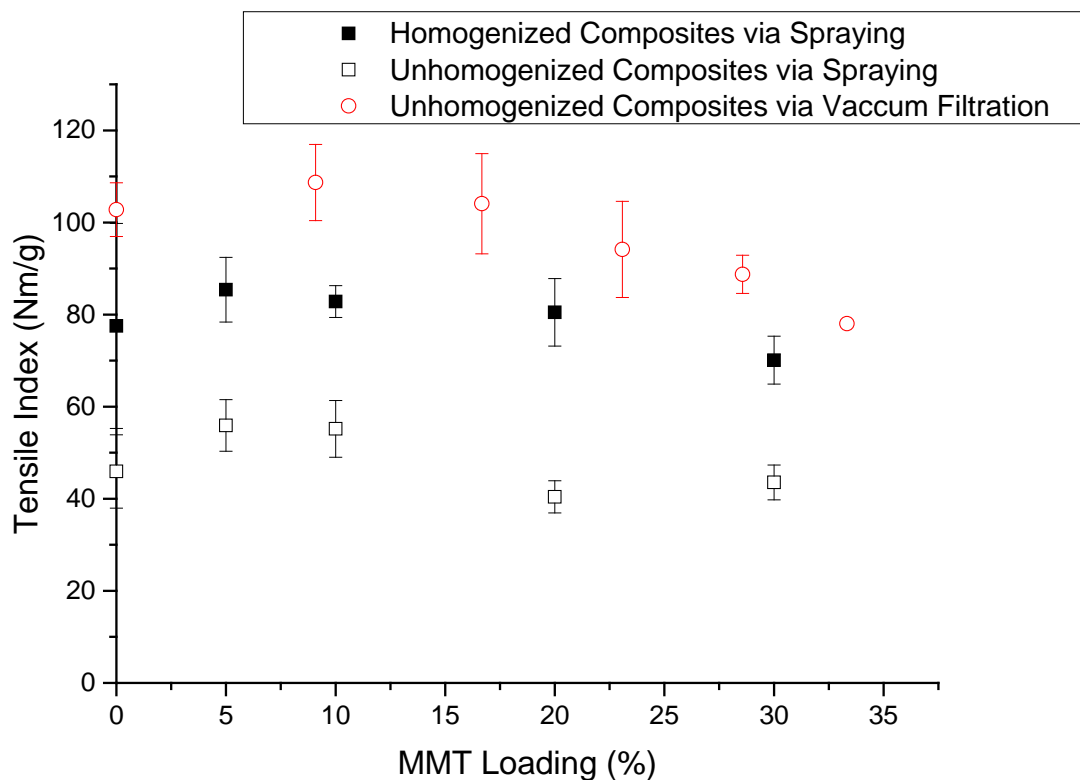
Figure.6.Tensile index of spray coated nanocomposites

5.7. DISCUSSION

Eco-friendly packaging is now required to combat the environmental consequences of synthetic plastics. 85% of plastic waste ended in landing filling [18] and disposed in oceans. To overcome these global problems, biodegradable, renewable and recyclable materials, such as paper, are a potential alternative. Due to swelling of fibrils and large pores in the fibrous network, the performance of paper and board as a barrier is poor. Nanocellulose (NC) films are a promising alternative to plastic packaging. They have reasonable barrier performance against water vapour under moderate humidity environments and are excellent barriers against oxygen. To utilize NC, we need to further improve the barrier performance with additives such as MMT and to develop a rapid and flexible production process.

There is no industrial method for making MMT/NC barrier films. The most common method for laboratory fabrication of MMT/NC composites is vacuum filtration. The addition of 30 wt. % MMT into the NC suspension increased the dewatering time from 30 mins to 24 hours. Moreover, peeling the nanocomposite from the filter or mesh, without introducing surface defects, is quite challenging. This drainage time makes it impossible to scale to commercial manufacture. Among fabrication techniques, spraying is relatively rapid in forming the NC film and flexible in handling high NC suspension consistencies when compared to vacuum filtration [12].

The novelty of this work is that the MMT-NC suspension is sprayed on an impermeable surface to produce the nanocomposite. This process easily controls the density of composites via tailoring thickness and basis weight of the composite. The operation time for spraying was less than 1 minute [13]. The spraying process could be scalable for production of self-standing composites or for a composite layer for laminating to a base sheet [19] . In the spraying process, the MMT addition in the NC suspension does not affect the time required for film formation, which is significantly lower compared with the time required for vacuum filtration. Compared with vacuum filtration, spray coating is a flexible process to tailor the properties of the nanocomposite without any effect of the addition of nanoclay on the spraying process.

Spraying can drastically reduce water consumption and water removal in sheet forming. The spraying of up to 9 wt. % suspensions on the metal surface was earlier reported to prepare free standing NC structures. However, it caused the formation of lumps of MFC due to the gel nature of MFC at a high solid concentration [20]. The maximum solids content that can be sprayed using our experimental set up was 2.4 wt. % NC with an additional 30 wt. % loading on an MMT mass/NC mass basis for an overall suspension solids content of 3.12%. Because of the higher concentration, spraying requires much less water for composite fabrication. For example, filtering a 0.3 wt. % NC suspension requires removal of 332 kg water/kg fibre, comparing with spraying of 3.12 wt. % NC + MMT which requires removal of 31 kg water/kg fibre. Even the best conditions investigated here, with 2 wt. % NC and a further 20% wt. % further MMT loading, for a total solids content of 2.4 wt. %, still only required the removal of 41 kg water/kg fibre, a reduction of 291 kg water/kg fibre over filtration. The advantages of spraying to produce nanocomposites with varying nanofillers are its simplicity in film formation, rapidity and achieving tailored composites with minimal operation time.

The vacuum filtration process takes a long time in the film formation via settling of cellulose nanofibrils on the filter mesh through draining the water, but there will be a higher solids content at the end of it. These higher solids content would reduce the overall time to dry it. The solids content in the sheet at the end of the formation process has not been measured, so the balance is not clear at the current time. However, forming sheets via vacuum filtration requires much more handling due to the difficulties of separating out the film from the filter.

The only significant negative for the spraying process was that the WVP increased. However, adding 20 wt. % MMT was able to reduce the WVP of homogenized nanocomposite nearly to that of the pure vacuum filtered composites as the MMT platelets were well distributed in the composites and aligned in the plane of the cellulose of the composite film. Paper is made from wood fibres in a continuous process by vacuum filtration through a moving filter mesh. However, this process is impractical to make continuous NC films or layers, as the small size of the NC fibres strongly hinders drainage. Even with relatively large NC fibres, drainage takes minutes to hours [21]. In comparison, the spraying process we have developed here is flexible and scalable and would be readily adaptable to spraying a continuous barrier layer onto a paper substrate. The remarkable reduction in water that has to be removed in drying would also substantially the processing speed for drying.

5.8. CONCLUSION

A rapid and industrially scalable process based on spray coating is developed to engineer high performance cellulosic nanocomposites for barrier applications. The process consists of spray coating a blend of nanocellulose fibres and nanoclay onto a substrate. The composites developed showed high mechanical strength and low water vapour permeability. Spraying process is a robust and can accommodate wide range of MMT concentration in NC suspension. Homogenization of NC with MMT, delaminating the stacked MMT in the suspension, significantly enhances the tortuous pathway in the cellulose nanofibril network of the composite. This investigation confirms spray coating as a rapid, flexible and scalable process to manufacture flexible and strong, high barrier performance composites. The process can be used to produce free-standing films or to produce composite barrier layers on the cellulose fibre substrates, such as paper.

5.9. ACKNOWLEDGEMENTS

5.10. REFERENCE

[1] Silvestre C, Duraccio D, Cimmino S. Food packaging based on polymer nanomaterials. Progress in Polymer Science. 2011;36(12):1766-1782.

[2] Berk Z. Chapter 27 - Food Packaging. In: Berk Z, editor. Food Process Engineering and Technology (Second Edition), San Diego: Academic Press; 2013. p. 621-636.

[3] Henriksson M, Berglund LA, Isaksson P, Lindström T, Nishino T. Cellulose Nanopaper Structures of High Toughness. Biomacromolecules. 2008;9(6):1579-1585.

[4] Nair SS, Zhu J, Deng Y, Ragauskas AJ. High performance green barriers based on nanocellulose. Sustainable Chemical Processes. 2014;2(1):23.

[5] Spoljaric S, Salminen A, Dang Luong N, Lahtinen P, Vartiainen J, Tammelin T, et al. Nanofibrillated cellulose, poly(vinyl alcohol), montmorillonite clay hybrid nanocomposites with superior barrier and thermomechanical properties. Polymer Composites. 2014;35(6):1117-1131.

[6] Azeredo HMCd. Nanocomposites for food packaging applications. Food Research International. 2009;42(9):1240-1253.

[7] Liu A, Berglund LA. Clay nanopaper composites of nacre-like structure based on montmorrilonite and cellulose nanofibers—Improvements due to chitosan addition. Carbohydrate Polymers. 2012;87(1):53-60.

[8] Liu A, Walther A, Ikkala O, Belova L, Berglund LA. Clay Nanopaper with Tough Cellulose Nanofiber Matrix for Fire Retardancy and Gas Barrier Functions. Biomacromolecules. 2011;12(3):633-641.

[9] Jochen W, Paul T, Julian MD. Functional Materials in Food Nanotechnology. Journal of Food Science. 2006;71(9):R107-R116.

[10] Uyama H, Kuwabara M, Tsujimoto T, Nakano M, Usuki A, Kobayashi S. Green Nanocomposites from Renewable Resources: Plant Oil−Clay Hybrid Materials. Chemistry of Materials. 2003;15(13):2492-2494.

[11] Garusinghe UM, Varanasi S, Raghuwanshi VS, Garnier G, Batchelor W. Nanocellulose-montmorillonite composites of low water vapour permeability. Colloids and Surfaces A: Physicochemical and Engineering Aspects. 2018;540:233-241.

[12] Shanmugam K, Varanasi S, Garnier G, Batchelor W. Rapid preparation of smooth nanocellulose films using spray coating. Cellulose. 2017;24(7):2669–2676.

[13] Shanmugam K, Doosthosseini H, Varanasi S, Garnier G, Batchelor W. Flexible spray coating process for smooth nanocellulose film production. Cellulose. 2018;25(3):1725–1741.

[14] Beneventi D, Chaussy D, Curtil D, Zolin L, Bruno E, Bongiovanni R, et al. Pilot-scale elaboration of graphite/microfibrillated cellulose anodes for Li-ion batteries by spray deposition on a forming paper sheet. Chem Eng J. 2014;243:372-379.

[15] Krol LF, Beneventi D, Alloin F, Chaussy D. Microfibrillated cellulose-SiO2 composite nanopapers produced by spray deposition. Journal of Materials Science. 2015;50(11):4095-4103.

[16] Shanmugam K, Doosthosseini H, Varanasi S, Garnier G, Batchelor W. Nanocellulose films as air and water vapour barriers: A recyclable and biodegradable alternative to polyolefin packaging. Sustainable Materials and Technologies. 2019;22:e00115.

[17] Raj P, Mayahi A, Lahtinen P, Varanasi S, Garnier G, Martin D, et al. Gel point as a measure of cellulose nanofibre quality and feedstock development with mechanical energy. Cellulose. 2016;23(5):3051-3064.

[18] North EJ, Halden RU. Plastics and environmental health: the road ahead. Reviews on environmental health. 2013;28(1):1-8.

[19] Mirmehdi S, Hein PRG, de Luca Sarantópoulos CIG, Dias MV, Tonoli GHD. Cellulose nanofibrils/nanoclay hybrid composite as a paper coating: Effects of spray time, nanoclay content and corona discharge on barrier and mechanical properties of the coated papers. Food Packaging and Shelf Life. 2018;15:87-94.

[20] Magnusson J. Method for spraying of free standing 3D structures with MFC: Creation and development of a method. 2016.

[21] Varanasi S, Batchelor WJ. Rapid preparation of cellulose nanofibre sheet. Cellulose. 2013;20(1):211-215.

CHAPTER 6

ENGINEERING SURFACE ROUGHNESS OF

NANOCELLULOSE FILM VIA SPRAYING TO

PRODUCE SMOOTH NC SUBSTRATES

THIS PAGE HAS BEEN INTENTIONALLY LEFT BLANK

Contents

ENGINEERING SURFACE ROUGHNESS OF NANOCELLULOSE FILM VIA SPRAYING TO PRODUCE SMOOTH NC SUBSTRATES

Kirubanandan Shanmugam, Humayun Nadeem, Christine Browne, Gil Garnier and Warren Batchelor,

Department of Chemical Engineering,

Bioresource Processing Research Institute of Australia (BioPRIA),

Monash University, Melbourne, Vic 3800, Australia.

*Corresponding Author, E-mail: Warren.Batchelor@monash.edu

6.1. GRAPHICAL ABSTRACT
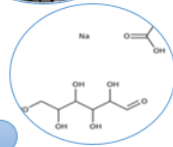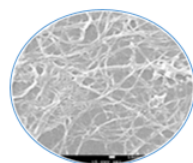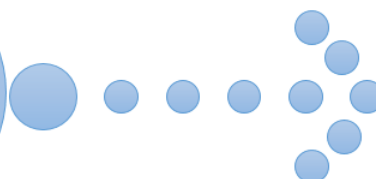
6.2. ABSTRACT

Due to the requirements of smooth cellulose substrates for printing electronic circuits to have proper conductance, nanocellulose (NC) have been used as a substrate for electronic material such as solar panels, supercapacitors and flexible electronics etc. Recently we developed a process to produce smooth NC films by spraying onto an impermeable substrate. The spray coated NC film has a shiny and glossy smooth surface where it was in contact with the substrate. In this study, we investigated the effect of i) substrates surface chemistry, ii) its substrate roughness, iii) NC fibre diameter and iv) addition of carboxymethyl cellulose (CMC) in NC suspension on the roughness of the smooth surface of NC film. The three parameters

controlling the roughness of the resultant NC films were the roughness of the substrate surface, the fibril diameter of the NC and CMC addition.

Adding 1.5 wt. % CMC had only a small effect with very smooth substrates but had a larger effect with rougher substrates. The lowest roughness obtained is 336±117 nm at a 259.1 µm x 259.9 µm inspection area when spraying of 1.5 wt. % CMC in 1.75wt. % NC suspension on the super polished stainless steel (SSS). The controlling order of roughness of NC films was found to be 1.5 wt. % CMC addition in NC suspension>fibril diameter>base substrate. The addition of CMC in the NC suspension decreases the surface roughness of the spray coated film.

This study has shown that spraying of NC on base substrates produce a smooth NC film in a rapid film formation process, with a smoothness that can be tailored across fibrils.

6.3. KEYWORDS

Surface roughness; base substrates; fibril diameter; homogenization; carboxymethyl cellulose (CMC); smooth NC film.

6.4. INTRODUCTION

Developing flexible electronic substrates from eco-friendly and biodegradable natural polymers can be helpful in designing and printing circuits for electronic devices. The smoothness of the substrate controls the conductive ink spreading on the surface and avoids forming discontinuities within the ink once on the substrates. Synthetic plastics can also be used as base substrates for printed electronics, however, these are not biodegradable, and require surface treatment to achieve a suitable smoothness. Moreover, the increased awareness of sustainability and environmental issues among people has driven researchers towards the replacement and reduction of the use of plastic materials [1]. Paper can be used as a low-cost substrate for fabricating electronic materials and offers the advantage of removing the plastic-based components from the current devices. However, paper substrates are susceptible to moisture absorption, have a high surface roughness and can be highly porous, which limits their use in high-performance electronic materials [2].

Nanocellulose (NC) can be used as a sustainable and eco-friendly substrate in the fabrication of printed electronics [3] and when mixed with inorganic fillers, it could control and reduce the surface roughness [4]. NC has a high aspect ratio, with the fibre diameter ranging from 20 nm to 100 nm and length to a few micrometres. NC has high strength and the ability

to form a compact network with considerable resistance to air, oxygen and water vapour permeance [5]. Due to the good barrier performance of NC, it could be a potential substrate with a suitable roughness for printing electronic circuits.

The surface roughness of NC film determines its glossy appearance as a finishing quality of the film. Lowest roughness NC film could replace the synthetic plastics as base substrates for printing circuits. The main applications of smooth NC films from laboratory methods investigated its use in the fabrication of Radiofrequency Identification device (RFID) tags, Organic Light Emitting Diode OLEDs, photovoltaic (PV) cells, electronic paper, cellulose-based batteries [6], membranes for water filtration [7], substrate for biosensors, diagnostics and bioactive interfaces [8].

Vacuum filtration is a conventional method for preparing NC films [9]. The surface of mesh in the vacuum filtration produces a film with a considerable roughness and also transfers filter marks to the film which results in high roughness on both sides [10]. In comparison, casting is a laboratory method for preparing NC films and the roughness of the NC film produced via this method depends on the fibre size and surface of the base material. However, this method is limited to laboratory scale production of NC films [11]. Time consumption for fabricating NC film by casting varied from days to weeks.

Calendering is a conventional process of smoothening cellulose macrofibres materials such as paper sheets with the compression of fibres with heated rolls. The cellulose sheet produced via this process is smooth and glossy. This is a final step in the industrial finishing of paper that could reduce the surface roughness [12] and porosity of the sheet. Calendering was implemented to smooth the surface of micro fibrillated cellulose (MFC) filler composites for flexible electronics applications. The mean surface roughness of the calendered MFC films varied from 470 nm to 341 nm at an inspection length of 30 mm in the film and has achieved a surface smoothness lower than that of a photo paper [4]. Whilst, calendering is a high temperature technique that produces sheets, which have a smoother surface, the other properties of sheets such as thickness, strength and stiffness are compromised.

Recently, we developed a new method of spraying of nanocellulose on the polished stainless-steel surface to produce smooth nanocellulose films. The measured RMS roughnesses were 389 nm and 81.1 nm at an inspection area of 1 cm x 1 cm from optical profilometry and 10 μm X10 μm for AFM evaluation [10]. These values confirm spray coating

as an appropriate method to engineer the roughness of NC films. It is flexible in the processing of NC film and film uniformity and properties can be controlled by suspension concentration and process variables in spraying [13].

This paper investigates the factors that control the roughness of NC films prepared by spraying. This includes the study of the effect of substrate roughness, NC fibre diameter and the addition of a water-soluble polymer to reduce the fibre-fibre friction during film formation. This will be a platform for the production of NC films with controlled smoothness for specific high-performance applications.

6.5. MATERIALS AND METHODS

6.5.1. PREPARATION OF NANOCELLULOSE (NC) SUSPENSION

The nomenclature for nanocellulose has not been reported consistently within the literature. It has been called microfibrillated cellulose (MFC), cellulose nano-fibrils, cellulose micro-fibrils and nano-fibrillated cellulose (NFC). In this paper, we use NC as the generic term for the cellulose nanomaterials used. The NC used was supplied from DAICEL Chemical Industries Limited (Celish KY-100S) at 25 wt. % solids content. This NC has cellulose fibrils with an average diameter of approximately 73 nm with a wide distribution of fibre diameter, and an average aspect ratio of 142 ± 28 [14]. NC suspension was prepared by diluting the original concentration of 25 wt. % to 1.75 wt. % NC suspension with de-ionized water and disintegrating for 15,000 revolutions at 3000 rpm in a disintegrator.

6.5.2. SELECTION OF BASE SUBSTRATES

The base substrates used for tuning the roughness of the nanocellulose films were ordinary stainless-steel plate (OSSS) (220 mm × 220 mm), ordinary stainless-steel circular (OSSC) (159 mm diameter), super mirror stainless steel plate (SSS) (220 mm X 220mm) and silicon wafer (SW) (152.4 mm diameter). The surface of OSSS contains many scratches and lines which elevates the roughness. The OSSC has more refined polishing than OSSS and therefore, a lower surface roughness. The silicon wafer is GAS06 -Size 6 " Silicon Wafer, Type P, 111 (Boron–1 primary flat) with a resistance of 1 to 30 Ohms from Pro Science Technology Central Queensland Australia. The silicon wafer has been polished with one side having a roughness of 2 A°. The thickness of this 6-inch wafer varies from 600±20 to 690±20 µm. The super mirror polished stainless steel from Rimex Metals (Australia) Pty Ltd, Somersby, NSW 2250, Australia, has 316 grade and it is surface mechanical polished to a mirror glass standard, with surface reflectivity of greater than 90%. The surface roughness of these substrates is

mentioned in Table 1 and their surface images are shown in Figure S3 in supplementary information.

Table 1- Types of substrates and its surface roughness

Types of Substrates	Average Roughness (Sa) nm	RMS Roughness Sq nm
Ordinary stainless-steel square	333	432
Ordinary stainless-steel circular	131	195
Silicon Wafer	17	25
Super polished stainless steel	18	22

6.5.3. PREPARATION OF SMOOTH NC FILMS VIA SPRAYING

The experimental set-up for a bench scale spray coating system with experimental conditions is shown in Figure 1. The NC spray coated film is prepared according to the reported method [13] by spraying onto a base substrate of interest, which has been placed on a moving conveyor at a fixed velocity 1.25±0.15 cm/sec. The NC suspension was sprayed using a Professional Wagner spray system (Model number 117) at a pressure of 100 bar. The type 317 spray tip used in the spray system produced an elliptical spray jet and the spray jet angle and beam width are 50° and 22.5 cm, respectively. The spray distance is 50.0±1.0 cm from the spray nozzle to the base substrate. Prior to the spraying of NC on the substrates, the pressure driven spray system was run for sufficient time to allow the system to reach equilibrium. After spraying, the film on the plate was dried under standard laboratory conditions for at least 24 hours. The dried NC film was readily peeled from the substrates.

6.5.4. TUNING ROUGHNESS OF NC FILMS

The following variables were investigated:

1. Varying the substrate roughness using the materials listed in Table 1.
2. Varying the cellulose nanofibril diameter via high-pressure homogenization of NC sprayed on the surfaces i) first pass with pressure of 1000 bar ii) second pass with pressure of 800 bar.
3. Adding 1.5 wt.% carboxymethyl cellulose (CMC) into 1.75 wt.% NC suspension and spraying on the substrates.

6.5.5. HIGH-PRESSURE HOMOGENIZATION OF NC

1.75 wt. % NC content in the suspension was fibrillated in GEA Niro Soavi (Laboratory scale) high-pressure homogeniser and subjected to 1 or 2 passes before spraying. The

number of passes that the NC suspension goes through the homogenizer controls the diameter of cellulose nanofibrils in NC. The pressure in homogenizer was at 1000 bar in first pass and 800 bar in the second pass.

6.5.5.1. EVALUATING NC FIBRIL DIAMETER AND ASPECT RATIO

A drop of 0.2 wt. % of homogenized NC suspension was cast on the silicon wafer and then dried in a controlled laboratory environment. The dried suspension on the silicon wafer was coated with iridium. Micrographs were taken with a FEI Magellan 400 FEG SEM using the Through Lens Detector (TLD) at a voltage of 5 keV. The micrographs were taken at a scale bar of 1 µm and magnification of 150000 x. The diameter distribution of NC fibres were measured with Image J (1.51 K National Institute of Health (NIH) USA). The data reports an average diameter of NC with 95% confidence interval. The diameter of NC after 1st and 2nd pass homogenization are ≈40nm and ≈20 nm. The aspect ratio of NC fibrils was evaluated by the sedimentation method [14].

6.5.6. CMC ADDITION IN NC SUSPENSION:

Carboxymethyl Cellulose (CMC) (Finnfix grade 10 from CP Kelco , USA) was used to prepare NC films containing CMC via spraying. To avoid the formation of agglomerates, 15 grams of dry carboxy methyl cellulose (CMC) was slowly added into 915g of distilled water whilst being agitated at 600 rpm with a mixer. The resultant solution is 930 g of suspension. To this is added 70 g of DAICEL NC (Default NC) at 25 wt. % solids content to make 1 kg of suspension with 1.75 wt. % of nanocellulose fibre in the suspension and 1.5 wt. % of CMC, for a total solids content of 3.25 wt.% NC-CMC.This suspension was disintegrated at 3000 RPM in a disintegrator for 15000 revs.

6.5.7. OPTICAL PROFILOMETRY

The size of specimen area from smooth NC films was 100 mm^2 selected from uniform film free from surface defects and pinholes. The NC film peeled from the substrate was the smooth surface of the NC film and the side exposed to air was the rough side. The spraying of 1.75 wt. % NC suspension on these surfaces produce a basis weight 55 g/m^2 and thickness 108.9 µm of NC film. An optical profiler (Olympus OLS 5000 Laser Confocal Microscope) was used to evaluate the area roughness of a 259 µm x 259 µm area of the NC films of both the rough and smooth sides. The average area roughness, Sa and root mean square (RMS) roughness, Sq of both sides of NC films were evaluated from the instrument software. Six

films were taken for measuring the roughness parameters. The minimum six locations on each film were considered for area roughness evaluation.

6.5.8. Scanning Electron Microscopy of Smooth NC Films

The surface morphology and topography of the smooth surface of the NC film were studied with FEI Nova NanoSEM 450 FEGSEM using a TLD. The sample were coated with a thin layer of iridium metal prior to imaging. The images were captured with magnification varying from 80000 x to 150000 x in secondary electron mode-II of FEI Novo SEM.
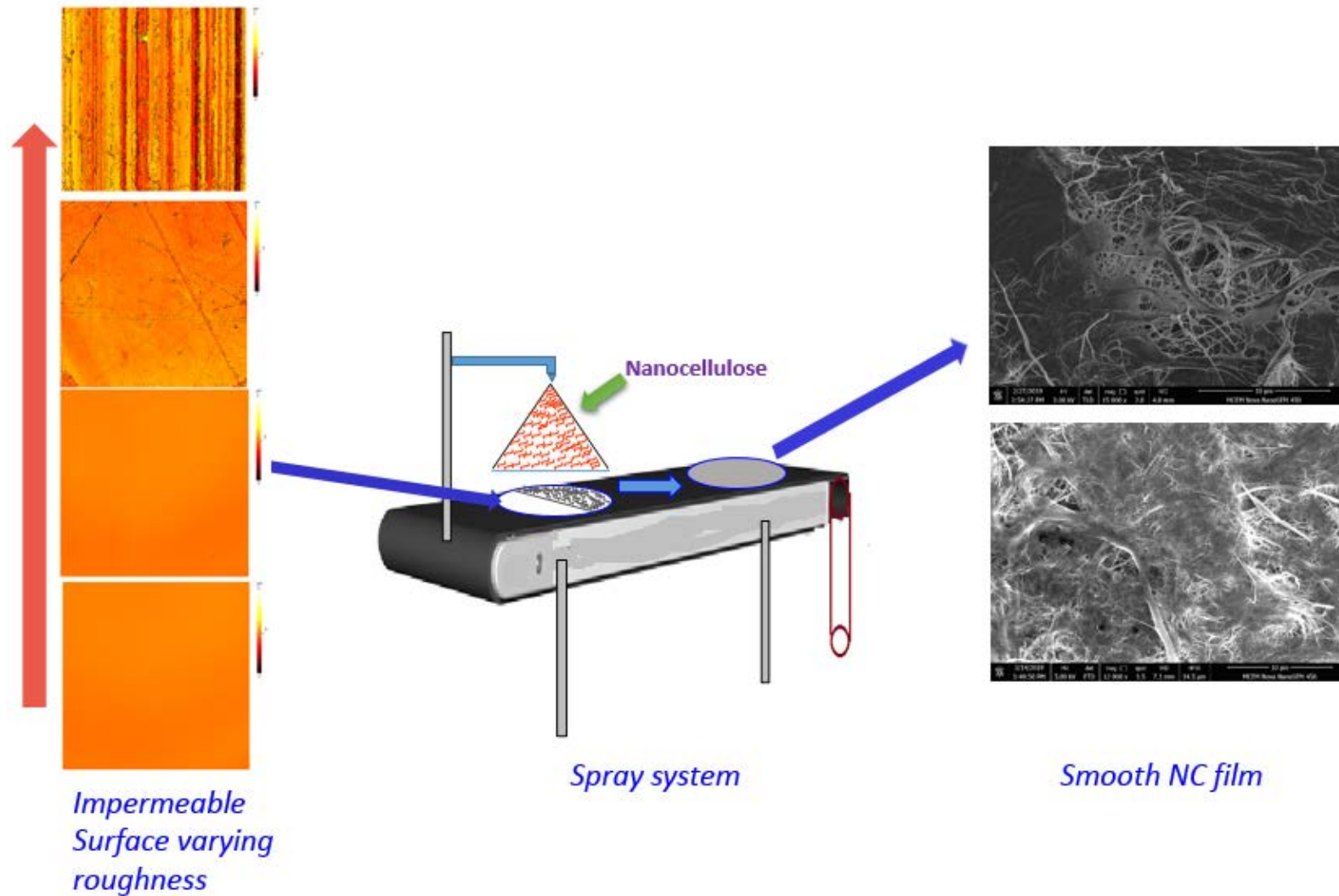
Figure 1: Experimental Set-up for Smooth NC production. The spraying of NC on the base substrates produce smooth NC films.

6.6. RESULTS

The area roughness parameters of NC films were evaluated from the statistical analysis of optical profiler images. The surface roughness of NC film derives from irregularities or unevenness and coarse texture produced by cellulose nanofibrils, imprints transcribed from the base substrates and also aggregates formed in the spraying process. It evaluates the vertical deviation from the actual surface through the parameters such as an average roughness (Sa) and root mean square roughness (RMS), Sq. Sa is an arithmetic mean of the height of the surface profile on the NC film [15]. Sa provides statistically stable and more accurate measurement with optical profilometry. However, it has limitations to differentiate between peaks and valleys on the surface. Sq is more sensitive to peaks and valleys than that of Sa because it is a square of height at the surface. RMS roughness Sq, provides authentic information about surface height variations on cellulose substrates and is considered as a quality indicator of the surface [16] [17]. In this work, both Sa and Sq have been reported.

The roughness of all the impermeable substrates was measured using optical profilometry at an inspection size of 259 μm x 259 μm. Table 2 lists the results on the roughness of smooth side of NC film. The OSSS and OSSC substrates show a significant difference between Sa and Sq due to presence of scratches and marks on their surfaces. This elevates the roughness of the NC film produced on OSSS via imprinting these markings on the film. When compared to OSSS, OSSC is a quite polished substrate, which yields a low film roughness. The optical profilometry images of these substrates are added in the supplementary information.

The data set in Table 2 is the average from different experiments at three different solids contents (The solid content used 1.25 wt. %, 1.75 wt. % and 2.25 wt. %), while the data in Figure 04, gives the data obtained at 1.75 wt. % only. The high-pressure homogenization of 1.75 wt. % was performed to make films. The suspension exceeds 2.wt. % solid content for difficulty in homogenization such as jelly nature of suspension and clogging.

Table 2-Surface Roughness of Spray Coated Side of NC Film

Controlling Parameters	Average Roughness Sa of NC film in nm		
	Substrates		
	OSSS	SSS	SW
Only Base Substrate (Ave Diameter of NC ≈70 nm)	1055±79	402±23	479±31
Fibre Diameter (≈40 nm)	1338	443±81	405±36
Fibre Diameter (≈20 nm)	1038±218	362	368±32
CMC addition	396±28	262±26	310±31
RMS Roughness, Sq of NC film in nm			
Only Base Substrate	1400±269	550±36	610±51
Fibre Diameter (≈40 nm)	1339±167	585±106	558±61
Fibre Diameter (≈20 nm)	1318±261	471±20	491±42
CMC addition	508±34	345±37	336±117

6.6.1. OPTICAL PROFILOMETRY INVESTIGATION

Factors	Highest Roughness NC Film (OSSS)	Lowest Roughness Film (SSS)
Base Substrate Fibril Diameter ≈70nm		
Fibril Diameter ≈20 nm		
CMC Fibril Diameter ≈70 nm		
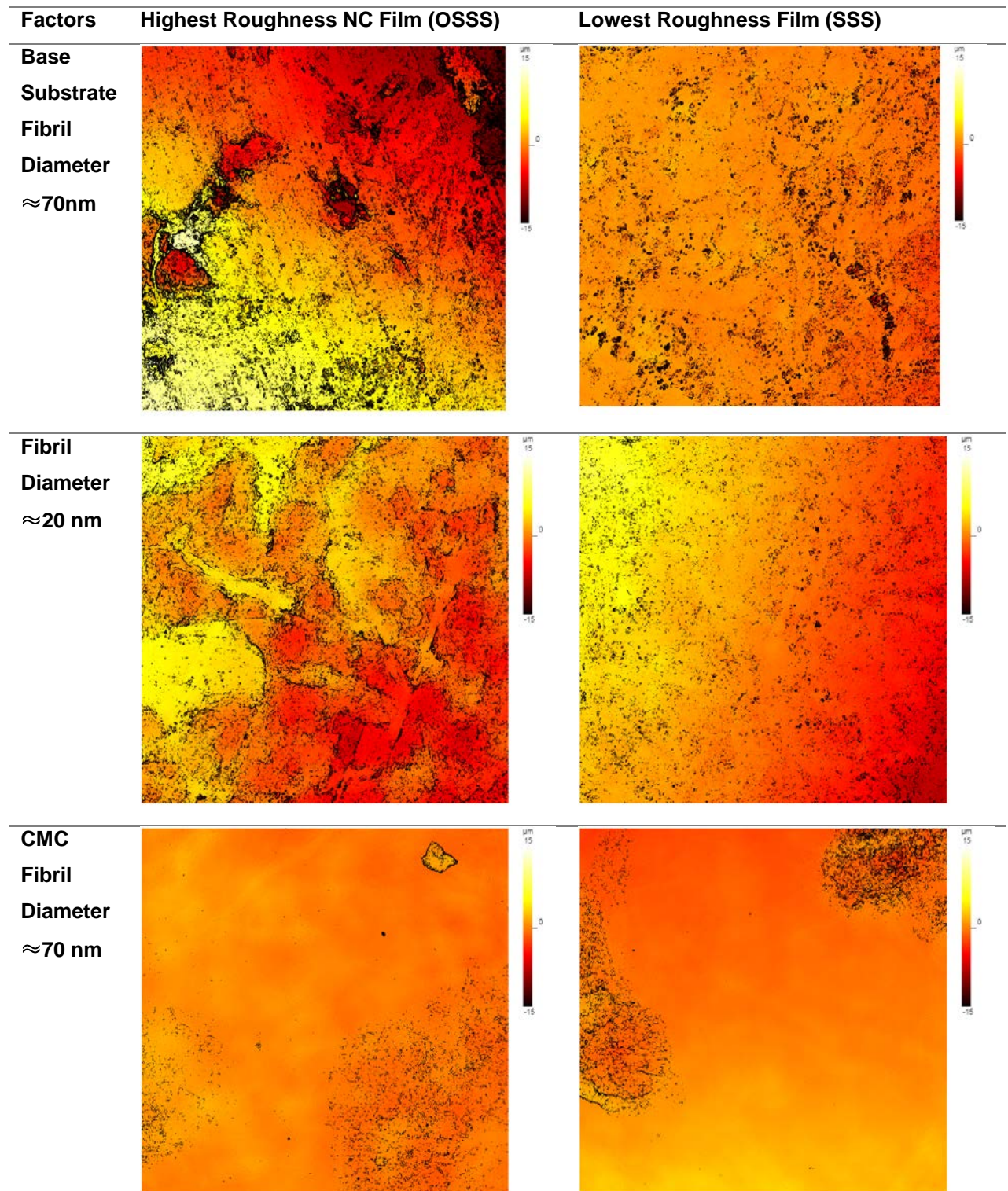
Figure 2: Optical profilometry images of NC film (50X magnification). The inspection size of specimen is 259 μm x 259 μm. The height is shown by the colour given in the legend.

6.6.2. SEM INVESTIGATION
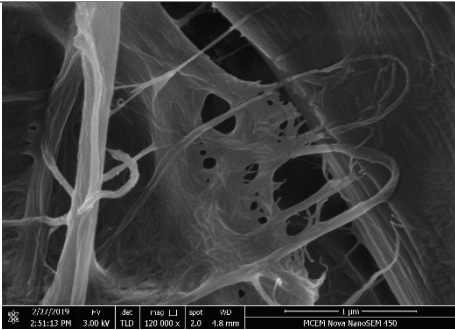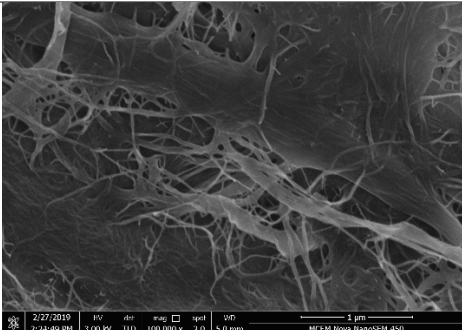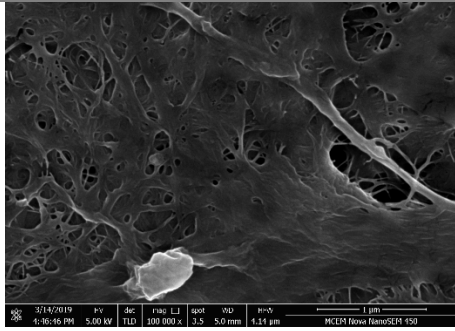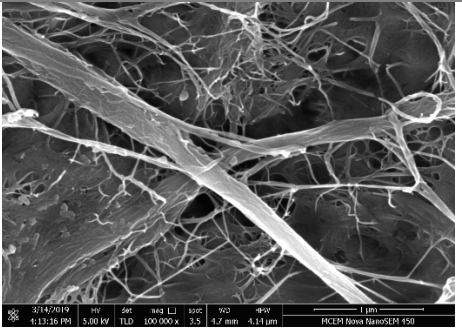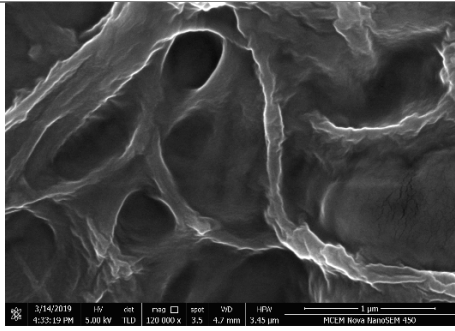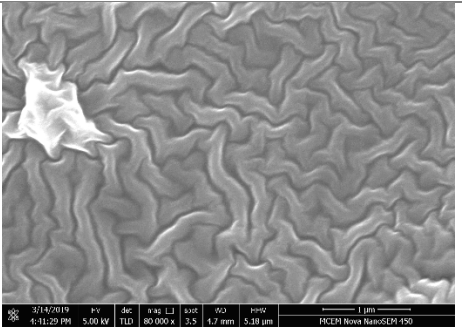
Factors	Highest Roughness NC Film (OSSS)	Lowest Roughness Film (SSS)
Base Substrate Fibril Diameter ≈70nm		
Fibril Diameter ≈20 nm		
CMC Fibril Diameter ≈70 nm		

Figure 3: SEM micrographs of smooth NC film via spraying.

Figure 2 shows optical profilometry images of smooth NC film and confirms the increase in surface smoothness of NC film when spraying on smoother base substrates. Additional images of the base substrate and smooth NC film from were added in Figure S1 and S2 in the supplementary information.

The SEM Micrographs of smooth NC films are shown in Figure 3. The surface of the NC film peeled from super polished and CMC added film has the lowest smoothness for

printed electronics applications compared the NC film from OSSS. The smooth NC film has a compact network of compressed fibrils with a glossy surface and less porosity than the rough surface of the film.

6.6.3. EFFECT OF SURFACE SUBSTRATES

Figure 4 shows the effect of the base substrate on the Sa and Sq surface roughness of the NC film peeled from the different base substrates with varying roughness. The results show that the substrate roughness has a significant influence on the film roughness, but that the extrapolated roughness for spraying on an infinitely smooth substrate is not zero.

The trends of the plot between film surface roughness and base substrate roughness have two components. One was the roughness of the underlying substrate and the other is the roughness created by the packing of the fibres on that substrate. The slope of the data in the plots are 2.04 and 1.95 for RMS roughness and average roughness, respectively. The fact that these slopes are greater than 1.0 shows that there are synergistic effects between substrate roughness and fibre network induced roughness

The peeling of NC film from the silicon wafer is quite challenging due to the strong interaction of fibres with the hydrophilic surface of the silicon wafer. Its surface is more hydrophilic than stainless steel surfaces. Therefore, since the RMS roughness of the SW was slightly higher than the SSS, the Sa of the NC film from the SW is also slightly higher than the film peeled from SSS. The correlations between the area surface roughness of NC film and base substrate are as follows.

$$Sa_{film} = 426 + 1.95 \, SRa_{base} \qquad \{1\}$$

$$Sq_{film} = 562 + 2.04 \, SRq_{base} \qquad \{2\}$$

Where Sa_{film} and Sq_{film} are the average roughness and RMS of spray coated NC film with these substrates. SRa_{base} and SRq_{base} are the average roughness and RMS roughness of the base substrate. The intercept of the plot indicates the minimum surface area roughness of spray coated NC films. The fibres in spray coated NC film have an average diameter of $\approx$ 70nm and an aspect ratio of 142 ± 28 [18]. The minimum average surface roughness, Sa and RMS roughness, Sq of spray coated NC film are 426 nm and 562 nm.
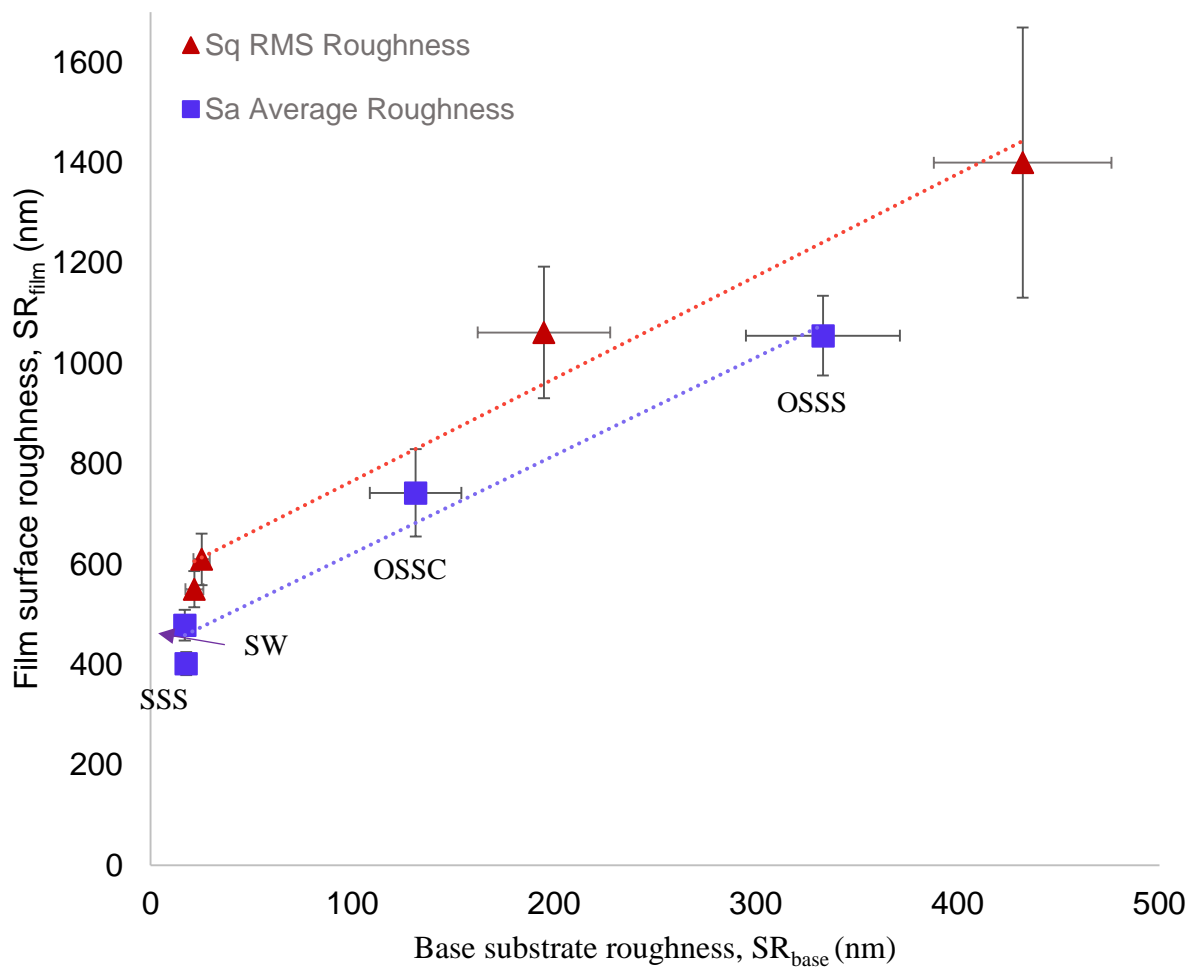
Figure 4: Effect of the substrate surface roughness on the film surface roughness of the NC samples (Sa and Sq)

The roughness of the free side of spray coated NC film was measured and added in the supplementary information. Moreover, the macro scale roughness of spray coated NC film is evaluated with Parker Print Surface instrument shown in Figure S9 and S10 and added in the supplementary information. This data confirms the smoothness of the NC film increased when sprayed on the solid substrates with decreasing roughness.

6.6.4. EFFECT OF HOMOGENIZATION OF NC AND CMC ADDITION:

Figure 5 and 6 show the effect of homogenization and CMC addition respectively on Sa and Sq. The two hypotheses tested are a) that the reduction of fibrils diameter and its length via high pressure homogenization will better allow the fibrils to conform to the base substrate and b) the addition of the CMC will reduce the friction between the fibrils to allow them to conform better, creating a smoother surface. The NC fibres were homogenised either

for 1 or 2 passes. Single pass homogenization reduced the fibre diameter from 70 to 40 nm. The diameter was further reduced to 20 nm with 2 pass homogenization. The diameter distribution results are shown in Figure 5.

Default NC

Average Diameter ≈70nm
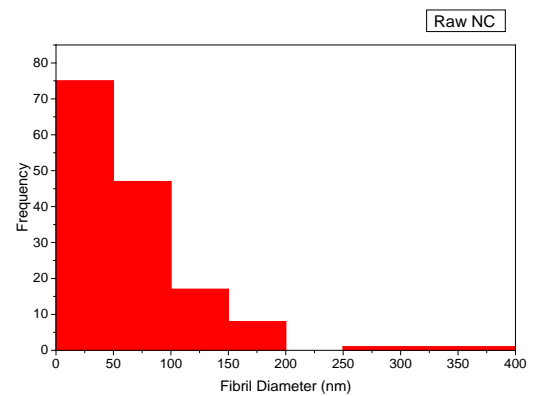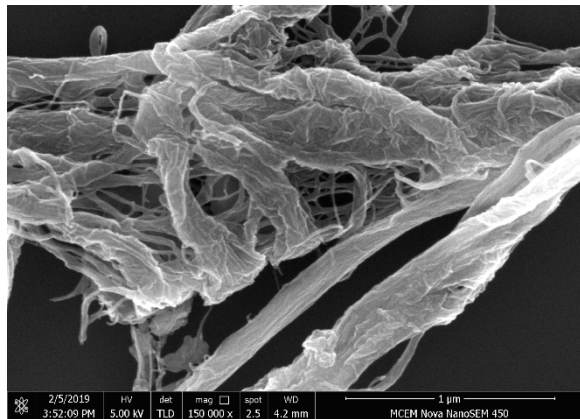
NC from First Pass Homogenization

Average Diameter ≈40nm
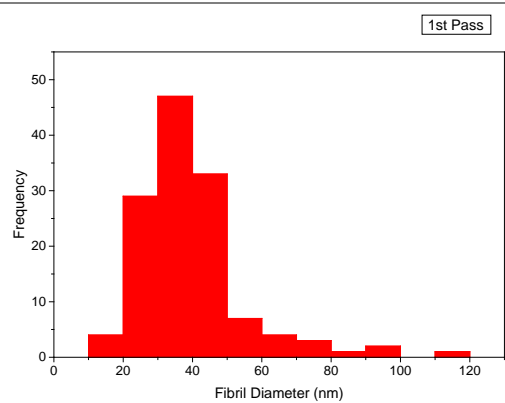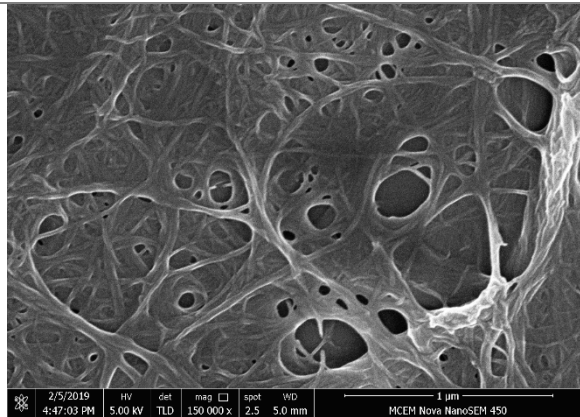
NC from Second Pass Homogenization

Average Diameter ≈20nm
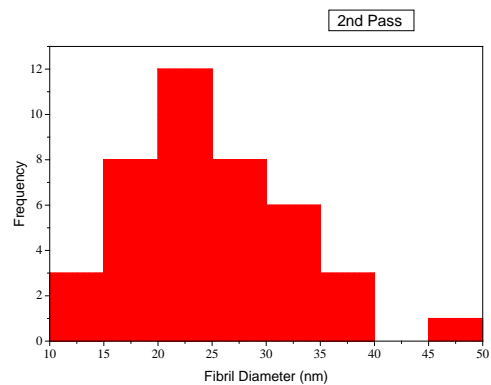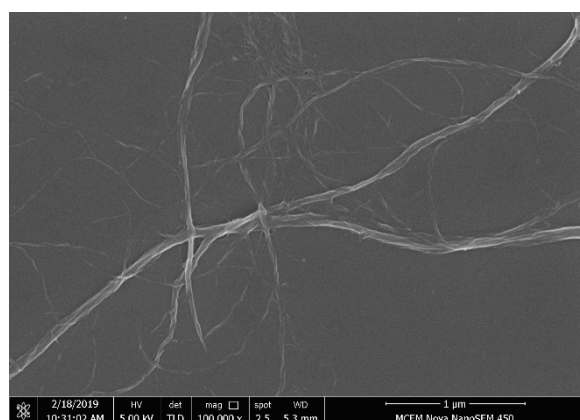
Figure 5: SEM Micrographs of Raw NC and homogenized NC with fibril distribution.
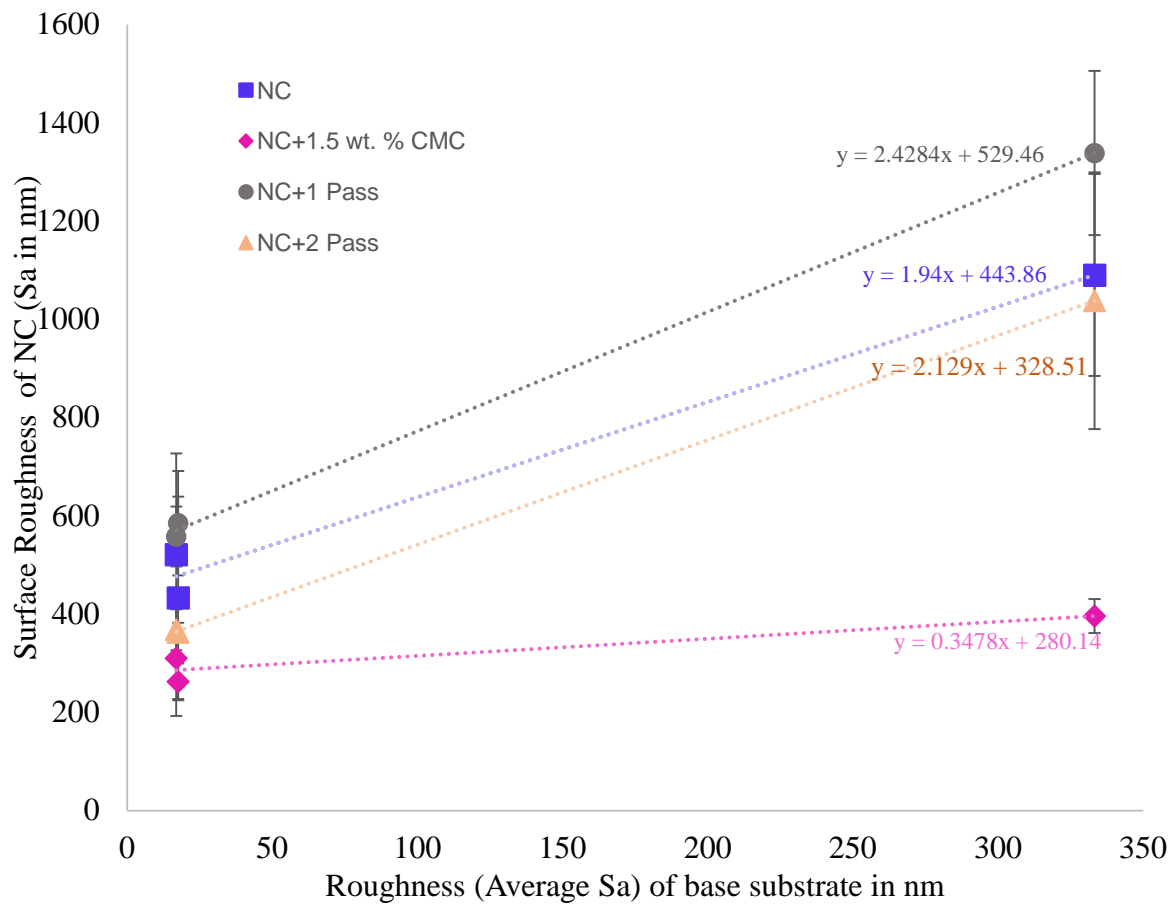
Figure 6: Effect of homogenization and CMC addition in NC suspension on the surface roughness (Sa) of NC film.

The nanoscale average roughness (Sa) of the NC film on the base substrate varied from 465 to 362 nm with SSS, when the nanofibril diameter varied $\approx$70 nm to $\approx$20 nm. It confirms the diameter of cellulose nanofibrils as another important controlling parameter on surface roughness. The correlation of each condition has been shown in Figure 7 and 8. Each intercept from the plot is the minimum surface roughness of NC film that could be achieved. It depends on the diameter of cellulose nanofibrils and its aspect ratio. Simultaneously, the roughness decreases with the fibre diameter as the lines with smaller fibre diameter are below the untreated NC. That means that decreasing the fibre diameter decreases the roughness, but that the roughness is still modifiable by changing the substrates. However, the high-pressure homogenization of cellulose nanofibers has small effect on the surface roughness of film
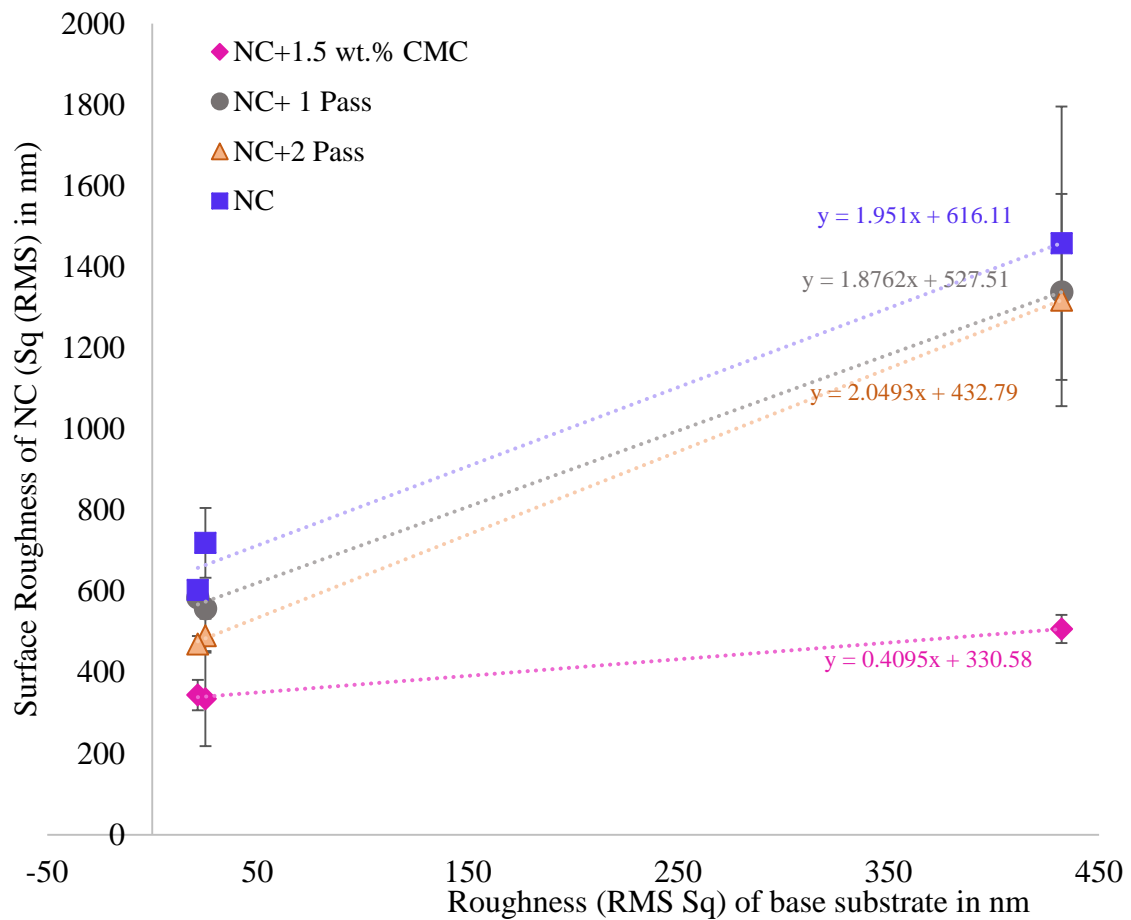
Figure 7: Effect of Homogenization and CMC addition in NC suspension on the RMS surface roughness. Sq of NC film.

The CMC results were very interesting. Both the slope and the intercept decreased when CMC was added with surface roughness which was much lower than the other three types of NC. The lower slope indicates that with the addition of CMC, the roughness becomes less dependent on the substrate roughness. Moreover, it will be worthwhile to investigate the addition of varying amounts of CMC and establish the minimum level of smoothness that is attainable using this method.

The plot between surface roughness of NC film and fibril diameter are shown in Figure 8 and 9. The intercept and slope of the correlation depends on the fibre diameter and aspect ratio which both decreased with number of passes in the high-pressure homogenization. High pressure homogenization consumes significant energy for fibrillation of fibres and increases the viscosity of the NC suspension, which could cause clogging in a homogenizer. Additionally,

the increased viscosity of NC suspension caused difficulties with spraying. Sometimes, the highly viscous NC suspension blocks the nozzle in the spray gun and results in poor spray jet of NC suspension. Adding carboxymethyl cellulose (CMC) to the unhomogenized NC suspension reduces fibre friction and enhance the smoothness of the film.
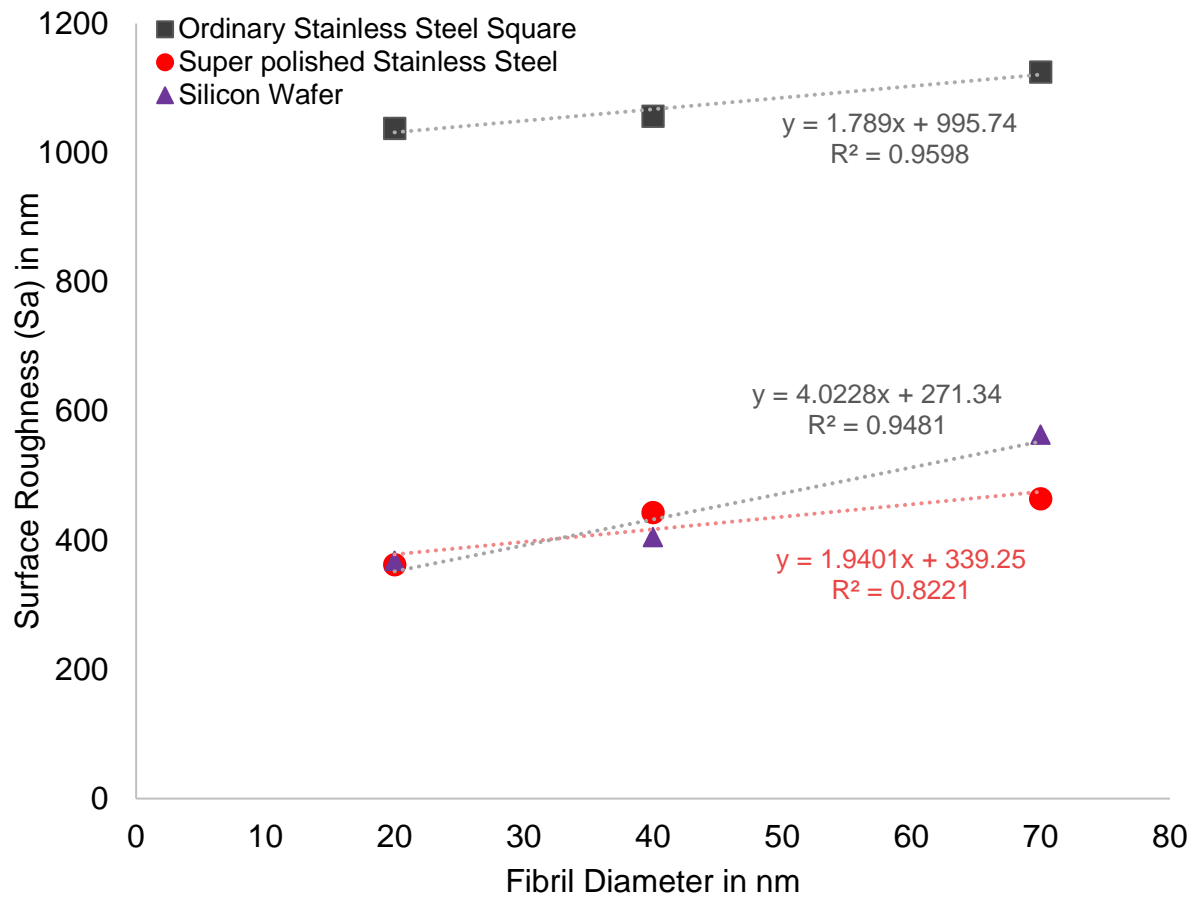
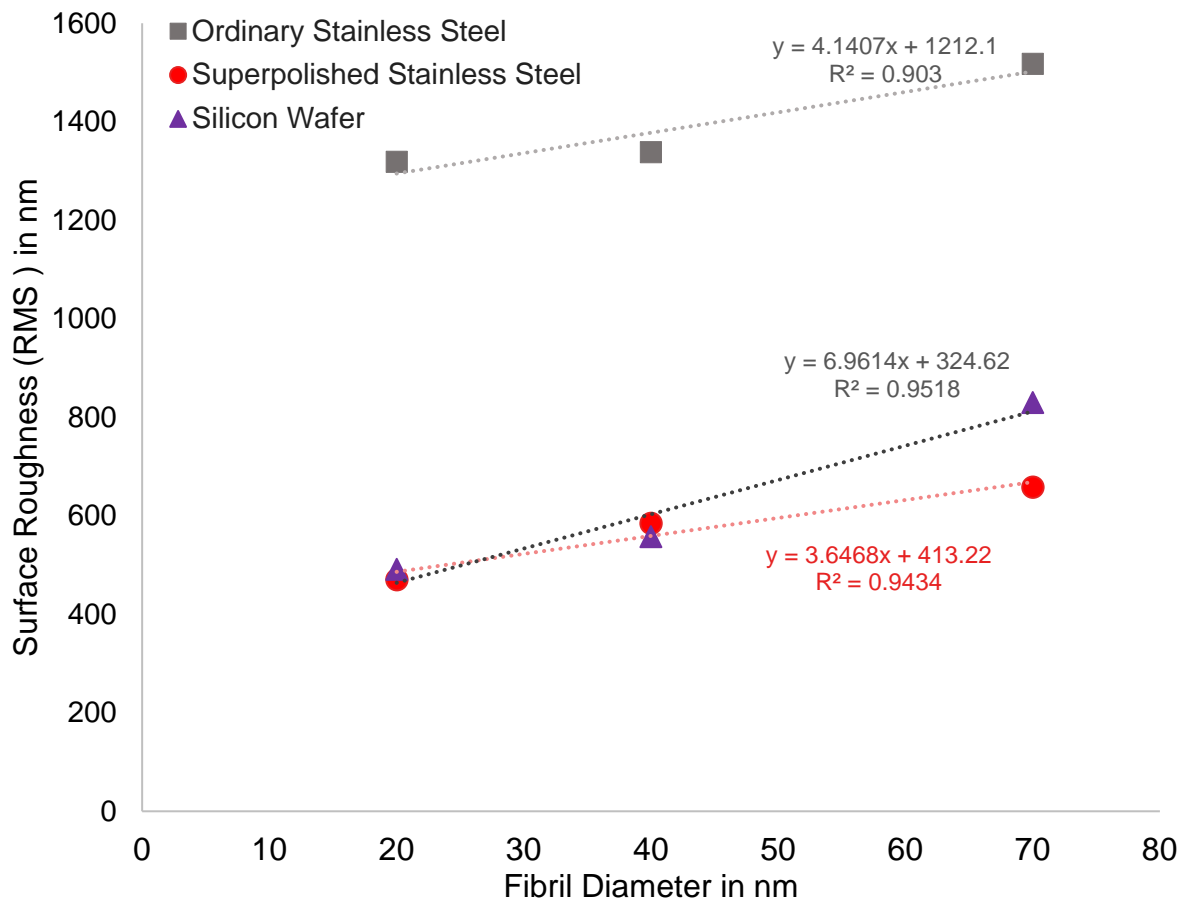Figure 8: Effect of fibril diameter of NC on roughness, Sa of NC film

Figure 9: Effect of fibril diameter of NC on RMS roughness, Sq of NC film

6.7. DISCUSSION

Spraying is a rapid process to form the NC film and can retain part of the smoothness of the base substrate. It is a single step process and the spraying time is independent of NC suspension concentration. The parameters controlling the smoothness of NC film are surface roughness of base substrates, fibril diameter of NC and friction modifiers such as carboxymethyl cellulose (CMC). The RMS roughness, Sq, of the NC film via spraying on the steel substrates varied from 1400 nm to 550 nm and was reduced to 336 nm with a loading of 1.5 wt.% CMC. The lowest value is under the maximum surface roughness of cellulose nanofibre material required for electronic applications, which is in the range of 310 nm to 470 nm [4]. This is comparable with the maximum surface roughness of plastic substrates, which is normally 400 nm, for fabricating electronic circuits. The smooth surface and texture of the base substrate like plastic material can be also replicated on the nanocellulose film [19, 20] produced via either solvent casting method or roll to roll method. The average roughness from

AFM measurements of the NC film via roll to roll method is $\approx$450 nm on the base substrate side and $\approx$800 nm on the free side of the film [21]. The surface roughness of NC film via vacuum filtration as a conventional method is 418 nm on free side and 331 nm on the filter side [10]. Sometimes, the NC film via filtration contains filter markings on the surface of the film affecting its roughness. Spray coating is a rapid method to prepare a suitable smooth NC films for developing functional electronic devices. The RMS roughness evaluated by AFM of rough side of spray coated NC film at an inspection area of 10 μm x 10 μm is 414 nm and 81 nm on the smooth side of film. The RMS roughness from optical profiler of NC film via vacuum filtration is 2673 nm on free side and 3753 nm on the filter side. The RMS for spray coated NC film is 389 nm on the side peeled from steel surface and 2087 nm on free side [10].

The NC suspension has strong inter-fibrillar interactions between cellulose nanofibrils and shows non-Newtonian thixotropic behaviour. It requires high shear force to decrease the viscosity of suspension. Due to this characteristic of NC, it could elevate the surface roughness of film via forming flocks or aggregation of fibrils in the film. Therefore, adding CMC into suspensions of NC reduces the friction between the surfaces of cellulose fibrils and enhances the dispersion of nanofibrils in the suspension [22-24]. The fibril interaction and friction in NC is reduced via ionic repulsion between nanofibrils resulting in good packing of the fibrils [25-27]. The ionic repulsion occurred between the carboxyl group of CMC and surface hydroxyl group of NC [28].

The surface roughness of NC film could be reduced by high pressure homogenization, which reduced the fibre diameter and length. When spraying on the SSS substrate, the RMS roughness was reduced from 550 to 470 nm after 2 passes through the homogenizer. However, beyond 2nd pass homogenization, the viscosity of the NC suspension increases and crosses the sprayable limits of Wagner 117 professional spray system, causing nozzle blockage in the spray gun. High pressure homogenization is also an extremely energy intensive process. The base substrates such as polished stainless steel and silicon wafer are also quite expensive. The most interesting finding was the effect of CMC. When this was added to raw NC suspension to reduce fibre friction and surface roughness of the film, the Sa and Sq for CMC – NC film decreased from 396±28 nm to 262±26 nm, 508±34 nm to 345±37 nm respectively, when spraying on ordinary stainless steel. This is very close to the range required for application as a plastic substrate for electronics.

The mechanism of replication of surface roughness from substrates to NC film remains obscure. Possibly, the mechanism can be explained with adhesion of fibrils and inter-fibre bonding with the substrate. Currently there are three different mechanisms proposed regarding the adhesion of cellulose fibres. Cellulose fibres have irregular surfaces and the interaction between the rough surfaces and interlocking of the fibres can produce adhesion. The interactions of the fibres and the base substrate is also influenced by the intermolecular diffusion of the cellulose chains and finally all of these components are controlled by force interactions. The interactions such as hydrogen bonding, van der Waals and electrostatic forces are important in cellulose fibres and can not only occur between the fibres and the substrate but also between the individual fibres themselves [29] [30].

Mechanical interlocking of cellulose nanofibres with substrates would be a common mechanism of replication of roughness from ordinary stainless-steel plate containing many complex scratches and lines. Both the square and circular stainless-steel plates, were not even and their surfaces had significant asperities compared to the silicon wafer and super polished stainless-steel surface. These larger asperities were imprinted on the NC films and produced rougher surfaces. Therefore, spray coated cellulose nanofibres were easier to peel from these surfaces. For the super polished stainless-steel surface, the height of asperities was much smaller and highly smooth surfaces were created due to the lack of large asperities. Super polished stainless-steel surface has an average Sa and Sq roughness of 17 nm and 22 nm, respectively and reflectivity of greater than 90% The surface hydroxyl groups of cellulose nanofibres interacts well with the surface resulting in a smoother NC film.

The silicon wafer used also has an ultra-smooth hydrophilic surface having an average Sa and Sq roughness of 17 nm and 25 nm, respectively. The surface hydroxyl groups of the NC interact with silicon surface via chemical bonding such as hydrogen bonding, van der Waals and electrostatic forces. Due to the formation of hydrogen bonds among the cellulosic nanofibrils, the fibril surfaces are in contact with the base substrate in the distance of molecular level. The reported molecular distances varies from 0.15 to 0.35 nm [31] [32] [29]. These values are much smaller than the actual dimension of the surface roughness of fibres. Thus, the roughness can drastically limit the molecular contact between adjacent surfaces [33].

It is found that 1.5 wt. % CMC added into NC suspension drastically reduced the surface roughness of NC film via spraying. CMC is a water soluble polysaccharide that could modify rheology of the NC suspension and by adsorbing onto the surface of NC [34] [35].

6.8. CONCLUSION

Highly smooth NC films were prepared via a one step process of spraying on the impermeable substrates. Their smoothness can be engineered by simply changing the base substrate roughness and part of its surface roughness is replicated on the NC film. Smoothness of the film was further increased via spraying of reduced NC fibril diameter suspension and also adding polymers into NC suspension. The parameters controlling the roughness of the NC film is in the order of CMC addition >fibril diameter >base substrate. The results confirm spraying as a rapid and one step process for engineering the surface roughness of NC film for commercial applications.

6.9. ACKNOWLEDGEMENTS

6.10. REFERENCE

1. Ummartyotin, S., M. Sain, and P. Qvintus, Cellulose in Printed Electronics, in HANDBOOK OF GREEN MATERIALS: 2 Bionanocomposites: processing, characterization and properties. 2014, World Scientific. p. 237-252.
2. Hübler, A., B. Trnovec, T. Zillger, M. Ali, N. Wetzold, M. Mingebach, A. Wagenpfahl, C. Deibel, and V. Dyakonov, Printed paper photovoltaic cells. Advanced Energy Materials, 2011. **1**(6): p. 1018-1022.
3. Sabo, R., J.-H. Seo, and Z. Ma. Cellulose nanofiber composite substrates for flexible electronics. in 2012 TAPPI International Conference on Nanotechnology for Renewable Materials. 2012.
4. Torvinen, K., J. Sievänen, T. Hjelt, and E. Hellén, Smooth and flexible filler-nanocellulose composite structure for printed electronics applications. Cellulose, 2012. **19**(3): p. 821-829.
5. Berk, Z., Chapter 27 - Food Packaging, in Food Process Engineering and Technology (Second Edition), Z. Berk, Editor. 2013, Academic Press: San Diego. p. 621-636.
6. Kantola, V., J. Kulovesi, L. Lahti, R. Lin, M. Zavodchikova, and E. Coatanéa, 1.3 Printed Electronics, Now and Future. Bit Bang, 2009. **63**.

7. Mautner, A., K.-Y. Lee, T. Tammelin, A.P. Mathew, A.J. Nedoma, K. Li, and A. Bismarck, Cellulose nanopapers as tight aqueous ultra-filtration membranes. Reactive and Functional Polymers, 2015. **86**: p. 209-214.

8. Salas, C., T. Nypelö, C. Rodriguez-Abreu, C. Carrillo, and O.J. Rojas, Nanocellulose properties and applications in colloids and interfaces. Current Opinion in Colloid & Interface Science, 2014. **19**(5): p. 383-396.

9. Varanasi, S. and W.J. Batchelor, Rapid preparation of cellulose nanofibre sheet. Cellulose, 2013. **20**(1): p. 211-215.

10. Shanmugam, K., S. Varanasi, G. Garnier, and W. Batchelor, Rapid preparation of smooth nanocellulose films using spray coating. Cellulose, 2017. **24**(7): p. 2669–2676.

11. Aulin, C., M. Gällstedt, and T. Lindström, Oxygen and oil barrier properties of microfibrillated cellulose films and coatings. Cellulose, 2010. **17**(3): p. 559-574.

12. Vernhes, P., M. Dubé, and J.F. Bloch, Effect of calendering on paper surface properties. Applied Surface Science, 2010. **256**(22): p. 6923-6927.

13. Shanmugam, K., H. Doosthosseini, S. Varanasi, G. Garnier, and W. Batchelor, Flexible spray coating process for smooth nanocellulose film production. Cellulose, 2018. **25**(3): p. 1725–1741.

14. Varanasi, S., R. He, and W. Batchelor, Estimation of cellulose nanofibre aspect ratio from measurements of fibre suspension gel point. Cellulose, 2013. **20**(4): p. 1885-1896.

15. De Oliveira, R., D. Albuquerque, T. Cruz, F. Yamaji, and F. Leite, Measurement of the nanoscale roughness by atomic force microscopy: basic principles and applications, in Atomic force microscopy-imaging, measuring and manipulating surfaces at the atomic scale. 2012, IntechOpen.

16. Xu, R., P.D. Fleming, A. Pekarovicova, and V. Bliznyuk, The effect of ink jet paper roughness on print gloss. Journal of imaging science and technology, 2005. **49**(6): p. 660-666.

17. Xu, R., P.D. Fleming, and A. Pekarovicova. The effect of ink jet papers roughness on print gloss and ink film thickness. in NIP & Digital Fabrication Conference. 2004. Society for Imaging Science and Technology.

18. Raj, P., A. Mayahi, P. Lahtinen, S. Varanasi, G. Garnier, D. Martin, and W. Batchelor, Gel point as a measure of cellulose nanofibre quality and feedstock development with mechanical energy. Cellulose, 2016. **23**(5): p. 3051-3064.

19. Chinga-Carrasco, G., D. Tobjörk, and R. Österbacka, Inkjet-printed silver nanoparticles on nano-engineered cellulose films for electrically conducting structures and organic transistors: concept and challenges. Journal of Nanoparticle Research, 2012. **14**(11): p. 1-10.

20. Tammelin, T., A. Salminen, and U. Hippi, Method for the preparation of NFC films on supports. WO, 2013. **2013060934**: p. A2.

21. Peresin, M.S., J. Vartiainen, V. Kunnari, T. Kaljunen, T. Tammelin, and P. Qvintus. Large-scale nanofibrillated cellulose film: an overview on its production, properties, and potential applications. in Book of abstracts international conference of pulping, papermaking and biotechnology. 2012.

22. Yan, H., T. Lindstrom, and M. Christiernin, Some ways to decrease fibre suspension flocculation and improve sheet formation. Nordic Pulp and Paper Research Journal, 2006. **21**(1): p. 36.

23. Ahola, S., P. Myllytie, M. Österberg, T. Teerinen, and J. Laine, Effect of polymer adsorption on cellulose nanofibril water binding capacity and aggregation. BioResources, 2008. **3**(4): p. 1315-1328.

24. Zauscher, S. and D.J. Klingenberg, Friction between cellulose surfaces measured with colloidal probe microscopy. Colloids and Surfaces A: Physicochemical and Engineering Aspects, 2001. **178**(1-3): p. 213-229.

25. Yoshiharu, N., K. Shigenori, W. Masahisa, and O. Takeshi, Cellulose microcrystal film of high uniaxial orientation. Macromolecules, 1997. **30**(20): p. 6395-6397.

26. Ebeling, T., M. Paillet, R. Borsali, O. Diat, A. Dufresne, J. Cavaille, and H. Chanzy, Shear-induced orientation phenomena in suspensions of cellulose microcrystals, revealed by small angle X-ray scattering. Langmuir, 1999. **15**(19): p. 6123-6126.

27. Orts, W., L. Godbout, R. Marchessault, and J.-F. Revol, Enhanced ordering of liquid crystalline suspensions of cellulose microfibrils: a small angle neutron scattering study. Macromolecules, 1998. **31**(17): p. 5717-5725.

28. Filpponen, I., E. Kontturi, S. Nummelin, H. Rosilo, E. Kolehmainen, O. Ikkala, and J. Laine, Generic method for modular surface modification of cellulosic materials in aqueous medium by sequential "click" reaction and adsorption. Biomacromolecules, 2012. **13**(3): p. 736-742.

29. Gardner, D.J., G.S. Oporto, R. Mills, and M.A.S.A. Samir, Adhesion and surface issues in cellulose and nanocellulose. Journal of adhesion science and technology, 2008. **22**(5-6): p. 545-567.

30. Fornué, E.D., G.G. Allan, H.J.C. Quiñones, G.T. González, and J.T. Saucedo, Fundamental aspects of adhesion between cellulosic surfaces in contact–a review. O Papel, 2011. **72**(9): p. 85-90.

31. Pelton, R., On the design of polymers for increased paper dry strength-a review. Appita Journal: Journal of the Technical Association of the Australian and New Zealand Pulp and Paper Industry, 2004. **57**(3): p. 181.

32. Linhart, F., Some thoughts on the mode of action of paper strength agents. Wochenblatt fur Papierfabrikation, 2005. **133**(11-12): p. 662-+.

33. Hubbe, M.A., Bonding between cellulosic fibers in the absence and presence of dry-strength agents–A review. BioResources, 2007. **1**(2): p. 281-318.

34. Liu, Z., H. Choi, P. Gatenholm, and A.R. Esker, Quartz Crystal Microbalance with Dissipation Monitoring and Surface Plasmon Resonance Studies of Carboxymethyl Cellulose Adsorption onto Regenerated Cellulose Surfaces. Langmuir, 2011. **27**(14): p. 8718-8728.

35. Orelma, H., I. Filpponen, L.-S. Johansson, M. Österberg, O.J. Rojas, and J. Laine, Surface Functionalized Nanofibrillar Cellulose (NFC) Film as a Platform for Immunoassays and Diagnostics. Biointerphases, 2012. **7**(1): p. 61.

CHAPTER 7

CONCLUSION AND FUTURE PERSPECTIVE

THIS PAGE HAS BEEN INTENTIONALLY LEFT BLANK

Contents

THIS PAGE HAS BEEN INTENTIONALLY LEFT BLANK

7. CONCLUSION

Nowadays there is the pressure to replace synthetic plastic films with natural polymers. Nanocellulose is readily available biomaterial from lignocellulosic biomass and has the potential for developing many functional materials. Nanocellulose films have suitably low oxygen and reasonably low water vapour permeability for food packaging applications. The existing methods for the production of nanocellulose films limit commercialization. These methods are not as fast as for manufacturing plastic films. Therefore, there is a necessity for the rapid production of nanocellulose films for commercialization in various functional applications. Spraying is a fast process for forming nanocellulose either as a barrier layer on the cellulosic substrates or as a self-standing sheet. However, the previously reported method in the literature still requires considerable time as it uses conventional filtration after spraying.

This thesis focus on a new concept on nanocellulose film preparation via spraying of NC on the polished impermeable metal surface. This concept has successfully translated into a laboratory scale process for the production of nanocellulose film. This method greatly enhanced operator productivity through the confirming operation time less than a minute. Spraying provides a reduction in an order of magnitude in time in film formation than vacuum filtration process. This process has been effectively implemented to produce composites as high-performance barrier materials and to produce smooth nanocellulose films for flexible electronics. Additionally, the recyclability of spray-coated nanocellulose film has been confirmed. The following sections give the major achievements of this thesis.

7.1. THE FUNDAMENTAL CONCEPT OF SPRAYING NC ON STAINLESS STEEL PLATES

The rapid preparation of NC films was developed through the spraying of NC fibres on stainless steel plates. This method reduced time consumption for forming a film from 10 mins in vacuum filtration to 1 minute. The basis weight and thickness of the NC film could be tailored by suspension concentration. The spraying process was not affected by suspension concentration from 1 wt.% to 2. wt.%. It was observed that the RMS roughness of spray-coated side NC film was 389 nm evaluated from an optical profiler and 81 nm from AFM. It is an added advantage in this method to engineer the surface of a film without any further treatments.

7.2. FLEXIBLE SPRAYING PROCESS AND SUSTAINABILITY

The base concept was further extended into a flexible spraying process to produce a uniform NC film. The properties of spray coated NC film were comparable with films produced from vacuum filtration. The bulk properties of spray coated NC film were independent on the process variables such as suspension consistency and process variables in spray coating. The uniformity of the NC film was controlled by these variables. The uniformity of the film increased when spraying of NC suspension at solids concentrations between 1.5 wt. % to 1.75 wt. % and was higher than that of the film prepared via vacuum filtration. The good uniform spray-coated NC film has a higher tensile index than that of a vacuum filtered film. Given this correspondence, spray coating is a more efficient process for the production of NC film.

The sustainability and recyclability of spray-coated NC films should also be an important consideration. Nano-cellulose films, created via spraying, were evaluated for barrier performance and strength and were recycled into similar NC film via vacuum filtration. The fourth chapter explored a sustainable pathway to producing barrier films.

7.3. APPLICATION OF SPRAYING PROCESS

The developed spraying process was implemented to develop two functional materials namely high barrier performance nanocomposite and smooth NC film. The high barrier performance nanocomposite was produced via spraying of NC-MMT on the stainless steel plates. Unlike vacuum filtration, the operation time for the spraying process was independent of MMT concentration in the NC suspension.

7.3.1. HIGH-PERFORMANCE NANOCOMPOSITE

The nanocomposite from nanocellulose and MMT (Sodium Bentonite) via a flexible spray coating process is developed. The effect of nanoclay (MMT) addition and homogenization on mechanical and barrier properties of the nanocomposite were studied. Additionally, the interaction of MMT with nanocellulose was evaluated as a function of MMT loading in the nanocomposite and size of the cellulose fibrils after high-pressure homogenization. Critical issues were addressed include the structure size and orientation of the nanoclay within the nanocellulose matrix and the relationship to barrier performance. The lowest WVP of the 20 wt.% MMT loaded and homogenized composite was reported to be 8.3 x 10^{-12} g/m.s.pa and comparable with synthetic plastics.

7.3.2. SMOOTH NANOCELLULOSE FILM

This chapter explores another application of spray coating to produce smooth nanocellulose films and focuses on engineering its surface smoothness. This smoothness of the nanocellulose film should play a major role in the performance of the material in the fabrication of various cellulose-based functional materials such as printed electronics, designing of bioactive papers as diagnostics, cellulose-based transformers and solar panel, fabrication of organic LED and the development of piezoelectric sensors and nanocellulose based transistors.

Spraying nanocellulose on the surfaces with low to high surface roughnesses were used to quantify the factors controlling the surface smoothness/roughness of the NC film. The factors that control the surface roughness and uniformity of nanocellulose film, including nanofibre diameter, substrate surface roughness and processing conditions, are investigated and given as the 6th chapter of the thesis.

This work enhances the scope of nanocellulose as high-performance barrier materials and a potential alternative for synthetic plastic packaging. Through spray coating, the operation time for forming nanocellulose film is less than a minute. This method has excellent potential for fast forming of multiple sheets when compared with vacuum filtration. However, the drying of spray-coated wet film takes more than 24 hours under air drying in a controlled laboratory environment. Improving the drying process on the wet film is a future research work and out of the scope of the thesis work. The formation of film via spraying is the predominant objective in this research and compared the quality of the spray coated film with the film prepared from vacuum filtration. The drying of the wet film formed via spraying is outside of the scope of the research and further research on drying of spray-coated wet film is required. The drying of the wet film takes much longer than the film formation. Spraying of nanocellulose on the polished impermeable surface produced the films with a shiny surface, which could be a platform for the numerous functional devices with a sustainable approach.

7.4. FUTURE PERSPECTIVE

7.4.1. RE-ENGINEERING OF SPRAY COATING SYSTEM

The spray system should be automated to increase the productivity of NC film production and to automate the control the basis weight and thickness of the film. It should be

operated via a control panel with the help of data acquisition software such as Lab View. A computational and experimental analysis of the spray jet from the spray nozzle should be performed and correlated with NC film properties. Spraying fibrous material is quite different from spraying a homogenous solution of particles and it is recommended to further investigate the mechanism of film formation on the base surface. With the support of a high-speed camera, the spraying pattern from the nozzle should be investigated. Computational fluid dynamics (CFD) analysis of spray jet from the nozzle should be performed. A correlation with spray patterns and NC film properties should be developed and used to design a spray system for NC or any fibrous material. This could then be used for scaling up the spraying process at an industrial level.

The removal of water from wet film formed via spray coating is a serious limitation in this technology. The air drying of the wet film is a feasible technique to remove the water from the spray-coated suspension and consumes 1 hour in a laboratory trial in an air oven. The temperature of an air oven was maintained at 105°C. But 24 hour was taken to dry spray-coated wet film in an open-air drying.

Recently, additional studies showed that the time taken for drying of the spray-coated wet film varied from 4 hours to 2 hours under an air oven-drying at 50°C and 75°C respectively. The spraying of NC onto a continuous steel substrate followed by rapid drying on the same substrates would be a feasible process. In industrial practice, the waste heat recovered to dry the wet film from spraying through the tunnel dryer. Additionally, Yankee dryer and Condebelt technology can be applied for continuous drying process of wet film (Stenström, 2019).

7.4.2. INVESTIGATE THE STRUCTURE OF SPRAY COATED NC FILM

The structure of spray-coated NC film should be investigated with X-Ray Tomography and TEM Tomography to view 3D and 4D of the spray coated film and compare it with the film from vacuum filtration. Numerous properties of spray-coated NC films should be investigated for proving their functional applications including as barriers, or as bioactive films for controlled delivery of drugs. The structure-activity relationship of NC film can be investigated.

7.4.3. PROCESSING OF NEW MATERIALS VIA SPRAYING

Spraying can provide a new platform for processing of new materials such as films, composites and coating on the base material, although these applications are still in the

laboratory stage of development. Spraying fibrous material such as collagen, keratin and chitosan, alone or with nanocellulose, on the metal surface could be utilized to fabricate films, scaffolds and bioactive coatings.

7.4.4. PROCESSING OF BARRIER LAYERS ON THE BASE SHEET

When comparing with vacuum filtration, spraying is the fastest process to produce materials such as barrier coatings on the base sheets, bioactive coatings on the implant metals, composite with an inorganic coating on the base sheet and antimicrobial coatings on the cellulosic substrates. This spray application limitations in the removal of water from the coated surface and required a rapid drying process. These active coatings enhance their barrier properties, antimicrobial properties and strength for packaging applications.

In vacuum filtration, the drainage time for removal of the water in the suspension takes a lot of time. The drainage time depends on the type of filter used and cellulose nanofiber suspension. The handling of high solid content suspension is quite difficult in filtration to prepare the nanocellulose film. In addition, it is likely that the solids content achievable with vacuum filtration alone is likely to be much lower than what can be achieved when preparing conventional wood fibre sheets, due to the much smaller pores in the structure. In laboratory sheet making, it can be difficult to separate nanocellulose sheets from the filter to press and dry them.

On the other hand with spraying, the initial solid content can be increased significantly over vacuum filtration. The solid content in the suspension varied from 1.00 wt.% to 2.00 wt.% to prepare the pure NC film via spraying in this research. The maximum solids content of the pure NC film that could be sprayed was 2.5 wt.%, although these experiments were not routinely done due to the increased chance of plugging the spraying system. The solid content can be also increased beyond this range through the use of additives such as carboxymethylcellulose. The maximum solids content achieved in the work in this thesis was 3.25 wt. % by spraying 1.75 wt. % NC, together with 1.5 wt. % CMC. This then will require the removal of 29.7 g of water/ g of nanofibers, which is much lower than the 199 g of water/g of NC that must be removed when forming nanocellulose sheets using vacuum filtration at 0.5 wt.%. Further increases in solids content could be achieved by upgrading the spray system to operate with a pressure-driven feed and increasing the pressure of spraying. It is still an

open question as to the maximum solids that can be achieved, and how much lower this is than the solids content at the end of the vacuum filtration process.

Using the spraying process, the basis weight of the film can be tailored through simply adjusting the solid concentration in the suspension or the conveyor speed, while with vacuum filtration, the filtration time goes up exponentially with basis weight of the film.

The weakness of the spraying process is that the drying process will take more time than with vacuum filtration, because of the higher initial solids content. While this is not necessarily a problem at the laboratory scale, it remains a critical issue to be addressed before spraying technology can be scaled up. Possible options might be contactless drying such infrared ray drying method which is normally used in the drying of coatings on the paper. Yankee and Condebelt technologies could be used, as discussed in one of the previous options.

7.4.5. PROCESSING OF FUNCTIONAL COMPOSITES

The preparation of nanocomposite via spraying, functionalized by the addition of specific nanoparticles/nanofillers in the nanocellulose suspension, would be an important application of spray coating and allow the production of sustainable composites in a rapid manner, while boosting its functional properties. The addition of nanoparticles into the NC suspension does not affect the operation time of the spraying process. Spraying could provide a potential platform for developing functional composites such as fire-retardant materials, photocatalytic composites, photo luminescent composites, antimicrobial composite, heat insulating composites for flexible electronics with nano inorganics.

7.4.6. PROCESSING OF NC FILM FROM RECYCLED FIBRES

Spray coating can provide the fastest process to make NC film from recycled fibres and barrier layers of recycled NC on the base sheet. The recycled films showed reduced strength and increased water vapour permeability. The effect of recycling processing conditions, such as number of revolutions and temperature of disintegration should be investigated. The aim would be to identify the processing conditions that would allow the original properties to be preserved. Furthermore, the recycling of spray coated NC composites are so far not explored and the effect of recycling on the barrier performance and strength of

the composites is not investigated. Spraying recycled fibres with inorganics from composites to prepare recycled composite film will be a new application.

REFERENCE

Stenström, S. (2019). Drying of paper: A review 2000–2018. *Drying Technology*, 1-21. doi: 10.1080/07373937.2019.1596949

APPENDIX I

SUPPLEMENTARY INFORMATION

SUPPLEMENTARY INFORMATION

FOR

RAPID PREPARATION OF SMOOTH NANOCELLULOSE FILMS USING SPRAY COATING

Kirubanandan Shanmugam, Swambabu Varanasi, Gil Garnier and Warren Batchelor [*]

Department of Chemical Engineering, Australian Pulp and Paper Institute, Monash University, Melbourne, Vic 3800, Australia.

[*]E-mail: Warren.Batchelor@monash.edu

Scanning Electron Microscopy of Spray Coated NC Film
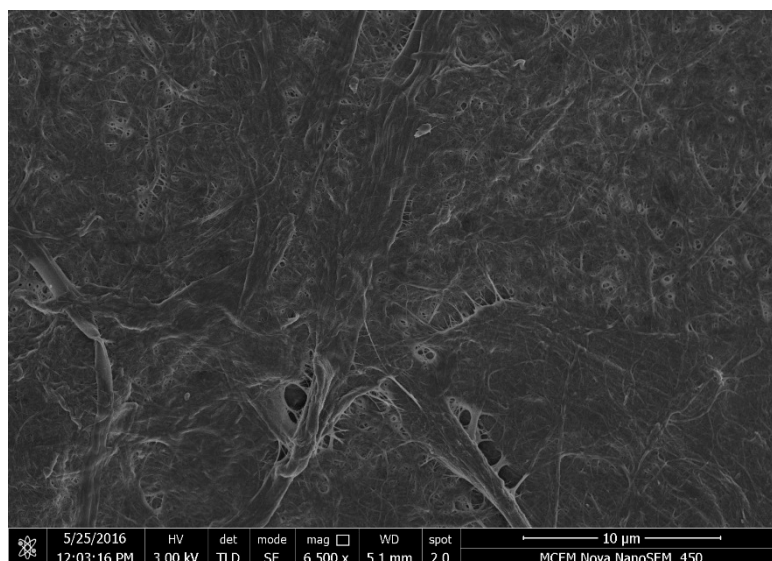
Free Surface

Surface exposed to metal
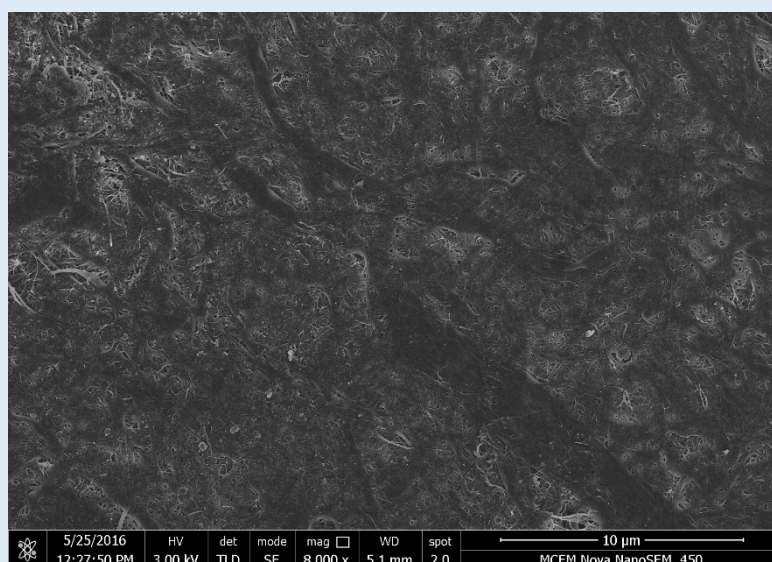
Figure A1: The micrograph of spray coated NC film at 10µm. The free surface of the film has significant roughness when compared to the smooth surface.

Atomic force micrographs of the spray coated NC Film:
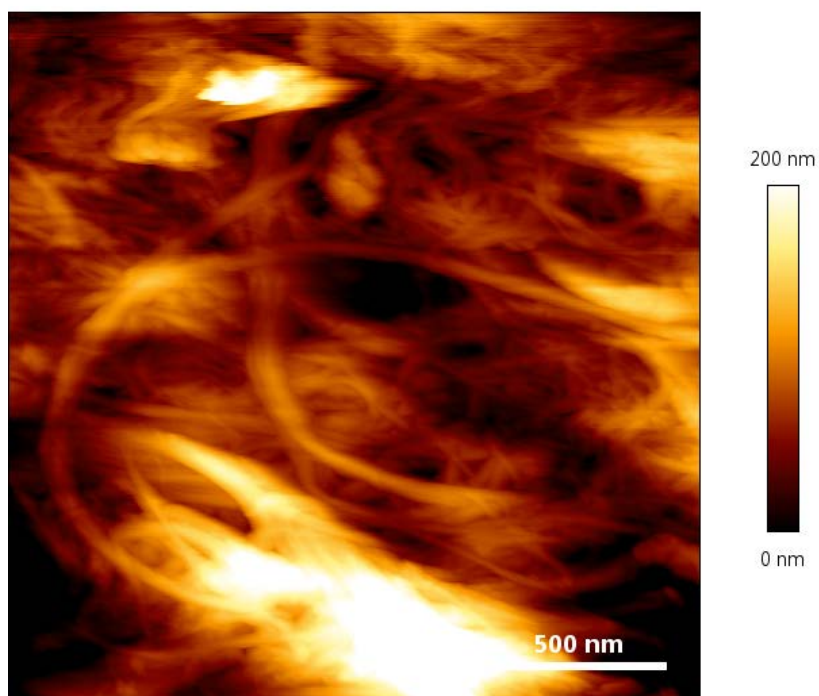
Free
Surface

Surface
Exposed
to steel
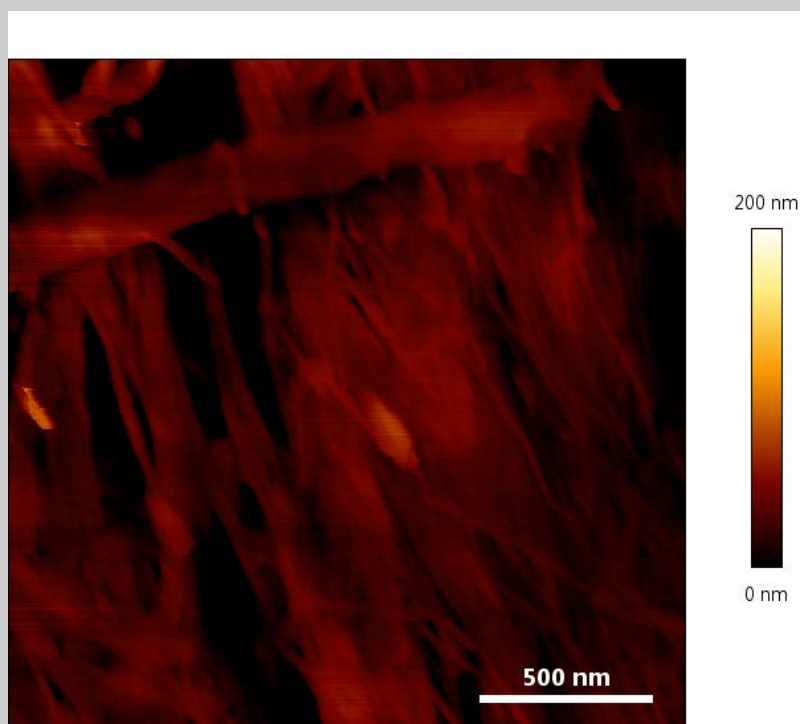
Figure A2: AFM image of spray coated NC Film. The film prepared by 1.5 wt. % NC Spraying on the base surface.

Atomic force micrographs of the spray-coated NC Film:
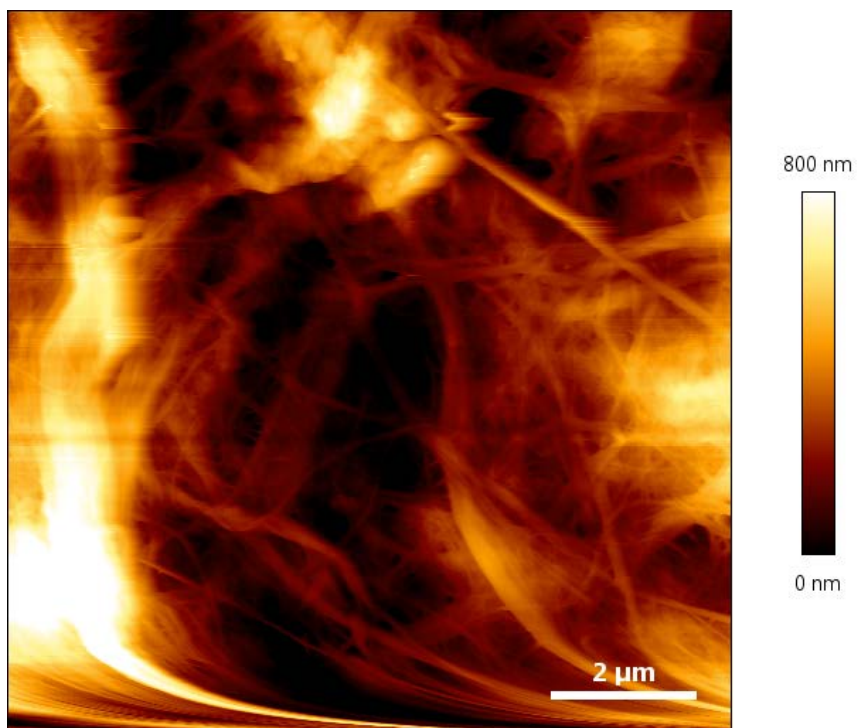
Free
Surface

Surface
Exposed
to steel
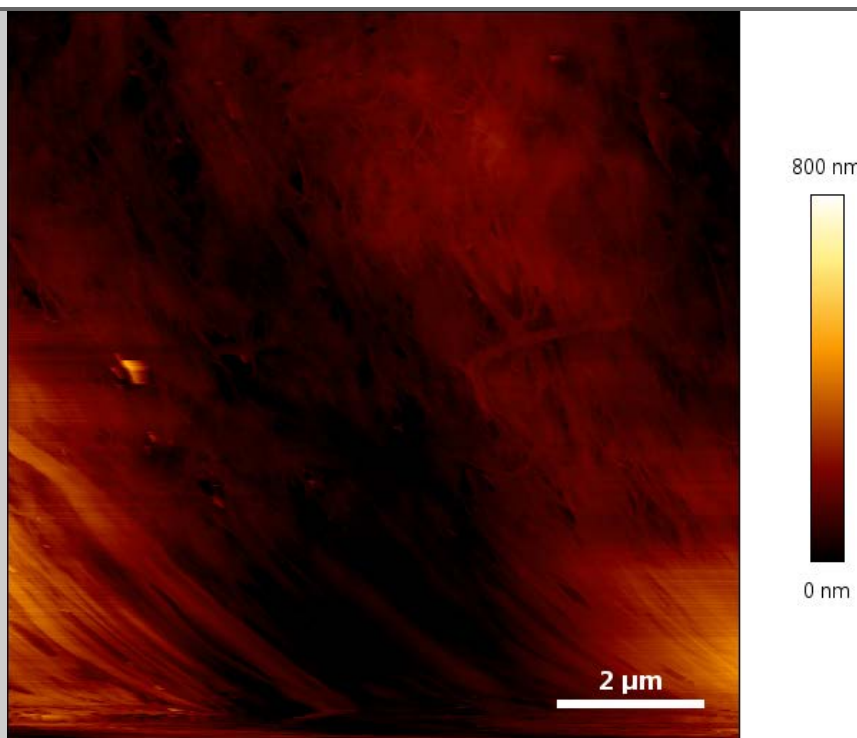
Figure A3: AFM image of spray coated NC Film. The NC film prepared by 1.5 wt. % NC Spraying on the base surface.

Atomic force micrographs of NC Film Prepared by Vacuum Filtration
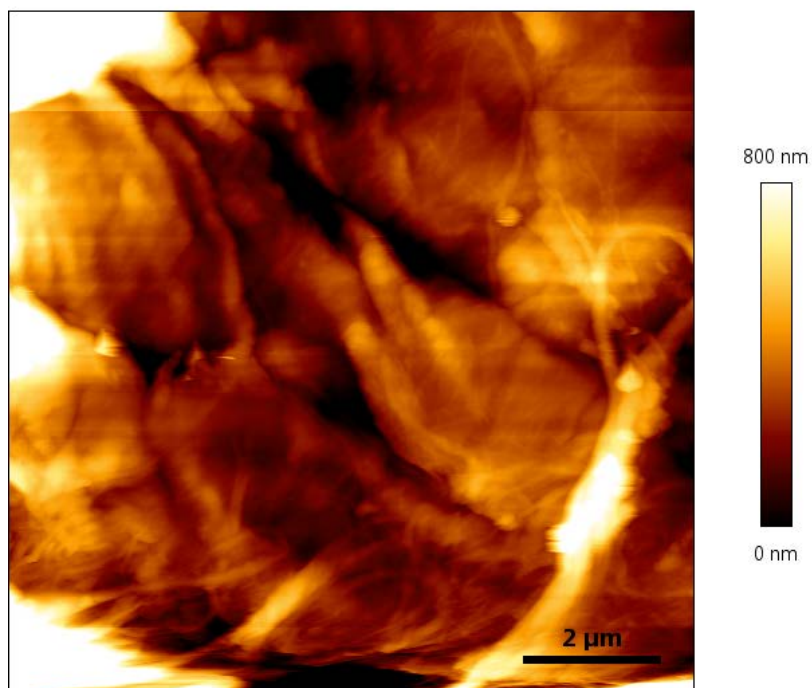
Free
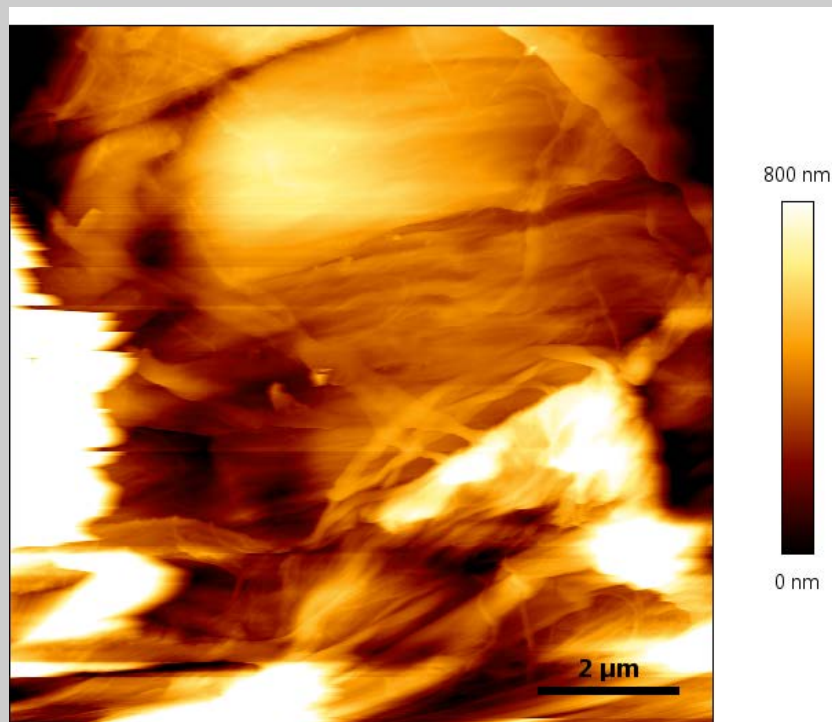
Filter
Surface

Figure A4 : AFM image of the film prepared via Vacuum filtration. The nano-cellulose film prepared by this method is used 0.2wt% nanocellulose suspension.

Atomic force micrographs of NC film Prepared by Vacuum filtration

Free
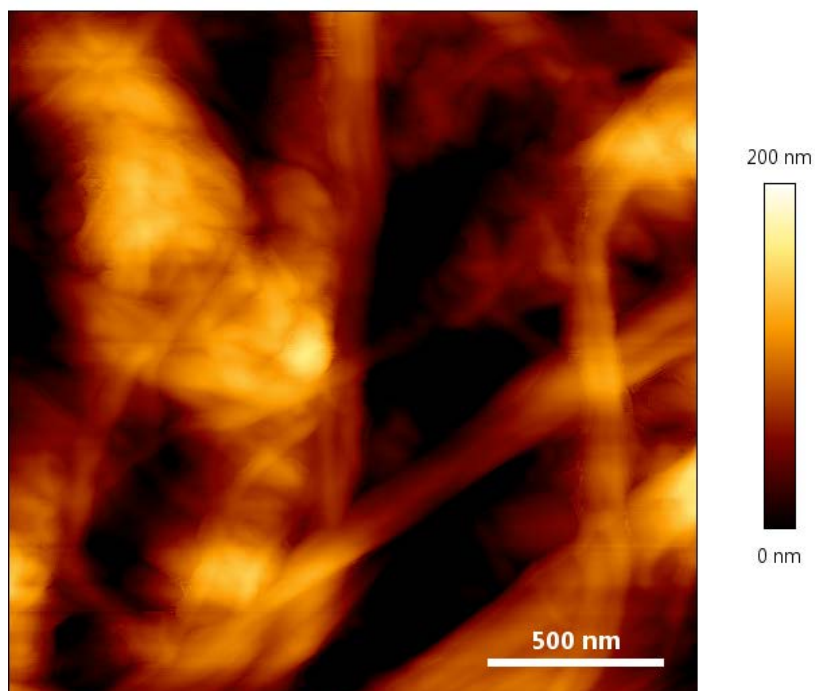
Filter
Surface
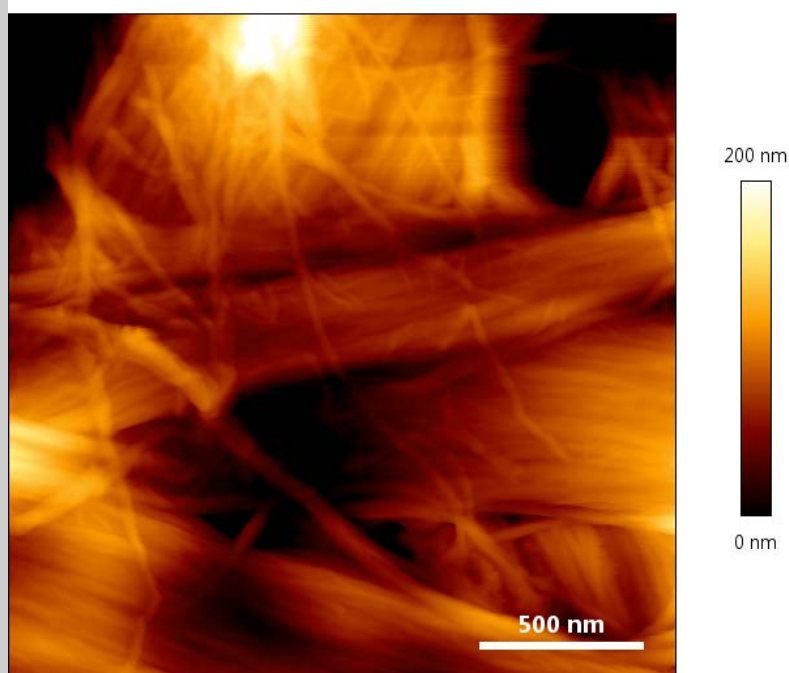
Figure A5 :AFM image of the film prepared via Vacuum filtration. The nano-cellulose film prepared by this method is used 0.2 wt. % NC suspension.

Table 1 and 2 – Thickness profile of the spray coated NC Film and NCFilm Prepared via vacuum filtration.

Data used for Thickness mapping of Spray Coated Film:

An 6 x 6 cm square section in the middle of spray coated NC film was tested for thickness (in microns) variation by measuring a matrix of 4x4 evenly spaced points

151	134	114	111
119	125	134	126
126	130	140	133
120	115	129	139

Table 2: Thickness Profile of the sheet prepared via Vacuum Filtration.

Data used for Thickness mapping of Sheet prepared via Vacuum Filtration:

An 6 x 6 cm square section in the middle of cellulose NC film prepared via vacuum filtration was tested for thickness (in microns) variation by measuring a matrix of 4x4 evenly spaced points,

128	116	116	113
117	111	110	113
113	112	112	114
116	109	109	122

Optical Profilometry Image of NC Film prepared via vacuum filtration:

Side 1

Label	Value	Units
Average	61.698	nm
Data Points	307200	
Percent Data Points	100	%
Ra	2149.87	nm
Rp	9229.153	nm
Rq	2672.966	nm
Rt	19937.212	nm
Rv	-10708.059	nm
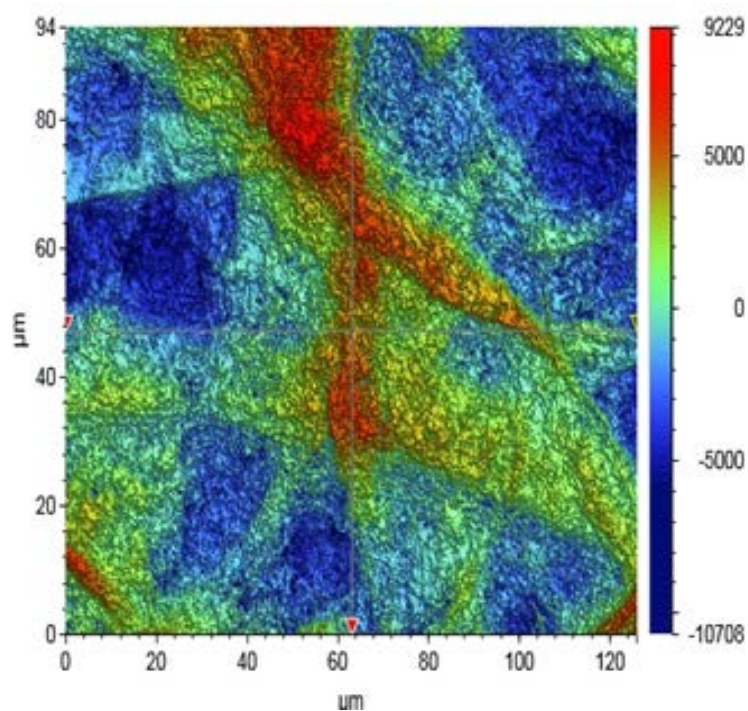
Side 2

Label	Value	Units
Average	114.429	nm
Data Points	307199.008	
Percent Data Points	100	%
Ra	3014.445	nm
Rp	14764.641	nm
Rq	3750.662	nm
Rt	27113.396	nm
Rv	-12348.754	nm
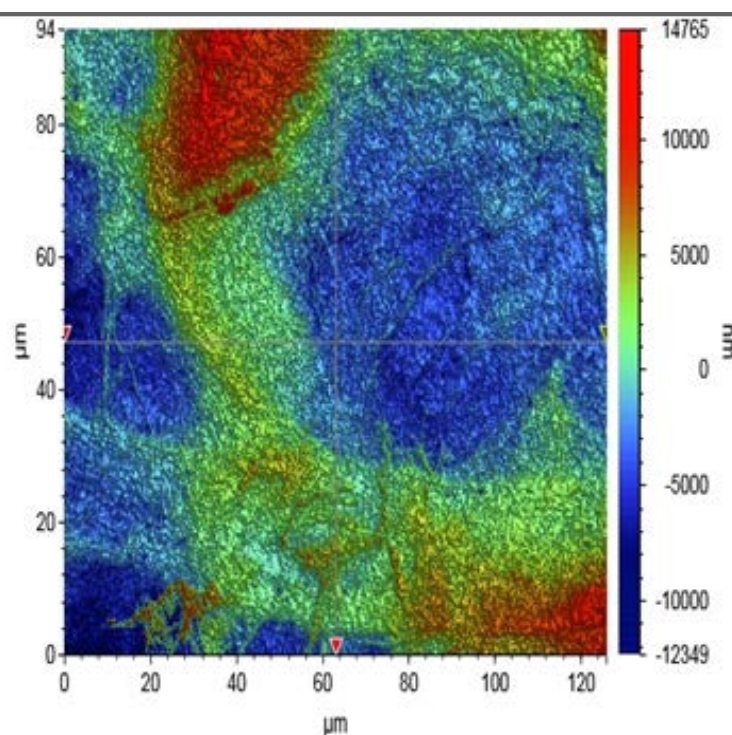
Figure A6: Optical profilometry image of nanocellulose film prepared via vacuum filtration

FLEXIBLE SPRAY COATING PROCESS FOR SMOOTH NANOCELLULOSE FILM PRODUCTION

Kirubanandan Shanmugam, Hamid Doosthosseini, Swambabu Varanasi, Gil Garnier, *Warren Batchelor

Bioresource Processing Research Institute of Australia, Department of Chemical Engineering, Monash University, Melbourne, Vic 3800, Australia.

*Corresponding Author, E-mail: Warren.Batchelor@monash.edu
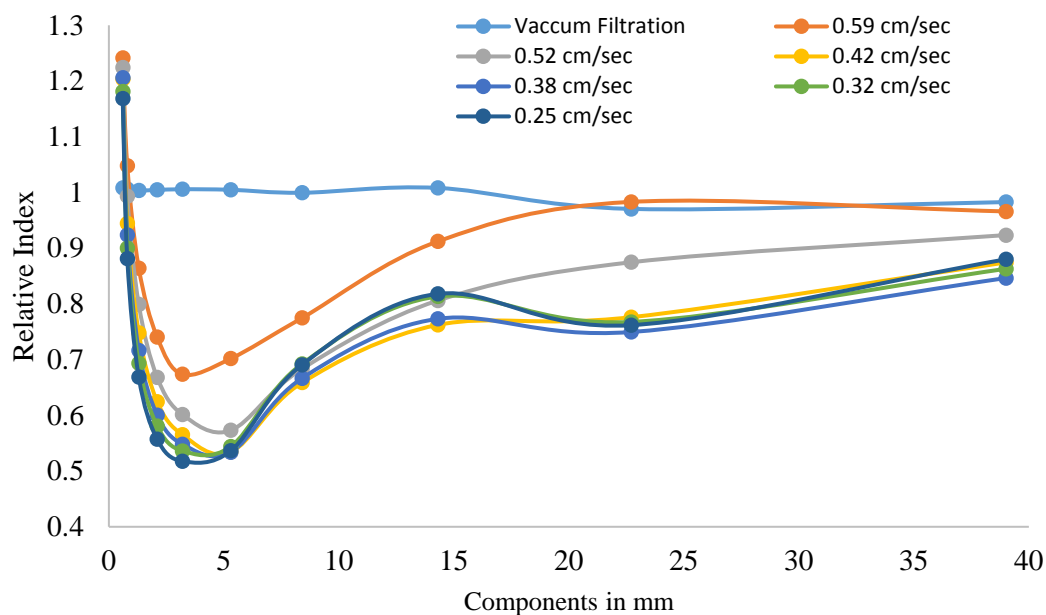
Figure B1 : Effect of Velocity on Optical Uniformity of Spray Coated NC Film at 1.5 wt. % solids concentration (series 1)
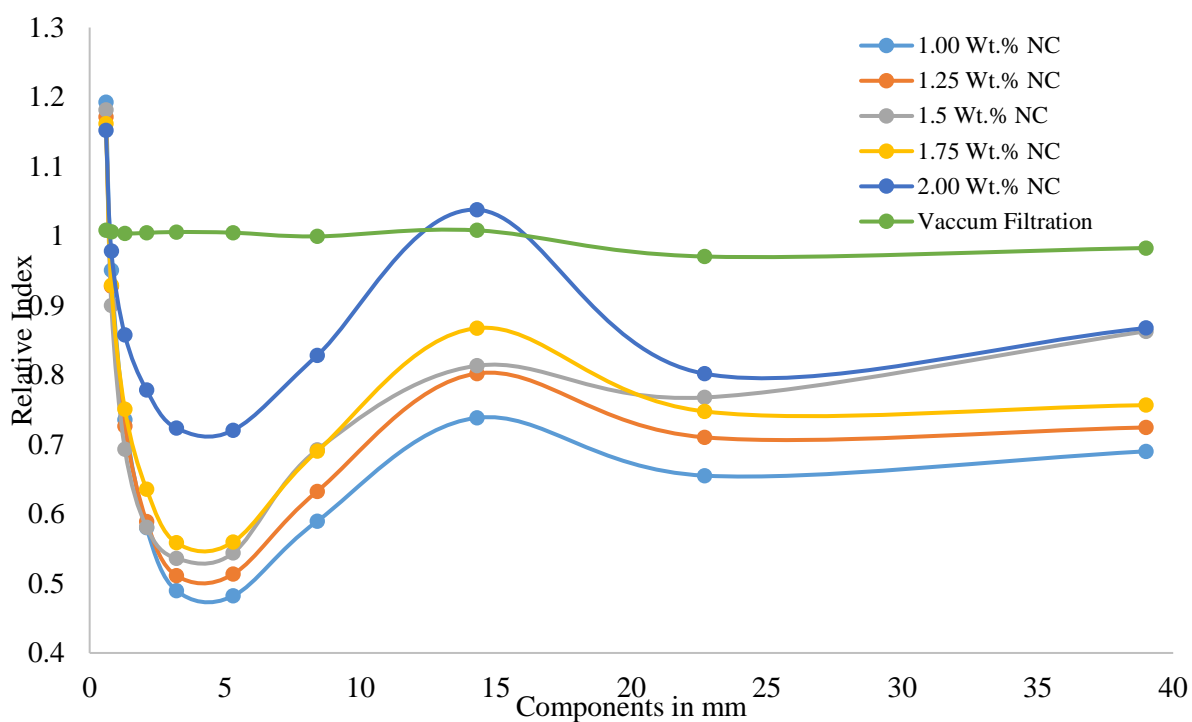
Figure.B2 –Effect of NC Suspension Concentration on the Optical Uniformity of Spray Coated NC film at a speed of 0.32 cm/s
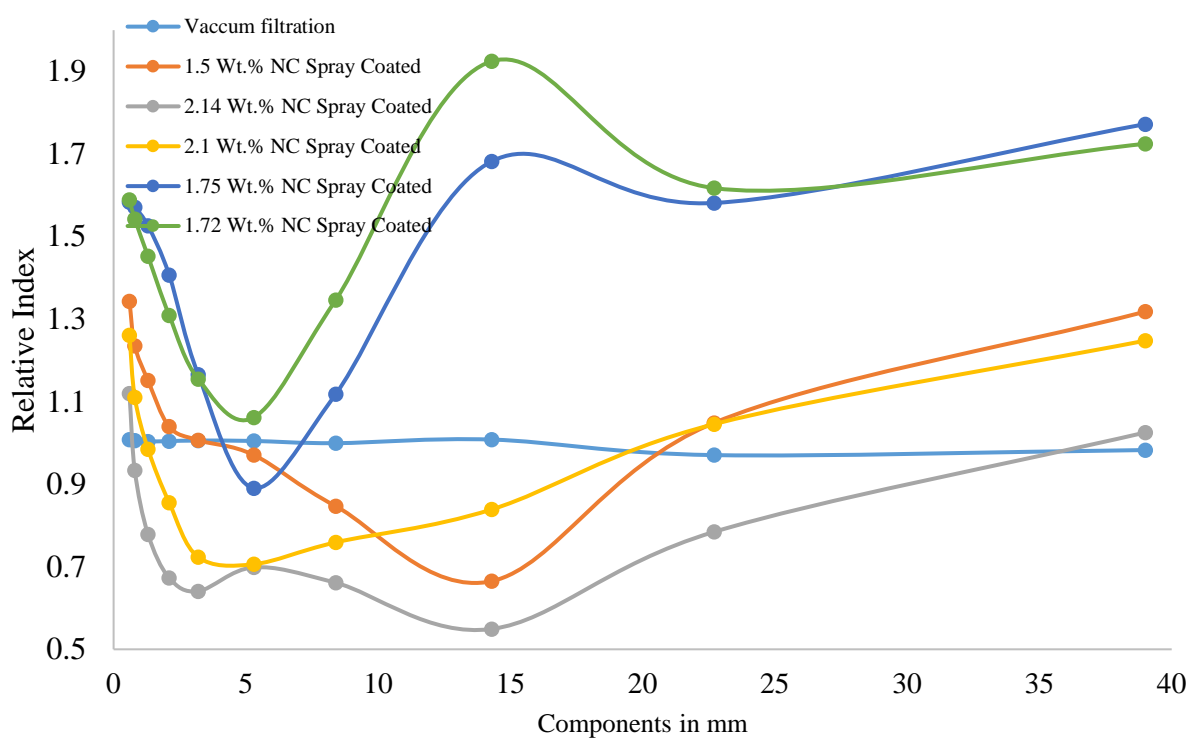
Figure B3: Optical Uniformity of Spray Coated NC film prepared Series 3 –Modified configuration in experimental set up.

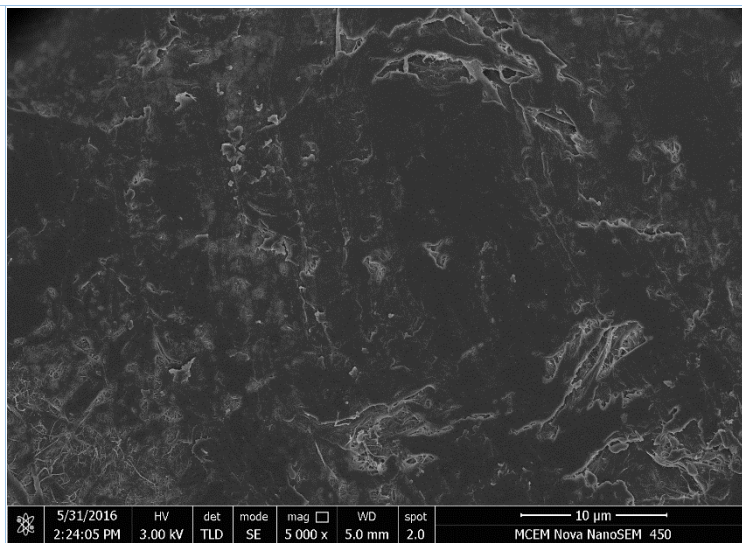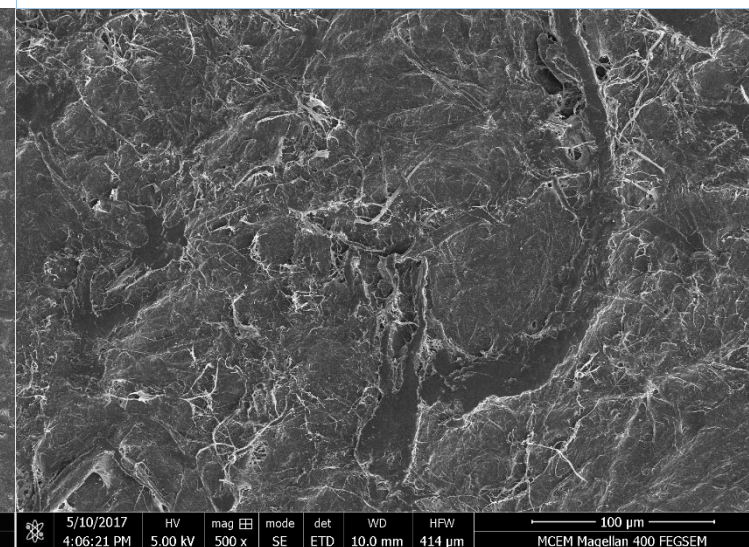| Scale	Spray Coated NC Film (Rough Side)	Vacuum Filtered NC Film (Side 1)
10µm		
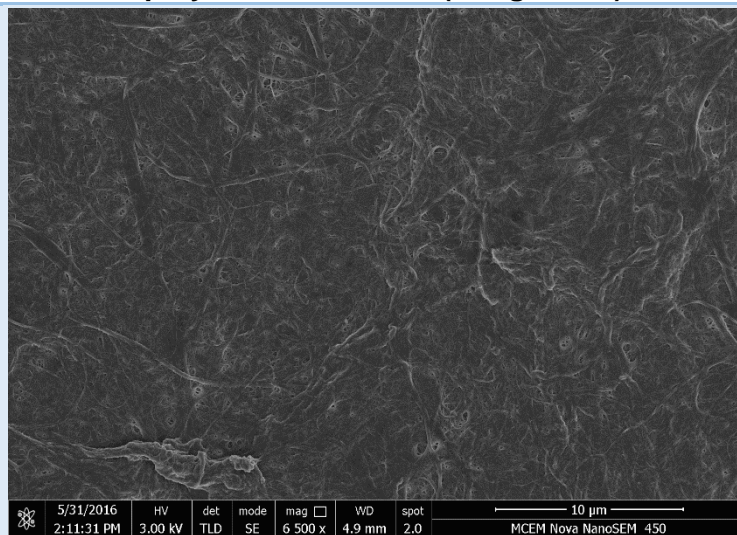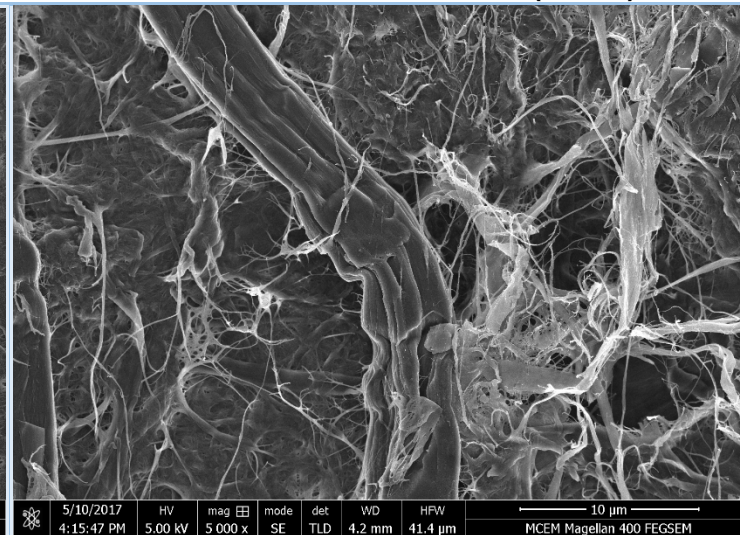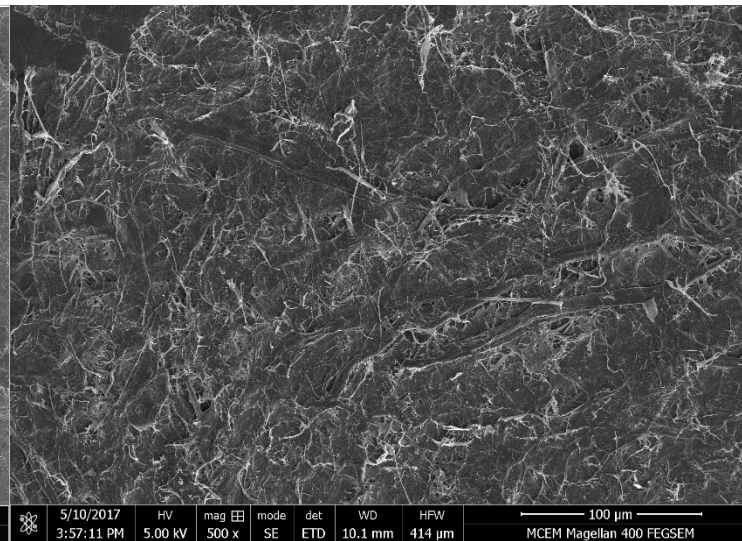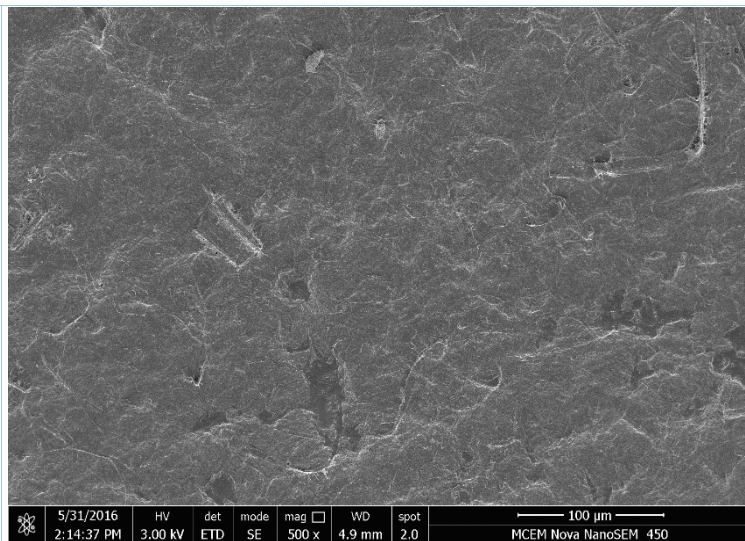
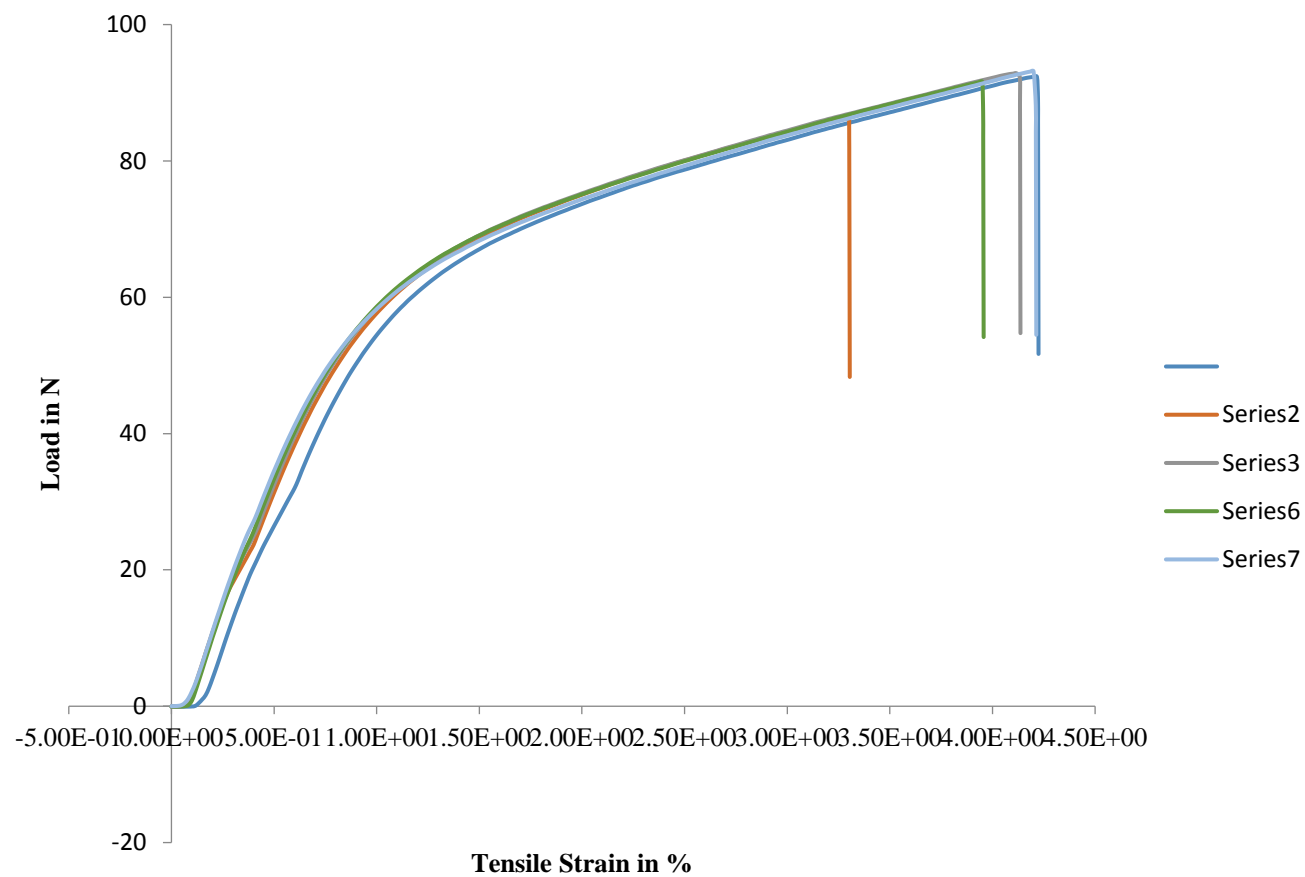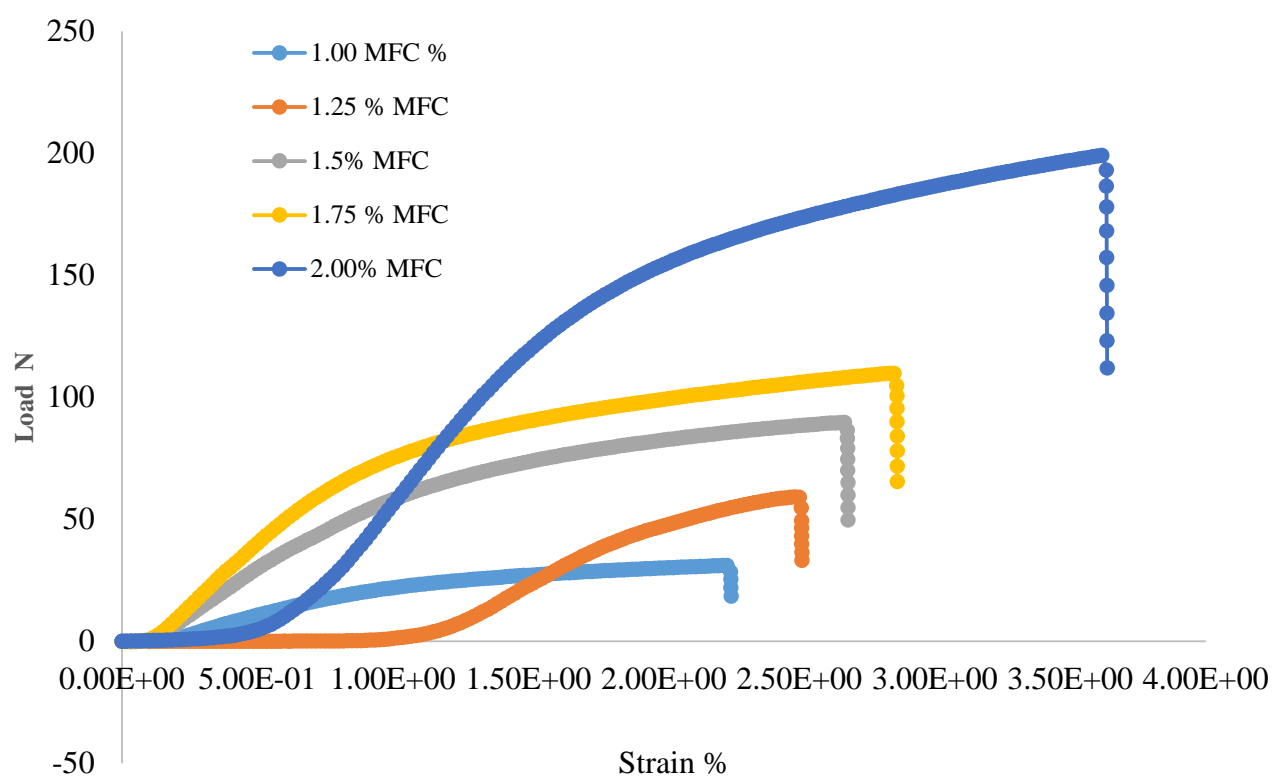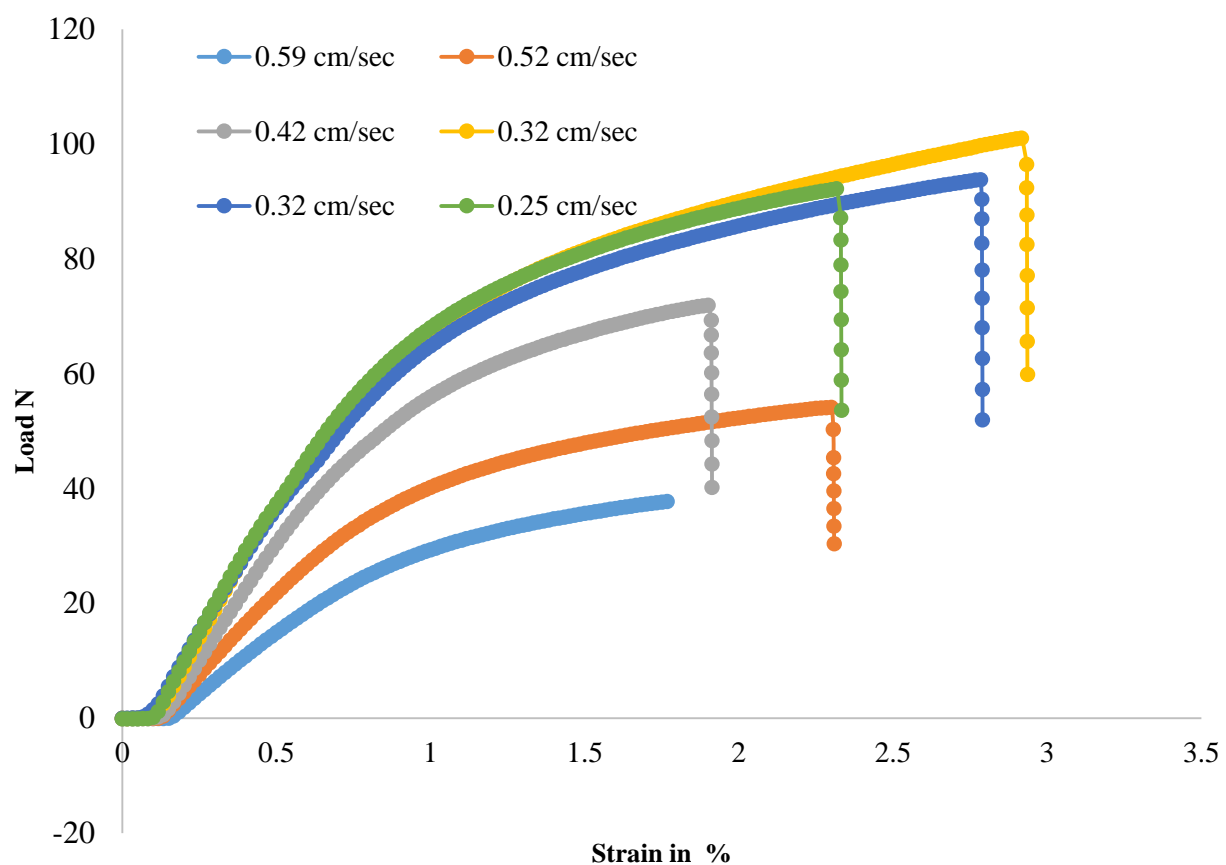| Scale | Spray Coated NC Film (Smooth Side) | Vacuum Filtered NC Film (Side 2 –Filter Side) |

100µm

10µm
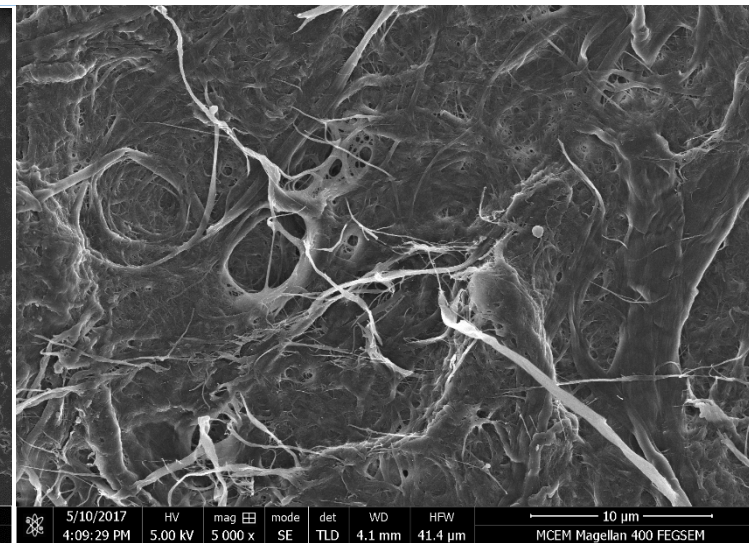
100µm
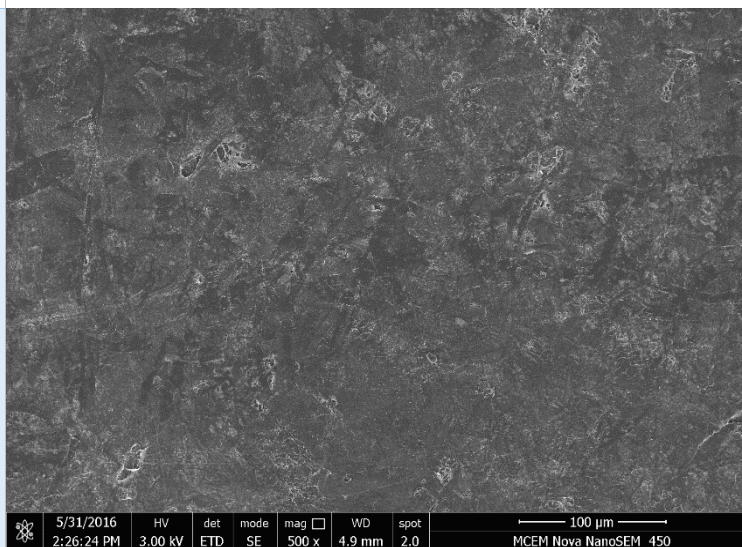
Figure – 4- Spray Coated NC film and Vacuum Filtered NC Film

Figure 5- Load- Strain Curve for 80 g/m² NC Film via Vacuum Filtration
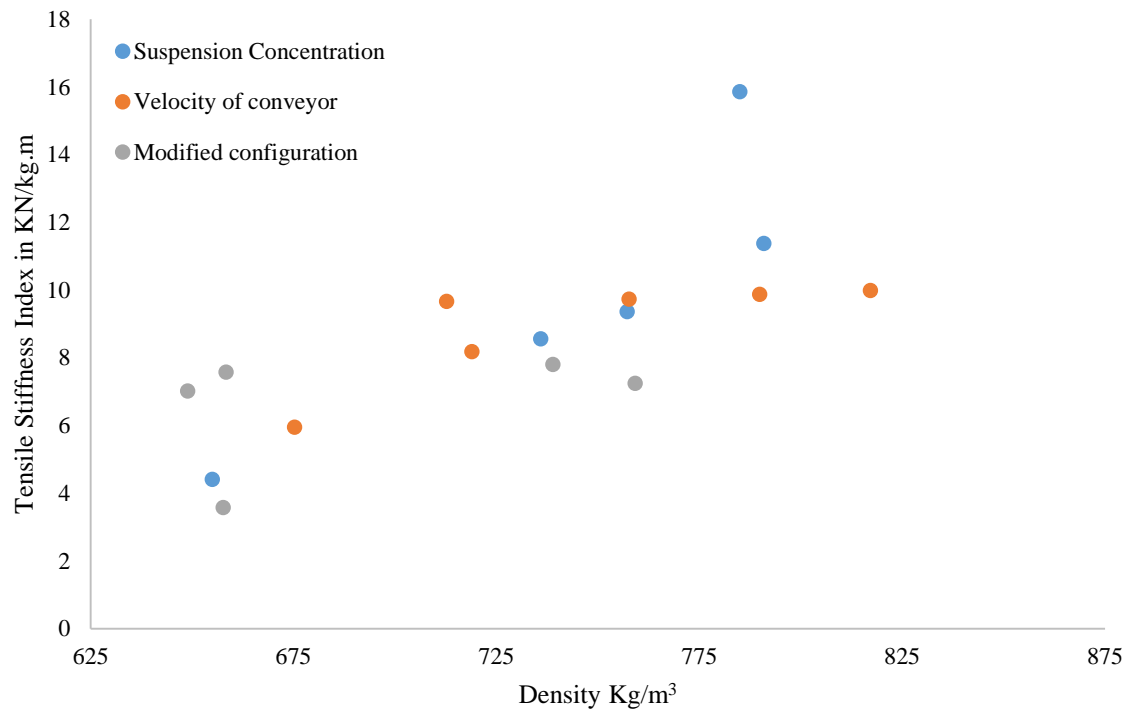
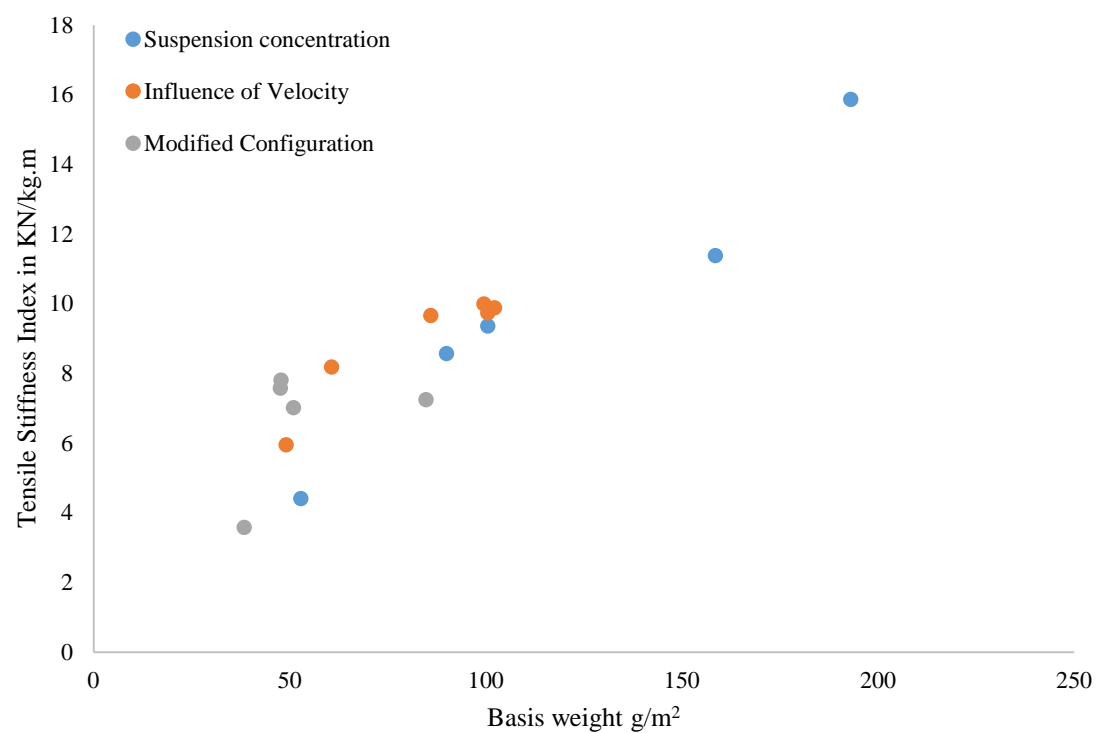**Figure B6: Load-Strain Curve for Spray coated NC Film prepared different NC Suspension.**

Figure B7: Load-Strain Curve for Spray coated NC Film prepared different velocity.

Tensile Stiffness Index of the NC films:

Figure B8. Tensile Stiffness Index of spray coated NC film.

SUPPLEMENTARY INFORMATION

ON

NANOCELLULOSE FILMS AS AIR AND WATER VAPOUR BARRIERS: A RECYCLABLE AND BIODEGRADABLE ALTERNATIVE TO POLYOLEFIN PACKAGING

Kirubanandan Shanmugam, Hamid Doosthosseini, Swambabu Varanasi, Gil Garnier, Warren Batchelor

Bioresource Processing Research Institute of Australia, Department of Chemical Engineering, Monash University, Melbourne, Vic 3800, Australia.

Address correspondence to E-mail: Warren.Batchelor@monash.edu

Comparison with WVP of Synthetic Polymers:

The comparisons of WVTR of spray coated NC film with numerous synthetic and biobased polymers are listed in Table C1.

Table 1: Comparison of WVTR of Barrier Polymers

Barrier Polymers	Water Transmission Rate (g/m² day)	Average Thickness of the film (μm)	Water Vapour Permeability (g/m.s.Pa)	Reference/Testing conditions
The NC Film Vacuum Filtration (100 g/m²)	52.9±1.2	119.4	4.97×10^{-11}	Present Investigation/ 50% RH, 23°C.
Recycled Cellulose film from Spray coated NC	89.5	133±3.92	9.83×10^{-11}	Present Investigation/ 50% RH, 23°C.
Cellulose Nano fibrils	234	42	8.12×10^{-11}	(Rodionova, Lenes, Eriksen, & Gregersen, 2011), 50% RH
Acetylated CNF (Acetylation Time-30 mins)	167	46	6.35×10^{-11}	(Rodionova et al., 2011), 50% RH
Polyvinylidene Chloride	3.07	12.7	1.27×10^{-13}	(Steven & Hotchkiss, 2002), 100% RH
Polyethylene (PE)	16.8	18.3	1.00×10^{-12}	(Steven & Hotchkiss, 2002), 100% RH
Plasticized (PVC)	118.56	12.7	4.90×10^{-12}	(Steven & Hotchkiss, 2002), 100% RH

Aluminium Foil			$1.42*10^{-13}$	(Steven & Hotchkiss, 2002), 100% RH
	2.376	18.3		
LDPE			$8.75*10^{-13}$	
	18	25		38°C, 90% RH*
HDPE			$4.37*10^{-13}$	
	9	25		38°C, 90% RH*
Oriented Nylon 6			$7.59*10^{-12}$	
	260	15		38°C, 90% RH*
Oriented Polystyrene	170	25	$8.27*10^{-12}$	38°C, 90% RH*
EVA	70	25	$3.41*10^{-12}$	38°C, 90% RH*
EVOH	22 -124	25	$1.07*10^{-12} - 6.032*10^{-12}$	(Bhunia et al., 2013), 38°C 90% RH
PA	155	25	$7.54*10^{-12}$	(Bhunia et al., 2013), 38°C 90% RH
PET	16-23	25	$7.78*10^{-13} - 1.12*10^{-12}$	(Bhunia et al., 2013), 38°C 90% RH
PC	139.5	25	$6.78*10^{-12}$	(Bhunia et al., 2013), 38°C 90% RH
PS	109 to 155	25	$5.30*10^{-12} - 7.54*10^{-12}$	(Bhunia et al., 2013), 38°C 90% RH
PP	6	25	$2.94*10^{-13}$	(Bhunia et al., 2013), 38°C 90% RH

*Data taken from DuPont Teijin Films, http://usa.dupontteijinfilms.com
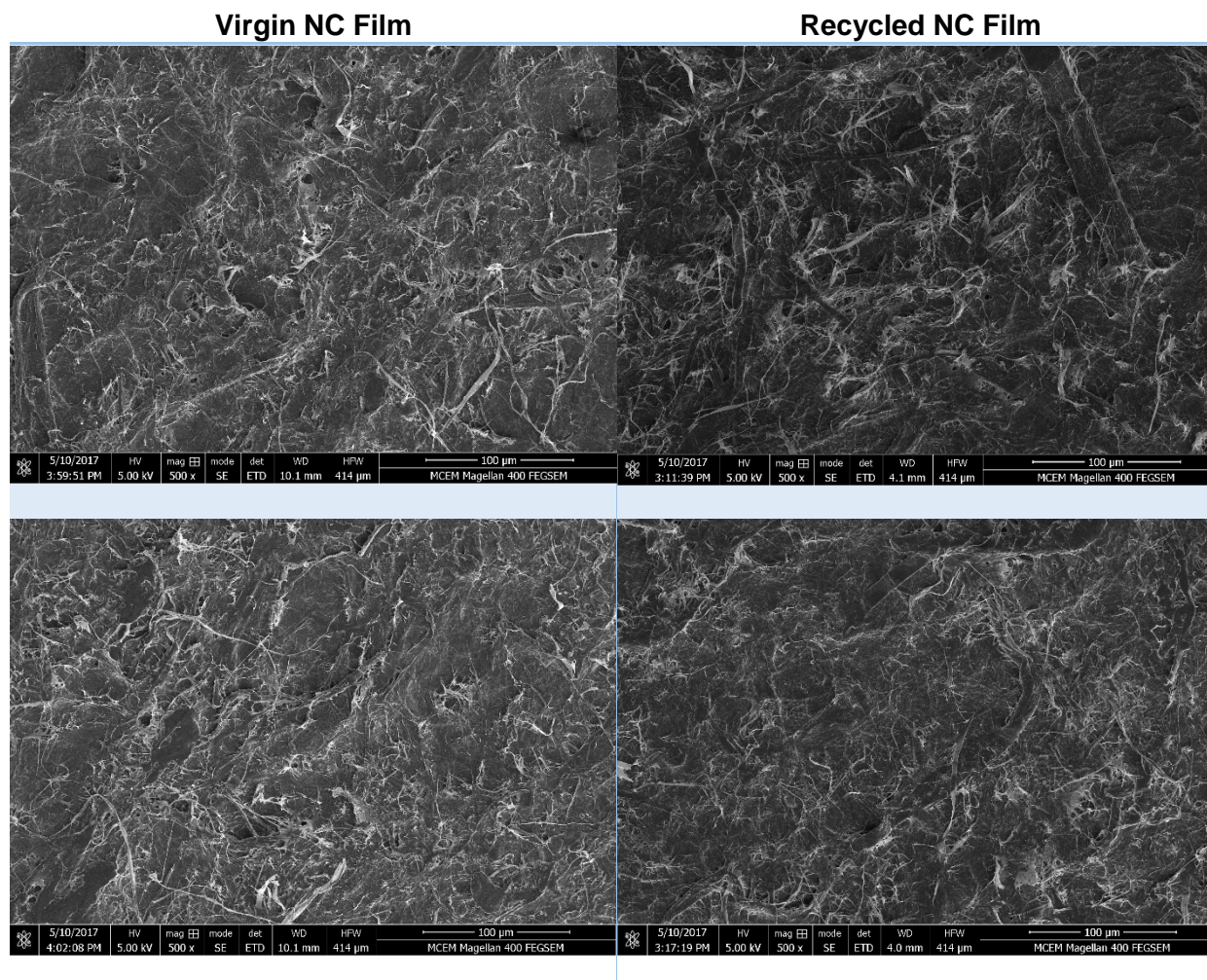
Virgin NC Film **Recycled NC Film**

Figure C1:SEM Micrographs of 100 µM Scale bar of Virgin NC Film and recycled NC film via Vacuum filtration (First Column– Free and Filter side for Raw NC film and Second Column – Free and Filter side of recycled sheet)
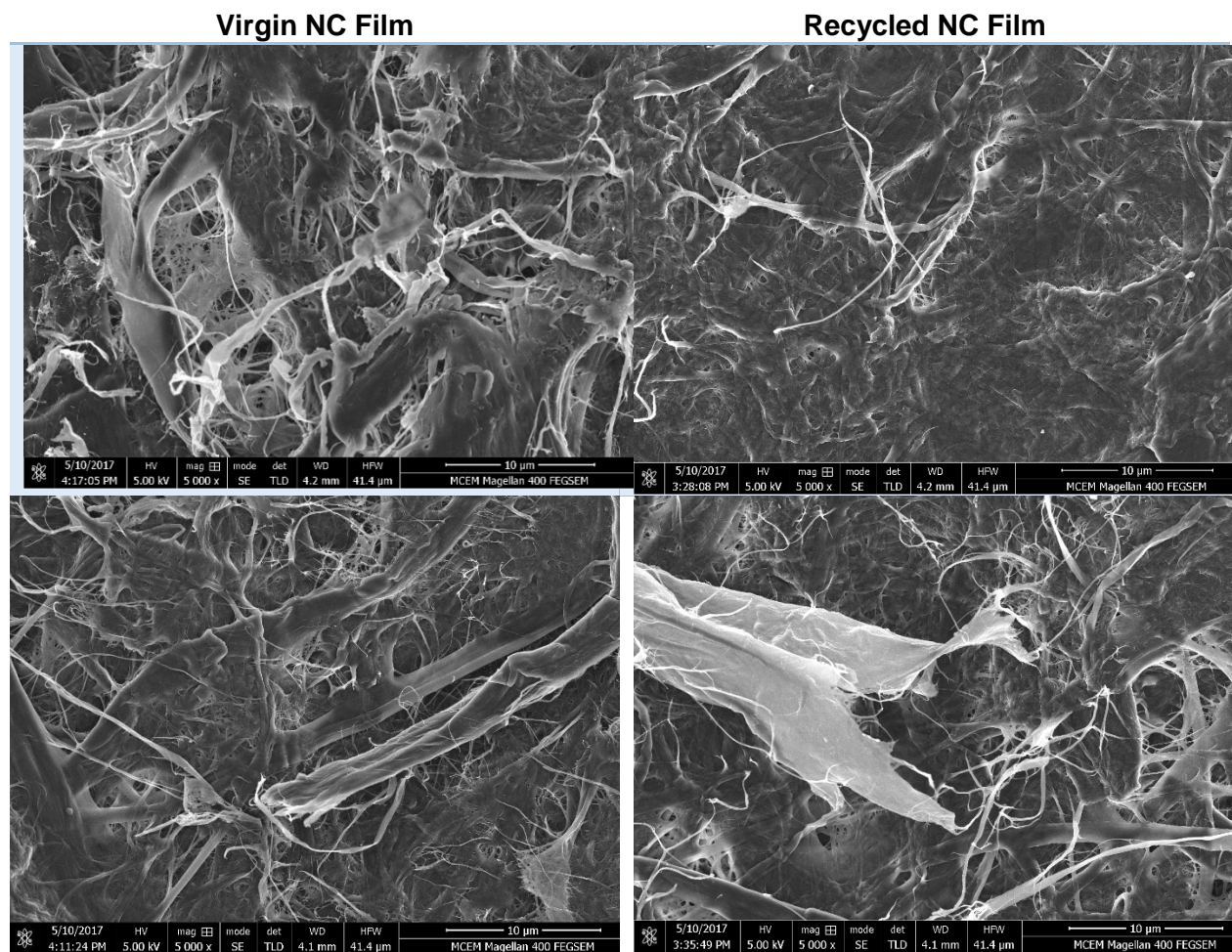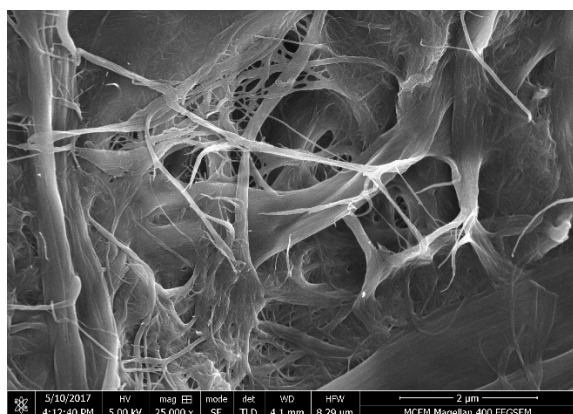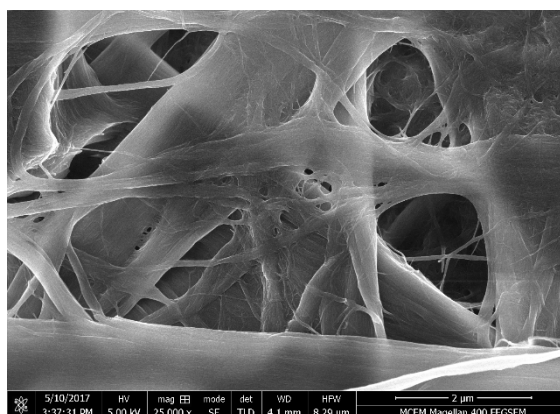
Virgin NC Film   **Recycled NC Film**

Figure C2: SEM Micrographs at 10μm of Raw NC film and Recycled film via vacuum filtration.
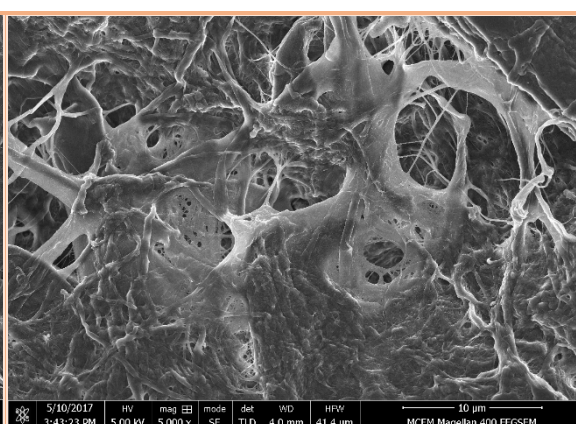
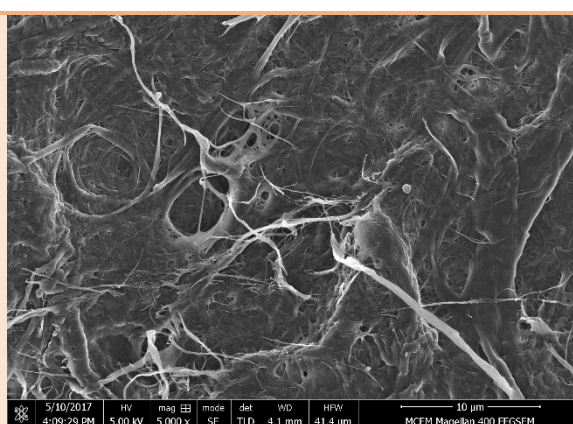Virgin NC Film   Recycled NC Film

Figure C3 SEM Micrographs of Virgin NC and Recycled Film. The micrographs of 2μm and 10μm scale bar confirm that there is a surface agglomeration of cellulose fibrils in the recycled film.
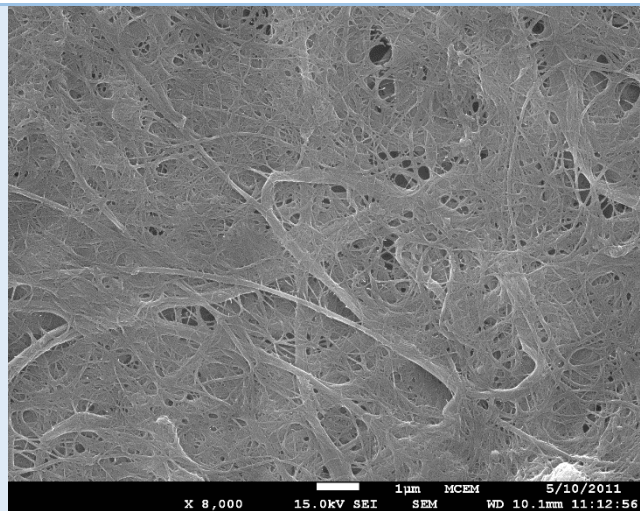
Virgin Fibres   **Recyled Fibres**
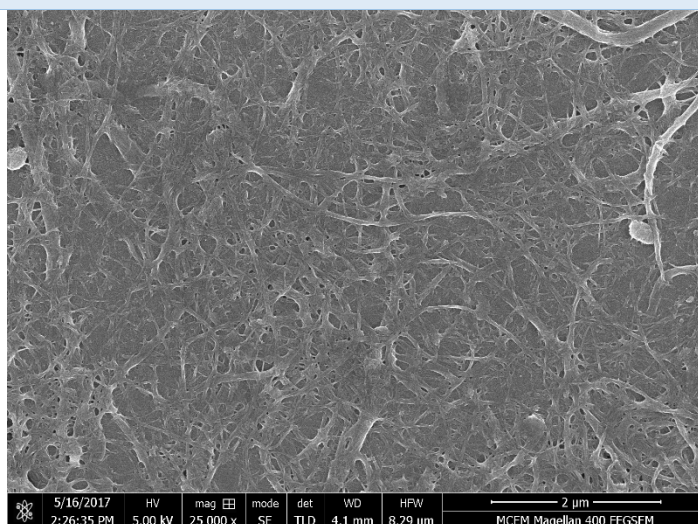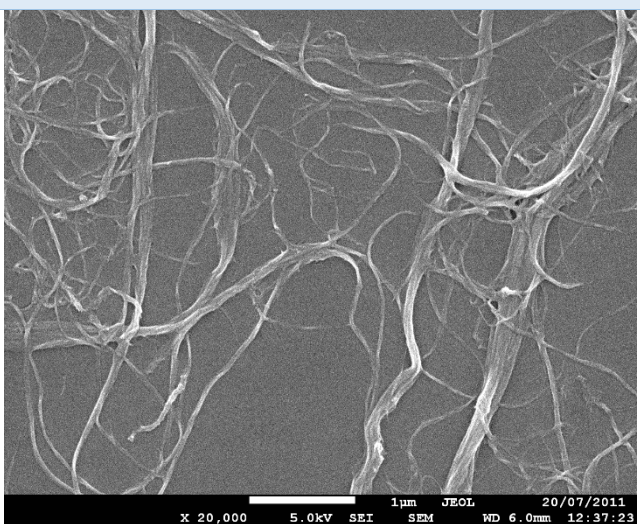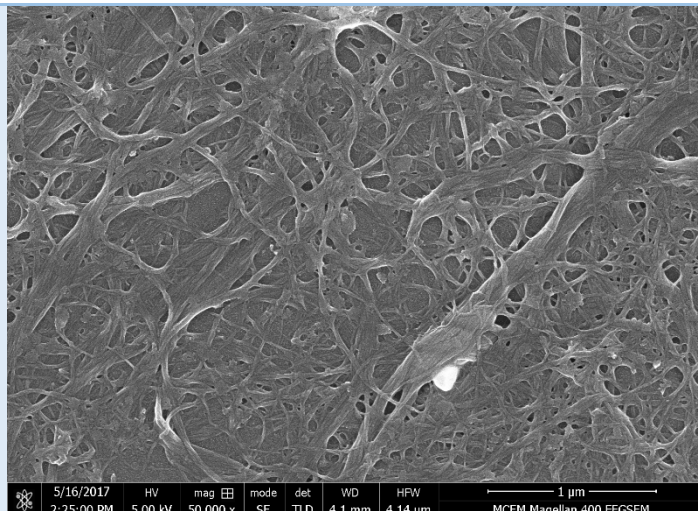
Figure C4 – SEM Micrographs of virgin and recycled nanocellulose fibres (1µm)

Recycled Fibres
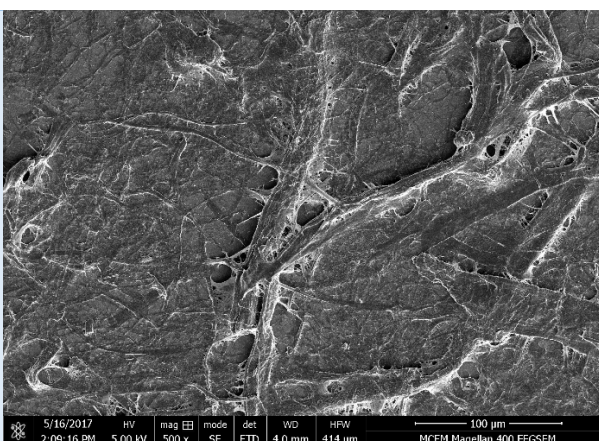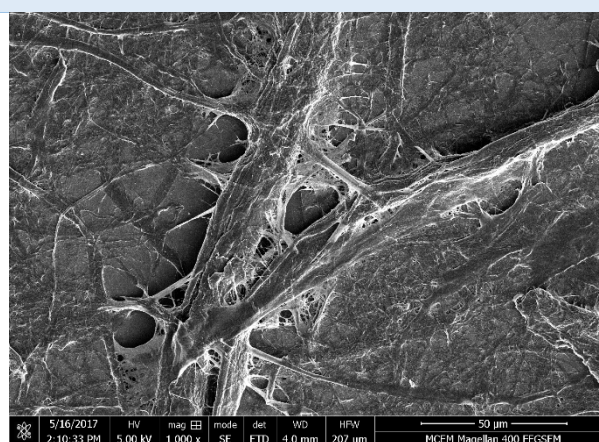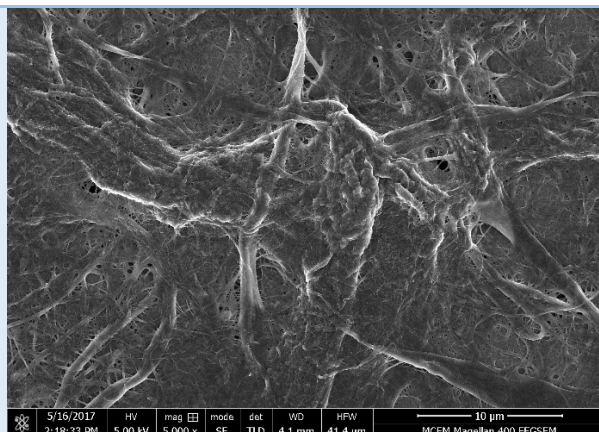
Figure C5- SEM Micrographs of Recycled Fibres (10 , 50, 100µm)

Virgin Fibres   **Recycled Fibres**
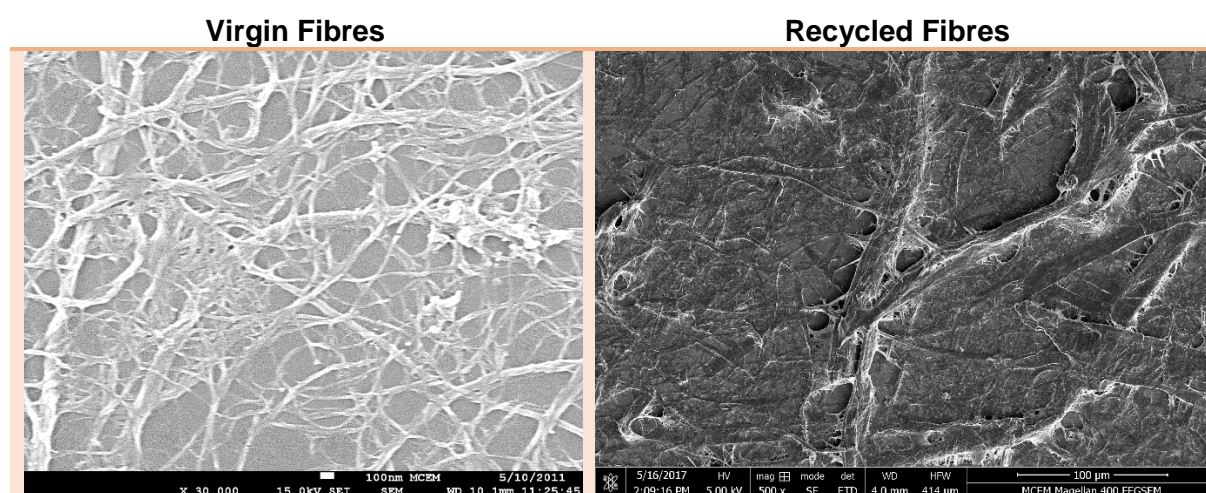
Figure C6 – SEM Micrographs of Virgin and Recycled NC Fibres (100µm)
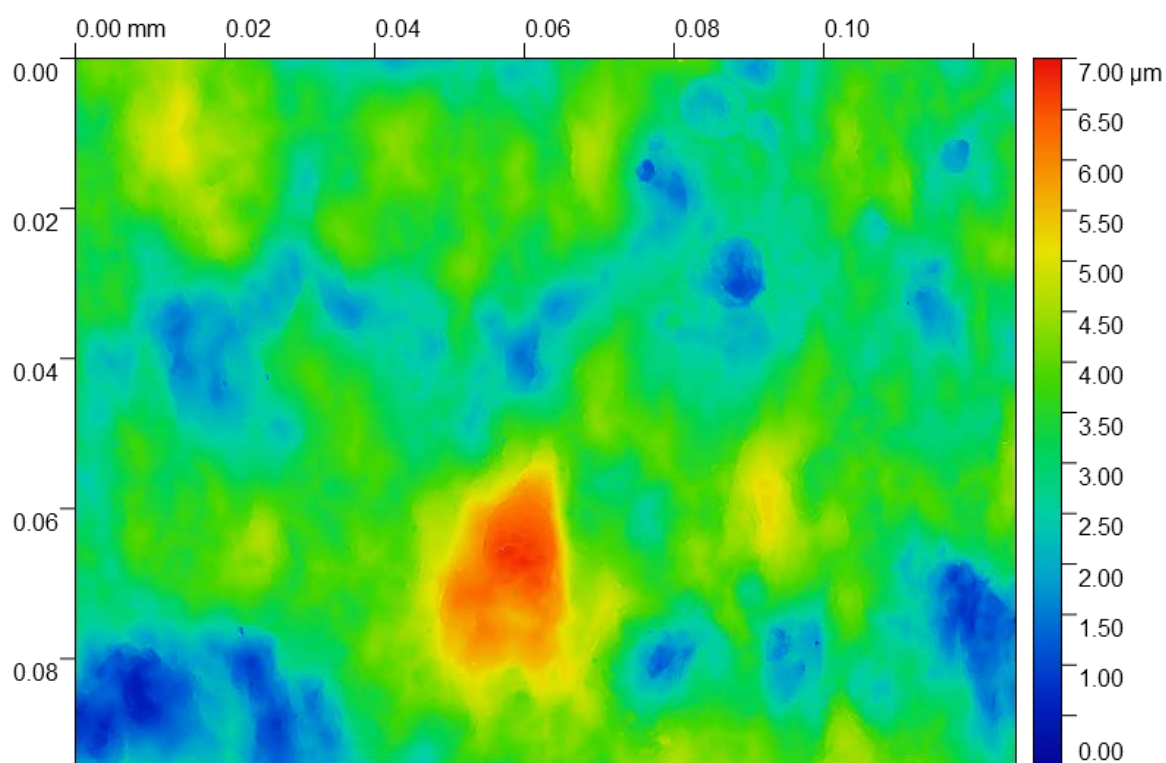
Filter Side of the Recycled Film
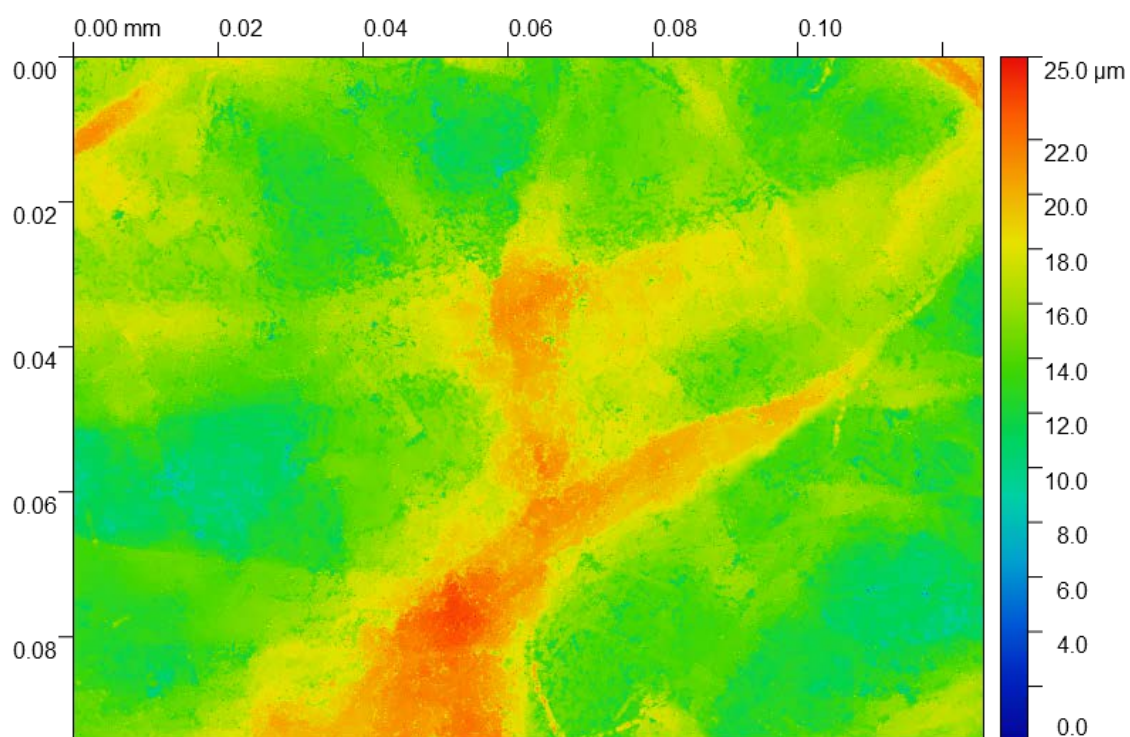
Filter Side of Virgin NC Film

Figure C7 – Optical Profilometry images (50 x magnification) of Virgin and recycled NC film

Virgin –NC Film Side -1

Recycled NC Film Side -1
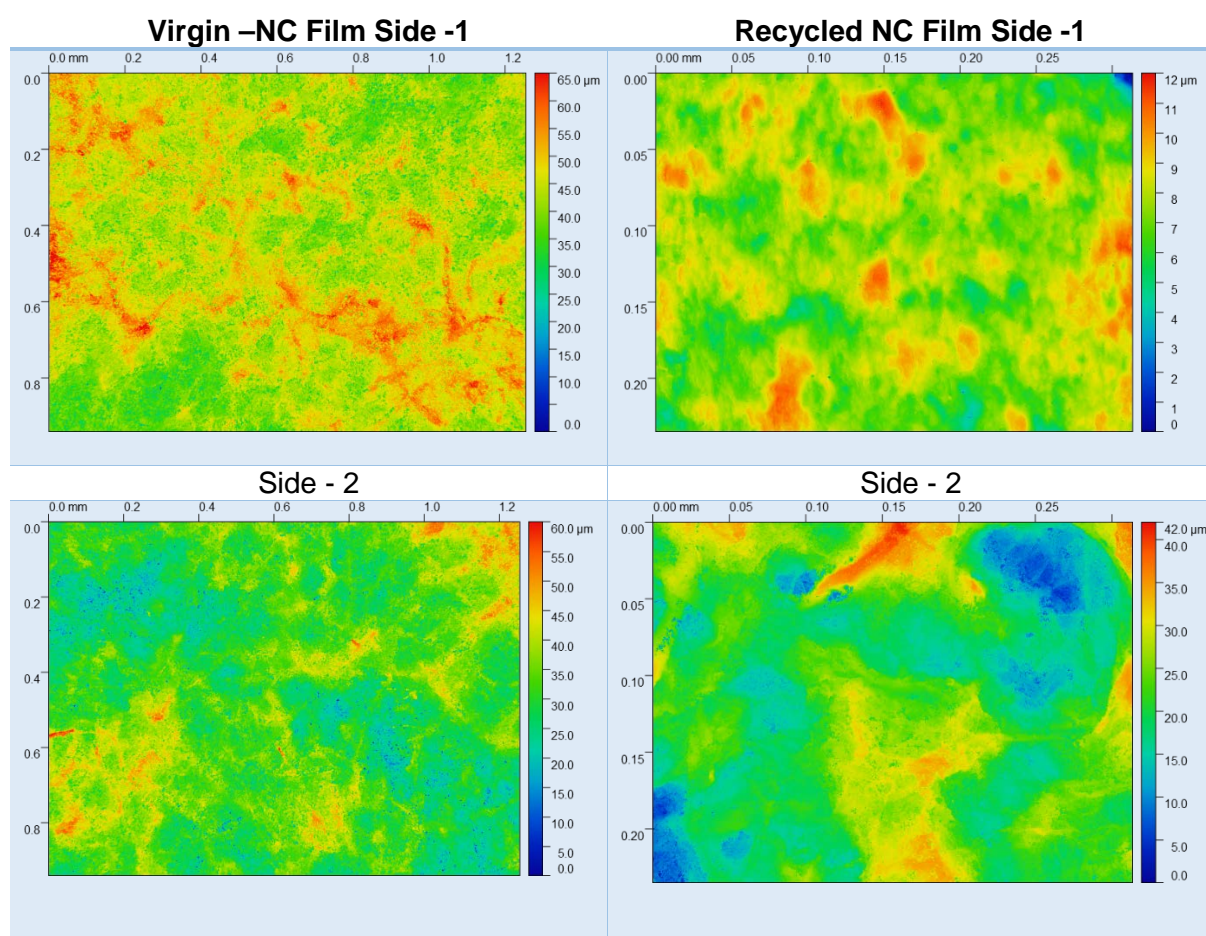
Side - 2

Side - 2

Figure C8 –Optical Profilometry Images (5x Magnification) of Virgin and Recycled NC Film. The surface roughness of virgin and recycled NC film are summarized in Table 2.

Table C2 – RMS of Virgin and Recycled NC Film

Films Types	Side 1	Side 2
Virgin NC Film	5.90002 µm	6.55052 µm
Recycled NC Film	5.12584 µm	5.93251 µm
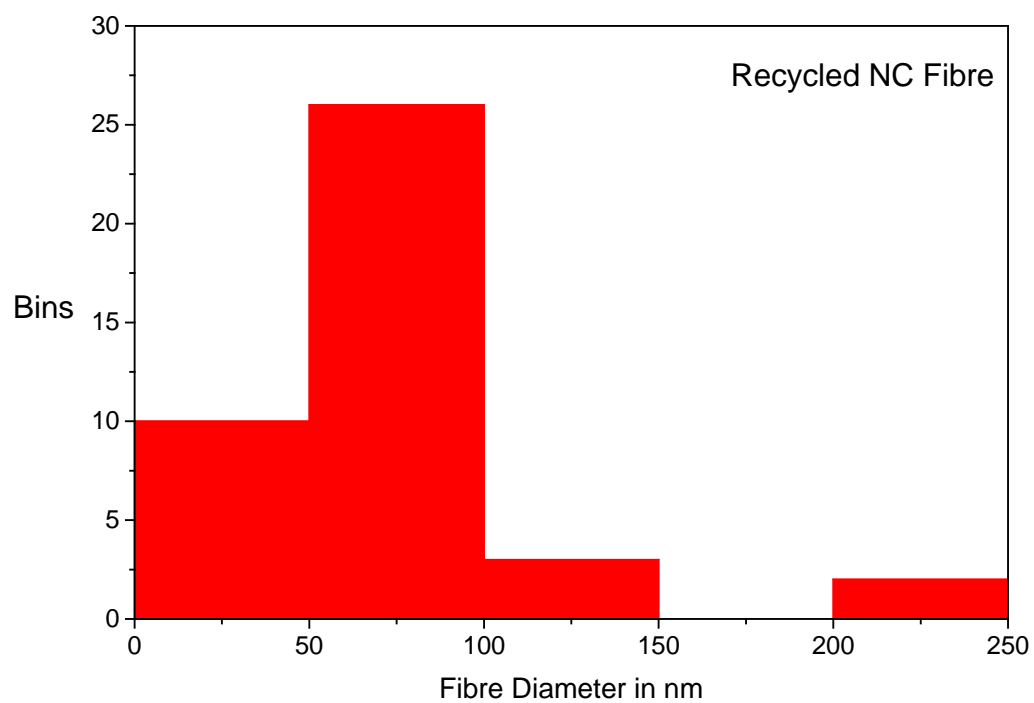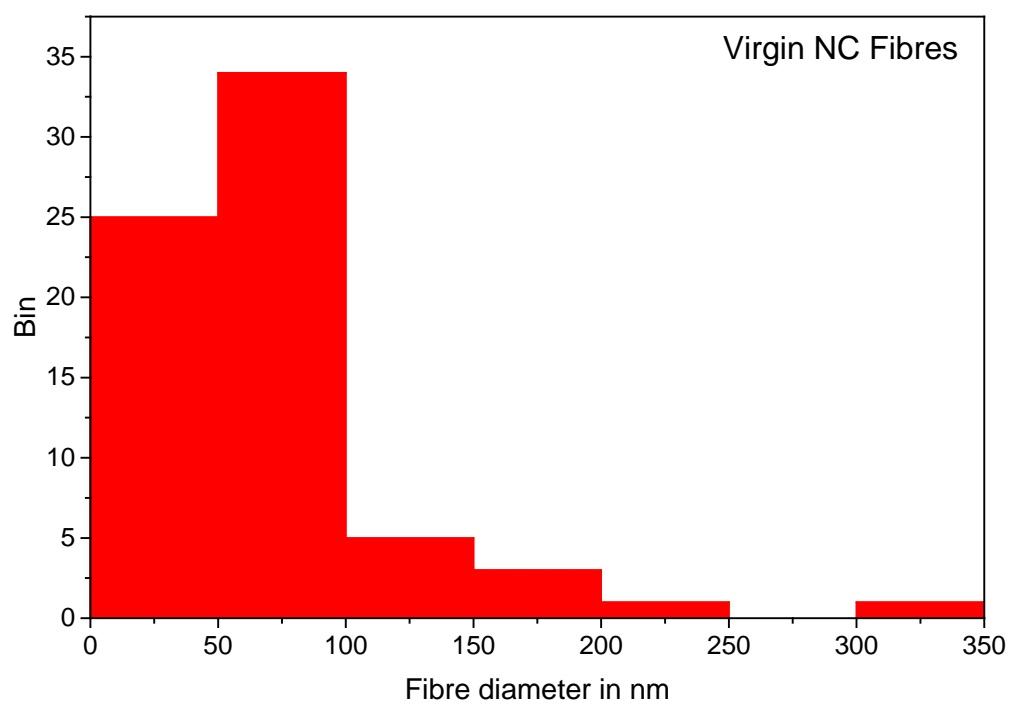
Figure C9 - Diameter Distribution of Virgin and Recycled NC fibres

SUPPLEMENTARY INFORMATION

ON

FLEXIBLE SPRAY COATING PROCESS FOR PREPARATION OF NANOCOMPOSITE

Homogenized (Rough)   *Homogenized (Smooth)*
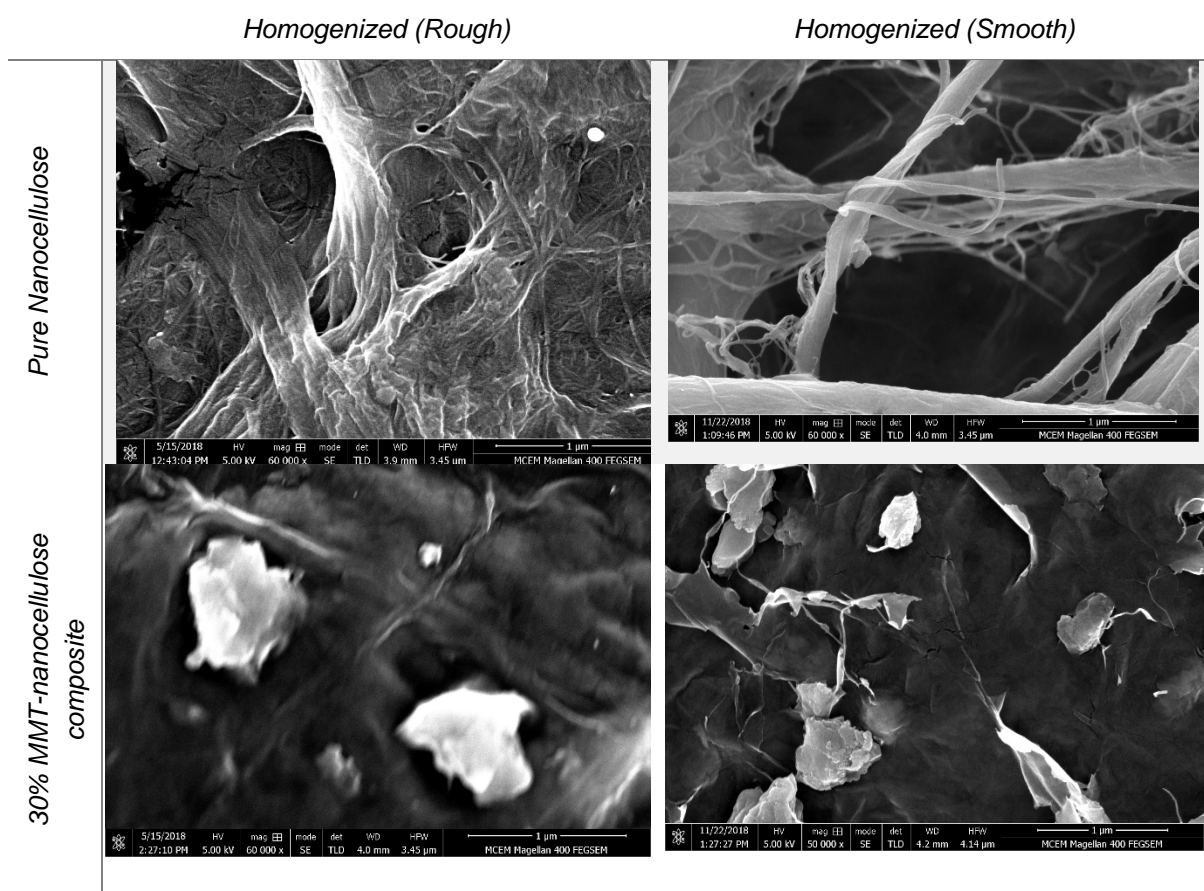
Figure D1: Rough and Smooth side of spray coated homogenized composite and pure NC film.

Homogenized

Pure Nanocellulose

30% MMT-nanocellulose composite
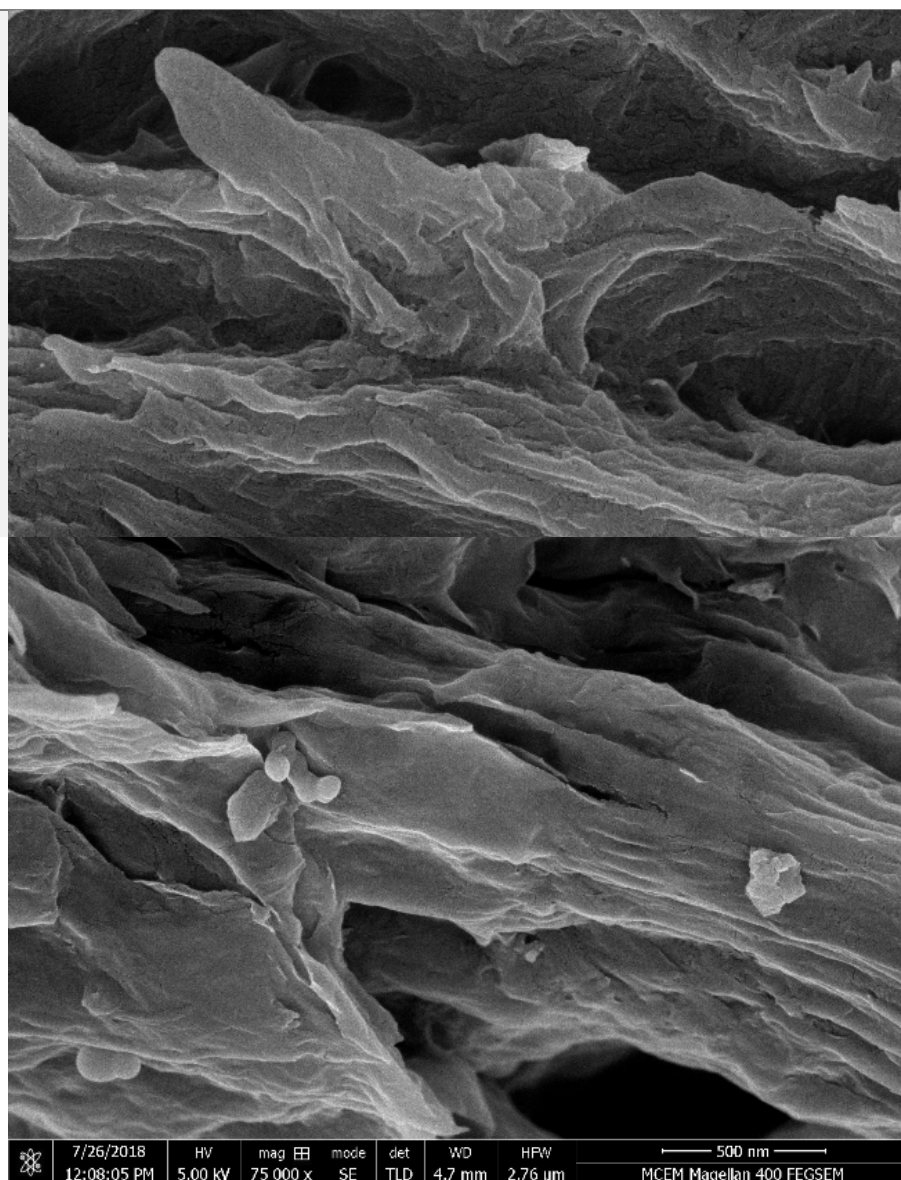
Figure D2: Cross-sectional view of spray coated homogenized composite and pure NC film.
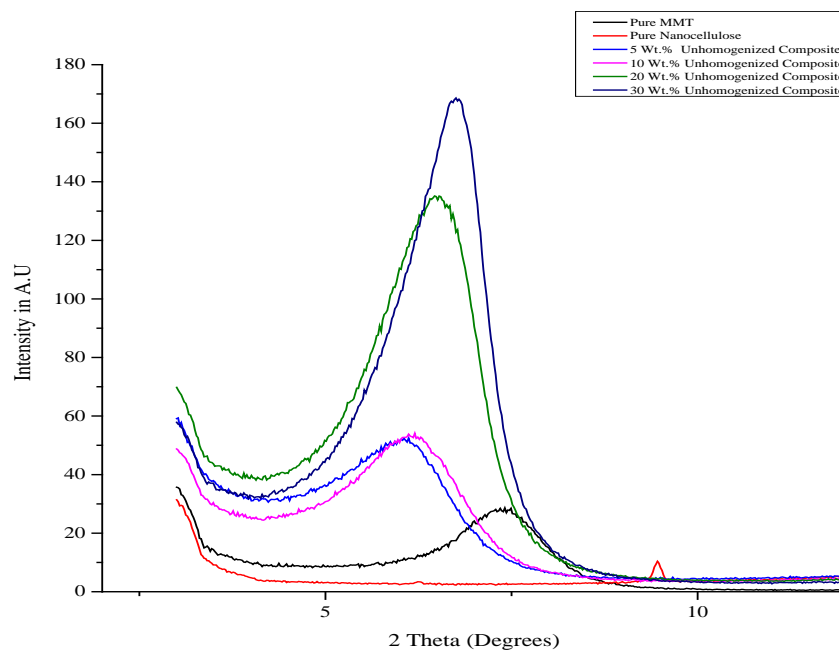
Figure D3: First peak of XRD Spectrum of Unhomogenized Nanocomposite.
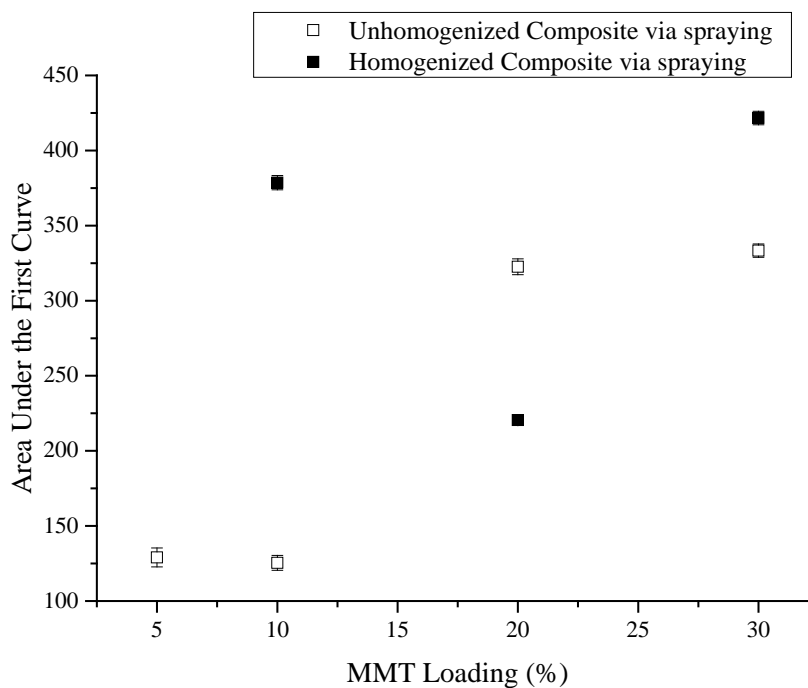
Figure D4: Area under the first curve of the XRD spectrum of Unhomogenized and Homogenized Composites

D) Mechanical Properties of Nanocomposites:
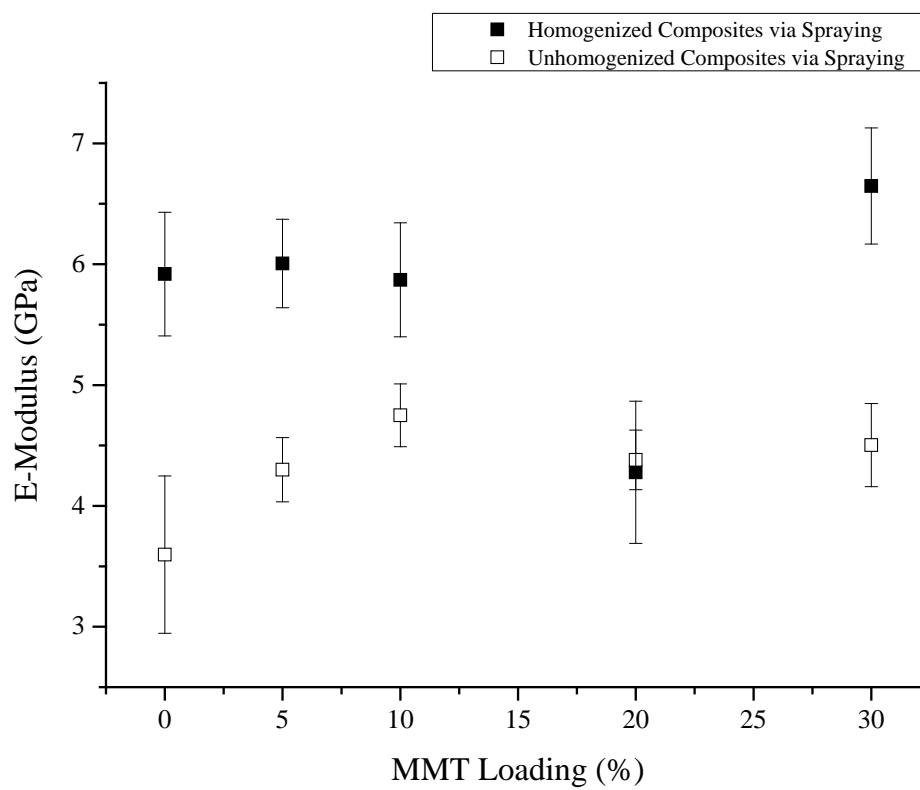
Figure D5: E-Modulus of Spray coated composites
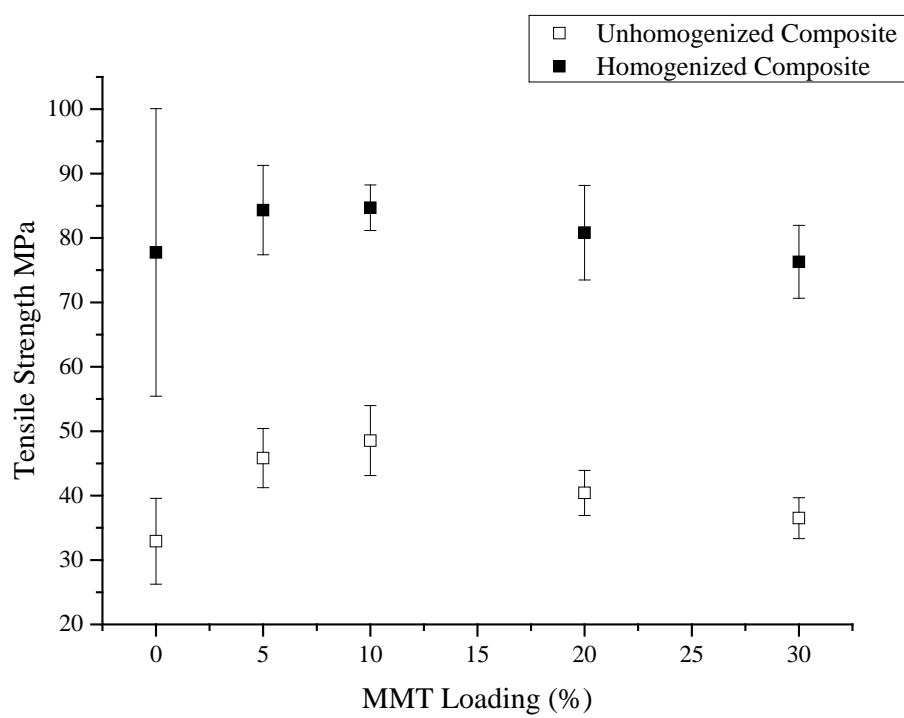
Figure D6: Tensile strength of spray coated composites

SUPPLEMENTARY INFORMATION

ON

ENGINEERING SURFACE SMOOTHNESS OF NANOCELLULOSE FILMS VIA SPRAYING
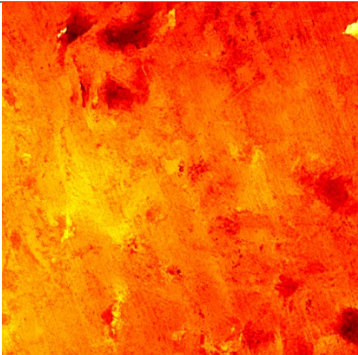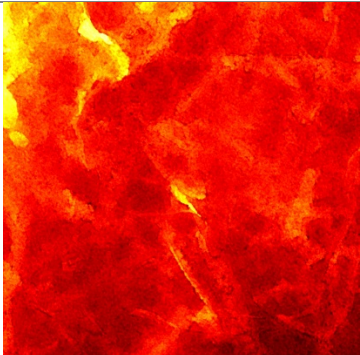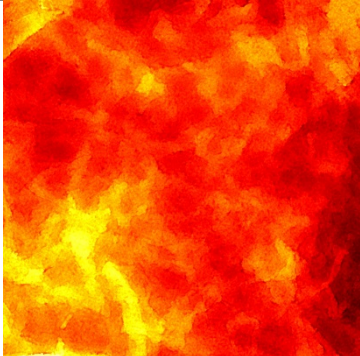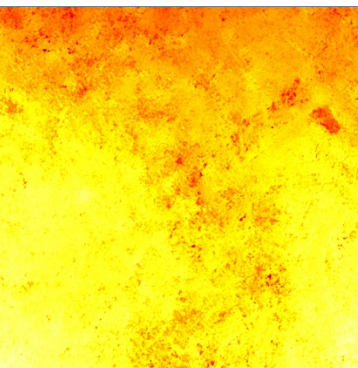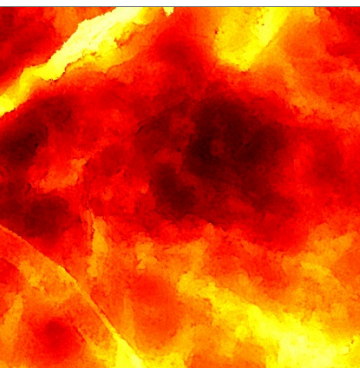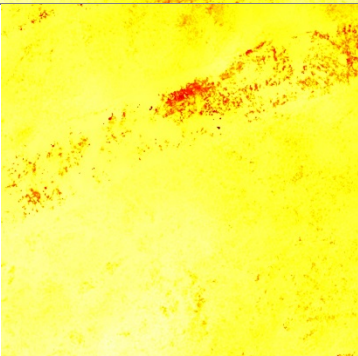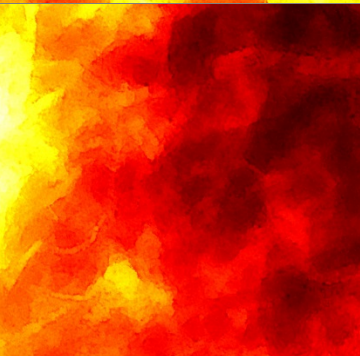
Base Substrate	Smooth Side of NC film	Rough Side of NC film
Ordinary Stainless Steel - Square		
Ordinary Stainless Steel - Circular		
Super Polished Stainless Steel		
Silicon Wafer		

Figure E1 :Optical Profiler Images of NC films from Spraying of 1.75 Wt.% NC (Unhomogenized) on various substrates. 50x Magnification. The height ranges from 10 to -10 μm.

	OSSS	SSS	SW
Raw NC			
Raw NC+ 1st Pass Homogenization			
Raw NC+ 2nd Pass Homogenization			
Raw NC+4 wt,% CMC			
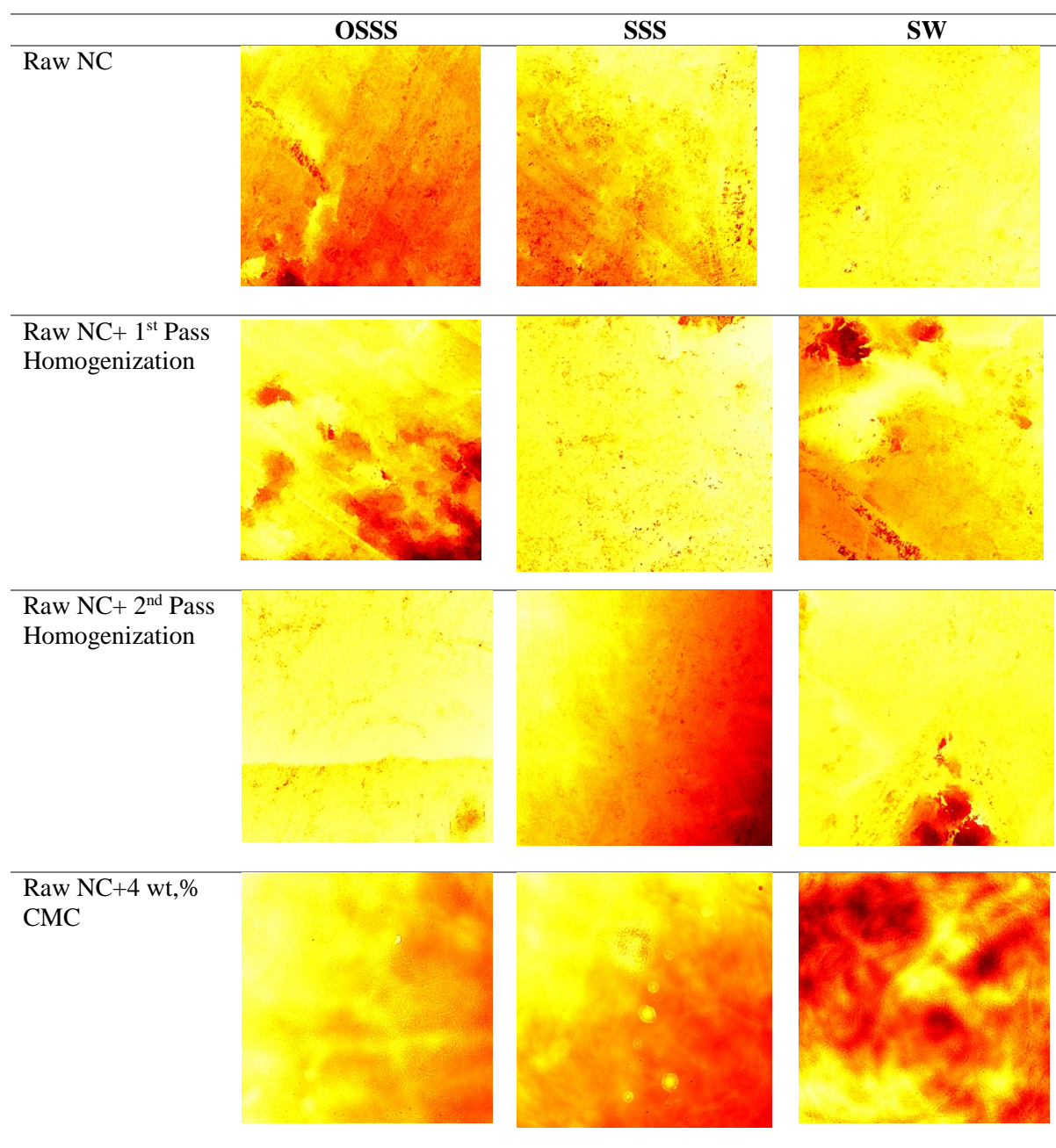
Figure E2: Optical Profiler images of Raw NC film, Homogenized NC , CMC added Spray coated NC film
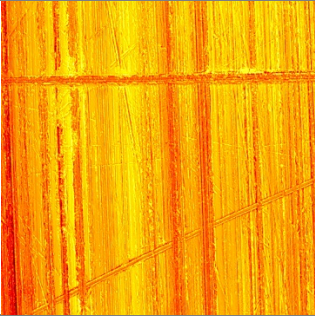
Base Surface	Surface of Base	Surface Roughness in nm
Ordinary Stainless Steel - Square		Sa=333 Sq=432
Ordinary Stainless Steel Circular		Sa=131 Sq=195
Super Polished Stainless Steel		Sa=18 Sq=22
Silicon Wafer		Sa=17 Sq=25

Figure E3 :Optical Profiler Images (50X Magnification) of Base Surface having high roughness to low roughness. The height ranges in the images ranges from 5μm to -5μm.

Surface Roughness of Spray Coated NC Film (Free Side)

Roughness of Free Side of NC film via spraying:
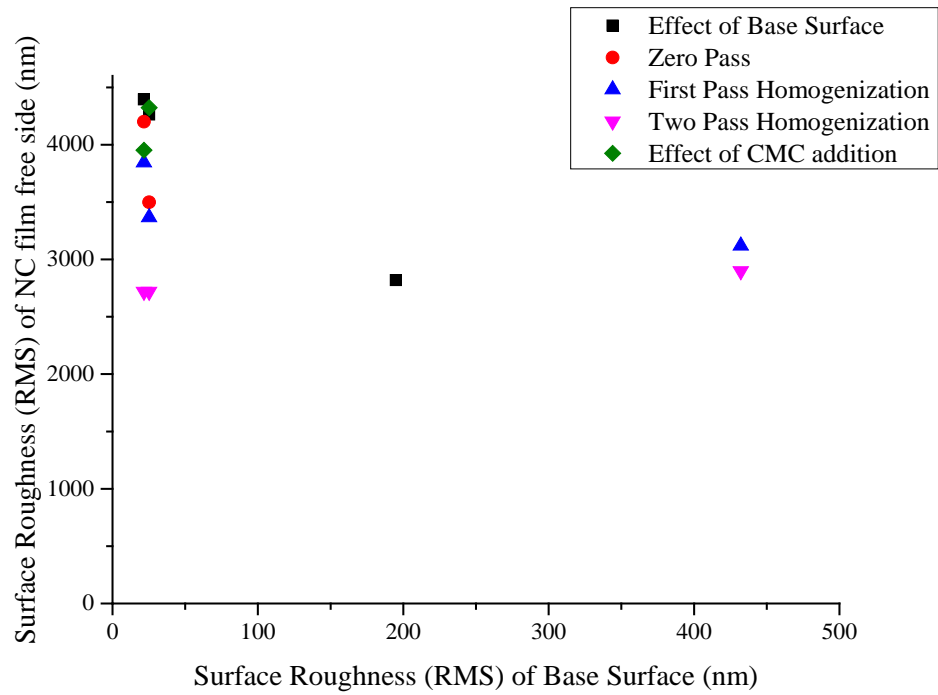
Figure E4: Surface roughness of free side of NC film
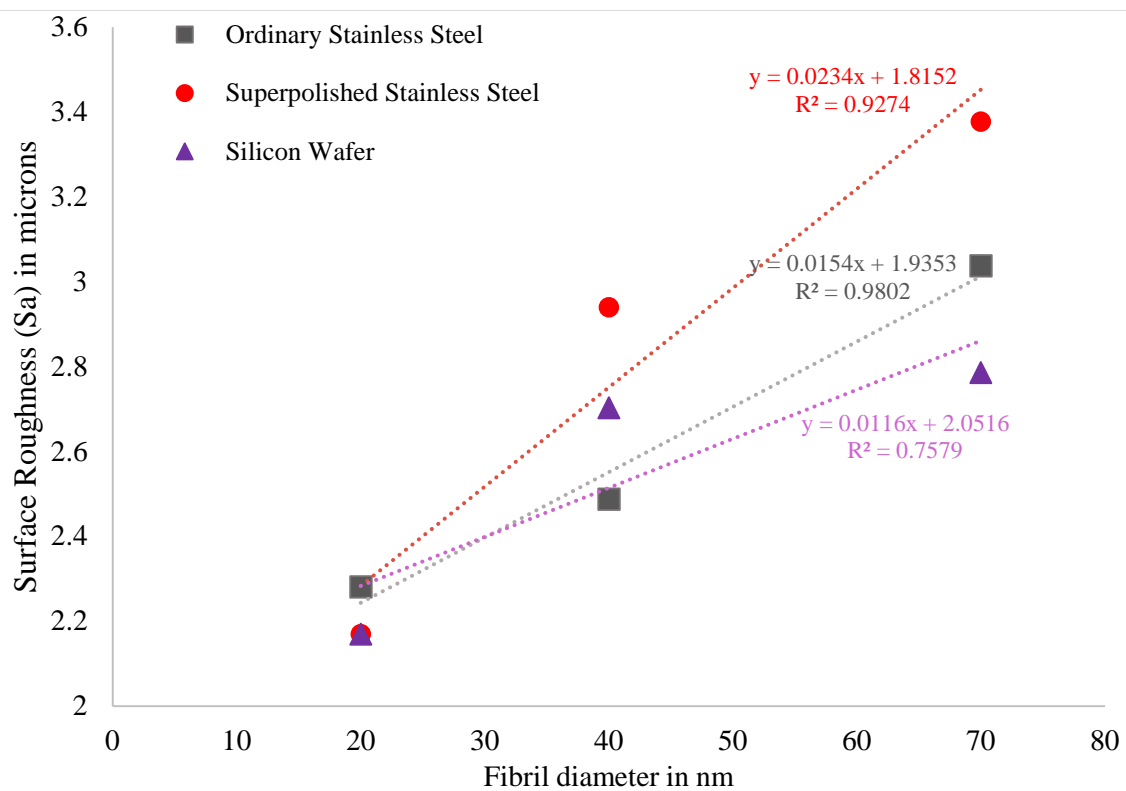
Figure E5: Effect of fibril diameter on the surface roughness of free side of the NC film
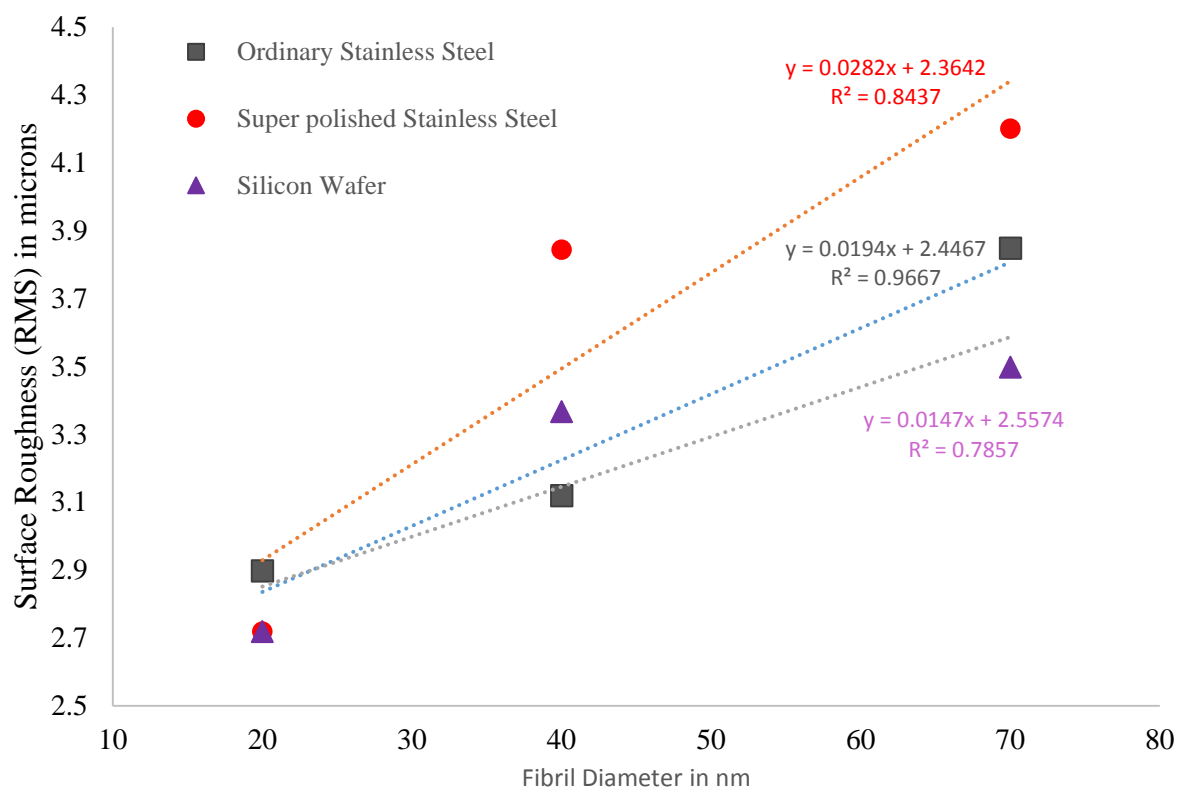
Figure E6: Effect of fibril diameter on the surface roughness (RMS) of free side of the NC film

Macroscale Roughness from Parker Print Surface Instrument:
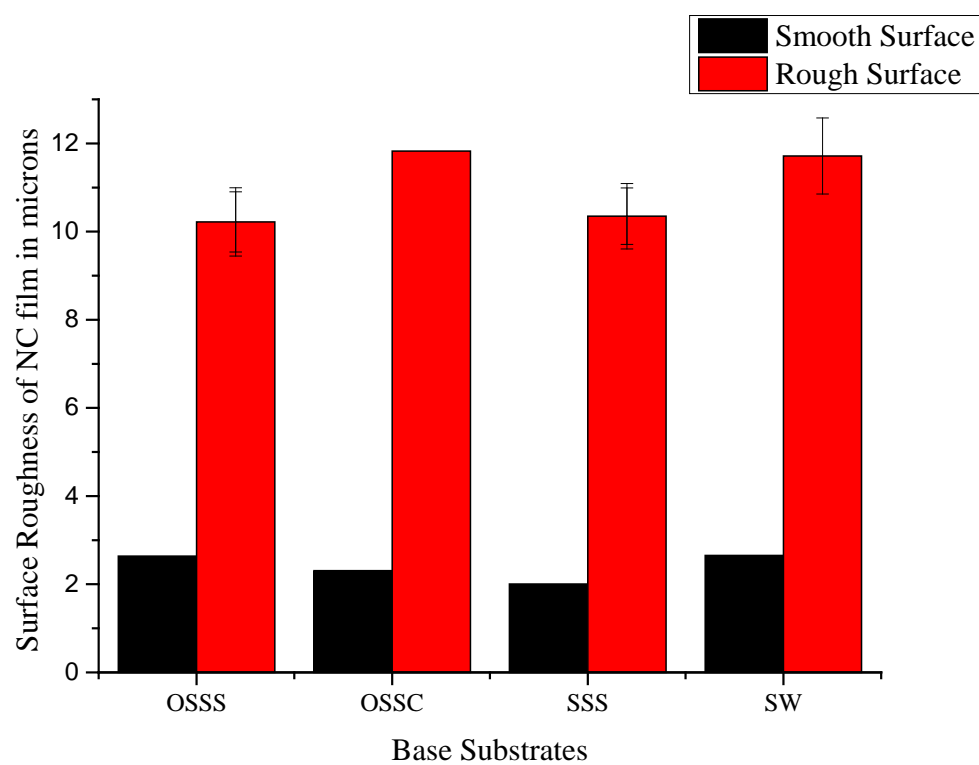
Figure E7 – Effect of base surface on the surface roughness of NC film
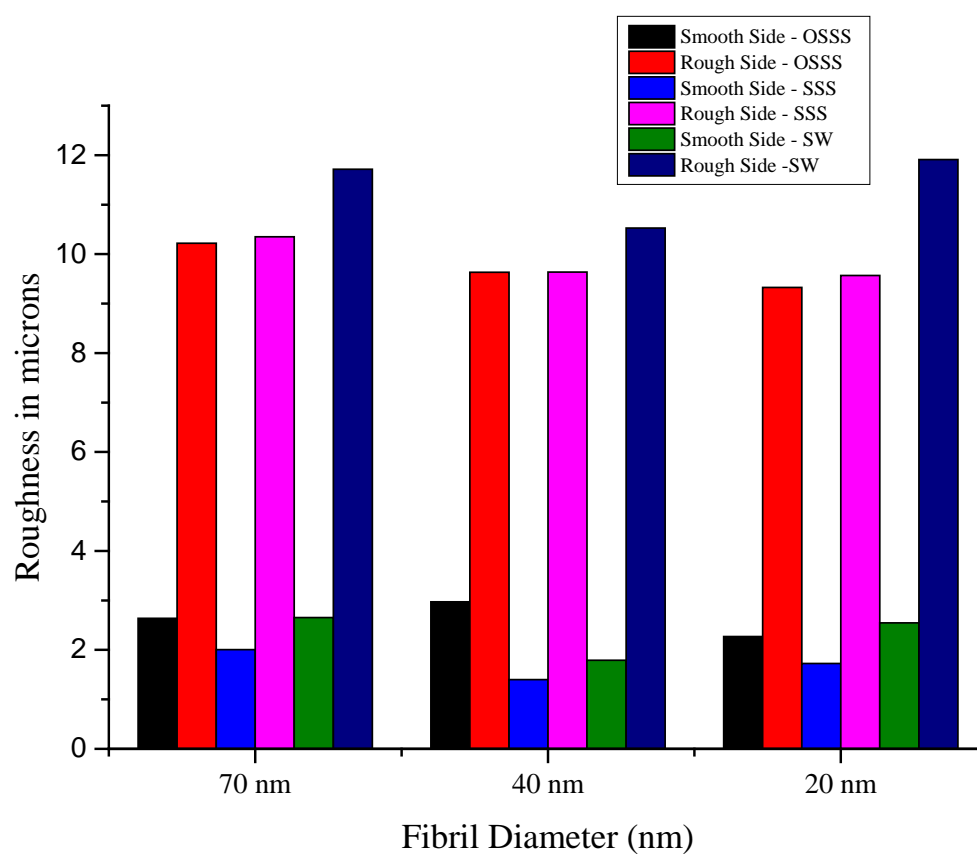
Figure E8: Effect of fibril diameter on the surface roughness of NC film

APPENDIX II

LIST OF PUBLISHED PAPERS

CrossMark

COMMUNICATION

Rapid preparation of smooth nanocellulose films using spray coating

**Kirubanandan Shanmugam · Swambabu Varanasi · Gil Garnier ·
Warren Batchelor**

Abstract Spraying of nanocellulose (NC) on a solid surface to prepare films is an alternative technique to vacuum filtration, which requires a long drainage time and produces films which can sometimes be difficult to separate from the filter. This letter reports a rapid preparation technique for nano-cellulose films using a bench scale system spray coating nanocellulose suspension onto stainless steel plates. After spraying NC suspension onto a smooth steel plate travelling on a constant velocity conveyor, the films can be dried directly on the plates using standard laboratory procedures, saving processing time and effort. By adjusting the suspension consistency, we were able to reproducibly make films with a basis weight ranging from 52.8 ± 7.4 to 193.1 ± 3.4 g/m^2 when spraying on to a plate moving at a velocity of 0.32 cm/s. The operator preparation time for the nanocellulose film was 1 min, independent of the sample basis weight, which compares to production times reported in the literature of 10 min using filtration techniques. The films made by spray coating showed higher thickness, but comparable uniformity, to those made by vacuum filtration. Optical profilometry measurements showed that over a 1 cm × 1 cm inspection area that the surface roughness (RMS) of the NC film is only 389 nm on the spray coated side in contact with the steel plates, compared to 2087 nm on the outside surface. Thus, the reduction in preparation time for producing the nanocellulose film recommends this spray coating technique as a rapid and flexible method to produce NC films at the laboratory scale.

Keywords Nanocellulose (NC) · Spray coating · Nanocellulose film · Uniformity · Roughness

Introduction

Nanocellulose is a promising renewable, biodegradable nanomaterial available in large quantities in nature. The interest in nanocellulose material is growing due to outstanding properties such as high specific strength, thermal stability, hydrophilicity, and easy chemical functionalization. Nanocellulose materials can provide an excellent alternative material for most plastic films which have limitations in recycling and biodegradability. Films prepared from nanocellulose have outstanding mechanical, optical and structural properties enabling the fabrication of many functional materials and devices such as organic transistors and conducting materials (Chinga-Carrasco et al. 2012), or immunoassays and diagnostics tests

K. Shanmugam · S. Varanasi · G. Garnier ·
W. Batchelor (✉)
Department of Chemical Engineering, Australian Pulp and Paper Institute, Monash University, Melbourne, VIC 3800, Australia
e-mail: Warren.Batchelor@monash.edu

(Orelma et al. 2012). The surface chemistry of nanocellulose can be easily tailored for applications such as photonics, biomedical scaffolds, optoelectronics and developing barrier materials (Abitbol et al. 2016). Recently, nano cellulose film has been investigated for use as filters (Metreveli et al. 2014; Varanasi et al. 2015), adsorbents, catalyst (Koga et al. 2010), cell culture substrates, thermal insulators and drug carriers (Huang et al. 2013).

Even though the nanocellulose films have potential uses in many areas, progress and applications are significantly hindered by the difficulty of simply and reproducibly preparing nanocellulose films both at the laboratory and industrial scales. Stand-alone nanocellulose films have been prepared using either vacuum filtration or casting. Casting is a time-consuming process which typically requires three days for the film to dry and wrinkling is difficult to control (Shimizu et al. 2014). Vacuum filtration is a considerably quicker process when compared to the casting method. Laboratory film preparation time for light weight films less than 60 g/m^2 has been reduced from 3 to 4 h (Nogi et al. 2009) to 10 min (Varanasi and Batchelor 2013; Zhang et al. 2012) by increasing the solids content above the gel point and using polyelectrolytes to increase the size and strength of the flocs to reduce filter resistance. However, there can be significant issues in separating the film from the filter and subsequent handling before it is finally dried. Vacuum filtration is also a manufacturing method with a limited range of film basis weight as the filtration time increases exponentially with film thickness (basis weight).

Spraying of nanocellulose on permeable substrates is an alternative technique for making nanocellulose films that has been used to produce continuous nanocellulose films by spraying onto a fabric or to produce composite laminates by spraying onto a base sheet (Beneventi et al. 2014). Spraying has significant advantages such as contour coating and contactless coating with the base substrate. The topography of the surface of the base substrate does not influence the coating process. The range of basis weight achievable with spraying is much higher than has been obtainable with filtration. A maximum mass of the film of 124 g/m^2 was obtained by spraying nanocellulose onto a nylon fabric running at a speed of 0.5 m/min (Beneventi et al. 2015). So far, spraying of nanocellulose on fabric or paper has been used to prepare sheets and

barrier layers, respectively. Spraying has also been used to prepare multilayer nanocomposites for electrodes (Krol et al. 2015; Zolin 2017).

Spraying of cellulose microfibres onto impermeable substrates has also been investigated. In a recent study, spraying was used to produce free-standing micro-fibrillated cellulose film with 3D structures on preheated metal surfaces (Magnusson 2016). The spray coated MFC film had a basis weight from 59 to 118 g/m^2 and thickness of the sheet varied from 46 to 68 μm. The major reported disadvantage of the approach was the formation of cracks in the film. In an earlier study, ethyl cellulose dispersed in water with plasticizer was sprayed on Teflon plates and produced a uniform film with better tensile strength and elastic modulus than a cast film (Obara and McGinity 1994). However, this method required extensive pre-treatment of the cellulose prior to spraying in comparison to our method, where the cellulose nano fibrils are directly used for spraying without additional preparation.

Spraying can also be performed at a higher solids content compared to filtration, reducing the amount of water to be removed by drying. Spraying has not so far been used to make discrete films for laboratory investigations, or for small scale products. It is still an open question about the sheet quality produced by spraying compared to handsheets made by laboratory vacuum filtration. It is the purpose of this paper to describe a new and efficient method for the laboratory production of nanocellulose films by spraying nanocellulose directly onto smooth steel plates. The nanocellulose films thus formed can subsequently be dried in many ways: in air under restraint, heat contact, etc. The uniformity of spray coated nanocellulose films is evaluated by thickness mapping and then compared with the thickness mapping of a nanocellulose film prepared via vacuum filtration.

Experimental method

Materials

The nomenclature for nanocellulose has not been reported in a consistent manner in the previous scientific investigations. As well as nanocellulose (NC), it is also called micro fibrillated cellulose (MFC), cellulose nano-fibrils, cellulose micro-fibrils

and nano-fibrillated cellulose (NFC). In this paper, we use NC as the generic term for all the cellulose nanomaterials used.

NC supplied from DAICEL Chemical Industries Limited (Celish KY-100S) was used to prepare films. NC samples were used at consistencies ranging from 1.0 to 2.0 wt%, prepared by diluting the original concentration of 25 wt% with distilled water and mixing for 15,000 revolutions in a disintegrator. The viscosity of the NC suspension was evaluated by the flow cup method, which evaluates coating fluid flow through an orifice, to be used as a relative measurement of kinematic viscosity, with the results expressed in seconds of flow time in DIN-sec.

Preparation of nanocellulose films through spray coating and vacuum filtration methods

The experimental system for a lab scale spray coating system is shown in Fig. 1. The NC suspension was sprayed on a circular stainless steel plate moving on a variable speed conveyor using a Professional Wagner spray system (Model number 117) at a pressure of 200 bar. The type 517 spray tip gave an elliptical spray jet. The spray jet angle and beam width are 50° and 22.5 cm, respectively. The spray distance is 30.0 ± 1.0 cm from the spray nozzle to the circular steel plate. The conveyor was operated at a constant speed of 0.32 cm/s for the spraying of NC on the plate surface. During the spraying, the pressure driven spray system was run for 30 s before forming the first film, so as to allow the system to reach equilibrium.

After spraying, the film on the plate was air dried under restraint at the edges for at least 24 h. The NC film can then be readily peeled from the stainless steel plate and stored at 23 °C and 50% RH for further testing. For comparison, NC films were also prepared using vacuum filtration method as reported in (Varanasi and Batchelor 2013). In brief, 1000 g of NC suspension with 0.2 wt% concentration was poured into a cylindrical container having a 150 mesh filter at the bottom and then filtered until it formed a wet film on the mesh. The wet film was carefully separated using blotting papers and then dried at 105 °C in a drum drier for around 10 min. The film prepared by this method is used as a reference film to compare the uniformity and thickness of the spray coated film. The basis weight (g/m^2) of each NC film was calculated by dividing the weight of the film, after 4 h drying in the oven at a temperature of 105 °C, by the film area.

Evaluation of thickness distribution and thickness mapping

The NC film thickness was measured utilizing L&W thickness analyzer (model no 222). The circular NC film was divided into six regions and thickness was measured in six evenly spaced locations in each region. The thickness mapping of a centre square region of the circular film is done by plotting a contour plot using Origin Pro 9.1. The visual explanation is given in Fig. 2. The mean thickness of all the films is plotted against the suspension concentration of nanocellulose. The mass of the film per unit area is evaluated for various concentration of nanocellulose sprayed on the stainless steel plate.

Fig. 1 Experimental set up for laboratory scale spray coating system for preparation of nanocellulose film. **a** The rough surface of the NC film, **b** the smooth surface of the NC film

Stainless steel plate

Conveyor and Professional Spray system

Spray coated nanocellulose film
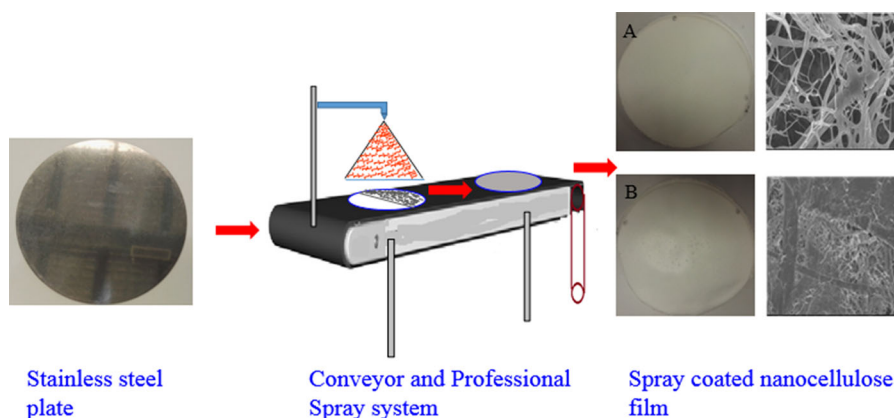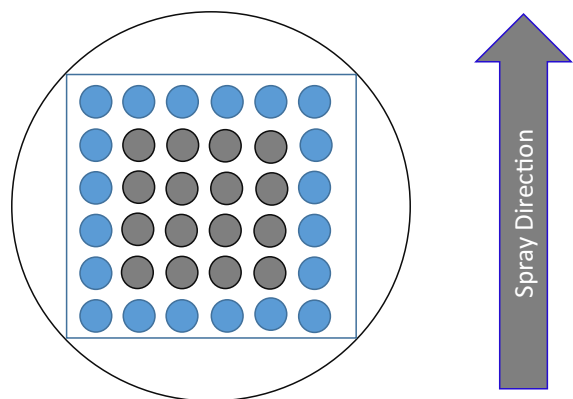
Fig. 2 Mapping of thickness of the NC film. The thickness is measured in the centre region of the film. The *square section* of centre part of the film is used for *contour plotting*. The *grey points* are used for mapping to confirm the uniformity of the film

Evaluation of tensile strength and air permeance

The strength of the nanocellulose films were evaluated by an Instron model 5566. The test specimen were 100 mm in length and 15 mm width and were conditioned for 24 h at 23 °C and 50% RH. The barrier properties of the 100.5 g/m^2 spray coated film and film prepared via vacuum filtration were evaluated by air permeance through an L&W Air permeance tester.

Surface topography of nanocellulose film

The surface morphology and topography of the iridium coated NC film were measured with a FEI Novo SEM450. The images of both surfaces of the nanocellulose films are captured at magnifications from 500 to 50,000 in secondary electron mode-II. Furthermore, the surface roughness of both sides of the film at nanoscale was evaluated by atomic force microscopy (JPK Nanowizard 3) and optical profilometry (Bruker Contour GT-I).

Results and discussion

The operational range for spraying NC suspension was between 1.0 and 2.0 wt%. Below 1 wt%, the suspension was too dilute and flowed over the metal surface producing an uneven film, which was difficult to peel from the plate after drying. Above 2 wt%, the suspension becomes too viscous to spray. The lower

and upper limits, corresponded to suspension viscosities of 17.0 ± 0.6 and 32.2 ± 0.9 DIN sec, respectively.

Figure 3 shows the effect of NC suspension concentration on the basis weight of the film and mean thickness of the film. Each point is the average of 4 replicates of NC film with the error bars providing the standard deviation. Both film basis weight and thickness increased approximately linearly with increasing NC concentration. Basis weight ranged from 52.8 ± 7.4 to 193.1 ± 3.4 g/m^2 by spraying suspension with a concentration of 1.0 and 2.0 wt%, respectively. The significant reduction in variability is most likely due to the more rigid suspension at 2.0 wt% consistency, which produces a more stable suspension sprayed onto the surface of the plate. The film thicknesses were 83.9 ± 13.9 and 243.2 ± 6.6 μm for the lowest and highest consistencies.

Figure 4 presents the contour plot of the thickness distribution of the 1.5 wt% spray coated film compared with a film made by the established method of vacuum filtration. The basis weight of the film prepared by spray coating and vacuum filtration are almost identical at 100.5 ± 3.4 and 95.2 ± 5.2 g/m^2, respectively. The direction of conveyor movement was from bottom to top. Compared to spray coating, vacuum filtration required a much higher dewatering time of 15 min to produce the film. When compared to the film made from vacuum filtration, the spray coated nanocellulose film is slightly thicker, even when correcting for the slight difference in basis weight. The apparent density of the spray coated film and film prepared via vacuum filtration were 793 and 834 kg/m^3, respectively. In addition, there is a somewhat wider distribution of thickness for the spray-coated film. The thickness of the NC film prepared via vacuum filtration process and spray drying were 113.4 ± 5.4 and 127.1 ± 12.1 μm, respectively. The uncertainties give the standard deviation of the distribution of measured thickness.

Figure 5 shows the surface morphology and topography of both surfaces of the spray coated NC film investigated by scanning electron microscopy and optical prolifometry. The AFM images are given in the supplementary material. At all the length scales investigated, the surface in contact with the stainless steel plate is notably smoother and less porous than the reverse side, where some fibre clumps from the suspension were retained on the film surface as it dried.

Fig. 3 Effect of suspension concentration on the basis weight and thickness of the nanocellulose film prepared using spray coating
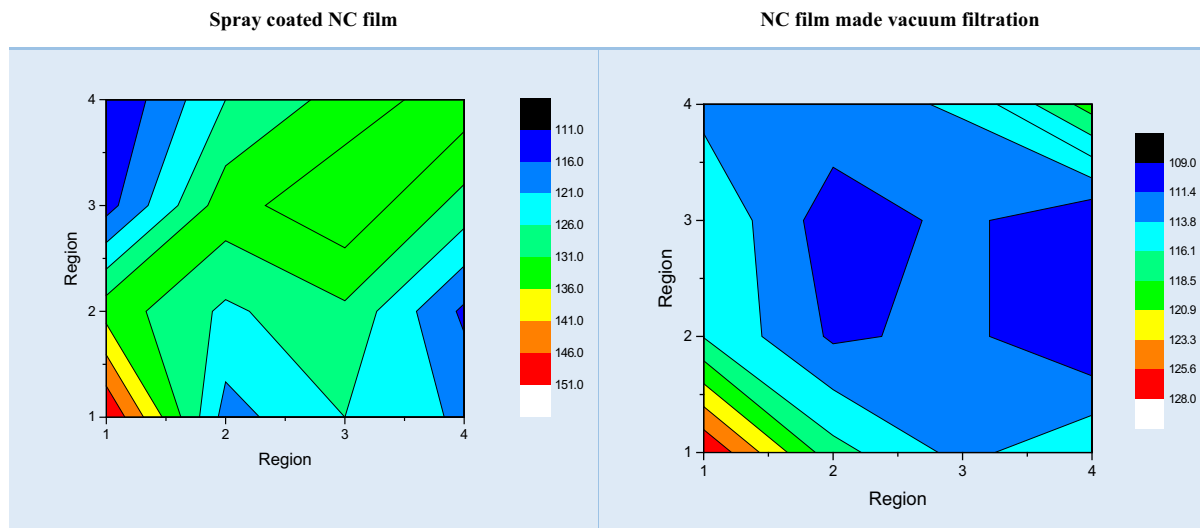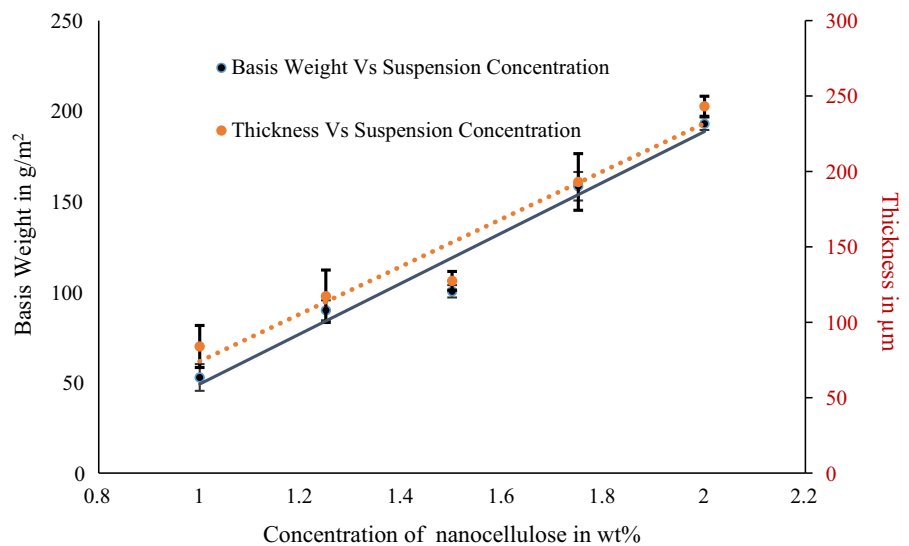
Fig. 4 Thickness distribution of the NC films—spray coated at conveyor velocity of 0.32 cm/s and vacuum filtration

Visually the smooth surface of the sprayed film has a glossy, shiny appearance. The RMS roughness from the AFM images of the rough side is 414.0 nm for 10 μm × 10 μm film area and 51.4 nm for 2 μm × 2 μm film area whereas the RMS surface roughness of the smooth side is only 81.1 nm for 10 μm × 10 μm film area and 16.7 nm for 2 μm × 2 μm film area. AFM measurements of the film prepared by filtration are also given in the Supplementary information and show the sides had a surface roughness of 417.7 nm (Side 1) and 330.8 nm (Side 2) at an inspection are of 10 μm × 10 μm, which

is approximately the same as the rough side of the film prepared by spray coating. Similarly, the RMS roughness of the spray-coated NC film measured using the optical profilometry at an inspection area of 1 cm × 1 cm is 2087 nm on the rough side and 389 nm on the spray coated side when comparing with NC Film prepared via vacuum filtration which had a RMS roughness of 2673 nm on side 1 and of 3751 nm on side 2.

The results reported in this investigation confirm that laboratory scale spraying NC on a stainless steel plate is viable for the rapid preparation of NC film with
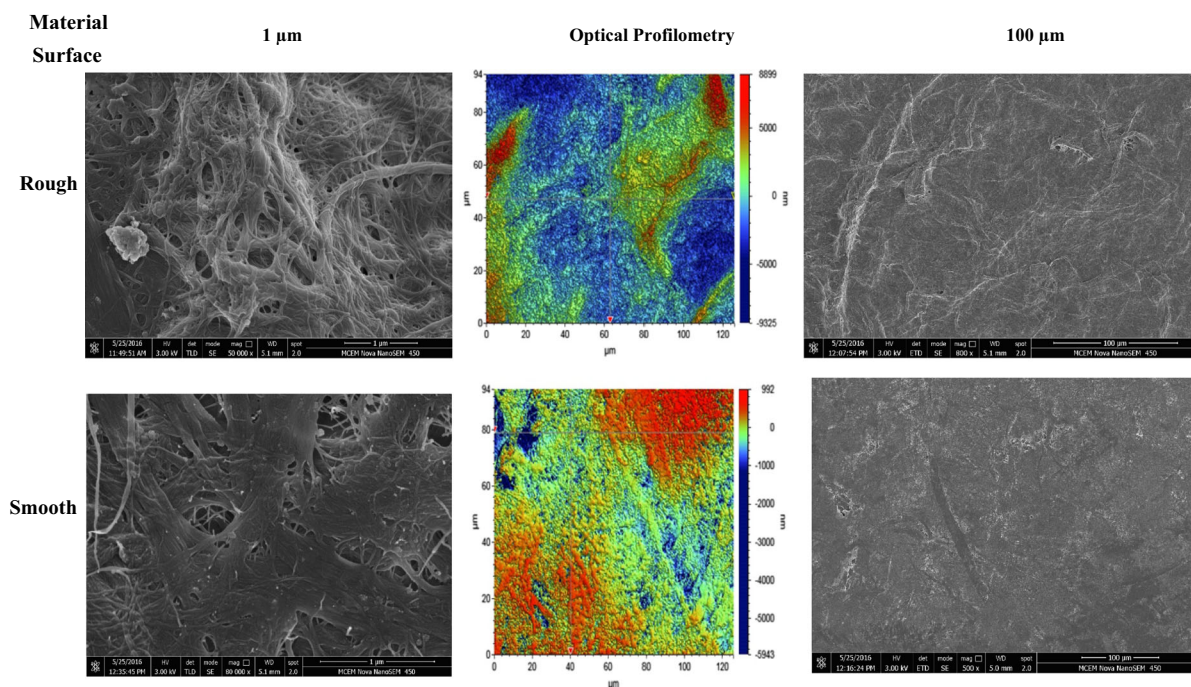
Fig. 5 SEM image of the sprayed NC film—rough and smooth surface and optical profilometry image of both sides of the NC film

a basis weight ranging from 53 to 193 g/m^2. The basis weight of the NC film was readily controlled by the concentration of nanocellulose suspension sprayed.

In our investigation of spraying, the processing time was 50.2 s to spray 15.9 cm diameter films, independent of the basis weight from 53 to 193 g/m^2. The quickest time reported in the literature for sheet/film formation with filtration was from work in our group (Varanasi and Batchelor 2013), where 2.8 min was required for filtering a low basis weight of 56.4 g/m^2, formed from 0.6 wt% suspension. In contrast, the 95.1 g/m^2 film formed at 0.2 wt%, made for the work in this paper, took 15 min to filter.

When the mechanical properties of the spray-coated and vacuum filtered films were compared, it was found that they were the same within the uncertainties. The tensile index of a 104.03 g/m^2 of film prepared via vacuum filtration was 62.3 ± 3.4 Nm/g while the tensile strength of the 100.5 g/m^2 of spray coated nanocellulose film was 60.2 ± 1.5 Nm/g. The tensile stiffness values were also the same within uncertainties at 946 ± 86 and 941 ± 78 kN/m, for the spray coated film and film prepared via vacuum filtration, respectively. The uncertainties give the 95% confidence interval. It is interesting to note that the tensile index of the 100 g/m^2 sheet prepared vacuum filtration is somewhat lower than 60 g/m^2 sheet made via vacuum filtration or spray coating/filtration of 72 Nm/g (Varanasi and Batchelor 2014) and 79 Nm/g (Beneventi et al. 2015), respectively. The air permeance of both the spray coated and vacuum filtered films were less than the measurement limit of the instrument of 0.003 µm/Pa s. This value confirms that the spray coated sheet is highly impermeable.

The current spray coating method is innovative because it allows the production of flat films with uniform thickness. These films require less operator time to produce than films prepared either by filtration or spraying onto porous media (Beneventi et al. 2014) and can be prepared without cracking unlike the moulded structures produced by Magnusson (2016). In addition, in contrast to Obara and McGinity (1994) we have created a cellulose film with one very smooth surface without regenerating or in any way chemically treating or modifying the cellulose.

After filtering, the nanocellulose films can often be difficult to separate from the filter, taking additional time to complete the transfer to the blotting paper without destroying the film. Drying the filtered film then requires repeatedly manually feeding the film into

a rotating drum dryer until dry, with the overall process taking at least 10 min from the start of filtration. In the spray coating method, the drying time for nano cellulose films in ambient conditions is from 24 to 48 h, which is reduced to 30–60 min when drying in an oven at 105 °C. While the total time to prepare and dry a film is longer with spray coating onto a stainless steel plate, the key strength of the method is the reduction in operator time. Leaving aside, the preparation of the nanocellulose suspension, which is common for the two methods, preparing ten 100 g/m^2 sheets requires less than 9 min of operator time with spraying compared to 220 total minutes with filtration.

Conclusion

We have developed a method of spraying a nanocellulose suspension onto a polished stainless steel plate to rapidly make smooth films with a basis weight ranging from 50 to 200 g/m^2, simply by adjusting the suspension consistency. This method greatly reduces the operator time to produce nanocellulose films. Further, spray-coating on to stainless steel creates a two-sided film structure with a very smooth surface in contact with the stainless steel plate.

Supporting information

SEM image of spray coated NC film; AFM image of Spray coated NC film and film prepared via vacuum filtration; Data set for thickness mapping; Optical prolifometry image of NC film prepared via vacuum filtration.

References

Abitbol T, Rivkin A, Cao Y, Nevo Y, Abraham E, Ben-Shalom T et al (2016) Nanocellulose, a tiny fiber with huge applications. Curr Opin Biotechnol 39:76–88. doi:10.1016/j.copbio.2016.01.002

Beneventi D, Chaussy D, Curtil D, Zolin L, Gerbaldi C, Penazzi N (2014) Highly porous paper loading with microfibrillated cellulose by spray coating on wet substrates. Ind Eng Chem Res 53(27):10982–10989. doi:10.1021/ie500955x

Beneventi D, Zeno E, Chaussy D (2015) Rapid nanopaper production by spray deposition of concentrated microfibrillated cellulose slurries. Ind Crops Prod 72:200–205. doi:10.1016/j.indcrop.2014.11.023

Chinga-Carrasco G, Tobjörk D, Österbacka R (2012) Inkjet-printed silver nanoparticles on nano-engineered cellulose films for electrically conducting structures and organic transistors: concept and challenges. J Nanopart Res 14(11):1–10. doi:10.1007/s11051-012-1213-x

Huang L, Chen X, Nguyen TX, Tang H, Zhang L, Yang G (2013) Nano-cellulose 3D-networks as controlled-release drug carriers. J Mater Chem B 1(23):2976–2984. doi:10.1039/C3TB20149J

Koga H, Tokunaga E, Hidaka M, Umemura Y, Saito T, Isogai A, Kitaoka T (2010) Topochemical synthesis and catalysis of metal nanoparticles exposed on crystalline cellulose nanofibers. Chem Commun 46(45):8567–8569. doi:10.1039/C0CC02754E

Krol LF, Beneventi D, Alloin F, Chaussy D (2015) Microfibrillated cellulose-SiO$_2$ composite nanopapers produced by spray deposition. J Mater Sci 50(11):4095–4103. doi:10.1007/s10853-015-8965-5

Magnusson J (2016) Method for spraying of free standing 3D structures with MFC. Master Thesis, Karlstad University

Metreveli G, Wågberg L, Emmoth E, Belák S, Strømme M, Mihranyan A (2014) A size-exclusion nanocellulose filter paper for virus removal. Adv Healthc Mater 3(10):1546–1550. doi:10.1002/adhm.201300641

Nogi M, Iwamoto S, Nakagaito AN, Yano H (2009) Optically transparent nanofiber paper. Adv Mater 21(16):1595–1598. doi:10.1002/adma.200803174

Obara S, McGinity JW (1994) Properties of free films prepared from aqueous polymers by a spraying technique. Pharm Res 11(11):1562–1567. doi:10.1023/a:1018949502392

Orelma H, Filpponen I, Johansson L-S, Österberg M, Rojas OJ, Laine J (2012) Surface functionalized nanofibrillar cellulose (NFC) film as a platform for immunoassays and diagnostics. Biointerphases 7(1):61. doi:10.1007/s13758-012-0061-7

Shimizu M, Saito T, Fukuzumi H, Isogai A (2014) Hydrophobic, ductile, and transparent nanocellulose films with quaternary alkylammonium carboxylates on nanofibril surfaces. Biomacromol 15(11):4320–4325. doi:10.1021/bm501329v

Varanasi S, Batchelor WJ (2013) Rapid preparation of cellulose nanofibre sheet. Cellulose 20(1):211–215. doi:10.1007/s10570-012-9794-1

Varanasi S, Batchelor W (2014) Superior non-woven sheet forming characteristics of low-density cationic polymer-

cellulose nanofibre colloids. Cellulose 21(5):3541–3550. doi:10.1007/s10570-014-0370-8

Varanasi S, Low Z-X, Batchelor W (2015) Cellulose nanofibre composite membranes—biodegradable and recyclable UF membranes. Chem Eng J 265:138–146. doi:10.1016/j.cej.2014.11.085

Zhang L, Batchelor W, Varanasi S, Tsuzuki T, Wang X (2012) Effect of cellulose nanofiber dimensions on sheet forming

through filtration. Cellulose 19(2):561–574. doi:10.1007/s10570-011-9641-9

Zolin L (ed) (2017) Electrode preparation exploiting the spray coating technique. In: Large-scale production of paper-based Li-ion cells. Springer International Publishing, Cham, pp 77–94. doi:10.1007/978-3-319-39016-1_6

CrossMark

ORIGINAL PAPER

Flexible spray coating process for smooth nanocellulose film production

Kirubanandan Shanmugam · Hamid Doosthosseini · Swambabu Varanasi · Gil Garnier · Warren Batchelor

Abstract A novel rapid method for high throughput production of smooth nanocellulose (NC) films by spray coating was communicated recently. In this method, we employed spray coating to produce wet films on stainless steel plates moving on a conveyor, forming free-standing films with interesting structural, mechanical and surface properties upon drying. In this research, we investigate the range of mechanical and physical properties of nanocellulose films prepared by spraying. Furthermore, a comparison with NC films prepared via conventional vacuum filtration was conducted to evaluate the suitability of this method as an alternative film preparation process. One set of experiments was completed where the solids concentration of the suspension was fixed at 1.5 wt% and the conveyor velocity was varied, while two series of experiments were completed where the solids concentration of the suspension was varied and the conveyor speed was fixed at either 0.32 or 1.05 cm/ s. By varying speed and solids concentration, spray-coating was found to allow efficient production of films with basis weights ranging from 38 to 187 g/m², with film thicknesses ranging from 58.4 to 243.2 μm, respectively. There was a universal linear relationship between the thickness and basis weight, independent of the process conditions. The optical uniformity of film was also noticeably dependent on the spraying process. The optical uniformity index of films, relative to vacuum filtered films, increased with conveyor speed at 1.5 wt% solids concentration and was independent of solids concentration at low speed. Forming at the higher speed of 1.05 cm/s produced a maximum in optical uniformity in the range 1.5–1.75%, with these films being more uniform than conventional films produced through vacuum filtration. The most uniform films produced by spraying also had a similar tensile index to films made via vacuum filtration. With an understanding of these parameters and effects, we demonstrate this method to be a more time efficient alternative method to produce uniform films where the properties can be tailored to the required application.

K. Shanmugam · H. Doosthosseini · S. Varanasi · G. Garnier · W. Batchelor (✉)
Department of Chemical Engineering, Bioresource Processing Research Institute of Australia, Monash University, Melbourne, VIC 3800, Australia
e-mail: Warren.Batchelor@monash.edu

Introduction

Throughout the past decade, there has been notable growth in the use of micro fibrillated cellulose/nanocellulose films as sustainable substrates for the development of a variety of functional materials (Abitbol et al. 2016). The literature on this topic has confirmed the applicability of nanocellulose films for nanocomposites, anti-microbial films and barrier materials (Dufresne 2013) among others. Films made from nanocellulose are strong and show good oxygen barrier properties; they also have the capacity for a broad range of chemical modifications which can attain varied and desirable properties. Additionally, this material is biodegradable, renewable, non-toxic and readily available in large quantities (Klemm et al. 2011).

Nanocellulose films are commonly prepared using either vacuum filtration, whereby fibre suspensions are filtered using a mesh filter and fibres gather in the form of a film, or casting, where the suspension is poured onto a surface and left to dry. Casting is a very time-consuming process as it typically requires three days for drying and can cause wrinkling of the film which is difficult to control (Shimizu et al. 2014). It is another laboratory method used for producing nanocellulose film (Rebouillat and Pla 2013). The strength of cast nanocellulose films is lower than that of films prepared using vacuum filtration method, which is a conventional process in paper-making industries (Sehaqui et al. 2010). Vacuum filtration is quicker than casting, however, time consumption is still significant (Siró and Plackett 2010). There are also difficulties in separating the film from the filter mesh and subsequent handling before final drying.

Modifications have improved filtration by increasing the solids content above the gel-point to reduce filtration time, increasing the size of the filter openings to reduce filter resistance and by using polyelectrolytes (Varanasi and Batchelor 2014). Laboratory film preparation time for light weight films less than 60 g/m^2 has been reduced from 3 or 4 h (Nogi et al. 2009) to 10 min (Varanasi and Batchelor 2013; Zhang et al. 2012). Despite these modifications, there are still significant issues as larger filter openings can result in a loss of material rendering it difficult to control the basis weight of the product and decreasing yield. Vacuum filtration processes reported in literature require a film preparation time ranging from 45 min to 3–4 h (Nogi et al. 2009) when finer filters are used. In addition, bulky cellulose film preparation via vacuum filtration is challenging; dewatering time increases exponentially with increased basis weight leading to high operation and labour costs. As such, the range of film basis weights that can be manufactured is limited.

Recently spraying nanocellulose (NC) has emerged as a viable alternative method of NC film preparation (Beneventi et al. 2014, 2015), while a rapid laboratory scale method for spray coating of NC suspension on a polished stainless steel (SS) plates to create free-standing recyclable films has been reported. Spray coating results in a very uniform deposition layer of nanocellulose on the base surface; the amount of NC increases with an increase in the suspension concentration or decrease in the velocity of the conveyor. Most significantly, spraying can substantially decrease operating time (Shanmugam et al. 2017).

The present work investigates the effects of process variables on the properties of free-standing NC films prepared by spraying on stainless steel plates. The effects of conveyor velocity, NC suspension concentration and setup configuration are evaluated. The properties of spray coated films are compared with films prepared via vacuum filtration and the effects of process parameters on these properties are quantified. The spraying of nanocellulose on the base surface is hypothesized to produce a stable and uniform distribution of nanocellulose, leading to free-standing films of high optical uniformity. Obtaining quantifiable relationships between process parameters and product properties will allow for tuning product properties such as uniformity and designing processes for desired products.

Experimental method

Materials

Micro-fibrillated cellulose, also commonly referred to as Nanocellulose in this paper was used for film preparation. Both spray coating and the conventional vacuum filtration methods were employed. From here on, Nanocellulose will be referred to as NC; nanocellulose films prepared by vacuum filtration, VF-NC; and Spray coated films, SC–NC. NC was supplied from DAICEL Chemical Industries Limited (Celish

KY-100S) with an initial concentration of 25 wt% cellulose fibres. DAICEL NC has fibrils with an average diameter of ∼ 70 nm with a wide distribution of fibril diameter, mean length of fibre around 8 μm and an average aspect ratio of 142 ± 28. The crystallinity of the NC sample was measured as 78% (Raj et al. 2016). NC was diluted to the concentration ranges from 1.00 to 2.50 wt% and disintegrated in a Messmer disintegrator Model MK III C for 15,000 revolutions at 3000 RPM. The viscosity of the NC suspension was evaluated by the flow cup method, i.e. measuring coating fluid flow through an orifice as a relative measure of kinematic viscosity expressed in seconds of flow time in DIN-Sec.

Spray coating

NC suspension was sprayed onto stainless steel plates using Wagner spray system (Model number 117). The experimental set up for spray coating is shown in Fig. 1. It is mainly consisting of variable speed conveyor and pressure driven spray system with a knob for adjusting/controlling pressure. The spraying of nanocellulose is performed on two different geometries like square stainless steel square plate (220 mm × 220 mm) and circular plate (Diameter—159 mm). Experiments were conducted in 3 series.

In experimental series 1, the spray jet angle was 50° and the spray width was 30 cm at a spray distance and pressure of 200 bar, respectively. Suspension concentration was kept constant at 1.5 wt% and conveyor speed was varied from 0.25 to 0.59 cm/s. 30 s time was allowed for pressure driven spray system to reach steady state. (Shanmugam et al. 2017).

In experimental series 2, the spray system setup was similar to series 1; however, the conveyor speed was kept constant at 0.32 cm/s and suspension concentration was varied from 1 to 2 wt%.

In experimental series 3, the conveyor system was changed, as was spray nozzle to attain a jet angle of 30° and beam width of 22.5 cm at a spray distance of 50.0 ± 1.0 cm and 100 bar pressure. The conveyor speed was kept constant at 1.05 cm/s and suspension concentration varied from 1.5 to 2.5 wt%.

After spraying, each film was dried on its plate for 24–48 h at ambient conditions, and subsequently removed from the plate and stored at 23 °C and 50% RH before testing.

Vacuum filtration

NC films were prepared using vacuum filtration as reported previously (Varanasi and Batchelor 2013). In brief, NC suspension with 0.2 wt% concentration was poured into a cylindrical container with 125 mesh at
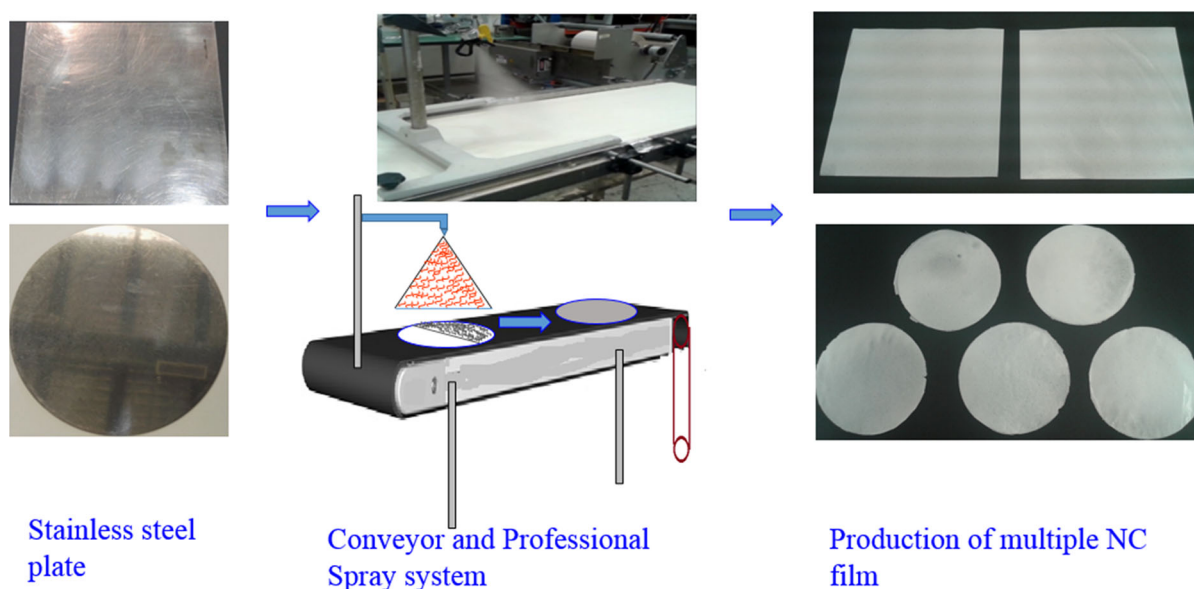
Fig. 1 An experimental setup for spraying NC suspension on a stainless steel plate to make multiple films

the bottom and filtered, forming a wet film on the mesh. After couching, the wet film was carefully separated using blotting papers, wet pressed at 0.4 MPa by sheet press (Type 5-1, AB Lorentzen & Wettre) for 7 min and drum dried at 105 °C. The drying of the film took up to 10 min. The film prepared by this method is used as a standard reference film to compare the optical uniformity and strength of the spray coated film.

Characterization of the NC films

Basis weight of NC films

The basis weight was evaluated by weighing a standard area of the film after 4 h drying in the oven at a temperature of 105 °C.

Thickness of NC films

The thickness of the spray coated films was determined using a Thickness Tester Type 21 from Lorentzen & Wettre AB, Stockholm, Sweden. The thickness was measured for at least 36 points on each of the spray coated and vacuum filtered NC films and averaged. The thickness of NC film was measured according to Australian/New Zealand standard method 426.

Apparent density

The apparent density of the NC films was evaluated through dividing basis weight by mean thickness of the film and followed Australian/New Zealand standard method 208.

Tensile strength

An Instron model 5566 was used to measure the tensile strength of the NC films. The tensile strength test samples were 100 mm in length and 15 mm width. The samples of NC films are equilibrated and conditioned for at least 24 h at 23 °C and 50% RH before dry tensile testing based on the Australian/New Zealand Standard Methods 448 and 437 s. All thickness and tensile tests were done at 23 °C and 50% RH. The samples were tested at a constant rate of elongation of 10 mm/min. The Tensile Index (TI) of the samples was calculated from the tensile strength (expressed in Nm^{-1}) divided by basis weight (gm^{-2}). The mean value was obtained from six to seven valid tests and the error bars in plots indicate standard deviation. The elastic modulus was calculated from the maximum slope in the stress–strain curve determined by the software.

Surface investigation

The surface morphology and topography was studied using Scanning Electron Microscopy of iridium coated NC-films. Images were sampled at magnifications of $500\times$ to $50,000\times$ in secondary electron mode-II of FEI Novo SEM 450 for Spray Coated NC film and FEI Magellan 400 FEGSEM for NC film prepared via vacuum filtration. The surface roughness of NC films were evaluated by the Parker print surface roughness tester (M590, Testing machines Inc), Atomic force microscopy (JPK Nanowizard 3) and optical profilometry (Bruker Contour GT-I).

Formation analysis

The optical uniformity of NC film was measured by the Paper Perfect Formation (PPF) tester (Op Test Equipment Inc, Canada), which measures the optical uniformity of light transmitted through the sample. In brief, the PPF consists of a black and white camera based image analyser and uses a CCD camera interfaced with 256 gray levels and 65 μm/pixel resolution. The analyser uses a diffuse quartz halogen light source with IR filters and automatic intensity control. The PPF classifies formation quality over 10 length scales ranging from 0.5 to 60 mm. The data reported here is the Relative Formation Value (RFV) of each component relative to one of the films made by vacuum filtration, which was used as a reference film. Three to six films were measured for each condition, with the results averaged. RFV value less than 1 means that the optical uniformity of the NC film tested is worse than the reference film at that length scale.

Results

The operational range of the conveyor's velocity, from 0.25 to 0.59 cm/s, was studied in series 2 of SC–NC experiments where the effects of velocity were studied

and suspension concentration was kept constant at 1.5 wt%. Within these bounds, basis weight ranged from 49.1 ± 5.4 to 102.2 ± 7.5 g/m^2 and thickness ranged from 70. 5 ± 2.9 to 130.3 ± 11.3 μm. Figure 2 shows the results for Series 2. At low velocity from 0.37 to 0.25 cm/s, the basis weight of the film is relatively constant at ∼ 100 ± 3 g/m^2 for 1.5 wt% consistency, representing a limit to the amount of suspension that remains on the plate after spraying. The plateau in film basis weight with reducing speed indicates that the carrying capacity of the plate has been reached and that excess material is likely to be flowing off the plate. Interestingly no such flow is observable in the films after they have dried, either in the thickness profiles reported in our previous paper (Shanmugam et al. 2017) or, as will be discussed later, in the transmitted light images captured to measure optical uniformity. The most likely explanation is that the fluid on the plate has levelled while the plate is held stationary as the film dried.

Beyond 0.37 cm/s, the basis weight of the film decreases as velocity increases in inverse proportions. In other words, less NC is deposited on the stainless steel when moving at a faster speed, resulting in the formation of a low basis weight NC film due to low suspension consistency of the NC.

The basis weight and thickness of NC films are controlled by the velocity of the conveyor and the consistency of the suspension. Assuming constant flow output of the spray system and positive displacement pump, it may be assumed that deposited mass per unit time would have a positive linear relation with suspension consistency, C_0. From the spray system manual, the spray flow is estimated to be 1.00 L/min or $\dot{m} = 17 \times 10^{-3}$ kg/s, assuming a suspension density of 1000 kg/m^3. If the film width is w, the mass consistency is C_0 (kg fibre/kg of suspension) and the conveyor velocity is υ then the film basis weight, B, is given by the Eq. (1).

$$B = \eta \frac{C_0}{\upsilon} \frac{\dot{m}}{w} \qquad (1)$$

where η is an efficiency factor, which includes losses from spraying over the width of the plate, suspension flow and any reduction in flow as suspension viscosity increases.

Figure 3 shows data for three series of experiments of SC–NC demonstrating basis weight as a function of C_0/v. It can be seen that in series 3, the optimized configuration shows a higher value for x, representing a higher efficiency in the process, which is the result of decreased pressure, change of nozzle and change in setup configuration. The negative values for the y-intercept represent losses of constant value, such as aerosol loss of material. It should be noted that in calculation of trend line for series 2, values below conveyor velocity of 0.38 cm/s were not considered. From Fig. 2, it was inferred that maximum deposition is reached at 0.38 cm/s and lowering velocity further results in any additional material flowing off the steel plates.

When the results for thickness are plotted in Fig. 4, it can be seen that there is a linear relation between thickness and basis weight of films. This relationship

Fig. 2 Influence of the conveyor velocity on the basis weight of SC–NC
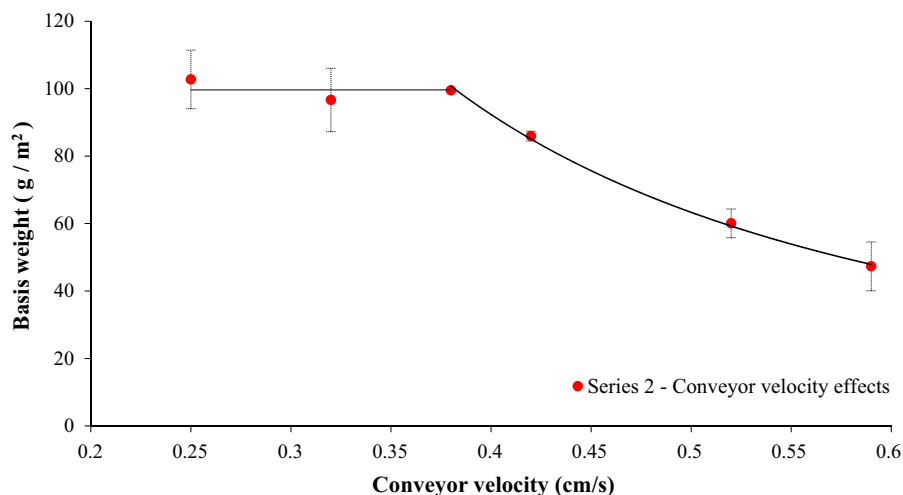
Fig. 3 Basis weight as proportional to $\frac{C_0\,(g/g)}{v\,(cm/s)}$
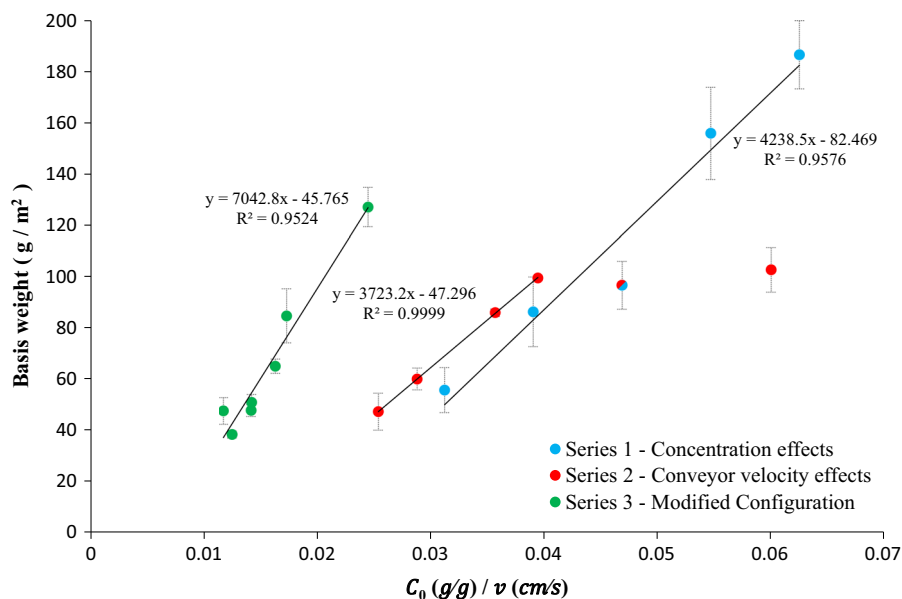
Fig. 4 Effect of NC suspension concentration and velocity of conveyor on Basis weight and thickness of spray coated NC film
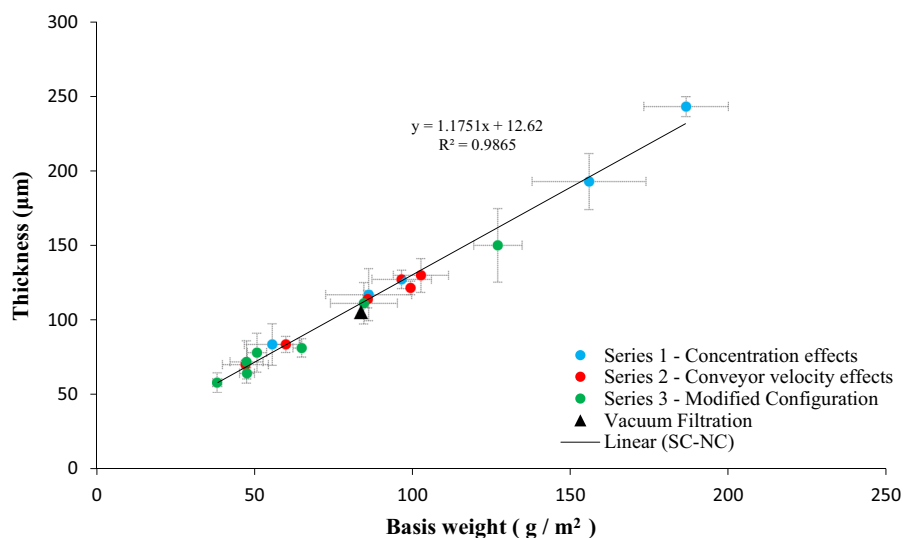
is maintained irrespective of configuration and process parameter changes.

The basis weight and thickness of the NC film can be tailored by two parameters, namely NC concentration and conveyor velocity. Though both can be varied independently, the relationship between thickness and basis weight is a characteristic of these SC–NC films. The figures show that the thickness of VF-NC also lies on the same trend line, irrespective of the fundamentally different production procedure. To calculate the error bars for thickness, all the values measured for a

given film were averaged. The average values for the set of films was then used to calculate the overall average shown here, with error bars calculated as the standard deviation of these film averages. The basis weight was only measured once for each film.

The apparent density of films was calculated based on the basis weight and mean thickness of NC films. Figure 5 shows the apparent density as a function of basis weight. It can be seen that for films of basis weight around or higher than 100 g/m^2, apparent density is constant. However, for lower basis weights,

Fig. 5 Relationship between apparent density and basis weight of the films
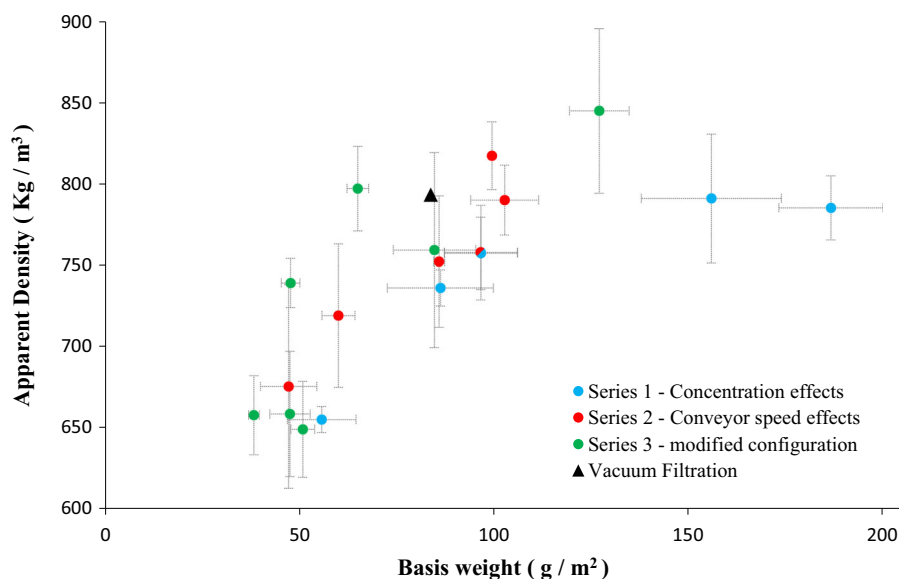
apparent density is lower demonstrating the effects of agglomerates and surface non-uniformity fibre clumps which become more significant as basis weight is decreased. This is also reflected by the non-zero y-intercept in Fig. 4.

The apparent densities of SC–NC close to 100 g/m^2, (99.5 $\pm$ 0.1, 102.7 $\pm$ 8.7 g/m^2) are 817.2 $\pm$ 20.9 and 789.9 $\pm$ 21.5 kg/m^3 respectively. Measurements for VF-NC films of 100 g/m^2 were found to be 822.5 $\pm$ 14.6 kg/m^3, within the same range and comparable to SC–NC considering the uncertainties.

Optical uniformity

Within the operational range of the conveyor and spray system, the effects of both velocity and suspension concentration were studied. These parameters were found to distinctly affect the optical uniformity of the films obtained. The optical uniformity of nanocellulose films were quantified at different length scales and analysed with the relative values defined using one of the VF-NC films as a reference. To simplify the presentation, the results are presented as firstly the average of all inspection zone sizes smaller than 1.8 mm and secondly of all inspection zone sizes between 1.8 and 12 mm. It should be noted that some spray coated films contain air bubbles and visible ripples, as can be observed in Figs. 10 and 11. These reduce the measured optical uniformity, although the contribution of bubbles and ripples, in comparison to

flocculation driven non-uniformity, is hard to quantify. Our major interest here is to use the measurement to identify the experimental conditions where the optical uniformity is equivalent to or better than the films formed through vacuum filtration. The uniformity of the smaller components of formation of the film tends to strongly influence the print quality while larger components of the film influence its strength.

Figures 6 and 7 show the optical uniformity of SC–NC films, at large and small inspection zones, respectively, as a function of conveyor velocity at 1.5 wt% suspension concentration. Detailed graphs can be found in the supplementary information.

The results show that as conveyor velocity increases, the films obtained are more uniform in both larger and smaller component sizes. The relative optical uniformity of all SC–NC is higher for smaller components than for larger components.

Figures 8 and 9 show the optical uniformity of SC–NC films as a function of suspension concentration at their respective constant velocities (0.32 m/s for series 2 and 1.05 cm/s for series 3), detailed graphs can be found in the supplementary information.

With increasing suspension concentration, an increased amount of agglomerated fibres is expected which would lead to lower optical uniformity. However, a thicker film with higher basis weight is obtained at higher concentrations leading to more overlapped fibres and higher optical uniformity. This compound effect determines the variation in optical

Fig. 6 Average Optical Uniformity Index of larger components (1.8–12 mm) as a function of conveyor velocity with vacuum filtered film as reference
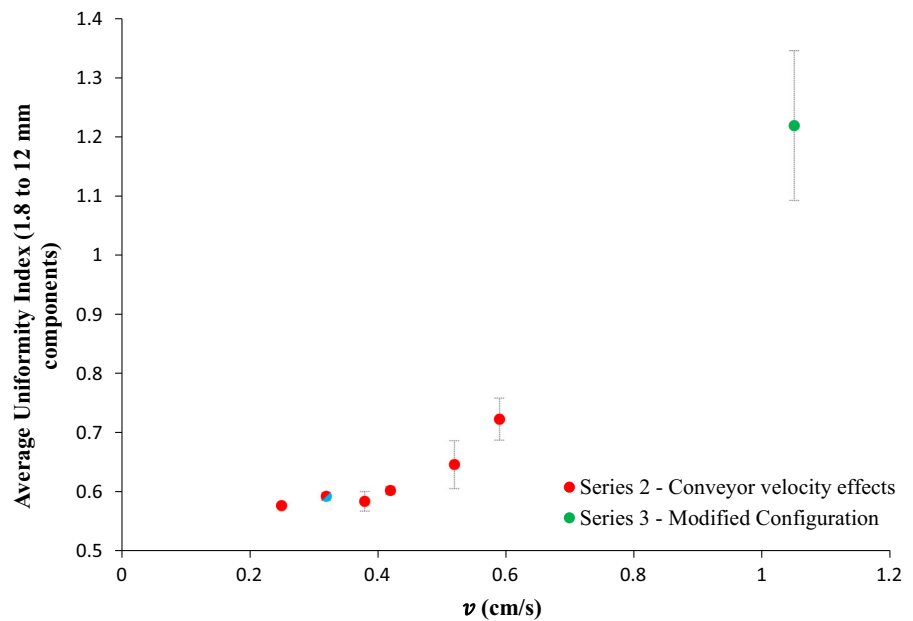
Fig. 7 Average Optical Uniformity Index of smaller components (< 1.8 mm) as a function of conveyor velocity with vacuum filtered film as reference
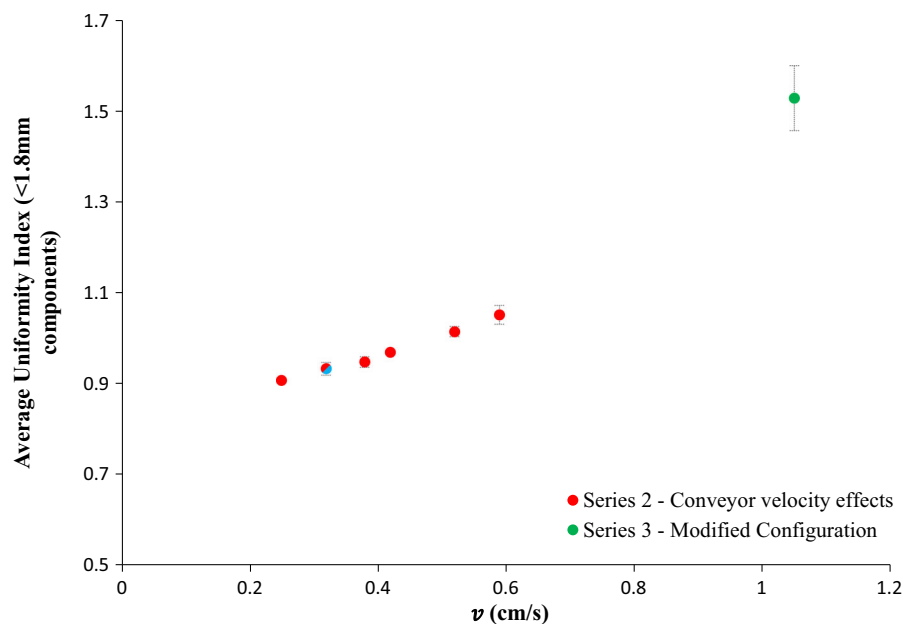
uniformity as a function of concentration. Figure 8 shows that at a constant velocity of 0.32 cm/s, higher optical uniformity in larger components is observed with increasing suspension concentration. This trend seems to be less pronounced for smaller components in Fig. 9.

One of the vacuum filtered NC films was used as a reference for all the Paper Perfect Formation comparisons and all data were normalised by the reference film value at each length scale. The values for the vacuum filtered films in Figs. 6, 7, 8, and 9 are all close to but not equal to 1.0 as the complete set of data for all vacuum filtered films was averaged, including the one reference NC film.

Results for series 3 show no universal trend in optical uniformity with the change of concentration,

Fig. 8 Average Optical Uniformity Index of larger components (1.8–12 mm) as a function of suspension concentration with vacuum filtered film as reference
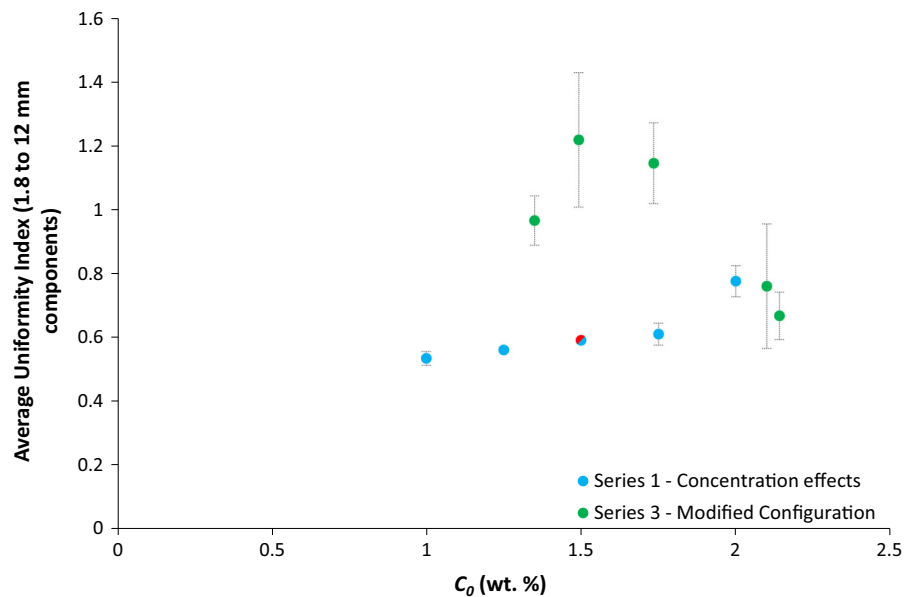
Fig. 9 Average Optical Uniformity Index of smaller components (< 1.8 mm) as a function of suspension concentration with vacuum filtered film as reference
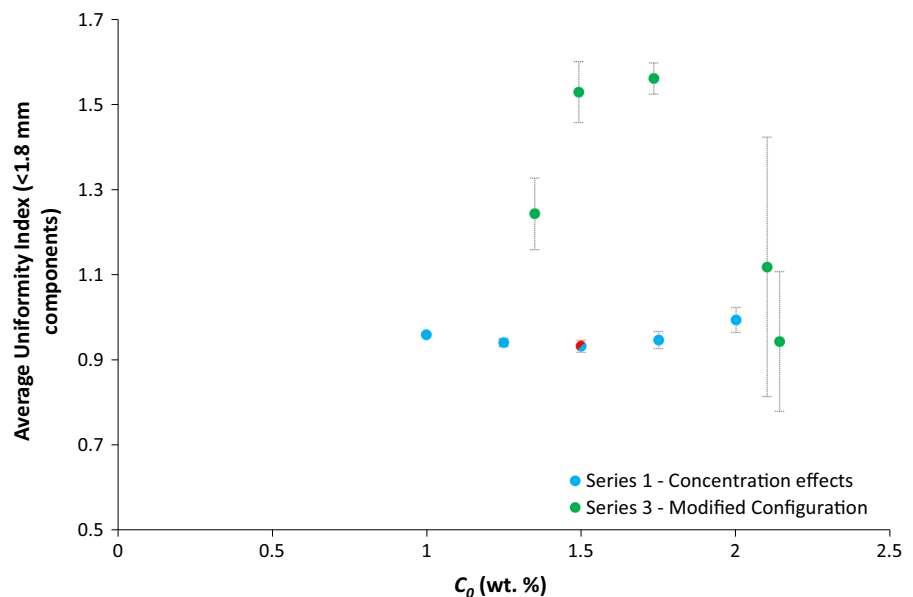
however, it is noteworthy that these films made at an increased velocity of 1.05 cm/s show higher uniformities in general. This was also demonstrated in Figs. 6 and 7. It is shown that to attain constant basis weight films, operating at higher velocities and higher suspension concentration creates more uniform films across all component sizes.

With the modified configuration operating at a higher conveyor velocity in series 3, the range of uniformities is as high as and above that of the VF-NC film; the spray coated NC film no longer visually shows the presence of non-uniformities and contains pinholes, whereas these could be observed for series 1 and series 2 experiments.

Figures 10 and 11 shows the images captured by the Paper Perfect Tester of NC films prepared via spray coating and vacuum filtration. Each image was recorded of an area of 6.75 cm × 6.75 cm. The optical uniformity of formed NC film worsened upon decreasing suspension concentration and the velocity

| VF – NC Film as Reference | Velocity -0.59 cm/sec | Velocity- 0.52 cm/sec | Velocity -0.42 cm/sec |
| Velocity -0.38 cm/sec | | | |

| VF – NC Film as Reference | Velocity -0.38 cm/sec | Velocity – 0.32 cm/sec | Velocity – 0.25 cm/sec |
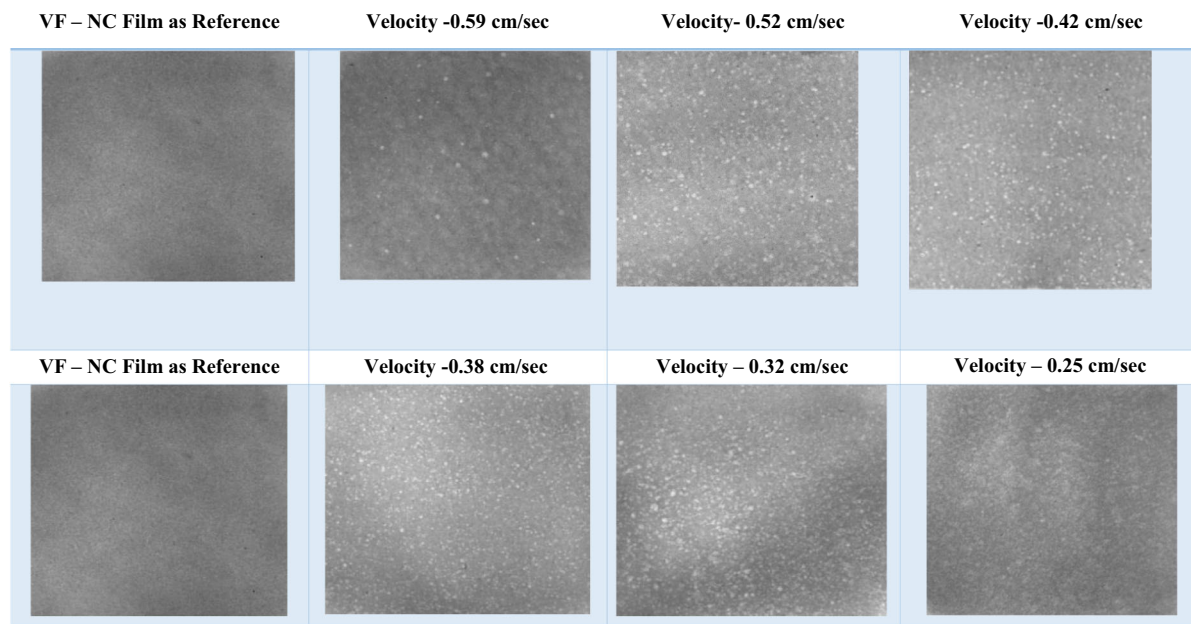
Fig. 10 Paper formation test for Nanocellulose films prepared spray coating at a different velocity (series 2)

of the conveyor, especially at larger components around 5 mm. Additionally, the 1% wt. NC spray coated film has ripples in the film while the surface of the film remains smooth. The ripples are formed by the transverse flow of the 1% wt suspension NC on the stainless steel plate after the spray impacts the surface. This problem was overcome by increasing the suspension concentration.

It can also be seen that apart from the ripples at low solids concentration, there is no evidence of fluid flow during the forming process, even though the plateau in film basis weight with decreasing velocity, shown in Fig. 2, strongly suggests that such flow must be occurring. As we previously mentioned, the most likely explanation for the apparent discrepancy is that the fluid film on the plate has levelled while the plate is held stationary during drying.

Figure 12 shows the spray coated film prepared via modified configuration and the films are free from glossy points and surface irregularities. Figures 1, 2, and 3 in the supplementary information reveal the relative formation value of each component of spray coated NC films prepared via adjusting NC concentration and velocity of the conveyor and relative to the NC film prepared via vacuum filtration. RFV value of NC film from series 1 is mostly lower than 1 and the NC film made 1.75 wt% is higher than 1

confirming good optical uniformity and formation quality in the film.

Mechanical properties

The mechanical properties of NC films were investigated by tensile strength testing. Figure 13 shows the tensile index of SC–NC as a function of basis weight and error bars concluding the standard deviation of six films. The actual Load Vs Strain curves of the spray coated films are available in the supplementary information. It can be seen that there is some indication that for series 2, a higher tensile index of a film is associated with a higher basis weight. However, considering standard deviation of measurements, no statistically meaningful difference can be inferred between series 1 and series 2. It can be seen that the SC–NC films from series 3, using the higher spraying efficiency configuration, show somewhat higher tensile strengths, with values equivalent to VF-NC. This is probably due to the higher optical uniformity of these films compared to the series 1 and series 2 films.

Higher basis weight films are significantly more rigid. This was investigated by evaluating the relationships between stress and strain, represented in Figure 14 as Elasticity (E-modulus). The relationship

VF-NC Film   **2.0 % N C Wt. SC-Film**   **1.75 % Wt. NC-Film**

1.50 % NC Wt. SC –Film   **1.25 % NC Wt. SC-Film**   **1.00 % NC Wt. SC-Film**

Fig. 11 Paper formation test for NC-film prepared via spraying different NC concentration (Series 1)

VF-NC Film   1.75 Wt% SC- NC Film 1   1.72 Wt% SC-NC Film 2

Fig. 12 Paper formation test for spray coated NC film prepared via modified configuration (Series 3)

Fig. 13 Tensile Index of NC films as a function of basis weight
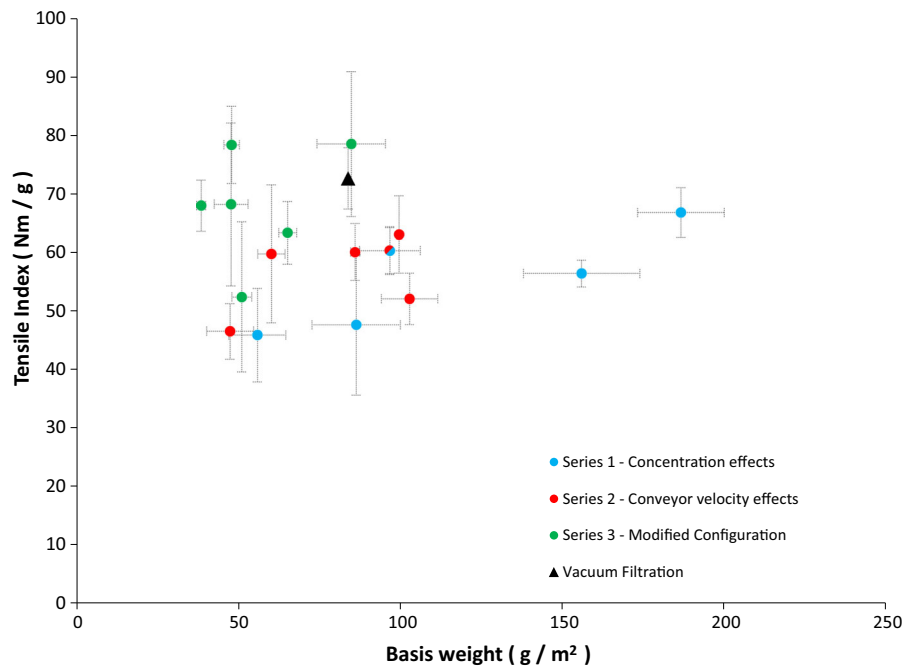
Fig. 14 Elastic modulus of NC films as a function of basis weight
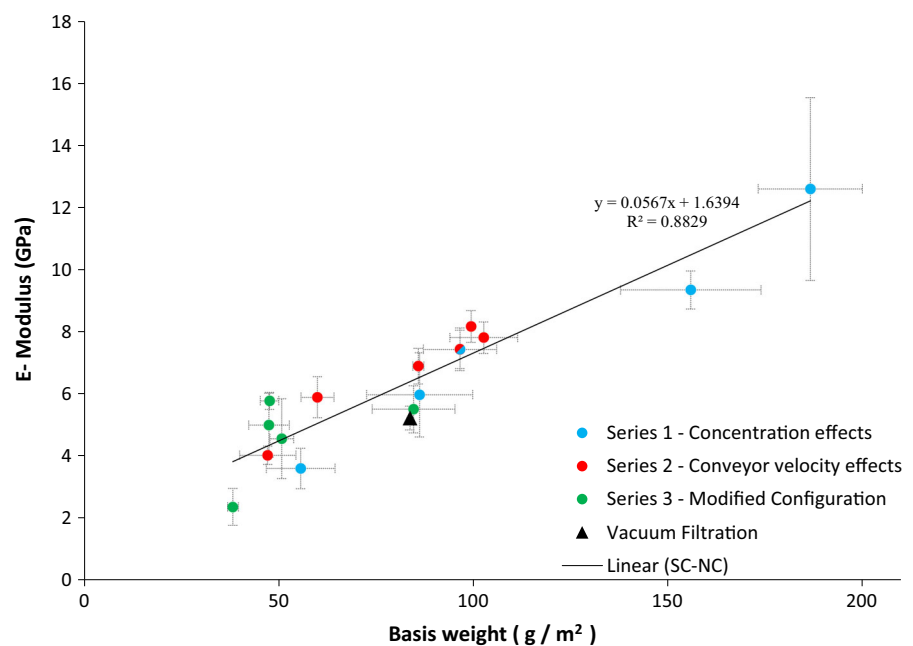
between the E-modulus and basis weight was found to be linear over the basis weight range investigated.

Figure 14 shows the elastic modulus of NC films against its basis weight, showing a linear increase with increasing basis weight. The E-modulus of the 83.8 g/m^2 VF-NC film is 5.22 $\pm$ 0.38 GPa, which is slightly

lower than that of SC–NC films of similar basis weight. One effect that is certainly contributing to this result is that Fig. 5 shows that film density increases with the basis weight rising from 650 to 850 kg/m^3 as basis weight increases. This increase in density will reduce the cross-sectional area for a given basis

weight, thus increasing strength, even if the breaking load has not changed. The second effect that may be important is that a denser fibre network will produce a higher number of fibre–fibre bonds, which for films from conventional cellulose fibres from wood has been theoretically and experimentally established to increase elastic modulus due to an improvement in the stress transfer efficiency in the network (Niskanen 1998). To clarify the effects of density, the data in Fig. 14 has been recalculated as the tensile stiffness index which is independent of thickness and has been plotted against film density and added as Fig. 9 in the supplementary information.

Figure 15 shows the SEM images of the NC films surfaces. It can be seen that the rough side of spray coated NC film is more porous than that of smooth side. Additionally, the spray coated NC film

are of similar roughness to vacuum filtered films on the air side, while being much smoother on the spray coated side. The surface roughness of 100.5 ± 3.4 and 95.2 ± 5.2 g/m^2 NC film measured via Parker surface instrument reveals 10.7 ± 0.4 μm on the rough side and 6.1 ± 1.8 μm on smooth side (95% confidence interval) for the spray coated (series 1 condition) compared with 10.67 ± 0.3 μm on filter side and 9.88 ± 0.15 μm on the free side of the vacuum filtered NC film.

Figures 16 and 17 shows the optical profilometry images of both surfaces of spray coated (100.5 ± 3.4 g/m^2 via series 1) and vacuum filtered (95.2 ± 5.2 g/m^2) NC films. The nanoscale RMS surface roughness of the spray coated NC film evaluated via an optical profiler (20× magnification with an inspection area of 235 μm × 310 μm) is

Side 1
(Rough side for Spray Coated NC film)

Side 2
(Smooth side for spray coated NC film)

(A)

(B)

(C)

(D)

Fig. 15 SEM micrographs of **a**, **b** two sides of VF-NC films, **c** the rough side of SC–NC film and **d** smooth side of SC–NC film

Rough

Smooth

2371 nm on the rough side and 682 nm on a smooth side. The smooth side roughness is much lower compared with the vacuum filtered film, where the roughness at filter side and free sides are 2877 and 4253 nm respectively.

We previously reported AFM measurements of the spray coated (100.5 ± 3.4 g/m^2 via series 1) NC film showed a RMS surface roughness of 414.0 nm for 10 μm × 10 μm film area and 51.4 nm for 2 μm × 2 μm film area on the rough side. This compared with a RMS roughness of only 81.1 nm for 10 μm × 10 μm film area and 16.7 nm for 2 μm × 2 μm film area on the spray coated side. When compared with the vacuum filtered 95.2 ± 5.2 g/m^2 NC film, the sides had a surface

roughness of 417.7 nm (Filter side) and 330.8 nm (air side) at an inspection area of 10 μm × 10 μm, which is approximately the same as the rough side of the film prepared by spray coating (Shanmugam et al. 2017).

Discussion

Spray coating has been proven to be a rapid and scalable method for the preparation of NC films, rendering it an exciting alternative for vacuum filtration which has many limitations (Shanmugam et al. 2017). To fully understand this process and allow for its implementation, a deeper understanding of the process parameters and properties of spray coated NC

Fig. 17 Optical Profilometry Images of both surface of vacuum filtered NC Film-×20 magnification
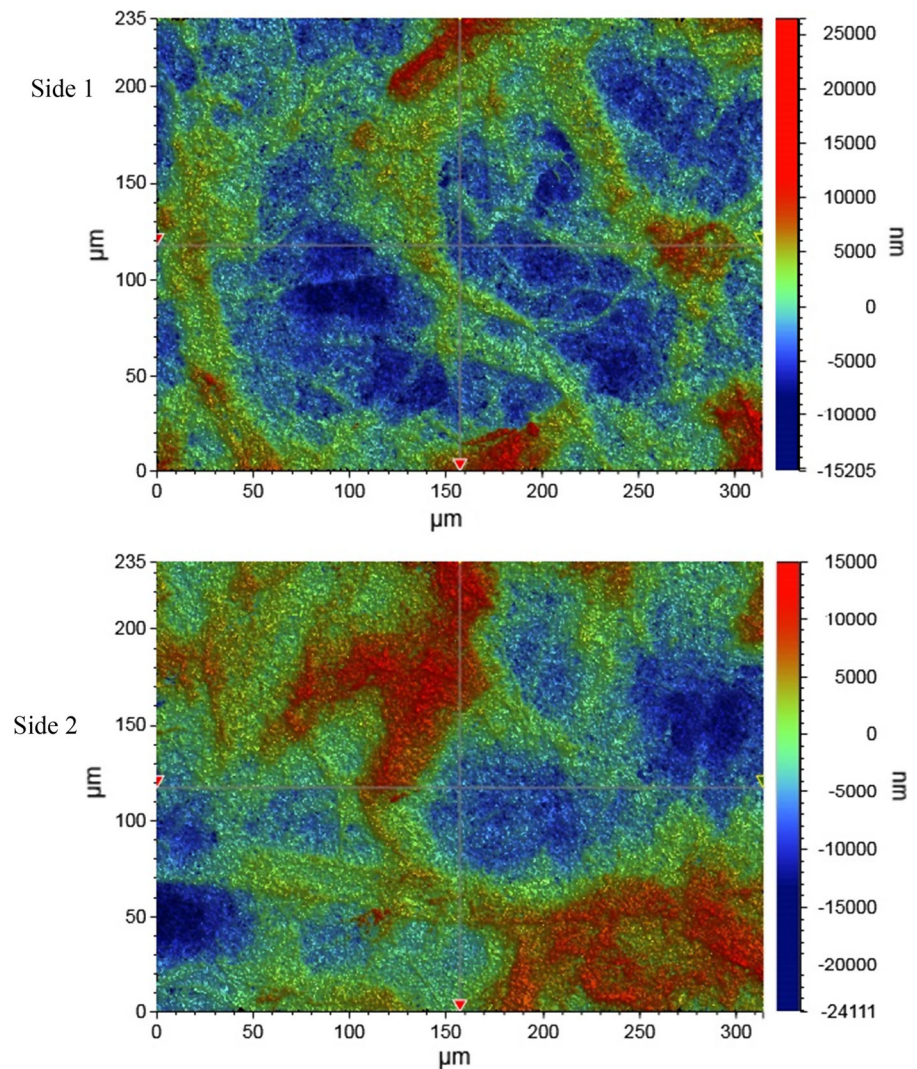
film was required, which this research addresses. Various combinations of conveyor velocity and suspension concentration can be used to produce the film with a given basis weight. Film density and E-Modulus were shown to be linearly related to basis weight of the film, but it was not possible to control film density and E-Modulus independently of each other. It was shown that thickness and basis weight are linearly related, independent of the process (whether vacuum filtration or spray coating) or experimental setup. Spray coating produced NC films with very reproducible thickness and basis weight between films, as shown in Fig. 5. Our previous publication also showed good thickness uniformity within the films,

demonstrating the suitability of the spraying process as an alternative to vacuum filtration (Shanmugam et al. 2017).

Certain properties of NC films, including printability and strength, are strongly interlinked to the optical uniformity of the NC film (Varanasi and Batchelor 2014). The optical uniformity of the films was evaluated with a PPF tester, which evaluates the NC film over a range of length scales from 0.5 to 39 mm reporting a formation values as a ratio to the reference film which was film prepared via vacuum filtration. The optical uniformity of spray coated NC films were shown to be adjustable via changing NC concentration and varying velocity of the conveyor. It was found that

increasing suspension concentration and conveyor velocity both increase the optical uniformity within different ranges of component size and that under optimal conditions, the optical uniformity of the spray-coated films was comparable to the reference NC film produced by vacuum filtration. It is noteworthy that with increased conveyor velocity, the operating time is also proportionally decreased.

The most uniform NC films were prepared by spray coating at the highest velocity of 1.05 cm/s using the modified setup. The images are shown in Fig. 12. Figure 16 shows that its optical uniformity evaluated by the PPF is better than the vacuum filtered NC films at both small and large inspection sizes.

In comparison to vacuum filtration, spraying of NC suspension produced films of similar density and mostly lower tensile strength and elasticity. The process setup was shown to have an effect on these properties, correlating lower tensile strength and elasticity with a lower apparent density for series 1 and 2.

A change of nozzle, optimized setup configuration and operation at a decreased pressure in series 3 resulted in a slight increase in the apparent density and an increase in the tensile index of the films to be approximately equal to that produced by vacuum filtration. Notably, the optical uniformity of NC film via modified configuration is actually better than the reference NC film via vacuum filtration. This indicates a change in the formation of a wet film on the stainless steel plate resulting in a more compact structure. It should also be noted that with the optimized configuration, waste was decreased allowing for higher throughput and rapid production of films.

Previous data on spray coating of NC on nylon fabric (Beneventi et al. 2015), showed the tensile index of spray coated NC film ranging from 45 to 104 Nm/g, within the range of the data reported here. However, these literature values are reported for homogenized NC which show better fibrillation potentially leading to an increase in mechanical strength (Syverud and Stenius 2008).

The strength of the spray coated NC film could be tailored by adjusting NC concentration or varying the velocity of the conveyor. In the case of vacuum filtration, the forming of film with high basis weight requires high dewatering time and tailoring film properties is a challenging task.

Conclusion

Spray coating, a rapid method to produce a strong, dense and robust NC films was examined in depth and process parameters were studied. Basis weight of NC films can be easily tailored with combinations of conveyor velocity and suspension concentration. The strength of the spray coated NC film is up to 45% lower than the strength of NC film via vacuum filtration and the optical uniformity of the spray coated film could be controlled by the adjusting the process setup. Under optimum conditions, both measured optical uniformity and strength were comparable to films prepared by vacuum filtration. The results confirm spraying to be a suitable alternative for fabricating NC films, allowing for high throughput mass production and the tailoring of properties for desired characteristics or applications.

Supplementary information

The supplementary information includes: 1) the data of film optical uniformity from the Paper Perfect formation tester and 2) SEM micrographs of films at lower magnification, 3) Load-strain curve for NC films and 4) Plot between tensile stiffness index and basis weight and density of NC film.

References

Abitbol T et al (2016) Nanocellulose, a tiny fiber with huge applications. Curr Opin Biotechnol 39:76–88

Beneventi D, Chaussy D, Curtil D, Zolin L, Gerbaldi C, Penazzi N (2014) Highly porous paper loading with microfibrillated

cellulose by spray coating on wet substrates. Ind Eng Chem Res 53:10982–10989. https://doi.org/10.1021/ie500955x

Beneventi D, Zeno E, Chaussy D (2015) Rapid nanopaper production by spray deposition of concentrated microfibrillated cellulose slurries. Ind Crops Prod 72:200–205. https://doi.org/10.1016/j.indcrop.2014.11.023

Dufresne A (2013) Nanocellulose: a new ageless bionanomaterial. Mater Today 16:220–227. https://doi.org/10.1016/j.mattod.2013.06.004

Klemm D, Kramer F, Moritz S, Lindström T, Ankerfors M, Gray D, Dorris A (2011) Nanocelluloses: a new family of nature-based materials. Angew Chem Int Ed 50:5438–5466. https://doi.org/10.1002/anie.201001273

Niskanen K (1998) Paper physics, papermaking science and technology book 16. Forest Products Engineers Finland, Helsinki, p 57

Nogi M, Iwamoto S, Nakagaito AN, Yano H (2009) Optically transparent nanofiber paper. Adv Mater 21:1595–1598. https://doi.org/10.1002/adma.200803174

Raj P, Mayahi A, Lahtinen P, Varanasi S, Garnier G, Martin D, Batchelor W (2016) Gel point as a measure of cellulose nanofibre quality and feedstock development with mechanical energy. Cellulose 23:3051–3064. https://doi.org/10.1007/s10570-016-1039-2

Rebouillat S, Pla F (2013) State of the art manufacturing and engineering of nanocellulose: a review of available data and industrial applications. J Biomater Nanobiotechnol 04(02):24. https://doi.org/10.4236/jbnb.2013.42022

Sehaqui H, Liu A, Zhou Q, Berglund LA (2010) Fast preparation procedure for large, flat cellulose and cellulose/inorganic nanopaper structures. Biomacromol 11:2195–2198

Shanmugam K, Varanasi S, Garnier G, Batchelor W (2017) Rapid preparation of smooth nanocellulose films using spray coating. Cellulose. https://doi.org/10.1007/s10570-017-1328-4

Shimizu M, Saito T, Fukuzumi H, Isogai A (2014) Hydrophobic, ductile, and transparent nanocellulose films with quaternary alkylammonium carboxylates on nanofibril surfaces. Biomacromolecules 15:4320–4325. https://doi.org/10.1021/bm501329v

Siró I, Plackett D (2010) Microfibrillated cellulose and new nanocomposite materials: a review. Cellulose 17:459–494

Syverud K, Stenius P (2008) Strength and barrier properties of MFC films. Cellulose 16:75–85. https://doi.org/10.1007/s10570-008-9244-2

Varanasi S, Batchelor WJ (2013) Rapid preparation of cellulose nanofibre sheet. Cellulose 20:211–215. https://doi.org/10.1007/s10570-012-9794-1

Varanasi S, Batchelor W (2014) Superior non-woven sheet forming characteristics of low-density cationic polymer-cellulose nanofibre colloids. Cellulose 21:3541–3550. https://doi.org/10.1007/s10570-014-0370-8

Zhang L, Batchelor W, Varanasi S, Tsuzuki T, Wang X (2012) Effect of cellulose nanofiber dimensions on sheet forming through filtration. Cellulose 19:561–574. https://doi.org/10.1007/s10570-011-9641-9

SILVER NANOWIRES: A VERSATILE TOOL FOR CONDUCTIVE PAPER

C. Czibula[1,2], C. Ganser[1,2], M. Kratzer[1], F. Brumbauer[3],
M. Kräuter[3], K. Shanmugam[4], W. Batchelor[4], M. Penn[3],
M. Ebner[3], M. Pramstrahler[3], F. Pilat[3], H.-T. Chien[3],
R. Schennach[2,3], B. Friedel[3,5] and C. Teichert[1,2]

[1] Institute of Physics, Montanuniversitaet Leoben, Austria
[2] CDL for Fibre Swelling and Paper Performance, Graz University
of Technology, Austria
[3] Institute of Solid State Physics, Graz University of Technology,
Austria
[4] Department of Chemical Engineering, Monash University,
Victoria, Australia
[5] Energy Research Center, Vorarlberg University of Applied Sciences,
Dornbirn, Austria

INTRODUCTION

Paper has a long tradition as a material in electronic components, for example, it is still used today as a dielectric in capacitors [1]. Here, like in many other applications of paper, one of the most important properties is that it is cheap. However, today many people consider paper as a renewable resource that should be used in a much broader scale in advanced materials (e.g. [2]). To get paper and other cellulose based materials established as an important building block in sustainable advanced materials, one needs to not only rethink paper properties. If paper should replace other materials, possibilities to adjust its properties to a certain device structure need to be further explored and investigated. Established views should be widened to allow a revival of paper as a material which is more than just a cheap substrate.

Applications of paper for microfluidic devices, e.g. [3], in sensors [4], in solar cells [5, 6] or as a dielectric in transistors [7] have been published recently. This demonstrates that paper can enter new scientific disciplines and markets successfully. In this

article, we will show that silver nanowires (AgNWs) are a very versatile tool to turn wood pulp paper [6], nanofibrillated (NF) paper, viscose fibres [8] and films made of regenerated cellulose conductive. Since all these various materials consist mainly of pure cellulose, a composite of an organic and an inorganic material is studied in detail. Our approach will increase the possible applications of paper in areas ranging from dielectrics towards conductors. Furthermore, results of the surface investigations of this interesting and exciting material combination with a special focus on atomic force microscopy (AFM) methods are presented giving a deeper insight into the surface morphology [9].

MATERIALS AND METHODS

Kraft pulp paper + AgNWs sample

20×20 mm^2 laboratory paper sheets with 16 g/m^2 were made of unbleached and unrefined kraft pulp (Monopol X, Frantschach, Austria) with a Rapid-Köthen sheet former (DIN EN ISO 5269–2:2004).

The AgNWs (diameter: 115 nm, length: 20–50 µm) were supplied by Sigma-Aldrich and dispersed in isopropanol (0.5 wt%). Via dip-coating (SDI company, Nano-DIP ND-0407) the AgNWs were deposited on the paper sheet [10].

NF paper + AgNWs sample

The nanofibrillated paper was produced by a rapid spray coating technique. A nanocellulose (Celish KY 100S, DAICEL Chemical Industries Limited) suspension with 1.5 wt% concentration was sprayed onto a polished stainless steel plate, which was moving on a conveyor at a velocity of 0.32 cm/s. After spraying, the sheet was air dried under restraint. The processing time to prepare spray coated nanofibrillated paper was approximately 1 min. The aspect ratio of the nanocellulose from sedimentation is 147 and the average fibre diameter obtained from SEM measurements is 73 nm [11, 12].

Ethylene glycol (>99 %), copper (II) chloride (99 %), polyvinylpyrrolidone (360,000 g/mol) (PVP) and silver nitrate (>99 %) have been purchased from Sigma-Aldrich and used without further purification. The AgNWs were synthesized similar to [13]. In brief, to the volume of 100 mL ethylene glycol as solvent, 0.6 mL of copper chloride solution (1.14 mg/mL) were added under stirring and heated to 144 °C. After adding 22.5 mL of PVP solution (25 mg/mL) the solution was cooled to 126 °C. Finally, growth of the silver nanowires was initiated by adding the precursor in form of 5 mL of silver nitrate solution (100 mg/mL) and heating at 150 °C for 50 min. After cooling to room temperature, the obtained AgNWs were

washed 5 times via centrifugation and dispersion in deionized water. The AgNWs were kept as a suspension in deionized water until further processing. Where applicable, the water was exchanged by ethanol for easier deposition.

Viscose fibre + AgNWs sample

Hollow viscose fibres with a length of about 40 mm were provided by Kelheim Fibres GmbH (Kelheim, Germany) and glued with nail polish [14] to a glass for better surface access for the AgNWs during the AgNW deposition.

The same AgNWs as for the kraft pulp paper sheet were used and deposited via dip-coating [10].

Cellulose film + AgNWs sample

The thin films of pure cellulose [15] were fabricated by spin coating a toluene solution of trimethylsilyl cellulose (TMSC) onto glass substrates according to the method published in [16]. After solvent exchange, the AgNW were added to the toluene solution. Subsequently to spin coating, these films were regenerated to cellulose by hydrolysis with gaseous HCl.

Characterization methods

Optical microscopy in reflection mode was performed using a Zeiss Axio Lab.A1 with an integrated Axiocam 105 color digital camera. Electron microscopy images were obtained with a NOVA 200 Nanolab FIB/SEM dual beam microscope. X-ray photoelectron spectroscopy analysis (XPS) was done at the Institute of Chemistry of Polymeric Materials at Montanuniversitaet Leoben, Austria using a K-Alpha™ + XPS system from Thermo Fisher Scientific Inc. The spectrometer is equipped with an Al X-ray source (1486.6 eV) operating at a base pressure in the range of 10^{-8} to 10^{-10} mbar. High resolution scans were acquired at a pass energy of 50 eV and a step size (resolution) of 0.1 eV. The instrument work function was calibrated to yield a binding energy (BE) of 83.96 eV for the Au 4f7/2 line for metallic gold. All measurements were performed at room temperature. The peaks were fitted utilizing Gaussian/Lorentzian mixed functions employing a linear background correction (program XPSPEAK41).

Electrical characterization of the AgNW-coated viscose fibre and regenerated cellulose films was carried out with electrical microprobes in argon atmosphere, using a Keithley 2636A source-measure unit. Here, droplets of silver paste are deposited on the sample in a distance of 2 mm and contacted by the microprobes. The electrical resistance of the kraft pulp and NF paper with AgNWs was measured using a home built two-point-probe measurement apparatus [10] (see Figure 4). It

consists of two metal clamps and an electrically isolating bottom plate. The distance between the clamps was about 1 cm. Due to the typically high contact resistance the sensitivity of the setup is limited and it is difficult to make clear statements about the influence of surface roughness and contamination effects.

AFM [17] was performed employing an Asylum Research MFP-3D device (Santa Barbara, CA, USA). The AFM system was equipped with a closed-loop planar x-y-scanner with a scanning range of 85×85 µm^2 and a z-range of 15 µm. Standard topography measurements were obtained in tapping mode with Olympus AC160-TS silicon probes. The cantilevers had a spring constant of about 30 N/m and the tips a radius of about 10 nm. Kelvin Probe Force Microscopy (KPFM) [18, 19] is an AFM based method for the determination of local contact potential differences (CPD) between probe and substrate. Here, probe tips with a conductive Pt/Ir coating and a tip radius of about 25 nm were used (Access EFM, AppNano). Bringing two materials with different work functions into contact results in a charge transfer between them in order to align their Fermi levels. As a result, a potential (CPD) is generated between them. The same holds true for the conductive AFM probe and the surface. The CPD between them causes an electric field influencing the tip movement. In KPFM, the CPD between tip and sample is compensated by applying a dc-voltage. Unlike in classical Kelvin probe, where the compensating current upon variation of the distance between substrate and electrode is nullified, KPFM uses the electrostatic force between tip and substrate. Since an AFM probe is a highly sensitive force sensor, this allows for high sensitivity in CPD measurement. In this case, the so called two-pass method is applied. First, the topography is scanned in standard intermittent contact mode and in a second pass this topography is retraced at a set lift height. During the second pass, the cantilever is electrically excited by the superposition of a DC voltage and an AC voltage close to the cantilever's resonance frequency ω. The DC voltage is adjusted by a feedback to nullify the capacitive force F_ω at frequency ω. The DC voltage – necessary to compensate F_ω at each tip position – corresponds to the CPD.

The mechanical shifting tests of the AgNWs were performed by taking advantage of the lithography and manipulation abilities of the MFP-3D software. In this software, it is possible to draw lines on the topography images which represent tip paths. Here, the applied force was about 18 µN, and the tip was dragged across the surface with a velocity of 1 µm/s. The data from all AFM measurements was processed with the open-source software Gwyddion [20].

RESULTS AND DISCUSSION

Electrically conductive paper can be fabricated in many different ways. One can metallize the surface of a sheet of paper, integrate carbon black, carbon nanotubes,

and graphene into paper sheets, or one can coat the paper with conductive inks as well as with conducting organic polymers. In all cases, one of the main problems is the adherence of the additives to the paper. Especially when aiming for a flexible device, it is crucial that the electrically conductive material adheres well to the paper. Another important problem is that if one needs specific optical properties, most of these methods fail because they darken the paper. Conductive inks and organic polymers lead to high conductivities, but always at the expense of transparency.

We have shown recently that a laboratory hand sheet made of unbleached kraft pulp fibres can become electrically conductive by integrating AgNWs [6]. Like all metallic nanowires, the AgNWs are stabilized in suspension via surface functionalization. Therefore, the interaction of this surfactant with the paper will determine the adherence of the AgNWs. In the case presented in [6], the commercial AgNWs showed a very good adherence to the paper. The resistivity of paper samples with the best balance between high optical transparency and low sheet resistance reached 38 Ω/sq [6], which is in the range of the common transparent conductor indium tin oxide (ITO). For comparison, an ITO film on glass has a sheet resistance of 5–15 Ω/sq, ITO on a plastic substrate has 30–60 Ω/sq, and most organic conductors like PEDOT:PSS or carbon nanotubes have around 200–800 Ω/sq [21].

Bulk silver has a resistivity of about $1.6*10^{-8}$ Ωm at room temperature. For the AgNW-coated kraft pulp sheet, a well conducting network was already established at low AgNW amounts. By varying the solid content of the AgNW dip-coating suspension between 0.05 and 0.50 wt%, it was possible to adjust the sheet resistance to values between 5 and 160 Ω/sq [6].

The AgNW network on the paper is presented in Figure 1 as optical micrographs and scanning electron microscopy (SEM) images. In Figure 1(a)–(b), one can see that the AgNWs increase the reflectivity of the paper, without much change in the other optical properties. In Figure 1(c), it becomes clear that the AgNWs tend to adhere well to the cellulose fibres and to each other.

A closer look on the AgNWs on the pulp fibre sheet is presented in AFM topography scans in Figure 2. One can clearly recognize the AgNWs on the cellulose fibre. Cellulose fibres are about 30 μm in diameter and have a length of roughly 4 mm. In comparison, the AgNWs diameter is about 115 nm and the length ranges from 20 μm–30 μm. In the SEM image (Figure 1(c)), it seems that the AgNWs are conforming very well to the pulp fibre surface. The AFM scans, however, suggest that the AgNWs have large distances between adjacent points of attachment and do not conform completely to the complex surface structure of the pulp fibres. Therefore, the AFM data suggests a stronger interaction between AgNWs and a weaker interaction between the AgNWs and the paper fibres. This is in contrast to what one would expect and interpret by only looking at the SEM
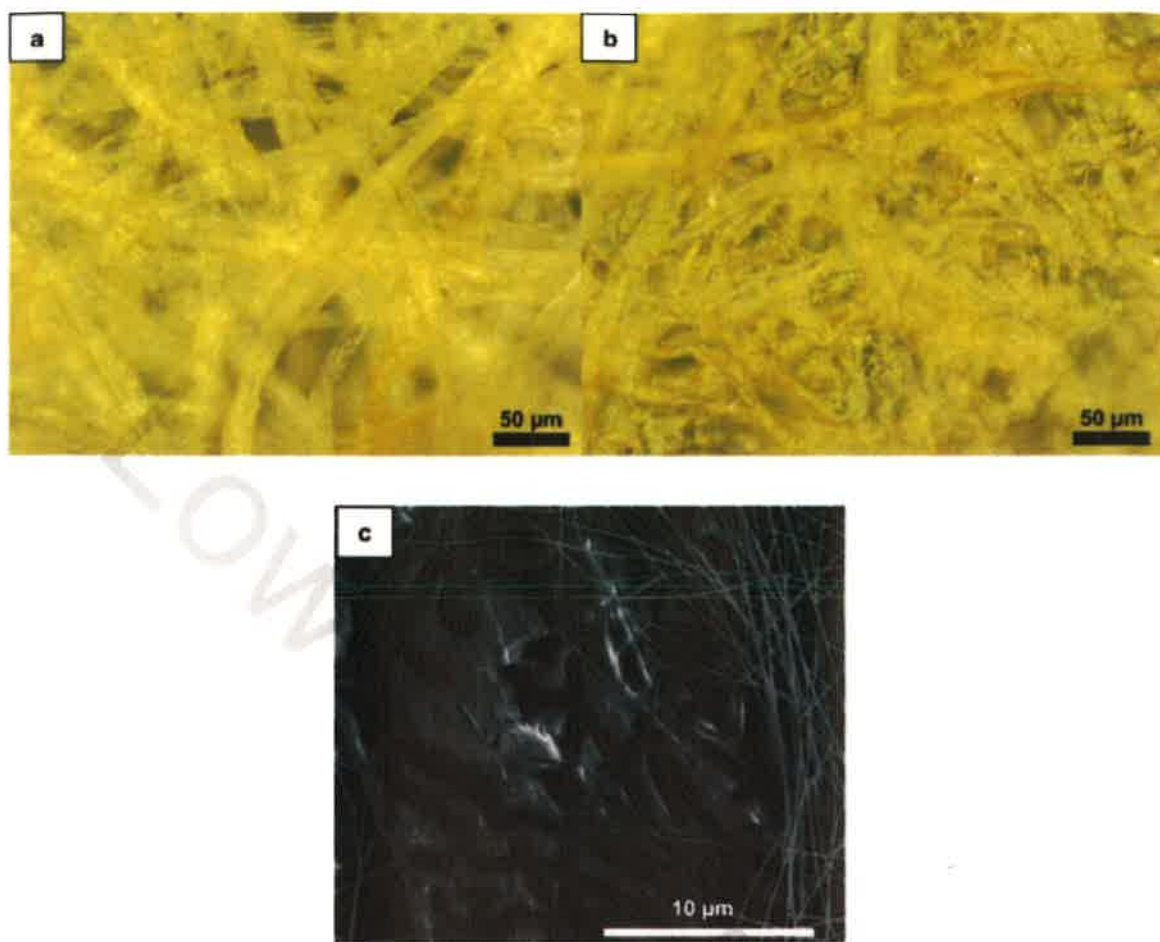
Figure 1. Optical microscopy images of: (a) the pristine soft wood kraft pulp fibre sheet; (b) the same sheet after dip coating with AgNWs; (c) SEM image of one AgNWs decorated cellulose fibre of the sheet shown in (a, b).

image. To further investigate the properties of AgNWs on cellulosic materials, KPFM was applied to measure CPDs as presented in Figure 3(b). The CPD values of the AgNW appear to be 40 mV above the cellulosic background. However, even though some individual AgNW are clearly distinguishable in the morphology, they exhibit a similar CPD value as the cellulose matrix. One explanation could be that these wires are coated by residuals originating from the preparation process (see red arrows in Figures 3(a)–(b)). Another possibility might be that these AgNWs are electrically insulated from the AgNW network. However, even in such a case a stronger difference in CPD values of charged AgNWs in comparison to those of the cellulose would be expected.

In another approach, it was also tried to turn nanofibrillated (NF) paper into a conductor by AgNW deposition. Here, conductivities comparable to standard transparent conducting oxide electrodes have been achieved. Also, bending of the
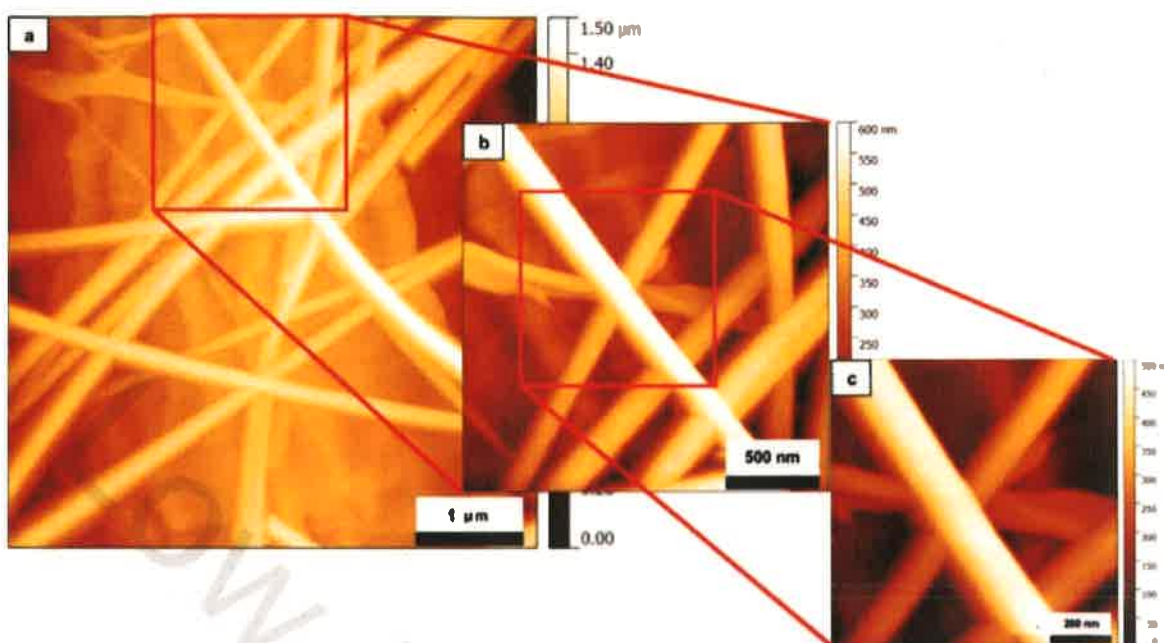
Figure 2. (a)–(c) AFM topography images of a AgNWs dip coated sheet of unbleached softwood kraft pulp [9].
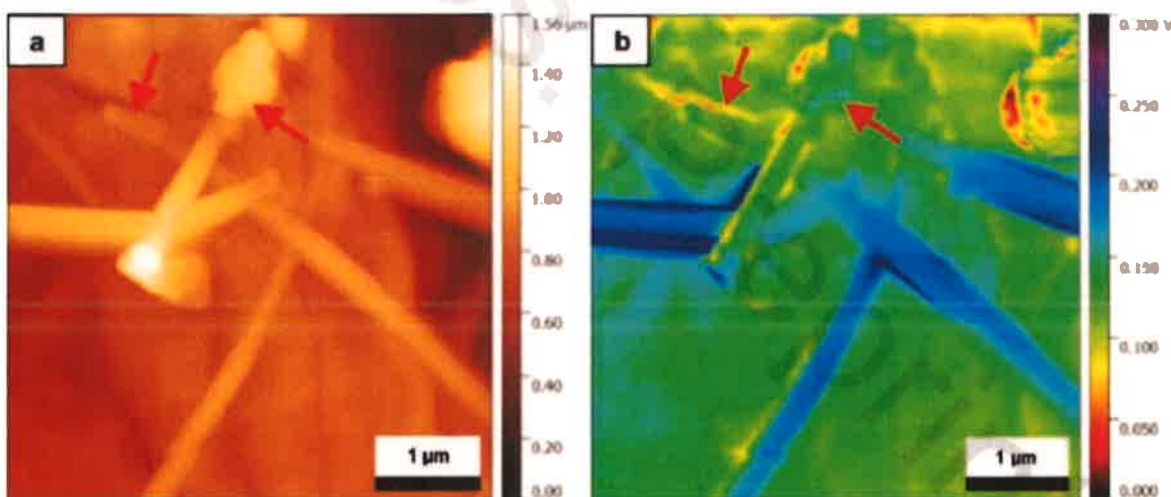
Figure 3. (a) 5 × 5 μm² AFM topography and (b) corresponding KPFM CPD image. (b) shows the contrast between AgNWs (blue) and the cellulose substrate (green). The red arrows indicate possible residuals from the preparation process [9].

NF paper sheet based electrode by 180° with a bending radius of about 2.5 mm as demonstrated in Figure 4 resulted in unaltered resistance. Before AgNW deposition, both sides of the NF paper sheet were investigated by optical microscopy as well as AFM to identify any differences in surface roughness. Optically, it was

Figure 4. Electrical characterization setup for the AgNW-coated NF paper. Here, also an example for the bending is presented.

possible to distinguish between both sides. This is due to the production of the paper by spray coating.

One side of the sheet seems smoother, which is probably the side in contact with the metal plate. However, AFM measurements revealed only a small difference in surface roughness, but still the apparent smoother side of the paper was used for the AgNW deposition. In Figure 5, optical microscopy images of a bare NF paper and one after deposition of AgNWs are shown.

Comparing Figure 5(a) with Figure 1(a), it is obvious that the kraft pulp paper sheet is a much rougher substrate than the bare NF paper sheet.

For the NF paper, also a detailed AFM topography study has been carried out.
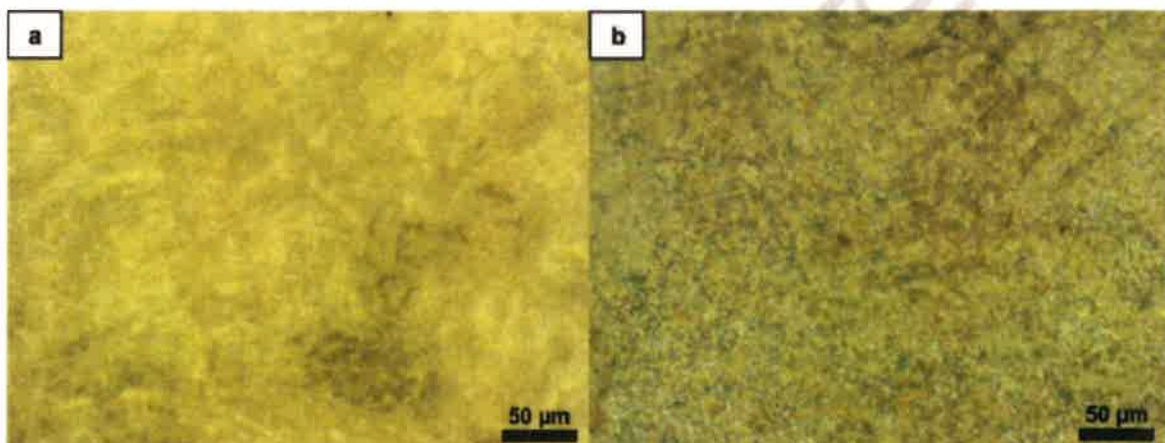
Figure 5. Optical microscopy images of the NF paper before (a) and after (b) the AgNW deposition.
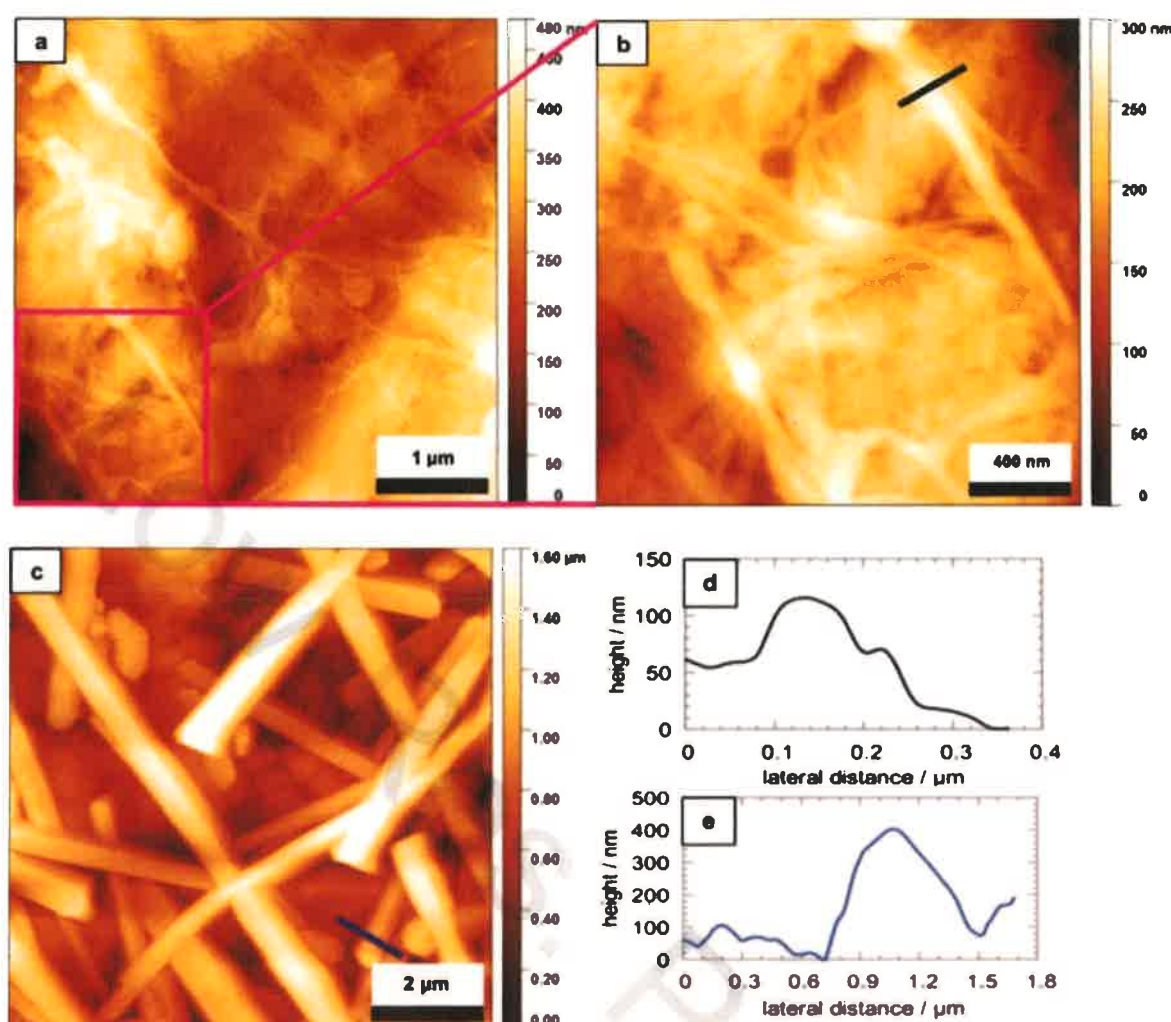
Figure 6. AFM topography images of the NF paper before (a), (b) and after (c) the AgNW deposition. (d) shows the corresponding line profile (indicated by the black line) in (b), (e) represents the corresponding line profile (blue line) in (c).

In Figure 6, exemplary AFM topography images of the NF paper before (6(a), (b)) and after (6(c)) the AgNWs deposition are shown. In larger topography images like in Figure 6(a), fibril bundles of up to 800 nm width and smaller randomly aligned fibrils are visible. Zooming in with an image size of 2×2 μm^2 (Figure 6(b)), it is very well visible that the surface is dominated by small fibrils with a lateral size of about 40 nm. The AgNWs are rather randomly distributed and sometimes seem to form agglomerates (Figure 6(c)). From line profiles in the topography images, the height (350 ± 190) nm and the width (310 ± 90) nm of the AgNWs were estimated. In comparison to AgNWs on the kraft pulp paper sample (Figures 2 and 3), the AgNWs deposited on the NF paper are shorter and broader. It should be noted that the dilation effect due to the finite
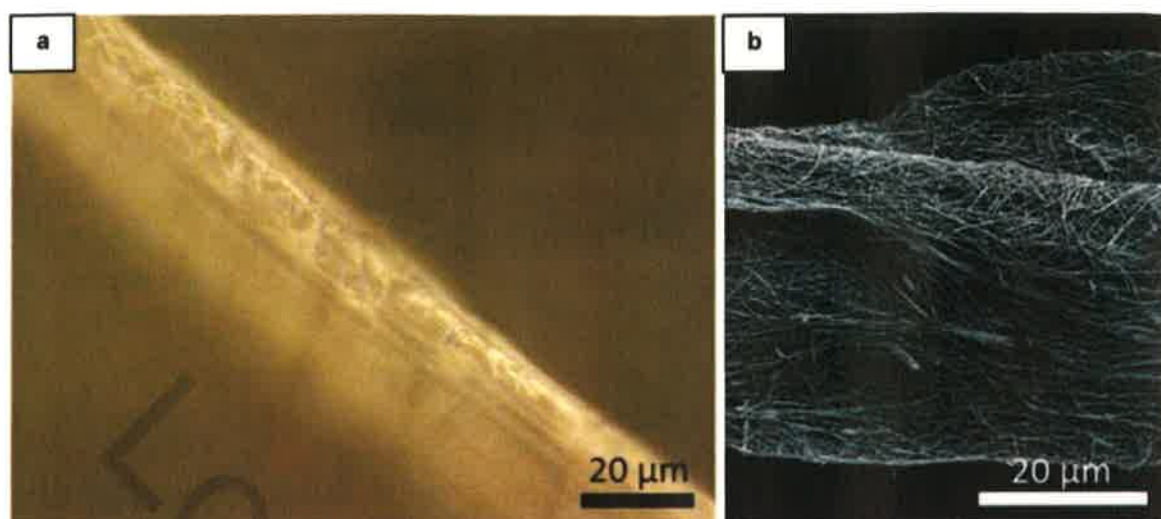
Figure 7. (a) Optical microscopy image and (b) SEM image of a AgNW dip coated viscose fibre taken from [8].

AFM tip size [22] contributes to the apparent width of all the measured surface features.

As expected, the RMS roughness σ increased after the AgNW deposition and showed large deviations. For the bare NF paper, $\sigma = (183 \pm 6)$ nm, with the AgNW on top the roughness increases to a value of $\sigma = (467 \pm 182)$ nm. Those values were obtained from six 10×10 μm^2 topography images.

For comparison with other cellulose-based materials, adsorption of AgNWs on viscose fibres has also been investigated [8]. Here, a conducting AgNW network on the fibre surfaces could be established as well. An optical microscopy image and an SEM micrograph of a single viscose fibre coated with AgNWs are presented in Figure 7. The enhanced reflectivity due to the AgNWs shown in Figure 1(b) is also observed on the viscose fibre. Therefore, one can assume a similar adhesion of the AgNWs to the viscose fibre surface. This is also indicated by the perfect Ohmic behaviour that these samples exhibit during electrical measurements. The resistance determined from measuring 11 fibres was (45 ± 11) Ω [8].

To further explore the interactions of AgNW with cellulose, we tried to incorporate the AgNW into thin cellulose films. As can be seen in AFM topography images in Figures 8(a)–(b), the AgNW are integrated within the cellulose film or are located at its surface. The AgNW are also covered by dot-like agglomerates with a lateral size of up to 200 nm. Some of the AgNW do react with the HCl gas forming AgCl which was confirmed via X-ray photoelectron spectroscopy analysis (XPS) of the films (Figure 8(c)). For conductivity measurements, the amount of AgNWs on the surface was not sufficient.
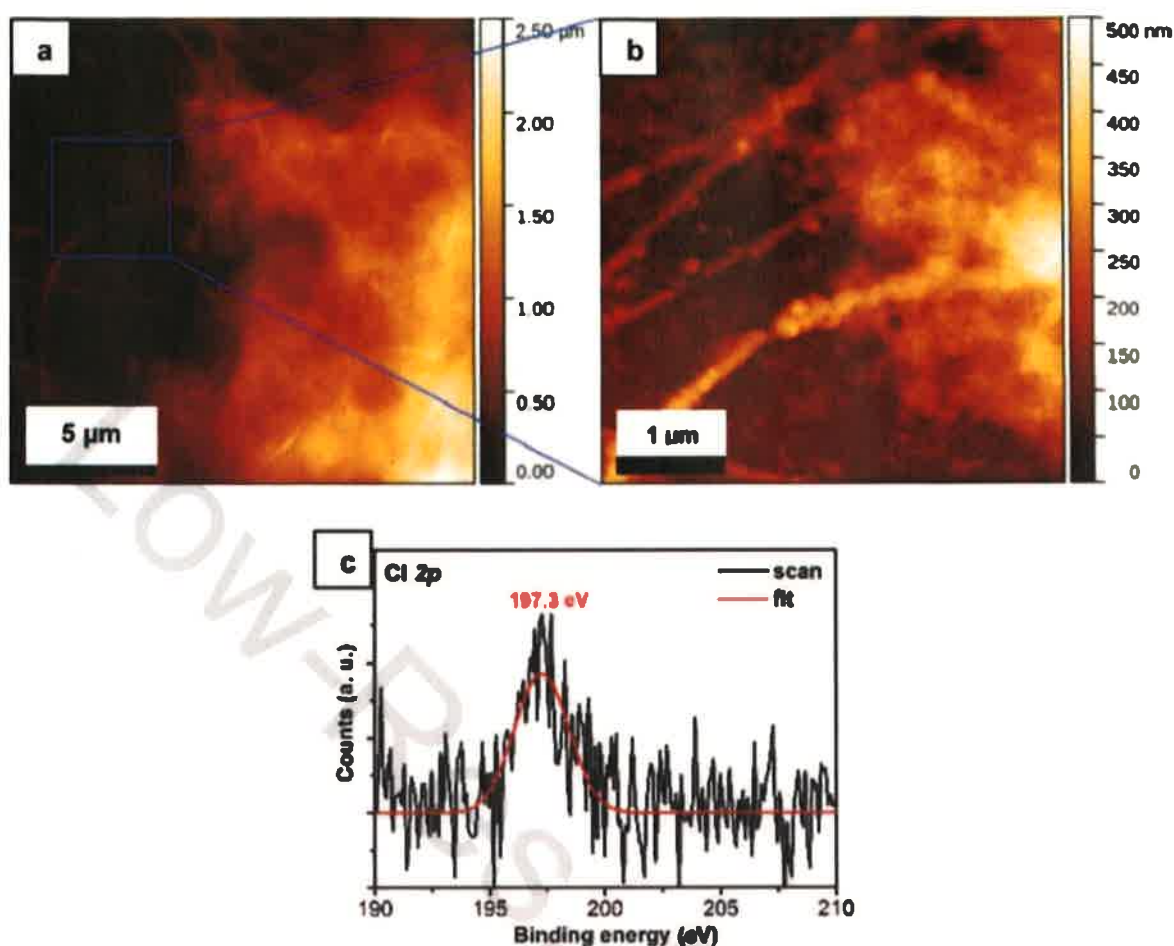
Figure 8. (a) 20 × 20 μm² AFM image of a regenerated cellulose film containing AgNWs; (b) A 5 × 5 μm² zoom-in AFM scan gives a closer look on the AgCl agglomerates formed on a AgNW; (c) XPS of the Cl 2p region.

OUTLOOK TO MECHANICAL TESTS

Further insight on how strongly the AgNWs are bound to the cellulosic surface can be obtained by pushing the AgNWs with the AFM probe and measure the necessary force. In Figure 9, first results are presented. Trial measurements without recording of the lateral force were performed to explore if it is even possible to move the large AgNWs with the AFM tip.

The AgNWs were mostly laterally moved during these experiments. However, in some cases, AgNWs seem bent afterwards. This is shown in Figure 9(c). Here, a 5 × 5 μm² image was recorded to get a closer look. It is still hard to distinguish, but the AgNW might have been broken or bent during the experiment or it was pushed underneath the other AgNW. The line profiles in Figure 9(d) indicate that
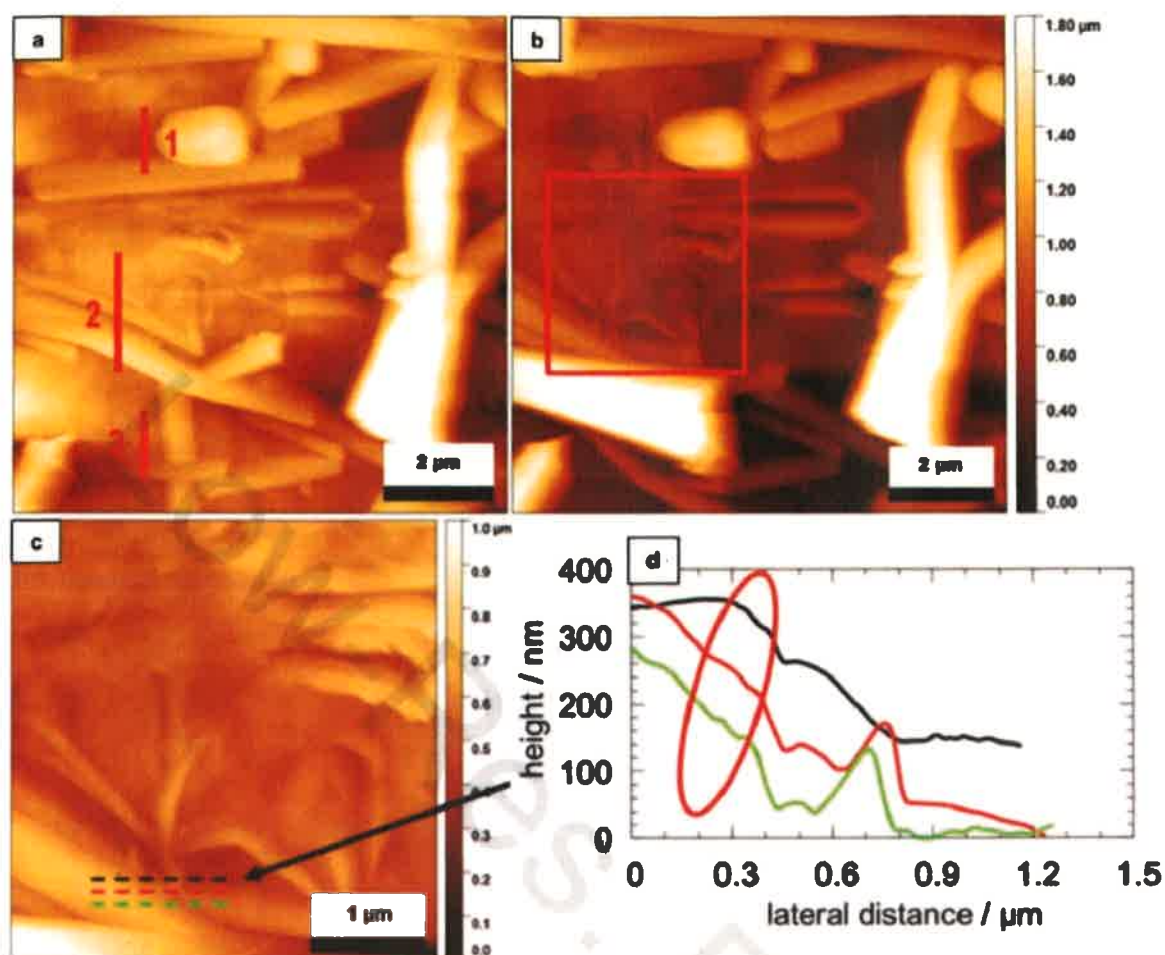
Figure 9. (a)–(b) $10 \times 10 \ \mu m^2$ topography images before (a) and after (b) AFM mechanical shifting experiments of the AgNW on NF paper. The red lines 1–3 in (a) indicate where the tip was dragged across the surface (always from top to bottom). (c) shows a $5 \times 5 \ \mu m^2$ zoom-in of (b) with corresponding line profiles in (d). The red ellipse in (d) indicates a scratch on the AgNW caused by dragging the AFM tip across it.

the tip even produced a notch in the AgNW. This observation of severe damage of the AgNW by the moving AFM probe indicates rather strong adhesion of the AgNWs to each other and to the surface.

By recording the lateral force signal and using different applied forces during these measurements, we expect in future experiments to get more insight on the level of adsorption.

CONCLUSIONS

It has been demonstrated that AgNWs are a very versatile and useful tool to add electrical conductivity to cellulose based materials. Commercially purchased or

self-synthesized AgNWs have been adsorbed to the surface of kraft pulp paper, NF paper sheets and also viscose fibres by dip coating. Together, cellulosic surfaces and AgNWs formed a conductive composite network with resistivity in the range of 38 Ω/sq which is comparable to the commonly used ITO. Additionally, optical and scanning probe microscopy methods have been proven to be appropriate for investigating the surface properties of these complex paper fibre-AgNWs composites. Optical microscopy investigations indicate that the AgNWs increase the reflectivity of the paper, without much change in other optical properties. This is an advantage compared to methods with conductive inks and organic polymers which always lead to a loss in transparency.

Although the samples are fairly rough, we also succeeded to study the surfaces of cellulosic materials with AgNWs by AFM in detail. In topography measurements, it was interesting to explore the alignment of the AgNWs along the rough cellulose fibres. KPFM investigations showed a difference in contact potential, which made it possible to distinguish between the cellulose background and the AgNWs. Finally, mechanical tests with an AFM probe have – at least qualitatively – proven a significant adhesion of the AgNWs to the paper surface.

One of the main future challenges is to build persistently good devices with a flat composite surface to avoid short circuits. Also, the flexibility of the composite needs to be further tested. As was demonstrated, it is possible to bend the AgNW-coated NF paper once and record similar conductivities but the long-term behaviour and cycling stabilities for applications in daily use are not yet clarified. Here, the strength of adhesion between the AgNWs and the cellulosic surface is crucial and needs to be further investigated, with the mechanical AFM tests presented here being the first step in this direction.

ACKNOWLEDGEMENTS

REFERENCES

1. J. Ho, S. Boggs and T. R. Jow. Historical Introduction to Capacitor Technology. *IEEE* **26**(1):20–25, 2010.
2. D. Tobjörk and R. Österbacka. Paper Electronics. *Adv. Mat.* **23**(17):1935–1961, 2011.

3. M. M. Thuo, R. V. Martinez, W. Lan, X. Liu, J. R. Barber, M. B. J. Atkinson, D. C. Bandarage, J. Bloch and G. M. Whitesides. Fabrication of Low-Cost Paper-Based Microfluidic Devices by Embossing or Cut-and-Stack Method. *Chem. Mater.* **26**(14):4230–4237, 2014.

4. F. Güder, A. Ainla, J. Redston, B. Mosadegh, A. Glavan, T. J. Martin and G. M. Whitesides. Paper-Based Electrical Respiration Sensor. *Angew. Chem. Int. Ed.* **55**(19):5727–5732, 2016.

5. M. Dasari, P. R. Rajasekaran, R. Iyer and P. Kohli. Calligraphic Solar Cells: Acknowledging Paper and Pencil. *J. Mat. Res.* **31**(19):2578–2589, 2016.

6. H. Kopeinik, R. Schennach, J. Gallik, H. Plank and B. Friedel. Photodiodes Based on Wood Pulp Fibre Networks. *Cellulose* **22**(5):3425–3434, 2015.

7. A. Wolfberger, A. Petritz, A. Fian, J. Herka, V. Schmidt, B. Stadlober, R. Kargl, S. Spirk and T. Griesser. Photolithographic Patterning of Cellulose: A Versatile Dual-Tone Photoresist for Advanced Applications. *Cellulose* **22**(1):717–727, 2015.

8. M. Ebner, R. Schennach, H.-T. Chien, C. Mayrhofer, A. Zankel and B. Friedel. Regenerated Cellulose Fibre Solar Cell. *Flex. Print. Electron.* **2**(1):014002, 2017.

9. C. Czibula, C. Ganser, M. Kratzer, R. Schennach, B. Friedel and C. Teichert. Exploring Paper/AgNW Based Composites for Photovoltaic Devices by Atomic Force Microscopy Methods. In proc. *Progress in Paper Physics Seminar 2016 Conference Proceedings*, pp. 213–216, Darmstadt, Germany, 2016.

10. H. Kopeinik. Organic Diodes and Photovoltaic Cells based on Conductive Cellulose Fibre Networks. Master Thesis, Institute of Solid State Physics, Graz University of Technology, Graz, 2014.

11. S.Varanasi, H. H. Chiam and W. Batchelor. Application and Interpretation of Zero and Short-Span Testing on Nanofibre Sheet Materials. *Nord. Pulp Pap. Res. J.* **27**(2):343–351, 2012.

12. S. Varanasi, R. He and W. Batchelor. Estimation of Cellulose Nanofibre Aspect Ratio from Measurements of Fibre Suspension Gel Point. *Cellulose* **20**(4):1885–1896, 2013.

13. N. Espinosa, R. R. Sondergaard, M. Jorgensen and F. C. Krebs. Flow Synthesis of Silver Nanowires for Semitransparent Solar Cell Electrodes: A Life Cycle Perspective. *ChemSusChem* **9**(8):893–899, 2016.

14. W. J. Fischer, A. Zankel, C. Ganser, F. J. Schmied, H. Schroettner, U. Hirn, C. Teichert, W. Bauer and R. Schennach. Imaging of the Formerly Bonded Area of Individual Fibre to Fibre Joints with SEM and AFM. *Cellulose* **21**(1):251–260, 2014.

15. E. Kontturi, P. C. Thüne and J. W. Niemantsverdriet. Cellulose Model Surfaces – Simplified Preparation by Spin Coating and Characterization by X-ray Photoelectron Spectroscopy, Infrared Spectroscopy, and Atomic Force Microscopy. *Langmuir* **19**(14):5735–5741, 2003.

16. S. Rohm, U. Hirn, C. Ganser, C. Teichert and R. Schennach. Thin Cellulose Films as a Model System for Paper Fibre Bonds. *Cellulose* **21**(1):237–249, 2014.

17. G. Binnig, C. F. Quate and C. Gerber. Atomic Force Microscope. *Phys. Rev. Lett.* **56**(9):930, 1986.

18. M. Nonnenmacher, M. P. O'Boyle and H. K. Wickramasinghe. Kelvin Probe Force Microscopy. *Appl. Phys. Lett.* **58**(25):2921–2923, 1991.

19. S. Sadewasser and T. Glatzel. Kelvin Probe Force Microscopy. Springer Verlag, Heidelberg, 2012.
20. D Nečas and P Klapetek. Gwyddion: An Open-Source Software for SPM Data Analysis. *Eur. J. Phys.* **10**(1):181–188, 2012.
21. Galagan Y, Andriessen R, Rubingh E, Grossiord N, Blom P, Veenstra S, Verhees W, Kroon J. Toward Fully Printed Organic Photovoltaics: Processing and Stability. In proc: *Electronics Convention LOPE-C Proceedings*, pp. 88–91, Frankfurt, Germany, 2010.
22. J. Villarrubia. Morphological Estimation of Tip Geometry for Scanned Probe Microscopy. *Surf. Sci.* **321**(3):287–300, 1994.

Contents lists available at ScienceDirect

Sustainable Materials and Technologies

Nanocellulose films as air and water vapour barriers: A recyclable and biodegradable alternative to polyolefin packaging

Kirubanandan Shanmugam, Hamid Doosthosseini, Swambabu Varanasi, Gil Garnier, Warren Batchelor *

Bio resource Processing Research Institute of Australia, Department of Chemical Engineering, Monash University, Melbourne, VIC 3800, Australia

ABSTRACT

Synthetic polymer packaging is neither reprocessable, renewable nor biodegradable and is difficult to recycle into useful barrier materials. Cellulose fibre based packaging is renewable, easily reprocessable, recyclable and biodegradable, however, it is a poor barrier material both before and after recycling, especially against air and water vapour. Nanocellulose (NC), formed by breaking down cellulose fibres into nanoscale diameter fibres, is a renewable alternative to synthetic polymer packaging barrier layers. This research investigates the recyclability of virgin NC films. Nanocellulose films were recycled and prepared into films, using standard dispersion-based laboratory papermaking techniques through mixing and vacuum filtration of the resultant suspension. The recycled films retained ~70% of the strength of the virgin films. Although the water vapour permeability (WVP) approximately doubled, increasing to 1.29×10^{-10} g.m^{-1}.s^{-1} Pa^{-1}, it is still comparable to synthetic polymer packaging materials such as Polyethylene(PE), Plasticized PVC, Oriented Nylon 6 and Polystyrene (PS). SEM micrographs reveal no fibre agglomeration and no damage to the fibres during the recycling process. The optical uniformity measurements of recycled NC film confirms a drop in uniformity of the film at smaller length scales and an increase in uniformity at larger length scales, compared with virgin NC film. The retained strength and barrier properties combined with easy reprocessability of the product promises a sustainable and recyclable alternative to conventional polyolefin packaging, providing a very attractive alternative for the packaging industry.

© 2019 Elsevier B.V. All rights reserved.

1. Introduction

The development of sustainable and recyclable barrier materials for packaging is a critical challenge arising from pressing environmental concerns with the widespread use of non-sustainable petroleum-derived polymers in the food, pharmaceutical, electronics and other industries. Sales of packaging materials is forecasted at US$997 billion by 2020 with a market growth of ~3.5% per year [1]. Presently, glass, aluminium, tin and petroleum-based polymers are extensively used as packaging materials. Throughout the industry, polyolefins have been widely adopted due to their effective barrier properties and simple and cheap processing. Despite these desirable properties, the majority of polyolefin packaging is not re-processable into their original form or into high value products. Petroleum polymers are neither sustainable nor biodegradable; their extensive use has had severe ecological impacts. Consequently, their disposal still raises environmental concerns and recycling requires complex and costly processes. Moreover, the recycle process involving blending the synthetic polymers into a processable melt is very dependent upon the chemical composition and molecular weight of the components; further, volatile organic compounds are emitted which can impact plants, animals and humans. The heat required for thermal recycling of plastics also generates various oxides of carbon that are the most responsible for global warming. Current polyolefin films cannot be reprocessed into the original product, as the recycled product would not yield suitable barrier properties [2–4]. During the recycling process, the mixing of different polymers together leads to a reduction in the quality and properties of the recycled plastic. Moreover, chemical compounds from synthetic packaging materials can affect the quality of food when exposed to post-packaging processes [5] and cause food contamination [6,7].

It is therefore imperative to pursue novel materials for packaging applications to address the ecological and environmental concerns with cost-effective, readily available and sustainable solutions. Bio-based polymers can produce humidity, oxygen and grease barriers for sustainable, biodegradable and compostable packaging [8]. Previously, bio-based materials have been processed into films, significantly enhancing shelf life and quality of foods and reducing waste from packaging. However, such biodegradable polymers have poor barrier performance and are noticeably brittle. As such, complications in processing these materials, such as low heat distortion, render them too expensive for industrial scale use [9].

* Corresponding author at: BioPRIA, Department of Chemical Engineering, 15 Alliance Lane, Monash University, Clayton, Melbourne, VIC 3800, Australia.
  E-mail address: warren.batchelor@monash.edu (W. Batchelor).

Cellulose fibre-based packaging materials, such as boxes, cartons and paper are renewable, recyclable and biodegradable but are poor barriers to oxygen and water. Laminating with polymers, such as LDPE, can yield products with sufficient barrier performance, but at the expense of recyclability and biodegradability [4].

One solution to improving the sustainability of paper-polymer laminates is to replace the polyolefin layer with a film of nanocellulose (NC). Nanocellulose is directly produced by defibrillating fibres from pulp and wood into their structural constituents [10]. NC can have widths ranging from 5 to 75 nm and lengths exceeding 5 μm. Nanocellulose fibrils show strong nanoscale interaction resulting in a high mechanical strength material with high resistance to diffusion. Nanocellulose and its composites were shown to have outstanding barrier properties against oxygen, air and reasonable barrier properties to water vapour [11]. Nanocellulose can be obtained at relatively low cost from renewable feedstocks, such as wood, rendering it particularly attractive for the development of sustainable barrier materials; the volume of research on NC has grown exponentially over recent years [12,13]. Though often hypothesized to be recyclable, the reprocessability of NC films has never been demonstrated.

This objective of this study is to evaluate the reprocessability and full recyclability of virgin NC films into a recycled NC film via vacuum filtration. By evaluating the barrier properties of virgin NC film and the effects of recycling on the barrier performance and strength of NC film, we aim to demonstrate that NC film is easily reprocessable and fully recyclable, and a suitable alternative to conventional packaging materials.

2. Materials and methods

The nomenclature for nanocellulose has not been reported consistently in the literature. As well as nanocellulose (NC), it is also called micro-fibrillated cellulose (MFC), cellulose nano-fibrils, cellulose micro-fibrils and nano-fibrillated cellulose (NFC). In this paper, we use NC as the generic term for the cellulose nanomaterials used. The NC used was supplied from DAICEL Chemical Industries Limited (Celish KY-100S) at 25% solids content. DAICEL NC (Celish KY-100S) has cellulose fibrils with an average diameter of ~73 nm with a wide distribution of fibre diameter, a mean length of fibre around 8 μm and an average aspect ratio of 142 ± 28 [14]. DAICEL KY-100S is prepared by micro fibrillation of cellulose with high-pressure water. The crystallinity index of DAICEL nanocellulose was measured to be 78% [15]. NC suspensions were prepared using by diluting the original concentration of 25 wt% to 1.5 wt% with de-ionized water and disintegrating for 15,000 revolutions at 3000 rpm in a disintegrator.

2.1. Preparation of nanocellulose film by vacuum filtration

The Virgin NC films were prepared using the conventional vacuum filtration method using British Handsheet Maker (BHM) as reported in the literature [16]. 600 ml of NC suspension with 0.2 wt% concentration was poured into a cylindrical container having a 150 mesh filter at the bottom and filtered to form a wet film on the mesh. The wet film was carefully separated using blotting papers and subsequently dried at 105 °C in a drum drier for around 10 min.

2.2. Recycling of nanocellulose film

Recently, a spray coating method to produce NC films on a smooth and polished stainless steel surface was developed and this method is capable of spraying a high solids NC suspension [17]. To make the large quantity of films required for recycling, we prepared 40 films according to this method [17,18] by spraying each film onto a smooth stainless steel plate on a moving conveyor at a fixed velocity 0.32 cm/s using a Professional Wagner spray system (Model number 117) at a pressure of 200 bar. The type 517 spray tip used in the spray system produce an elliptical spray jet and the spray jet angle and beam width are 50° and 22.5 cm, respectively. The spray distance is 30.0 ± 1.0 cm from the spray nozzle to the circular steel plate. After spraying, the film on the plate was dried under restraint at the edges for at least 24 h.

After drying, the nanocellulose films were dispersed and suspended in water following TAPPI standard T205 SP-02, where the films were torn into pieces of 1 cm × 1 cm dimensions and soaked in de-ionized water for 24 h. The soaked films were disintegrated for 75,000 revolutions at 3000 rpm in a disintegrator Model MK III C. The obtained suspension was then made into films according to the vacuum filtration method explained above. Fig. 1 shows the method of recycling of spray coated NC films.

2.3. Evaluating NC fibre diameter

A drop of 0.2 Wt% of recycled or virgin nanocellulose suspension was cast on the silicon chip and then dried in a controlled laboratory environment. The dried suspension on the silicon chip is coated with an iridium layer. Its surface was studied using secondary electron mode-II with FEI Magellan 400 FEGSEM for NC film at a voltage of 5 KV. The diameter distribution of the raw nanocellulose fibres and recycled NC fibres were measured with Image J. The data are reported as average diameter of NC with 95% confidence interval. The supplementary information gives the micrographs and the diameter distribution histograms of virgin and recycled nanocellulose fibres.

2.4. Evaluating NC film properties

All prepared virgin and recycled NC films prepared were stored at 23 °C and 50% RH for 24 h prior to further testing.

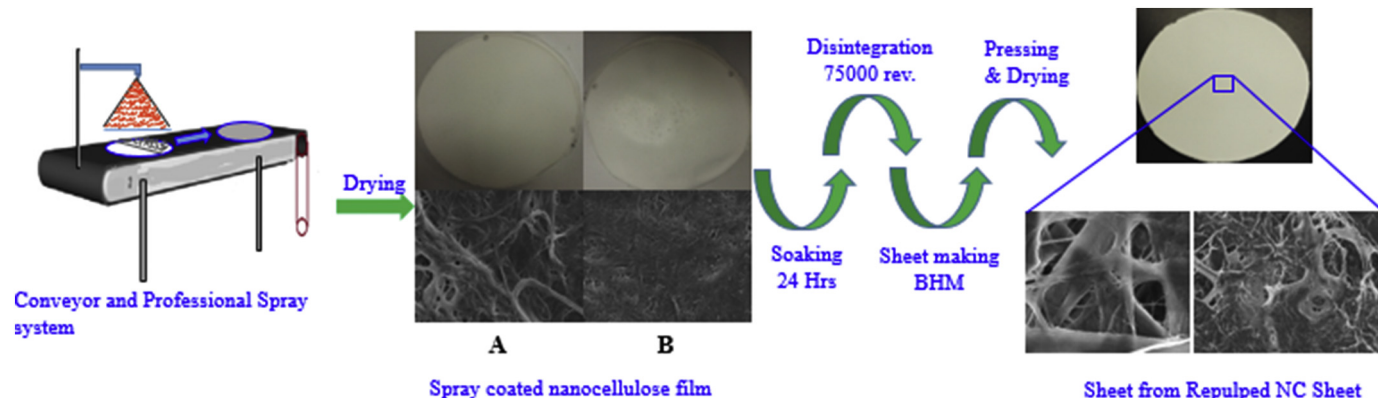**Fig. 1.** Method on recyling of spray coated virgin nanocellulose films.

2.5. Basis weight

The basis weight (g/m^2) of each nanocellulose film was calculated by dividing the weight of the film, after 4 h drying in the oven at a temperature of 105 °C, by the film area.

2.6. Thickness of NC films

The thickness of the virgin and recycled NC films was determined using a Thickness Tester Type 21 from Lorentzen & Wettre AB, Stockholm, Sweden. The thickness of each NC film was evaluated at fifteen points and averaged. The thickness of NC film was measured according to TAPPI T 411, 2015.

2.7. Apparent density

The apparent density of the NC films was evaluated through dividing basis weight by mean thickness of the film.

2.8. Air permeability

The air permeance of dried NC films was measured with a L&W air permeance tester with an operating range from 0.003 to 100 μm/Pa·S. The mean value of air permeance evaluated from 3 different areas of each NC film was reported. The Technical Association of the Pulp and Paper Industry (TAPPI) standard T 460 is used to measure the air permeance of the films.

2.9. Water vapour permeability

Water vapour permeability (WVP) was evaluated according to the American Society of Testing and Materials (ASTM) standard (E96/E96M-05) method using anhydrous Calcium Chloride ($CaCl_2$). In this method, NC film was dried for 24 h at a temperature of 105 °C in an air oven. ~40 g of dried anhydrous $CaCl_2$ was added into the cups and covered by the NC films. The increase in weight of the cups is caused by the absorption of water vapour by $CaCl_2$ in the cups through NC film. Test sample was weighed at standard time intervals. The variation in weight of the cups with time was noted and the WVTR calculated from the slope of the line between weight and time. The water vapour transmission rate were carried out at 23 °C and 50% Relative Humidity (RH). The water vapour transmission rate (WVTR) of NC film are normalised with thickness of the NC film and converted into WVP. The mean value of three replicates of each virgin NC film was reported. The value of four different recycled NC films were reported.

2.10. *Film uniformity analysis*

The uniformity of the NC films were evaluated using the Paper Perfect Formation (PPF) Tester (OpTest Equipment Inc., Canada) which measures the optical uniformity of light transmitted through the sample. In brief, the PPF consists of a black and white camera based image analyser and uses a CCD camera interfaced with 256 Gy levels, 65 μm/pixel resolution. The analyser uses a diffuse quartz halogen light source with IR filters and automatic intensity control. The PPF classifies formation quality over 10 length scales ranging from 0.5 mm to 60 mm. The data reported here is the Relative Formation Value (RFV) of each component relative to one of the films made by vacuum filtration, which was used as a reference film. Three films were measured for each condition, with the results averaged. RFV value less than 1 means that the optical uniformity of the NC film tested is worse than the reference film at that length scale.

2.11. Surface properties

The surface roughness of the NC films was evaluated by Parker surface instrument and optical profiler (Bruker Contour GT-I). The raw image from Optical profilometry is processed with the Gwyddion 2.49 software to accurately evaluate RMS of each film. Surface topography of the film was studied using secondary electron mode-II with FEI Magellan 400 for virgin and recycled NC film.

2.12. Mechanical properties

The strength of both virgin and recycled NC films were evaluated by an Instron model 5566 using test specimens of 100 mm length and 15 mm width, conditioned for 24 h at 23 °C and 50% RH before dry tensile testing based on the Australian/New Zealand Standard AS/NZS 1301.448S-2007. All thickness and tensile tests were done at 23 °C and 50% RH. The samples were tested at a constant rate of elongation of 10 mm/min. The Tensile Index (TI of the samples was calculated from the tensile strength (expressed in Nm^{-1}) divided by basis weight (gm^{-2}). The mean value was obtained from six to seven valid tests and the error bars in the plots indicate standard deviation.

The zero span tensile index of the films were evaluated with a Pulmac Troubleshooter using six samples 1.5 cm wide and 0.5 cm long for each test [19]. In brief, six samples of NC film were required for an individual investigation. A specimen of NC film was placed in the central clamping area of the tester and two other samples were kept under the two back steps of the clamping jaws to ensure proper jaw alignment under pressure. After each test, the samples were removed and replaced. Before the zero-span testing, optimum clamping pressures were determined. An optimum clamping pressure of 70 psi was used for nanocellulose film samples.

3. Results

3.1. Air permeability

The air permeability of the virgin NC film was less than 0.003 μm/Pa·S, which is the detection limit of the instrument, confirming the film is highly impermeable for packaging application. The air permeance of the recycled NC film was 0.0045 μm/Pa.S, which still provides a good impermeable film for packaging.

3.2. NC film density

The relationship between film density and basis weight is shown in Fig. 2, for all the sheets made in this study. The effects of reprocessing can be seen in a change in apparent density as shown in Fig. 2. The apparent density of NC films from virgin fibres is higher, demonstrating that a less compact structure is formed after recycling. It is noteworthy that the same process was used to make both the recycled film and virgin film by vacuum filtration, therefore, the decrease in apparent density after recycling is attributed to fibre properties and not to process.

The density of the NC film is approximately the same and independent of the NC film basis weight for both the recycled and virgin NC film, but it is statistically lower for the recycled NC film. The reason for the reduced density of recycled NC film is probably the formation of larger aggregates in the nanocellulose fibrous network that has hindered the compaction of the fibre network. As a result, recycled NC films have formed larger pores, which has caused an increase in permeation of water vapour and air through the pores. Drying of recycled cellulose fibres and fibre hornification may also have reduced the fibre swelling capacity and decreased the conformability of recycled fibres, which will also reduce the compaction of the fibre web as the film forms. This will also reduce the film density.

3.3. Water vapour permeability (WVP)

The Water Vapour Permeability (WVP) was measured in triplicate for all samples. The results are compared in Fig. 3 as a function of film basis weight. Fig. 3 shows that recycled cellulose films show higher
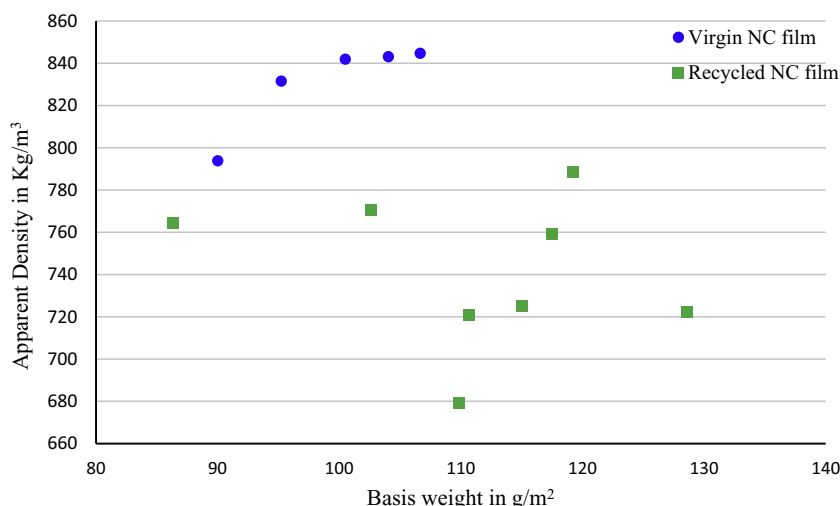
Fig. 2. Effect of recycling on the density of the NC films.

WVP than the virgin NC films, with an average increase of approximately 7.5×10^{-11} g.m^{-1}.s^{-1} Pa^{-1}.

Agglomerates from the incomplete breakdown of recycled films into separated nanofibers, produce non-uniformity in the film and will increase the size of both the surface and bulk pores elevating water vapour permeability and air permeance over than that of virgin NC film. These floc aggregates will also have a poorer bond to the separated cellulose fibrils resulting in a weaker recycled NC film. Additionally, the presence of agglomerates reduces the total surface area available for bonding thereby limiting film density, uniformity and compactness of the fibril network.

3.4. *Film uniformity analysis*

The formation test concludes the good uniformity of recycled NC films compared to the virgin NC film. Fig. 4 also shows that the recycled film is less uniform than that of the virgin NC film at lower inspection tiles of 15 mm and more uniform for areas greater than 15 mm.

3.5. *Mechanical properties of the recycled film*

The tensile strength of the virgin and recycled NC films was measured at both standard 100 mm test spans, in an Instron, and at zero-span. The zero span tensile index is a measure of the nanofibre film strength over a very short span [19]. Fig. 5 showed that the tensile index, at both long and short spans has decreased by 30% and ~28%, respectively, for the recycled film compared to the virgin film.

A loss in mechanical strength is expected in recycling of conventional cellulose fibres due to poorer hydrogen bonding between fibres and their hornification. The tensile index of the recycled film is affected by weaker inter-fibre bonds due to reduced conformability of the cellulose fibres [20].

3.6. *Effect of recycling on cellulose fibrils and cellulose film uniformity*

The effect of recycling on the nanocellulose fibres was evaluated with surface morphology, topography and diameter of the fibres measured with SEM micrographs. Fig. 6 shows SEM micrographs of the NC fibres before and after recycling, showing a wide distribution of fibre size in each sample. The average diameter of the nanocellulose was 69.8 ± 11.3 nm before recycling and 69.6 ± 12.6 nm after, showing no evidence of agglomeration at this smaller inspection area. SEM micrographs show a more compact structure after recycling, but no increase in average fibre diameter.

The surface topography and morphology of recycled films were evaluated by SEM micrographs and compared with virgin NC films in Fig. 7.
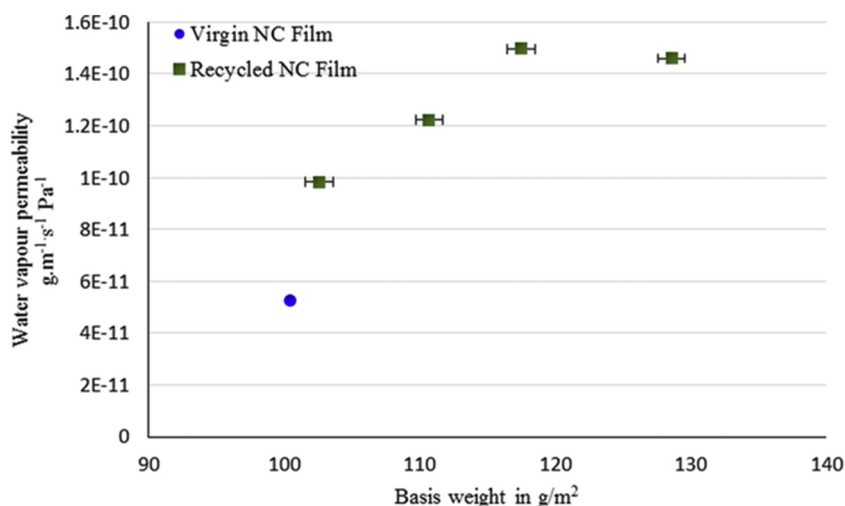

Fig. 3. Water Vapour permeability of Virgin and Recycled NC Film against basis weight of the film.
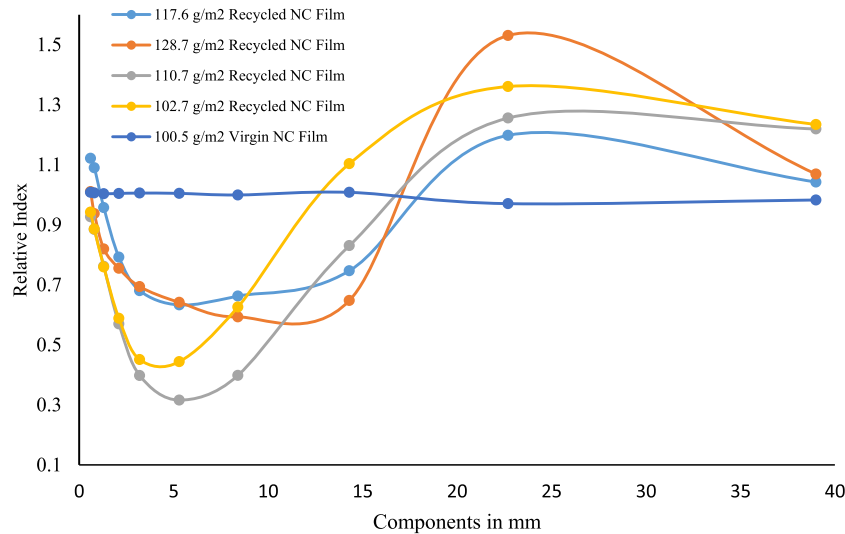
Fig. 4. Formation of Recycled NC film and its comparison with Virgin NC film.

The recycled films retained fibre morphology and topography, showing no significant damage to fibres. Cellulose fibrils were randomly distributed and orientated. In the recycled film, some larger pores were observed and might be a reason for increased air permeance and water vapour transmission. Additional micrographs of both virgin and recycled NC fibres and NC film from virgin and recycled NC fibres from 1 to 100 μm are in the supplementary information.

3.7. Surface roughness investigation

Fig. 8 shows the surface roughness of the recycled and virgin NC films measured using optical profilometry. For an inspection area of 125.7 μm × 94.2 μm, the RMS roughness of the recycled film was found to be 2624 nm and 3116 nm on filter side and free side, respectively, showing a similar roughness to the values of 2445 nm on filter side and 3113 nm on free side after recycling. Previously published data shows RMS roughness at 2673 nm and 3751 nm for NC film via vacuum filtration [17]. Additional optical profilometry images (5× magnification) for virgin and recycled NC are in the supplementary information, and also show similar surface roughness for virgin and recycled NC films.

4. Discussion

The effect of recycling on the NC fibres and NC films was tested at a range of length scales, and is summarised in Table 1. The effect of recycling on virgin NC fibres is predominantly observed at larger inspection areas affecting its properties such as zero-span strength, strength, WVP, air permeability and optical uniformity.

The change in the properties of recycled NC fibres cannot be explained by the traditional model of fibre hornification on recycling, which impacts the bonding between fibres and mostly reduces the strength of NC film. Our best explanation is that some of the agglomeration in initial film preparation has not been fully broken down, leaving small flakes. These flakes of material are probably at the 100 μm or so scale. If the structure is partly composed of flakes of materials connected with NC fibres, then this will not pack together as well as individual fibres, thus lowering density, reducing uniformity, and lowering strength at multiple length scales, while at the same time increasing permeability, with only a moderate decrease in density.

However, these effects are limited and recycling does not undermine the applicability of the reprocessed product, which is still both strong, with reasonable barrier performance. It should be noted that the properties of the recycled film might be further improved by optimising
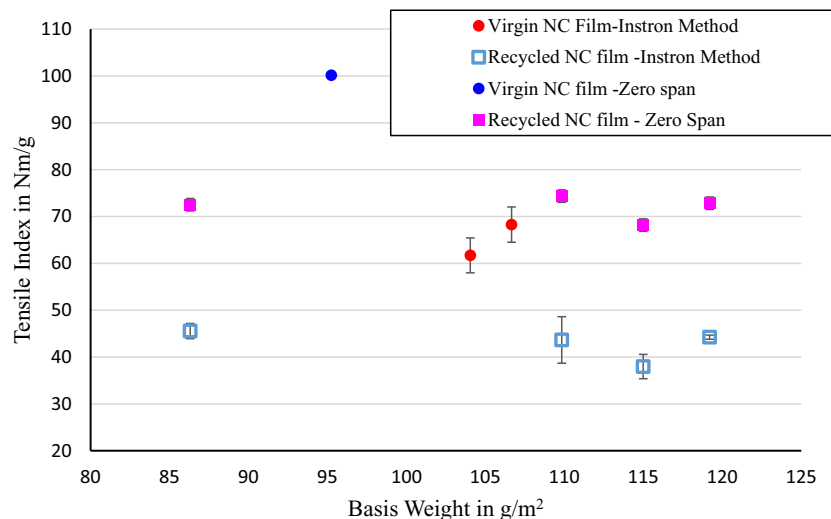

Fig. 5. Effect of basis weight and preparation process on Tensile Index and Zero Span Tensile Index of NC Film via Vacuum Filtration and recycled film.

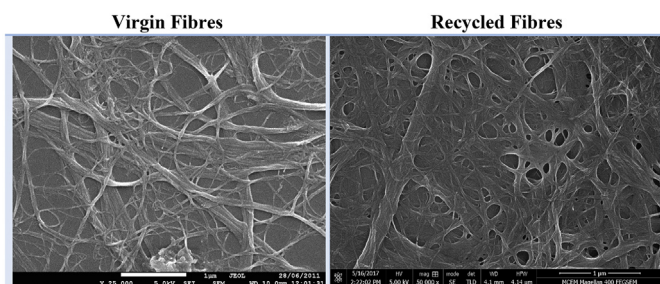**Virgin Fibres**   **Recycled Fibres**

Fig. 6. Scanning Electron Micrograph of nanocellulose before and after recycling.

the recycling conditions and processing. Possible strategies could be to increase the disintegration time or to use well established chemistry from the paper recycling process to improve the separation of the fibrils [21]. Homogenisation of the disintegrated fibres could also be used; this was an effective technology to break down clay agglomerates within a cellulose nanofiber suspension [22]. These additional processes could also reverse the effects of larger aggregates formation. Mixing recycled and virgin NC fibres could also produce films with enhanced barrier performance due to substantial increase of narrow pores in the films. From this investigation, it has been determined that fibrils are not impacted in the micro scale by recycling, retaining their structure and size. A limited negative impact on WVP and air permeability is observed and is likely due to the formation of small agglomerates. These may also have reduced the strength, although other factors such as hornification may be playing a role.

The potential of the recycled NC film as a packaging material can be evaluated through comparing with numerous synthetic and other cellulose polymers. The WVP of virgin NC films and recycled films of approximately 100 g/m^2 are 4.97×10^{-11} and 9.83×10^{-11} g/m.s.Pa, respectively. This is somewhat above WVPs for plastic packaging materials. For example, Ethylene-vinyl acetate (EVA), Polyamide (PA), Polycarbonate (PC), Low Density Poly-Ethylene (LDPE) and Poly Propylene (PP) have been reported at 3.41×10^{-12}, 7.54×10^{-12}, 6.78×10^{-12}, $8.75{*}10^{-13}$ and $2.94 {*}10^{-13}$ g/m.s.Pa respectively [[5], Data taken http://usa.dupontteijinfilms.com]. However, this difference can be overcome by using NC films of higher thickness. The standard thickness of plastics reported falls between 15 and 25 μm, whereas the thickness of standard 100 g/m^2 films prepared in this work are approximately 100 μm, which then attains WVTRs lower than that of PA and PC and almost equal to that of EVA. This demonstrates the applicability of recycled

Virgin Film-Filter side   **Recycled Film-Filter side**

Virgin Film-Free side   **Recycled Film-Free side**

Fig. 7. SEM Micrographs of Virgin and Recycled NC films 2 μm scale bar.

products and the suitability of the recycling process. The recycled NC films also have comparable WVP with the virgin NC films of cellulose nanofibrils (CNF) of 8.12×10^{-11} and acetylated CNF of $6.35{*}10^{-11}$ g/m.s.Pa previously reported in Rodionova, 2011 [23]. The full set of data is given in a table in supplementary information. Recycled NC film can be promised as a suitable alternative for synthetic packaging.

The strength of the recycled films is also impacted by the effects of recycling on fibres, however the recycling process retained 70% of film tensile strength. This, too, could possibly be further enhanced by procedures discussed above. The micrographs of recycled films confirm the presence of intact fibres. The roughness of the recycled film is similar to a film prepared via vacuum filtration and that of the rough side of the vacuum filtered NC Film. This is critical as the surface roughness and network of pores in NC films are controlling parameters in barrier performance and a change in roughness can cause differing behaviour in wettability of the NC surfaces [24].

Moreover, the recycling process used here is an eco-friendly and chemical free process and the simplicity and efficiency of reprocessing, i.e. soaking and disintegration, and ease of upscaling for recycling processes demonstrate the unique advantages obtained herein. Recycled NC film obtained can serve as an alternative to synthetic polymers where recycling and reprocessing is not possible or very difficult.

While plastics, such as LDPE are low cost and easy to fabricate into a desired form, they are produced from by-products of fossil fuel. Such plastics are neither renewable nor biodegradable and are a serious threat to the ecosystem. 322 million tonnes of plastics are produced every year and a substantial fraction of accumulates as waste in the environment as it is not biodegradable [25]. Recently the European Union has introduced new rules to reduce the amount of single-use plastics in applications such as packaging, which will reduce the cost advantages of plastic packaging [26,27]. Biopolymers are a potential choice to replace fossil-fuel derived plastics. However, biopolymers such as starch or chitosan have neither good enough strength nor appreciable barrier performance. Therefore, NC fibres, with better strength and barrier performance are being actively developed as barrier layer alternatives to conventional plastics [28].

Preliminary energy consumption analysis on a comparison of spray coating with vacuum filtration concludes that spray coating consumes 0.15 MJ for spraying 1 kg of dry NC film, compared with vacuum filtration which requires 0.56 MJ/Kg. The energy required for spraying the film is similar to that required to form a conventional film of Low-Density Polyethylene (LDPE).

The production of nanocellulose consumes ten times more energy than conventional packaging films [29,30], although significant research is being conducted to lower the energy consumption. In addition, it should be noted that the full scale production of NC is still in the early stages of development and that estimates of energy consumption have often been derived using laboratory scale production. Recent analysis has suggested that substantial savings in energy could be expected as production facilities are scaled up [31]. Growing biomass for nanocellulose will also have significantly higher land-use and water consumption, than is required to produce polyolefin products. From this particular comparison, it could easily conclude that conventional packaging films are more sustainable and the sustainability trade-off between petroleum-derived and bio-based derived packaging may only conserve the non-renewable resources. However, when it comes to recycling, only two third of the packaging films could be recycled and rest ends up in landfill or released to the environment [32]. Waste from packaging materials will overburden the landfills in the near future and poses significant environmental concerns. Work to include the impacts of plastic waste in life-cycle analysis is still in the very early stages of development [32]. It is also interesting to note that the recycling of polyolefin films such as LDPE consumes more than half of the energy in comparison to the energy required to produce these virgin films [33]. In contrast, the energy consumption for recycling
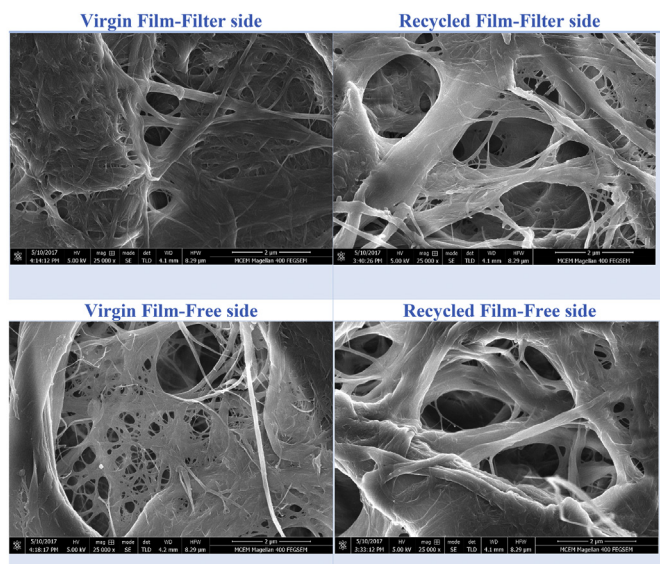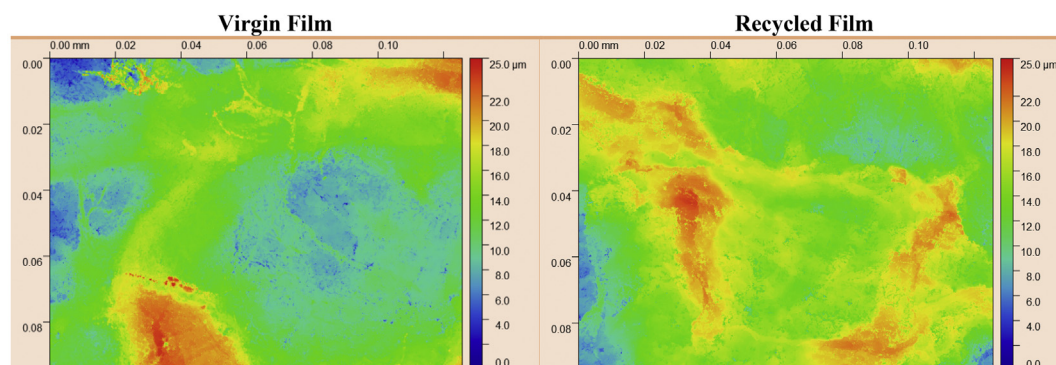
Fig. 8. Optical Profilometry of Free side of NC Film and Recycled NC Film (50 X Magnification).

nanocellulose is negligible in contrast to the energy emission from its production [29]. Thus, considered the end of life analysis, nanocellulose could be more sustainable and greener owing to its ease of recycling when compared to conventional packaging films, and certainly is worthy of active development.

5. Conclusion

Virgin NC films of low permeability and high uniformity were manufactured by standard approch. Virgin NC films were recycled using standard paper testing techniques and formed into films again. Results confirm that some of the agglomeration in initial film formation has not been fully broken down, leaving small flakes. The flakes did not pack together as well as individual fibres, thus lowering density, reducing uniformity, and lowering strength. However, the recycled NC barrier materials retained ~70% of the tensile strength and showed limited reductions in barrier performance and was still able to perform acceptably

for most synthetic packaging applications. Nanocellulose films can now provide an alternative to conventional packaging, and readily recycled and reprocessed into a potential barrier material. This process leads to global sustainability by replacing non-renewable polluting synthetic plastic packaging and laminates with a product that can be recycled directly into a barrier material or could be used in the conventional paper recycling process.

Acknowledgments

Appendix A. Supplementary data

Supplementary data to this article can be found online at https://doi.org/10.1016/j.susmat.2019.e00115.

Table 1
Effect of recycling on properties of NC fibres.

Measurement Technique	Area examined	Effect of Recyling compared to virgin fibres
SEM Measurement of Fibre diameter	1 μm scale bar	None
SEM Measurement of Film Surface	2 μm scale bar	Nothing conclusive
SEM Measurement of Film Surface	10 μm scale bar	None
Optical Profilometry roughness	100×90 μm	None
SEM Measurement of Film Surface	100 μm scale bar	None
Film thickness	159 mm diameter of film	Higher thickness at the same basis weight (g/m^2)
Zero-span strength	Estimated 300 μm span length	30% Less
PPF tester of optical uniformity	1–15 mm inspection areas 16–39 mm inspection areas	Decrease in uniformity at lower areas of Inspection Increase in uniformity at higher areas of Inspection
Water vapour permeability	63.5 mm diameter circle of film	Higher permeability ~ Doubled WVP
Air permeability	50 cm^2 sample	Higher permeability: permeability increased above the detection limit of the instrument.
Tensile strength via Instron Method	100 mm test span	30% less strength

References

[1] Smithers Pira, The Future of Global Packaging to 2020, (14 December 2015; Available from) http://www.smitherspira.com/industry-market-reports/packaging/the-future-of-global-packaging-markets-to-2020 2015.
[2] G. Davis, J.H. Song, Biodegradable packaging based on raw materials from crops and their impact on waste management, Ind. Crop. Prod. 23 (2) (2006) 147–161.
[3] A. Tukker, Plastic waste-feedstock recycling, chemical recycling and incineration, Rapra. Rev. Rep. 13 (4) (2002) 1–10.
[4] E. Bugnicourt, et al., Processing and validation of whey-protein-coated films and laminates at semi-industrial scale as novel recyclable food packaging materials with excellent barrier properties, Adv. Mater. Sci. Eng. 2013 (2013) 10.
[5] K. Bhunia, et al., Migration of chemical compounds from packaging polymers during microwave, conventional heat treatment, and storage, Compr. Rev. Food Sci. Food Saf. 12 (5) (2013) 523–545.
[6] O.-W. Lau, S.-K. Wong, Contamination in food from packaging material, J. Chromatogr. A 882 (1–2) (2000) 255–270.
[7] T.D. Lickly, K.M. Lehr, G.C. Welsh, Migration of styrene from polystyrene foam food-contact articles, Food Chem. Toxicol. 33 (6) (1995) 475–481.
[8] M.A. Hubbe, et al., Nanocellulose in thin films, coatings, and plies for packaging applications: a review, BioResources 12 (1) (2017) 2143–2233.
[9] R.N. Tharanathan, Biodegradable films and composite coatings: past, present and future, Trends Food Sci. Technol. 14 (3) (2003) 71–78.
[10] H.M.C. Azeredo, M.F. Rosa, L.H.C. Mattoso, Nanocellulose in bio-based food packaging applications, Ind. Crop. Prod. 97 (2017) 664–671.
[11] C. Aulin, M. Gällstedt, T. Lindström, Oxygen and oil barrier properties of microfibrillated cellulose films and coatings, Cellulose 17 (3) (2010) 559–574.
[12] J. Bras, S. Saini, 8 - nanocellulose in functional packaging A2 - Jawaid, Mohammad, in: S. Boufi, A.K. H.P.S (Eds.), Cellulose-Reinforced Nanofibre Composites, Woodhead Publishing 2017, pp. 175–213.
[13] H.P.S. Abdul Khalil, et al., A review on nanocellulosic fibres as new material for sustainable packaging: process and applications, Renew. Sust. Energ. Rev. 64 (2016) 823–836.

[14] S. Varanasi, R. He, W.J. Batchelor, Estimation of cellulose nanofibre aspect ratio from measurements of fibre suspension gel point, Cellulose 20 (4) (2013) 1885–1896.

[15] P. Raj, et al., Gel point as a measure of cellulose nanofibre quality and feedstock development with mechanical energy, Cellulose 23 (5) (2016) 3051–3064.

[16] S. Varanasi, W.J. Batchelor, Rapid preparation of cellulose nanofibre sheet, Cellulose 20 (1) (2013) 211–215.

[17] K. Shanmugam, et al., Rapid preparation of smooth nanocellulose films using spray coating, Cellulose 24 (7) (2017) 2669–2676.

[18] K. Shanmugam, et al., Flexible spray coating process for smooth nanocellulose film production, Cellulose 25 (3) (2018) 1725–1741.

[19] S. Varanasi, H.H. Chiam, W. Batchelor, Application and interpretation of zero and short-span testing on nanofibre sheet materials, Nordic Pulp Paper Res. J. 27 (2) (2012) 343.

[20] M. Delgado-Aguilar, et al., Are cellulose nanofibers a solution for a more circular economy of paper products? Environ. Sci. Technol. 49 (20) (2015) 12206–12213.

[21] M. Hietala, K. Varrio, L. Berglund, J. Soini, K. Oksman, Potential of municipal solid waste paper as raw material for production of cellulose nanofibres, Waste Manag. 80 (2018) 319–326 2018/10/01/.

[22] U. Garusinghe, S. Varanasi, V.S. Raghuwanshi, G. Garnier, W.J. Batchelor, Nanocellulose-montmorillonite composites of low water vapour permeability, Coll. Surf. A Physicochem. Eng. Aspects 540 (2018) 233–241.

[23] G. Rodionova, M. Lenes, Ø. Eriksen, Ø. Gregersen, Surface chemical modification of microfibrillated cellulose: improvement of barrier properties for packaging applications, Cellulose 18 (1) (2011) 127–134.

[24] Pieter Samyn, Wetting and hydrophobic modification of cellulose surfaces for paper applications, J. Mater. Sci. 48 (19) (2013) 6455–6498.

[25] Leonidas Milios, Aida Esmailzadeh Davani, Yi Yu, Sustainability impact assessment of increased plastic recycling and future pathways of plastic waste management in Sweden, Recycling 3 (3) (2018) 33.

[26] European Commission, Single use of Plastics, 28 May 2018; Available from: https://ec.europa.eu/commission/news/single-use-plastics-2018-may-28 2018.

[27] European Commision, Technical report on " A european strategy for plastics in a circular economy", 2018 , Available from http://ec.europa.eu/environment/circular-economy/pdf/plastics-strategy-brochure.pdf.

[28] Joo-Hyung Kim, et al., Review of nanocellulose for sustainable future materials, Int. J. Precision Eng. Manuf. Green Technol. 2 (2) (2015) 197–213.

[29] Qingqing Li, Sean McGinnis, Cutter Sydnor, Anthony Wong, Scott Renneckar, Nanocellulose life cycle assessment, ACS Sustain. Chem. Eng. 1 (8) (2013) 919–928.

[30] Sue Jackson, T. Bertényi, Recycling of plastics, ImpEE Project, Department of Engineering, University of Cambridge, 2006 , Available from; http://www-g.eng.cam.ac.uk/impee/topics/RecyclePlastics/files/Recycling%20Plastic%20v3%20PDF.pdf.

[31] F. Piccinno, R. Hischier, S. Seeger, C. Som, Predicting the environmental impact of a future nanocellulose production at industrial scale: application of the life cycle assessment scale-up framework, J. Clean. Prod. 174 (2018) 283–295, https://doi.org/10.1016/j.jclepro.2017.10.226.

[32] J. Rydz, M. Musioł, B. Zawidlak-Węgrzyńska, W. Sikorska, Present and future of biodegradable polymers for food packaging applications, Biopolymers for Food Design 2018, pp. 431–467.

[33] Bulim Choi, Seungwoo Yoo, Su-il Park, Carbon footprint of packaging films made from LDPE, PLA, and PLA/PBAT blends in South Korea, Sustainability 10 (7) (2018) 2369.
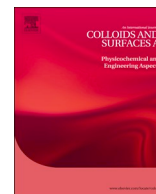
# Cellulose fibre- perlite depth filters with cellulose nanofibre top coating for improved filtration performance

Aysu Onur[a], Kirubanandan Shanmugam[a], Aaron Ng[b], Gil Garnier[a], Warren Batchelor[a],*

[a] Bioresource Processing Research Institute of Australia, Chemical Engineering Department, Monash University, Clayton, Australia
[b] 3M Australia, Sydney, Australia

GRAPHICAL ABSTRACT
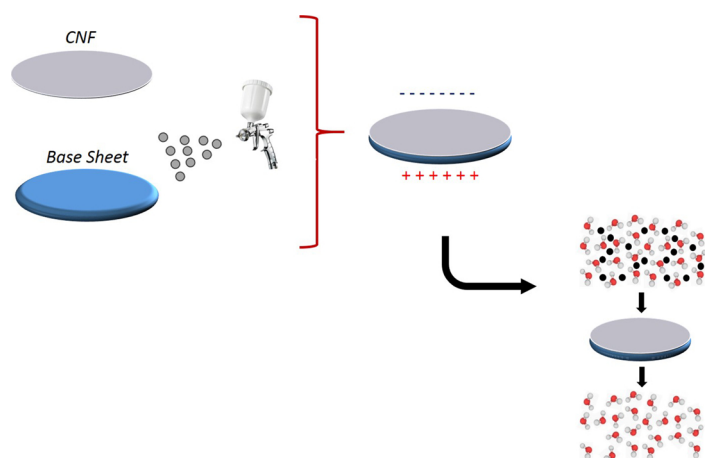
ARTICLE INFO

ABSTRACT

Depth type composite filters are used to remove contaminants from liquids by combining mechanical entrapment and adsorption. Commonly, depth filters can adsorb either anionic or cationic charged contaminants, but not both, as well as filter micron-sized particles. Therefore, there is still a need to improve the existing depth filter performance. In this study, we developed a two-layer filters with enhanced functionality by spray coating an anionically charged cellulose nanofibre (CNF) layer onto a cationically charged depth filter layer. The depth filter layer was prepared via papermaking technique of vacuum filtration from wood pulp fibres, perlite adsorbent and cationic polyamide-amine epichlorohydrin (PAE) wet strength resin. The CNF coat weight ranged from 4 to 30 g per square metre (gsm). The two layer filters were proven to have triple functionality, capable of adsorbing anionic molecules in the cationic depth filter layer, while the anionic CNF layer could adsorb cationic molecules and was also a microfiltration membrane. A gradual increase in CNF coat weight improved filtration performance but decreased the filter flux. The optimum performance was found at an 8 gsm CNF coat weight, where the membrane layer rejected 80% of 5000 kDa molecular weight polyethylene glycol, at a flux of 133 Litres per square meter per hour (LMH) under 1.5 bar pressure, while still achieving a good breakthrough curve when absorbing cationic methylene blue dye.

* Corresponding author at: Bioresource Processing Research Institute of Australia, Chemical Engineering Department, Monash University, Clayton, 3800, Australia.
E-mail address: warren.batchelor@monash.edu (W. Batchelor).

1. Introduction

Depth filters are porous filtering mediums that are retaining contaminants throughout the thickness by both size-based and adsorption-based separations [1]. These filters are composed of cellulose fibres, a type of filter aid and a charged wet-strength polymer and they are mainly used for clarification of food and beverages as well as pharmaceuticals [2,3] to remove yeast, cell cultures and trace of organic contaminants. These nonmembrane-based filters are typically employed for coarse separation and usually the solid content of suspension is very high where pre-filtration or recovery is targeted. Even though depth filters are commercially available and used in a filter cartridge form [1,4], there is still a need to improve the performance of the depth filters due to some limitations. For example, these filters are able to adsorb either anionic or cationic charged contaminants, but not both into one filter medium [5]. Furthermore, the current depth filters still have unresolved challenges with the cost-effective removal of relatively small molecules. There are different pressure-driven filtration processes: microfiltration [6], ultrafiltration [7], nanofiltration [8] and reverse osmosis [9] that are categorised based on their pore size distribution and application areas. While these filters can separate varying contaminants from suspended solids and bacteria to small organics and ions [10], depth filters are only limited to coarse filtration including suspended solids and bacteria.

All these limitations particularly were identified in our previous studies [11,12]. Filtration by size exclusion is restricted to very large particles due to the pore size distribution of our base sheet of (1–3 μm) [11,12] and we were not able to adsorb both positively and negatively charged molecules in the same filter medium. Ideally, all these challenges should be addressed with the aid of renewable and sustainable materials to reduce the impact on the environment. Recently, cellulose nanofibres (CNF) are seen as a good candidate to meet these challenges. CNF is an advantageous material due to high aspect ratio, low fibre diameter with high surface area and a web-like entangled structure [13]. The size of contaminants that are filtered can be reduced by using CNF [14] and increased surface area and bonding provided by CNF improves the wet strength of filters [15]. In addition, its largely crystalline nature and the ability to form dense percolating network of CNF result in low permeability [16].

The use of CNF in filters can particularly be seen in thin film nanofibrous composite (TFNC) membranes [17–21]. TFNC membranes typically consists of a multi-layered fibrous structure; a thin top barrier layer offering filtration function; a mid-layer fibrous scaffold made of electrospun nanofibres with large porosity and uniform continuous void structure minimizing the resistance of the membrane and giving a delicate support; and a bottom layer of a non-woven microfibrous substrate such as polyethylene terephthalate (PET) providing an overall mechanical support to the TFNC. However, the top barrier layer is the key component in these membranes for separation of solute and permeates and here the use of cellulose nanofibres as a barrier layer has been widely researched. The primary reason why cellulose is extensively studied for barrier properties is the cellulose crystalline regions. These regions are impermeable, which makes the length of the effective flow path of the air, water vapor or gas molecules through a cellulose nanofibre film significantly greater than the measured film thickness [22,23]. CNF not only can have a similar performance to conventional materials as a top barrier layer, but also be able to offer new opportunities in water purification [24–27]. For example, the ultrafine cellulose nanofibres can be used as an adsorbent with a high adsorption efficiency to remove charged molecules, such as positively charged contaminant adsorption [28]. The TFNC membrane concept has been proven to be energy efficient for membrane filtration, and a nanocomposite cellulose barrier layer could potentially further help in improving energy efficiency [24,25,29–31].

In a recent study, Roy et al. studied the CNF coating on top of a tissue paper to add excellent membrane separation functionality to tissue paper [32]. Modified CNF was coated on tissue paper by spray coating technique and they reported that coated tissue papers showed outstanding separation performances towards a variety of oil/water mixtures. Additionally, coated tissue papers exhibited improved dye adsorption capacity from aqueous solutions.

Following that, the same top layer approach could be applied to depth filters to improve their performance. Use of CNF as barrier layer could be a route for the performance improvement without any impact on environment thanks to the biodegradable and renewable nature of cellulose. Furthermore, an easy and eco-friendly technique, such as spray coating, should be employed for the coating of the barrier layer. Spray coating is an easily scalable, cheap and a rapid technique, that is capable of producing sheets with comparable uniformity to those produced by papermaking vacuum filtration [33,34]. In this study, we spray-coated CNF barrier layers with weights per unit area ranging from 4 to 30 g/m^2 onto depth filter base sheets and have investigated water permeation flux, cationic and anionic dye adsorption and polyethylene glycol (PEG) rejection to characterise the performance of the two layer filters.

2. Material and methods

2.1. Material

Unrefined northern softwood NIST RM 8495 bleached Kraft pulp from Procter and Gamble and Bleached radiata pine softwood Kraft pulp refined to 400 Canadian standard freeness (CSF) in a disk refiner are used for the base sheet preparation. The CNF grade used was microfibrillated cellulose (MFC) purchased from DAICEL Chemical Industries Limited, Japan, (grade Celish KY-100S). This was used as received for the top barrier layer preparation. MFC has 25% solids content and an average aspect ratio of 142 ± 28 with mean fibre diameter of 73 nm as reported in Varanasi et al. [35]. The MFC suspension, containing only cellulose and water, has a zeta potential of −22.3 mV [36].

Expanded perlite supplied by Dicalite Minerals Corp was used as inorganic fillers. Perlite is a low cost and an excellent filter aid made from a glassy volcanic rock [37]. It is an anionic adsorbent; the zeta potential is ranging between -40 to −50 mV [38]. The particle size distribution of perlite and its effect on the structure and porosity of filters was reported in a previous study [11,12]. Commercial PAE provided from Nopcobond Paper Technology Pty Ltd was used as wet strength resin. PAE is a positively charged polymer used to provide wet strength to the filters by crosslinking [15] as well as partial coverage to the negatively charged surface of perlite and cellulose fibres. Therefore, addition of PAE is important in terms of initiating electrostatic interaction between negatively charged contaminants and the filter medium.

Positively charged methylene blue (MB) and negatively charged metanil yellow (MY) dyes supplied from Sigma Aldrich were used to characterise the adsorption properties. MB has the amino group [39] and MY has the sulfonate group [40] that are providing the positive and negative charges, respectively, when they dissociate in water. Polyethylene glycol (PEG) of two molecular weights (600 and 5000 kDa) was provided by Dow Chemical for characterising the ultrafiltration capabilities of the filters.

2.2. Methods

2.2.1. Preparation of base sheets

200 gsm base sheets were prepared by using a standard British hand sheet maker. A particular fibre and perlite composition with a constant polymer (PAE) dosage was used to form the sheets. The composition is given below.

- 30% Fibre (1/3 refined pulp + 2/3 unrefined pulp) + 70% Perlite + 120 mg PAE

This composition was used in our previous studies [11,12];

however, due to its overall cationic charge it does not adsorb positively charged MB [11,12]. Preliminary experiments were also unable to detect any retention of PEG up to a molecular weight of 5000 kDa.

To prepare the base sheet, the perlite suspension (1.4 wt%) was mixed with refined pulp suspension (0.1 wt%). Following that, the mixture was added to the unrefined pulp suspension (0.08 wt%) and PAE (0.22% w/v) was added at a rate of 100 mg/g fibre on top of the finished slurry. As the last stage, the slurry was hand mixed and poured into British hand sheet maker chamber. A 150 μm size mesh was used in the chamber with a wet strengthened qualitative filter paper deposited on top. Filter paper is used to obtain uniformity and maximise the retention. The sheets were formed on top of the filter paper by draining water with gravity. After sheet formation, the wet sheets were taken out from the mesh and placed between dry blotting papers for pressing under 345 kPa for 5 min in a sheet pressing machine. This was followed by curing for 5 min at 150 °C. Curing is applied to develop wet strength in the base sheet through crosslinking the azetidinium groups of PAE with each other and with the cellulose [41]. Cured sheets were further air-dried in a humidity-controlled room (23 °C, 50% relative humidity) for at least 24 h.

2.2.2. Spray coating onto base sheets

CNF suspension for coating was prepared using MFC from DAICEL. 1 wt. % suspension was prepared by mixing pulp in water followed by disintegration in a model MKIIIC, Messmer Instruments Ltd disintegrator for 15,000 revolutions. Spray coating was performed using a Professional Wagner spray system (Model number 117) at a pressure of 200 bar. Before coating, the base sheets were placed onto stainless steel circular plates (diameter of 159 mm) and pre-wetted by dripping ultrapure water on them until the sheets were fully wetted, with no dry spots showing. This is done to improve the adhesion of the CNF layer. The detailed schematic of spray coating experimental setup is shown in Fig. 1. The spray nozzle used in this work was Wagner 317, producing a spray jet angle and a beam width around 30° and 15 cm, respectively. The spray nozzle size is 0.017 inch and this allowed the MFC to propagate easily. The spray distance from spray nozzle to the circular steel plate is 50.0 ± 1.0 cm. CNF suspension consistency was kept constant at 1 wt. % and the deposited mass of the CNF layer was controlled with varying conveyor speed levels which are 20, 40, 60, 80 and 100. The measured actual speeds of each levels are respectively 533, 1333, 2182, 2667, 3429 mm/min. After spray coating, the filters were left on the circular plates in drying racks and air-dried for 24 h. Drying racks help minimizing the sheet shrinkage and keep the sheets flat during drying. Following air-drying, samples were kept in the humidity-controlled room for another 24 h before any further testing. All experiments were performed with at least two repetitions. The variability in coat-weight added was determined by obtaining the weight of samples before and after spray coating and was typically less than 1 g/m^2.

2.2.3. Thickness and air flow testing

Thickness of the filters was measured before and after spray coating using Lorentzen & Wettre (L&W) Micrometer thickness tester. Average thickness of ten points was used to calculate the thickness of each sample. The weight of coated CNF layer was measured by weighing filters before and after spray coating. The grammage of each coating was then measured by dividing the weight of CNF layers by surface area of the filters. A L&W air permeance tester with an operating range from 0.003 to 100 μm/Pa.S was used to measure air permeance before and after coating. Two replicates were tested for each filter.

2.2.4. Scanning electron microscopy

FEI Magellan 400 FEG SEM were used to characterize surface and cross section morphology of filters. Samples were mounted onto a metal substrate using carbon tape and coated with a thin layer of Iridium. Secondary electron images of composites were captured. 2 kV of accelerating voltage was applied for magnification up to 10,000 X.

2.2.5. Adsorption and filtration properties

Adsorption and filtration experiments were carried out with a dead-end stirred cell from Merck Millipore Australia. For PEG filtration, a TOC (Total Organic Carbon) analyser manufactured by Shimadzu was used to analyse the PEG content of the filtrate. Dye concentration was measured at 10 s intervals with an ultraviolet-visible (UV–vis) spectrometer with a quartz micro flow cell with 10 mm optical path length. Mass flux for the effective membrane area (0.00418 m^2) was calculated by measuring the mass of permeate as function of time. The experimental procedure with a comprehensive schematic and flux equation can be found in our previous studies [11,12].

The experiments were performed at 1.5 bar for both adsorption and filtration experiments. Before any adsorption and filtration testing, water flux was measured on the sheets at 1.5 bar with 400 ml of ultrapure water. Adsorption experiments were conducted with 400 ml of either 5 ppm MY or MB dye solutions and PEG filtration was done with 50 ml of 0.1% (wt./v) of either 600 or 5000 kDa PEG. 0.1% (wt./v) PEG solution was prepared by adding 1 g of polymer into 1000 ml pure water and stirring overnight. Two replicates were tested for each sample.

3. Results

3.1. Cellulose nanofibre layer structure

3.1.1. Coated layer grammage

Fig. 2 shows the different grammage (g/m^2) of cellulose nanofibre (CNF) layer coated on top of the base sheets as a function of conveyor speed.

Fig. 2 shows that we could get a 30 gsm CNF layer coated onto base sheet with the slowest speed (533 mm/min). However, increasing speeds results in less material transfer onto base sheets, which in turn decreases the total gsm of final products. The lowest gsm coated onto filters is around 4 gsm with the highest speed (3429 mm/min).

The thickness of coated layers onto base sheets is shown in Fig. 3 in mm according to different coating grammages. The original base sheet thicknesses are ranging between 0.43 and 0.45 mm. The coated layer thicknesses onto base sheets are in the range of 0.0112 to 0.0405 mm; these thicknesses were obtained by CNF grammage between 4 and 30 gsm. The increase in thickness at 4 gsm is 28% of the increase in thickness at 30 gsm. The gradual increase indicates that CNF is not likely to intrude into the base layer. This can be also seen from the cross-section SEM image in the next section (Fig. 5). Moreover, this is also consistent with measurements of the gel-point [35], which show that at the sprayed solids content of 1 wt.%, the fibres in the suspension will form a connected network, preventing them from adsorbing into the base sheet layer.

3.1.2. Surface and cross section scanning electron microscopy images

Fig. 4 shows the surface morphology of base sheet and samples coated with different grammages of CNF layer. The base sheet has a lot of perlite particles protruding from the surface. However, CNF layer successfully provides almost full surface coverage from 8 gsm coating
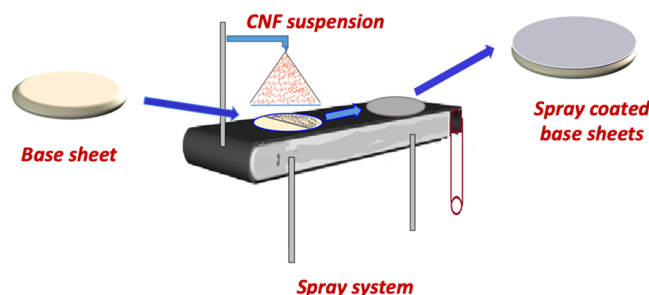

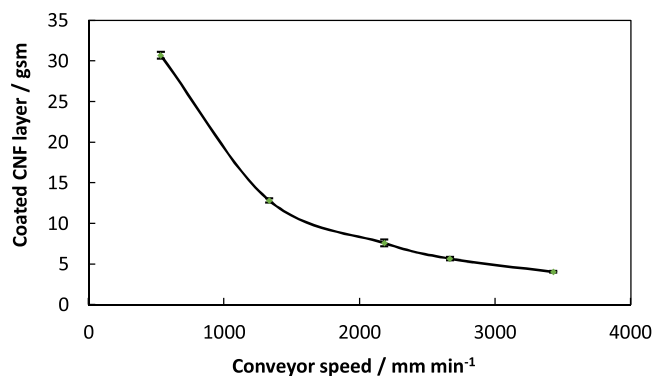**Fig. 1.** Spray coating experimental setup schematic [33,34].

Fig. 2. The grammage of top coating according to increasing conveyor speeds.
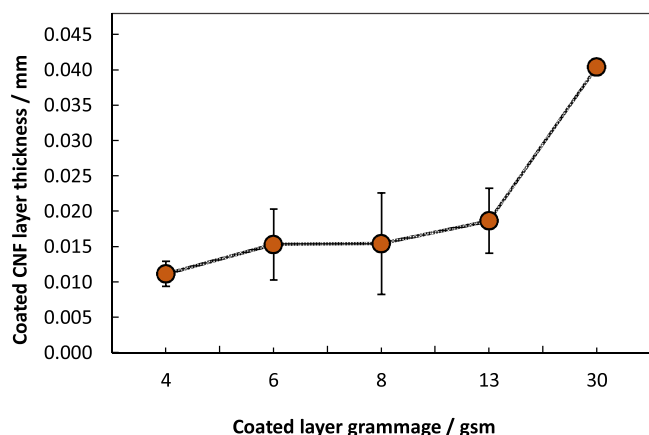

Fig. 3. Thickness of coated layers according to different grammages.

upwards; neither of the high gsm coatings (13 and 30 gsm) show visible particles protruding through the coating. However, perlite particles can be visibly seen protruding from the surface of 4 and 6 gsm CNF coated filters.

Fig. 5 shows a cross-section of the sample with 6 gsm CNF layer, with the CNF layer on the right-hand side of the image. The internal bonding between the CNF coating and base sheet can be seen in the image; the CNF layer is connected to the base sheet with extensive amount of bonding provided by the high surface area of CNF. However, there is no evidence of fibres intruding into the base sheet. The fibres seem to form a discrete smooth surface providing a full surface coverage on the base sheet. This is also in agreement with the gradual thickness increase of layers with increasing grammages (Fig. 3).

3.1.3. Air flow testing

Air flow testing is done to investigate the air barrier properties of samples that might be potentially improved by CNF coating. Fig. 6 shows the air permeability of each filter in µm/Pa.s. Base sheet is quite porous with high permeability around 2.39 µm/Pa.s. 4 gsm coating on top of base sheet reduced the air permeability significantly by 83%. The thickest coating, 30 gsm, has a permeability of less than 0.003 µm/Pa.s, which is the lower measurement limit of the instrument. All these results confirm that even the thinnest 4 gsm sprayed CNF layer has successfully formed a continuous barrier layer.

3.2. Filtration performance

3.2.1. Water flux

Water flux of samples, as a function of coating layer grammage, is shown in Fig. 7. The base sheet without any CNF layer (0 gsm) has the highest flux around 690 LMH. Even the lowest coating grammage (4 gsm) dropped flux by 51%. The gradual increase in the coating layer

grammage decreased the water flux gradually where the thickest coating layer (30 gsm) only has a flux of around 15 LMH, which is a substantial decrease by 98% compared to the base sheet. Our flux results are in a similar range with CNF membranes reported by Varanasi et al. [14]. Additionally, water permeance for 6–67 µm thick Cladophora CNF membranes was reported to be between 10–150 LMH [42,43]. While fibre dimension, pore size distribution and having a base sheet might cause differences in flux, our water flux results for 10–40 µm thick CNF coated filters are ranging between 15–334 LMH. This shows some similarities of our work with other studies.

3.2.2. Polyethylene glycol filtration

Separation experiments by molecular weight were conducted with two different molecular weights of polyethylene glycol (PEG) (600 kDa and 5000 kDa). The fraction rejected for each molecular weight is given in Fig. 8 as a function of the grammage of CNF coating. The 13 gsm sample was not tested for PEG rejection, as the major interest is the maximum rejection achievable. The highest rejection achieved was 84% and 86% for 600 and 5000 kDa PEG, respectively, at the thickest coating (30 gsm). The rejection for 5000 kDa PEG is slightly higher than 600 kDa for 6 and 8 gsm coatings. This is expected as 5000 kDa PEG molecules would be larger and more likely to be held by the filters. However, there is no rejection obtained with the base sheets for any of these molecular weights; these experiments were performed in our previous study [11,12]. Ultrafiltration membranes have molecular weight cut off (MWCO) reported in Dalton, ranging from 1000 Da to 1 MDa [44]. MWCO refers to the lowest molecular weight of a solute of which at least 90% can be retained by a membrane. 600 kDa can easily fall under ultrafiltration, where 5000 kDa is in the smaller size ranges of microfiltration. Therefore, 600 and 5000 kDa PEGs were particularly selected to represent molecular weights in the ultrafiltration and microfiltration ranges, respectively. Our results indicate that we could improve the rejection of different molecular weights by spraying CNF layer on top of the base filters. The full set of TOC results for each sample are given in the SI (Table S1).

3.2.3. Methylene blue adsorption

MB adsorption breakthrough curves are shown in Fig. 9. Base sheets originally have very steep adsorption breakthrough curves which correspond to very poor adsorption. This can be attributed to the positive charge characteristics of the filters due to the presence of positively charged polymer PAE. As a result of repulsion between the filter media and positively charged methylene blue, very little adsorption occurs onto filters. However, our filters are very successful in terms of adsorbing negatively charged contaminants thanks to the presence of PAE. The negatively charged metanil yellow adsorption breakthrough curve of base sheet is shown in Fig. 11. In this study, we also aim to improve the positively charged contaminant adsorption onto filters besides adding filtration capabilities. Fig. 9 shows that with the increasing CNF layer thickness, MB breakthrough curves are improving, and more adsorption occurs onto filters. This can be also seen with the photos taken after adsorption onto filters (Fig. 10a). The layers become darker from left to right with increasing CNF thicknesses which indicates more MB adsorption on filters. On the other hand, Fig. 10b demonstrates the back side of the filters after adsorption. The back side is the base sheet and they all have the same very light intensity of blue colour; this proves that the adsorption is mainly dependent on the top layer coating. The poor base sheet MB adsorption characteristics have not been impacted by the top coating, as expected. Methylene blue adsorption capacity of each filter was calculated by the trapezoid rule and shown in Table 1. Adsorption capacity of base sheet is 0.0033 mg/g, while it is increased tremendously up to 1.3610 mg/g by 13 gsm CNF coating. The 30 gsm coated sample was not shown in Fig. 9 and Fig. 10 as the flux was too slow to be practical for industrial applications.

Pictures of the sheet with 13 gsm CNF coating and the base sheet after MY adsorption are shown in Fig. 11a and b, respectively. Fig. 11c
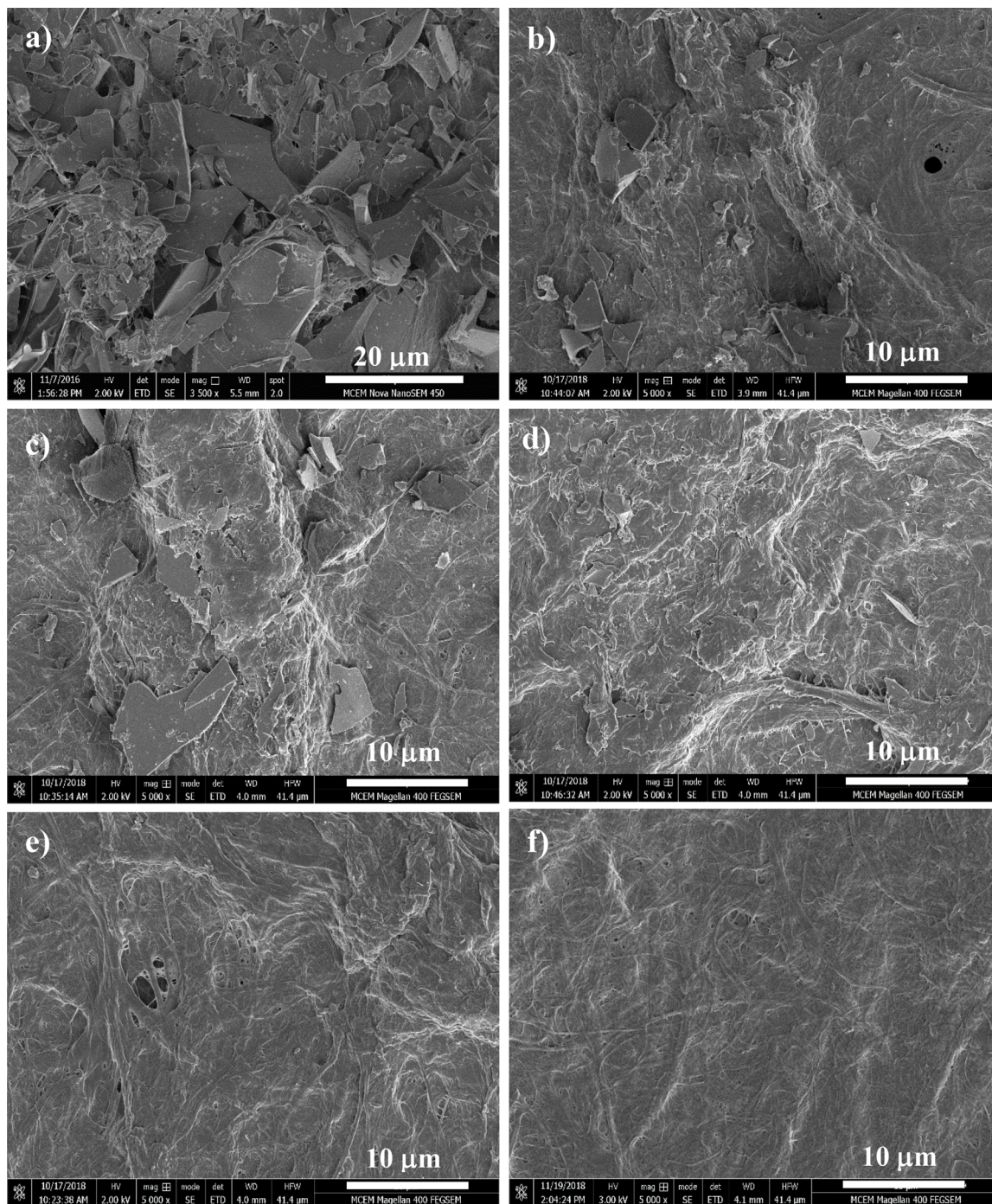
Fig. 4. Surface SEM images of **a)** base sheet **b)** 4 gsm **c)** 6 gsm) **d)** 8 gsm **e)** 13 gsm **f)** 30 gsm CNF layers.

shows metanil yellow adsorption breakthrough curve of the base sheet. There is no adsorption onto CNF layer; metanil yellow is adsorbed onto the base sheet only.

4. Discussion and future perspective

This new two-layer filter developed here shows remarkable performance. While the positively charged cellulose-perlite depth filters are a well-established solution for adsorbing negatively charged contaminants, we have previously established that they have no adsorption of positively charged contaminants. In addition, due to the large pore size distribution of our depth filters of 2–3 μm [11,12], the particle capturing is only limited to large particles. In this work, we have

prepared a dual layer system by spraying a top layer onto the previously developed depth filter. Spraying is a scalable and could readily be adapted for the production of these materials on an industrial scale.

Furthermore, the sprayed cellulose nanofibre layer is naturally negatively charged. The performance achieved has not required the use of any additional polyelectrolytes to control the charge. These negatively charged cellulose nanofibres have formed a layer that has effectively bonded to the depth filter layer due to firstly, the small size of the fibres, which means that they are able to conform to the base layer. Secondly, the electrostatic interaction between the positively charged base layer and the negatively charged cellulose nanofibre layer provides additional bonding between the layers.

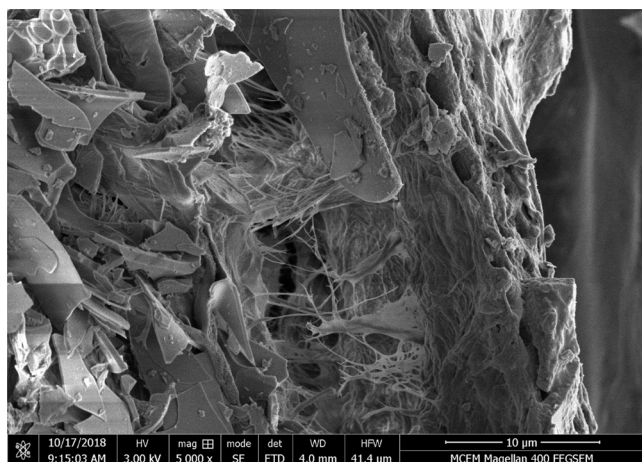The new dual layer structure gives a highly promising triple

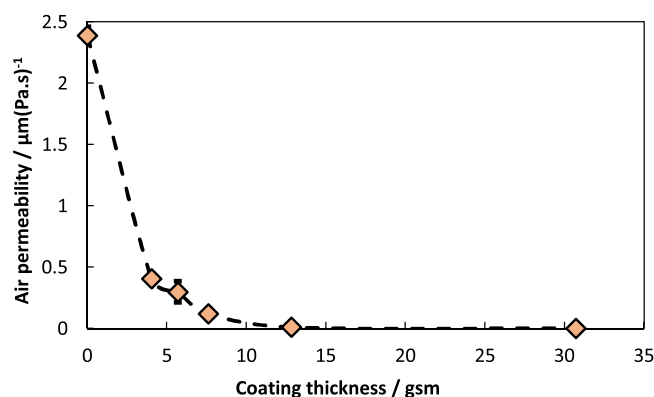**Fig. 5.** Cross section image of 6 gsm coated sample.

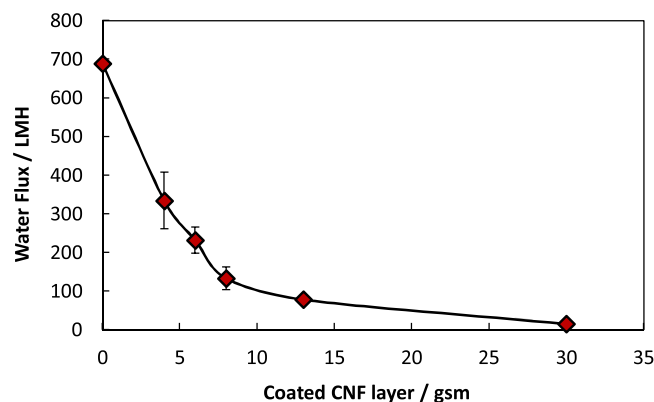**Fig. 6.** Air permeability of filters versus coating layer grammage.

Fig. 7. Water flux of samples versus coating layer grammage.

Fig. 8. PEG rejection results with respect to different coating layer grammage and two different molecular weights of PEG.

Fig. 9. Methylene blue adsorption breakthrough curves as a function of CNF layer thicknesses (For interpretation of the references to colour in this figure legend, the reader is referred to the web version of this article).

functionality: microfiltration performance to reject particles by size, adsorption of positively charged contaminants in the negatively charged cellulose nanofibre membrane top layer and adsorption of negatively charged contaminants in the depth filter layer by electrostatic interaction. In addition, the membrane layer protects the depth filter layer from becoming clogged from suspended particles.

The performance trade-off is in the reduction of flux. Selection of the appropriate barrier layer grammage needs to be made. After consideration of all the results, the best grammage to balance separation performance against flux would be an 8 gsm layer. While this layer has reduced the flux at 1.5 bar pressure from 689 to 133 LMH, the two layer structure has achieved nearly 80% rejection of 5000 kDa PEG and has not been fully saturated when filtering the positively charged dye.
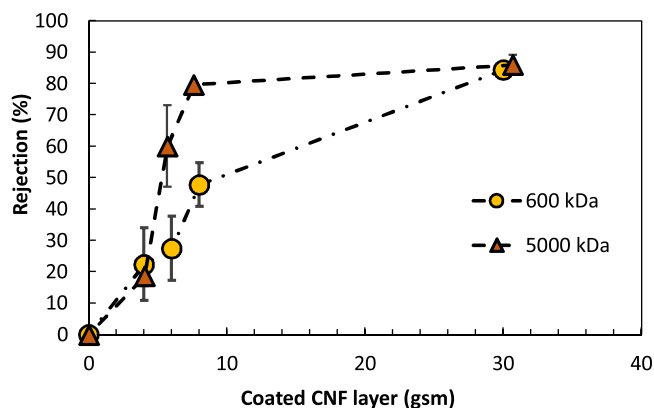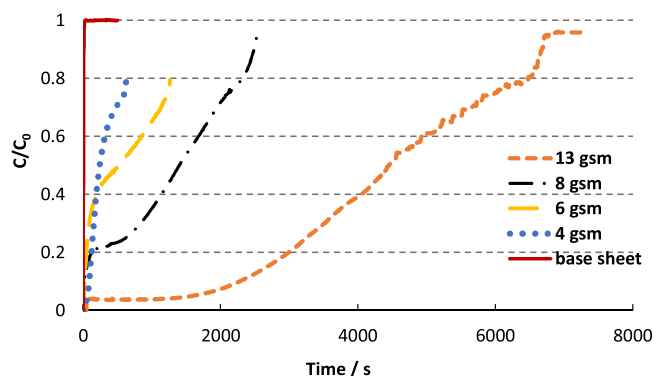
5. Conclusion

This study has focused on the development of new functionalities for depth type filters by coating a top barrier layer. Depth filters were made by papermaking technique composing of cellulose fibre, perlite and wet strength resin PAE and used as base sheets. Following this, we have investigated a novel filter material made by spraying an anionic CNF suspension as a membrane layer onto a cationically charged cellulose fibre-perlite depth filter. The resulting laminate is flexible, with excellent adhesion between the layers, even though no bonding agent was added. Different thickness of CNF layer was investigated for a variety of properties: water flux, adsorption and rejection of molecules by molecular weight. CNF is advantageous as a top barrier layer thanks to its highly connected network and smaller pore sizes. This helps holding smaller molecules that base sheets individually are not able to do. We could obtain around 84% cut-off for two different molecular weights of PEG only with 30 gsm top coating. Moreover, the negatively charged nature of CNF helps attracting positively charged molecules. MB dye breakthrough curves showed a remarkable improvement with increasing grammage of CNF layer. Surface and cross section morphologies were observed by SEM images and they indicate that CNF provides a smoother and more discrete surface coverage by increasing thickness of CNF.

Our study shows that CNF is a promising material to be used as a barrier layer on top of the filters, allowing us to fine-tune performance of the filters by tuning surface area and surface charge of the filters. CNF's biodegradable and renewable nature also ensure that our filters are tailored without any chemical impact on the environment.
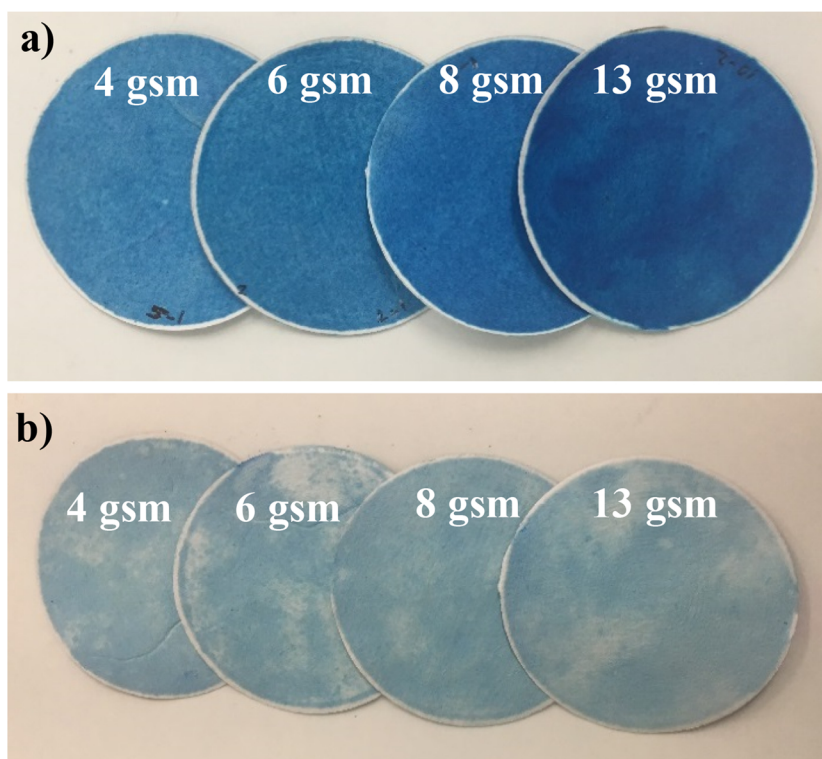
Fig. 10. Pictures taken after methylene blue adsorption from **a)** the front side **b)** the back side of filters with different thicknesses of CNF layer (For interpretation of the references to colour in this figure legend, the reader is referred to the web version of this article).
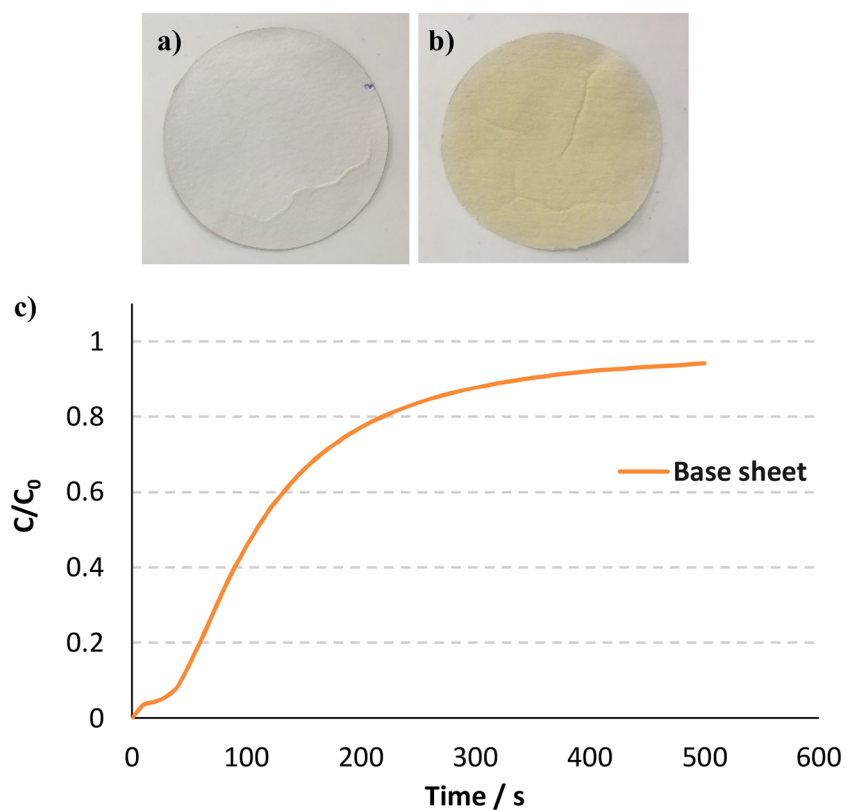
Fig. 11. a) Composite sheet 13 gsm CNF layer after metanil yellow (MY) adsorption **b)** base sheet after MY adsorption **c)** Base sheet metanil yellow breakthrough curve [11,12] (For interpretation of the references to colour in this figure legend, the reader is referred to the web version of this article).

Table 1
Methylene blue adsorption capacity of samples.

Sample	Adsorption Capacity (mg/g)
Base sheet	0.0033
4 gsm	0.5632
6 gsm	0.6930
8 gsm	0.7730
13 gsm	1.3610

Declaration of Competing Interest

The authors declare that they have no known competing financial interests or personal relationships that could have appeared to influence the work reported in this paper.

Acknowledgements

References

[1] I.M. Hutten, Chapter 7 - liquid filter applications, Handbook of Nonwoven Filter Media, second edition, Butterworth-Heinemann, Oxford, 2016, pp. 409–450.

[2] K. Sutherland, Filtration overview: a closer look at depth filtration, Filtr. Sep. 45 (8) (2008) 25–28.

[3] A. Bennett, Pharmaceuticals and fine chemicals: filtration and separation in the diverse fine chemical sectors, Filtr. Sep. 50 (6) (2013) 30–33.

[4] M.K. M. Wang, R. Sale, M. Entezarian, Single-use depth-filtration system, GEN Genetic Eng. Biotechnology News 32 (2012).

[5] H. Sehaqui, P. Spera, A. Huch, T. Zimmermann, Nanoparticles capture on cellulose nanofiber depth filters, Carbohydr. Polym. 201 (2018) 482–489.

[6] G. dos Santos Bernardi, J.D. Magro, M.A. Mazutti, J.V. Oliveira, M. Di Luccio, G.L. Zabot, M.V. Tres, 13 - microfiltration for filtration and pasteurization of beers, in: A.M. Grumezescu, A.M. Holban (Eds.), Engineering Tools in the Beverage Industry, Woodhead Publishing, 2019, pp. 405–434.

[7] M. Bernal, M.O. Ruiz, R.M. Geanta, J.M. Benito, I. Escudero, Colour removal from beet molasses by ultrafiltration with activated charcoal, Chem. Eng. J. 283 (2016) 313–322.

[8] B. Van der Bruggen, C. Vandecasteele, Removal of pollutants from surface water and groundwater by nanofiltration: overview of possible applications in the drinking water industry, Environ. Pollut. 122 (3) (2003) 435–445.

[9] M. Sarai Atab, A.J. Smallbone, A.P. Roskilly, A hybrid reverse osmosis/adsorption desalination plant for irrigation and drinking water, Desalination 444 (2018) 44–52.

[10] B. Van der Bruggen, Chapter 2 - microfiltration, ultrafiltration, nanofiltration, reverse osmosis, and forward osmosis, in: P. Luis (Ed.), Fundamental Modelling of Membrane Systems, Elsevier, 2018, pp. 25–70.

[11] A. Onur, A. Ng, W. Batchelor, G. Garnier, Multi-layer filters: adsorption and filtration mechanisms for improved separation, Front. Chem. 6 (417) (2018).

[12] A. Onur, A. Ng, G. Garnier, W. Batchelor, Engineering cellulose fibre inorganic composites for depth filtration and adsorption, Sep. Purif. Technol. 203 (2018) 209–216.

[13] Q. Li, W. Chen, Y. Li, X. Guo, S. Song, Q. Wang, Y. Liu, J. Li, H. Yu, J. Zeng, Comparative study of the structure, mechanical and thermomechanical properties of cellulose nanopapers with different thickness, Cellulose 23 (2) (2016) 1375–1382.

[14] S. Varanasi, Z.-X. Low, W. Batchelor, Cellulose nanofibre composite membranes – biodegradable and recyclable UF membranes, Chem. Eng. J. 265 (2015) 138–146.

[15] A. Onur, A. Ng, G. Garnier, W. Batchelor, The use of cellulose nanofibres to reduce the wet strength polymer quantity for development of cleaner filters, J. Clean. Prod. 215 (2019) 226–231.

[16] A. Dufresne, Nanocellulose: a new ageless bionanomaterial, Mater. Today 16 (6) (2013) 220–227.

[17] H. Ma, K. Yoon, L. Rong, Y. Mao, Z. Mo, D. Fang, Z. Hollander, J. Gaiteri, B.S. Hsiao, B. Chu, High-flux thin-film nanofibrous composite ultrafiltration membranes containing cellulose barrier layer, J. Mater. Chem. 20 (22) (2010) 4692–4704.

[18] H. Ma, C. Burger, B.S. Hsiao, B. Chu, Fabrication and characterization of cellulose nanofiber based thin-film nanofibrous composite membranes, J. Memb. Sci. 454 (2014) 272–282.

[19] X. Wang, D. Fang, B.S. Hsiao, B. Chu, Nanofiltration membranes based on thin-film nanofibrous composites, J. Memb. Sci. 469 (2014) 188–197.

[20] Z. Wang, H. Ma, B.S. Hsiao, B. Chu, Nanofibrous ultrafiltration membranes containing cross-linked poly(ethylene glycol) and cellulose nanofiber composite barrier layer, Polymer 55 (1) (2014) 366–372.

[21] X. Wang, H. Ma, B. Chu, B.S. Hsiao, Thin-film nanofibrous composite reverse osmosis membranes for desalination, Desalination 420 (2017) 91–98.

[22] J.M. Lagaron, R. Catalá, R. Gavara, Structural characteristics defining high barrier properties in polymeric materials, Mater. Sci. Technol. 20 (1) (2004) 1–7.

[23] S. Amit, J.E. Thomas, K. Jeffrey, J.R. Arthur, High oxygen nanocomposite barrier films based on xylan and nanocrystalline cellulose, Nano-Micro Lett. 2 (4) (2010) 235–241.

[24] H. Ma, C. Burger, B.S. Hsiao, B. Chu, Ultra-fine cellulose nanofibers: new nano-scale materials for water purification, J. Mater. Chem. 21 (21) (2011) 7507–7510.

[25] H. Ma, C. Burger, B.S. Hsiao, B. Chu, Ultrafine polysaccharide nanofibrous membranes for water purification, Biomacromolecules 12 (4) (2011) 970–976.

[26] P.R. Sharma, A. Chattopadhyay, S.K. Sharma, B.S. Hsiao, Efficient removal of UO22 + from water using carboxycellulose nanofibers prepared by the nitro-oxidation method, Ind. Eng. Chem. Res. 56 (46) (2017) 13885–13893.

[27] P.R. Sharma, A. Chattopadhyay, S.K. Sharma, L. Geng, N. Amiralian, D. Martin, B.S. Hsiao, Nanocellulose from spinifex as an effective adsorbent to remove cadmium(II) from water, ACS Sustain. Chem. Eng. 6 (3) (2018) 3279–3290.

[28] H. Ma, B.S. Hsiao, B. Chu, Ultrafine cellulose nanofibers as efficient adsorbents for removal of UO22 + in water, ACS Macro Lett. 1 (1) (2012) 213–216.

[29] K. Yoon, B.S. Hsiao, B. Chu, Functional nanofibers for environmental applications, J. Mater. Chem. 18 (44) (2008) 5326–5334.

[30] H. Ma, C. Burger, B.S. Hsiao, B. Chu, Highly permeable polymer membranes containing directed channels for water purification, ACS Macro Lett. 1 (6) (2012) 723–726.

[31] H. Ma, B. Chu, B.S. Hsiao, Functional nanofibers for water purification, Functional Nanofibers and their Applications, (2012), pp. 331–370.

[32] S. Roy, L. Zhai, L. Van Hai, J.W. Kim, J.H. Park, H.C. Kim, J. Kim, One-step nanocellulose coating converts tissue paper into an efficient separation membrane, Cellulose 25 (9) (2018) 4871–4886.

[33] K. Shanmugam, S. Varanasi, G. Garnier, W. Batchelor, Rapid preparation of smooth nanocellulose films using spray coating, Cellulose 24 (7) (2017) 2669–2676.

[34] K. Shanmugam, H. Doosthosseini, S. Varanasi, G. Garnier, W. Batchelor, Flexible spray coating process for smooth nanocellulose film production, Cellulose 25 (3) (2018) 1725–1741.

[35] S. Varanasi, R. He, W. Batchelor, Estimation of cellulose nanofibre aspect ratio from measurements of fibre suspension gel point, Cellulose 20 (4) (2013) 1885–1896.

[36] P. Raj, A. Blanco, E. de la Fuente, W. Batchelor, C. Negro, G. Garnier, Microfibrilated cellulose as a model for soft colloid flocculation with polyelectrolytes, Colloids Surf. A Physicochem. Eng. Asp. 516 (2017) 325–335.

[37] M. Doğan, M. Alkan, Y. Onganer, Adsorption of methylene blue from aqueous solution onto perlite, Water Air Soil Pollut. 120 (1) (2000) 229–248.

[38] M. Alkan, Ö. Demirbaş, M. Doğan, Zeta potential of unexpanded and expanded perlite samples in various electrolyte media, Microporous Mesoporous Mater. 84 (1) (2005) 192–200.

[39] M. Doğan, M. Alkan, A. Türkyilmaz, Y. Özdemir, Kinetics and mechanism of removal of methylene blue by adsorption onto perlite, J. Hazard. Mater. 109 (1) (2004) 141–148.

[40] D.E. Jan, S. Raghavan, Adsorption of Metanil Yellow on a positively charge-modified nylon 66 membrane, Colloids Surf. A Physicochem. Eng. Asp. 92 (1) (1994) 1–7.

[41] T. Obokata, A. Isogai, The mechanism of wet-strength development of cellulose sheets prepared with polyamideamine-epichlorohydrin (PAE) resin, Colloids Surf. A Physicochem. Eng. Asp. 302 (1) (2007) 525–531.

[42] S. Gustafsson, P. Lordat, T. Hanrieder, M. Asper, O. Schaefer, A. Mihranyan, Millefeuille paper: a novel type of filter architecture for advanced virus separation applications, Mater. Horiz. 3 (4) (2016) 320–327.

[43] S. Gustafsson, A. Mihranyan, Strategies for tailoring the pore-size distribution of virus retention filter papers, ACS Appl. Mater. Interfaces 8 (22) (2016) 13759–13767.

[44] J. Liderfelt, J. Royce, Chapter 14 - filtration principles, Biopharmaceutical Processing, Elsevier, 2018, pp. 279–293.

Effect of Recycling on the properties of nanocellulose –Barrier and Mechanical Properties

Kirubanandan Shanmugam, Humayun Nadeem, Swambabu Varanasi, Gil Garnier, Warren Batchelor

Department of Chemical Engineering, Bioresource Processing Institute of Australia, Monash University, Melbourne, Vic 3800, Australia.

Address correspondence to E-mail: Warren.Batchelor@monash.edu

Abstract

Plastic based packaging causes significant problems in the environment. They are neither renewable nor biodegradable and plastics are accumulating in the environment, damaging the eco-system. Recycling also remains problematic. Sustainable, recyclable materials with outstanding barrier performance are required to replace these synthetic plastics. Nanocellulose is a potential candidate to replace synthetic polymers as packaging barrier layers. Nanocellulose films have low oxygen permeability and reasonable water vapour permeability. However, the effect on the fibres and material of recycling such films has not been widely investigated. In the work reported here, we made nanocellulose films via spray coating and then recycled them using disintegration, before forming into films with vacuum filtration. The formed films were compared virgin films also formed with vacuum filtration. The recycled films retained 70 % of the strength of the virgin films. The water vapour permeability (WVP) approximately doubled, increasing to 1.2×10^{-10} $g.m^{-1}.s^{-1}$ Pa^{-1}. Investigations across a range of length scales pinpointed that the likely difference was due to bundles of the cellulose nanofibers that had not fully separated in recycling.

Introduction

Currently, the synthetic polymers in food, medical and pharmaceutical packaging are neither renewable nor biodegradable and are accumulating in the environment, damaging the eco-system. Additionally, recycling of synthetic polymer is complex due to the contamination and the difficulty of separating synthetic polymers for reprocessing. For example, polyolefin films cannot be reprocessed into the original product, as the recycled product would not yield suitable barrier performance, failing to reuse the material. Cellulose fibre-based packaging materials, such as boxes, cartons and paper are renewable, recyclable and biodegradable but are poor barriers to oxygen and water due to the presence of wide pores. Laminating with polymers, such as LDPE, can yield products with sufficient barrier performance, but at the expense of recyclability and biodegradability). To combat this problem, nanocellulose is under widespread investigation.   It is biodegradeable and renewable and nanocellulose films possesses low oxygen (Aulin et al., 2010) and moderate water vapour permeability, something that can be improved by forming nanocellulose-nanoparticle composites (Varanasi et al., 2018). There remains the question of the recyclability of the films and the effect of recycling on the properties. This is addressed in this study.

Methods

The material tested was a commercial, never-dried Japanese MFC with an average diameter of 73 nm (Varanasi et al., 2013). A large number of virgin NC sheets were prepared by spraying (Shanmugam et al., 2018; Shanmugam et al., 2017). These virgin NC sheets were then recycled using laboratory dispersion techniques, under ISO standard conditions, to produce nanofibre suspensions. Following

dispersion, the nanofibre suspension was then formed into sheets using vacuum filtration. For comparison, another set of sheets from the virgin fibres was also formed.

The air permeance of dried films was measured with an L&W air permeance tester. Water vapour permeability was evaluated according to the ASTM standard (E96/E96M-05) method using anhydrous Calcium Chloride. Zero-span strength was measured with a Pulmac troubleshooter.

Result and Discussion

Table 1 summarises the results on the virgin and recycled fibres and films. The results are presented in order of the length scale over which they are measured. It can be seen that there is no evidence of observable differences in the films at the individual fibre level or at SEM under high magnification. The major differences show up at larger length scales. The recycled films are less dense and have poorer optical uniformity at smaller length scales. These differences are probably due to small aggregates from the virgin sheet that have failed to fully separate during the recycling process. These aggregates have hindered the uniform, dense packing of the nanofibers to form a sheet using vacuum filtration. This has then reduced the density of the sheet, increasing the water vapour permeability and decreasing the tensile strength at both small (Varanasi et al., 2012) and large (100 mm span) inspection scales.

Table 1 – Effect of Recycling on Properties of NC fibres

Measurement Technique	Area examined	Virgin film	Recycled film
SEM Measurement of Fibre diameter	1 micron scale bar	69 nm	69 nm
SEM Measurement of Film Surface	10 micron scale bar	No differences observed	No differences observed
Optical Profilometry roughness	100 x 90 microns	No differences observed	No differences observed
Film density	110 micron thick	831 kg/m3	741 kg/m^3
Zero-span strength	Estimated 300 micron span length	100 Nm/g	72 Nm/g
PPF tester of optical uniformity	1-15 mm inspection areas	More uniform	Less uniform
Water Vapour Permeability	63.5 mm diameter circle of film	5.5×10^{-11} g/m.s.Pa,	1.2×10^{-10} g/m.s.Pa,
Air permeability	50 cm^2 sample	<0.003 µm/Pa.S	0.045 µm/Pa.S
Tensile strength via Instron Method	100 mm test span	64 Nm/g	42 Nm/g

Conclusion:

The recycling of NC reduces strength and barrier performance. However, barrier performance is still much better than conventional cellulose based packaging. The major issue appears to be that the recycling process has not completely broken down the nanocellulose sheets into individual fibres.

Acknowledgements

Reference

Aulin, C., Gällstedt, M., Lindström, T. 2010. Oxygen and oil barrier properties of microfibrillated cellulose films and coatings. *Cellulose*, **17**(3), 559-574.

Shanmugam, K., Varanasi, S., Garnier, G., Batchelor, W. 2018. Flexible Spray Coating Process for Smooth Nanocellulose Film Production. *Cellulose*, **25**(3), 1725-1741.

Shanmugam, K., Varanasi, S., Garnier, G., Batchelor, W. 2017. Rapid Preparation of smooth nanocellulose films using spray coating. *Cellulose*, **24**(7), 2669-2676.

Varanasi, S., Chiam, H.H., Batchelor, W. 2012. Application and interpretation of zero and short-span testing on nanofibre sheet materials. *Nordic Pulp and Paper Research Journal*, **27**(2), 343-351.

Varanasi, S., Garusinghe, U., Simon, G.P., Garnier, G., Batchelor, W. 2018. Novel In-situ Precipitation Process to Engineer Low Permeability Porous Composite. *Scientific Reports*, **8**(1), 10747.

Varanasi, S., He, R., Batchelor, W.J. 2013. Estimation of cellulose nanofibre aspect ratio from measurements of fibre suspension gel point. *Cellulose*, **20**(4), 1885-1896.